

Fall 1994

Section I: Thermodynamic properties of hydrocarbon radicals, peroxy hydrocarbon and peroxy chlorohydrocarbon molecules and radicals  
Section II: Kinetics and reaction mechanisms for :  
(1) chloroform pyrolysis and oxidation (2) benzene and toluene oxidation under atmospheric conditions

Tsan-Horng Lay  
*New Jersey Institute of Technology*

Follow this and additional works at: <https://digitalcommons.njit.edu/dissertations>

 Part of the [Environmental Sciences Commons](#)

---

### Recommended Citation

Lay, Tsan-Horng, "Section I: Thermodynamic properties of hydrocarbon radicals, peroxy hydrocarbon and peroxy chlorohydrocarbon molecules and radicals Section II: Kinetics and reaction mechanisms for : (1) chloroform pyrolysis and oxidation (2) benzene and toluene oxidation under atmospheric conditions" (1994). *Dissertations*. 1101.  
<https://digitalcommons.njit.edu/dissertations/1101>

This Dissertation is brought to you for free and open access by the Theses and Dissertations at Digital Commons @ NJIT. It has been accepted for inclusion in Dissertations by an authorized administrator of Digital Commons @ NJIT. For more information, please contact [digitalcommons@njit.edu](mailto:digitalcommons@njit.edu).

## **Copyright Warning & Restrictions**

The copyright law of the United States (Title 17, United States Code) governs the making of photocopies or other reproductions of copyrighted material.

Under certain conditions specified in the law, libraries and archives are authorized to furnish a photocopy or other reproduction. One of these specified conditions is that the photocopy or reproduction is not to be “used for any purpose other than private study, scholarship, or research.” If a user makes a request for, or later uses, a photocopy or reproduction for purposes in excess of “fair use” that user may be liable for copyright infringement,

This institution reserves the right to refuse to accept a copying order if, in its judgment, fulfillment of the order would involve violation of copyright law.

**Please Note: The author retains the copyright while the New Jersey Institute of Technology reserves the right to distribute this thesis or dissertation**

Printing note: If you do not wish to print this page, then select “Pages from: first page # to: last page #” on the print dialog screen

The Van Houten library has removed some of the personal information and all signatures from the approval page and biographical sketches of theses and dissertations in order to protect the identity of NJIT graduates and faculty.

## ABSTRACT

### SECTION I: THERMODYNAMIC PROPERTIES OF HYDROCARBON RADICALS, PEROXY HYDROCARBON AND PEROXY CHLOROHYDROCARBON MOLECULES AND RADICALS

### SECTION II: KINETICS AND REACTION MECHANISMS FOR: (1) CHLOROFORM PYROLYSIS AND OXIDATION (2) BENZENE AND TOLUENE OXIDATION UNDER ATMOSPHERIC CONDITIONS

by  
Tsan-Horng Lay

Alkyl radicals are important active intermediates in gas phase photochemistry and combustion reaction systems. With the exception of a limited number of the most elementary radicals, accurate thermodynamic properties of alkyl radicals are either not available or only rough estimations exist. An H atom Bond Increment approach is developed and a data base is derived, for accurately estimating thermodynamic properties ( $\Delta H_f^{\circ}_{298}$ ,  $S^{\circ}_{298}$  and  $C_p(T)$ ) for generic classes of hydrocarbon radical species.

Reactions of alkyl radicals with molecular oxygen are one of the major reaction paths for these radicals in atmospheric photochemistry, oxidation of hydrocarbon liquids and combustion process. Alkyl hydroperoxides are subsequently formed through the alkyl peroxy radicals reactions with varied chemical species present in the reaction system. Thermodynamic properties of the alkyl hydroperoxides and related radicals are therefore frequently required in gas phase modeling and kinetic studies on these systems. The thermodynamic properties of alkyl hydroperoxides, alkyl peroxy radicals and



hydroperoxyl-1-ethyl radicals including the species with fluorine and chlorine substituents on the  $\alpha$ -carbon are evaluated using molecular orbital calculations.

Chloroform is used as a model chlorocarbon system with high Cl/H ratio to investigate thermal decomposition processes of chlorocarbons in oxidative and pyrolytic reaction environments. A detailed reaction mechanism is developed to describe the important features of products and reagent loss and is shown to predict the experimental data well. Reaction pathways and rate constants are developed for  $\text{CCl}_3$ ,  $\text{CCl}_2$  and  $\text{C}_2\text{Cl}_3$  radical addition to  $\text{O}_2$  and combination with O, OH,  $\text{HO}_2$  and ClO.

The reversible addition reaction of OH radical with benzene to form the hydroxyl-2,4-cyclohexadienyl (benzene-OH) adduct and the subsequent reactions of this benzene-OH adduct with  $\text{O}_2$  are important initial steps for the photooxidation of benzene and other aromatic species in the atmosphere. OH addition to the benzene ring, the subsequent reaction of  $\text{O}_2$  with the hydroxyl-2,4-cyclohexadienyl to form hydroxyl-2-peroxy-4-cyclohexenyl (benzene-OH- $\text{O}_2$  adduct), are chemical activation reactions and are a function of both pressure and temperature. The kinetics of these two reaction systems at various pressure & temperatures using a quantum version of Rice-Ramsperger-Kassel theory (QRRK) and a modified strong collision approach are analyzed and calculated. The analogue reaction system of toluene photooxidation is also analyzed. Reaction mechanisms are developed for initial steps of atmospheric oxidation of benzene and toluene, which include reverse reaction rates determined from thermodynamic parameters and microscopic reversibility. The model results show good agreement with the limited available experimental data.

**SECTION I: THERMODYNAMIC PROPERTIES OF HYDROCARBON  
RADICALS, PEROXY HYDROCARBON AND PEROXY  
CHLOROXYDROCARBON MOLECULES AND RADICALS**

**SECTION II: KINETICS AND REACTION MECHANISMS FOR:  
(1) CHLOROFORM PYROLYSIS AND OXIDATION  
(2) BENZENE AND TOLUENE OXIDATION UNDER ATMOSPHERIC  
CONDITIONS**

by  
**Tsan-Horng Lay**

**A Dissertation  
Submitted to the Faculty of  
New Jersey Institute of Technology  
in Partial Fulfillment of the Requirements for the Degree of  
Doctor of Philosophy**

**Department of Chemical Engineering,  
Chemistry and Environmental Science**

**January 1995**

Copyright © 1995 by Tsan-Horng Lay

ALL RIGHTS RESERVED

**APPROVAL PAGE**

**SECTION I: THERMODYNAMIC PROPERTIES OF HYDROCARBON  
RADICALS, PEROXY HYDROCARBON AND PEROXY  
CHLOROHYDROCARBON MOLECULES AND RADICALS**

**SECTION II: KINETICS AND REACTION MECHANISMS FOR:  
(1) CHLOROFORM PYROLYSIS AND OXIDATION  
(2) BENZENE AND TOLUENE OXIDATION UNDER ATMOSPHERIC  
CONDITIONS**

**Tsan-Horng Lay**

---

Dr. Joseph W. Bozzelli, Dissertation Advisor Date  
Distinguished Professor of Chemistry, NJIT

---

Dr. Barbara B. Kebbekus, Committee Member Date  
Professor of Chemistry, Associate Chairperson of the Department of Chemical  
Engineering, Chemistry and Environmental Science, NJIT

---

Dr. Lev N. Krasnoperov, Committee Member Date  
Associate Professor of Chemistry, NJIT

---

Dr. Richard Trattner, Committee Member Date  
Professor of Chemistry and Environmental Science, Associate Chairperson and  
Graduate Advisor for Environmental Science, NJIT

---

Dr. Carol A. Venanzi, Committee Member Date  
Professor of Chemistry, NJIT

---

Dr. Daniel J. Watts, Committee Member Date  
Executive Director of Emission Reduction Research Center, NJIT

---

Dr. William H. Green, Committee Member Date  
Senior Chemist, Exxon Research and Engineering Company

## BIOGRAPHICAL SKETCH

**Author:** Tsan-Horng Lay  
**Degree:** Doctor of Philosophy  
**Date:** January 1995

### Undergraduate and Graduate Education:

- Doctor of Philosophy in Environmental Science  
New Jersey Institute of Technology, Newark, NJ, 1995
- Bachelor of Science in Chemistry,  
National Cheng Kung University, Tainan, Taiwan

**Major:** Environmental Science

### Presentations and Publications:

Bozzelli, Joseph W., Lay, Tsan-Horng, Anderson, William R. and Sausa, Rosario C.,  
“CF<sub>2</sub>O Conversion / Burnout in CF<sub>3</sub>Br Inhibited CH<sub>4</sub> Flames: Reactions of OH and  
O with CF<sub>2</sub>O”, *Chemical and Physical Process in Combustion*, 1994, Proceeding  
of 1994 Technical Meeting at Clearwater, Florida, The Eastern States Section of  
The Combustion Institute, December 5-7, 1994.

Lay, Tsan-Horng and Bozzelli, Joseph W., “Detailed Analysis of Photochemical  
Oxidation of Benzene in the Atmosphere: Benzene + OH and the Adduct  
(Hydroxy-2,4-cyclohexadienyl) + O<sub>2</sub>”, *1994 AIChE Annual Meeting*,  
San Francisco, California, November 13-19, 1994.

Lay, Tsan-Horng and Bozzelli, Joseph W., “Thermodynamic Properties of Oxygenated  
Hydrocarbon Radical Species using Hydrogen Atom Bond Dissociation Groups”,  
*1994 AIChE Annual Meeting*, San Francisco, California, November 13-19, 1994.

- Lay, Tsan-Horng, Krasnoperov, Lev N., Venanzi, Carol and Bozzelli, Joseph W., “*Ab Initio* Study of Structures, Barriers for Internal Rotation, Vibrational Frequencies, and Thermodynamic Properties of Hydroperoxide Molecules:  $\text{CH}_3\text{CH}_2\text{OOH}$ ,  $\text{CH}_3\text{CHClOOH}$  and  $\text{CH}_3\text{CCl}_2\text{OOH}$ ”, *208th ACS National Meeting*, Washington, DC, August 21-25, 1994.
- Lay, Tsan-Horng and Bozzelli, Joseph W., “Pathways and Kinetic Evaluation of Benzene Oxidation in the Atmosphere: Benzene + OH and the Adduct (Hydroxy-2,4-cyclohexadienyl) +  $\text{O}_2$ ”, *ACS 7th BOC Priestley Conference*, Lewisburg, Pennsylvania, June 24-27, 1994
- Lay, Tsan-Horng and Bozzelli, Joseph W., “Thermodynamic Properties of Oxy-Hydrocarbons and Oxy-Hydrocarbon Radicals Species”, *1993 AIChE Annual Meeting*, St. Louis, Missouri, November 7-12, 1993.
- Lay, Tsan-Horng and Bozzelli, Joseph W., “Hydrogen Atom Bond Dissociation Groups for Calculation of Thermodynamic Properties of Oxy-Hydrocarbons Radicals Species”, *Chemical and Physical Process in Combustion, 1993*, Proceeding of 1993 Technical Meeting at Princeton, New Jersey, The Eastern States Section of The Combustion Institute, October 25-27, 1993.
- Lay, Tsan-Horng, Ritter, Edward and Bozzelli, Joseph W., “Hydrogen Atom Bond Dissociation Groups for Use in Calculation of Thermodynamic Properties of Radicals Species”, *Combustion Fundamentals and Applications, 1993*, Proceeding of 1993 Joint Technical Meeting at New Orleans, Louisiana, The Central and Eastern States Sections of The Combustion Institute, March 15-17, 1993.

This thesis is dedicated to  
Dad, Mom, Hsiu-Fen and Vincent

## ACKNOWLEDGMENT

The author wishes to express his earnest gratefulness to his advisor, Dr. Joseph W. Bozzelli, for his instruction, encouragement and friendship. Special appreciation to Dr. Lev N. Krasnoperov and Dr. Carol A. Venanzi for timely help and generous support. The author also thanks Dr. Barbara B. Kebbekus, Dr. Richard Trattner, Dr. Daniel J. Watts and Dr. William H. Green for serving as members of the committee and their valuable corrections.

It is the author's pleasure to acknowledge his colleagues at NJIT Thermodynamics and Kinetics Research Group: Mr. Hong-Ming Chiang, Mr. Hsien-Tsung Chern, Dr. Yo-Ping Wu, Dr. Yang Soo Won and Dr. Wen-Pin Ho who shared with me their experience and knowledge. The appreciation for friendship and assistance from current and past students in this research group cannot be exaggerated.

The author shall be endlessly grateful to his wife, Hsiu-Fen, and his parents for all they did. All of this would not have been possible without their constant support and encouragement.



## TABLE OF CONTENTS

Chapter	Page
SECTION I: THERMODYNAMIC PROPERTIES OF HYDROCARBON RADICALS, PEROXY HYDROCARBON AND PEROXY CHLOROHYDROCARBON MOLECULES AND RADICALS	
1 INTRODUCTION.....	1
1.1 Thermodynamic Properties of Hydrocarbon Radicals.....	1
1.2 Importance of Alkyl Peroxy Radicals and Alkyl Hydroperoxides in Gas Phase Kinetics.....	2
1.3 Thermodynamic Properties of Alkyl Hydroperoxides with and without Chlorine and Fluorine Substituents.....	4
1.4 <i>Ab Initio</i> Study.....	4
1.4.1 The General Performance of <i>Ab Initio</i> MO Calculations at HF/6-31G* Level of Theory.....	5
1.4.2 Comparison of Semiempirical and <i>Ab Initio</i> MO Calculations.....	6
1.5 Hindered Rotor.....	7
1.6 Modeling Study of Chloroform Pyrolysis and Oxidation: Effects of Added O <sub>2</sub> ....	9
1.7 Detailed Analysis of Initial Reactions of Photochemical Oxidation of Benzene and Toluene in the Atmosphere.....	9
2 HYDROGEN ATOM BOND INCREMENTS (HBI) FOR CALCULATION OF THERMODYNAMIC PROPERTIES OF HYDROCARBON RADICAL SPECIES.....	12
2.1 Introduction.....	12
2.2 Methodology and Calculations.....	16
2.2.1 Heats of Formation.....	16
2.2.2 Entropies (S° <sub>298</sub> ) and Heat Capacities (C <sub>p</sub> (T), 300≤T/K≤1500).....	17

**TABLE OF CONTENTS**  
(Continued)

Chapter	Page
2.2.3 Vibrational Frequencies .....	18
2.2.4 Hindered Internal Rotations.....	19
2.2.5 Spin Degeneracy and Symmetry.....	19
2.3 Calculation Details in Determining the Values of $\Delta S^{\circ}_{298}(\text{HBI})$ and $\Delta C_p(T)(\text{HBI})$ .....	20
2.3.1 <i>CCJ</i> , <i>RCCJ</i> , <i>ISOBUTYL</i> and <i>NEOPENTYL</i> .....	21
2.3.2 <i>CCJC</i> , <i>RCCJC</i> and <i>RCCJCC</i> .....	22
2.3.4 <i>TERTALKYL</i> .....	22
2.3.5 $C \equiv CJ$ .....	23
2.3.6 <i>VIN</i> .....	23
2.3.7 $C=C=CJ$ .....	23
2.3.8 <i>VINS</i> .....	24
2.3.9 <i>ALLYL_P</i> .....	24
2.3.10 <i>ALLYL_S</i> .....	25
2.3.11 <i>ALLYL_T</i> .....	25
2.3.12 <i>BENZYL_P</i> , <i>BENZYL_S</i> and <i>BENZYL_T</i> .....	25
2.3.13 Other Radicals.....	26
2.4 Discussion.....	28
2.5 Summary.....	32
2.6 Expressions Used in Thermodynamic Calculations.....	32

**TABLE OF CONTENTS**  
(Continued)

Chapter	Page
3	THERMODYNAMIC PROPERTIES OF GAS-PHASE ALKYL HYDROPEROXIDE COMPOUNDS WITH AND WITHOUT CHLORINE AND FLUORINE SUBSTITUENTS..... 35
3.1	Introduction..... 35
3.2	Calculation Method..... 37
3.2.1	Standard Enthalpy of Formation, $\Delta H_f^\circ_{298}$ ..... 37
3.2.2	Entropy ( $S^\circ_{298}$ ) and Heat Capacity ( $C_p^\circ(T)$ )..... 38
3.2.3	Comparison of Currently Available Thermodynamic Properties with Benson's Group Additivity Scheme..... 39
3.2.4	Scheme II..... 42
3.3	Results and Discussion..... 42
3.4	Conclusion..... 44
4	<i>AB INITIO</i> STUDY OF $\text{CH}_3\text{CH}_2\text{OOH}$ , $\text{CH}_3\text{CHClOOH}$ AND $\text{CH}_3\text{CCl}_2\text{OOH}$ : CONFORMATION ANALYSIS, INTERNAL ROTATION BARRIERS, VIBRATIONAL FREQUENCIES, AND THERMODYNAMIC PROPERTIES ..... 46
4.1	Introduction..... 46
4.2	Literature Survey..... 47
4.2.1	Molecular Structure of Hydroperoxides..... 47
4.2.2	Thermochemistry of Hydroperoxides..... 49
4.2.3	Comparison of Semiempirical and <i>Ab Initio</i> MO Calculations..... 50
4.3	Method..... 51
4.4	Results and Discussion..... 53

**TABLE OF CONTENTS**  
(Continued)

<b>Chapter</b>	<b>Page</b>
4.4.1 Molecular Geometries.....	53
4.4.2 Vibrational Frequencies.....	54
4.4.3 Rotational Barriers.....	54
4.4.4 Heat of Formation.....	56
4.4.5 Thermodynamic Properties.....	60
4.4.6 Coupling Effects of Internal Rotations.....	60
4.4.7 Comparison of MNDO/AM1 and PM3 Molecular Geometries and Vibrational Frequencies.....	61
4.5 Summary.....	62
5 <i>AB INITIO</i> STUDY OF $\alpha$ -CHLORINATED ETHYL PEROXY RADICALS, CH <sub>3</sub> CH <sub>2</sub> OO, CH <sub>3</sub> CHClOO AND CH <sub>3</sub> CCl <sub>2</sub> OO: CONFORMATIONAL ANALYSIS, INTERNAL ROTATION BARRIERS, VIBRATIONAL FREQUENCIES, AND THERMODYNAMIC PROPERTIES.....	64
5.1 Introduction.....	64
5.2 Method.....	66
5.3 Results and Discussion.....	68
5.3.1 Molecular Geometries.....	68
5.3.2 Vibrational Frequencies.....	69
5.3.3 Rotational Barriers.....	70
5.3.4 Heat of Formation.....	72
5.3.5 Thermodynamic Properties.....	74

**TABLE OF CONTENTS**  
(Continued)

<b>Chapter</b>	<b>Page</b>
5.3.6 Comparison of MNDO/AM1 and PM3 Molecular Geometries and Vibrational Frequencies.....	74
5.4 Summary.....	75
6 <i>AB INITIO</i> STUDY OF HYDROPEROXYL- 1-ETHYL AND 1-CHLORO-1-ETHYL RADICALS, CH <sub>3</sub> C.HOOH AND CH <sub>3</sub> C.CIOOH: CONFORMATIONAL ANALYSIS, INTERNAL ROTATION BARRIERS, VIBRATIONAL FREQUENCIES, AND THERMODYNAMIC PROPERTIES.....	77
6.1 Introduction.....	77
6.2 Method.....	78
6.3 Results and Discussion.....	78
6.3.1 Molecular Geometries.....	78
6.3.2 Vibrational Frequencies.....	79
6.3.3 Rotational Barriers.....	80
6.3.4 Enthalpies of Formation.....	82
6.3.4.1 Determination of $\Delta H_f^{\circ}_{298}(\text{CH}_3\text{C.HOOH})$ .....	82
6.3.4.2 Determination of $\Delta H_f^{\circ}_{298}(\text{CH}_3\text{C.HOOH})$ and $\Delta H_f^{\circ}_{298}(\text{CH}_3\text{C.CIOOH})$ .....	83
6.3.4.3 Difference of Bond Dissociation Energy of $\alpha\text{C-H}$ Bond.....	83
6.3.5 Thermodynamic Properties.....	85
6.3.6 Comparison of MNDO/AM1 and PM3 Molecular Geometries and Vibrational Frequencies.....	85
6.4 Summary.....	87

**TABLE OF CONTENTS**  
(Continued)

<b>Chapter</b>	<b>Page</b>
SECTION II: KINETICS AND REACTION MECHANISMS FOR:	
(1) CHLOROFORM PYROLYSIS AND OXIDATION	
(2) BENZENE AND TOLUENE OXIDATION UNDER ATMOSPHERIC CONDITIONS	
7	CHLOROFORM PYROLYSIS AND OXIDATION: EFFECTS OF ADDED O <sub>2</sub> ..... 88
7.1	Introduction..... 88
7.2	Experimental..... 91
7.2.1	Method..... 91
7.2.2	Result and Discussion..... 92
7.3	Quantum RRK Calculations..... 94
7.3.1	Chloroform Pyrolysis..... 95
7.3.2	Chloroform Oxidation..... 97
7.4	Mechanism..... 100
7.5	Comparison of Predictions with Observed Data..... 102
7.6	Conclusion..... 104
8	DETAILED ANALYSIS OF PHOTOCHEMICAL OXIDATION OF BENZENE AND TOLUENE IN THE ATMOSPHERE: BENZENE + OH AND THE ADDUCT (HYDROXYL-2,4-CYCLOHEXADIENYL) + O <sub>2</sub> TOLUENE + OH AND THE ADDUCT (HYDROXYL-2-METHYL-2,4-CYCLOHEXADIENYL) + O <sub>2</sub> ..... 106
8.1	Introduction..... 106

**TABLE OF CONTENTS**  
(Continued)

<b>Chapter</b>	<b>Page</b>
8.2 Calculations and Results of Benzene Photooxidation System.....	110
8.2.1 Chemical Activated Reactions of OH + Benzene.....	110
8.2.1.1 Thermodynamic Properties for Benzene-OH Adduct.....	110
8.2.1.2 Quantum RRK Calculation for Benzene + OH.....	112
8.2.2 Chemical Activated Reactions of Benzene-OH Adduct + O <sub>2</sub> .....	113
8.2.2.1 Thermodynamic Properties for Benzene-OH-O <sub>2</sub> Adduct.....	114
8.2.2.2 Thermodynamic Properties and Ring Strain Energy for Bicyclic Peroxy Species.....	115
8.2.2.2.1 Enthalpy and Ring Strain Energy.....	116
8.2.2.2.2 Entropy and Heat Capacities.....	119
8.2.2.3 Quantum RRK calculation of Benzene-OH Adduct + O <sub>2</sub> .....	120
8.2.2.4 Reactions of Ring Cleavage: Estimation of Beta-Scission Reaction Parameters (Transition State Study).....	122
8.2.2.4.1 Adduct IX => Butene-1,4-dial + CHOC.HOH.....	123
8.2.2.4.2 Adduct X => Butene-1,4-dial + CHOC.HOH.....	124
8.2.2.4.3 Adduct XI => 1-Hydroxy-Butene-4-al-1yl + Glyoxal.....	124
8.3 Calculations and Results of Toluene Photooxidation System.....	125
8.3.1 The Chemical Activated Reactions of OH + Toluene.....	125
8.3.2 The Chemical Activated Reactions of Toluene-OH Adduct + O <sub>2</sub> .....	126
8.3.2.1 Quantum RRK Calculation for Toluene-OH + O <sub>2</sub> .....	128
8.3.3 Ring Cleavage Reactions.....	128

**TABLE OF CONTENTS**  
**(Continued)**

<b>Chapter</b>	<b>Page</b>
8.4 Model Prediction.....	129
8.4.1 Benzene Photooxidation.....	130
8.4.2 Toluene Photooxidation.....	131
8.5 Discussion.....	132
8.6 Summary.....	134
APPENDIX A TABLES FOR SECTION I.....	136
APPENDIX B FIGURES FOR SECTION I.....	192
APPENDIX C TABLES FOR SECTION II.....	226
APPENDIX D FIGURES FOR SECTION II.....	249
REFERENCES.....	298



## LIST OF TABLES

Table	Page
2.1 Definition of HBI Group Term Name, Model Radicals and Corresponding Bond Energy of C-H Bond.....	136
2.2 Fundamental Vibration Frequencies ( $\text{cm}^{-1}$ ) for Model Stable Molecules and Free Radicals.....	139
2.3 Assignment of Vibration Frequency in this Work.....	140
2.4 Moments of Inertia ( $I_r$ ), Torsion Barriers ( $V$ ) and Foldness Numbers ( $\sigma$ ) to Hindered Rotation about Single Bonds.....	141
2.5 Calculation Details of HBI $\Delta S^\circ_{298}$ and $\Delta C_p(T)$ Values.....	142
2.6 Standard Entropy and Heat Capacities for Species Used Directly to Calculate HBI Group Values.....	147
2.7 Molecular Weight, Moments of Inertia for External Rotation and Fundamental Vibration Frequencies for the Radicals in Table 2.6.....	148
2.8 Data Base for HBI Group for Hydrocarbon Radicals.....	148
2.9 Comparison of Calculated Thermo Data from this Study with Literatures.....	149
3.1 Literature Survey of Standard Enthalpy of Formation (298K) (kcal/mol).....	151
3.2 Bond Energy of (O)O-H Bond in Hydroperoxides ( $D^\circ_{298}(\text{ROO-H})$ , kcal/mol).....	153
3.3 Vibration Frequencies, Barriers of Internal Hindered Rotations and Moments of Inertia ( $I_x$ , $I_y$ , $I_z$ ) for External Rotations of Stable Species.....	153
3.4 Potential Barriers for Hindered Internal Rotations ( $V(\text{HR})$ ) about Single Bonds.....	155
3.5 Thermodynamic Properties for Stable Molecules and Comparison.....	156
3.6 Consistence Study of Group Values of General Scheme GA Approach.....	157
3.7 Group Values of Scheme II.....	157

**LIST OF TABLES**  
(Continued)

<b>Table</b>	<b>Page</b>
4.1 Previous Studies on Geometry and Rotational Barriers of H <sub>2</sub> O <sub>2</sub> and D <sub>2</sub> O <sub>2</sub> as Determined by far IR, Microwave Spectroscopy and <i>Ab Initio</i> Study.....	158
4.2 Structure Parameters for CH <sub>3</sub> CH <sub>2</sub> OOH at HF/6-31G*.....	159
4.3 Structure Parameters for CH <sub>3</sub> CHClOOH at HF/6-31G*.....	160
4.4 Structure Parameters for CH <sub>3</sub> CCl <sub>2</sub> OOH at HF/6-31G*.....	161
4.5 Molecular Mulliken Charge Distribution Calculated at MP2/6-31G**.....	162
4.6 Harmonic Vibration Frequencies (cm <sup>-1</sup> ) of CH <sub>3</sub> CH <sub>2</sub> OOH Rotational Conformers.....	163
4.7 Harmonic Vibration Frequencies (cm <sup>-1</sup> ) of CH <sub>3</sub> CHClOOH Rotational Conformers.....	164
4.8 Harmonic Vibration Frequencies (cm <sup>-1</sup> ) of CH <sub>3</sub> CCl <sub>2</sub> OOH Rotational Conformers.....	165
4.9 Rotational Barriers.....	166
4.10 Coefficients of Fourier Expansions for Internal Rotations.....	167
4.11 Total Energy and Enthalpies of Formation for Species in Isodesmic Reactions and the Reaction Energies.....	168
4.12 Reaction Energies (kcal/mol) and Enthalpies of Formation (kcal/mol) for CH <sub>3</sub> CH <sub>2</sub> OOH, CH <sub>3</sub> CHClOOH and CH <sub>3</sub> CCl <sub>2</sub> OOH.....	168
4.13 Coamparison of difference of Bond dissociation energies for DH°(R-OH) - DH°(R-OOH).....	169
4.14 Ideal Gas Phase Thermodynamic Properties for CH <sub>3</sub> CH <sub>2</sub> OOH, CH <sub>3</sub> CHClOOH and CH <sub>3</sub> CCl <sub>2</sub> OOH.....	169
4.15 Comparison of Pitzer & Gwinn's and the Method Used in this Study for Calculation of Thermodynamic Properties of Molecules with Hindered Rotors.....	170

**LIST OF TABLES**  
**(Continued)**

<b>Table</b>	<b>Page</b>
4.16 Comparison of Bond Lengths (Angstrom) among Different Calculation Levels.....	171
4.17 Comparison of Bond Angles (degree) among Different Calculation Levels.....	172
4.18 Comparison of Dihedral Angles (degree) among Different Calculation Levels...	173
5.1 Optimized Molecular Geometry Parameters of CH <sub>3</sub> CH <sub>2</sub> OO Rotational Conformers.....	174
5.2 Optimized Molecular Geometry Parameters of CH <sub>3</sub> CHClOO Rotational Conformers.....	175
5.3 Optimized Molecular Geometry Parameters of CH <sub>3</sub> CCl <sub>2</sub> OO. Rotational Conformers.....	176
5.4 Molecular Mulliken Charge Distribution Calculated at UHF/6-31G*.....	177
5.5 Harmonic Vibration Frequencies (cm <sup>-1</sup> ).....	178
5.6 Rotation Barriers.....	179
5.7 Potential Constants (kcal/mol) of Fourier Expansions for Internal Rotations.....	179
5.8 Total Energy and Enthalpies of Formation for Species in Isodesmic Reactions and the Reaction Energies.....	180
5.9 Reaction Energies (kcal/mol) and Enthalpies of Formation (kcal/mol) for CH <sub>3</sub> CH <sub>2</sub> OO, CH <sub>3</sub> CHClOO and CH <sub>3</sub> CCl <sub>2</sub> OO.....	180
5.10 Ideal Gas Phase Thermodynamic Properties for CH <sub>3</sub> CH <sub>2</sub> OO, CH <sub>3</sub> CHClOO and CH <sub>3</sub> CCl <sub>2</sub> OO.....	181
5.11 Comparison of Pitzer & Gwinn's and the Method Used in this Study for Calculation of Thermodynamic Properties of Molecules with Hindered Rotors.....	182
5.12 Comparison of Bond Lengths at Different Calculation Levels.....	182

**LIST OF TABLES**  
(Continued)

<b>Table</b>	<b>Page</b>
5.13 Comparison of Bond Angles at Different Calculation Levels.....	183
5.14 Comparison of Dihedral Angles at Different Calculation Levels.....	184
6.1 Optimized Molecular Geometry Parameters of CH <sub>3</sub> C.HOOH Rotational Conformers.....	184
6.2 Optimized Molecular Geometry Parameters of CH <sub>3</sub> C.CIOOH Rotational Conformers.....	185
6.3 Molecular Mulliken Charge Distribution Calculated at UHF/6-31G*.....	185
6.4 The Out-of-plane Angle ( $\gamma$ , in degrees) for All Rotational Conformers.....	186
6.5 Harmonic Vibration Frequencies (cm <sup>-1</sup> ) for Rotational Conformers of CH <sub>3</sub> C.HOOH.....	186
6.6 Harmonic Vibration Frequencies (cm <sup>-1</sup> ) for Rotational Conformers of CH <sub>3</sub> C.CIOOH.....	187
6.7 Rotation Barriers.....	187
6.8 Potential Constants (kcal/mol) of Fourier Expansions for Internal Rotations.....	188
6.9 Total Energy and Enthalpies of Formation for Species in Isodesmic Reactions and the Reaction Energies.....	188
6.10 Reaction Energies (kcal/mol) and Enthalpies of Formation (kcal/mol) for CH <sub>3</sub> C.HOOH and CH <sub>3</sub> C.CIOOH.....	189
6.11 Ideal Gas Phase Thermodynamic Properties for CH <sub>3</sub> C.HOOH and CH <sub>3</sub> C.CIOOH.....	189
6.12 Comparison of Pitzer & Gwinn's and the Method Used in this Study for Calculation of Thermodynamic Properties of Molecules with Hindered Rotors.....	190
6.13 Comparison of Bond Lengths (Å) among Different Calculation Levels.....	190

**LIST OF TABLES**  
**(Continued)**

<b>Table</b>	<b>Page</b>
6.14 Comparison of Bond Angles and Dihedral Angles (in degrees) among Different Calculation Levels.....	191
7.1 Detailed mechanism for Chloroform Pyrolysis in Ar Bath (Model A).....	226
7.2 Detailed mechanism for Chloroform Oxidation in Ar Bath (Model B).....	229
7.A.1 Input Parameters for QRRK Calculation: CHCl <sub>3</sub> Decomposition.....	234
7.A.2 Input Parameters for QRRK Calculation: CCl <sub>2</sub> + CHCl <sub>3</sub> → Products.....	234
7.A.3 Input Parameters for QRRK Calculation: CCl <sub>2</sub> + CCl <sub>2</sub> → Products.....	235
7.A.4 Input Parameters for QRRK Calculation: CCl <sub>2</sub> + CCl <sub>3</sub> → Products.....	235
7.A.5 Input Parameters for QRRK Calculation: CCl <sub>3</sub> + CCl <sub>3</sub> → Products.....	236
7.A.6 Input Parameters for QRRK Calculation: CCl <sub>2</sub> + O <sub>2</sub> → Products.....	236
7.A.7 Input Parameters for QRRK Calculation: CCl <sub>2</sub> + O → Products.....	237
7.A.8 Input Parameters for QRRK Calculation: CCl <sub>2</sub> + OH → Products.....	237
7.A.9 Input Parameters for QRRK Calculation: CCl <sub>3</sub> + O <sub>2</sub> → Products.....	238
7.A.10 Input Parameters for QRRK Calculation: CCl <sub>3</sub> + O → Products.....	238
7.A.11 Input Parameters for QRRK Calculation: C <sub>2</sub> Cl <sub>4</sub> + O → Products.....	239
8.1 Ideal Gas Phase Thermodynamic Properties ΔH <sub>f</sub> <sup>°</sup> <sub>298</sub> ( kcal/mol), S <sup>°</sup> <sub>298</sub> (cal/mol-K) and Cp(T)'s (cal/mol-K, 300 ≤ T/K ≤ 1000).....	240
8.2 Selected HBI Group Values, ΔS <sup>°</sup> <sub>298</sub> and ΔCp(T) (cal/mol-K) in Use for Thermodynamic Properties of Radicals.....	242
8.3 Input Parameters for QRRK Calculation and the Results of Apparent Rate Constants.....	242

**LIST OF TABLES**  
**(Continued)**

<b>Table</b>	<b>Page</b>
8.4 Input Parameters for QRRK Calculation and the Results of Apparent Rate Constants.....	243
8.5 Input Parameters for QRRK Calculation and the Results of Apparent Rate Constants.....	244
8.6 Input Parameters for QRRK Calculation and the Results of Apparent Rate Constants.....	245
8.7 Reaction Mechanism of Benzene Photooxidation.....	246
8.8 Reaction Mechanism of Toluene Photo-Oxidation.....	247
8.9 Forward Rate constants, Concentration Equilibrium Constants and Backward Rate Constants for Benzene-OH + O <sub>2</sub> System of Reactions.....	248

## LIST OF FIGURES

Figure	Page
2.1 Example of HBI Approach.....	192
4.1 Previous Studies of Rotational Barriers for RO--OH.....	193
4.2 Definitions of Nomenclature Used in this Work.....	194
4.3 Optimized Geometries at HF/6-31G*.....	195
4.4 Calculated Potential Barriers for Internal Rotation about C-C Bond.....	196
4.5 Calculated Potential Barriers for Internal Rotation about C-O Bond.....	197
4.6 Calculated Potential Barriers for Internal Rotation about O-O Bond.....	198
4.7 Investigation of Potential Energy Surface for Rotation about C-O Bond in CH <sub>3</sub> CHClOOH.....	199
4.8 Coupling Effects for Rotational Barriers of CH <sub>3</sub> --CH <sub>2</sub> OOH.....	200
4.9 Coupling Effects for Rotational Barriers of CH <sub>3</sub> CH <sub>2</sub> --OOH.....	201
4.10 Coupling Effects for Rotational Barriers of CH <sub>3</sub> CH <sub>2</sub> O--OH.....	202
4.11 Comparison of Harmonic Vibrational Frequencies Calculated using Semiempirical and <i>Ab Initio</i> MO for CH <sub>3</sub> CH <sub>2</sub> OOH.....	203
4.12 Comparison of Harmonic Vibrational Frequencies Calculated using Semiempirical and <i>Ab Initio</i> MO for CH <sub>3</sub> CHClOOH.....	204
4.13 Comparison of Harmonic Vibrational Frequencies Calculated using Semiempirical and <i>Ab Initio</i> MO for CH <sub>3</sub> CCl <sub>2</sub> OOH.....	205
5.1 Definitions of Nomenclature Used in this Work.....	206
5.2 Difference of C-O and O-O Bond Length between ROO and ROOH.....	207
5.3 Rotational Barriers for CH <sub>3</sub> --CXYOO.....	208
5.4 Rotational Barriers for CH <sub>3</sub> CH <sub>2</sub> --OO.....	209

**LIST OF FIGURES**  
(Continued)

<b>Figure</b>	<b>Page</b>
5.5 Rotational Barriers for CH <sub>3</sub> CHCl--OO.....	210
5.6 Rotational Barriers for CH <sub>3</sub> CH <sub>2</sub> --OO.....	211
5.7 Comparison of Harmonic Vibrational Frequencies Calculated using Semiempirical and <i>Ab Initio</i> MO for CH <sub>3</sub> CH <sub>2</sub> OO.....	212
5.8 Comparison of Harmonic Vibrational Frequencies Calculated using Semiempirical and <i>Ab Initio</i> MO for CH <sub>3</sub> CHClOO.....	213
5.9 Comparison of Harmonic Vibrational Frequencies Calculated using Semiempirical and <i>Ab Initio</i> MO for CH <sub>3</sub> CCl <sub>2</sub> OO.....	214
6.1 Definitions of Nomenclature Used in this Work.....	215
6.2 Definition of Out-of-plane Angle.....	216
6.3 Difference of C-O and O-O Bond Length between (a) CH <sub>3</sub> CH.OOH and CH <sub>3</sub> CH <sub>2</sub> OOH (b) CH <sub>3</sub> CCl.OOH and CH <sub>3</sub> CHClOOH.....	217
6.4 Rotational Barriers for CH <sub>3</sub> --CH.OOH.....	218
6.5 Rotational Barriers for CH <sub>3</sub> --CCl.OOH.....	219
6.6 Rotational Barriers for CH <sub>3</sub> CH.--OOH.....	220
6.7 Rotational Barriers for CH <sub>3</sub> CCl.--OOH.....	221
6.8 Rotational Barriers for CH <sub>3</sub> CH.O--OH.....	222
6.9 Rotational Barriers for CH <sub>3</sub> CCl.O--OH.....	223
6.10 Comparison of Harmonic Vibrational Frequencies Calculated using Semiempirical and <i>Ab Initio</i> MO for CH <sub>3</sub> C.HOOH.....	224
6.11 Comparison of Harmonic Vibrational Frequencies Calculated using Semiempirical and <i>Ab Initio</i> MO for CH <sub>3</sub> C.ClOOH.....	225



**LIST OF FIGURES**  
(Continued)

<b>Figure</b>	<b>Page</b>
7.1 Comparison of $\text{CHCl}_3$ Decay vs Temperature at Pyrolytic and Oxidative Environments.....	250
7.2 $\text{CCl}_4$ Formed per mole of $\text{CHCl}_3$ in Presence and Absence of Added $\text{O}_2$ .....	251
7.3 $\text{C}_2\text{Cl}_4$ Formed per mole of $\text{CHCl}_3$ in Presence and Absence of Added $\text{O}_2$ .....	252
7.4 $\text{CHCl}_3$ Pyrolysis Product Distribution vs Temperature ( $\text{CHCl}_3/\text{Ar}$ ).....	253
7.5 Decay of $\text{CHCl}_3$ in Chloroform Pyrolysis ( $\text{CHCl}_3/\text{Ar}$ ).....	254
7.6 $\text{CHCl}_3$ Pyrolysis at 873 K ( $\text{CHCl}_3/\text{Ar}$ ).....	255
7.7 $\text{CHCl}_3$ Pyrolysis at 908 K ( $\text{CHCl}_3/\text{Ar}$ ).....	256
7.8 $\text{CHCl}_3$ Oxidation Product Distribution vs Temperature (1% $\text{CHCl}_3$ + 1% $\text{O}_2$ ).....	257
7.9 $\text{CHCl}_3$ Oxidation at 953 K (1% $\text{CHCl}_3$ + 1% $\text{O}_2$ ).....	258
7.10 $\text{CHCl}_3$ Oxidation at 1008 K (1% $\text{CHCl}_3$ + 1% $\text{O}_2$ ).....	259
7.11 $\text{CHCl}_3$ Oxidation Product Distribution vs Temperature (1% $\text{CHCl}_3$ + 3% $\text{O}_2$ )...	260
7.12 $\text{CHCl}_3$ Oxidation at 873 K (1% $\text{CHCl}_3$ + 3% $\text{O}_2$ ).....	261
7.A.1 Potential Energy Diagram and Arrhenius Plot for Reactions: $\text{CHCl}_3 \Rightarrow$ Products.....	262
7.A.2 Potential Energy Diagram and Arrhenius Plot for Reactions: $\text{CCl}_2 + \text{CHCl}_3 \Rightarrow$ Products.....	263
7.A.3 Potential Energy Diagram and Arrhenius Plot for Reactions: $\text{CCl}_2 + \text{CCl}_2 \Rightarrow$ Products.....	264
7.A.4 Potential Energy Diagram and Arrhenius Plot for Reactions: $\text{CCl}_2 + \text{CCl}_3 \Rightarrow$ Products.....	265
7.A.5 Potential Energy Diagram and Arrhenius Plot for Reactions: $\text{CCl}_3 + \text{CCl}_3 \Rightarrow$ Products.....	266

**LIST OF FIGURES  
(Continued)**

<b>Figure</b>	<b>Page</b>
7.A.6 Potential Energy Diagram and Arrhenius Plot for Reactions: CCl <sub>2</sub> + O <sub>2</sub> => Products.....	267
7.A.7 Potential Energy Diagram and Arrhenius Plot for Reactions: CCl <sub>2</sub> + O => Products.....	268
7.A.8 Potential Energy Diagram and Arrhenius Plot for Reactions: CCl <sub>2</sub> + OH => Products.....	269
7.A.9 Potential Energy Diagram and Arrhenius Plot for Reactions: CCl <sub>3</sub> + O <sub>2</sub> => Products.....	270
7.A.10 Potential Energy Diagram and Arrhenius Plot for Reactions: CCl <sub>3</sub> + O => Products.....	271
7.A.11 Potential Energy Diagram and Arrhenius Plot for Reactions: C <sub>2</sub> Cl <sub>4</sub> + O => Products.....	272
8.1 Potential Energy Diagram for Benzene + OH.....	273
8.2 Arrhenius Plot of Benzene + OH => Products.....	274
8.3 Potential Energy Diagram for Benzene-OH Adduct + O <sub>2</sub> .....	275
8.4 Analysis of Correlation Factor for PM3 Enthalpy to Experimental Enthalpy.....	276
8.5 Potential Energy Diagram for Channel BA: Benzene-OH Adduct + O <sub>2</sub> => 2,4-Hexadiene-1,6-dial + OH.....	277
8.6 Potential Energy Diagram for Channel BB: Benzene-OH Adduct + O <sub>2</sub> => Phenol + HO <sub>2</sub> .....	278
8.7 Arrhenius Plot of Benzene-OH + O <sub>2</sub> => Products.....	279
8.8 Potential Energy Diagram for Adduct IX β-Scission.....	280
8.9 Potential Energy Diagram for Adduct X β-Scission.....	281
8.10 Potential Energy Diagram for Adduct XI β-Scission.....	282

**LIST OF FIGURES**  
**(Continued)**

<b>Figure</b>	<b>Page</b>
8.11 Potential Energy Diagram for Toluene + OH.....	283
8.12 Arrhenius Plot of Toluene + OH => Products.....	284
8.13 Potential Energy Diagram for Toluene-OH Adduct + O <sub>2</sub> .....	285
8.14 Arrhenius Plot of Toluene-OH Adduct + O <sub>2</sub> => Products.....	286
8.15 Selected Species Profiles of Model BM1.....	287
8.16 Selected Species Profiles of Model BM2.....	288
8.17 Selected Species Profiles of Model BM3.....	289
8.18 Selected Species Profiles of Model TM1.....	290
8.19 Selected Species Profiles of Model TM2.....	291

## CHAPTER 1

### INTRODUCTION

#### 1.1 Thermodynamic Properties of Hydrocarbon Radicals

Alkyl radicals are important active intermediates in gas phase reaction systems. With the exception of a limited number of the most elementary radicals, however, the accurate thermodynamic properties of most alkyl radicals are not available or only rough estimations. This is because of the difficulty of using calorimetric measurements or in determining structure and spectroscopy on these unstable species.<sup>1</sup>

An H atom Bond Increment (HBI) approach is developed and a data base is derived in Chapter 2, for accurately estimating thermodynamic properties ( $\Delta H_f^\circ_{298}$ ,  $S^\circ_{298}$  and  $C_p(T)$ ,  $300 \leq T/K \leq 1000$ ) for generic classes of hydrocarbon (HC) radical species relevant to combustion, atmospheric chemistry and the general organic chemistry community. The HBI group technique is based on known thermodynamic properties of the parent molecule and calculated changes that occur upon formation of a radical via loss of a H atom. The HBI method incorporates

- (i) evaluated literature bond energies,
- (ii) calculated entropy and heat capacity ( $C_p(T)$ ) increments resulting from loss and change in vibration frequencies (including inversion),
- (iii) increments resulting from changes in barriers and reduced moments of inertia to internal rotation, and

(iv) increment resulting from the change in spin degeneracy.

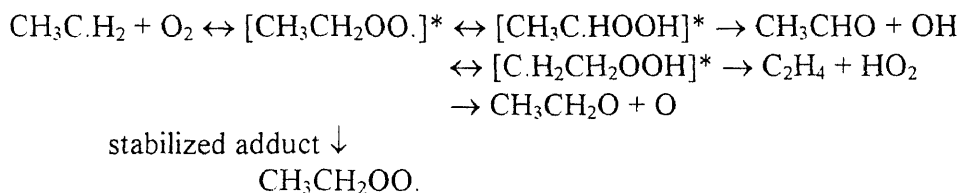
26 HBI groups are defined and the group values are calculated in this work. The HBI groups, when coupled with the thermodynamic properties of the appropriate "parent" molecules, yield accurate thermodynamic properties for the respective radicals. Corrections due to the change of translational and external rotation motions are considered only for small and light radicals where they are of significance. These HBI groups can be applied to determine accurate thermodynamic properties of any radical in the homology series.

### **1.2 Importance of Alkyl Peroxy Radicals and Alkyl Hydroperoxides in Gas Phase Kinetics**

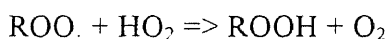
Reactions of alkyl radicals with molecular oxygen are one of the major reaction paths for these radicals in atmospheric photochemistry, oxidation of hydrocarbon liquid and in combustion process. These reactions are complex and their rates strongly depend on both pressure and temperature. An example for ethyl radical shows that, the energized adduct, ethyl peroxy [ $\text{CH}_3\text{CH}_2\text{OO}\cdot$ ]\* which is initially formed from the ethyl radical adding to  $\text{O}_2$  can undergo the following pathways:<sup>2</sup>

- (i) to be stabilized,
- (ii) to dissociate back to ethyl +  $\text{O}_2$  reactants,
- (iii) to isomerize by H atom shift to a hydroperoxyl-1-ethyl radical ( $\text{CH}_3\text{C}\cdot\text{HOOH}$ )
- (iv) to isomerize by H atom shift to a hydroperoxyl-2-ethyl radical ( $\text{C}\cdot\text{H}_2\text{CH}_2\text{OOH}$ ),
- (v) to dissociate to ethoxy + O atom.

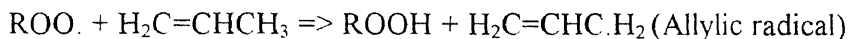
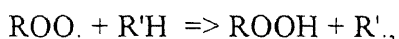
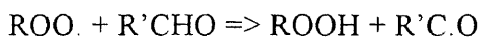
These pathways are often the major routes of transformation of alkyl radicals in combustion and atmospheric oxidation process. The products for ethyl radical can be summarized as following (\* denotes energized complex):



Alkyl hydroperoxides are subsequently formed through the alkyl peroxy radicals reactions with hydroperoxy radicals which are typically present in the reaction system.<sup>3,4,5,6</sup>



Alkyl hydroperoxides can also be produced via H atom abstraction of alkyl hydroperoxy radicals from aldehydes or other hydrocarbon species (chain propagation step in the reaction mechanism):<sup>7</sup>



The thermodynamic properties of the alkyl hydroperoxide and related radicals are therefore frequently required in gas phase kinetic studies. In this work the thermodynamic

properties of alkyl hydroperoxides (Chapter 3 and 4), alkyl peroxy radicals (Chapter 5) and hydroperoxyl-1-ethyl radicals (Chapter 6) including the species with fluorine (Chapter 3) and chlorine substitution on  $\alpha$ -carbon (Chapter 3-6) are studied.

### **1.3 Thermodynamic Properties of Alkyl Hydroperoxides with and without Chlorine and Fluorine Substituents**

A data base of thermodynamic properties ( $\Delta H_f^\circ$ ,  $S^\circ$ ,  $C_p^\circ(T)$ ,  $300 \leq T/K \leq 1000$ ) of gas-phase one to four carbon alkyl and monochloro and monofluoro hydroperoxides is presented in Chapter 3. Enthalpies of formation are obtained by evaluation of literature data. Entropies and heat capacities for stable species are calculated using the Rigid Rotor Harmonic Oscillator <sup>8</sup> approximation taking into account the contributions from translations, rotations, vibrations and internal rotations. Proper account is also taken for symmetry and optical isomers. Moments of inertia and fundamental frequencies are obtained using semiempirical, MNDO/PM3 <sup>9</sup> calculations in MOPAC6.0 <sup>10</sup> package. Barriers for internal rotations are adopted from appropriate experimental data or *ab initio* studies. Pitzer and Gwinn's <sup>11</sup> approach is used to calculate the contributions of hindered rotors. Group values for thermodynamic estimations are derived and allow applications to other hydroperoxide molecules and corresponding radicals.

### **1.4 *Ab Initio* Study**

The thermodynamic properties of  $\text{CH}_3\text{CH}_2\text{OOH}$ ,  $\text{CH}_3\text{CHClOOH}$ ,  $\text{CH}_3\text{CCl}_2\text{OOH}$  (in Chapter 4),  $\text{CH}_3\text{CH}_2\text{OO}$ ,  $\text{CH}_3\text{CHClOO}$ ,  $\text{CH}_3\text{CCl}_2\text{OO}$  (in Chapter 5)  $\text{CH}_3\text{C}\cdot\text{HOOH}$  and  $\text{CH}_3\text{C}\cdot\text{ClOOH}$  (in Chapter 6) are studied using *ab initio* Molecular Orbital (MO)

calculations. Conformational analysis, calculation of internal rotational barriers and vibrational frequencies are also carried out. The *ab initio* MO calculations are performed by means of the Gaussian92 system of programs<sup>12</sup> using the Hartree-Fock (HF) method and second order Møller-Plesset perturbation theory (MP2) with the 6-31G\* (6-31G(d)) and 6-31G\*\* (6-31G(d,p)) basis sets.<sup>13,14,15</sup> Unrestricted HF (UHF) is used for the calculations of open shell free radicals.

Several isodesmic reactions<sup>16,p271</sup> are constructed for evaluation of the enthalpies of formation on the above 8 species. The “isodesmic reactions” are defined as “transformations in which the numbers of bonds of each formal type are conserved and only the relationships among the bonds are altered”.<sup>16,p298</sup> All species involved in isodesmic reactions are calculated at the same level of theory. The use of isodesmic reactions for the calculation of reaction energies has been demonstrated by Hehre *et al.*<sup>16,p298-308</sup> as a generally accurate method. Thus determined reaction energies are combined with the known enthalpies of formation (experimentally determined) of species in reactions to obtain the unknown enthalpies of formation for the desired species.

#### **1.4.1 The General Performance of *Ab Initio* MO Calculations at HF/6-31G\* Level of Theory**

The performance of *ab initio* MO calculations using the Gaussian system of programs is studied by Hehre *et al.*<sup>16,p133-341</sup> The mean absolute bond lengths deviation from experiment is 0.014 Å for one-heavy-atom hydrides (AH<sub>n</sub> type molecules)<sup>16,p142</sup> at HF/6-31G\* level. The mean absolute error in bond lengths of single bonds between heavy atoms in two-heavy-atom hydrides (AH<sub>n</sub>-BH<sub>m</sub> type molecules) is 0.030 Å for 30 comparisons.



<sup>16,p164</sup> It is also found that single bonds involving second-row elements are well described using the HF/6-31G\* basis set and electron correlation effects are less significant in influencing the structures of these second-row systems than they are for the analogous first-row compounds. <sup>16,p154</sup> The mean absolute errors in calculated vs experimental bond lengths between heavy atoms are 0.023 Å for larger molecules than AH<sub>n</sub>-BH<sub>m</sub>. <sup>16,p165</sup>

The mean absolute percentage deviation from directly measured (anharmonic) values of the Hartree-Fock vibrational frequencies at the HF/6-31G\* level is 13.9%. When experimental anharmonic frequencies are corrected with harmonicity, the magnitude of the error is reduced to 9-11%. <sup>16,p260</sup>

It is also found <sup>16,p263</sup> that the rotational barriers calculated using 6-31G\* basis set reproduce observed trends in the methyl-group rotation barrier height reasonably well (CH<sub>3</sub>CH<sub>3</sub> > CH<sub>3</sub>NH<sub>2</sub> > CH<sub>3</sub>OH). For hydrogen peroxide (H<sub>2</sub>O<sub>2</sub>), the calculated *trans* barrier (0.9 kcal/mol) and *cis* barrier (9.2 kcal/mol) using the 6-31G\* level are reasonably close to experimental values (1.1 kcal/mol and 7.0 kcal/mol, respectively). <sup>16,p265</sup>

#### 1.4.2 Comparison of Semiempirical and *Ab Initio* MO Calculations

The general performance of semiempirical MO calculations for the molecules calculated in this work is also of interest since the two methods, MNDO/AM1 <sup>17</sup> or PM3 <sup>28</sup> are often used for calculations on large molecules, where *ab initio* calculations are not feasible.

The MNDO <sup>17</sup> method with standard AM1 and PM3 parameters in the MOPAC6.0<sup>10</sup> package is used to perform the semiempirical MO calculations. The equilibrium molecular geometries are calculated using AM1 and PM3, and the results are

compared to those obtained by *ab initio* studies at the (U)HF/6-31G\* level of theory. Harmonic vibrational frequencies are also calculated using AM1 and PM3 and compared to the Hartree-Fock frequencies. The keyword "PRECISE" is used to set up a more strict criteria of  $10^{-8}$  for the self-consistent-field (SCF) convergence in the geometry optimization process.

### 1.5 Hindered Rotor

One of the most uncertain aspects in calculating thermodynamic functions is the method for calculating the contribution of hindered internal rotations. Pitzer and Gwinn's method and tables<sup>11</sup> are widely used to calculate this contribution of hindered internal rotors to free energy, entropy and heat capacity of a molecule. However, Pitzer and Gwinn's approach is applicable only for a sinusoidal hindered potential (uniform barrier). In most cases the calculated potential for internal rotations actually cannot be represented by the single sine or cosine function. Here it is found that the use of Pitzer and Gwinn's tables lead to significant errors in internal rotor contributions to the thermodynamic functions (see Chapter 4,5,6).

A technique for calculation of thermodynamic functions from hindered rotations with arbitrary potentials therefore has been developed.<sup>18</sup> This technique employs expansion of the hindrance potential in Fourier series, calculation of the Hamiltonian matrix in the basis of free rotation wave functions and subsequent calculation of energy levels by direct diagonalization of the Hamiltonian matrix.

The following form of the Fourier series is often used for conventional representation of the dependence of hindered potential on torsional angle:<sup>19,20,21</sup>

$$V(\phi) = \frac{1}{2}V_1(1 - \cos\phi) + \frac{1}{2}V_2(1 - \cos2\phi) + \frac{1}{2}V_3(1 - \cos3\phi) + \frac{1}{2}V'_1\sin\phi + \frac{1}{2}V'_2\sin2\phi \quad (E1)$$

In this work the torsional potential calculated at a discrete torsional angle is fitted by a truncated Fourier series in the following:

$$V(\phi) = a_0 + a_1 \cos\phi + a_2 \cos2\phi + a_3 \cos3\phi + b_1 \sin\phi + b_2 \sin2\phi \quad (E2)$$

The matrix elements of individual sine and cosine terms in the basis of free rotor wave functions have a simple appearance. The terms  $\sin(m\phi)$  and  $\cos(m\phi)$  induce transitions with  $\Delta K = \pm m$ , where  $K$  is the rotational quantum number. Moreover, the matrix element does not depend on  $K$ , which leads to a simple form of the Hamiltonian matrix. The matrix has a band structure and consists of diagonal terms that are equal to those of the free rotor and subdiagonals of constant values that correspond to a different terms in the potential expansion, (E2).

The Hamiltonian matrix can therefore be truncated to the size of  $2K_{\max}+1$ , where  $K_{\max}$  is the maximum rotational quantum number. The truncated matrix (in reduced dimensionless form) is diagonalized, and calculated eigenvalues are used to calculate partition function, entropy, heat capacity, etc., using direct summation over the calculated

energy levels. This description briefly outlines the procedure used. A detailed description with examples and comparisons will be published by Krasnoperov, Lay and Shokhirev.<sup>18</sup>

### 1.6 Modeling Study of Chloroform Pyrolysis and Oxidation

Chloroform is used by Won<sup>22</sup> as a model chlorocarbon system with high Cl/H ratio to investigate thermal decomposition processes of chlorocarbons over oxidative and pyrolytic reaction environments. The reactions are studied in tubular flow reactors at a pressure of 1 atm with residence times of 0.3 - 2.0 seconds in the temperature range 535 - 800 °C. Chloroform decay and product distributions are distinctly different in the absence and presence of added O<sub>2</sub>. Increases in O<sub>2</sub> are observed to speed chloroform loss and increase CCl<sub>4</sub> and CO production, while decreasing C<sub>2</sub>Cl<sub>4</sub>. In CHCl<sub>3</sub>/O<sub>2</sub>, the products are C<sub>2</sub>Cl<sub>4</sub>, HCl, CCl<sub>4</sub>, C<sub>2</sub>HCl<sub>5</sub>, C<sub>2</sub>HCl<sub>3</sub>, CO and CO<sub>2</sub> over a wide temperature range. A detailed reaction mechanism to describe the important features of products and reagent loss is developed. Reaction pathways and rate constants are developed for CCl<sub>3</sub>, CCl<sub>2</sub> and C<sub>2</sub>Cl<sub>3</sub> radical addition to O<sub>2</sub> and chlorocarbon radical combination with O, OH, HO<sub>2</sub> and ClO.

### 1.7 Detailed Analysis of Initial Reactions of Photochemical Oxidation of Benzene and Toluene in the Atmosphere

The reversible addition reaction of OH radical with benzene to form the hydroxyl-2,4-cyclohexadienyl (benzene-OH) adduct and the subsequent reactions of this benzene-OH adduct with O<sub>2</sub> are important initial steps for the photooxidation of benzene and all other aromatics in the atmosphere (see references in Chapter 8). The OH addition to benzene ring, the subsequent reaction of O<sub>2</sub> with the hydroxyl-2,4-cyclohexadienyl to form

hydroxyl-2-peroxy-4-cyclohexenyl (benzene-OH-O<sub>2</sub> adduct), are chemical activation reactions and are a function of both pressure and temperature. The atmospheric oxidation process for the aromatic ring in toluene is analogous to the reactions of benzene in many ways. The kinetics of these two reaction systems at various pressure & temperature using a quantum version of Rice-Ramsperger-Kassel theory (QRRK) and a modified strong collision approach are analyzed and calculated in Chapter 8. The analogue reaction system of toluene photooxidation is also analyzed.

Potential energy diagrams of the reactions and thermodynamic properties ( $H_f^\circ$ ,  $S^\circ_{298}$ , and  $C_p(T)$ 's) of reactants, intermediates and products are calculated. Group Additivity (GA) techniques are used to calculate thermodynamic properties of stable molecules. When GA method is not adequate, the semiempirical Molecular Orbital (MO) calculation, MNDO/PM3 is used to derive the required Group values for specific species like the bicyclic benzene-OH-O<sub>2</sub> adducts. Several Hydrogen Atom Bond Increment groups (HBI) are introduced to allow calculations of the thermodynamic properties for the relevant free radical intermediates.

Rate constants for elementary reaction steps are determined from literature values or estimated from Transition State Theory and principles of thermochemical kinetics. Apparent rate constants are calculated for conditions of atmospheric oxidation as well as other temperature and pressure regimes. Two short reaction mechanisms are developed for initial steps of atmospheric oxidation of benzene and toluene, which include reverse reaction rates determined from thermodynamic parameters and microscopic reversibility. The results for atmospheric conditions are compared with available experimental data.

Calculated kinetic and mechanistic data in this study can be used in modeling of photochemical oxidation of combustion and aromatic compounds in atmosphere. Results show that calculation and consideration of equilibrium levels of benzene-OH and benzene-OH-O<sub>2</sub> adducts (or toluene-OH and toluene-OH-O<sub>2</sub> adducts), and other active species in the systems are important in the determining conversion of the aromatic species as well as nature of specific products.

## CHAPTER 2

### HYDROGEN ATOM BOND INCREMENTS (HBI) FOR CALCULATION OF THERMODYNAMIC PROPERTIES OF HYDROCARBON RADICAL SPECIES

#### 2.1 Introduction

Detailed kinetic reaction models using mechanisms based upon fundamental thermodynamic and kinetic principles are presently used and being developed by researchers attempting to optimize or more fully understand a number of systems comprised of many elementary chemical reactions. These include pyrolysis, combustion<sup>2,23</sup>, ignition<sup>24</sup>, atmospheric smog formation and transport<sup>25,26</sup>, stratospheric ozone depletion, municipal and hazardous waste incineration<sup>27-29</sup>, chemical vapor deposition and semiconductor etching<sup>30</sup>, rocket propulsion,<sup>31</sup> and other related fields. One important requirement for reliable simulation of these systems is accurate thermodynamic property data for the molecular and radical species in the chemical mechanism. This data allows determination of the thermodynamic feasibility of reaction paths, equilibrium constants ( $K_{eq}$ ), as well as reverse rate constants ( $k_r$ ) from the forward rate constant ( $k_f$ ) and  $K_{eq}$ . It also serves a vital role in estimating rate constants for endothermic reactions.

Benson's Group Additivity (GA) estimation technique is an accurate method for the estimation of ideal gas phase heat capacities, heats of formation, and entropies of stable molecules. This technique is discussed in Benson's **Thermochemical Kinetics**<sup>32</sup> and other reference sources<sup>33,34</sup>. The method assumes that the properties for a chemical substance are the sum of the contributions from each group or polyvalent atom (central

atom) in that molecule. It is referred to as a second order estimation technique since next-nearest-neighbor corrections, and to some extent, chemical structure, are accounted for. Estimations based upon chemical bond additivity alone are known as first order estimation techniques, while those based upon atomic contributions alone are referred to as zero order techniques.<sup>33</sup> The second order estimates are naturally more accurate than lower order techniques; but also requires a larger data base. Several other estimation techniques based upon group contribution principles are presented in Reid, Prausnitz, and Sherwood<sup>33</sup>, and Pedley, Naylor and Kirby<sup>35</sup> (for enthalpies only). Benson's method is the most widely accepted one because of its ease of use and relative accuracy when compared with other techniques. In addition Benson's GA approach has been programmed<sup>36,37</sup> for use in computer codes.

Group contributions (Group Values for GA) were derived by Benson and co-workers<sup>11</sup> and various other researchers<sup>34,37,38</sup> by dividing similar molecules with known thermodynamic properties into their constituent groups and then performing multivariable linear regressions to find group contributions which gave the best fit to available experimental property data. The enthalpy group values for this GA approach were comprehensively reviewed and updated by Cohen and Benson<sup>39</sup> in 1993 to make the prediction results more consistent with current experimental data.

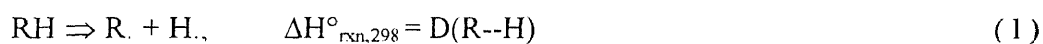
Benson and co-workers also derived several corresponding group values for estimating thermodynamic properties ( $\Delta H_f^\circ$ ,  $S^\circ$  and  $C_p(T)$ 's) for free radicals in the same manner as for stable molecules.<sup>11,39</sup> Two classes of radical groups were derived: (i) groups for the radical-centered atoms and (ii) groups for radical-adjacent atoms. Every



radical contains at least one of the two radical type groups plus the normal groups for atoms not next to radical center. The values for several radical-related groups for alkyl radicals were revised by Cohen.<sup>34</sup>

In this work, we present an alternative approach, i.e. a single group, to estimate the thermodynamic properties ( $\Delta H_f^\circ_{298}$ ,  $S^\circ_{298}$  and  $C_p(T)$ ,  $300 \leq T/K \leq 1500$ ) for hydrocarbon free radicals. Our method utilizes the thermodynamic properties of the parent molecules incorporated with a H-atom Bond Increment (HBI) for each respective property of the parent which reflects the change due to loss of an H atom. We demonstrate that HBI groups are based on fundamental principles of statistical mechanics and thermochemistry. An advantage of this approach is the straightforward modification of the group if improved molecular data are developed.

Consider the following homolytic reaction :



The radical enthalpy of formation can be written as:

$$\Delta H_f^\circ_{298}(R.) = D(R\text{--}H) + \Delta H_f^\circ_{298}(RH) - 52.1 \text{ kcal/mol}, \Delta H_f^\circ_{298}(H.) \quad (2)$$

Thus one can calculate  $\Delta H_f^\circ_{298}(R.)$  if one has a value for the bond strength for the bond broken to form the radical. The values of bond energies,  $D(R\text{--}H)$  in HBI data base for the corresponding radicals are adopted from evaluation of the literature.

To some extent, the molecular structure of a radical (R.) is similar to that of corresponding stable molecule (RH). The unpaired electron at the radical-centered atom of the free radical is replaced by an H atom in the stable molecule while the rest of the atom sequence and chemical bonds are basically the same for the two species. If all the differences of molecular structures for R. and RH are properly taken into account, one could expect that  $S^{\circ}_{298}$  and  $C_p(T)$  of R. can be calculated from those of corresponding RH plus the values of increments,  $\Delta C_p(T)$  and  $\Delta S^{\circ}_{298}$  as:

$$S^{\circ}_{298}(\text{R.}) = S^{\circ}_{298}(\text{RH}) + \Delta S^{\circ}_{298} \quad (3)$$

$$C_p(T)(\text{R.}) = C_p(T)(\text{RH}) + \Delta C_p(T) \quad (4)$$

The increments of  $\Delta S^{\circ}_{298}$  and  $\Delta C_p(T)$  ( $300 \leq T/K \leq 1500$ ) are group values and termed Hydrogen atom Bond Increment (HBI) ( $\Delta S^{\circ}_{298}(\text{HBI})$  and  $\Delta C_p(T)(\text{HBI})$ ), since they are used to calculate  $S^{\circ}_{298}$  and  $C_p(T)$ 's for a free radical formed from its parent molecule. The values we report for  $\Delta S^{\circ}_{298}$  and  $\Delta C_p(T)$  are obtained by applying the principles of the Rigid-Rotor-Harmonic-Oscillator (RRHO)<sup>19</sup> model to account for the differences of molecular structures between R. and the corresponding RH (parent). They may, however, also be determined from accurate literature data on the respective properties of a parent molecule and the corresponding radical when available.

The classification of HBI terms is based on the generic types of R--H bonding. In addition, a change in the potential barriers of internal rotations about C-C bond next to the

radical center are taken into account. This work considers 26 types of hydrocarbon radicals.

This analysis approach incorporates the following:

- Evaluated literature data corresponding to the bond energies,  $D(R-H)$  of the specific R-H bond; e.g. primary, secondary, tertiary....etc.
- Entropy and heat capacity increments accounting for loss and for the differences in vibrational frequencies of a parent molecule losing an H atom to form the radical,
- Gain of inversion frequencies at radical centers of carbon atoms,
- Entropy and heat capacity corrections accounting for the differences of rotational barriers of internal rotors in parent and radical,
- Entropy corrections for electron spin degeneracy,
- Corrections to translational and rotational entropy for small molecules where a change in this property results from loss of the H atom,

Entropy corrections accounting for changes in symmetry are not included in the HBI group values, as they need to be considered separately for each radical and parent molecule.

## 2.2 Methodology and Calculations

### 2.2.1 Heats of Formation

The calculation of  $\Delta H_f^\circ_{298}(R\cdot)$  for a specific radical species uses literature values or Group Additivity (GA) values of enthalpy for the parent molecule ( $\Delta H_f^\circ_{298}(RH)$ ) and an evaluated bond energy (BDE),  $D(R-H)$ , for the specific H atom removed from the parent molecule to form the desired radical, see equation (2). Table 2.1 lists the BDE values.

### 2.2.2 Change in Vibrational Frequencies and Rotational Barriers

The  $S^\circ_{298}$  and heat capacities  $C_p(T)$ 's of free radicals are calculated by applying HBI values ( $\Delta S^\circ_{298}$  and  $\Delta C_p(T)$ 's) via the equation (3) and (4). The change in both entropy and heat capacity values, due to loss of a hydrogen atom, are selected, because R--H bond properties are typically the most accurately known. The loss of one H atom from the parent molecule causes the daughter radical to lose 3 degrees of freedom for intramolecular motions (vibrations plus internal rotations) relative to the parent molecule (RH).

As an example, consider formation of  $C_2H_5$  from  $C_2H_6$ , Figure 2.1 illustrates the calculation of  $\Delta S^\circ_{298}$  and  $\Delta C_p(T)$ 's values. The loss of a hydrogen atom results in the loss of one C-H stretch, two H-C-H bend and one H-C-C bend. The radical center in ethyl is no longer the normal tetrahedral structure, and it becomes more flexible. The flexibility of radical center is coupled with the appearance of one low frequency<sup>40,41</sup> in the spectrum of ethyl, corresponding to inversion of the radical center. The loss of four frequencies and the gain of one frequency are taken into account for the difference of frequencies between the ethyl and ethane.

The description of changes which occur in the loss of an H atom from ethane is still not complete. The rotational barriers about the C-C bond are very different for ethyl<sup>41</sup> and ethane.<sup>42</sup> The difference of rotational barriers accounts for the significant fraction of HBI  $\Delta S^\circ_{298}$  and  $\Delta C_p(T)$ 's contributions. The correction of spin degeneracy is added to the value of  $\Delta S^\circ_{298}$ .

### 2.2.3 Vibrational Frequencies

The assignment of fundamental frequencies is adopted in part from the analysis of molecular vibrational frequencies by Shimanouchi<sup>43</sup> and other studies of hydrocarbon radical structure and spectra. These studies include ethyl, *n*-propyl, *i*-propyl and *t*-butyl by Pacansky and co-workers,<sup>40,44,45</sup> *sec-n*-butyl by Chen *et al.*,<sup>46</sup> C<sub>2</sub>H (<sup>2</sup>Σ<sub>-</sub>) by Kiefer *et al.*<sup>47</sup> All of the vibrational frequencies needed in this study are unfortunately not all available. We therefore performed MNDO/PM3<sup>9</sup> Molecular Orbital (MO) calculations using the MOPAC 6.0<sup>10</sup> program to obtain vibrational frequencies via normal mode analysis of nuclear coordinates for model radicals on which the information is sparse, e.g. CH<sub>2</sub>=C.H, CH<sub>2</sub>=C.CH<sub>3</sub> and CH<sub>2</sub>=C=C.H. The vibrational frequencies of several stable molecules and free radicals are listed in Table 2.2. These data help determine the differences and similarities for vibrations between a radical species and the parent molecule.

A data base of fundamental frequencies is assembled for relevant vibrational modes in Table 2.3. The harmonic vibration frequencies for bond stretching and bond bending motions assigned and listed in Table 2.3 originate from Benson (Table A.13. in ref. 11). Most assignments adopt an average value of characteristic frequencies identified in previous studies<sup>11,43</sup> representing the standard stretching or bending motions. For the PM3 vibrational frequencies we use the animation analysis in the Hyperchem package<sup>48</sup> for assistance in the assignment of the approximate type of mode. This is helpful for frequencies of hydrocarbon radicals not well characterized in the literature. Vibrations with low wavenumber, e.g.  $\leq 1000\text{ cm}^{-1}$ , have a larger contribution to the values of  $\Delta S^\circ_{298}$  and  $\Delta C_p(T)$  ( $300 \leq T/K \leq 1500$ ) than high frequency vibrations. Cohen also points out that

the low-frequency out-of-plane methylene bend ( $541\text{ cm}^{-1}$ ) in the ethyl radical ( $\text{C}_2\text{H}_5$ ) and ( $530\text{ cm}^{-1}$ ) in n-propyl ( $\text{C}_3\text{H}_7$ ) are very important in determining the values of  $\Delta S^\circ_{298}$  and  $\Delta C_p(T)$ 's for these two radicals.<sup>34</sup> We assign an inversion mode of  $550\text{ cm}^{-1}$  to this low-frequency vibration. We also assign inversion modes for C-C-H-C ( $420\text{ cm}^{-1}$ ) and C-(C)3 ( $200\text{ cm}^{-1}$ ) based on the spectra data determined by Pacansky and co-workers for isopropyl radical<sup>44</sup> and for *tert*-butyl radical.<sup>45</sup>

#### 2.2.4 Hindered Internal Rotations

Barriers to hindered internal rotation adjacent to a radical center are another very important contribution factor to  $\Delta S^\circ_{298}$  and  $\Delta C_p(T)$  in the term values. The rotational barrier about the C-C bond in the ethyl radical,  $\text{C}_2\text{H}_5$ , has an upper limit of  $0.1\text{ kcal/mol}$ <sup>34</sup> while that in ethane is  $2.9\text{ kcal/mol}$ .<sup>42</sup> The barriers of hindered internal rotations for stable molecules and free radicals considered in this work are listed in Table 2.4. The majority of data on rotational barriers in Table 2.4 are results of experimental determinations or *ab initio* quantum mechanical calculations. When literature data are not available, the barriers are assigned by interpolation of the values from similar, studied internal rotor systems. The method and tables of Pitzer and Gwinn<sup>11</sup> were then used to calculate the contribution of hindered internal rotations to the thermodynamic functions.

#### 2.2.5 Spin Degeneracy and Symmetry

All free radicals estimated in this approach are considered to have only one unpaired electron (doublet) and assumed spin degeneracy equal to 2 ( $S=2$ ). The occupied orbitals of

stable molecules in their ground state generally have paired electrons ( $S=1$ ). The correction factor for spin degeneracy in the entropy increment is, therefore,  $R \ln 2$  ( $R$  is Ideal Gas Constant) which has been added into all group values of  $\Delta S^\circ_{298}$ .

Entropy corrections accounting for changes in symmetry are not included in the HBI group values, as they need to be considered separately for each radical and parent molecule. The symmetry is not included in the values of  $\Delta S^\circ_{298}(\text{HBI})$ , therefore the calculation of  $S^\circ_{298}$  for radicals is :

$$S^\circ_{298}(\text{R.}) = S^\circ_{298}(\text{RH}) + \Delta S^\circ_{298}(\text{HBI}) - R \ln(\sigma_{\text{radical}}/\sigma_{\text{parent}}) \quad (5)$$

where  $\sigma_{\text{radical}}$  and  $\sigma_{\text{parent}}$  are the symmetry number for radical and the corresponding parent molecule, respectively.

No further correction is required for the calculation of  $C_p(T)$  using HBI term values:

$$C_p(T)(\text{R.}) = C_p(T)(\text{RH}) + \Delta C_p(T)(\text{HBI}) \quad (6)$$

### 2.3 Calculation Details in Determining the Values of $\Delta S^\circ_{298}(\text{HBI})$ and $\Delta C_p(T)(\text{HBI})$

The values of  $\Delta S^\circ_{298}$  and  $\Delta C_p(T)$ 's that result from changes in the vibration frequencies and internal rotation barriers between a radical and its parent are presented in Table 2.5 for each HBI group. Contributions to  $\Delta S^\circ_{298}$  and  $\Delta C_p(T)$ 's are listed for each vibrational frequency and internal rotor, in addition to the sum of the respective contributions.

Assignment of frequencies lost and gained, and adjustment in potential barriers of internal rotation for the HBI  $\Delta S^{\circ}_{298}$  and  $\Delta C_p(T)$ 's are discussed below.

### 2.3.1 Primary Alkyl Radicals (*CCJ*, *RCCJ*, *ISOBUTYL* and *NEOPENTYL*)

These four groups are all for primary alkyl radicals,  $C(C)_xH_{3-x}-C.H_2$ . The difference between the four groups is the number of substituted alkyl groups on the  $\alpha$ -carbon (carbon next to the radical center), i.e. no alkyl substitution on *CCJ*, one for *RCCJ*, two for *ISOBUTYL* and three for *NEOPENTYL*. The adjustments in frequencies accounting for loss of an H atom are based on the comparison of vibrational frequencies for ethane and ethyl as illustrated in Figure 2.1 and discussed above. Frequencies lost and gained are assumed identical for all four. Rotational barriers account for the differences in the three HBI terms.

The rotational barriers of the methyl group (C-CH<sub>3</sub>) vary in this series (see Table 2.4): ethane (2.9 kcal/mol), propane (3.3 kcal/mol), isobutane (3.8 kcal/mol), and neopentane (4.7 kcal/mol). The barriers for methylene group (C-C.H<sub>2</sub>) are similar for ethyl (<0.1 kcal/mol), *n*-propyl (<0.1 kcal/mol), isobutyl (0.17 kcal/mol) and neopentyl (0.16 kcal/mol).<sup>34</sup> This difference in rotational barriers of methyl group (C-CH<sub>3</sub>) in the parent molecules is the primary reason that one needs four HBI terms to account for all types of primary alkyl radicals.



### 2.3.2 Secondary Alkyl Radicals (*CCJC*, *RCCJC* and *RCCJCC*)

The adjustments in frequencies are based on analysis of fundamental vibrations for *n*-propane and isopropyl (see Table 2.2). One C-H stretch, one H-C-H bend and two H-C-C bends are lost from C-CH<sub>2</sub>-C to C-C.H-C. The H-C-C bend in methylene group is assigned a higher wavenumber (1150 cm<sup>-1</sup>) than that in the methyl group (850 cm<sup>-1</sup>) based on the experimental observations,<sup>43</sup> see Table 2.3. Gain of the frequency associated with inversion of the radical center (C-C.H-C) which was determined as 420 cm<sup>-1</sup> is included.

The barriers for C.-C bond rotations in secondary alkyl radicals (R-C.H-R') have very different values, 0.7 kcal/mol for the isopropyl radical CH<sub>3</sub>-(C.HCH<sub>3</sub>), (or 0.51 kcal/mol for CH<sub>3</sub>-C.HCH<sub>2</sub>CH<sub>3</sub>), and 2.16 kcal/mol for CH<sub>3</sub>C.H-CH<sub>2</sub>CH<sub>3</sub>, see Table 2.4 and references therein. The methyl group is nearly a free rotor about the CH<sub>3</sub>-(C.HC) bond, while the ethyl group in the iso-butyl radical has a significant rotational barrier. The rotational barrier of the ethyl group is only about 1 kcal/mol lower than that in the parent molecule. Three secondary HBI terms are needed to account for all types of secondary alkyl radicals.

### 2.3.4 Tertiary Alkyl Radicals (*TERTALKYL*)

Isobutane and *tert*-butyl are the model parent and radical for the calculation of the *TERTALKYL* group. The spectra for *tert*-butyl vibrational frequencies were reported by Pacansky *et al.*,<sup>45</sup> while the assignment of vibrational frequencies for *tert*-butane are studied in this work by means of PM3 MO calculations. One C-H stretch and three H-C-C bends are lost from (C)<sub>3</sub>CH to (C)<sub>3</sub>C., and one frequency, inversion of radical center, (200

cm<sup>-1</sup>) is gained. In addition the frequencies for CCC symmetric and asymmetric bending are very different for *tert*-butane and the *tert*-butyl radical. The rotational barrier of methyl rotors in *tert*-butane is 4.7 kcal/mol while that in the *tert*-butyl radical is only 1.5 kcal/mol.

### 2.3.5 Acetylenic Radicals (C≡CJ)

C<sub>2</sub>H<sub>2</sub> and C<sub>2</sub>H (<sup>2</sup>Σ<sup>+</sup>) are the model parent and radical. The vibrational frequencies for C<sub>2</sub>H (<sup>2</sup>Σ<sup>+</sup>) were determined by Kiefer *at al.*,<sup>47</sup> while the assignment of frequencies for C<sub>2</sub>H<sub>2</sub> is taken from Schimonouchi.<sup>43</sup> The H-C≡C bending frequency substantially shifts from 420 cm<sup>-1</sup> in C<sub>2</sub>H<sub>2</sub> to 310 cm<sup>-1</sup> in C<sub>2</sub>H.

### 2.3.6 Vinyl Radicals (VIN)

The model parent and radical are CH<sub>2</sub>=CH<sub>2</sub> and CH<sub>2</sub>=C.H. The vibrational frequencies of C<sub>2</sub>H<sub>3</sub> were determined by an *ab initio* MO study.<sup>49</sup> Like the case of C<sub>2</sub>H<sub>2</sub> and C<sub>2</sub>H, the frequency of the H-C=C bend significantly shifts from 1050 cm<sup>-1</sup> in C<sub>2</sub>H<sub>4</sub><sup>43</sup> to 785 cm<sup>-1</sup> in C<sub>2</sub>H<sub>3</sub>.<sup>49</sup>

### 2.3.7 Allenic Radicals (C=C=CJ)

This group is very different from *VIN*. The value of D(CH<sub>2</sub>CC(H)--H) was determined to be 89 kcal/mol,<sup>51</sup> which is different from the bond energy of C-H bond in C<sub>2</sub>H<sub>4</sub> (111.2 kcal/mol),<sup>35</sup> The H-C=C bending frequency in allene<sup>43</sup> is 840 cm<sup>-1</sup> while in ethylene it is 1050 cm<sup>-1</sup>.<sup>43</sup>

### 2.3.8 Secondary Vinyl Radicals (*VINS*)

The group is for vinyl radicals with a alkyl group substituted at the radical carbon (secondary vinyl). 1-Propene and  $\text{CH}_2=\text{C}\cdot\text{CH}_3$  are the model parent and radical. The bond energy  $D(\text{CH}_2\text{C}(\text{CH}_3)\text{--H})$  is evaluated from  $D(\text{CH}_2\text{C}(\text{H})\text{--H})$  plus the difference between  $D(\text{CH}_3\text{C}(\text{H}_2)\text{--H})$  and  $D(\text{CH}_2\text{CH}(\text{CH}_3)\text{--H})$ ,  $111.2 + (98.45-101.1) = 108.6$  kcal/mol, see Table 2.1.

The vibrational frequencies for  $\text{CH}_2=\text{C}\cdot\text{CH}_3$  are calculated in this study by PM3 as given in Table 2.2. The frequency of the C=C-C bend is found to shift from  $420\text{ cm}^{-1}$  in the parent to  $310\text{ cm}^{-1}$  in the radical. The internal rotation of the methyl group in 1-propene is a three-fold rotation, with a moderate barrier height, 2.1 kcal/mol,<sup>52</sup> which is assumed to be identical for the secondary vinyl radical,  $\text{CH}_2=\text{C}\cdot\text{CH}_3$ .

### 2.3.9 Primary Allyl Radicals (*ALLYL\_P*)

1-Propene and allyl are the model parent and radical. Like the case of *CCJ* group, one C-H stretch, two H-C-H bends and one H-C-C bend are lost from C-CH<sub>3</sub> to C-C<sub>2</sub>H<sub>2</sub>. In addition the frequencies of C-C ( $1000\text{ cm}^{-1}$ ) and C=C stretch ( $1650\text{ cm}^{-1}$ ) in 1-propene are both shifted to an intermediate value ( $1350\text{ cm}^{-1}$ ) for C.-C (one and half bond) stretch in allyl. The H-C-H wag of the vinyl group of 1-propene ( $950\text{ cm}^{-1}$ ) is also different from that in allyl ( $500\text{ cm}^{-1}$ , termed as H-A-H wag), see Table 2.3 and Table 2.5. Another important change from the parent to the radical is the lose of methyl rotor and gain of one H-A-H wag.

### 2.3.10 Secondary Allyl Radicals (*ALLYL\_S*)

1-Butene and  $\text{CH}_2=\text{CHC}\cdot\text{HCH}_3$  are the model parent and radical. Similar to *CCJC*, one C-H stretch, one H-C-H bend and two H-C-C bends are lost from C-CH<sub>2</sub>-C to C-C·H-C. The frequencies of the C-C and C=C stretch in the parent are shifted to an intermediate value for C-C stretch in the radical, analogous to *ALLYL\_P*. The most important change, however, is about the internal rotations. The ethyl group rotation in 1-butene is replaced by the torsion motion about the C-C 1.5 order bond (termed as H-A-C, see Table 2.3) in the radical. The barrier height of the methyl group changes from 3.3 kcal/mol in 1-butene to 2.1 kcal/mol in  $(\text{CH}_2=\text{CHC}\cdot\text{H})-\text{CH}_3$  which is estimated from that of 1-propene.

### 2.3.11 Tertiary Allyl Radicals (*ALLYL\_T*)

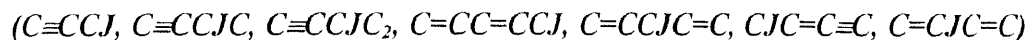
3-Methyl-1-butene and  $\text{CH}_2=\text{CHC}\cdot(\text{CH}_3)_2$  are the model parent and radical. One C-H stretch and three H-C-C bends are lost from (C)<sub>3</sub>-CH to (C)<sub>3</sub>-C·, in addition to the shift of C-C and C=C stretches to two C-C stretches, parallel to *ALLYL\_P* and *ALLYL\_S*. The rotation iso-propyl group in the parent is replaced by the torsion motion about the C-C 1.5 order bond (termed as C-A-C, see Table 2.3) in the radical. The rotational barriers of the two methyl groups change from 3.3 kcal/mol in the parent to 2.1 kcal/mol in radical as in *ALLYL\_S*.

### 2.3.12 Benzyl Radicals (*BENZYL\_P*, *BENZYL\_S* and *BENZYL\_T*)

*BENZYL\_P*, *BENZYL\_S* and *BENZYL\_T* are for primary, secondary and tertiary benzyl radicals with zero, one and two alkyl groups substituted at the radical carbon, respectively.

Toluene, ethylbenzene and iso-propylbenzene are the three model parents, while Ph-C.H<sub>2</sub>, Ph-C.HCH<sub>3</sub> and Ph-C.(CH<sub>3</sub>)<sub>2</sub> (Ph- equal to C<sub>6</sub>H<sub>5</sub>-) are the three model radicals, respectively. The calculations for *BENZYL\_P*, *BENZYL\_S* and *BENZYL\_T* follow the *ALLYL\_P*, *ALLYL\_S* and *ALLYL\_T*. See Table 2.5 for the calculation details. The most significant difference between the *BENZYL\_P* and *ALLYL\_P* is that the methyl rotor on the benzene ring (Ph-CH<sub>3</sub>) is nearly a free rotor,<sup>11,42</sup> while that in propene ((CH<sub>2</sub>=CH)-CH<sub>3</sub>) has a barrier as 2.1 kcal/mol.<sup>52</sup> This also holds for *BENZYL\_S* and *BENZYL\_T*.

### 2.3.13 Other Radicals



Application of the above procedures relies on the similarity of the fundamental vibration modes and internal rotations for the respective radicals and the corresponding parents. These processes based on the similarity of molecular structures are not as feasible for radicals with conjugated electronic resonance structure, like C.H<sub>2</sub>CH=CHCH=CH<sub>2</sub> and C.H<sub>2</sub>CH=CHC≡CH. An alternative method is to obtain ΔS°<sub>298</sub> and ΔCp(T) HBI values by “direct subtraction”, i.e. subtracting the S°<sub>298</sub> and Cp(T)’s values of the radical from the corresponding values of its parent.

The ΔS°<sub>298</sub> and ΔCp(T)’s values of seven HBI groups in this work are derived by this direct subtraction method:



$$\Delta S^{\circ}_{298}(C\equiv CCJ) = S^{\circ}_{298}(\text{HC}\equiv\text{CCH}_3) - S^{\circ}_{298}(\text{HC}\equiv\text{CC.H}_2),$$

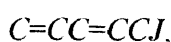
$$\Delta \text{Cp(T)}(C\equiv CCJ) = \text{Cp(T)}(\text{HC}\equiv\text{CCH}_3) - \text{Cp(T)}(\text{HC}\equiv\text{CC.H}_2),$$



$$\Delta S^{\circ}_{298} \text{ \& } \Delta C_p(T)(C\equiv CCJC) = S^{\circ}_{298} \text{ \& } C_p(T)(HC\equiv CCH_2CH_3) \\ - S^{\circ}_{298} \text{ \& } C_p(T)(HC\equiv CC.HCH_3),$$



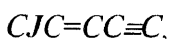
$$\Delta S^{\circ}_{298} \text{ \& } \Delta C_p(T)(C\equiv CCJC_2) = S^{\circ}_{298} \text{ \& } C_p(T)(HC\equiv CCH(CH_3)_2) \\ - S^{\circ}_{298} \text{ \& } C_p(T)(HC\equiv CC.(CH_3)_2),$$



$$\Delta S^{\circ}_{298} \text{ \& } \Delta C_p(T)(C=CC=CCJ) = S^{\circ}_{298} \text{ \& } C_p(T)(H_2C=CHCH=CHCH_3) \\ - S^{\circ}_{298} \text{ \& } C_p(T)(H_2C=CHCH=CHC.H_2),$$



$$\Delta S^{\circ}_{298} \text{ \& } \Delta C_p(T)(C=CCJC=C) = S^{\circ}_{298} \text{ \& } C_p(T)(H_2C=CHCH_2CH=CH_2) \\ - S^{\circ}_{298} \text{ \& } C_p(T)(H_2C=CHC.H_2CH=CH_2),$$



$$\Delta S^{\circ}_{298} \text{ \& } \Delta C_p(T)(CJC=CC\equiv C) = S^{\circ}_{298} \text{ \& } C_p(T)(CH_3CH=CHC\equiv CH) \\ - S^{\circ}_{298} \text{ \& } C_p(T)(C.H_2CH=CHC\equiv CH),$$



$$\Delta S^{\circ}_{298} \text{ \& } \Delta C_p(T)(C=CJC=C) = S^{\circ}_{298} \text{ \& } C_p(T)(H_2C=CHCH=CH_2) \\ - S^{\circ}_{298} \text{ \& } C_p(T)(H_2C=C.-CH=CH_2),$$

Data of  $S^{\circ}_{298}$  and  $C_p(T)$ ' for above stable molecules and free radicals are listed in Table 2.6.  $S^{\circ}_{298}$  and  $C_p(T)$ 's of stable molecules are taken from literature, or calculated in

this work using Group Additivity.<sup>37</sup> Data for  $S^{\circ}_{298}$  and  $C_p(T)$ 's of free radicals are determined in this work as follows.

$CH\equiv CC.H_2$ ,  $CH\equiv CC.HCH_3$  and  $CH\equiv CC.(CH_3)_2$  have the resonance structures as  $C.H=C=CH_2$ ,  $C.H=C=CHCH_3$  and  $C.H=C=C(CH_3)_2$ , respectively. We obtain their  $S^{\circ}_{298}$  and  $C_p(T)$ 's by applying the approach of  $C=C=CJ$  HBI values on each parent,  $CH_2=C=CH_2$ ,  $CH_2=C=CHCH_3$  and  $CH_2=C=C(CH_3)_2$ , respectively. This series allow us to evaluate the usefulness of the HBI Group data base where only one  $C=C=CJ$  HBI term is used to calculate the thermodynamic properties of the above three radicals. The calculated  $S^{\circ}_{298}$  and  $C_p(T)$  values for  $CH\equiv CC.H_2$ ,  $CH\equiv CC.HCH_3$  and  $CH\equiv CC.(CH_3)_2$  are listed in Table 2.6.

For  $CH_2=C.CH=CH_2$ ,  $CH_2=CHCH=CHC.H_2$  ( $CH_2=CHC.HCH=CH_2$ ) and  $CH\equiv CCH=CHC.H_2$ , we perform PM3 MO calculations using the MOPAC 6.0 program with standard parameters to obtain their  $S^{\circ}_{298}$  and  $C_p(T)$ 's values. The parameters needed to calculate thermodynamic properties for these three radicals, which includes moments of inertia for external rotation and fundamental vibration frequencies are listed in Table 2.7.

## 2.4 Discussion

The HBI Groups have one simplifying advantage that only one HBI term is needed for a given generic class radical. In the normal GA scheme a radical group is needed for each radical site, in addition to the groups for each central atom adjacent to the radical center.

It is important to note that the first requirement in obtaining thermodynamic property data on radical species using the HBI Group approach is to acquire the

corresponding properties of the parents. It means the absolute accuracy of thermodynamic data for radicals using HBI Group approach also relies on the accuracy of the data for the corresponding stable molecules. The discussion of the accuracy of current thermodynamic data for the hydrocarbon (HC) compounds is beyond the scope and context of this paper. In most cases the thermodynamic data for HC stable molecule are determined by experiments or high level *ab initio* MO calculations which are more reliable than values for the HC free radicals. Benson's GA approach has been proven to be an very accurate alternative for thermodynamic properties of HC stable molecules. Errors in the determination of the thermodynamic properties of the corresponding free radicals using our HBI procedure resulting from the errors of parent's thermodynamic data should be minor. When the thermodynamic data of the parent molecules are not correct, equilibrium calculations for free radicals relative to the parent will not be affected, but both will be in error relative to other radicals and molecules.

$\Delta S^{\circ}_{298}$  and  $\Delta C_p(T)$  ( $300 \leq T/K \leq 1500$ ) values in the HBI data base are strongly affected by low frequency motions. We evaluate the frequencies of inversion at radical centers from literature data. We also rely on semiempirical MO calculations, MNDO/PM3, to obtain the fundamental vibration frequencies for the model radicals which have not been studied previously. PM3 is easily accessible, not CPU time expensive; and a number of systematic studies<sup>56</sup> show that PM3 generally provides an acceptable match of vibrational frequencies across the entire spectrum without any empirical adjustment required. The harmonic vibrational frequencies calculated by *ab initio* MO theory at the intermediately high level of theory, such as (U)HF/6-31G\* level, however, need to be scaled by 0.89 for



use in thermodynamic calculations.<sup>38</sup> We understand that there may exist some error in the vibrational frequencies using PM3 MO calculations, especially in the region of wavenumber lower than 1000  $\text{cm}^{-1}$ . But PM3 is a reasonable choice to derive the HBI values without the availability of experimental or higher level calculations. The HBI data base will be improved when more reliable data are available.

The potential barriers to internal rotation are also significant in determining the  $\Delta S^\circ_{298}$  and  $\Delta C_p(T)$  values. For some HBI terms like *TERTALKYL*, the loss of high barrier (>3 kcal/mol) rotors and gain of low barrier rotors accounts for major increases in  $\Delta S^\circ_{298}$  and decreases in  $\Delta C_p(T)$  ( $300 \leq T/K \leq 1500$ ).

Some assumptions included in our calculation scheme may be considered to limit its accuracy. For example, we use one frequency for the C-H stretch, and one for the H-C-H bend, where literature indicates that there are actually ranges covering several hundred  $\text{cm}^{-1}$  for these vibrations. C-H stretches, for example typically range from 2800 to 3200  $\text{cm}^{-1}$  and H-C-H bends typically range from 1300 to 1500  $\text{cm}^{-1}$ . These effects on  $\Delta S^\circ_{298}$  and  $\Delta C_p(T)$  ( $300 \leq T/K \leq 1500$ ) are fortunately very small. Frequencies ranging from 1000 to 2000  $\text{cm}^{-1}$  effect  $\Delta S^\circ_{298}$  and  $\Delta C_p(T)$  only by  $\leq 0.1$  cal/mol, and they effect  $\Delta C_p(T)$  less at higher temperature.

A second assumption is that we only consider a select number of changes - trying to focus on the most significant, while in actuality loss of an H atom may effect the vibrations of the entire molecule. Fortunately H is a light atom and its loss is usually accurately described by the vibrations, inversion frequencies and internal rotation changes we have included.

The objective of developing the HBI data base is to develop an accessible and fundamental approach to estimate thermodynamic properties for radicals for which data are not currently available. A comparison to data in literature with the data determined in this work is presented in Table 2.9.

A computer code **THERM** (Thermo Estimation for Radicals and Molecules) for IBM PC's and PC compatibles can be used to estimate this thermodynamic property data for gas phase radicals and molecules, using Benson's group additivity method.<sup>37</sup> Thermodynamic properties are generated in NASA polynomial format for compatibility with the CHEMKIN<sup>53</sup> reaction modeling code or the NASA equilibrium code<sup>54</sup>. In addition, thermodynamic, kinetic and equilibrium analysis are also performed by the code.

One valuable aspect of **THERM** is its ability to easily estimate thermodynamic properties for a wide range of organic radical species, using the HBI values presented in this work and the thermodynamic properties of the stable parent. In this paper we present an initial data base for a number of such HBI terms for hydrocarbon radicals relevant to hydrocarbon chemistry for the combustion and atmospheric modeling communities. Details on methods utilized in determining these Hydrogen atom Bond Increment and comparisons with literature data are presented for evaluation and reference. Improvements in our knowledge and understanding of vibration and inversion frequencies, internal rotation barriers, their symmetry and reduced moments, as well as bond energies can be readily implemented by substitution into the data files and recalculation.

## 2.5 Summary

We have evaluated HBI values, which when applied to the respective thermodynamic properties of a parent hydrocarbon molecule, determine the thermodynamic properties ( $\Delta H_{f,298}^\circ$ ,  $S_{298}^\circ$  and  $C_p(T)$ ,  $300 \leq T/K \leq 1500$ ) of a radical corresponding to loss of an H atom, based on the principles of statistical mechanics. Databases on vibrational frequencies and internal rotational barriers in both stable molecules and radicals are also developed.

The Enthalpy term ( $\Delta H_{f,298}^\circ$ ) in HBI data base is related to the bond energy (BDE) of the corresponding C-H bond for each radical groups. The Entropy term ( $\Delta S_{298}^\circ$ ) and Heat Capacity terms ( $\Delta C_p(T)$ ) in HBI data base are to be added to the corresponding properties of the parent molecule, to obtain the thermodynamic properties of the radical. The corrections are included for changes in barriers of internal rotations and vibrational frequencies (including frequencies of radical center inversions). The entropy values include correction for the electron spin degeneracy, but do not include symmetry corrections in going from the parent to the radical.

## 2.6 Expressions Used in Thermodynamic Calculations

For stable molecules (without electronic degeneracy), entropy and heat capacities are calculated by:

$$S^\theta(\text{tot}) = S^\theta(\text{trans}) + S^\theta(\text{ext-rot}) + \sum_j S_j^\theta(\text{int-rot}) + \sum_n S_n^\theta(\text{vib}) \quad (\text{E1})$$

$$C_p^\theta(\text{tot}) = C_p^\theta(\text{trans}) + C_p^\theta(\text{ext-rot}) + \sum_j C_{p,j}^\theta(\text{int-rot}) + \sum_n C_{p,n}^\theta(\text{vib}) \quad (\text{E2})$$

where (trans) is translation, and (ext-rot) and (int-rot) are external and internal rotation, respectively.

The molar translational and rotational components of the entropy and heat capacities are given by: <sup>8</sup>

$$S^{\theta}(\text{trans}) = (5/2)R + R \ln\{(2\pi mkT / h^2)^{3/2} (RT / p^{\theta} NA)\} \quad (\text{E3})$$

$$S^{\theta}(\text{ext-rot}) = (3/2)R + R \ln\{(\pi^{1/2}/\sigma)(8\pi^2 kT/h^2)^{3/2} (I_x I_y I_z)^{1/2}\} \quad (\text{E4})$$

$$Cp^{\theta}(\text{trans}) = (5/2)R \quad (\text{E5})$$

$$Cp^{\theta}(\text{ext-rot}) = R \text{ for linear molecules; } (3/2)R \text{ for non-linear molecules} \quad (\text{E6})$$

where

$m$  is molecular mass,  $T$  is temperature,  $R$  is ideal gas constant,

$I_x, I_y, I_z$  are the main moments of inertia,  $\sigma$  is the symmetry number for external rotations,

$h$  is Planck's constant,  $k$  is Boltzmann constant,

$p^{\theta}$  is the standard pressure ( $p^{\theta} = 1 \text{ atm} = 101325 \text{ Pa}$  was used in this work). The vibrational contribution of the  $n$ th frequency to the entropy and heat capacity is given by:

$$S^{\circ}_{\text{vib},n} = (U_{\text{vib},n} - F_{\text{vib},n}) / T; Cp^{\circ}_{\text{vib},n} = R u_n^2 \exp(u_n) / (\exp(u_n) - 1)^2 \quad (\text{E7})$$

$$U_{\text{vib},n} = RT u_n / (\exp(u_n) - 1) \quad (\text{E8})$$

$$F_{\text{vib},n} = -RT \ln Q_{\text{vib},n} \quad (\text{E9})$$

$$Q_{\text{vib},n} = 1 / (1 - \exp(-u_n)) \quad (\text{E10})$$

$$u_n = ch\nu_n / kT \quad (\text{E11})$$

where

$\nu_i$  is vibration frequency in wavenumbers ( $\text{cm}^{-1}$ ),  $c$  is speed of light.

There is no simple equation to express  $S^{\theta}(\text{int-rot})$  and  $Cp^{\theta}(\text{int-rot})$ . These parameters are calculated using the method and tables of Pitzer and Gwinn. <sup>11</sup>

According to equation (E1) to (E6), the differences of entropy and heat capacity between parent molecule and daughter free radical are:

$$\begin{aligned} \delta S^\theta(\text{tot}) = & \delta S^\theta(\text{trans}) + \delta S^\theta(\text{ext-rot}) + \delta S_j^\theta(\text{int-rot}) + \delta S_n^\theta(\text{vib}) \\ & + \delta S^\theta(\text{spin degeneracy}) \end{aligned} \quad (\text{E12})$$

$$\delta C_p^\theta(\text{tot}) = \delta C_p_j^\theta(\text{int-rot}) + \delta C_p_n^\theta(\text{vib}), (\delta C_p(\text{trans}) = \delta C_p(\text{ext-rot}) = 0) \quad (\text{E13})$$

$$\delta S^\theta(\text{trans}) = (3/2)R \ln\{(M-1)/M\} + R \ln(\text{OI of radical}) - R \ln(\text{OI of parent}) \quad (\text{E14})$$

$$\delta S^\theta(\text{ext-rot}) = \delta \{ R [\ln(I_x I_y I_z)^{1/2} - \ln \sigma] \} \quad (\text{E15})$$

$$\delta S^\theta(\text{spin degeneracy}) = R \ln 2 \quad (\text{E16})$$

where M is the molecular mass of the parent molecule, OI is the number of optical isomers and the other symbols are the same as those used and defined in (E1) to (E11).  $\delta S^\theta(\text{trans})$  and  $\delta R \ln(I_x I_y I_z)^{1/2}$  are usually quite small and are neglected in this study. Spin degeneracy of free radicals is assumed to be equal to 2.  $\delta S^\theta(\text{tot})$  and  $\delta C_p^\theta(\text{tot})$  therefore can be expressed as:

$$\delta S^\theta(\text{tot}) = -R \ln (\sigma_{\text{radical}}/\sigma_{\text{parent}}) + \delta S_j^\theta(\text{int-rot}) + \delta S_n^\theta(\text{vib}) + R \ln 2 \quad (\text{E17})$$

$$\delta C_p^\theta(\text{tot}) = \delta C_p_j^\theta(\text{int-rot}) + \delta C_p_n^\theta(\text{vib}) \quad (\text{E18})$$

$\delta S(\text{HBI})$  and  $\delta C_p(\text{HBI})$  are defined as:

$$\delta S(\text{HBI}) = \delta S(\text{tot}) - R \ln (\sigma_{\text{radical}}/\sigma_{\text{parent}}) = \delta S_j^\theta(\text{int-rot}) + \delta S_n^\theta(\text{vib}) + R \ln 2 \quad (\text{E19})$$

$$\delta C_p(\text{HBI}) = \delta C_p(\text{tot}) = \delta C_p_j^\theta(\text{int-rot}) + \delta C_p_n^\theta(\text{vib}) \quad (\text{E20})$$

## CHAPTER 3

### THERMODYNAMIC PROPERTIES OF GAS-PHASE ALKYL HYDROPEROXIDE COMPOUNDS WITH AND WITHOUT CHLORINE AND FLUORINE SUBSTITUENTS

#### 3.1 Introduction

Alkyl hydroperoxides and their corresponding alkyl and peroxy radicals are critical intermediates in combustion of hydrocarbons, in atmospheric photochemical smog formation, oxidation and degradation of liquid hydrocarbons, low temperature oxidations and internal combustion.<sup>57,58,59</sup>

The study of standard entropy ( $S^{\circ}_{298}$ ) and heat capacities ( $C_p^{\circ}(T)$ 's) of these species has, however, experienced little activity since the review of Shaw and Benson<sup>38</sup> in 1970 where the generic data of  $S^{\circ}_{298}$  and  $C_p^{\circ}(T)$ 's of HOOH were available and used to derive data for all other alkyl hydroperoxides. Baldwin had reviewed the thermochemistry of peroxides in 1983<sup>60</sup> which updated some of the  $\Delta H_f^{\circ}_{298}$  of alkyl hydroperoxides and hydroperoxy radicals, but the  $S^{\circ}_{298}$  and  $C_p^{\circ}(T)$ 's remained identical to those estimated by Shaw and Benson.

Benson's Group Additivity (GA) approach has proven to be a useful method for the estimation of thermodynamic properties of molecules.<sup>32,33</sup> The approach is based on the assumption that the specific thermodynamic property of a chemical substance is the sum of the contributions from each group or polyvalent atom (central type atom) in the molecule. It is referred to as a second order estimation technique since next-nearest-

neighbor corrections, and to some extent, chemical structure are accounted for. Second order estimates consider more factors and therefore are more accurate than lower order, bond and atom additivity, techniques.<sup>33</sup> Benson's GA approach has been programmed<sup>61</sup> for use in computer codes and has become widely accepted due to its ease of use and relative accuracy when compared to other techniques.<sup>33</sup>

Benson's GA scheme utilized the generic thermodynamic data of HOOH, CH<sub>3</sub>OOCH<sub>3</sub> and alkyl hydroxides (ROH) to estimate the corresponding alkyl hydroperoxides (ROOH).<sup>62</sup> These values were widely used in thermodynamics and kinetics studies related to these species.<sup>60,63,64</sup> Baldwin reported that  $\Delta H_f^\circ_{298}$  of dialkyl peroxides and alkyl hydroperoxides can be well reproduced by Benson's GA scheme and group values.<sup>60</sup> The  $S^\circ_{298}$  and  $C_p^\circ(T)$  data estimated by Benson's GA has, however, not been verified by substantial generic data from experimental results or theoretical calculations. Group values required to estimate the thermodynamic properties of fluoro and chloro hydroperoxides and vinyl hydroperoxides with or without chlorine substitutions are in addition not available at present.

In this study generic  $S^\circ_{298}$  and  $C_p^\circ(T)$ 's ( $300 \leq T/K \leq 1000$ ) of monochloro- and monofluoro- hydroperoxides, primary, secondary and tertiary alkyl hydroperoxides and vinyl hydroperoxides, with or without fluorine or chlorine substituents, were calculated using the Rigid Rotor Harmonic Oscillator method (RRHO).<sup>8</sup> The RRHO contributions to  $S^\circ_{298}$  and  $C_p^\circ(T)$ 's adopt harmonic vibration frequencies and moments of inertia from the semiempirical quantum Molecular Orbital (MO) calculations. Specifically, the MNDO/PM3<sup>9</sup> method in MOPAC6.0<sup>10</sup> computer package. Hindered internal rotations

are treated by the approximation method of Pitzer and Gwinn<sup>11</sup> with reduced moments of inertia and barriers derived from experimental data or high level *ab initio* calculations. These  $S^\circ_{298}$  and  $C_p^\circ(T)$ 's data, when combined with corresponding enthalpies of formation ( $\Delta H_f^\circ_{298}$ ) determined by evaluation of literature data, are used to derive group values in a modified GA scheme.

### 3.2 Calculation Method

Thermodynamic properties considered in this paper are referred to a standard state of an ideal gas at 1 atm. The standard state for molecules with optical isomers is defined as an equilibrium mixture of enantiomers at the total pressure 1 atm.

#### 3.2.1 Standard Enthalpy of Formation, $\Delta H_f^\circ_{298}$

Literature data and the data estimated from literature results on standard enthalpies of formation ( $\Delta H_f^\circ_{298}$ ) of stable molecules are listed in Table 3.1. The  $\Delta H_f^\circ_{298}$  data marked by subscript "a" in Table 3.1 are adapted into the data base of this work.

Gutman and co-workers<sup>65,66,67</sup> have studied a series of  $R + O_2 = ROO$  reactions that include  $R = CH_3, CH_2Cl, CHCl_2, CCl_3, C_2H_5$  and  $CH_3CHCl$ . Boyd, S. L. *et al.*<sup>68</sup> have studied theoretically the bond energy of  $(CH_3)C-OO$  and  $CH_2=CH-OO$ . The bond energy of the  $R-OO$ , determined in those experiments or theoretical studies combined with the  $\Delta H_f^\circ_{298}$  of corresponding alkyl radicals are used to obtain the  $\Delta H_f^\circ_{298}$  of  $ROO$  radicals (see Table 3.1). These data can serve as a primary source to obtain  $\Delta H_f^\circ_{298}$  of  $ROOH$  if the bond dissociation energy of the corresponding  $ROO-H$  bond, ( $D^\circ(ROO-H)$ ) can be



presumed. Some  $D^\circ(\text{ROO-H})$  bond energies are listed in Table 3.2. We use 88 kcal/mol as the generic value of  $D^\circ(\text{ROO-H})$  in this work for all alkyl hydroperoxides with and without chlorine and fluorine substituents with one exception. This is value of 95.1 kcal/mol reported for the bond energy of  $D^\circ(\text{CF}_3\text{OO-H})$  based on Melius's MAC/MP4 calculations<sup>69</sup> (see Table 3.2).

### 3.2.2 Entropy ( $S^\circ_{298}$ ) and Heat Capacity ( $C_p^\circ(T)$ )

While the standard enthalpies of formation of some alkyl hydroperoxides and some alkyl peroxy radicals are investigated by experiment or theoretical calculation on the MO level (see Table 3.1 and references therein), there have been no or very few measurements or reports of standard entropies and heat capacities of these species since the review of Shaw and Benson.<sup>38</sup> In this work we calculate the generic  $S^\circ_{298}$  and  $C_p^\circ(T)$  of these alkyl hydroperoxides listed in Table 3.3 using RRHO<sup>8</sup> which then allows calculation of the contributions of from translation, external rotation, vibrations and internal rotations of molecules. The detailed expressions used to calculate  $S^\circ_{298}$  and  $C_p^\circ(T)$  are described in the Appendix of Chapter 2.

Optimized molecular geometry and vibrational frequencies were obtained using PM3<sup>9</sup> in the MOPAC<sup>10</sup> computer package. These geometries were then used to determine moments of inertia for external rotation. The Restricted Hartree-Fock (RHF) method with Self Consistent Field (SCF) Molecular Orbital (MO) treatment using the PM3 parameter set is employed for the calculations of all close shell molecules. Systematic studies<sup>56,70,72</sup> of MNDO calculations have shown that it provides reliable molecular

structures and vibration frequencies with good overall agreement between calculated values and experimental ones. The calculated frequencies and moments of inertia are listed in Table 3.3. The torsion vibration modes were replaced by hindered internal rotors when calculating  $S^{\circ}_{298}$  and  $C_p^{\circ}(T)$ . The method of Pitzer and Gwinn <sup>11</sup> was used to calculate the contribution of hindered internal rotations to the thermodynamic functions. Data on rotation barriers listed in Table 3.4 are either results of experimental studies or estimated from available data of *ab initio* theoretical calculations. Results of our calculations using GAUSSIAN92 <sup>30</sup> on the RHF/ or UHF/6-31G\* level corrected by second order Møller-Plesset (MP2) perturbation theory on 6-31G\*\* (MP2/6-31G\*\*//HF/6-31G\*) (see Chapter 4) are also included in Table 3.4. The correction of zero point vibration energies (ZPVE) by HF/6-31G\* frequencies was included in calculating the potential barriers for internal rotations. The thermodynamic properties data calculated in this study are illustrated in Table 3.5.

### 3.2.3 Comparison of Currently Available Thermodynamic Properties with Benson's Group Additivity Scheme

Group Additivity approach assumes that the specific thermodynamic properties ( $\Delta H_f^{\circ}_{298}$ ,  $S^{\circ}_{298}$ ,  $C_p^{\circ}(T)$ ) of a molecule can be represented by the sum of the contributions from each group which is an analogy of the polyvalent atom in the molecule together with its ligands.

For example, CH<sub>3</sub>CH<sub>2</sub>OH can be represented by:

C/C/H<sub>3</sub>: group of the carbon bonded to 1 carbon and 3 hydrogens,

C/C/H<sub>2</sub>/O: group of the carbon bonded to 1 carbon, 2 hydrogens and 1 oxygen,

O/C/H: group of the oxygen bonded to 1 carbon and 1 hydrogen.

Benson assumed the thermodynamic properties of alkyl hydroperoxides can be reproduced by the general GA scheme as exemplified above.<sup>62</sup> This general GA scheme is currently used<sup>63,64,2</sup> to estimate the  $\Delta H_f^\circ_{298}$ ,  $S^\circ_{298}$  and  $C_p^\circ(T)$  of most alkyl hydroperoxides. A comparison of thermodynamic data obtained in this work with the data obtained from Benson's GA scheme is performed and listed in Table 3.5.

An evaluation of Benson's GA scheme can be performed using the thermodynamic properties for these alkyl hydroperoxides where data are measured or calculated at a high level of theory (e.g. *ab initio* MO theory). First we verify the GA scheme using currently available  $\Delta H_f^\circ_{298}$  data of HOOH, CH<sub>3</sub>OOCH<sub>3</sub> and CH<sub>3</sub>OOH (see Table 3.1):

$$\Delta H_f^\circ_{298}(\text{CH}_3\text{OOCH}_3) = \Delta H_f^\circ_{298}\{(\text{C}/\text{H}3/\text{O}) + 2(\text{O}/\text{C}/\text{O})\} \quad (\text{G1})$$

$$\Delta H_f^\circ_{298}(\text{CH}_3\text{OOH}) = \Delta H_f^\circ_{298}\{(\text{C}/\text{H}3/\text{O}) + (\text{O}/\text{C}/\text{O}) + (\text{O}/\text{H}/\text{O})\} \quad (\text{G2})$$

Therefore, (G2) - 1/2 \* (G1) =  $\Delta H_f^\circ_{298}(\text{O}/\text{H}/\text{O})$ . The  $\Delta H_f^\circ_{298}(\text{HOOH})$  can also be expressed as :

$$\Delta H_f^\circ_{298}(\text{HOOH}) = 2\Delta H_f^\circ_{298}(\text{O}/\text{H}/\text{O}) \quad (\text{G3})$$

and thus  $\Delta H_f^\circ_{298}(\text{O}/\text{H}/\text{O})$  can also be obtained from 1/2 \*  $\Delta H_f^\circ_{298}(\text{HOOH})$ .

According to values listed in Table 3.1, the  $\Delta H_f^\circ_{298}(\text{O}/\text{H}/\text{O})$  obtained from (G2) - 1/2 \* G(2) = -14.62 kcal/mol, however, this is not equal to that obtained from 1/2 \*  $\Delta H_f^\circ_{298}(\text{HOOH}) = -16.3$  kcal/mol (see Table 3.6).

The consistency of group values between alkyl hydroxides (ROH) and corresponding alkyl hydroperoxides (ROOH) can also be verified. Benson's GA approach can be applied to CH<sub>3</sub>OH, CH<sub>3</sub>OOH, CH<sub>3</sub>CH<sub>2</sub>OH and CH<sub>3</sub>CH<sub>2</sub>OOH :

$$\Delta H_f^\circ{}_{298}(\text{CH}_3\text{OH}) = \Delta H_f^\circ{}_{298}\{(\text{C}/\text{H}_3/\text{O}) + (\text{O}/\text{C}/\text{H})\} \quad (\text{G4})$$

$$\Delta H_f^\circ{}_{298}(\text{CH}_3\text{OOH}) = \Delta H_f^\circ{}_{298}\{(\text{C}/\text{H}_3/\text{O}) + (\text{O}/\text{C}/\text{O}) + (\text{O}/\text{H}/\text{O})\} \quad (\text{G2})$$

$$\Delta H_f^\circ{}_{298}((\text{CH}_3)_3\text{COH}) = \Delta H_f^\circ{}_{298}\{3(\text{C}/\text{C}/\text{H}_3) + (\text{C}/\text{C}_3/\text{O}) + (\text{O}/\text{C}/\text{H})\} \quad (\text{G5})$$

$$\Delta H_f^\circ{}_{298}((\text{CH}_3)_3\text{OOH}) = \Delta H_f^\circ{}_{298}\{3(\text{C}/\text{C}/\text{H}_3) + (\text{C}/\text{C}_3/\text{O}) + (\text{O}/\text{C}/\text{O}) + (\text{O}/\text{H}/\text{O})\} \quad (\text{G6})$$

The value of  $\Delta H_f^\circ{}_{298}\{(\text{O}/\text{C}/\text{O}) + (\text{O}/\text{H}/\text{O}) - (\text{O}/\text{C}/\text{H})\}$  is 14.88 kcal/mol by subtracting (G4) from (G2) which is 5 kcal/mol different from that obtained by subtracting (G5) from (G6), 19.89 kcal/mol. More examples of these comparisons are illustrated in Table 3.6.

In the above calculations,  $\Delta H_f^\circ{}_{298}$  of HOOH, CH<sub>3</sub>OOCH<sub>3</sub>, CH<sub>3</sub>OH, (CH<sub>3</sub>)<sub>3</sub>COH and (CH<sub>3</sub>)<sub>3</sub>COOH are experimentally measured values,  $\Delta H_f^\circ{}_{298}(\text{CH}_3\text{OOH})$  is derived from the experimentally measured  $\Delta H_f^\circ{}_{298}(\text{CH}_3\text{OO}\cdot)$  under the assumption of bond dissociation energy  $D^\circ(\text{ROO}-\text{H})$  equal to 88 kcal/mol. In using Benson's scheme for peroxide species the discrepancy can be up to 5 kcal/mol. This can be caused by using the enthalpy of (CH<sub>3</sub>)<sub>3</sub>COH which is not accurately determined, or the general failure of the original additivity scheme. Therefore an alternative GA scheme (Scheme II) is developed in this work.

### 3.2.4 Scheme II

An alternative GA scheme for alkyl hydroperoxides hereafter defined as Scheme II is based on treatment of -OO- as one polyvalent atom, e.g. in this scheme the expressions for  $\Delta H_f^\circ_{298}$  of  $\text{CH}_3\text{OOCH}_3$ ,  $\text{CH}_3\text{OOH}$  and  $\text{CH}_3\text{CH}_2\text{OOH}$  in scheme II are:

$$\Delta H_f^\circ_{298}(\text{CH}_3\text{OOCH}_3) = \Delta H_f^\circ_{298}\{(\text{C}/\text{H3}/\text{OO}) + (\text{OO}/\text{C2})\} \quad (\text{G7})$$

$$\Delta H_f^\circ_{298}(\text{CH}_3\text{OOH}) = \Delta H_f^\circ_{298}\{(\text{C}/\text{H3}/\text{OO}) + (\text{OO}/\text{C}/\text{H})\} \quad (\text{G8})$$

$$\Delta H_f^\circ_{298}(\text{CH}_3\text{CH}_2\text{OOH}) = \Delta H_f^\circ_{298}\{(\text{C}/\text{C}/\text{H3}) + (\text{C}/\text{C}/\text{H2}/\text{OO}) + (\text{OO}/\text{C}/\text{H})\} \quad (\text{G9})$$

The discrepancy in Benson's GA scheme illustrated in Table 3.6 can thus be avoided. The  $S^\circ_{298}$  and  $C_p^\circ(T)$ 's can also be treated by Scheme II as the illustration of (G7), (G8) and (G9).

The group values for the calculations of thermodynamic properties of peroxides using Scheme II are listed in Table 3.7. The thermodynamic properties of four molecules (*n*-propyl, *n*-butanyl, *i*-butyl and  $\alpha$ -methyl propyl hydroperoxide) listed in Table 3.5 are calculated using Scheme II with these group values.

## 3.3 Results and Discussion

Vibration frequencies and moments of inertia obtained by MNDO/PM3 are listed in Table 3.3. The accuracy of vibration frequencies determined by MNDO/PM3 was examined by Coolidge *et al.*<sup>56</sup> Their results indicate that for vibration frequencies of closed shell molecules, "PM3 generally gives an acceptable match across the entire spectrum" ; "PM3

provides values that can be compared directly to experiment".<sup>56</sup> The estimate of average systematic error based on the 61 small molecules with a total of 674 calculated vibration frequencies is  $-2.6 \text{ cm}^{-1}$  and the average relative deviation of the calculated from the experimental value is  $-2.6\%$ . It should be noted that PM3 does not predict the frequencies of O-H stretching modes accurately,<sup>56</sup> typically  $3900 \text{ cm}^{-1}$  instead of  $3200 \text{ cm}^{-1}$  to  $3600 \text{ cm}^{-1}$ . However, these frequencies are large and this deviation does not cause any significant error in calculating entropies and heat capacities over the temperature range 300K - 1000K.

Higher level *ab initio* calculations using Gaussian92 provide more accurate predictions of molecular geometry. However, the consistency of experimental and calculated vibration frequencies using Gaussian92 at the HF/6-31G\* level is not very good. According to a systematic study by Hehre *et al.*<sup>16</sup> on the performance of various basis sets, 'The mean absolute percentage deviations of 3-21G(\*) and 6-31G\* frequencies from directly measured values are 12.4% and 13.9% respectively', and if the comparison are performed with experimental harmonic frequencies the deviation of 6-31G\* is about +12.8%.

Since usually *ab initio* methods are considered to be a more preferable approach compared to semiempirical MO calculations (like PM3), we performed a limited comparison of vibrational frequencies calculated by PM3 with those calculated by HF/6-31G\* on  $\text{CH}_3\text{CH}_2\text{OOH}$ ,  $\text{CH}_3\text{CHClOOH}$  and  $\text{CH}_3\text{CCl}_2\text{OOH}$  molecules (see Chapter 4). Our comparison indicates that there is no reason to use higher level calculation to acquire

vibration frequencies for calculations of the corresponding vibrational contributions to thermodynamic properties.

Barriers for internal rotations used in this work are listed in Table 3.3. These barriers were directly adapted or estimated from literature data, see Table 3.4. Internal rotations of molecules are often treated either as harmonic torsional vibrations, or as a free rotations with application of classical statistics in calculating thermodynamic properties. These approximations could result in a significant error in entropies and heat capacities. Pitzer and Gwinn's analysis and tabulated thermodynamic properties present a more accurate method to account for hindered internal rotors than the approximations using torsional frequencies or free-rotor model.

The thermodynamic properties of gas-phase, one to four carbon, alkyl, monochloro- and monofluoro- hydroperoxides are listed in Table 3.5. Group values derived in this work are listed in Table 3.7. Groups obtained in this work can be used for calculation of thermodynamic properties of other alkyl hydroperoxide molecules that are not considered here.

### 3.4 Conclusion

We have developed a data base of thermodynamic properties ( $\Delta H_f^\circ_{298}$ ,  $S^\circ_{298}$ ,  $C_p^\circ(T)$ ) for gas-phase alkyl, monochloro- and monofluoro- hydroperoxides, where experimental or accessible literature data are not available. Enthalpies of formation are evaluated using experimental and theoretical literature data. Contributions to entropies and heat capacity were determined using calculated molecular parameters: optimized geometry of molecular

structure, moments of inertia, vibrational frequencies and potential barriers for internal rotations. Group values of an alternative scheme of Group Additivity have also been derived.



## CHAPTER 4

### ***AB INITIO* STUDY OF CH<sub>3</sub>CH<sub>2</sub>OOH, CH<sub>3</sub>CHClOOH AND CH<sub>3</sub>CCl<sub>2</sub>OOH: CONFORMATIONAL ANALYSIS, INTERNAL ROTATION BARRIERS, VIBRATIONAL FREQUENCIES, AND THERMODYNAMIC PROPERTIES**

#### **4.1 Introduction**

There have been few studies on determination of thermodynamic properties of alkyl hydroperoxides (see Chapter 3). One reason is the difficulty in defining the experimental structures with accuracy due to the strong influence of intramolecular and intermolecular forces in the condensed phase (solvent effects, crystal packing effect...etc.), the rapid interaction of conformers, and the inherent instability of alkyl hydroperoxides.<sup>73</sup> The facts that hydroperoxides usually dissociate to alkoxy (RO.) and hydroxy (OH) under condition of high temperature, or rapidly react with other active species, and thus do not appear in the product profiles of gas phase reactions, also contribute to the reasons for lack of the thermodynamic studies of alkyl hydroperoxides.

The objective of this work was primarily proposed to calculate thermodynamic functions ( $\Delta H_f^\circ_{298}$ ,  $S^\circ_{298}$  and  $C_p(T)$ ,  $300 \leq T/K \leq 5000$ ) for CH<sub>3</sub>CH<sub>2</sub>OOH (**a**), CH<sub>3</sub>CHClOOH (**b**) and CH<sub>3</sub>CCl<sub>2</sub>OOH (**c**) using *ab initio* MO theory for the analysis of molecular conformations, barriers to internal rotation, and harmonic vibrational frequencies.

## 4.2 Literature Survey

### 4.2.1 Molecular Structure of Hydroperoxides

HOOH was the first molecule in the hydroperoxide family which has been studied extensively. Cremer<sup>74</sup> has reviewed the experimental results for the conformational analysis and rotational barrier for H<sub>2</sub>O<sub>2</sub> and D<sub>2</sub>O<sub>2</sub>. This is organized as Table 4.1 which includes the results of Cremer's *ab initio* study. The *skew* conformation of HOOH with a dihedral angle about 110° to 120° is the most stable. The potential energy surface, however, is rather flat in the region of HOOH internal rotation around the *trans* conformation ( $\angle\text{HOOH}=180^\circ$ , see Table 4.1 and Figure 1) with a ca. 1 kcal/mol barrier height. The potential barrier of the *cis* conformation ( $\angle\text{HOOH}=0^\circ$ ) was determined as 7.03 kcal/mol by Hunt et al.<sup>75</sup> using infrared spectroscopy, compared to 7.94 kcal/mol reported by Radom *et al.*<sup>21</sup> and 7.4 by Cremer<sup>74</sup> using an intermediate level of theory, HF/4-31G and (11s6p2d/6s2p) basis sets, respectively. The O-O bond length ( $r_{\text{OO}}$ ) in H<sub>2</sub>O<sub>2</sub> was determined as 1.475 Å by Redington *et al.*<sup>76</sup> using IR spectroscopy and was interpreted as 1.463 Å by Cremer,<sup>74</sup> compared to the value of 1.452 Å which was reported by Khacuruzov and Przhevalskii.<sup>77</sup> Cremer's *ab initio* calculations<sup>74</sup> were basically in good agreement with experimental results in the prediction of HOOH geometry (see Table 4.1). It is notable that using higher level of theory than HF/4-31G<sup>21</sup> does not improve the agreement with experimental values for the rotational barrier and  $r_{\text{OO}}$  of HOOH. Hehre *et al.*<sup>16</sup> reported 9.2 kcal/mol as the barrier height for *cis* conformations and 1.393 Å as  $r_{\text{OO}}$  for the equilibrium structure at HF/6-31G\* level.

There were several studies using MO calculations to determine the molecular geometries and rotational barriers for FOOH and ClOOH,<sup>21,78</sup> but no experimental results have been reported. Radom *et al.*<sup>21</sup> predicted that the rotational barriers for FOOH were 3.33 kcal/mol for the *cis* conformation and 7.39 for the *trans* (see Fig. 1) using a 4-31G basis set. This result gives a quite different feature of the potential energy surface for internal rotation of FOOH compared to that for HOOH's. The former has a maximum barrier at the *trans* conformation and the latter at the *cis*. Francisco *et al.*<sup>78</sup> optimized the geometry for ClOOH at a high level of theory, CCSD(T)/TZ2P. The *skew* conformation was determined as the most stable at all theory levels.<sup>78</sup> The *trans* conformation of ClOOH was predicted to have a barrier height ranging from 3.1 to 3.8 kcal/mol<sup>78</sup> depending on the basis set used in the calculation. The rotational barrier for the *cis* conformation of ClOOH was calculated to be 7.0 kcal/mol at the MP2/6-31G\* level, 5.7 at the CCSD(T)/TZ2P level, and 5.1 at the CCSD(T)/ANO4 level, the highest level of the calculations.<sup>78</sup> The O-O bond length ( $r_{OO}$ ) at the *skew* conformation was determined as 1.437 Å, 1.408 Å and 1.443 Å at the MP2/6-31G\*, MP2/6-311G\*\* and CCSD(T)/TZ2P levels, respectively.<sup>78</sup> In such cases as the study of ClOOH<sup>78</sup> where there is experimental data, it is rather difficult to select the values of  $r_{OO}$  and barrier height for the *cis* conformation for use in calculation of thermodynamic functions.

The equilibrium geometry for CH<sub>3</sub>OOH was determined experimentally to be the COOH *skew* conformation with the values as follows: 1.443 Å and 1.437 Å as  $r_{OO}$  and  $r_{CO}$ , respectively; 114° as the COOH dihedral angle.<sup>79,80</sup> No experimental data for rotational barriers for CH<sub>3</sub>OOH has been published. Several studies using *ab initio* MO calculations

have been performed for  $\text{CH}_3\text{OOH}$ .<sup>73,21,80</sup> The COOH dihedral angle in the *skew* conformation was calculated as  $140^\circ$  at the HF/4-31G level of theory,<sup>21</sup> and  $118.8^\circ$  at the HF/6-31G\* level. The rotational barrier for the COOH *cis* conformation was determined as 7.80 kcal/mol at the HF/4-21G level,<sup>80</sup> 7.99 kcal/mol at the HF/4-31G<sup>21</sup> level and 7.74 kcal/mol at the HF/6-31G\* level.<sup>73</sup> Another internal rotation for  $\text{CH}_3\text{OOH}$  was about C-O bond which barrier height was determined as 2.93 at the HF/4-21G level.<sup>80</sup>

A recent comparison<sup>81</sup> of *ab initio* MO calculations to experimental data for peroxides concluded that there was no general computational procedure that will yield accurate molecular geometries. Large basis sets including polarization functions predict correct *skew* conformations, but give too short O-O bond lengths. Inclusion of electron correlation corrections can improve O-O bond length yet bond angles were hardly affected.<sup>73,81</sup> The recommended procedure<sup>81</sup> was MP2 or MP4 single point calculation at the HF/3-21G-optimized molecular geometries.

To our knowledge neither experimental nor *ab initio* MO studies have been published for the determination of molecular structures, rotational barriers and vibrational frequencies for alkyl hydroperoxides with more than 2 carbons.

#### 4.2.2 Thermochemistry of Hydroperoxides

Few heats of formation ( $\Delta H_f^\circ_{298}$ ) for alkyl hydroperoxides have been studied experimentally. The experimental values of  $\Delta H_f^\circ_{298}$  were available for only  $\text{CH}_3\text{OOH}$ ,  $\text{C}_2\text{H}_5\text{OOH}$ , *i*- $\text{C}_3\text{H}_7\text{OOH}$  and *t*- $\text{C}_4\text{H}_9\text{OOH}$  according to a recent review.<sup>73</sup> The only known experimental value of  $\Delta H_f^\circ_{298}$  for ethyl hydroperoxide was measured in 1940,<sup>82</sup> and the

reported number contained a high uncertainty, i.e.  $45 \pm 12$  kcal/mol.<sup>82,83</sup> The  $\Delta H_f^\circ$ ,<sup>298</sup>,  $S^\circ$ ,<sup>298</sup> and  $C_p(T)$  for the alkyl hydroperoxides are generally estimated using Benson's Group Additivity (GA) scheme and Group Values,<sup>60</sup> if experimental data or the values from high level of MO calculations are not available. Benson's GA approach has proven to be an useful method for the estimation of thermodynamic properties of most molecules. The accuracy of Benson's GA scheme for (chloro-) alkyl hydroperoxide, however, was not comprehensively assessed since limited reliable thermodynamic property data exist. (See Chapter 3 for review of Benson's GA scheme for alkyl hydroperoxides)

#### 4.2.3 Comparison of Semiempirical and *Ab Initio* MO Calculations

The general performance of semiempirical MO calculations on alkyl hydroperoxides is also of interest since these methods, like CNDO,<sup>84</sup> MNDO/AM1<sup>17</sup> or PM3,<sup>9</sup> are often used when *ab initio* MO calculations were not accessible nor economical. A study by Ohkubo *et al.*<sup>85</sup> showed that the O-O bond length in HOOH, CH<sub>3</sub>OOH and CH<sub>3</sub>OOCH<sub>3</sub> cannot be correctly predicted by some semiempirical MO methods. INDO and CNDO/2 seriously underestimate the  $r_{OO}$  for equilibrium geometries, while the former gives 1.22 Å for that of HOOH and the latter yields 1.23 Å for that for CH<sub>3</sub>OOH.<sup>85</sup> This situation is improved by using MINDO/2' which gives 1.404 Å for  $r_{OO}$  of HOOH and 1.414 Å for  $r_{OO}$  of CH<sub>3</sub>OOH. However, MINDO/2' predicts a too large HOO bond angle in HOOH (+21°), and too large COO bond angle (+14°) in CH<sub>3</sub>OOH.<sup>85</sup> The authors concluded that 'the slight underestimation of  $r_{OO}$  was mainly attributable to the underestimate of the lone pair-lone pair interactions between the two oxygen atoms (caused by the neglect of two center integrals

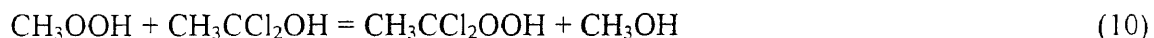
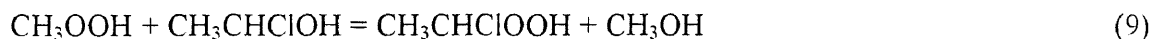
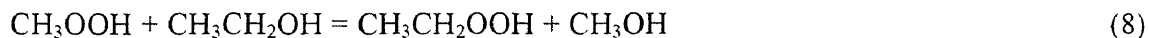
involving one-centered overlap), while the overestimation of the bond angles was due to an insufficient parameterization for the heteroatom.”<sup>85</sup>

### 4.3 Method

All *ab initio* calculations were performed using Gaussian92 system of programs<sup>12</sup> on the Cray YMP at Pittsburgh Supercomputing Center (PSC) and the Vax-6430 at New Jersey Institute of Technology. Equilibrium and saddle-point geometries were completely optimized at the close shell restricted Hartree-Fock (RHF) level of theory with analytical gradients<sup>86</sup> using the 6-31G\* (6-31G(d)) basis set (HF/6-31G\*).<sup>13,14,15</sup> Then single-point energies for all rotational conformers were calculated using second-order Møller-Plesset perturbation theory at the 6-31G\*\* (6-31G(d,p)) level<sup>13,14,15</sup> (MP2/6-31G\*\*//HF/6-31G\*). Vibrational frequencies were calculated for all rotational conformers using analytical second derivatives at HF/6-31G\* level. Zero-point vibrational energies (ZPVE) were scaled by 0.9 for all calculations because the HF-SCF harmonic vibrational frequencies were found to be overestimated by about 10% in a study of systematic performance.<sup>16</sup>

To calculate the rotational barriers, the potential energy surface (PES) was first calculated for the selected dihedral angle for each internal rotation. For instance, a PES was calculated for changes in the HCCO dihedral angle to study the barriers for the internal rotation about CH<sub>3</sub>--CH<sub>2</sub>OOH bond. In this case, the frequency of CH<sub>3</sub>--CH<sub>2</sub>OOH torsional motion in the equilibrium structure (staggered) was not included in the calculation of ZPVE.

Three isodesmic reactions<sup>16</sup> were used to study the enthalpies of reactions:



The total energies for  $\text{CH}_3\text{OH}$ ,  $\text{CH}_3\text{OOH}$ ,  $\text{CH}_3\text{CH}_2\text{OH}$ ,  $\text{CH}_3\text{CHClOH}$  and  $\text{CH}_3\text{CCl}_2\text{OH}$  were calculated at the same level of theory as that used for the title species, MP2/6-31G\*\*//HF/6-31G\*. The energies of the reactions were obtained from the total energies of the reactants and products with the corrections of the scaled (x0.9) ZPVE. The calculated reaction energies were then combined with experimental data or evaluated values of  $\Delta H_f^\circ_{298}$  for  $\text{CH}_3\text{OH}$ ,  $\text{CH}_3\text{OOH}$ ,  $\text{CH}_3\text{CH}_2\text{OH}$ ,  $\text{CH}_3\text{CHClOH}$  and  $\text{CH}_3\text{CCl}_2\text{OH}$  to obtain the enthalpies of formation for  $\text{CH}_3\text{CH}_2\text{OOH}$  (**a**),  $\text{CH}_3\text{CHClOOH}$  (**b**) and  $\text{CH}_3\text{CCl}_2\text{OOH}$  (**c**).

The standard entropies ( $S^\circ_{298}$ ) and heat capacities ( $C_p(T)$ ,  $300 \leq T/K \leq 5000$ ) as function of temperature were calculated using the Rigid-Rotor-Harmonic-Oscillator (RRHO) model.<sup>8</sup> A method described in Chapter 1 was used to calculate contributions of hindered rotors to the entropy and heat capacities.

The AM1<sup>17</sup> and PM3<sup>9</sup> methods in the MOPAC6.0<sup>10</sup> package were used to perform the semiempirical MO calculations. The molecular geometries in the equilibrium states for title species were calculated with AM1 and PM3 parameters, and the results were compared to those obtained from *ab initio* studies at the HF/6-31G\* level of theory.

The harmonic vibrational frequencies of MNDO/AM1 and PM3 were also calculated using normal mode analysis of nuclear coordinates and were compared to Hartree-Fock frequencies.

## 4.4 Results and Discussion

### 4.4.1 Molecular Geometries

The definition and nomenclature for all rotational conformers in this work are illustrated in Figure 4.2. The optimized geometries for the rotational conformers of  $\text{CH}_3\text{CH}_2\text{OOH}$  (**a**),  $\text{CH}_3\text{CHClOOH}$  (**b**) and  $\text{CH}_3\text{CCl}_2\text{OOH}$  (**c**) are listed in Table 4.2, Table 4.3 and Table 4.4, respectively. The equilibrium structures for **a**, **b**, and **c** are further illustrated in Figure 4.3. C-C bond lengths are quite consistent in the equilibrium states, while the C-O bond length decreases consistently from 1.406 Å in **a**, to 1.374 Å in **b** and 1.368 Å in **c**. The O-O bond length also decreases in this series from 1.393 Å in **a**, to 1.387 in **b** and 1.364 Å in **c**.

The *skew* conformations are the most stable in all cases, with the COOH dihedral angles as  $116.52^\circ$ ,  $97.89^\circ$  and  $97.54^\circ$  for **a**, **b** and **c**, respectively. These results are consistent with the former studies for HOOH and  $\text{CH}_3\text{OOH}$  (see Figure 4.1). The *trans* conformation of  $(\text{CH}_3)\text{CHCl-O}(\text{OH})$  and  $(\text{CH}_3)\text{CCl}_2\text{-O}(\text{OH})$  (dihedral angle CCOO  $\approx 180^\circ$ ) are more stable than the *gauche* (CCOO  $\approx 60^\circ$  or  $-60^\circ$ ), indicating that the electronic repulsion between  $\text{C}_1$  and  $\text{O}_8$  was stronger than that between  $\text{O}_8$  and H atom or  $\text{C}_1$  atom for these two molecules. The atomic Mulliken charge<sup>16</sup> distributions for each molecule are listed in Table 4.5.



#### 4.4.2 Vibrational Frequencies

Harmonic vibrational frequencies were calculated for all rotational conformers and the unscaled frequencies are listed in Table 4.6, 4.7 and 4.8. The equilibrium structures, which are supposed to be the local minimum point on energy surface, were confirmed by no appearance of imaginary frequencies. The presence of one and only one imaginary frequency was an index of the transition state being located. All vibrational frequencies and ZPVE were scaled by 0.9 for all following calculations in this work<sup>16</sup> due to the 10% overestimation of HF-SCF procedure.

Three frequencies of torsion motions were assigned through the normal mode analysis of nuclei coordinates, which represent the torsions about C-C, C-O and O-O bonds. In the rotational transition states, the corresponding torsion frequencies are imaginary. For instance, the frequencies for the torsion motions about C-O and O-O bonds are 138 and 215  $\text{cm}^{-1}$  in aSTS, 146 and 219  $\text{cm}^{-1}$  in aETS, respectively, while the frequency, 262  $\text{cm}^{-1}$  in aSTS and the imaginary frequency, -256  $\text{cm}^{-1}$  in aETS represents the torsional motion about C-C bond in **a**. The location of all rotational conformers on the potential energy surface can be further checked in this manner (see Table 4.6, 4.7, 4.8).

#### 4.4.3 Rotational Barriers

The calculated energy, ZPVE (unscaled) and rotational barrier (i.e. the energy difference compared to the equilibrium state) for each conformer are given in Table 4.9. The following discussion is based on the values of barriers calculated at MP2/6-31G\*\*//HF/6-31G\* level with the corrections of scaled ZPVE ( $\times 0.9$ ) unless otherwise noted.

The barriers of the methyl group rotations increase from 3.32 kcal/mol in **a** to 4.39 kcal/mol in **b** and 4.65 kcal/mol in **c**, reflecting the increase of electronic repulsion with the increase of chlorine substitution on the  $\alpha$ -carbon. The eclipse of methyl groups with groups of  $\alpha$ -carbon also makes the C-C bond length longer than that in the staggered conformation; increases are 0.0146 Å, 0.0157 Å, 0.0214 Å for **a**, **b** and **c**, respectively.

The barriers for internal rotations about the C-O bond are more complex. The most stable form for **a** is aSTS, 0.38 kcal/mol lower than aSGS at the HF/6-31G\*\*//6-31G\* level. However, the total energies calculated at the MP2/6-31G\*\*//HF/6-31G\* level indicate that aSTS is 0.11 kcal/mol higher than aSGS. The maximum rotational barrier about C-O bond in **a** occurs at aSE<sub>C</sub>S which is 3.24 kcal/mol higher than aSE<sub>H</sub>S.

For **b** the potential energy surface of the CCOO dihedral angle from 60° to 120° is rather flat. A scan calculation of rotational energy surface as a function of CCOO dihedral angle at the HF/6-31G\* level was performed keeping all the parameters fixed and varying CCOO at 15° intervals, to confirm the location of the transition state, see Figure 4.7. The barriers of rotations on the scanned potential energy surface using the rigid geometries are higher than those calculated by allowing geometry optimization. However, the scan investigation indicates that there is no obvious saddle point (local maximum) in the range of the CCOO dihedral angle from 60° to 180° and that the energy diagram fitted from our calculations of rotational barriers about C-O bond is reliable.

The maximum rotational barrier about the C-O bond in **b** occurs at bSE<sub>C</sub><sub>1</sub>S, 3.23 kcal/mol higher than bSE<sub>C</sub>S. It is also notable that the barrier for the rotation across the

overlap of  $O_8$  and  $C_1$  at  $C_2$  from the equilibrium state ( $\text{CCOO} = 180^\circ$ ) in **c** is lower than that in **b** by about 2.7 kcal/mol.

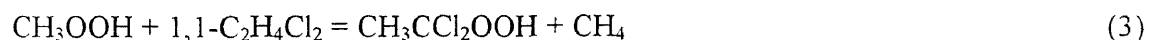
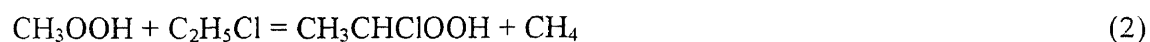
The COOH *skew* conformations are the most stable form in all cases. This is consistent with the fact that the orthogonal conformation of X-O-O-Y allows for the delocalization of lone pair electrons more than coplanar conformations (*cis* and *trans*).<sup>21</sup> The internal rotational barriers about the O-O bond in alkyl hydroperoxides are strongly dependent on the  $\alpha$ -carbon substituent groups. However, the rotational barriers for the *cis* and *trans* conformation do not increase with the increase of the number of substituent chlorine atoms on the  $\alpha$ -carbon. The bSTC has the highest barrier at 8.43 kcal/mol while aSTC and cSTC have lower barriers of 6.67 and 5.35 kcal/mol, respectively.

The values of the Fourier expansion components (see Chapter 1),  $V_i$  and  $V'_i$  in equation (E1) and  $a_i$  and  $b_i$  in equation (E2) are obtained by curve fitting at  $3^\circ$  intervals for entire potential energy surface. These values are given in Table 4.10.

#### 4.4.4 Heat of Formation

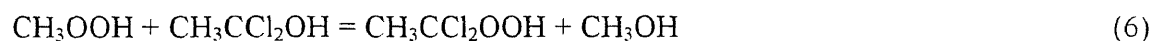
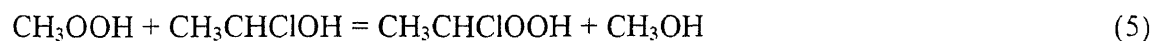
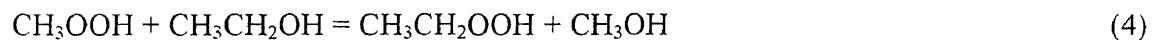
Two sets of isodesmic reactions may be used to study the enthalpies of reactions theoretically. The first option is the reaction with alkane and  $\text{CH}_3\text{OOH}$  as the reactants and the desired alkyl hydroperoxide and  $\text{CH}_4$  as products.

##### Scheme I



One other alternative is reaction with the alcohol and  $\text{CH}_3\text{OOH}$  as reactants and the desired alkyl hydroperoxide and  $\text{CH}_3\text{OH}$  as products:

### Scheme II



Scheme II should be the better choice than Scheme I for the isodesmic reactions. But to our knowledge there are no reliable data for  $\Delta H_f^\circ_{298}$  of  $\text{CH}_3\text{CHClOH}$  and  $\text{CH}_3\text{CCl}_2\text{OH}$ , while  $\Delta H_f^\circ_{298}$  for all alkane species in the reactions in Scheme I is more precisely known. We performed both two sets of calculations in order to compare the results of the schemes.

For Scheme II, we need to have the values of  $\Delta H_f^\circ_{298}(\text{CH}_3\text{CHClOH})$  and  $\Delta H_f^\circ_{298}(\text{CH}_3\text{CCl}_2\text{OH})$ . The  $\Delta H_f^\circ_{298}(\text{CH}_3\text{CHClOH})$  and  $\Delta H_f^\circ_{298}(\text{CH}_3\text{CCl}_2\text{OH})$  are estimated from  $\Delta H_f^\circ_{298}$  of  $(\text{C}_2\text{H}_5\text{CHClOH})$  as 20.20 kcal/mol and  $\Delta H_f^\circ_{298}(\text{CH}_3\text{CCl}_2\text{OH})$  as 18.80 kcal/mol, (results of BAC/MP4 calculation by Melius),<sup>69</sup> with  $\Delta H_f^\circ_{298}(\text{H})$  equal to 52.1 kcal/mol and the average bond dissociation energy of primary C-H bond as 101.1 kcal/mol.<sup>88</sup>

The total energies, ZPVE (unscaled) and experimental data or evaluated values of  $\Delta H_f^\circ_{298}$  for the species in all isodesmic reactions are given in Table 4.11. The reaction

energies and the calculated  $\Delta H_f^\circ_{298}$  for  $\text{CH}_3\text{CH}_2\text{OOH}$  (**a**),  $\text{CH}_3\text{CHClOOH}$  (**b**) and  $\text{CH}_3\text{CCl}_2\text{OOH}$  (**c**) are listed in Table 4.12.

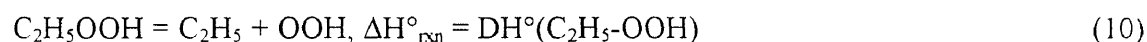
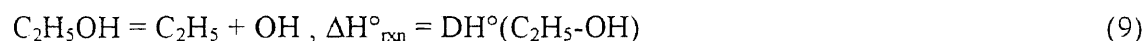
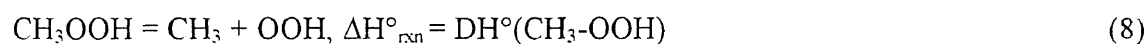
The results of  $\Delta H_f^\circ_{298}$  for ethyl hydroperoxide using the Scheme I and Scheme II isodesmic reactions are consistent, but the discrepancy between the values for the two schemes dramatically increases for  $\text{CH}_3\text{CHClOOH}$  and  $\text{CH}_3\text{CCl}_2\text{OOH}$ . Since the isodesmic reactions in Scheme II are better choices than those in Scheme I, the data calculated from the  $\Delta H^\circ_{\text{rxn}}$  of reactions in Scheme II are recommended.

The  $\Delta H_f^\circ_{298}$  of  $\text{CH}_3\text{CH}_2\text{OOH}$  is calculated to be -39.42 kcal/mol using reaction (4) in scheme 2, while the  $\Delta H_f^\circ_{298}$  of  $\text{CH}_3\text{OOH}$  is equal to -31.3 kcal/mol. It is -41.32 kcal/mol while  $\Delta H_f^\circ_{298}$  of  $\text{CH}_3\text{OOH}$  is equal to -33.2 kcal/mol. The latter result is in good agreement with another value, -41.09 kcal/mol,<sup>89</sup> which is evaluated using the experimentally-determined  $\Delta H_f^\circ_{298}$  of  $\text{CH}_3\text{CH}_2\text{OO}$ , -5.19 kcal/mol<sup>67</sup> and the average bond energy  $D^\circ(\text{ROO-H})$ , 88 kcal/mol.<sup>89</sup> The isodesmic reactions in scheme 2 and the value of  $\Delta H_f^\circ_{298}(\text{CH}_3\text{OOH}) = -33.2$  kcal/mol is also used to evaluate the enthalpies of formation for  $\text{CH}_3\text{CHClOOH}$  and  $\text{CH}_3\text{CCl}_2\text{OOH}$ .

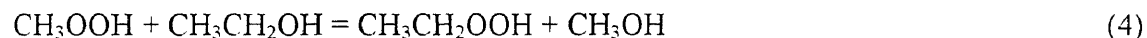
The calculated  $\Delta H_f^\circ_{298}(\text{CH}_3\text{CHClOOH})$  is -49.26 kcal/mol using  $\Delta H^\circ_{\text{rxn}}$  of reaction (5) and  $\Delta H_f^\circ_{298}(\text{CH}_3\text{CHClOH}) = -64.2$  kcal/mol. It is consistent with the value -48.98 kcal/mol, which is evaluated from  $\Delta H_f^\circ_{298}(\text{CH}_3\text{CHClOO}) = -13.08$  kcal/mol<sup>90</sup> and the average bond energy  $D^\circ(\text{ROO-H}) = 88$  kcal/mol.<sup>89</sup>

$\Delta H_f^\circ_{298}(\text{CH}_3\text{CCl}_2\text{OOH})$  is calculated as -52.84 kcal/mol. This value is calculated using  $\Delta H^\circ_{\text{rxn}}(6)$  and  $\Delta H_f^\circ_{298}(\text{CH}_3\text{CCl}_2\text{OH}) = -71.8$  kcal/mol. No comparable data are known for  $\Delta H_f^\circ_{298}(\text{CH}_3\text{CCl}_2\text{OOH})$ .

We are also interested in bond dissociation energy differences between  $DH^\circ(R-OOH)$  and  $DH^\circ(R-OH)$  which are useful information for estimating the enthalpies of formation for alkyl hydroperoxides with  $\alpha$ -chlorine substituted from the that of corresponding alcohols. These values can be calculated by following procedure:



$$(8) + (9) = (7) + (10),$$



$$\Delta H^\circ_{rxn} = DH^\circ(CH_3-OOH) + DH^\circ(C_2H_5-OH) - DH^\circ(C_2H_5-OOH) - DH^\circ(CH_3-OH)$$

The  $\Delta H^\circ_{rxn}$  of isodesmic reaction (4) is therefore equal to  $\{DH^\circ(CH_3-OOH) - DH^\circ(CH_3-OH)\} + \{DH^\circ(C_2H_5-OH) - DH^\circ(C_2H_5-OOH)\}$ . The value of  $\{DH^\circ(C_2H_5-OH) - DH^\circ(C_2H_5-OOH)\}$  can be obtained with the known data of  $\Delta H^\circ_{rxn}(4)$  and  $\{DH^\circ(CH_3-OOH) - DH^\circ(CH_3-OH)\}$ . The values of  $\{DH^\circ(CH_3CHCl-OH) - DH^\circ(CH_3CHCl-OOH)\}$  and  $\{DH^\circ(CH_3CCl_2-OH) - DH^\circ(CH_3CCl_2-OOH)\}$  can also be obtained in the same manner. The results of the bond strength differences are given in Table 4.13. The data indicate that the bond energies of the C-O bond in alkyl hydroperoxides (ROOH) are higher than those in alcohols (ROH) by about 20 to 26 kcal/mol. The differences of bond strength for the two kinds of C-O bond are about 21.6 kcal/mol for  $CH_3CH_2-OOH$  vs

$\text{CH}_3\text{CH}_2\text{-OH}$  and  $\text{CH}_3\text{CHCl-OOH}$  vs  $\text{CH}_3\text{CHCl-OH}$ , but it is 25.8 kcal/mol for  $\text{CH}_3\text{CCl}_2\text{-OOH}$  vs  $\text{CH}_3\text{CCl}_2\text{-OH}$ .

#### 4.4.5 Thermodynamic Properties

The thermodynamic properties are listed in Table 4.14. The contribution of entropies and heat capacities from internal hindered rotors are calculated by direct diagonalization of the Hamiltonian Matrix. The difference of using this technique and Pitzer and Gwinn's approximation and Tables are illustrated in Table 4.15.

#### 4.4.6 Coupling Effects of Internal Rotations

The calculation of entropies and heat capacities is based on the assumption that the internal hindered rotations are not coupled. The contribution of entropies and heat capacities from hindered rotors are calculated separately and summed to give the total entropies and heat capacities. There is one important concern in the calculations of thermodynamic functions using the above procedure, *i.e.* for these three molecules, how much can the three internal rotors affect each other, or, what would be the rotational barriers if the rotations are coupled.

It obviously requires a great deal of computer CPU time to calculate the total energies for all possible rotational conformers at a level of theory like HF/6-31G\* in order to partly answer these questions. However, we performed the calculations at the smaller 3-21G\* basis set to scan the possible coupling effects of rotational barriers for  $\text{CH}_3\text{CH}_2\text{OOH}$ . The calculations were performed at the MP2/3-21G\*\*//HF/3-21G\* level

with scaled ZPVE (0.9) for all theoretically local maximum and minimum points on the different potential energy surfaces. The coupling effects were investigated by calculating the total energies of conformers with various dihedral angles. The results are illustrated in Figure 4.8, 4.9 and 4.10.

Generally speaking, the shapes of PES of internal rotations remain and the barrier heights vary when coupling is considered. For the rotation about C-C bond, the barriers increase to about 6 kcal/mol (from 3 kcal/mol) with the dihedral angle CCOO and COOH both equal to 0°. They increase to about 4 kcal/mol when CCOO is equal to 0° with COOH in the *skew* conformation.

For the rotation about the C-O bond, the barriers increase to about 7 kcal/mol with the dihedral angle COOH equal to 0° and HCCO in the staggered conformation. The rotational barriers about the O-O bond remain on the same scale while the dihedral angle CCOO is varied. These scan studies indicate that the rotations coupled with the COOH *cis* conformation have the most significant effects for rotational barriers.

The coupling effects of internal rotations for CH<sub>3</sub>CHClOOH and CH<sub>3</sub>CCl<sub>2</sub>OOH were not investigated due to limited computer resources.

#### **4.4.7 Comparison of MNDO/AM1 and PM3 Molecular Geometries and Vibrational Frequencies**

The comparison of bond lengths between *ab initio* and semiempirical MO calculations is given in Table 4.16. The results indicate that the O-O bond length is highly underestimated by AM1 as an average 0.10 Å shorter, but overestimated by PM3 as 0.13 Å longer, compared to geometries optimized in the HF/6-31G\* basis set. The C-O bond lengths in



the alkyl hydroperoxides are also not correctly predicted by both AM1 and PM3 Hamiltonians. Here the PM3 gives a more consistent C-O(OH) bond with an average deviation of  $-0.02 \text{ \AA}$ , whereas AM1 yields a C-O(OH) bond length too large by  $0.066 \text{ \AA}$  on average. The comparison of bond angles and dihedral angles is given in Table 4.17.

The comparison of vibrational frequencies is illustrated in Figure 4.11, 12 and 13. Very large deviations occur at the three lowest frequencies. But in practical consideration, these three frequencies which correspond to the three torsion motions are not included in the calculations of entropies and heat capacities. The entropies and heat capacity contributed from vibrational frequencies ( $S^{\circ}_{298,\text{vib}}$  and  $C_{p500,\text{vib}}$ ) are also compared in these three figures. The mean absolute deviation of  $S^{\circ}_{298,\text{vib}}$  from AM1 to 6-31G\* is  $-0.75 \text{ cal/mol-K}$ , and it is  $+0.40 \text{ cal/mol-K}$  from PM3 to 6-31G\*. The mean absolute deviation of  $C_{p298,\text{vib}}$  from AM1 to 6-31G\* is  $-1.03 \text{ cal/mol-K}$ , and it is  $+0.63 \text{ cal/mol-K}$  from PM3 to 6-31G\*. This indicates that when the resources for sophisticated *ab initio* calculations are not available, the semiempirical PM3 Hamiltonian is a fairly good alternative for the calculation of vibrational frequencies and thus  $S_{\text{vib}}$  and  $C_{p,\text{vib}}$ .

#### 4.5 Summary

The molecular geometries of equilibrium states and rotational transition states for  $\text{CH}_3\text{CH}_2\text{OOH}$ ,  $\text{CH}_3\text{CHClOOH}$  and  $\text{CH}_3\text{CCl}_2\text{OOH}$  were calculated at the HF/6-31G\* level. Potential barriers of internal rotations were calculated at MP2/6-31G\*\*/HF/6-31G\* level. The potential constants for Fourier expansions were derived. Standard entropies ( $S^{\circ}_{298}$ ) and heat capacities ( $C_p(T)$ 's,  $300 \leq T/\text{K} \leq 5000$ ) were calculated using the RRHO

model and the information obtained from the *ab initio* studies, accompanied with the method described in section 1.5 for handling the energy levels of hindered internal rotations. The enthalpies of formation for these three molecules were calculated by means of isodesmic reactions. The  $\Delta H_f^\circ$  of  $\text{CH}_3\text{CH}_2\text{OOH}$ , **-41.32** kcal/mol, calculated by the method of isodesmic reactions is in very good agreement with previously published values. The  $\Delta H_f^\circ$  for  $\text{CH}_3\text{CHClOOH}$  and  $\text{CH}_3\text{CCl}_2\text{OOH}$  were calculated to be **-49.26** kcal/mol and **-52.74** kcal/mol, respectively. The major uncertainty in above two values arises from the uncertainty of the estimated data of  $\Delta H_f^\circ(\text{CH}_3\text{CHClOH})$  and  $\Delta H_f^\circ(\text{CH}_3\text{CCl}_2\text{OH})$ . The accuracy for  $\Delta H_f^\circ$  of  $\text{CH}_3\text{CHClOOH}$  and  $\text{CH}_3\text{CCl}_2\text{OOH}$  can definitely be further improved when more reliable data of  $\Delta H_f^\circ(\text{CH}_3\text{CHClOOH})$  and  $\Delta H_f^\circ(\text{CH}_3\text{CCl}_2\text{OOH})$  are obtained.

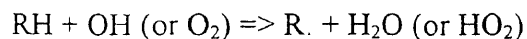
Semiempirical MO calculations with the AM1 and PM3 Hamiltonians were also compared with the *ab initio* HF-SCF results. The comparisons show that neither AM1 nor PM3 can predict correct molecular geometries for alkyl hydroperoxides, while the vibrational frequencies calculated by PM3 were ,on average, within an acceptable range.

## CHAPTER 5

### ***AB INITIO* STUDY OF $\alpha$ -CHLORINATED ETHYL PEROXY RADICALS, CH<sub>3</sub>CH<sub>2</sub>OO, CH<sub>3</sub>CHClOO AND CH<sub>3</sub>CCl<sub>2</sub>OO: CONFORMATIONAL ANALYSIS, INTERNAL ROTATION BARRIERS, VIBRATIONAL FREQUENCIES, AND THERMODYNAMIC PROPERTIES**

#### 5.1 Introduction

The alkyl peroxy radicals have received a lot of attention recently in the study of combustion<sup>2,65-67,91-95</sup> and atmospheric photochemistry<sup>96, 97</sup> of hydrocarbon compounds, because they are the primary adducts while the alkyl radicals react with molecular oxygen (see Chapter 1):



Enthalpies of formation for CH<sub>3</sub>OO<sup>98</sup>, CH<sub>2</sub>ClOO<sup>99</sup>, CHCl<sub>2</sub>OO<sup>99</sup>, CCl<sub>3</sub>OO<sup>100</sup>, CH<sub>3</sub>CH<sub>2</sub>OO,<sup>67</sup> and CH<sub>3</sub>CHClOO<sup>90</sup> was reported by Gutman and co-workers. They reported that the bond strength (DH<sup>o</sup><sub>298</sub>) of the C-O bond in alkyl peroxy radicals decreased from 32.5 kcal/mol<sup>98</sup> in CH<sub>3</sub>-O<sub>2</sub> to 19.8 kcal/mol<sup>100</sup> in CCl<sub>3</sub>-O<sub>2</sub> with intermediate values of 28.9 kcal/mol<sup>99</sup> for CH<sub>2</sub>Cl-O<sub>2</sub> and 25.3 kcal/mol<sup>99</sup> for CHCl<sub>2</sub>-O<sub>2</sub>. The DH<sup>o</sup><sub>298</sub> of the C-O bond for CH<sub>3</sub>CH<sub>2</sub>-O<sub>2</sub><sup>67</sup> and CH<sub>3</sub>CHCl-O<sub>2</sub><sup>90</sup> were also determined as 34.1 and 31.3 kcal/mol, respectively.

Vibrational frequencies were determined experimentally for the  $\text{CH}_3\text{CH}_2\text{OO}$  radical.<sup>101</sup> Conformational analysis and vibrational frequency assignment for  $\text{CH}_3\text{OO}$ <sup>68</sup>,  $\text{CH}_3\text{CH}_2\text{OO}$ <sup>68,102</sup>,  $\text{CH}_3\text{CHClOO}$ <sup>90</sup>,  $(\text{CH}_3)_2\text{CHOO}$ <sup>68</sup> and  $(\text{CH}_3\text{CH}_2)_2\text{CHOO}$ <sup>68</sup> were also carried out using a high level basis set and electron correlation theory.

Besler *et al.*<sup>103</sup> reported that the  $\text{CH}_3$  group rotation in  $\text{CH}_3\text{OO}$  has a very low barrier of 0.43 kcal/mol at the MP2/6-31G\* level of theory and should behave nearly as a free rotor at room temperature,<sup>103</sup> although a quite different number, 1.3 kcal/mol<sup>103</sup> as this barrier height calculated at the UHF/6-31G\* level was also reported in the same article.

Using DZP/CISD level of theory, Quelch *et al.*<sup>102</sup> found the potential energy surface (PES) of the rotation about C-O bond in  $\text{CH}_3\text{CH}_2\text{OO}$  ( $\text{CH}_3\text{CH}_2\text{--OO}$  rotation) to be a triple well with one higher peak and two lower peaks. The maximum rotation barrier of  $\text{CH}_3\text{CH}_2\text{--OO}$  rotation occurs at the CCOO *cis* conformation, as 2.7 kcal/mol, while the eclipse of the  $\alpha$ -hydrogen with terminal oxygen has a lower barrier of 1.0 kcal/mol. The PES for the methyl group rotation about the C-C bond in  $\text{CH}_3\text{CH}_2\text{OO}$  ( $\text{CH}_3\text{--CH}_2\text{OO}$  rotation) was a periodic triple well with a barrier of 2.9 kcal/mol at the DZP/CISD level.<sup>102</sup>

For  $\text{CH}_3\text{CHClOOH}$ , the PES of the rotation about the C-O bond was determined to be more like a double well with one broad and one narrow minimum at the MP2/6-31G\*\*//UHF/6-31G\* level of theory.<sup>90</sup> The maximum of the sharper peak is found around the dihedral angle ClCOO close to  $0^\circ$  with the barrier of 4.46 kcal/mol.<sup>90</sup> The maximum of the broader peak is found around the dihedral angle ClCCO equal to  $0^\circ$  with

a barrier of 2.96 kcal/mol.<sup>90</sup> The PES around dihedral angle  $\alpha\text{HCOO} = 0^\circ$  has a rather flat potential energy surface (see Figure 4.5). The barrier of rotation about the C-C bond ( $\text{CH}_3\text{--CHClOO}$  rotation) was determined to be 3.89 kcal/mol.<sup>90</sup>

The objective of this study is performed primarily for determining the thermodynamic functions, ( $\Delta\text{H}_f^\circ_{298}$ ,  $\text{S}^\circ_{298}$  and  $\text{Cp}(\text{T})$ ,  $300 \leq \text{T}/\text{K} \leq 5000$ ) for the ethyl peroxy radicals with chlorine substitution on the  $\alpha$ -carbon.  $\text{CH}_3\text{CH}_2\text{OO}$  (**a**),  $\text{CH}_3\text{CHClOO}$  (**b**) and  $\text{CH}_3\text{CCl}_2\text{OO}$  (**c**) were selected to study the substitution effect of chlorine on the  $\alpha$ -carbon. Although the enthalpies of formation for  $\text{CH}_3\text{CH}_2\text{OO}$ <sup>67</sup>,  $\text{CH}_3\text{CHClOO}$ <sup>90</sup> have been determined by experiment, the theoretical calculations were performed to further analyze these values.

## 5.2 Method

All *ab initio* calculations were performed using Gaussian92 system of program<sup>12</sup> on the Cray YMP at Pittsburgh Supercomputing Center (PSC) or the Vax-6430 at New Jersey Institute of Technology. Equilibrium and saddle-point geometries were completely optimized at the open shell unrestricted Hartree-Fock (UHF) level of theory with analytical gradients<sup>86</sup> using the 6-31G\* basis set (UHF/6-31G\*).<sup>13,14,15</sup> Single-point energies for all rotational conformers were then calculated using second-order Møller-Plesset perturbation theory at 6-31G\*\* level (MP2/6-31G\*\*//UHF/6-31G\*). Vibrational frequencies were calculated for all rotational conformers using analytical second derivatives at UHF/6-31G\* level. Zero-point vibrational energies (ZPVE) were scaled by

0.9 for all calculations because the HF-SCF harmonic vibrational frequencies were found to be overestimated by about 10% in a study of systematic performance.<sup>16</sup>

To calculate the rotational barriers, the potential energy surface (PES) was first calculated for the selected dihedral angle for each internal rotation. For example, a PES was calculated for changes in the CCOO dihedral angle to study the barriers for the internal rotation about CH<sub>3</sub>CH<sub>2</sub>--OO bond. In this case, the corresponding frequency of CH<sub>3</sub>CH<sub>2</sub>--OO torsion motion for each equilibrium structure was not included in the calculation of ZPVE. Several isodesmic reactions were used to evaluate the enthalpies of reactions.

The total energies for CH<sub>3</sub>O, CH<sub>3</sub>OO, CH<sub>3</sub>CH<sub>2</sub>O, CH<sub>3</sub>CHClO and CH<sub>3</sub>CCl<sub>2</sub>O were calculated at the same level of theory as that used for the title species, MP2/6-31G\*\*//UHF/6-31G\*. The energies of the reactions were obtained from the total energies of the reactants and products with the corrections of the scaled (x0.9) ZPVE. The calculated reaction energies were then combined with experimental data or evaluated values of  $\Delta H_f^\circ_{298}$  for CH<sub>3</sub>O, CH<sub>3</sub>OO, CH<sub>3</sub>CH<sub>2</sub>O, CH<sub>3</sub>CHClO and CH<sub>3</sub>CCl<sub>2</sub>O to obtain the enthalpies of formation for CH<sub>3</sub>CH<sub>2</sub>OO (**a**), CH<sub>3</sub>CHClOO (**b**) and CH<sub>3</sub>CCl<sub>2</sub>OO (**c**).

The standard entropies ( $S^\circ_{298}$ ) and heat capacities ( $C_p(T)$ ,  $300 \leq T/K \leq 5000$ ) as function of temperatures were calculated using the Rigid-Rotor-Harmonic-Oscillator (RRHO) model<sup>8</sup> which utilizes the calculated harmonic vibrational frequencies, moments of inertia, and the hindered internal rotations. For the contributions of hindered rotors to entropies and heat capacities, the effects of coupled internal rotations with each other were assumed to be insignificant. The contributions of each hindered rotor were calculated

separately with the corresponding potential energy surface and summed into the total entropies and heat capacities.

The MNDO<sup>17</sup> semiempirical MO calculations were performed using MOPAC6.0<sup>10</sup> package with standard AM1<sup>10</sup> and PM3<sup>9</sup> parameters at UHF level of theory. The keyword 'PRECISE' was used to set up a more strict criteria of  $10^{-8}$  for the self-consistent-field (SCF) convergence in the geometry optimization process. The molecular geometry and vibrational frequencies of the equilibrium states for the three title species were calculated and compared with the values from *ab initio* studies.

## 5.3 Results and Discussion

### 5.3.1 Molecular Geometries

Definition and nomenclature for rotational conformers in this work are illustrated in Figure 5.1. Although the conformational studies of CH<sub>3</sub>CH<sub>2</sub>OO were previously carried out at about the same or higher level,<sup>68, 102</sup> we still list the all optimized molecular geometries calculated in this work at the UHF/6-31G\* level for the purpose of comparison.

The calculations by Knyazev *et al.* for CH<sub>3</sub>CHClOO<sup>90</sup> are actually at the same level as this work, but the rotational transition states locating method is slightly different here. The rotational transition states calculated by Knyazev *et al.* are saddle points on potential energy surfaces (PES's) with all geometric parameters fully optimized.<sup>90</sup> The geometries of the eclipsed structures defined in this work are optimized with one specific dihedral angle fixed at 0°, (i.e. CCOO = 0° for bCis<sub>C</sub>, HCOO = 0° for bCis<sub>H</sub> and ClCOOH = 0° for bCis<sub>Cl</sub>), and all other parameters relaxed. The transition state (4)<sup>90</sup> in the work of

Knyazev *et al.* is analogous to bCis<sub>C</sub> here and has the CCOO dihedral angle equal to  $-14^\circ$ , while it is manually fixed at  $0^\circ$  in bCis<sub>C</sub>. It is valuable to show the difference between these two approaches, since the approach used here has the advantage of less calculation time, and thus is widely used to study the rotational barriers,<sup>104</sup> and the one used by Knyazev *et al.* is theoretically more correct in finding the rotational transition states.

The optimized geometries for rotational conformers of CH<sub>3</sub>CH<sub>2</sub>OO (**a**), CH<sub>3</sub>CHClOO (**b**) and CH<sub>3</sub>CCl<sub>2</sub>OO (**c**) are listed in Table 5.1, Table 5.2 and Table 5.3, respectively. Table 5.4 presents the Mulliken charge distribution for the three radicals.

C-C bond and O-O lengths are consistent in the equilibrium states (CCOO *trans* conformations) of **a**, **b** and **c**, while the C-O bond length decreases consistently from 1.42490 Å in **a**, 1.40095 Å in **b** and 1.39605 Å in **c**. Another interesting feature is the comparison of C-O and O-O bond lengths in the  $\alpha$ -chlorinated ethyl peroxy radicals with those in the corresponding hydroperoxides calculated at the RHF/6-31G\* level of theory<sup>38</sup> (see Figure 5.2). The O-O bond lengths in the ROO radical are shorter than in ROOH by  $-0.092$  Å for R=C<sub>2</sub>H<sub>5</sub>,  $-0.08$  Å for R = CH<sub>3</sub>CHCl, and  $-0.075$  Å for R = CH<sub>3</sub>CCl<sub>2</sub>. The C-O bond lengths in ROO radical are longer than those in ROOH molecules by 0.019 Å for R=C<sub>2</sub>H<sub>5</sub>, 0.027 Å for R=1-Cl-C<sub>2</sub>H<sub>4</sub>, 0.019 Å for R=1,1-di-Cl-C<sub>2</sub>H<sub>3</sub>.

### 5.3.2 Vibrational Frequencies

Harmonic vibrational frequencies are calculated for all rotational conformers and the unscaled frequencies are listed in Table 5.5. The presence of one imaginary frequency is an index for location of the transition-state. Two frequencies of torsion motions about C-C



and C-O bond are assigned for each conformer. For each rotational transition-state, one specific torsion frequency is imaginary. For instance, the frequency for the torsion motion about C-C bond is  $252.2\text{ cm}^{-1}$  in aCis<sub>H</sub>, and the imaginary frequency,  $-101.6\text{ cm}^{-1}$  presents the torsion motion about the C-O bond.

### 5.3.3 Rotational Barriers

The calculated energy, ZPVE (unscaled) and the energy difference compared to the equilibrium state for rotational barriers of each conformer are given in Table 5.6. Spin contamination are determined to be not important as the unrestricted HF procedure is applied for each conformers, as the theoretical  $S^2$  values given in Table 5.6. The following discussions are based on the values of barriers calculated at the MP2/6-31G\*\*//HF/6-31G\* level with the corrections of scaled ZPVE (x0.9) if not otherwise noted.

The rotational barriers about the C-C bond for **a** and **b** are adopted from the work by Quelch *et al.*<sup>102</sup> and Knyazev *et al.*,<sup>90</sup> respectively, and that for **c** is calculated in this work. The PES's for the methyl rotors in **a**, **b**, and **c** are periodic triple wells, which are illustrated in Figure 5.3. The barrier of methyl group rotation increases from 2.7 kca/mol<sup>102</sup> in **a** to 3.89 kcal/mol<sup>90</sup> in **b** and 4.68 kcal/mol in **c**, reflecting the increase of electronic repulsion with the increase of chlorine substitution on the  $\alpha$  carbon.

The PES's of internal rotations about the C-O bond are more complex. The PES of the rotation about the C-O bond for **a** is a triple well with one higher barrier and two lower barriers, see Figure 5.4. The most stable structure for **a** is aTrans, a 0.10 kcal/mol lower potential energy than aGauch at HF/6-31G\*//6-31G\*, while the total energies

calculated at the MP2/6-31G\*\* level indicate that aTrans is 0.42 kcal/mol higher than aGauch. The maximum rotational barrier about the C-O bond in **a** occurs at aCIS<sub>C</sub> which is 1.54 kcal/mol higher than aCis<sub>H</sub>. The PES constructed from the values of rotational barriers by Quelch *et al.*<sup>102</sup> at DZP/CISD level of theory is also illustrated in Table 5.6 and Figure 5.4 for comparison.

For **b**, the PES of the CCOO dihedral angle from 60° to 120° is rather flat because the relative energies of bG<sub>C-H</sub> and bCis<sub>H</sub> are similar, see Figure 5.5. The maximum rotational barrier about the C-O bond in **b** occurs at bCis<sub>Cl</sub> which is 1.51 kcal/mol higher than bCis<sub>C</sub>. The relative energies for the rotational conformers of CH<sub>3</sub>CHClOO calculated by Knyazev *et al.*<sup>90</sup> are listed in Table 5.6 for comparison with the barriers calculated in this work. The values are almost identical to each other at the MP2/6-31G\*\* level of theory although the slightly different approaches are used to search the saddle points on PES (see 5.3.1).

The PES for rotation about the C-O bond in **c** is a triple well with one lower barrier and two higher barriers, see Figure 5.6. The barrier for the rotation across the overlap of O8 and Cl at C2 (ClCCO=0°) from the equilibrium state (CCOO=180°) in **c** is lower than that in **b** by about 0.9 kcal/mol.

The PES of rotation about the C-O bond for the  $\alpha$ -chlorinated ethyl hydroperoxides corresponding to **a**, **b** and **c** (CH<sub>3</sub>CH<sub>2</sub>OOH, CH<sub>3</sub>CHClOOH, CH<sub>3</sub>CCl<sub>2</sub>OOH, respectively) calculated at the MP2/6-31G\*\*//RHF/6-31G\* level<sup>38</sup> are also illustrated in Figure 5.4, 5.5 and 5.6. These three figures illustrate the difference in rotational barriers about the C-O bond, with and without a hydrogen on the peroxy group.

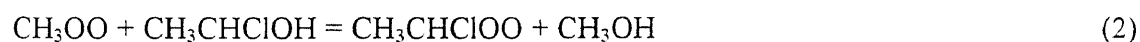
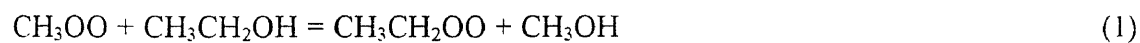
The results indicate that there is significant decrease in the CCOO rotational barriers from ROOH to ROO $\cdot$ , with the difference as large as 8 kcal/mol, see bCisCl in Figure 5.5. The shorter C-O bond length in ROOH vs ROO $\cdot$  (see Figure 5.2) partly explains the reduced barrier when ROOH loses its hydrogen.

The values of Fourier expansion components (see Chapter 1),  $V_i$  and  $V'_i$  in (E1) and  $a_i$  and  $b_i$  in (E2) are obtained by curve fitting for each PES, see Table 5.7.

### 5.3.4 Heat of Formation

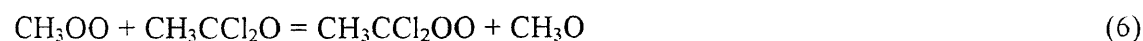
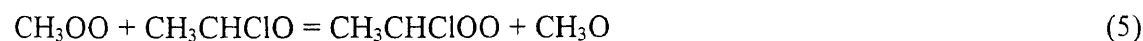
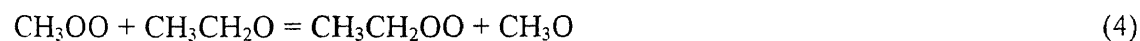
Two sets of isodesmic reactions may be used to study the enthalpies of reactions. The first option is the reaction with R-OH (R = C<sub>2</sub>H<sub>5</sub> for **a**, R = CH<sub>3</sub>CHCl for **b** and R = CH<sub>3</sub>CCl<sub>2</sub> for **c**) and CH<sub>3</sub>OO as the reactants and ROO and CH<sub>3</sub>OH as products, respectively.

#### Scheme I



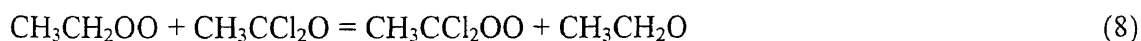
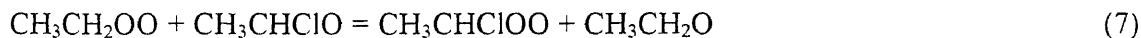
A second alternative is RO and CH<sub>3</sub>OO as reactants and the desired ROOH and CH<sub>3</sub>O as products:

#### Scheme II



Two other reactions can be used to validate the consistency of the above theoretical enthalpies using experimental data of  $\Delta H_f^\circ_{298}(\text{CH}_3\text{CH}_2\text{OO})$ :<sup>67</sup>

### Scheme III



The total energies, ZPVE (unscaled) along with experimental data or evaluated values of  $\Delta H_f^\circ_{298}$  for the species in all isodesmic reactions are given in Table 5.8. The reaction energies and the calculated  $\Delta H_f^\circ_{298}$  for  $\text{CH}_3\text{CH}_2\text{OO}$  (**a**),  $\text{CH}_3\text{CHClOO}$  (**b**) and  $\text{CH}_3\text{CCl}_2\text{OO}$  (**c**) are listed in Table 5.9.

Using reaction(1)  $\Delta H_f^\circ_{298}(\text{CH}_3\text{CH}_2\text{OO})$  is calculated as -5.37 kcal/mol which is in excellent agreement with the experimental value, -5.19 kcal/mol.<sup>67</sup> The value of  $\Delta H_f^\circ_{298}(\text{CH}_3\text{CH}_2\text{OO})$  is calculated to be -6.69 kcal/mol using reaction(4) and  $\Delta H_f^\circ_{298}(\text{CH}_3\text{CH}_2\text{O}) = -4$  kcal/mol.<sup>32</sup> If  $\Delta H_f^\circ_{298}(\text{CH}_3\text{CH}_2\text{O})$  is adjusted to be **-2.5** kcal/mol, the experimental value of  $\Delta H_f^\circ_{298}(\text{CH}_3\text{CH}_2\text{OO})$ , -5.19 kcal/mol can be fitted using reaction(4).

All three schemes cannot predict  $\Delta H_f^\circ_{298}(\text{CH}_3\text{CHClOO})$  to be in good agreement with experimental value, -13.07 kcal/mol.  $\Delta H_f^\circ_{298}(\text{CH}_3\text{CHClOO})$  is calculated as -14.01 kcal/mol by reaction(2); -10.87 kcal/mol by reaction(5); and -9.27 kcal/mol by reaction(7). The deviation of the calculated  $\Delta H_f^\circ_{298}(\text{CH}_3\text{CHClOO})$  from experimental data result from the uncertainty of  $\Delta H_f^\circ_{298}$  of  $\text{CH}_3\text{CHClOH}$  and  $\text{CH}_3\text{CHClO}$ . If the measured value,

$\Delta H_f^\circ_{298}(\text{CH}_3\text{CHClOO}) = -13.07 \text{ kcal/mol}$  <sup>90</sup> is used to validate  $\Delta H_f^\circ_{298}(\text{CH}_3\text{CHClOH})$  using reaction(1), and  $\Delta H_f^\circ_{298}(\text{CH}_3\text{CHClO})$  using reaction(4), the  $\Delta H_f^\circ_{298}(\text{CH}_3\text{CHClOH})$  appears as **-63.25 kcal/mol**,  $\Delta H_f^\circ_{298}(\text{CH}_3\text{CHClO})$  appears as **-14.5 kcal/mol**.

No comparable data have been reported for  $\Delta H_f^\circ_{298}(\text{CH}_3\text{CCl}_2\text{OO})$ . Since the reaction(8) is the best choices as an isodesmic reaction, the  $\Delta H_f^\circ_{298}(\text{CH}_3\text{CCl}_2\text{OO})$  calculated using Scheme III are recommended, as **-16.16 kcal/mol**.

### 5.3.5 Thermodynamic Properties

The thermodynamic properties are listed in Table 5.10. The contribution of entropies and heat capacities from internal hindered rotors are calculated by directly diagonalization of the Hamiltonia Matrix. The difference between using this technique and Pitzer and Gwinn's approximation and Tables are illustrated in Table 5.11.

### 5.3.6 Comparison of MNDO/AM1 and PM3 Molecular Geometries and Vibrational Frequencies

A comparison of bond length between *ab initio* and semi-empirical MO calculations is listed in Table 5.12. The results indicate that the O-O bond length is highly underestimated by AM1, an average 0.15 Å shorter, and by PM3 only 0.05 Å shorter, than predicted at UHF/6-31G\*. The C-O bond lengths in the alkyl peroxy are also not correctly predicted by both the AM1 and PM3 Hamiltonians. The PM3 method gives a more consistent C-O(O.) bond length with an average deviation of +0.05 Å, whereas AM1 on the average gives a C-O(O.) bond length too large by +0.1 Å. The comparison of bond angles and dihedral angles are given in Table 5.13 and Table 5.14.

Comparison of vibrational frequencies are illustrated in Figure 5.7, 5.8 and 5.9 which do not include two torsion frequencies. The contributions of vibrational frequencies to entropies and heat capacities ( $S_{\text{vib}}$  at 298K and  $C_{\text{p,vib}}$  at 500K) are also compared in the three figures. The results clearly indicate that when sophisticated *ab initio* calculations are not available, the semi-empirical MNDO/PM3 Hamiltonian is a fairly good alternative to calculate vibrational frequencies and thus  $S_{\text{vib}}$  and  $C_{\text{p,vib}}$  when the torsion frequencies are excluded.

#### 5.4 Summary

Molecular geometries of equilibrium states and rotational transition states for  $\text{CH}_3\text{CH}_2\text{OO}$ ,  $\text{CH}_3\text{CHClOO}$  and  $\text{CH}_3\text{CCl}_2\text{OO}$  were calculated at UHF/6-31G\*. The potential barriers of internal rotations were calculated at MP2/6-31G\*\*//HF/6-31G\* and the potential constants for Fourier expansions were derived. Standard entropies ( $S^\circ_{298}$ ) and heat capacities ( $C_{\text{p}}(T)$ 's,  $300 \leq T/\text{K} \leq 5000$ ) were calculated using the RRHO model which was incorporated with the information obtained in the *ab initio* studies, and a new technique for calculating the energy levels of hindered internal rotations.

The enthalpies of formation for  $\text{CH}_3\text{CH}_2\text{OO}$ ,  $\text{CH}_3\text{CHClOO}$  and  $\text{CH}_3\text{CCl}_2\text{OO}$  were calculated by means of isodesmic reactions. The  $\Delta H_f^\circ_{298}$  of  $\text{CH}_3\text{CH}_2\text{OO}$  calculated by the method of isodesmic reactions as **-5.37** kcal/mol, is in very good agreement with experimental values. If the  $\Delta H_f^\circ_{298}(\text{CH}_3\text{CHClO})$  is adjusted to be **-14.5** kcal/mol, and  $\Delta H_f^\circ_{298}(\text{CH}_3\text{CHClOH})$  is adjusted to be **-63.25** kcal/mol, the experimental value of  $\Delta H_f^\circ_{298}(\text{CH}_3\text{CHClOO})$ , 13.07 kcal/mol, can be reproduced using isodesmic reactions.

$\Delta H_f^\circ(\text{CH}_3\text{CCl}_2\text{OO})$  is calculated to be **-16.16** kcal/mol with  $\Delta H_f^\circ(\text{CH}_3\text{CCl}_2\text{O})$  equal to -19.9 kcal/mol. The major uncertainty in the value of  $\Delta H_f^\circ(\text{CH}_3\text{CCl}_2\text{OO})$  arises from the uncertainty in  $\Delta H_f^\circ(\text{CH}_3\text{CCl}_2\text{O})$ . The accuracy of  $\Delta H_f^\circ(\text{CH}_3\text{CCl}_2\text{OO})$  can be further improved when a more reliable value of  $\Delta H_f^\circ(\text{CH}_3\text{CCl}_2\text{O})$  is obtained.

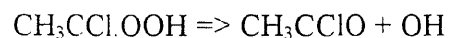
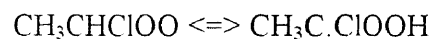
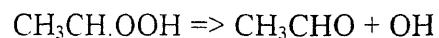
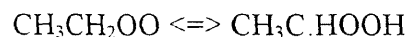
Semiempirical MO calculations with MNDO/AM1 and PM3 were also compared and evaluated with *ab initio* HF-SCF calculation results. The comparisons show that neither AM1 nor PM3 can predict correct molecular geometries for alkyl peroxy radicals, while the vibrational frequencies calculated by MNDO/PM3 were generally within an acceptable range.

## CHAPTER 6

### ***AB INITIO* STUDY OF HYDROPEROXYL-1-ETHYL AND 1-CHLORO-1-ETHYL RADICALS, CH<sub>3</sub>C.HOOH AND CH<sub>3</sub>C.CIOOH: CONFORMATIONAL ANALYSIS, INTERNAL ROTATION BARRIERS, VIBRATIONAL FREQUENCIES, AND THERMODYNAMIC PROPERTIES**

#### 6.1 Introduction

The ethyl peroxy radicals are formed from reactions of alkyl radicals with molecular oxygen (see Chapter 1). The ethyl peroxy radicals can isomerize to corresponding hydroperxyl ( $\alpha$ -chlorinated) 1-ethyl radicals which then rapidly undergo an exothermic beta-scission to the corresponding alkanals plus OH radical.



This study is performed primarily to determine the thermodynamic functions, ( $\Delta H_f^\circ_{298}$ ,  $S^\circ_{298}$  and  $C_p(T)$ ,  $300 \leq T/K \leq 5000$ ) for the hydroperoxyl 1-ethyl and 1-chloro-1-ethyl radicals, and to estimate the bond strength of the  $\alpha$ C-H bond of  $\text{CH}_3\text{CH}_2\text{OOH}$  and  $\text{CH}_3\text{CHClOOH}$ .



## 6.2 Method

The calculation procedure is fully described in Chapter 5, section 5.2.

## 6.3 Results and Discussion

### 6.3.1 Molecular Geometries

Definition and nomenclature for all rotational conformers in this work are illustrated in Figure 6.1. The optimized geometries for the rotational conformers of  $\text{CH}_3\text{C.HOOH}$  (**a**) and  $\text{CH}_3\text{C.CIOOH}$  (**b**) are listed in Tables 6.1 and 6.2, respectively. The Mulliken charge distribution in the equilibrium state (aSTS and bSTS) of the two radical species are given in Table 6.3.

The radical centers are non-planar for both radicals, with the out-of-plane (OOP) angle ( $\gamma$ )  $41.3^\circ$  for aSTS and  $45.1^\circ$  for bSTS. (see Figure 6.2 for definition of OOP angle,  $\gamma$ ) The OOP angle at the radical center varies with each rotational conformer since the relaxed model is used to study the rotational barriers, see Table 6.4. The OOP angle for **a** varies from  $41.3^\circ$  (aSTS) to  $28.8^\circ$  (aSE<sub>C</sub>S), and for **b**, from  $45.1^\circ$  (bSTS) to  $37.3^\circ$  (bSE<sub>C</sub>S).

The COOH *skew* conformations are the most stable in both species with the CCOO dihedral angle about  $100^\circ$  ( $-254^\circ=106^\circ$  in aSTS and  $-256^\circ=104^\circ$  in bSTS). This is consistent with the higher delocalization of lone pair electrons in the orthogonal conformation of X-O-O-Y relative to coplanar conformations (*cis* and *trans*) (see section 4.2.1 for further discussion).

When the  $\alpha$ -hydrogen in  $\text{CH}_3\text{C.HOOH}$  is substituted by chlorine (**b**,  $\text{CH}_3\text{C.ClOOH}$ ), the C-C bond length remains nearly constant, the C-O bond length decreases from 1.3695 Å (aSTS) to 1.3481 Å (bSTS), and O-O bond lengths increase slightly from 1.3895 Å to 1.3933 Å.

Comparisons of bond lengths are also made between the radicals and the corresponding saturated hydroperoxides,  $\text{CH}_3\text{CH}_2\text{OOH}$  and  $\text{CH}_3\text{CHClOOH}$ . Molecular geometries of  $\text{CH}_3\text{CH}_2\text{OOH}$  and  $\text{CH}_3\text{CHClOOH}$  are calculated at the MP2/6-31G\*\*//RHF/6-31G\* level of theory, see Chapter 4. These comparisons show that when the  $\alpha$ -hydrogen is lost from the saturated (chlorinated) alkyl hydroperoxides, the C-C bond lengths slightly decrease (-0.0229 Å in **a**, -0.0159 Å in **b**). The C-O bond lengths also decrease (-0.0365 Å in **a**, and -0.0258 Å in **b**). The O-O bond lengths are unchanged, see Figure 6.3.

### 6.3.2 Vibrational Frequencies

Harmonic vibrational frequencies are calculated for all rotational conformers and the unscaled frequencies are listed in Table 6.5 and Table 6.6. Three frequencies (including the imaginary ones) corresponding to torsion motions about the C-C, C-O and O-O bonds are assigned for each conformer. One specific torsion frequency is imaginary for each rotational transition-state, e.g. the frequency for the torsion motion about C-C bond as  $136.7\text{ cm}^{-1}$  is imaginary in aE<sub>H</sub>TS. All vibrational frequencies and Zero-point vibrational energies (ZPVE) are scaled by 0.9.

### 6.3.3 Rotational Barriers

Calculated total energy, ZPVE (unscaled) and rotational barrier for each conformer are given in Table 6.7. The following discussions are based on the values of barriers calculated at MP2/6-31G\*\*//UHF/6-31G\* with the corrections of scaled ZPVE (x0.9) unless further noted.

#### 6.3.3.1 Rotation about the C-C Bonds

We first perform scan studies of potential energy surfaces (PES's) of the rotation about the C-C bond. The rotational PES's as a function of  $\text{H}_3\text{C}_1\text{C}_2\text{O}_7$  dihedral angle are calculated at UHF/6-31G\* level of theory using fixed geometries (rigid model) varying the HCCO dihedral angle at  $10^\circ$  intervals, see Figure 6.4 for **a** and Figure 6.5 for **b**. These two PES's calculated using rigid geometries illustrate a triple well for the methyl group rotation in both **a** and **b**. Corrections of ZPVE are not included in the scan calculations.

Rotational barriers about the C-C bonds are also calculated using a relaxed model, yielding 1.83 kcal/mol for **a** (see Figure 6.4) and 2.02 kcal/mol for **b** (see Figure 6.5). These calculations include the corrections of ZPVE. The barriers calculated using relaxed geometries are close to those using rigid geometries.

Figure 6.4 and Figure 6.5 also illustrate the rotational barriers about the C-C bond of the stable molecules,  $\text{CH}_3\text{CH}_2\text{OOH}$  and  $\text{CH}_3\text{CHClOOH}$ , respectively. Comparison shows that when one  $\alpha$ -hydrogen is removed from  $\text{CH}_3\text{CH}_2\text{OOH}$ , the rotational barrier about the C-C bond decreases from 3.3 kcal/mol to 1.8 kcal/mol. The rotational barrier

about the C-C bond decreases from 5.3 kcal/mol in  $\text{CH}_3\text{CHClOOH}$  to 2.0 kcal/mol of  $\text{CH}_3\text{C}(\text{Cl})\text{OOH}$ .

### 6.3.3.2 Rotation about the C-O Bonds

The PES's for rotation about the C-O bonds are determined to be a double well with two different barriers, see Figures 6.6 and 6.7 for **a** and **b**, respectively. The conformer of dihedral angle  $\text{CCOO} = 0^\circ$  ( $\text{aSE}_{\text{C}}\text{S}$ ) for **a** has a higher barrier (2.67 kcal/mol) than that of  $\text{HCOO} = 0^\circ$  ( $\text{aSE}_{\text{H}}\text{S}$ , 0.5 kcal/mol). The high barrier for **b** occurs at the dihedral angle  $\text{ClCOO} = 0^\circ$  ( $\text{aSE}_{\text{Cl}}\text{S}$ ), 6.22 kcal/mol, while  $\text{CCOO} = 0^\circ$  has a barrier 3.52 kcal/mol.

### 6.3.3.3 Rotation about the O-O Bonds

The  $\text{COOH}$  *skew* conformation is the most stable form for both radicals, the *cis* conformation has a higher barrier and the *trans* conformation has a much lower barrier. It is significant that the barrier of the  $\text{COOH}$  *cis* conformation for **a** ( $\text{aSTC}$ ), 5.23 kcal/mol, is higher than that for **b** ( $\text{bSTC}$ ), 4.21 kcal/mol, although **b** has a larger  $\alpha$ -substituent, i.e. the Cl atom rather than H in **a**, see Figures 6.8 and 6.9.

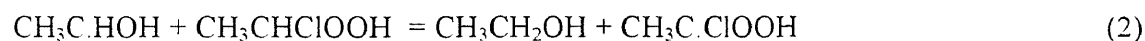
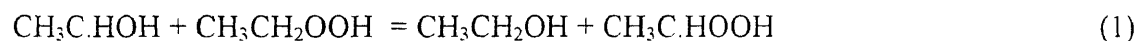
The loss of an  $\alpha$ -H in saturated alkyl hydroperoxides also affects the rotational barriers about the O-O bond. Comparison of the rotational barriers about the O-O bond between **a** and  $\text{CH}_3\text{CH}_2\text{OOH}$ , **b** and  $\text{CH}_3\text{CHClOOH}$ , are illustrated in Figure 6.8 and 6.9, respectively. The maximum rotational barrier about the O-O bond (*cis*) decreases from 6.67 kcal/mol in  $\text{CH}_3\text{CH}_2\text{OOH}$  to 5.23 kcal/mol in **a** when  $\text{CH}_3\text{CH}_2\text{OOH}$  loses its  $\alpha$ -H.

The decrease of the rotational barrier about the O-O bond from  $\text{CH}_3\text{CHClOOH}$  (8.43 kcal/mol) to **b** (4.21 kcal/mol) is more significant.

Values of Fourier expansion components (see Chapter 1),  $V_i$  and  $V'_i$  in (E1) and  $a_i$  and  $b_i$  in (E2) are obtained by curve fitting for each PES, see Table 6.8.

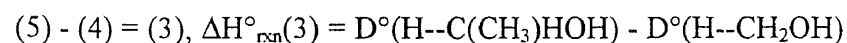
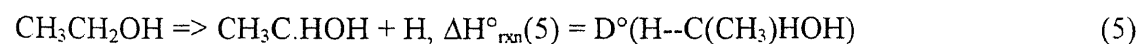
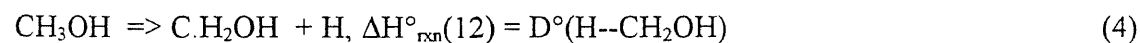
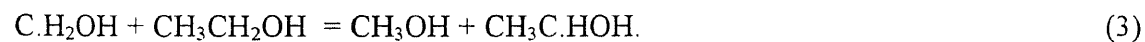
### 6.3.4 Enthalpies of Formation ( $\Delta H_f^\circ_{298}$ )

Two isodesmic reactions are used to study the enthalpies of hydroperoxyl 1-ethyl and 1-chloro-1-ethyl radicals:



#### 6.3.4.1 Determination of $\Delta H_f^\circ_{298}(\text{CH}_3\text{C.HOOH})$

The  $\Delta H_f^\circ_{298}(\text{CH}_3\text{C.HOH})$  was calculated as -14.3 kcal/mol<sup>3</sup> by Melius using the BAC/MP4 approach. We also estimate this data from experimentally measured value of bond energy of  $D^\circ(\text{H--CH}_2\text{OH})$  and the results of *ab initio* studies for the following isodesmic reaction:



Two very different numbers have been reported for the value of  $D^\circ(\text{H--CH}_2\text{OH})$ : 93.9 kcal/mol by Benson and Golden,<sup>107</sup> and 98.0 kcal/mol by Seetula and Gutman.<sup>108</sup> The latter number is adopted in the following calculations.

The difference of  $D^\circ(\text{H--C}(\text{CH}_3)\text{HOOH}) - D^\circ(\text{H--CH}_2\text{OH})$  is thus determined to be -0.8 kcal/mol using isodesmic reaction (3) and the results of *ab initio* calculations by Pardo *et al.*<sup>109</sup> at the MP2/6-31G\*\*//UHF/6-31G level of theory.  $D^\circ(\text{H--C}(\text{CH}_3)\text{HOH})$  is thus determined to be 96.3 kcal/mol using  $D^\circ(\text{H--CH}_2\text{OH}) = 98.0$  kcal/mol. Using  $D^\circ(\text{H--C}(\text{CH}_3)\text{HOH}) = 96.2$  kcal/mol<sup>55</sup> and  $\Delta H_f^\circ{}_{298}(\text{CH}_3\text{CH}_2\text{OH}) = -56.12$  kcal/mol,<sup>55</sup>  $\Delta H_f^\circ{}_{298}(\text{CH}_3\text{C.HOH})$  is determined to be -11.9 kcal/mol, which is 2.4 kcal/mol different from the value, -14.3 calculated by Melius.<sup>69</sup>

#### 6.3.4.2 Determination of $\Delta H_f^\circ{}_{298}(\text{CH}_3\text{C.HOOH})$ and $\Delta H_f^\circ{}_{298}(\text{CH}_3\text{C.ClOOH})$

The total energies, ZPVE (unscaled) and the experimental derived or evaluated values of  $\Delta H_f^\circ{}_{298}$  for the species in all isodesmic reactions are given in Table 6.9. The  $\Delta H_f^\circ{}_{298}$  for **a** and **b** are determined as 5.0 kcal/mol and -1.0 kcal/mol, as given in Table 6.10, using isodesmic reactions (1) and (2) and  $\Delta H_f^\circ{}_{298}(\text{CH}_3\text{C.HOH}) = -11.9$  kcal/mol.

#### 6.3.4.3 Difference of Bond Dissociation Energy for the $\alpha\text{C-H}$ Bonds

Reactions (1) and (2) also provide a way to calculate the difference of the  $\alpha\text{C-H}$  bond dissociation energy.

$$\Delta H^\circ_{\text{rxn}}(1) = D^\circ(\text{H--C}(\text{CH}_3)\text{HOOH}) - D^\circ(\text{H--C}(\text{CH}_3)\text{HOH})$$

$$\Delta H^\circ_{\text{rxn}}(2) = D^\circ(\text{H--C}(\text{CH}_3)\text{ClOOH}) - D^\circ(\text{H--C}(\text{CH}_3)\text{HOH})$$

The values of  $D^\circ(\text{H--C}(\text{CH}_3)\text{HOOH}) - D^\circ(\text{H--C}(\text{CH}_3)\text{HOH})$  and  $D^\circ(\text{H--C}(\text{CH}_3)\text{ClOOH}) - D^\circ(\text{H--C}(\text{CH}_3)\text{HOH})$  are determined to be 2.08 kcal/mol and 4.14 kcal/mol.  $D^\circ(\text{H--C}(\text{CH}_3)\text{HOOH})$  and  $D^\circ(\text{H--C}(\text{CH}_3)\text{ClOOH})$  are then determined to be 98.4 kcal/mol and 100.4 kcal/mol using 96.3 kcal/mol as  $D^\circ(\text{H--C}(\text{CH}_3)\text{HOH})$ . These results indicate that the relative order of the  $\alpha$  C-H bond strength is:



The degree of stabilization by hybridization of the unpaired electron at  $\alpha$ -carbon with the connected oxygen atom is lowest in  $\text{CH}_3\text{C}\cdot\text{ClOOH}$ , intermediate in  $\text{CH}_3\text{C}\cdot\text{HOOH}$  and in  $\text{C}\cdot\text{H}_2\text{OH}$ , and highest in  $\text{CH}_3\text{C}\cdot\text{HOH}$ .

The difference of  $D^\circ(\text{H--C}(\text{CH}_3)\text{ClOOH}) - D^\circ(\text{H--C}(\text{CH}_3)\text{ClOH})$  can also be calculated:



$$\Delta H^\circ_{\text{rxn}}(6) = D^\circ(\text{H--C}(\text{CH}_3)\text{ClOOH}) - D^\circ(\text{H--C}(\text{CH}_3)\text{ClOH})$$

$D^\circ(\text{H--C}(\text{CH}_3)\text{ClOOH}) - D^\circ(\text{H--C}(\text{CH}_3)\text{ClOH})$  is calculated to be 0.53 kcal/mol, as the data given in Table 6.10, indicating that Cl atom stabilizes C-H bond on the  $\alpha$ -carbon by about 0.5 kcal/mol.

### 6.3.5 Thermodynamic Properties

The radical centers in **a** and **b** are considered more flexible than saturated carbons which have more rigid structure of tetrahedral bonding. The radical centers can have umbrella bending or inversion oscillation motions. The calculations of entropy and heat capacities do not consider the effects of hindered internal rotations coupled with inversion (or umbrella bending) at the radical center. Fortunately the out-of-plane (OOP) angle at radical center of each rotational conformer only varies within a small range, ca.  $\pm 6.3^\circ$  for **a** and  $\pm 3.7^\circ$  for **b**, see Table 6.4. In this case, the coupling effects of umbrella bending to internal rotations are considered to be insignificant. Contributions to  $S^\circ_{298}$  and  $C_p(T)$  ( $300 \leq T/K \leq 5000$ ) from each internal rotation of **a** and **b** are calculated separately and summed to total entropies and heat capacities.

The thermodynamic properties are listed in Table 6.11. The contribution of entropies and heat capacities from internal hindered rotors are calculated by directly diagonalization of the Hamiltonian Matrix. The difference of using this technique versus Pitzer and Gwinn's method is illustrated in Table 6.12.

### 6.3.5 Comparison of MNDO/AM1 and PM3 Molecular Geometries and Vibrational Frequencies

Comparisons of bond length between *ab initio* and semiempirical MO calculations, AM1 and PM3 are given in Table 6.13. Results indicate that the O-O bond length is underestimated by AM1 on the average by 0.09 Å, and is highly overestimated by PM3 on the average by 0.63 Å, in comparison with geometries optimized at the UHF/6-31G\* level. It is significant that PM3 gives 1.93 Å as the O-O bond length of the radicals such as



hydroperxyl 1-ethyl. The C-O bond length predicted by PM3 is 1.21 Å which is too short, more like a C=O double bond. Comparison of bond angles and dihedral angles are given in Table 6.14. PM3 again fails to predict the COOH *skew* conformation as the most stable with the dihedral angle COOH close to 180° in the equilibrium state. The use of PM3 to perform the general studies for such hydroperxyl 1-ethyl radical species therefore seems to be unacceptable. The geometries calculated by AM1 are generally more consistent with *ab initio* results at the UHF/6-31G\* level of theory.

The comparison of vibrational frequencies calculated by the AM1 and PM3 methods with those by the UHF/6-31G\* method are illustrated in Figure 6.10 and Figure 6.11 which have three torsion frequencies removed. The frequencies predicted by AM1 are not consistent with scaled *ab initio* frequencies for the entire spectra, especially in the region below 1400 cm<sup>-1</sup> where values of entropy and heat capacity are most sensitive. The discrepancy between the PM3 and UHF/6-31G\* frequencies is even larger, because PM3 tends to treat the C.-O bonds as C=O along with the long O-O bond (i.e. with a leaving OH group) for both hydroperoxyl 1-ethyl radicals. The contributions of vibrational frequencies to entropies and heat capacities ( $S_{\text{vib}}$  at 298K and  $C_{\text{p,vib}}$  at 500K) are also compared and given in Figure 6.10 and 6.11. AM1 tends to overestimate frequencies below 1400 cm<sup>-1</sup> and underestimates  $S_{\text{vib}}$  and  $C_{\text{p,vib}}$ . PM3 highly underestimates the frequencies in the region below 1400 cm<sup>-1</sup> and highly overestimate  $S_{\text{vib}}$  and  $C_{\text{p,vib}}$ .

## 6.4 Summary

Molecular geometries of the equilibrium states and rotational transition states for  $\text{CH}_3\text{C.HOOH}$  and  $\text{CH}_3\text{C.CIOOH}$  are calculated at the UHF/6-31G\* level. Potential barriers to internal rotations are calculated at the MP2/6-31G\*\*//UHF/6-31G\* level and potential constants for Fourier expansions are derived. Standard entropies ( $S^\circ_{298}$ ) and heat capacities ( $C_p(T)$ 's,  $300 \leq T/K \leq 5000$ ) are calculated using the RRHO model and the information obtained in the *ab initio* studies.

The enthalpies of formation for these two free radicals are calculated using isodesmic reactions.  $\Delta H_f^\circ_{298}$  of  $\text{CH}_3\text{C.HOOH}$  and  $\text{CH}_3\text{C.CIOOH}$  are determined as **5.86** kcal/mol and **-0.12** kcal/mol, respectively. The  $\Delta H_f^\circ_{298}$  of  $\text{CH}_3\text{C.HOH}$  is also calculated as **-11.0** kcal/mol. The bond dissociation energies,  $D^\circ(\text{H--C}(\text{CH}_3)\text{HOH})$ ,  $D^\circ(\text{H--C}(\text{CH}_3)\text{HOOH})$ ,  $D^\circ(\text{H--C}(\text{CH}_3)\text{ClOH})$  and  $D^\circ(\text{H--C}(\text{CH}_3)\text{ClOOH})$  are calculated as 96.3 kcal/mol, 98.4 kcal/mol, 99.9 kcal/mol, and 100.4 kcal/mol, respectively, using the experimental data, 98.0 kcal/mol for  $D^\circ(\text{H--CH}_2\text{OH})$ ,<sup>108</sup> and the isodesmic reactions.

Semiempirical MO calculations with MNDO/AM1 and PM3 are also compared and evaluated with *ab initio* HF-SCF calculation results. The comparisons show that PM3 does not predict correct molecular geometries for both hydroperoxyl 1-ethyl radical species, with severely short C-O bonds and long O-O bonds. AM1 gives more consistent results for molecular geometries and vibrational frequencies than does PM3. However, with AM1 the O-O bond lengths, and  $S_{\text{vib}}$  and  $C_{p,\text{vib}}$  are underestimated.

## CHAPTER 7

### CHLOROFORM PYROLYSIS AND OXIDATION: EFFECTS OF ADDED O<sub>2</sub>

#### 7.1 Introduction

Hazardous waste incineration involving chlorine compounds merits attention because the behavior of chlorine is unique among the halogenated compounds. Organic chlorine compounds serve as a source of chlorine atoms, which readily abstract H atoms from other organic hydrocarbons accelerating the onset reactions. Chlorine, as HCl, can inhibit combustion through reactions like  $\text{OH} + \text{HCl} \Rightarrow \text{H}_2\text{O} + \text{Cl}$ , which depletes OH needed for CO burnout<sup>1</sup>.

Several investigations into the thermal decomposition of chloroform have been conducted. Semeluk and Bernstein<sup>2</sup> investigated the decomposition kinetics of chloroform where they estimated a 72 kcal/mol upper limit for the activation energy of a proposed initiation reaction:  $\text{CHCl}_3 \Rightarrow \text{CHCl}_2 + \text{Cl}$ .

Kung and Bissinger<sup>3</sup> studied the pyrolysis of chloroform in cyclohexene. They reported on the formation of dichloronorane (insertion of dichlorocarbene into the double bond to form a 1,1 dichlorocyclopropane ring) in addition to toluene, which is a known decomposition product from dichloronorane. This suggested that  $\text{CCl}_2$ , dichlorocarbene, was the major intermediate from unimolecular dissociation of chloroform.

Chloroform pyrolysis reaction and an elementary mechanism were previously studied extensively by Won in this NJIT Kinetics Research Group. His mechanism used a

value of  $\Delta H_f^\circ_{298}({}^1\text{CCl}_2)$  of 39 kcal/mol. We have since learn that the accurate value of  $\Delta H_f^\circ_{298}({}^1\text{CCl}_2)$  is 53 kcal/mol. It is critically important to note that the use of an incorrect  $\Delta H_f^\circ_{298}({}^1\text{CCl}_2)$  value off by more than 13 kcal/mol resulted in a mechanism that was not a thermodynamically correct or accurate reaction set. All of the chemical activated and other elementary reactions involving  ${}^1\text{CCl}_2$  would have not been properly accounted to this 13 kcal/mol.

A revised mechanism for both pyrolysis and oxidation is therefore required. This new mechanism has each reaction of  ${}^1\text{CCl}_2$  (the key radical in  $\text{CHCl}_3$  reaction system) re-evaluated. The chemical activated reactions for combination, insertion, addition and reaction with  $\text{O}_2$  are of particular importance.

Three studies (Benson and Spokes<sup>4</sup>, Schug *et al.*<sup>5</sup>, Herman, Lee *et al.*<sup>6</sup>) were directed at determining the activation energy and pathway of the initial step in chloroform thermal decomposition. Benson and Spokes favor an Arrhenius A factor of ca.  $5.0\text{E}13$  with an  $E_a$  greater than 56 kcal/mol for HCl elimination of chloroform from a very low pressure pyrolysis study. They also reported that when oxygen was added to reaction system, the products yielded a pair of mass peaks at 63 and 65 amu, possibly due to  $\text{COCl}$  from phosgene. This was an expected product from the reaction of dichlorocarbene with  $\text{O}_2$ ,  $:\text{CCl}_2 + \text{O}_2 \Rightarrow \text{CCl}_2\text{O} + \text{O}$ .

Schug *et al.*<sup>5</sup> measured the appearance of  $\text{C}_2\text{Cl}_4$  by ultraviolet adsorption after a shock tube pulse, reporting a 54.5 kcal/mol activation energy at 1200 K. The photolysis of chloroform by Herman *et al.*<sup>6</sup> examined the pulsed  $\text{CO}_2$  laser (11  $\mu\text{m}$ ) multiple-photon dissociation of deuterated chloroform ( $\text{CDCl}_3$ ) in a molecular beam. The only observed

dissociation pathway was hydrogen chloride (HCl) elimination (>99.1%), with no evidence of simple chloride atom cleavage (<0.9%).

Taylor and Dellinger <sup>7</sup> evaluated the thermal degradation characteristics of the four chloromethanes as pure compounds as a function of feed composition and fuel/air equivalence ratio. Their results indicated chloroform was the most fragile molecule, and methyl chloride was the least fragile under both pyrolytic and oxidative conditions.

The reaction of chloroform diluted in hydrogen and water vapor has been studied in the temperature range 550 - 1200 °C by Chuang and Bozzelli. <sup>8</sup> The major products of chloroform pyrolysis in H<sub>2</sub> at temperatures above 1100 °C were HCl, C(s) and CH<sub>4</sub>. The most stable chlorocarbon products observed were chloromethane and C<sub>2</sub>H<sub>3</sub>Cl for the reaction of chloroform with excess hydrogen. This study also demonstrated that selective formation of HCl can result from thermal reaction of chloroform under an atmosphere of hydrogen.

In the present study, we focus on variations in chloroform decay rates and product distributions in presence and absence of added oxygen, but with no added hydrogen fuel source. Future research will incorporate H<sub>2</sub>O, H<sub>2</sub>, CH<sub>4</sub> and supplemental hydrogen sources, which are most important to obtain quantitative HCl formation as well as application to actual incineration problems. A revised mechanism is developed from analysis of the experimental data and thermochemical principles, for chloroform pyrolysis and oxidation.

## 7.2 Experimental

### 7.2.1 Method

The thermal reaction of  $\text{CHCl}_3$  in both oxidative and pyrolytic reaction environments was studied by Won<sup>9</sup> in a tubular flow reactor at 1 atm pressure. Reactant mole ratios were:  $\text{CHCl}_3$  (1%),  $\text{O}_2$  (0-3 %), Ar bath. Experiments were performed using a tubular flow reactor which has been described in detail in Won's thesis.<sup>9</sup>

Small amounts of  $\text{O}_2$  (0 - 3%) were added to the  $\text{CHCl}_3/\text{Ar}$  flow. A quartz reactor tube, 10.5 mm ID, was housed within a three zone electric tube furnace 46 cm length. Temperature profiles were obtained using a type K thermocouple probe moved coaxially within the reactor under representative flows. The reactor effluent stream was analyzed by an on-line gas chromatograph with flame ionization detector (FID). A catalytic convertor was employed to increase the accuracy of quantitative analysis for CO and  $\text{CO}_2$ . The 5% ruthenium on alumina (30/40 mesh) at 315 °C was used to catalyze CO and  $\text{CO}_2$  reduction with  $\text{H}_2$  (10 ml/min).

Quantitative analysis of HCl was performed for each run; reactor effluent was diverted through a dual bubbler train containing 0.01 M NaOH before being exhausted to a fume hood. The HCl was then calculated based upon titration of the combined bubbler solutions with 0.01 M HCl to the phenolphthalein endpoint. The NaOH solution also collected  $\text{CO}_2$  and the  $\text{CO}_2/\text{FID}$  results were used to correct for this.

### 7.2.2 Result and Discussion

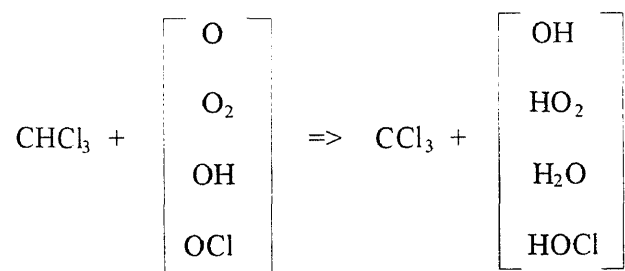
The thermal decomposition of the three reactant ratio sets were studied by Won to determine important chlorocarbon reaction pathways before initiating development of the detailed reaction mechanism.

Study 1:  $\text{CHCl}_3 : \text{Ar} = 1 : 99$

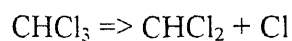
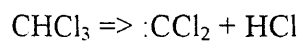
Study 2:  $\text{CHCl}_3 : \text{O}_2 : \text{Ar} = 1 : 1 : 98$

Study 3:  $\text{CHCl}_3 : \text{O}_2 : \text{Ar} = 1 : 3 : 96$

Figure 7.1 compares chloroform decay as a function of temperature in Ar bath gas at 1.0 sec reaction time for each reaction environment.  $\text{O}_2$  has a significant effect on the decomposition of parent  $\text{CHCl}_3$  in this reaction system; higher  $\text{O}_2$  results in faster  $\text{CHCl}_3$  decay. The accelerated decomposition of  $\text{CHCl}_3$ , when  $\text{O}_2$  is present results from the bimolecular reactions of  $\text{O}_2$  and  $\text{O}$  with  $\text{CHCl}_3$  to  $\text{HO}_2 + \text{CCl}_3$  and  $\text{OH} + \text{CCl}_3$  products respectively.



These reactions occur in parallel with the unimolecular dissociation of chloroform.



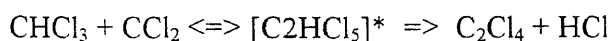
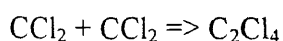
Increases in  $O_2$  concentration consistently increased reagent loss which is also observed in chlorobenzene oxidation.<sup>10</sup> The O responsible for the increased reaction with  $O_2$  is from  $CCl_2 + O_2 \Rightarrow CCl_2O + O$ , where O can then react with  $CHCl_3$  and  $CCl_2$  results from reaction (1).

The OH radical is not as important to the destruction of  $CHCl_3$  since limited hydrogen is available when no supplemental fuel is added. In fact only small (ca 1%) amounts of hydrogen substituted products are found in the presence of  $O_2$ .

Data in Figure 7.2 indicate that oxygen has a significant effect on the formation of  $CCl_4$ ; the level of  $CCl_4$  in oxidative reaction is higher than in pyrolysis. The hydrogen atom present in the parent chloroform is lost by reaction with O,  $O_2$  and OH, resulting in the  $CCl_3$  radical as shown above. The presence of  $O_2$  results in higher  $CCl_3$ , and consequently higher  $CCl_4$ , which is formed by Cl addition to  $CCl_3$  and Cl abstraction by  $CCl_3$ .



$C_2Cl_4$  is the main product observed over a wide range of temperatures for all cases as shown in Figure 7.3, where the symbols represent experimental data and the lines represent model prediction. This product mainly results from combination of two  $:CCl_2$  radicals and insertion of  $CCl_2$  into  $CHCl_3$  as reported by Won and Bozzelli.<sup>9</sup>





There is, however, significantly less  $C_2Cl_4$  formed when  $O_2$  is added. This implies that the reaction,  $:CCl_2 + O_2 \Rightarrow CCl_2O + O$ , suppresses the formation of  $C_2Cl_4$ . Here the  $C_2Cl_4$  yield is decreased relative to its yield in  $CHCl_3$  pyrolysis in argon as shown in Figure 7.4. The presence of  $O_2$ , therefore, results in suppressed  $C_2Cl_4$  formation and faster decomposition of  $C_2Cl_4$  as illustrated in Figures 3 and 4. The production of  $C_2Cl_4$  increases with increasing temperature to a maximum near  $680\text{ }^\circ\text{C}$  and then drops when CO begins to increase as indicated in Figures 5 and 6.

The  $C_2Cl_4$  reaches a steady state value accounting for almost 100 % of the parent  $CHCl_3$  carbon between  $680$  and  $800\text{ }^\circ\text{C}$  in pyrolysis (1.0 second reaction time).  $C_2Cl_4$  is apparently thermodynamically stable in the pyrolysis throughout this time and temperature regime. There is, in addition, limited hydrogen available to undergo reaction with this species and chlorine abstraction by Cl is unlikely, due to the large endothermicity. This indicates that chlorinated compounds (such as  $C_2Cl_4$  and  $CCl_4$ ) have a relatively high degree of stability up to  $800\text{ }^\circ\text{C}$  in reaction systems, which are deficient of  $O_2$  and hydrogen source. Data of Tirey *et al.*<sup>11</sup> reported that  $C_2Cl_4$  exhibited only minimal degradation at  $800\text{ }^\circ\text{C}$  and 2.0 second reaction time in a  $C_2Cl_4/He$  system and further observed that poly-aromatic compounds were formed above  $900\text{ }^\circ\text{C}$ .

### 7.3 Quantum RRR Calculations

The minor products of the C2 species ( $C_2HCl_3$ ,  $C_2HCl_5$ ,  $C_2H_2Cl_2$  ...etc.) observed in this reaction system are formed as a consequence of C1 radicals ( $CHCl_2$ ,  $CCl_3$  and  $CCl_2$ ) which undergo combination and insertion processes (formation of chemically activated adducts)

as discussed by Won and Bozzelli.<sup>12</sup> The reaction versus stabilization of these adducts are strongly pressure- and temperature-dependent and we find the Quantum Rice-Ramsperger-Kassel (QRRK) statistical analysis (Dean *et al.*)<sup>13</sup> important to analyze the rate constants as a function of pressure and temperature.

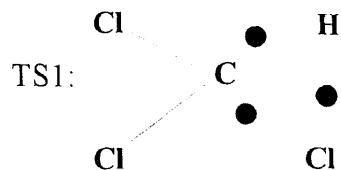
All input parameters for QRRK calculations of important reactions considered in the reaction systems of pyrolysis and oxidation are listed in the Appendix as Table 7.A.1 through Table 7.A.11. The potential energy diagram accompanied with Arrhenius plots which present the results of QRRK calculations are given as Figures 7.A.1 through 7.A.11.

### 7.3.1 Chloroform Pyrolysis

Figure 7.A.1 presents the potential energy diagram and Arrhenius plot for three possible pathways of chloroform decomposition:



The reaction rate of (1) is sensitive to the rates of  $\text{CHCl}_3$  decay and  $\text{CCl}_2$  is the active intermediate of most importance in the pyrolysis system. The adjustment of the A factor and the reaction barrier of (1) will cause a dramatic change in the modeling prediction. The HCl elimination for  $\text{CHCl}_3$  is expected via a three center Transition State (TS1).

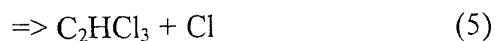
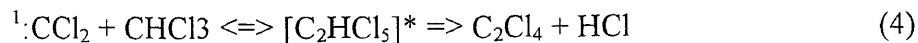


The semiempirical MO calculation, MNDO/PM3<sup>14</sup> is used to define the molecular structure of TS1 and to obtain the vibrational frequencies, moments of inertia of external rotations, and thus the entropy of TS1. From conventional transition state theory, the pre-exponential factor, A is calculated by:

$$A = (eh_p T/k_b) \exp(\Delta S^\ddagger),$$

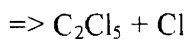
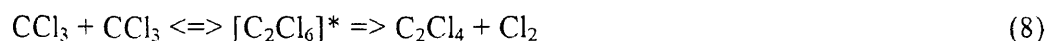
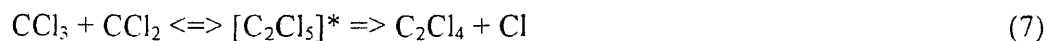
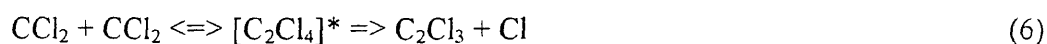
where  $h_p$  is Planck's constant,  $k_b$  is the Boltzmann constant, T is the temperature and  $\Delta S^\ddagger$  is the entropy difference between the product and the TS. The PM3 calculations give  $\Delta S^\ddagger_{298} = 5.18$  cal/mol,<sup>15</sup> yielding  $A = 7.18E14$  s<sup>-1</sup> at the average temperature 950 K. The barrier,  $E_{a1}$ , equal to 57.5 kcal/mol is the result of the best fit of modeling to the experimental data of  $\text{CHCl}_3$  pyrolysis in the Ar bath. This value of  $E_{a1}$  implies that the insertion of singlet dichlorocarbene,  $^1\text{CCl}_2$  into HCl to form  $\text{CHCl}_3$ , as the backward reaction of (1), has a small barrier, c.a. 3.3 kcal/mol.

Another important reaction is the insertion of the primary product,  $^1\text{CCl}_2$ , into  $\text{CHCl}_3$  (see Figure 7.A.2):



Reaction (4) is also sensitive to the rates of  $\text{CHCl}_3$  decay and is an important path of  $\text{C}_2\text{Cl}_4$  formation. The input parameters for QRRK calculations are listed in Table 7.A.2.

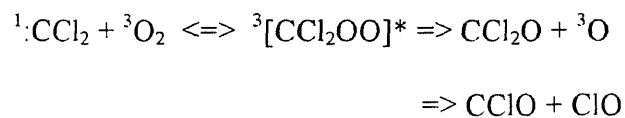
Three other important paths of  $\text{C}_2\text{Cl}_4$  formation, (6), (7) and (8), are also analyzed. See Figure 7.A.4 to 7.A.5 and Table 7.A.3 to 7.A.5 for reaction (6), (7) and (8), respectively.



### 7.3.2 Chloroform Oxidation

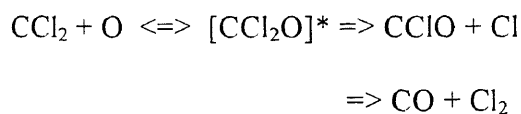
Oxygen obviously plays an important role in limiting formation of heavy chlorocarbons under fuel lean combustion conditions. The reactions of the oxygen molecule and the oxygen atom with chlorocarbon radicals relevant to this study are important to the development of mechanism. These are addition and combination reactions and are analyzed using QRRK calculations.

The reaction paths of dichlorocarbene,  $^1\text{CCl}_2 + \text{O}_2$ , is analyzed as the potential energy diagram presented in Figure 7.A.6. The input parameters of the QRRK calculations are given in Table 7.A.6.



The barrier of  $^1\text{CCl}_2$  addition to  $\text{O}_2$  is determined to be 14 kcal/mol, from the best model fit to experimental data. The well depth is estimated to be 12.4 kcal/mol. The energized complex  $[\text{CCl}_2\text{OO}]^*$  is expected to immediately beta-scission to  $\text{CCl}_2\text{O} + \text{O}$ , because the reaction  $\text{CCl}_2\text{OO} \Rightarrow \text{CCl}_2\text{O} + \text{O}$  has low barrier and is highly exothermic. One other possible pathway,  $[\text{CCl}_2\text{OO}]^* \Rightarrow \text{CClO} + \text{ClO}$  is estimated to be hindered by a high reaction barrier (c.a. 28.6 kcal/mol), see potential energy diagram and the calculated Arrhenius plot in Figure 7.A.6.

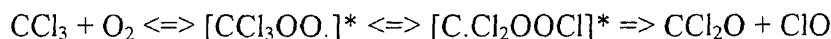
The chemical activated combination reaction of  $\text{CCl}_2 + \text{O}$  is analyzed with the potential energy diagram presented in Figure 7.A.7.



The energized complex  $[\text{CCl}_2\text{O}]^*$  mainly dissociates to  $\text{CO}$  and  $\text{Cl}_2$ , which is identified as the important path of  $\text{CO}$  formation in the modeling prediction of  $\text{CHCl}_3$  oxidation.

$\text{CCl}_2 + \text{OH}$  presents a more complex situation as the analysis of reaction paths given in Figure 7.A.8. Although the reactions of  $\text{OH}$  are not so important in our reaction system (see Section 7.2.2), it is important in flame, and it is analyzed for completeness of the mechanism.  $\text{CCl}_2 + \text{OH} \Rightarrow \text{CCl}_2\text{O} + \text{H}$  is the dominate path of the chemical activated reaction of  $\text{CCl}_2 + \text{OH} \Rightarrow$  products.

The reaction of  $O_2$  with  $CCl_3$ , another important radical fragment of  $CHCl_3$  is analyzed as Figure 7.A.9:



The  $[CCl_3OO]^*$  energized complex can be stabilized, decompose back to initial reactants, decompose to  $CCl_3O + O$ , or isomerize (via Cl shift) to  $CCl_2OOCl$ , which immediately dissociates to  $CCl_2O + ClO$ . The reaction to  $CCl_3O + O$  does not occur due to thermodynamic limitations (high energy barrier) as shown in Figure 7.A.9. The  $[C.Cl_2OOCl]^*$ , if formed, will rapidly decompose to  $CCl_2O + ClO$ , but there is a barrier here also and the primary reaction of this adduct is the dissociation back to reactants. Addition of  $CCl_3$  to  $O_2$  was determined to have a shallow well, 19.9 kcal/mol.<sup>16</sup> This shallow well limits adduct formation and only a fraction of the collisions proceed to  $CCl_2O + ClO$  at temperature  $> 1000$  K, see the Arrhenius plot in Figure 7.A.9.

In contrast to the situation of  $CCl_3 + O_2$ , the reaction of  $CCl_3 + O$  has a deep energy well (c.a. 79 kcal/mol), see the potential energy diagram in Figure 7.A.10. The combination-beta-scission channel  $CCl_3 + O \Rightarrow CCl_2O + Cl$  is the dominate path of the chemical activated reaction  $CCl_3 + O \Rightarrow$  products, as the Arrhenius plot shows in Figure 7.A.10.

## 7.4 Mechanism

Two elementary reaction sets describe the high temperature pyrolysis (Ar bath) and oxidation of  $\text{CHCl}_3$ , and are presented in Tables 7.1 and 7.2, respectively. The mechanisms are listed together with the rate parameters for the forward reaction paths and references for the rate constants. Reverse reaction rates were calculated from thermodynamics and microscopic reversibility (MR). In the initial phase of model development, the thermal decomposition of  $\text{CHCl}_3$  in argon bath gas was studied to determine the rate constants of the initiation reaction of  $\text{CHCl}_3$ . The pyrolysis reaction system is the most straightforward ( $\text{CHCl}_3/\text{Ar}$  only) and it does not include the more complex effects from additive fuels and  $\text{O}_2$  on decay of  $\text{CHCl}_3$ . The second phase of model development considers the effects of  $\text{O}_2$  addition to the  $\text{CHCl}_3/\text{Ar}$  system.

The detailed oxidative/pyrolysis mechanism was constructed by systematically considering the elementary reactions of  $\text{CHCl}_3/\text{O}_2/\text{Ar}$  and intermediate stable species consistent with experimental observations. Recommended rate parameters based on recent experimental data or evaluations are used whenever possible. Kinetic data do not, however, exist for some of the needed elementary reactions, consequently, kinetic parameters were estimated for these by using thermodynamics, micro-reversibility, Transition State Theory<sup>17</sup> and by generic analysis of the reaction, i.e. comparison of the reaction to a similar one where the rate parameters are known.

For reactions such as radical addition to an unsaturated species and radical-radical combination, where pressure and temperature effects can be important to determine the reaction paths of a chemically activated adduct, kinetic parameters were calculated using

Quantum RRK Theory (Dean *et al.*).<sup>13,18</sup> Examples are described above for  $\text{CHCl}_3$  dissociation,  $\text{CCl}_3$  and  $\text{CCl}_2$  additions to  $\text{O}_2$ . The mechanism development also includes the analysis on the combination reactions of  $\text{CCl}_2$  and chlorinated hydrocarbon radicals (e.g.  $\text{CCl}_3$  and  $\text{CHCl}_2$ ) with  $\text{OH}$ ,  $\text{O}$ ,  $\text{HO}_2$  to correctly describe the temperature and pressure dependencies of plausible reaction pathways. Simple dissociation and isomerization reactions are analyzed with unimolecular QRRK analysis for treatment of the fall-off dependency.

The CHEMKIN computer program package (Kee *et al.*<sup>19,20</sup>) is used in interpreting and integrating the detailed reaction mechanisms (models) of the systems studied. Thermochemical data are required to determine the energy balance in chemical reactions, and in determining the Gibbs Free Energy of a reaction as a function of temperature. The thermodynamics also provide a convenient way to determine reverse reaction rate constants from the calculated equilibrium constant of the reaction and the known forward rate<sup>21</sup> and play a very important role in determination of rate constants (A factors and activation energies).

The thermochemical information was acquired from the recent literature values. Data for some of the species in the mechanism are not available. Consequently, they were estimated by Benson's Group Additivity methods or THERM,<sup>22</sup> a computer code which utilizes the Benson's Group Additivity scheme and the HBI estimation method (see Chapter 2 for example) based on bond dissociation energies and loss of a H atom from the corresponding parent of the radical. Bond energies for radicals can be obtained from evaluations of current literature. Entropies and heat capacities (versus temperature) are



calculated using thermochemical methods incorporating loss of the appropriate vibrational frequencies, changes in symmetry, spin and rotational barrier changes. The values determined are checked or compared with similar compounds or series of species to verify they are reasonably accurate. The thermodynamic properties and references listed in ref. 9 and 12 have been validated in this work.

### 7.5 Comparison of Model Predictions with Experimental Data

The thermal decomposition of  $\text{CHCl}_3$  in argon ( $\text{CHCl}_3/\text{Ar}$ ) was first studied to determine the rate constants of  $\text{CHCl}_3$  dissociation and to develop a mechanism for the pyrolysis system. The detailed reaction mechanism for  $\text{CHCl}_3$  pyrolysis in argon is listed in Table 7.1.

Figure 7.4 compares and shows good agreement between the pyrolysis experimental data and model predictions for  $\text{CHCl}_3$  decay plus product distributions versus temperature at 1 second reaction time. The lines represent model prediction and the symbols are the experimental data. Figure 7.5 presents the modeling prediction of  $\text{CHCl}_3$  decay in a pyrolytic environment versus reaction time (0 to 2.0 sec) at five reaction temperatures. Figure 7.6 and Figure 7.7 illustrate model prediction and experimental data for product distribution versus reaction time at 873 K and 908 K, respectively.

Modeling  $\text{CHCl}_3$  oxidation required the listed reactions in Table 7.2 in addition to the pyrolysis mechanism in Table 7.1. Experimental data for  $\text{CHCl}_3$  oxidation, initial 1%  $\text{CHCl}_3 + 1\% \text{O}_2$  in Ar bath, are compared with model predictions in Figures 7.8 for  $\text{CHCl}_3$  decomposition and product distributions as function of temperature at 1 second reaction

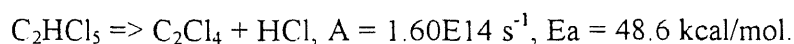
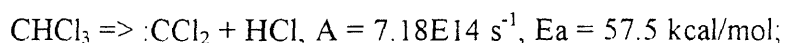
time. Figure 7.9 and Figure 7.10 further compare the experimental data for the 1%  $\text{CHCl}_3$  + 1%  $\text{O}_2$  initial conditions with model prediction versus reaction time at 953 K and 1008 K, respectively.

Experimental data for  $\text{CHCl}_3$  oxidation, initial 1%  $\text{CHCl}_3$  + 3%  $\text{O}_2$  in Ar bath, are compared with model predictions in Figures 7.11, for product distributions versus temperature at 1 second reaction time. Figure 7.12 presents the model prediction of product distribution as function of time at 673 K in 1%  $\text{CHCl}_3$  + 3%  $\text{O}_2$  initial concentration.

The predictions shown are quite reasonable in all three cases. The  $\text{CHCl}_3$  pyrolysis mechanism is a subset of the  $\text{CHCl}_3$  oxidation mechanism which fits all of the pyrolysis data. Rate parameters for a few reactions appearing in Table 7.1 were varied over small intervals to give a better fit to our experimental data. For example, one important value optimized was the reaction barrier,  $E_{a1}$  of chloroform dissociation to  $^1\text{:CCl}_2 + \text{HCl}$ . Here it was found that only  $\pm 0.5$  kcal/mol dramatically changed to the reaction predictions. The references to each elementary reaction listed in Table 7.1 and Table 7.2 actually describe the sources or how the rate constants were estimated. There is slight modification of a few key rate constants to fit our experimental results, if they are not accurately known from previous studies. The shape of the experimental  $\text{CHCl}_3$  loss and product profiles over a wide range of temperature, are reproduced quite well by the model.

## 7.6 Conclusion

The elementary reaction mechanisms are revised for chloroform pyrolysis and oxidation, which were previously studied in tubular flow reactors at 1 atm with a residence time 0.3 to 2.0 seconds in the temperature range 535 - 800 °C. The thermodynamic data for the species in the reaction systems are updated. Bimolecular Quantum RRK calculations for important reactions have been recalculated with the input parameters (high pressure limit rate constants) which are based on revised thermodynamic properties or taken from more recently reported kinetic data. High pressure limit rate constants have been evaluated for the following:



A barrier, 14 kcal/mol is determined for  $\cdot\text{CCl}_2 + \text{O}_2 \Rightarrow$  products from best model-fitting to experimental data.

Chloroform decay and product distributions are distinctly different in the absence and presence of added  $\text{O}_2$ . The presence of  $\text{O}_2$  was observed to speed reagent loss, decrease  $\text{C}_2\text{Cl}_4$  formation and increase CO production. The major products from  $\text{CHCl}_3/\text{O}_2/\text{Ar}$  oxidation are  $\text{C}_2\text{Cl}_4$ ,  $\text{CCl}_4$ ,  $\text{HCl}$ ,  $\text{CO}$  and  $\text{CO}_2$  over a wide temperature range. Minor products include  $\text{C}_2\text{HCl}_3$  and  $\text{C}_2\text{HCl}_5$ .

An elementary reaction mechanism to describe the important features of product formation and reagent loss in pyrolysis and oxidation of chloroform with no added fuel has

been validated. The mechanism consists of 82 species and 198 elementary reactions and is based on thermochemical principles. Mechanism development includes QRRK analysis for the combination of  $\text{CCl}_3 + \text{CCl}_3$ ,  $\text{CCl}_3 + \text{CCl}_2$ ,  $\text{CCl}_2 + \text{CCl}_2$ , and chlorinated hydrocarbon radicals with OH, O,  $\text{HO}_2$ , ClO and radical addition to  $\text{O}_2$ .

## CHAPTER 8

### **DETAILED ANALYSIS OF PHOTOCHEMICAL OXIDATION OF BENZENE AND TOLUENE IN THE ATMOSPHERE: BENZENE + OH AND THE ADDUCT (HYDROXYL-2,4-CYCLOHEXADIENYL) + O<sub>2</sub> TOLUENE + OH AND THE ADDUCT (HYDROXYL-2,4-METHYLCYCLOHEXADIENYL) + O<sub>2</sub>**

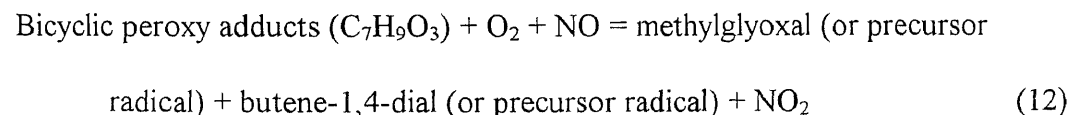
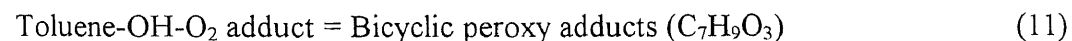
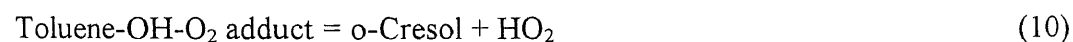
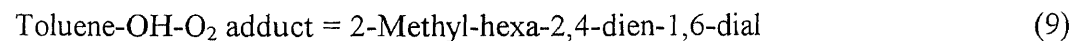
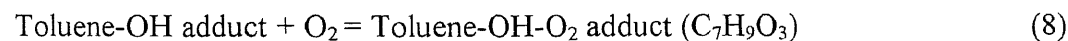
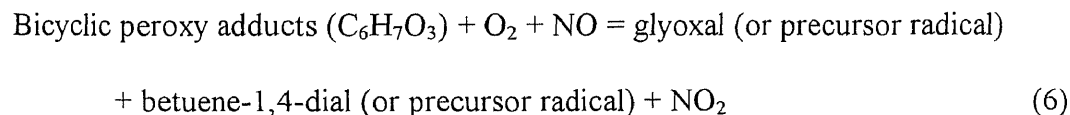
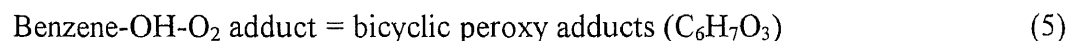
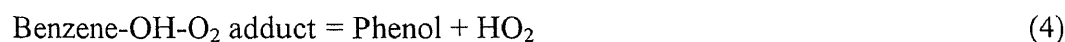
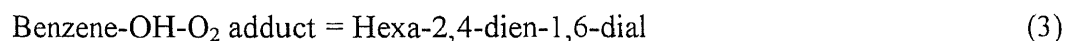
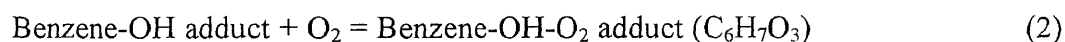
#### **8.1 Introduction**

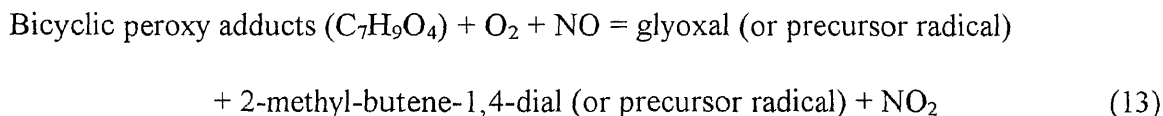
A number of researchers have studied photochemical oxidation of aromatic hydrocarbons, such as benzene,<sup>23,24,25</sup> toluene<sup>23-30</sup> and xylenes,<sup>23,28,31,32</sup> since aromatics comprise a substantial portion of the reactive hydrocarbon in the urban atmosphere.<sup>30,33,34</sup> Toluene represents one-third of the atmospheric aromatics and probably is the most extensively studied aromatic up to date.<sup>30,33</sup> Several reaction mechanisms were proposed for the interpretation of the experimental data of toluene photooxidation,<sup>26,30,35-37</sup> and the model prediction of formation and decay of a limited number of products appear to fit the observed major features.<sup>26,30</sup>

Detailed interpretations of experimental results using reaction mechanisms are limited due in part to the paucity of thermodynamic property data and barriers to formation of the key intermediates in the reaction systems.<sup>26,38,39</sup> The evaluations of rate constants are difficult and sometimes questionable without the available enthalpies and entropies of reactants and products. In addition, the reaction mechanisms currently used for modeling of photooxidation of toluene and other aromatics contain only apparent rate constants for many important reactions, due in part to the difficulty in determination of

absolute rate constants from overall reaction rates without required thermodynamic data, and also to lack of microscopic reversibility in the rate parameters.

Absolute rate constants for the initial reactions of aromatic oxidation of the benzene and toluene, especially the reactions of benzene and toluene + OH, and the adducts (benzene-OH and toluene-OH) + O<sub>2</sub>,<sup>25,26,38</sup> are derived and validated in this study. Reaction path analysis, reaction barriers, Arrhenius A factors, and energy well depth of each reaction step have been calculated for:





One important requirement in the evaluation of reaction rate constants and derivation of detailed mechanisms is the thermodynamic properties ( $\Delta H_f^\circ$ ,  $S^\circ$ ) of reactants, intermediates and products in the reactions studied. We calculate values of  $\Delta H_f^\circ$ ,  $S^\circ$  and  $C_p(T)$ 's ( $T = 300\text{K}$  to  $1500\text{K}$ ) for species including:

- aromatic stable molecule and free radicals
- OH-aromatic adduct
- peroxy adducts and radicals (data not previously available)
- bicyclic ring species resulting from OO internal addition across the rings
- radicals and stable species resulting from reactions of the above species with NO<sub>x</sub>
- radicals and stable species resulting from beta scission of the above species,

We also develop elementary kinetic mechanisms, including microscopic reversibility for each step, for production of species like glyoxal and butene-dial and the intermediates leading to them.

The thermodynamic properties of bicyclic peroxy rings adducts are particularly important to evaluate the kinetic factors for ring opening steps which lead to the final stable products. Examples include: the bicyclic-(benzene-OH-O<sub>2</sub>) adduct in benzene system and the bicyclic-(toluene-OH-O<sub>2</sub>) adduct in the toluene system. Calculations of ring strain energy and thermodynamic properties of these species are also carried out.

Quantum Rice-Ramsperger-Kassel (QRRK) analyses<sup>13</sup> which incorporate the modified strong collision ( $\beta$ -collision) approach of Gilbert, Luther and Troe for fall off, are performed on chemical activated reactions (1)-(5), (7)-(11) for pressure and temperature dependence. Results are presented here only for 1atm pressure. High pressure limit kinetic parameters (A factor and Ea's) of the reactions used as input of the QRRK calculations are taken from generic reactions in the literature or estimated from thermodynamic and kinetic principles, e.g. Transition State Theory (TST). The estimation of kinetic factors for ring opening and  $\beta$ -scission reactions in the photooxidation of benzene and toluene are also carried out.

Modeling calculations on selected limited reaction sets are performed. It is important to note that in these modeling calculations:

- All reactions are elementary or treated in a way that the elementary reaction steps are properly incorporated.
- All reactions are reversible
- Reverse reaction rates are calculated from thermodynamics and microscopic reversibility (MR) principles.

The reasons for using MR, i.e. considering reverse reactions, are both thermodynamically consistent and resulting in more accurate determination of species concentrations near steady state. Inclusion of MR allows use of accurate elementary rate constants. Inclusion of reverse reactions eliminates the need to use adjusted or apparent rate constants for reactions where the reverse reaction is important. These adjustments are

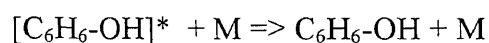


often just the values of average estimate or the estimated conversion rate, and are usually not correct at all operating condition over a given experimental study.

## 8.2 Calculations and Results of Benzene Photooxidation System

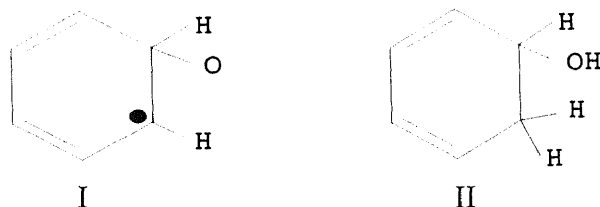
### 8.2.1 Chemical Activated Reactions of OH + Benzene

The addition of the OH radical to the aromatic ring of benzene forms an energized benzene-OH adduct (I). This energized benzene-OH adduct can dissociate back to reactants, be stabilized, or react to form phenol + H atom via  $\beta$ -scission.



#### 8.2.1.1 Thermodynamic Properties for Benzene-OH Adduct

The thermodynamic properties of the benzene-OH adduct (I) are estimated from those of hydroxyl 2,4-cyclohexadiene (II) which are calculated using the Group Additivity (GA) method.<sup>17,22</sup> The hydroxyl-2,4-cyclohexadiene (II) stable molecule, is called the parent molecules for the free radical, hydroxyl-2,4-cyclohexadienyl (benzene-OH) (I).



The above oxyhydrocarbons, both daughter radical and parent molecule, closely parallel to cyclohexadienyl and cyclohexadiene whose thermochemistry have been extensively studied.<sup>1,40-44</sup> The HC-H bond energy for cyclohexadienyl was evaluated by Tsang as 76.0 kcal/mol (318 kJ/mol)<sup>44</sup> which is adopted in this work.  $\Delta H_f^\circ_{298}(\text{II})$  is calculated using GA method as -13.73 kcal/mol. This results in  $\Delta H_f^\circ_{298}(\text{I})$  of 10.17 kcal/mol, using Tsang's HC-H bond energy and  $\Delta H_f^\circ_{298}(\text{H.})$  (52.1 kcal/mol).<sup>45</sup>

The entropy ( $S^\circ_{298}$ ) and heat capacities ( $C_p(T)$ ,  $300 \leq T/K \leq 1000$ ) for I are also evaluated from II, by applying the incremental values of  $S^\circ_{298}$  and  $C_p(T)$ 's from cyclohexadiene to cyclohexadienyl. This approach is termed as the "Hydrogen Atom Bond Increment" (HBI) group,<sup>46</sup> which is based on known thermodynamic properties of the parent and calculated changes that occur upon formation of a radical via loss of a H atom. The HBI group values for radicals of cyclohexadienyl type (HBI(*CHD*)) is applied to compound I to obtain entropies and heat capacities of radical II.

The values of  $S^\circ_{298}$  and  $C_p(T)$ 's for 1,3-cyclohexadiene are taken from the work of Dorofeeva *et al.*<sup>47</sup> The entropies and heat capacities of cyclohexadienyl were evaluated by Tsang<sup>44</sup> using the vibrational frequencies which were assessed from those of benzene and 1,4-cyclohexadiene. The selection of frequencies for cyclohexadienyl by Tsang was desired to fit the experimental value of entropy at 550 K equal to 89.7 cal/mol-K. We separately performed a semiempirical MO calculation, MNDO/PM3 (PM3)<sup>14</sup> using MOPAC 6.0<sup>48</sup> to further determine the vibrational frequencies of cyclohexadienyl and thus the  $S^\circ_{298}$  and  $C_p(T)$ 's of cyclohexadienyl as given in Table 8.1. Our values of  $S^\circ_{298}$  and  $C_p(T)$ 's are slightly different from Tsang's. The PM3 MO calculation gives 90.1

cal/mol-K as the entropy of cyclohexenyl at 550 K which is in excellent agreement with the experimental data, without any further adjustment. The  $S^{\circ}_{298}$  and  $C_p(T)$ 's of the PM3 MO calculation for cyclohexadienyl and the work of Dorofeeva *et al.* for 1,3-cyclohexadiene are therefore used to derive the groups values ( $\Delta S^{\circ}_{298}$  and  $\Delta C_p(T)$ 's) of HBI(*CHD*) by subtracting the intrinsic entropy ( $S_{\text{int}}^{\circ}_{298}$ ) and heat capacities ( $C_p(T)$ 's) of cyclohexadiene from those of cyclohexadienyl, e. g.

$$\Delta S^{\circ}_{298}(\text{CHD}) = S_{\text{int}}^{\circ}_{298}(1,3\text{-cyclohexadiene}) - S_{\text{int}}^{\circ}_{298}(\text{cyclohexadienyl}) = -0.68 \text{ cal/mol-K.}$$

$$\Delta C_{p300}(\text{CHD}) = C_{p300}(1,3\text{-cyclohexadiene}) - C_{p300}(\text{cyclohexadienyl}) = -0.80 \text{ cal/mol-K,}$$

and so on for  $\Delta C_{p400}(\text{CHD})$  to  $\Delta C_{p1000}(\text{CHD})$ .

And  $S^{\circ}_{298}$  and  $C_p(T)$ 's for I are calculated as:

$$S_{\text{int}}^{\circ}_{298}(\text{I}) = S_{\text{int}}^{\circ}_{298}(\text{II}) + \Delta S^{\circ}_{298}(\text{CHD}) \text{ and } C_p(T)(\text{I}) = C_p(T)(\text{II}) + \Delta C_p(T)(\text{CHD})$$

The thermodynamic properties for species I and II are given in Table 8.1.

### 8.2.1.2 Quantum RRK Calculation for Benzene + OH

The potential energy diagram for the reaction of benzene + OH is illustrated in Figure 8.1.

The well depth for OH addition to benzene is 19.1 kcal/mol according to our thermochemical calculation. The high pressure limit rate constant of reaction (B1) needed for the QRRK input parameters has the pre-exponential factor (A factor) estimated to be  $2.29\text{E}12 \text{ cc/mol-s}$  with a small barrier 0.68 kcal/mol following the recommendation of

Baulch *et al.*<sup>49</sup>  $k_{B1}$  is calculated via the principle of microscopic reversibility (MR)<sup>17</sup> using the thermodynamic data given in Table 8.1. The rate constant for addition of the H atom to benzene is used to evaluate  $k_{B2}$  and then  $k_{B3}$ :



The value of  $A_{B3}$  is reported<sup>50</sup> as  $3.98\text{E}13$  mol/cc-s with a barrier,  $E_{aB3} = 4$  kcal/mol.  $A_{B2}$  and  $E_{aB2}$  are assumed equal to  $A_{B3}$  and  $E_{aB3}$ , and thus  $A_{B2}$  and  $E_{aB2}$  can be determined via MR. The input data for the QRRK calculation of benzene + OH and the calculation results are give in Table 8.3. The calculated apparent rate constants as a function of temperature are also listed in Table 8.3. The Arrhenius plot for the apparent rate constants is illustrated in Figure 8.2.

As Figure 8.2 illustrates, the stabilization channel is dominant at room temperature and 1 atm. The apparent rate constant of benzene + OH  $\Rightarrow$  benzene-OH adduct at 298 K is calculated to be  $7.23\text{E}11$  mol/cc-s which is identical to the value measured by means of flash photolysis-resonance fluorescence technique.<sup>23</sup> The formation of phenol is obviously the minor reaction path in the temperature regime lower than 500 K, although it is important at high temperature.

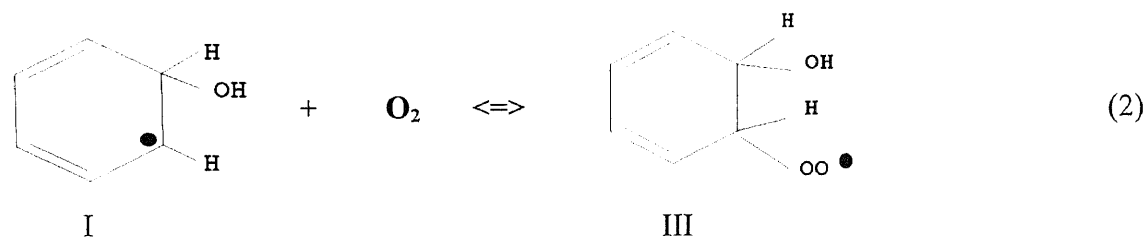
### 8.2.2 Chemical Activated Reactions of Benzene-OH Adduct + O<sub>2</sub>

The addition of the benzene-OH adduct to O<sub>2</sub> first forms the benzene-OH-O<sub>2</sub> adduct (hydroxyl-2,4-cyclohexadienyl-6-peroxy). This adduct can dissociate back to reactants,

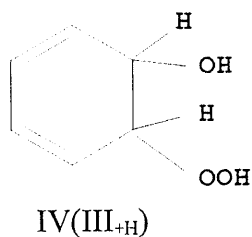
isomerize to one of several bicyclic adducts, or react via hydrogen transfer following  $\beta$ -scission to form 2,4-hexadienyl-1,6-dial + OH, or to phenol + HO<sub>2</sub>, see Figure 8.3. Calculation of the thermodynamic properties of these species, and the evaluations of the kinetic parameters are carried out as follows.

### 8.2.2.1 Thermodynamic Properties for Benzene-OH-O<sub>2</sub> Adduct

The benzene-OH-O<sub>2</sub> adduct is formed via the addition of benzene-OH + O<sub>2</sub>. The addition reactions can happen at either position 2 or 4 of the ring.<sup>26,38</sup> However, we only discuss the addition at position 2 to form adduct V as the primary adduct as a mean to simplify the reaction system and the further detailed analyses of the reactions of the peroxy adduct.



The thermodynamic properties of the parent molecule of III, e.g. the hydroperoxide IV (or marked as III<sub>+H</sub>) is first calculated using the GA method. The enthalpy for IV appears as -37.3 kcal/mol. The average bond energy  $D^{\circ}_{298}(\text{ROO}-\text{H})$  was determined as 88.0 kcal/mol (R is an alkyl group)<sup>51,52</sup> which leads to -1.2 kcal/mol for  $\Delta H_f^{\circ}_{298}$  of III.



The entropy and heat capacities for III are estimated from IV by using the HBI PEROXY group (HBI(*PEROXY*)).<sup>46</sup> e.g.

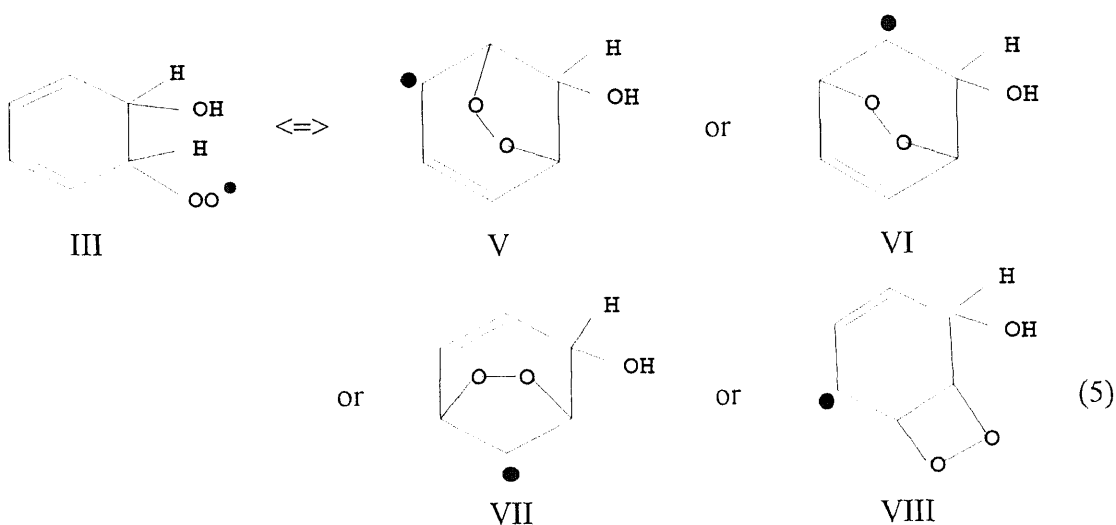
$$S_{\text{int}}^{\circ}{}_{298}(\text{IV}) = S_{\text{int}}^{\circ}{}_{298}(\text{III}) + \Delta S^{\circ}{}_{298}(\text{PEROXY})$$

$$C_p(T)(\text{IV}) = C_p(T)(\text{III}) + \Delta C_p(T)(\text{PEROXY}), 300 \leq T/\text{K} \leq 1000$$

The group values for HBI(*PEROXY*) as given in Table 8.2 are the  $S^{\circ}{}_{298}$  and  $C_p(T)$ 's increments resulting from loss and/or change in vibration frequencies and changes in barriers to internal rotation, from alkyl hydroperoxide (ROOH) to alkyl peroxy radical (ROO.). The  $S^{\circ}{}_{298}$ ,  $C_p(T)$ 's and  $\Delta H_f^{\circ}{}_{298}$  for species III and IV are given in Table 8.1.

### 8.2.2.2 Thermodynamic Properties and Ring Strain Energy for Bicyclic Peroxy Species

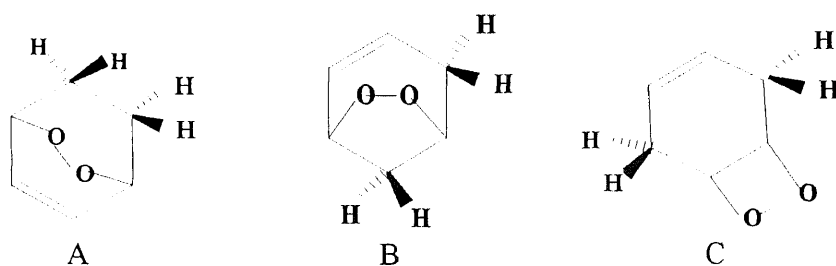
Adduct III can isomerize to bicyclic species via the addition of the peroxy radical to a double bond of the ring:



The thermodynamic properties ( $\Delta H_f^\circ_{298}$  and  $S^\circ_{298}$ ) of these bicyclic peroxy radicals are extremely important in evaluating the kinetic parameters of consequent reactions of benzene-OH + O<sub>2</sub>. Unfortunately, the thermodynamic properties of these species have not been previously studied, and the corresponding group values for use in GA method are not available. We calculate the thermodynamic properties of their parent (stable) molecules prior to calculating the thermodynamic properties of the bicyclic radicals. Ring strain energies are required in estimating the thermodynamic properties of the parent molecules by our GA approach. These are also evaluated from the calculated enthalpies of these bicyclic molecules. Several HBI groups (see Chapter 2) are then used to estimate the thermodynamic properties of the radical adducts V to VIII, after parameters of the corresponding parent molecules are obtained.

#### 8.2.2.2.1 Enthalpy and Ring Strain Energy of the Bicyclic Peroxides

MO calculations of the three bicyclic compounds were carried out to investigate the ring strain energies, e.g.



We utilized the PM3 MO method to determine the theoretical enthalpies ( $\Delta H_f^\circ_{298,PM3}$ ) of A, B and C. An analysis was performed to determine a correlation factor

for the  $\Delta H_f^\circ_{298,PM3}$  with the experimental values of  $\Delta H_f^\circ_{298}$  ( $\Delta H_f^\circ_{298,expt.}$ ) for relevant monocyclic and bicyclic hydrocarbons. A plot of this correlation,  $\Delta H_f^\circ_{298,expt.}$  vs.  $\Delta H_f^\circ_{298,PM3}$  is illustrated in Figure 8.4. The regressed line is found to pass through (0,0) with a slope 0.83, resulting  $\Delta H_f^\circ_{298,expt.} = 0.83 \times \Delta H_f^\circ_{298,expt.}$ . The empirical factor 0.83 is used to scale the  $\Delta H_f^\circ_{298,PM3}$  values of A, B and C.

The PM3 values for enthalpy of formation are:  $\Delta H_f^\circ_{298,PM3}(A) = -2.37$  kcal/mol,  $\Delta H_f^\circ_{298,PM3}(B) = -5.73$  kcal/mol and  $\Delta H_f^\circ_{298,PM3}(C) = +24.08$  kcal/mol. The scaled values are:  $\Delta H_f^\circ_{298}(A) = -1.97$  kcal/mol,  $\Delta H_f^\circ_{298}(B) = -4.76$  kcal/mol and  $\Delta H_f^\circ_{298}(C) = +20.00$  kcal/mol. The total ring strain energy (R.S.) can be obtained using the GA groups<sup>22</sup> for centered atoms in the molecules.

The enthalpy of formation of compound A is expressed by groups in GA approach as,  $\Delta H_f^\circ_{298}(A) = \Delta H_f^\circ_{298}\{2(C_d/C/H) + 2(C/C/C_d/H/O) + 2(O/C/O) + (C/C2/H/O) + (O/C/H) + (C/C2/H2)\} + \text{Ring Strain of A (R.S.(A))}$ ; where the symbol  $C_d/C/H$ ,  $C/C/C_d/H/O$ ,..... etc. are the terms of the GA approach used in THERM package.<sup>22</sup> The ring strain energy of compound A is therefore calculated as:

$$\text{R.S.(A)} = \Delta H_f^\circ_{298}(A) - \Delta H_f^\circ_{298}\{2(C_d/C/H) + 2(C/C/C_d/H/O) + 2(O/C/O) + (C/C2/H/O) + (O/C/H) + (C/C2/H2)\}, \text{ and so on for the R.S.(B) and R.S.(C).}$$

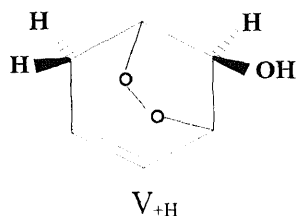
The calculated total ring strain energies are:  $\text{R.S.(A)} = 14.77$  kcal/mol,  $\text{R.S.(B)} = 13.01$  kcal/mol and  $\text{R.S.(C)} = 38.80$  kcal/mol. These enthalpy increments due to ring strain



are assigned to three new GA groups, BCY/C2E/O2/C2, BCY/C3E/O2/C1 and BCY/C4E/O2/0 in use for the type A, B and C bicyclic peroxy hydrocarbons, respectively.

Enthalpies of the hydroxyl bicyclic peroxides (the parent molecules for radical adducts V to VIII, identified as  $V_{+H}$ ,  $VI_{+H}$ ,  $VII_{+H}$ ,  $VIII_{+H}$ ) are calculated using the GA method coupled with the three groups developed above. The enthalpy of  $V_{+H}$  (the parent molecule of V), for example, is calculated as:

$$\Delta H_f^\circ{}_{298}(V_{+H}) = \Delta H_f^\circ{}_{298}\{2(C_d/C/H) + (C/C/C_d/H_2) + (C/C/C_d/H/O) + 2(O/C/O) + (C/C_2/H/O) + (O/C/H) + (BCY/C3E/O2/C1)\}$$



The  $\Delta H_f^\circ{}_{298}$  of each hydroxyl bicyclic radical (V, VI, VII, VIII) is obtained from the  $\Delta H_f^\circ{}_{298}$  of the parent hydroxyl cyclic peroxide ( $V_{+H}$ ,  $VI_{+H}$ ,  $VII_{+H}$ ,  $VIII_{+H}$ ) and the corresponding C--H bond energy,  $D^\circ{}_{298}(C--H)$ . The secondary  $D^\circ{}_{298}(C--H)$ , 98.45 kcal/mol,<sup>53</sup> is used to estimate  $\Delta H_f^\circ{}_{298}(VI)$  and  $\Delta H_f^\circ{}_{298}(VII)$ . The  $\Delta H_f^\circ{}_{298}(VI_{+H})$  is determined as -42.14 kcal/mol using the GA method, which leads to a  $\Delta H_f^\circ{}_{298}(VI)$  equal to 3.86 kcal/mol.

Adducts V and VIII are allylic and the secondary allylic C--H bond energy is estimated to be 85.6 kcal/mol.<sup>54</sup>  $\Delta H_f^\circ{}_{298}(V) = -13.2$  kcal/mol is estimated from  $\Delta H_f^\circ{}_{298}$  of its parent ( $V_{+H}$ ), -44.93 kcal/mol with this secondary allylic bond energy.

### 8.2.2.2 Entropy and Heat Capacities

PM3 in the MOPAC 6.0 package was used to calculate the entropies and heat capacities for compound A, B and C. These data were used to derive the group values of  $S^{\circ}_{298}$  and  $C_p(T)$ 's for above three new groups, BCY/C2E/O2/C2, BCY/C3E/O2/C1 and BCY/C4E/O2/0.  $S^{\circ}_{298}(\text{BCY/C2E/O2/C2})$  is obtained, for example, by taking the increment of  $S^{\circ}_{298}$  and  $C_p(T)$ 's for this bicyclic ring form  $S_{\text{int}}^{\circ}_{298}(\text{A})$  minus the  $S^{\circ}_{298}$  group values of all the centered atoms:

$$S^{\circ}_{298}(\text{BCY/C2E/O2/C2}) = S_{\text{int}}^{\circ}_{298}(\text{A}) - S^{\circ}_{298}\{2(\text{C}_d/\text{C}/\text{H}) + 2(\text{C}/\text{C}/\text{C}_d/\text{H}/\text{O}) + 2(\text{O}/\text{C}/\text{O}) + (\text{C}/\text{C2}/\text{H}/\text{O}) + (\text{O}/\text{C}/\text{H}) + (\text{C}/\text{C2}/\text{H2})\},$$

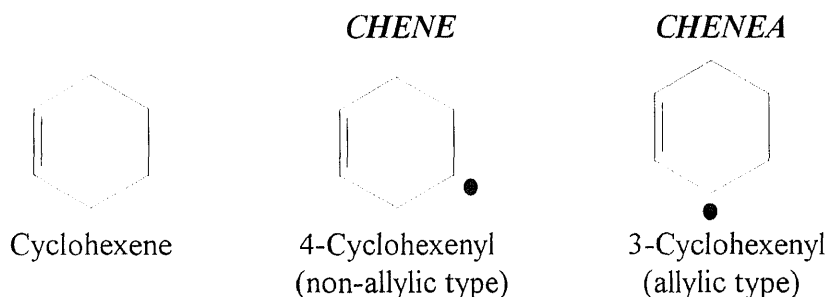
and so on for  $S^{\circ}_{298}(\text{BCY/C3E/O2/C1})$  and  $S^{\circ}_{298}(\text{BCY/C4E/O2/0})$  and the  $C_p(T)$  group values.

The availability of the  $S^{\circ}_{298}$  and  $C_p(T)$ 's group values for BCY/C2E/O2/C2, BCY/C3E/O2/C1 and BCY/C4E/O2/0 enable the calculation of corresponding parameters for the hydroxyl bicyclic peroxides,  $\text{V}_{+\text{H}}$ ,  $\text{VI}_{+\text{H}}$ ,  $\text{VII}_{+\text{H}}$  and  $\text{VIII}_{+\text{H}}$  (parent molecules of V to VIII) using the GA method. The  $S^{\circ}_{298}$  and  $C_p(T)$ 's of the bicyclic radical adducts, V, VI, VII and VIII are then estimated from the properties of their parent molecules and HBI group. Two HBI groups are introduced to carry out these calculations.

The HBI groups *CHENE* (secondary cyclohexadienyl) and *CHENEA* (allylic cyclohexadienyl) were used in the estimation of the  $S^{\circ}_{298}$  and  $C_p(T)$ 's for the 4-cyclohexenyl type and 3-cyclohexenyl type of radicals, respectively. Group values ( $\Delta S^{\circ}_{298}$  and  $\Delta C_p(T)$ 's) of HBI(*CHENE*) and HBI(*CHENEA*) were determined as the increments of  $\Delta S^{\circ}_{298}$  and  $\Delta C_p(T)$ 's from cyclohexene to 4-cyclohexenyl and 3-cyclohexenyl,

respectively. The  $\Delta S^{\circ}_{298}$  and  $\Delta C_p(T)$ 's data for cyclohexene were taken from the work of Dorofeeva *et al.*, the these parameters of two cyclohexenyl radicals are obtained using PM3 MO calculations.

HBI group



$S^{\circ}_{298}$  and  $C_p(T)$ 's of adducts V and VIII were calculated using the HBI(*CHENEA*) group. The HBI(*CHENE*) group is used to determine those properties of adducts VI and VII. Entropies, heat capacities and enthalpies of formation of the radical species and their parent molecules are given in Table 8.1.

### 8.2.2.3 Quantum RRK Kinetic Calculation of Benzene-OH Adduct + O<sub>2</sub>

The potential energy diagram for the benzene-OH adduct reaction with O<sub>2</sub> is illustrated in Figure 8.3. The well depth of benzene-OH + O<sub>2</sub> => benzene-OH-O<sub>2</sub> is determined as 10.17 kcal/mol. The first reaction path considered of this benzene-OH-O<sub>2</sub> adduct is the hydrogen transfer from the OH group to peroxy group with a subsequent  $\beta$ -scission to form 2,4-hexadiene-1,6-dial + OH, see channel BA in Figure 8.3 and Figure 8.5. The first step (hydrogen transfer) from the peroxy radical to the 1-hydroperoxyl-2-oxy radical has a

reaction barrier of 16 kcal/mol, see Figure 8.5. This is the rate-determining step because the following steps are thermochemical favorable  $\beta$ -scissions with lower barriers.

The second reaction path considered is H transfer from the carbon with OH substitution (C1) to the peroxy group, and subsequent beta-scission to form phenol + HO<sub>2</sub>., see channel BB in Figure 8.3 and Figure 8.6. This reaction path has a lower barrier than channel BA because the C-H bond is doubly allylic with a much lower bond energy (80 kcal/mol) than O-H bond (104 kcal/mol).

Channels BC, BD, BE and BF involve the cyclization of the peroxy group to form the 4 bicyclic adducts V, VII, VI and VIII, respectively. The reaction barriers for cyclization channels result primarily from the potential energy increment of ring strain and the peroxy radical addition to a C=C double bond. Since the adducts V, VI and VII have the similar RS energy (13 ~ 15 kcal/mol) and the adduct VIII has much higher RS energy (39 kcal/mol), channel BF is much less thermochemically favorable than the other three cyclization channels.

Evaluations of the A factors and Ea's for the benzene-OH + O<sub>2</sub> reaction system for the QRRK input parameters are based on thermodynamic properties and literature data as listed in Table 8.4. The results of QRRK calculations are also listed in Table 8.4 and the Arrhenius plot is illustrated in Figure 8.7. The apparent rate constant for benzene-OH + O<sub>2</sub> => benzene-OH-O<sub>2</sub> adduct is calculated to be 6.58E11 cc/mol-s, while  $k_{BB}$ ,  $k_{BC}$ ,  $k_{BD}$ , and  $k_{BE}$  are about of the same order, 10<sup>6</sup> cc/mol-s at 1 atm and 298.15 K. Channel BB could be the major pathway for the formation of phenol in benzene photooxidation system. The three bicyclic adducts V, VII and VI formed via channel BC, BD and BB could be the

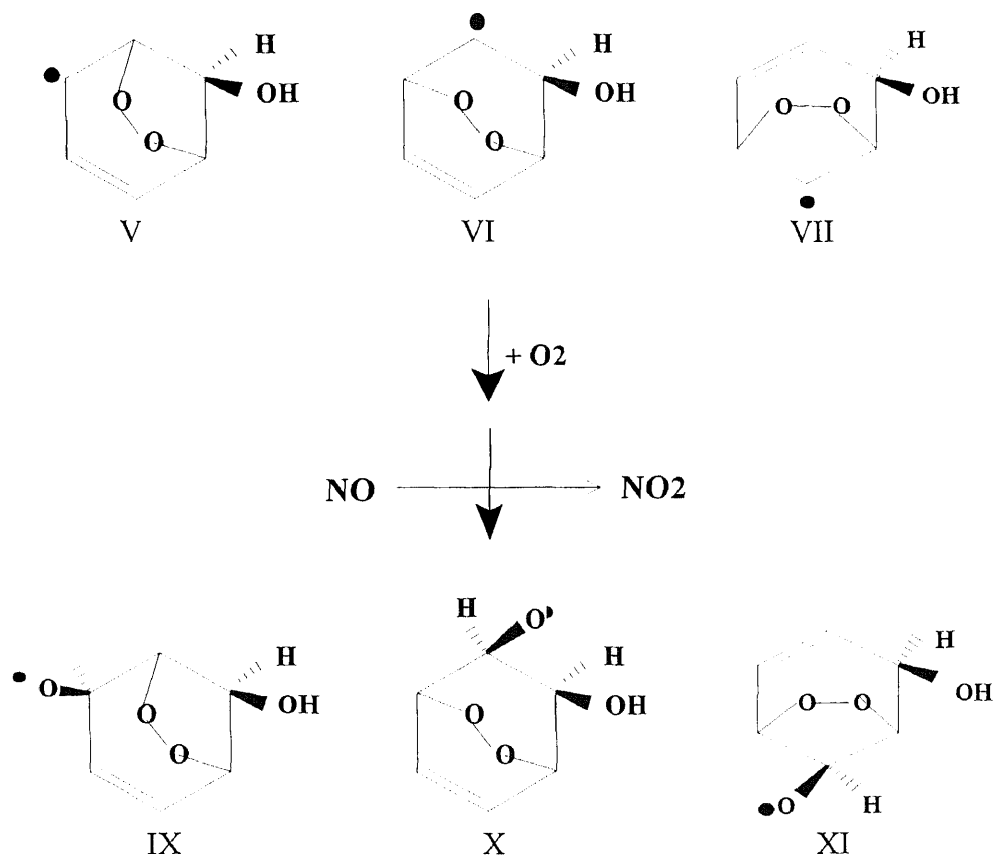
important precursors of the ring cleavage products, which will be discussed later. Formation of 2,4-cyclohexadiene-1,6-dial (channel BA) and the bicyclic adduct VIII (channel BF) is relatively slow at room temperature. The low  $k_{BA}$  is consistent with the experimental product data which indicate that 2,4-cyclohexadiene-1,6-dial is not the primary product of benzene photooxidation. Channel BF is not thought to compete with other reaction channels in the system, thus further reactions of adduct VIII will be excluded from further discussion.

#### **8.2.2.4 Reactions of Ring Cleavage: Estimation of $\beta$ -Scission Reaction Parameters (Transition State Study)**

The bicyclic benzene-OH-O<sub>2</sub> adducts, V, VI and VII formed from reaction (5) will react with the O<sub>2</sub> to form a second series of peroxy radicals. These will subsequently become oxy radicals after one oxygen is abstracted by NO.<sup>4,38</sup>

The calculation details of thermodynamic properties follow the procedure described above. The HBI(*ALKOXY*) group was used for estimating thermodynamic properties of these oxy radicals along with the corresponding values of the parent molecules. The thermodynamic parameters are listed in Table 8.1 and the group values of HBI(*ALKOXY*) are listed in Table 8.2.

The ring opening of adduct IX occurs through several  $\beta$ -scission steps in series, see Figure 8.8. Potential energy analysis indicates that the first reaction should be rate-determining. The reaction paths are similar for the cases of adducts X and XI, see Figure 8.9 and 8.10, respectively. The estimations of rate constants for these  $\beta$ -scission process are described as follows.



#### 8.2.2.4.1 Adduct IX $\Rightarrow$ Butene-1,4-dial + CHOC.HOH

There are limited or no experimental data on such kind of reactions of bicyclic species from which to estimate the corresponding kinetic factors ( $A$  and  $E_a$ ). We use Transition State (TS) theory to determine the rate constants. The determination of the TS structure of the first step (see Figure 8.8) for adduct IX  $\beta$ -scission was carried out using the semiempirical PM3 method, and identified by the existence of one and only one imaginary frequency in the harmonic vibration normal mode analysis. The PM3 vibrational frequencies were used to determine the entropy difference ( $\Delta S_{298}^\ddagger$ ) between adduct IX and the TS, since  $\Delta S_{298}^\ddagger \approx \Delta S_{298, \text{vibration}}^\ddagger$ .<sup>55</sup>

From conventional transition state theory,<sup>17</sup> the pre-exponential factor, A for a unimolecular reaction is calculated by,  $A = (eh_p T/k_b) \exp(\Delta S^\ddagger)$ , where  $h_p$  is Planck's constant,  $k_b$  is the Boltzmann constant, T is the temperature and  $\Delta S^\ddagger$  is the entropy difference between the product and the TS. The PM3/UHF calculations give  $\Delta S^\ddagger_{298} = 1.18$  cal/mol. Therefore  $A = 3.07E13 \text{ s}^{-1}$  at  $T = 298 \text{ K}$  for the adduct IX ring opening reaction.

The PM3 enthalpies of formation of adduct IX and the TS were used to determine the reaction barrier of the  $\beta$ -scission. The activation energy for the  $\beta$ -scission of adduct IX is calculated as:

$$\begin{aligned} E_a &= [\text{Hf}^\circ_{\text{PM3}}(\text{TS}) - \text{Hf}^\circ_{\text{PM3}}(\text{reactant})] \\ &= -17.42 - (-25.6) = 8.18 \text{ kcal/mol.} \end{aligned}$$

The same procedure was applied for the ring opening reactions of adducts X and XI to obtain the corresponding A's and  $E_a$ 's which are listed below.

#### 8.2.2.4.2 Adduct X => Butene-1,4-dial + CHOC.HOH

$$\Delta S^\ddagger_{298} = 0.96 \text{ cal/mol-K, } A = 2.75E13 \text{ s}^{-1},$$

$$E_a = -18.56 - (-27.19) = 8.63 \text{ kcal/mol (see Figure 8.9 for the potential energy diagram).}$$

#### 8.2.2.4.3 Adduct XI => 1-Hydroxy-Butene-4-al-1yl + Glyoxal

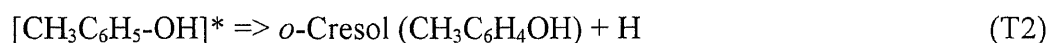
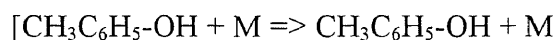
$$\Delta S^\ddagger_{298} = 1.41 \text{ cal/mol-K, } A = 3.45E13 \text{ s}^{-1},$$

$$E_a = -22.4 - (-30.42) = 8.02 \text{ kcal/mol (see Figure 8.10 for the potential energy diagram).}$$

### 8.3 Calculations and Results for the Toluene Photooxidation System

#### 8.3.1 The Chemical Activated Reactions of OH + Toluene

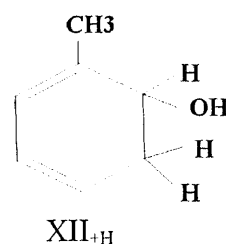
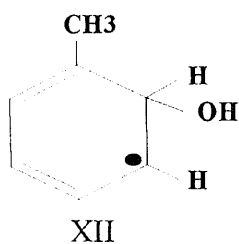
The reactions for the energized toluene-OH adduct resulting from the reaction of toluene with OH radical are parallel to those for benzene-OH adduct: dissociation back to reactants, stabilization and beta-scission to *o*-cresol + H atom, see Figure 8.11. The OH addition to the aromatic ring of toluene was presumed to occur primarily at the ortho position based on the available experimental product data.<sup>4,8,38</sup>



The thermodynamic properties of the toluene-OH adduct (XII, hydroxyl-1-methyl-2,4-cyclohexadien-6-yl) were estimated from its parent molecule (XII<sub>+H</sub>).  $\Delta H_f^\circ_{298}(\text{XII})$  is estimated using bond energy  $DH(\text{HC--H})$  equal to 76.0 kcal/mol and  $HBI(\text{CHD})$  was used to calculate the  $S^\circ_{298}$  and  $C_p(T)$ 's of XII:

$$S_{\text{int}}^\circ_{298}(\text{XII}) = S_{\text{int}}^\circ_{298}(\text{XII}_{+\text{H}}) + \Delta S^\circ_{298}(\text{CHD})$$

$$C_p(T)(\text{XII}) = C_p(T)(\text{XII}_{+\text{H}}) + \Delta C_p(T)(\text{CHD}), 300 \leq T/\text{K} \leq 1000.$$

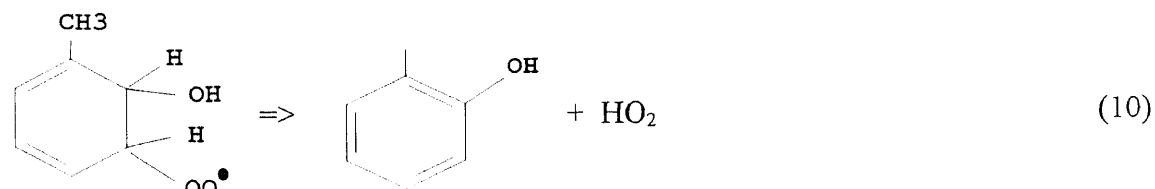
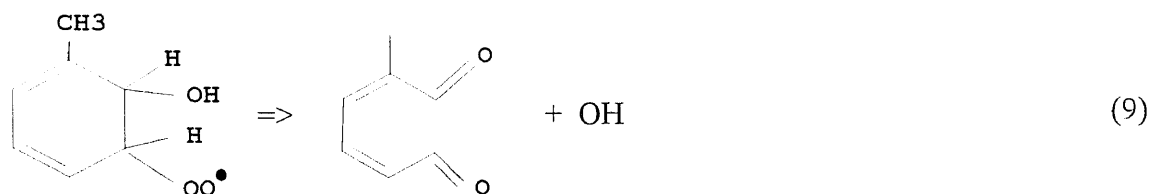
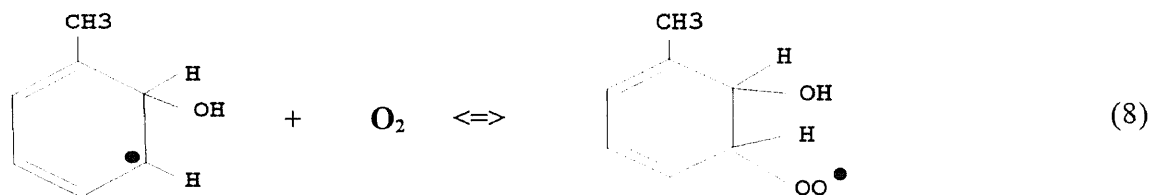


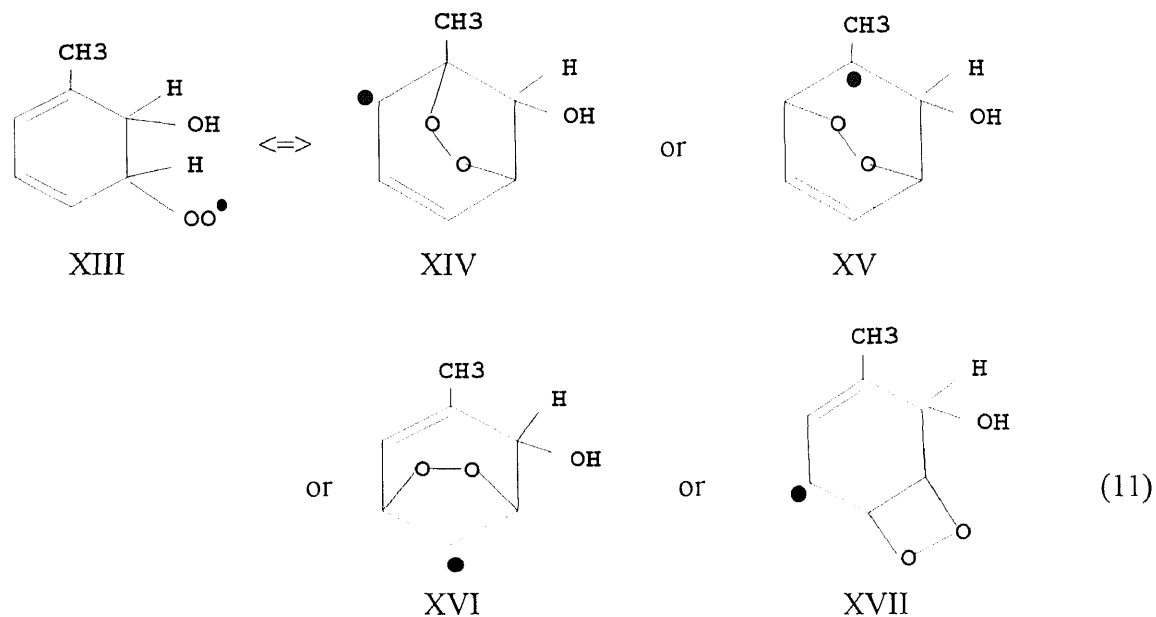


The well depth for toluene + OH  $\Rightarrow$  toluene-OH adduct is calculated to be 19.6 kcal/mol and the potential energy diagram is illustrated in Figure 8.11. The evaluation of A factors and activation energies for (T1), (-T1) and (T2) were carried out following the reaction of benzene + OH. The input data for the QRRK calculation of toluene + OH are give in Table 8.5 where the calculated apparent rate constants are also included. The Arrhenius plot for the apparent rate constants is illustrated in Figure 8.12. The calculated apparent  $k_{f,298}$  of toluene + OH  $\Rightarrow$  toluene-OH adduct is 4.12E12 mol/cc-s which is close to the experimental data, 3.85E12 mol/cc-s.<sup>1</sup> The formation of cresol is the minor reaction path in the temperature regime lower than 500 K.

### 8.3.2 The Chemical Activated Reactions of Toluene-OH Adduct + O<sub>2</sub>

The chemical activated reactions for toluene-OH + O<sub>2</sub> are parallel to benzene-OH + O<sub>2</sub> system, see Figure 8.13 for potential energy diagram for the reaction paths.





The entropies and heat capacities of the above radical adducts were calculated using the GA method (for their parent molecules) incorporated with HBI approach such as the calculations described in section 8.2.2.2. For instance, the entropies of adduct XIII and XIV are calculated as follows:

$$S_{\text{int}}^{\circ}{}_{298}(\text{XIV}) = S_{\text{int}}^{\circ}{}_{298}(\text{XIV}_{+\text{H}}) + \Delta S^{\circ}{}_{298}(\text{CHENEA})$$

$$S_{\text{int}}^{\circ}{}_{298}(\text{XV}) = S_{\text{int}}^{\circ}{}_{298}(\text{XV}_{+\text{H}}) + \Delta S^{\circ}{}_{298}(\text{CHENE})$$

The enthalpies of the above radical adducts were estimated from the GA method (for parent molecules) and the corresponding bond energies,  $D^{\circ}{}_{298}(\text{C--H})$ . The tertiary C--H bond energy (96.30 kcal/mol)<sup>53</sup> was used to estimate  $\Delta H_{\text{f}}^{\circ}{}_{298}(\text{XV})$  after the  $\Delta H_{\text{f}}^{\circ}{}_{298}(\text{XV}_{+\text{H}})$  was determined as -52.93 kcal/mol (using the GA method). Therefore  $\Delta H_{\text{f}}^{\circ}{}_{298}(\text{XV})$  is equal to -8.7 kcal/mol. The adducts XIV and XVII are allylic radicals, and

the secondary allylic C--H bond energy (85.6 kcal/mol)<sup>54</sup> was used to estimate  $\Delta H_f^\circ_{298}(\text{XIV})$  and  $\Delta H_f^\circ_{298}(\text{XVII})$  from  $\Delta H_f^\circ_{298}(\text{XIV}_{+\text{H}})$  and  $\Delta H_f^\circ_{298}(\text{XVII}_{+\text{H}})$ , respectively. The  $\Delta H_f^\circ_{298}(\text{XV})$  was estimated from  $\Delta H_f^\circ_{298}(\text{XV}_{+\text{H}})$  and secondary C--H bond energy (98.45 kcal/mol).<sup>53</sup>

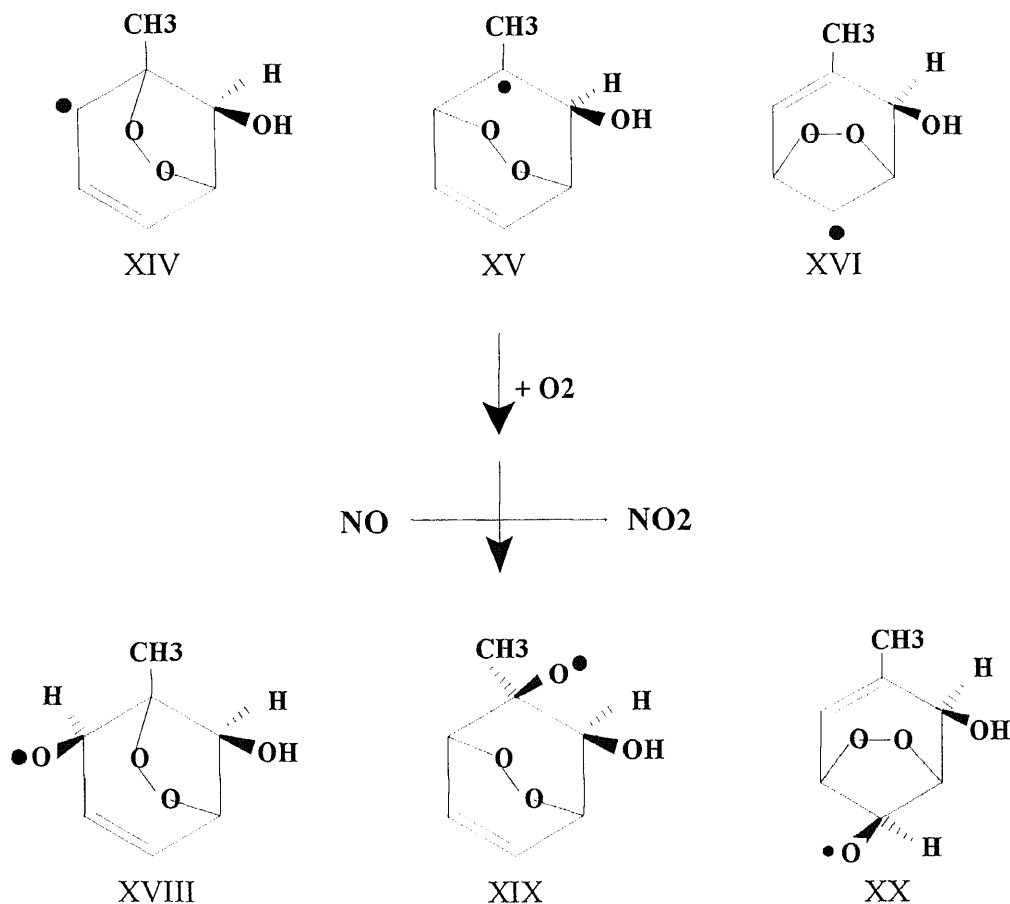
### 8.3.2.1 Quantum RRK Calculation for Toluene-OH + O<sub>2</sub>

The reaction system of toluene-OH + O<sub>2</sub> is similar to that of benzene-OH + O<sub>2</sub>. The potential energy diagram is illustrated in Figure 8.13, and the QRRK input parameters and calculation results are given in Table 8.6. The Arrhenius plot for each reaction channel of the toluene-OH + O<sub>2</sub> reaction system is presented as Figure 8.14. Channel TB is considered to be the major pathway for the formation of *o*-cresol in the toluene photooxidation system. Bicyclic adduct XIV is the key intermediate for subsequent ring opening reactions. Channel TF has very low rate constant due to the high barrier resulting from high ring strain energy and adduct XVII is therefore excluded from further discussion.

### 8.3.3 Ring Cleavage Reactions

The three oxy radicals, XVIII, XIX and XX are formed via the addition of O<sub>2</sub> molecule to adduct XIV, XV and XVI and the subsequent abstraction of one O atom by NO radical. The bicyclic oxy radicals further react via a series of  $\beta$ -scission reactions which lead to the ring cleavage and the formation of final dicarbonyl products and their precursors. The

determination of rate constants for these  $\beta$ -scission reactions are similar to that for adduct IX, X and XI in benzene oxidation system, see section 8.2.2.4.



#### 8.4 Modeling Prediction

The kinetic modeling which contain the important initial reaction mechanisms of atmospheric oxidation of benzene and toluene are given in Table 8.7 and Table 8.8, respectively. The initial concentrations of species in modeling study are [OH]:  $1.0E-8$  ppm, [benzene] or [toluene]: 1 ppm and [NO]: 1 ppm. The selection of [OH]

concentration is based on the average [OH] profile in troposphere, 2.0E5 to 5.0E6 molecule  $\text{cm}^{-3}$ .<sup>58</sup> The first two reactions in Table 8.7 and Table 8.8 are two dummy reactions used to maintain the steady state (SS) of OH concentration, where the AA and BB are two dummy molecules.

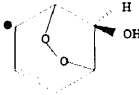
It is important to note that in these modeling calculation:

- All reactions are elementary or treated in a way that the elementary reaction steps are properly incorporated.
- All reactions are reversible
- Reverse reaction rates are calculated from thermodynamics and microscopic reversibility principles in the numerical integration code CHEMKIN<sup>19</sup> and thus automatically incorporated into the mechanisms.

#### **8.4.1 Benzene Photooxidation**

The modeling work is performed to evaluate the effects of the selected reactions to the whole reaction system. Submodel BM1 contains reactions #1 to #6 in Table 8.6 which are mainly the reaction system of benzene + OH plus two dummy reactions for preserving [OH] equal to  $10^{-8}$  ppm. The calculated product profile of submodel BM1 is illustrated in Figure 8.15. Benzene-OH adduct reaches a steady state (SS) within 3 minutes, where the SS presents the equilibrium of forward and backward reactions of benzene + OH = benzene-OH. Phenol grows steadily since no further reactions included in BM1 can consume benzene-OH adduct which decomposes back to reactants and eventually decomposes to phenol + H.

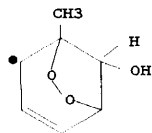
Submodel BM2 includes the mechanism of BM1 plus reactions #7 to #18 in Table 8.7 which are the reactions following benzene-OH + O<sub>2</sub>. Figure 8.16 presents the calculated product profile of submodel BM2. It is surprising to find the adduct V is the only one bicyclic adduct which can be accumulated to significant concentration while the apparent rate constants of the formation of the three bicyclic adducts, V, VI and VII, are estimated in the same order. Adduct V is the primary intermediate in this step with a concentration higher than phenol. The benzene-OH-O<sub>2</sub> adduct is in SS with concentration (10<sup>-7</sup> ppm) one order higher than the benzene-OH adduct (10<sup>-8</sup> ppm). The bicyclic adducts other than adduct V are of inconsiderable amount as adducts VI and VII are in SS of 10<sup>-12</sup>

and 10<sup>-13</sup> ppm, respectively. Adduct V,  is therefore the only one effective bicyclic adduct which leads to ring opening products in benzene photooxidation system.

Model BM3 includes the reactions of ring cleavage. The concentration of selected species as a function of reaction time using model BM3 are illustrated in Figure 8.17. The products of ring fragments are 2-butene-1,4-dial (BDA) and glyoxal (GLY) which are of the same concentration. The subsequent reactions of phenol, BDA, and GLY with the active species in the system.

#### 8.4.2 Toluene Photooxidation

The submodel TM1 which is analogous to BM2 of benzene oxidation contains the reaction systems of toluene + OH and toluene-OH + O<sub>2</sub> (reactions #1 to #21 in Table 8.8) without including the ring opening reactions. The product profile is illustrated in Figure



8.18. Adduct XIV is found to be the only one effective bicyclic adduct of the following ring opening reactions. The *o*-cresol and benzaldehyde are in less concentrations than adduct XIV. The product profile of the entire mechanism listed in Table 8.8 including the ring opening reactions is illustrated as Figure 8.19.

### 8.5 Discussion

An analysis is performed to interpret the fact adduct V is the only one effective bicyclic adduct of the following ring opening reactions in benzene reaction system. The forward rate constants, concentration equilibrium constants and reverse rate constants at 298 K and 1 atm pressure for elementary reactions following benzene-OH + O<sub>2</sub> are listed in Table 8.9.

The rate constant of reaction (A) in Table 8.9 is about 5 orders of magnitude higher than those of BB, BC, BD and BE. Therefore benzene-OH-O<sub>2</sub> is the primary intermediate in the reaction sequence of benzene-OH + O<sub>2</sub>. The benzene-OH-O<sub>2</sub> adduct can either dissociate back to reactants, benzene-OH + O<sub>2</sub> or to phenol + HO<sub>2</sub> through (C1), or isomerize to bicyclic adducts through (C2), (C3) and (C4), see Table 8.9. The benzene-OH-O<sub>2</sub> adduct can also react with NO resulting an oxy radical (ROO. + NO => RO. + NO<sub>2</sub>), but the low concentration of NO (usually ≤ 1 ppm) in the atmosphere makes this reaction path less important than the isomerization of benzene-OH-O<sub>2</sub> to form bicyclic adducts.

The forward reactions of (BA) and (BB) are much more thermodynamically favorable than the corresponding backward reactions. Channels (BA) and (BB) are in fact less reversible at room temperature.

The major reaction pathway of adducts V, VI and VII is the further addition to an oxygen molecule. The rate constant for addition of radicals to O<sub>2</sub> is typically c.a. 5.0E12 cm<sup>3</sup>/mol-s. The reaction rates of adduct V, VI and VII addition to O<sub>2</sub> are therefore  $\leq 4.5E7 \text{ s}^{-1}$  with the concentration of O<sub>2</sub> in the atmosphere, being about 9.0E-6 mol/cm<sup>3</sup> (22% V/V). The backward reaction of channel BE ( $k_{\text{BE}}=8.23E8 \text{ s}^{-1}$ ) and BD ( $k_{\text{BD}}=7.70E8 \text{ s}^{-1}$ ) occurs before the addition of oxygen to adducts VI and VII occurs. Adduct VI and VII therefore cannot be effective to further ring opening reactions under atmospheric condition. The backward constant of channel BC has a rather low rate constant, 8.6E-3 s<sup>-1</sup>, and thus adduct V is the effective intermediate leading to the occurrence of ring cleavage.

The situations of the toluene oxidation system are similar to benzene oxidation system. The experimental works like the smog chamber which simulates the oxidation of toluene under tropospheric conditions resulting in the product profiles: ~0.25 yield of cresols, ~0.10 yield of benzaldehyde and ~0.25 yield of the fragments of aromatic ring cleavage and 0.40 unknown products.<sup>30</sup> Our model includes only the important initial steps of toluene photooxidation, and the results are not completely comparable. However, the features of our model present a good connection to the experimental data.



## 8.6 Summary

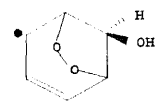
We have applied the Group Additivity and semiempirical Molecular Orbital methods to the determinations of thermodynamic properties and Transition State structures for the study of benzene and toluene photooxidation. These properties, along with literature experimental data on kinetics, have been utilized to determine rate constants for reactions relevant to photooxidation of aromatics species.

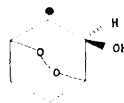
Quantum Rice-Ramsperger-Kassel (QRRK) calculations were performed to evaluate pressure effects and to obtain apparent rate constants of reactions from adduct formation. The data are then used to develop components of reaction mechanisms for benzene and toluene photooxidation in the atmosphere. These mechanisms are used in CHEMKIN2<sup>19</sup> interpreter and integrator. All reactions in the mechanisms are considered by the integrator in both forward and reverse directions via principles of Microscopic Reversibility (MR).

The equilibrium controlled by kinetic parameters which incorporate the enthalpy and entropy of reactants, reaction adducts and products at room temperature are found to play a significant role in the overall reactions. Section 8.5 interprets how the microscopic equilibrium effects the overall rates of the benzene-OH adduct + O<sub>2</sub> reactions.

According to our initial analysis, only one effective channel will lead to ring cleavage in benzene photo-oxidation. The key bicyclic intermediate leading to ring

cleavage products, for example, in benzene oxidation system is adduct V,





which was frequently assumed to be adduct VI, in most other previous studies. The reason adduct V is the favored species of importance is that V is an allylic radical (i.e. resonance stabilized) with a intermediate ring strain energy (c.a. 14 kcal/mol, see section 8.2.2.2.1) while other bicyclic adducts (adduct VI and adduct VII) are not allylic radicals with the similar ring strain energy or allylic (adduct VIII) with a high ring strain energy (c.a. 39 kcal/mol).

APPENDIX A

TABLES FOR SECTION I

**Table 2.1** Definition of HBI Group Term Name, Model Radicals and Corresponding Bond Energy of C-H Bond

<i>HBI</i> <sup>a</sup>	<i>BDE</i> <sup>b</sup> <i>D(R--H)</i> ( <i>kcal/mol</i> )	<i>Definition</i>	<i>Model Radicals</i>
<i>CCJ</i>	101.1	primary alkyl radicals	CH <sub>3</sub> C.H <sub>2</sub>
<i>RCCJ</i>	101.1	primary alkyl radicals	CH <sub>3</sub> (CH <sub>2</sub> ) <sub>n</sub> C.H <sub>2</sub>
<i>ISOBUTYL</i>	101.1	primary alkyl radicals	(CH <sub>3</sub> ) <sub>2</sub> CHC.H <sub>2</sub>
<i>NEOPENTYL</i>	101.1	primary alkyl radicals	(CH <sub>3</sub> ) <sub>3</sub> CC.H <sub>2</sub>
<i>CCJC</i>	98.45	secondary alkyl radicals	CH <sub>3</sub> C.HCH <sub>3</sub>
<i>RCCJC</i>	98.45	secondary alkyl radicals	CH <sub>3</sub> (CH <sub>2</sub> ) <sub>n</sub> C.HCH <sub>3</sub>
<i>RCCJCC</i>	98.45	secondary alkyl radicals	CH <sub>3</sub> (CH <sub>2</sub> ) <sub>n</sub> C.HCH <sub>2</sub> CH <sub>3</sub>
<i>RCJR</i>	98.45	secondary alkyl radicals, (large molecules)	CH <sub>3</sub> (CH <sub>2</sub> ) <sub>n</sub> C.H(CH <sub>2</sub> ) <sub>n</sub> -CH <sub>3</sub> , n>1
<i>TERTALKYL</i>	96.3	tertiary alkyl radicals	(CH <sub>3</sub> ) <sub>3</sub> C.
<i>VIN,</i>	111.2	vinyl radicals	CH <sub>2</sub> =C.H
<i>VINS,</i>	109	1-alkyl vinyl radicals	CH <sub>2</sub> =C.CH <sub>3</sub>
<i>ALLYL_P,</i>	88.2	allyl radicals	CH <sub>2</sub> =CHC.H <sub>2</sub>
<i>ALLYL_S,</i>	85.6	1-alkyl allyl radicals	CH <sub>2</sub> =CHC.HCH <sub>3</sub>
<i>ALLYL_T,</i>	83.4	1,1-diallyl radicals	CH <sub>2</sub> =CHC.(CH <sub>3</sub> ) <sub>2</sub>
<i>BENZYL_P,</i>	88.5	benzyl radicals	(C <sub>6</sub> H <sub>5</sub> )-C.H <sub>2</sub>
<i>BENZYL_S,</i>	85.9	1-alkyl benzyl radicals	(C <sub>6</sub> H <sub>5</sub> )-C.HCH <sub>3</sub>
<i>BENZYL_T,</i>	83.8	1,1-dialkyl benzyl radicals	(C <sub>6</sub> H <sub>5</sub> )-C.(CH <sub>3</sub> ) <sub>2</sub>
<i>C≡CJ</i>	132.7	acetylenic	HC≡C.
<i>C≡CCJ</i>	89.4	propargyl	HC≡CC.H <sub>2</sub>
<i>C≡CCJC</i>	87.0	secondary propargyl	HC≡CC.HCH <sub>3</sub>
<i>C≡CCJC2</i>	84.5	tertiary propargyl	HC≡CC.(CH <sub>3</sub> ) <sub>2</sub>
<i>C=C=CJ</i>	89.0	allenic	CH <sub>2</sub> =C=C.H
<i>C=CJC=C</i>	99.8		CH <sub>2</sub> =C.CH=CH <sub>2</sub>
<i>C=CCJC=C</i>	76.0		CH <sub>2</sub> =CHC.HCH=CH <sub>2</sub>
<i>C=CC=CCJ</i>	80.0		CH <sub>2</sub> =CHCH=CHC.H <sub>2</sub>
<i>CJC=CC=C</i>	81.0		C.H <sub>2</sub> CH=CHC≡CH

<sup>a</sup> 'J' in HBI Group ID indicates the radical center located on carbon just before J, for example, *CJC* = C.H<sub>2</sub>CH<sub>3</sub>. <sup>b</sup> BDE = bond dissociation energy of corresponding C-H bond for the imagined parent molecule which the radical is generated through the reaction: RH => R. + H.

Literature Sources for the Bond Energies in HBI data base:

1. **CCJ, RCCJ, ISOBUTYL, NEOPENTYL, CCJC, RCCJC, RCCJCC, RCJCR, TERTALKYL**

The bond energies are evaluated from the following literature data:

- (1) Seakins, P. W., Pilling, M. J., Nitranen, J. T., Gutman, D., Krasnoperov, L. N., *J. Phys. Chem.* **1992**, *96*, 9847,
- (2) Nicovich, J. M., van Dijk, C. A., Kreutter, K. D., and Wine, P. H., *J. Phys. Chem.* **1991**, *95*, 9890,
- (3) Russell, J. J., Seetula, J. A., Gutman, D., *J. Am. Chem. Soc.* **1988**, *110*, 3092,
- (4) Gutman, D., *Acc. Chem. Res.* **1990**, *23*, 375,
- (5) CH<sub>3</sub>C.HCH<sub>3</sub>. Chen, Y., Rauk, A., and Tschuikow-Roux, E., *J. Phys. Chem.* **1990**, *94*, 2775.  
CH<sub>3</sub>CH<sub>2</sub>C.HCH<sub>3</sub>, *ibid.* **1990**, *94*, 6250.

2. **VINYL**

- (1) Ervin, K. M., Gronert, S., Barlow, S. E., Gilles, M. K., Harrison, A. G., Bierbaum, V. M., Depuy, C. H., Lineberger, c., Ellison, B., *J. Am. Chem. Soc.* **1990**, *112*, 5750;
- (2) Wu, C. J., and Carter, E. A., *J. Phys. Chem.* **1991**, *95*, 8352;
- (3) Curtiss, L. A., and Pople, J. A., *J. Chem. Phys.* **1988**, *88*, 7405;
- (4) Defrees, D. J., McIver Jr. R. T., Hehre, W. J., *J. Am. Chem. Soc.* **1980**, *102*, 3334.

3. **VINS**

Vinyl adjusted for difference between primary and secondary in alkyls

4. **ALLYL\_P**

Tsang, W., *J. Phys. Chem.* **1992**, *96*, 8378

5. **ALLYL\_S**

Roth, R. W., Bauer, F., Beitat, A., Ebbecht, T., Wustefeld, M., *Chem. Ber.* **1991**, *124*, 1453;

6. **ALLYL\_T**

Tertiary allylic adjusted to have same difference from allyls as tertiary from secondary. Trends reported in McMillen, D. F., and Golden, D. M., *Ann. Rev. Phys. Chem* **1982**, *33*, 493.

7. **BENZYL\_P**

- (1) Gunion, R., Gilles, M., Polak, M. and Lineberger, W. C., *Int. J. Mass Spectrometry and Ion Physics* **1993**
- (2) Defrees, D. J., McIver Jr, R. T., Hehre, W. J., *J. Am. Chem. Soc.* **1980**, *102*, 3334.
- (3) Robaugh, D. A., and Stein, S. E., *J. Am. Chem. Soc.* **1986**, *108*, 3224,
- (4) Tsang, W., Walker, J., *J. Phys. Chem.* **1990**, *94*, 3324

8. **BENZYL\_S, BENZYL\_T**

- (1) Robaugh, D. A., and Stein, S. E., *J. Am. Chem. Soc.* **1986**, *108*, 3224,
- (2) Hippler, H. and Troe, J., *J. Phys. Chem.* **1990**, *94*, 3803.

9. **PHCJPH**

Ajusted from **BENZYL\_P**

10. **C≡CJ**

- (1) Ervin, K. M., Gronert, S., Barlow, S. E., Gilles, M. K., Harrison, A. G., Bierbaum, V. M., Depuy, C. H., Lineberger, c., Ellison, B., *J. Am. Chem. Soc.* **1990**, *112*, 5750.
- (2) Curtiss, L. A., and Pople, J. A., *J. Chem. Phys.* **1988**, *88*, 7405;
- (3) Kiefer, J. H., Sidhu, S. S., Kern, R. D., Xie, K., Chen, H. and Harding, L. B., *Combust. Sci. and Tech.* **1992**, *82*, 101.

(4) Wagner, A., and Keifer, J., *24th Symposium (International) on Combustion (Proc.)*, The Combustion Institute, **1992**, 1107.

11.  $C\equiv CCJ$

(1) Tsang, W., *J. Phys. Chem. Ref. Data* **1988**, 17, 109;

(2) Orlov, Y. D., and Lebedev, Y. A., *Russian. J. Phys. Chem.* **1991**, 65, 153.

12.  $C\equiv CCJC$ ,  $C\equiv CCJC_2$

Orlov, Y. D., and Lebedev, Y. A., *Russian. J. Phys. Chem.* **1991**, 65, 153.

13.  $CJ=C=C$

Miller, J. A., Melius, K. F., *24th Symposium (International) on Combustion (Proc.)*, The Combustion Institute, **1992**.

14.  $C=CCJ=C$

(1) Melius, K. F., and Miller, J. A., *23th Symposium (International) on Combustion (Proc.)*, The Combustion Institute, **1990**;

(2) Kuhnel, V. W., Gey, E., Ondruschka, B., *Z. Phys. Chemie, Leipzig* **1987**, 268, 23.

15.  $C=CCJC=C$ ,  $C=CC=CCJ$

(1) McMillen, D. F., and Golden, D. M., *Ann. Rev. Phys. Chem.* **1982**, 33, 493.

(2) Holmes, J., *J. Phys. Org. Chem.* **1992**

16.  $CJC=CC\equiv C$

Green, I. G. and Walton, J. *Chem. Soc., Perkin Trans II* **1984**, 1253.

**Table 2.2** Fundamental Vibration Frequencies ( $\text{cm}^{-1}$ ) for Model Stable Molecules and Free Radicals

Molecule	Frequencies	Note	Radical	Frequencies	Note
$\text{C}_2\text{H}_2$	612(x2), 730(x2), 1974, 3289, 3374	ref. 23	$\text{C}_2\text{H}$	( $2\Sigma^+$ ) 371.6(x2), 1840, 3328 ( $2\Pi$ ) 560(x2), 1850, 3460	ref. 27
$\text{C}_2\text{H}_4$	826, 943, 949, 1023, 1236, 1342, 1444, 1623, 2989, 3103, 3106, 3206	ref. 23	$\text{CH}_2=\text{C}\cdot\text{H}$	785, 825, 920, 1185, 1445, 1670, 3115, 3190, 3265	ref. 34
$\text{C}_2\text{H}_6^*$	822(x2), 955, 955, 1190(x2), 1379, 1388, 1468(x2), 1469(x2), 2954, 2969(x2), 2985(x2)	ref. 23	$\text{C}_2\text{H}_5$	541, 713, 948, 1123, 1206, 1370, 1427, 1445, 1462, 2842, 2920, 2987, 3033, 3112	ref. 20, 21
$\text{CH}_2=\text{C}=\text{CH}_2$	328(x2), 633(x2), 931, 1053(x2), 1382, 1452(x2), 2142, 2918, 3008(x2), 3334	ref. 23	$\text{CH}_2=\text{C}=\text{C}\cdot\text{H}$	378, 392, 708, 747, 801, 946, 1151, 1342, 1996, 3000(x3)	b
Propene* ( $\text{C}_3\text{H}_6$ )	428, 575, 912, 914, 945, 990, 1045, 1174, 1298, 1378, 1419, 1443, 1459, 1653, 2932, 2953, 2973, 2991, 3017, 3091	a	$\text{CH}_2=\text{CHC}\cdot\text{H}_2$ (allyl)	426, 503, 530, 763, 781, 912, 969, 1018, 1201, 1235, 1378, 1463, 1467, 3041, 3062, 3074, 3167, 3174	c
			$\text{CH}_2=\text{C}\cdot\text{CH}_3$	241, 385, 805, 899, 912, 945, 1023, 1246, 1359, 1363, 1369, 1905, 3000(x5)	b
$\text{C}_3\text{H}_8$ ( 2 internal rotors )	369, 748, 869, 922, 940, 1054, 1158, 1192, 1278, 1472, 1338, 1378, 1392, 1451, 1462, 1464, 1476, 2887, 2887, 2962, 2967, 2968, 2968, 2973, 2977	ref. 23	$i\text{-C}_3\text{H}_7$ ( 1 internal rotors )	337, 426, 836, 917, 932, 1029, 1089, 1159, 1342, 1408, 1411, 1460, 1467, 1470, 1475, (2900x7)	ref. 24
			tert-Butyl	200, 541(x2), 733, 992(x2), 1126, 1189(x2), 1252(x2), 1279, 1370(x3), 1455(x6), 2825(x2), 2931(x6)	ref. 25

\* Molecule has one internal rotor.

<sup>a</sup> Dewar, M. J. S. and Ford, G. P., *J. Am. Chem. Soc.* **1977**, *99*, 1685. <sup>b</sup> This work, PM3 MO calculations.<sup>c</sup> Sim, F. *et al.*, *J. Chem. Phys.* **1991**, *95*, 4317.

**Table 2.3** Assignment of Vibration Frequency in this Work

<i>Symbol</i>	<i>Freq.<sup>a</sup></i>	<i>Approximate type of mode</i>
CT-H	3400	C-H stretch (next to C≡C triple bond)
CD-H	3100	C-H stretch (next to C=C double bond)
C-H	3000	C-H stretch (next to C-C single bond)
H-C-H	1400	H-C-H bend (CH <sub>3</sub> or CH <sub>2</sub> deform)
H-V-H,W	950	H-C-H wag in C=CH <sub>2</sub> vinyl group
H-A-H	500	H-C-H wag in C=C-C.H <sub>2</sub> allyl group
H-C-C	1150	H-C-C bend (CH <sub>3</sub> , CH <sub>2</sub> twist & wag)
H-C-C,TR	850	CH <sub>3</sub> rock in methyl group -CH <sub>3</sub>
H-C-C,R	750	CH <sub>2</sub> rock in chain -CH <sub>2</sub> - group
H-A-C	500	C=C-C.HC wag in allyl group
H-C#C,u <sup>b</sup>	730	C-H bond bend (symmetric, u) in C≡CH
H-C#C,g	610	C-H bond bend (symmetry g) in C≡CH
H-C#C.	372	H-C#C. bend, ethynyl radical
H-C=C	1050	H-C=C bend, (CH <sub>2</sub> wag & twist)
H-C.=C	785	H-C.=C bend, 2 ½ CC bond
=C=C-H	840	CH <sub>2</sub> wag in allene
C=CC.,OP	770	C=C-C. bend in allyl group
CH,BEND	500	C-H bend
CCC,S	370	C-C-C deform, symmetric
CCC,A	440	C-C-C deform, asymmetric
CC.C,S	540	C-C-.C deform in allyl group, symmetric
CC.C,A	730	C-C-.C deform in allyl group, asymmetric
C-C=C	420	C-C=C deform, single bond & double bond
C-C.=C	310	C-C.=C deform, single bond & 2 ½ bond
C-A-C	540	C=C-C.C <sub>2</sub> wag in allyl group
C=C	1650	C=C double bond stretch
C=C.	1900	C=C. 2 & ½ bond stretch
C-C	1000	C-C single bond stretch
C-.C	1350	C-.C 1 & ½ bond stretch
C=C,TR	1000	torsion of double bond
H <sub>2</sub> C=CC,TR	800	torsion of double bond
PH-CH <sub>2</sub>	450	torsion of PH-C.H <sub>2</sub>
PH-CHC	260	torsion of PH-C.HC
PH-C <sub>2</sub>	200	torsion of PH-C.C <sub>2</sub>
INV-H <sub>3</sub>	600	inversion of C.H <sub>3</sub>
INV-CH	420	inversion of -C.HC
INV-H <sub>2</sub>	550	inversion of -C.H <sub>2</sub>
INV-C <sub>2</sub>	200	inversion of -C.C <sub>2</sub>

<sup>a</sup> Frequency in cm<sup>-1</sup>, <sup>b</sup> # represents triple bond.

Reference source of the assignment: ref. 11, ref. 23-27 and MNDO/PM3 semiempirical Molecular Orbital calculation, see text.

**Table 2.4** Moments of Inertia ( $I_r$ )<sup>a</sup>, Torsion Barriers ( $V$ )<sup>b</sup> and Foldness Numbers ( $\sigma$ )<sup>c</sup> to Hindered Rotation about Single Bonds

Rotor	$I_r$	$V$	$\sigma$	Source*	Comment
MOLECULE:					
CH3-CH3	1.6	2.9	3	1	
RCH2-CH3	3.1	3.3	3	2	large molecule
CH3-C2H5	2.85	3.3	3	1	
RCH2-C2H5	20.76	3.3	3	1	
(CH3)2CH-CH3	3.07	3.8	3	1	
RCH(CH3)-CH3	3.1	3.8	3	Assigned	large molecule
R2CH-CH3	3.1	3.8	3	Assigned	large molecule
CH3-C(CH3)3	3.1	4.7	3	1	
CH3-VIN	2.81	2.1	3	3	VIN: -CH=CH2
CH3-VINR	3.1	2.1	3	Assigned	large molecule
CC-VINR	20.76	2.1	3	Assigned	large molecule
CH3-PH	3.09	0	6	1	PH: phenyl, -C6H5
C2H5-PH	20.24	0	2	Assigned	
(CH3)2CH-PH	40.55	0	2	Assigned	
CH3-BENZYL	3.14	1.65	3	1	BENZYL: -CH2(C6H5)
RADICAL:					
CH3-CH2	1.15	0.1	6	2	
RCH2-CH2	1.77	0.1	2	Assigned	
CH2-C2H5	1.68	0.1	6	2	
CH2-CH(CH3)2	1.77	0.17	6	2	
CH2-C(CH3)3	1.78	0.16	6	2	
CH3-C.HCH3	2.89	0.7	3	2	
CH3-C.(CH3)2	3.03	1.5	3	2	
CH3C.H-C2H5	13.1	2.16	3	2	

<sup>a</sup> Unit: amu-Å<sup>2</sup>. <sup>b</sup> Unit: kcal/mol. <sup>c</sup> number of maximum points in potential energy surface of internal rotation from torsion angle 0° to 360°. <sup>d</sup> barriers are assigned approximately in this work.

\* Source of rotational barriers (for general review of hindered internal rotations, see ref. 22.):

1. ref. 11
2. ref. 13
3. ref. 37



**Table 2.5** Calculation Details of HBI  $\Delta S^{\circ}_{298}$  and  $\Delta C_p(T)$  Values

<i>CCJ</i>							
	$S^{\circ}_{int\ 298}$	$C_{p300}$	$C_{p400}$	$C_{p500}$	$C_{p600}$	$C_{p800}$	$C_{p1000}$
- 1 x C-H _ 3000cm <sup>-1</sup> :	0	0	-0.005	-0.025	-0.075	-0.26	-0.51.0
- 2 x H-C-H _ 1400cm <sup>-1</sup> :	-0.035	-0.212	-0.653	-1.176	-1.66	-2.391	-2.855
- 1 x H-C-C.TR _ 850cm <sup>-1</sup> :	-0.167	-0.573	-0.954	-1.228	-1.416	-1.638	-1.754
+ 1 x INV-H2 _ 550cm <sup>-1</sup> :	0.538	1.14	1.444	1.616	1.72	1.831	1.885
- 1 x rotor _ CH3-CH3 :	-3.864	-2.018	-2.041	-1.936	-1.801	-1.562	-1.404
+ 1 x rotor _ CH3-CH2 :	4.756	1.008	1.002	1	0.998	0.995	0.995
Total Increment	1.228	-0.654	-1.207	-1.75	-2.235	-3.024	-3.634
<i>RCCJ</i>							
	$S^{\circ}_{int\ 298}$	$C_{p300}$	$C_{p400}$	$C_{p500}$	$C_{p600}$	$C_{p800}$	$C_{p1000}$
- 1 x C-H _ 3000cm <sup>-1</sup> :	0	0	-0.005	-0.025	-0.075	-0.26	-0.501
- 2 x H-C-H _ 1400cm <sup>-1</sup> :	-0.035	-0.212	-0.653	-1.176	-1.66	-2.391	-2.855
- 1 x H-C-C.TR _ 850cm <sup>-1</sup> :	-0.167	-0.573	-0.954	-1.228	-1.416	-1.638	-1.754
+ 1 x INV-H2 _ 550cm <sup>-1</sup> :	0.538	1.14	1.444	1.616	1.72	1.831	1.885
- 1 x rotor _ RCH2-CH3 :	-4.283	-2.13	-2.19	-2.099	-1.96	-1.7	-1.512
+ 1 x rotor _ RCH2-CH2 :	5.183	1.006	1.001	0.999	0.997	0.996	0.995
Total Increment	1.236	-0.769	-1.357	-1.914	-2.395	-3.162	-3.741
<i>ISOBUTYL</i>							
	$S^{\circ}_{int\ 298}$	$C_{p300}$	$C_{p400}$	$C_{p500}$	$C_{p600}$	$C_{p800}$	$C_{p1000}$
- 1 x C-H _ 3000cm <sup>-1</sup> :	0	0	-0.005	-0.025	-0.075	-0.26	-0.501
- 2 x H-C-H _ 1400cm <sup>-1</sup> :	-0.035	-0.212	-0.653	-1.176	-1.66	-2.391	-2.855
- 1 x H-C-C.TR _ 850cm <sup>-1</sup> :	-0.167	-0.573	-0.954	-1.228	-1.416	-1.638	-1.754
+ 1 x INV-H2 _ 550cm <sup>-1</sup> :	0.538	1.14	1.444	1.616	1.72	1.831	1.885
- 1 x rotor _ CH3-IPROPYL :	-3.558	-1.899	-2.092	-2.102	-2.023	-1.805	-1.612
+ 1 x rotor _ CH2-IPROPYL :	4.756	1.008	1.003	1.000	0.998	0.995	0.995
Total Increment	1.534	-0.536	-1.257	-1.916	-2.458	-3.267	-3.842
<i>NEOPENTYL</i>							
	$S^{\circ}_{int\ 298}$	$C_{p300}$	$C_{p400}$	$C_{p500}$	$C_{p600}$	$C_{p800}$	$C_{p1000}$
- 1 x C-H _ 3000cm <sup>-1</sup> :	0	0	-0.005	-0.025	-0.075	-0.26	-0.501
- 1 x H-C-H _ 1400cm <sup>-1</sup> :	-0.017	-0.106	-0.326	-0.588	-0.83	-1.195	-1.427
- 1 x H-C-H _ 1400cm <sup>-1</sup> :	-0.017	-0.106	-0.326	-0.588	-0.83	-1.195	-1.427
- 1 x H-C-C.TR _ 850cm <sup>-1</sup> :	-0.167	-0.573	-0.954	-1.228	-1.416	-1.638	-1.754
+ 1 x INV-H2 _ 550cm-1:	0.538	1.14	1.444	1.616	1.72	1.831	1.885
- 1 x rotor _ CH3-TBUTYL :	-3.864	-1.953	-2.156	-2.231	-2.212	-2.039	-1.831
+ 1 x rotor _ CH2-TBUTYL :	5.182	1.008	1.001	0.999	0.998	0.997	0.996
Total Increment	1.654	-0.59	-1.323	-2.046	-2.646	-3.499	-4.059

**Table 2.5** Calculation Details of HBI  $\Delta S^{\circ}_{298}$  and  $\Delta C_p(T)$  Values (continued)

<i>CCJC</i>		$S^{\circ}_{int\ 298}$	$C_{p300}$	$C_{p400}$	$C_{p500}$	$C_{p600}$	$C_{p800}$	$C_{p1000}$
- 1 x	C-H _ 3000cm <sup>-1</sup> :	0	0	-0.005	-0.025	-0.075	-0.26	-0.501
- 1 x	H-C-H _ 1400cm <sup>-1</sup> :	-0.017	-0.106	-0.326	-0.588	-0.83	-1.195	-1.427
- 1 x	H-C-C _ 1150cm <sup>-1</sup> :	-0.049	-0.24	-0.554	-0.849	-1.086	-1.403	-1.586
- 1 x	H-C-C,R _ 750cm <sup>-1</sup> :	-0.248	-0.737	-1.113	-1.361	-1.524	-1.709	-1.803
+ 1 x	INV-CH _ 420cm <sup>-1</sup> :	0.884	1.427	1.645	1.76	1.826	1.894	1.927
- 2 x	rotor _ CH3-C2H5 :	-8.417	-4.228	-4.362	-4.184	-3.913	-3.395	-3.021
+ 2 x	rotor _ CH3-C.HCH3 :	10.98	2.584	2.351	2.229	2.159	2.088	2.052
	Total Increment	3.132	-1.301	-2.364	-3.02	-3.444	-3.979	-4.359
<i>RCCJC</i>		$S^{\circ}_{int\ 298}$	$C_{p300}$	$C_{p400}$	$C_{p500}$	$C_{p600}$	$C_{p800}$	$C_{p1000}$
- 1 x	C-H _ 3000cm <sup>-1</sup> :	0	0	-0.005	-0.025	-0.075	-0.26	-0.501
- 1 x	H-C-H _ 1400cm <sup>-1</sup> :	-0.017	-0.106	-0.326	-0.588	-0.83	-1.195	-1.427
- 1 x	H-C-C _ 1150cm <sup>-1</sup> :	-0.049	-0.24	-0.554	-0.849	-1.086	-1.403	-1.586
- 1 x	H-C-C,R _ 750cm <sup>-1</sup> :	-0.248	-0.737	-1.113	-1.361	-1.524	-1.709	-1.803
+ 1 x	INV-CH _ 420cm <sup>-1</sup> :	0.884	1.427	1.645	1.76	1.826	1.894	1.927
- 1 x	rotor _ RCH2-CH3 :	-4.283	-2.13	-2.19	-2.099	-1.96	-1.7	-1.512
- 1 x	rotor _ RCH2-C2H5 :	-6.081	-2.296	-2.291	-2.166	-2.007	-1.727	-1.527
- 1 x	rotor _ R-C3H8 :	-6.945	-2.314	-2.302	-2.174	-2.013	-1.729	-1.529
+ 1 x	rotor _ RCC.H-CH3 :	5.577	1.295	1.177	1.116	1.08	1.044	1.026
+ 1 x	rotor _ RCH2-C.HCH3 :	7.417	1.326	1.191	1.125	1.086	1.048	1.029
+ 1 x	rotor _ R-CC.C :	7.499	2.232	1.993	1.772	1.603	1.384	1.259
	Total Increment	3.755	-1.545	-2.775	-3.491	-3.901	-4.351	-4.644
<i>RCCJCC</i>		$S^{\circ}_{int\ 298}$	$C_{p300}$	$C_{p400}$	$C_{p500}$	$C_{p600}$	$C_{p800}$	$C_{p1000}$
- 1 x	C-H _ 3000cm <sup>-1</sup> :	0	0	-0.005	-0.025	-0.075	-0.26	-0.501
- 1 x	H-C-H _ 1400cm <sup>-1</sup> :	-0.017	-0.106	-0.326	-0.588	-0.83	-1.195	-1.427
- 1 x	H-C-C _ 1150cm <sup>-1</sup> :	-0.049	-0.24	-0.554	-0.849	-1.086	-1.403	-1.586
- 1 x	H-C-C,R _ 750cm <sup>-1</sup> :	-0.248	-0.737	-1.113	-1.361	-1.524	-1.709	-1.803
+ 1 x	INV-CH _ 420cm <sup>-1</sup> :	0.884	1.427	1.645	1.76	1.826	1.894	1.927
- 1 x	rotor _ RCH2-CH3 :	-4.208	-2.114	-2.181	-2.092	-1.956	-1.698	-1.511
- 1 x	rotor _ RCH2-C2H5 :	-6.081	-2.296	-2.291	-2.166	-2.007	-1.727	-1.527
- 2 x	rotor _ R-C3H8 :	-13.889	-4.628	-4.604	-4.347	-4.025	-3.458	-3.057
+ 1 x	rotor _ RC.C-CH3 :	4.803	2.101	1.918	1.724	1.571	1.369	1.251
+ 2 x	rotor _ RCC.-CC :	14.834	2.652	2.382	2.249	2.172	2.096	2.057
+ 1 x	rotor _ R-CC.CC :	7.499	2.232	1.993	1.772	1.603	1.384	1.259
	Total Increment	3.527	-1.711	-3.135	-3.924	-4.333	-4.705	-4.917

**Table 2.5** Calculation Details of HBI  $\Delta S^{\circ}_{298}$  and  $\Delta C_p(T)$  Values (continued)

<i>TERTALKYL</i>							
	$S^{\circ}_{\text{int } 298}$	$C_{p300}$	$C_{p400}$	$C_{p500}$	$C_{p600}$	$C_{p800}$	$C_{p1000}$
- 1 x C-H _ 3000cm <sup>-1</sup> :	0	0	-0.005	-0.025	-0.075	-0.26	-0.501
- 1 x CCC,S _ 370cm <sup>-1</sup> :	-1.071	-1.534	-1.715	-1.808	-1.86	-1.914	-1.94
- 2 x CCC,A _ 440cm <sup>-1</sup> :	-1.638	-2.767	-3.232	-3.478	-3.621	-3.771	-3.842
- 3 x H-C-C _ 1150cm <sup>-1</sup> :	-0.148	-0.721	-1.662	-2.548	-3.258	-4.208	-4.757
+ 2 x CC,C,S _ 540cm <sup>-1</sup> :	1.118	2.325	2.92	3.255	3.457	3.673	3.778
+ 1 x CC,C,A _ 730cm <sup>-1</sup> :	0.268	0.774	1.146	1.388	1.545	1.722	1.812
+ 1 x INV-C2 _ 200cm <sup>-1</sup> :	2.123	1.84	1.903	1.932	1.949	1.965	1.973
- 3 x rotor _ CH3-IPROP :	-12.275	-6.201	-6.612	-6.556	-6.259	-5.527	-4.917
+ 3 x rotor _ CH3-C.(CH3)2 :	15.485	5.502	4.781	4.288	3.97	3.575	3.377
Total Increment	3.861	-0.783	-2.476	-3.551	-4.154	-4.745	-5.017
<i>HC=C(2Σ')</i>							
	$S^{\circ}_{\text{int } 298}$	$C_{p300}$	$C_{p400}$	$C_{p500}$	$C_{p600}$	$C_{p800}$	$C_{p1000}$
- 1 x C-H _ 3000cm <sup>-1</sup> :	0	0	-0.005	-0.025	-0.075	-0.26	-0.501
- 2 x H-C#C,G _ 610cm <sup>-1</sup> :	-0.854	-2.023	-2.69	-3.085	-3.329	-3.594	-3.726
- 2 x H-C#C,U _ 730cm <sup>-1</sup> :	-0.536	-1.547	-2.292	-2.776	-3.089	-3.444	-3.624
+ 2 x H-C#C _ 372cm <sup>-1</sup> :	2.126	3.06	3.425	3.612	3.718	3.827	3.879
Total Increment	0.735	-0.511	-1.561	-2.275	-2.775	-3.471	-3.972
<i>VIN</i>							
	$S^{\circ}_{\text{int } 298}$	$C_{p300}$	$C_{p400}$	$C_{p500}$	$C_{p600}$	$C_{p800}$	$C_{p1000}$
- 1 x C-H _ 3000cm <sup>-1</sup> :	0	0	-0.005	-0.025	-0.075	-0.26	-0.501
- 1 x H-C-H _ 1400cm <sup>-1</sup> :	-0.017	-0.106	-0.326	-0.588	-0.83	-1.195	-1.427
- 1 x H-V-H,W _ 950cm <sup>-1</sup> :	-0.112	-0.436	-0.806	-1.097	-1.306	-1.563	-1.702
- 1 x H-C=C _ 1050cm <sup>-1</sup> :	-0.075	-0.326	-0.672	-0.97	-1.195	-1.484	-1.645
+ 1 x H-C=C _ 785cm <sup>-1</sup> :	0.216	0.677	1.057	1.315	1.487	1.684	1.787
Total Increment	0.012	-0.192	-0.753	-1.365	-1.92	-2.818	-3.489
<i>C=C=CJ</i>							
	$S^{\circ}_{\text{int } 298}$	$C_{p300}$	$C_{p400}$	$C_{p500}$	$C_{p600}$	$C_{p800}$	$C_{p1000}$
- 1 x C-H _ 3000cm <sup>-1</sup> :	0	0	-0.005	-0.025	-0.075	-0.26	-0.501
- 1 x H-C-H _ 1400cm <sup>-1</sup> :	-0.017	-0.106	-0.326	-0.588	-0.83	-1.195	-1.427
- 1 x H-V-H,W _ 950cm <sup>-1</sup> :	-0.112	-0.436	-0.806	-1.097	-1.306	-1.563	-1.702
- 1 x =C=CH2 _ 840cm <sup>-1</sup> :	-0.174	-0.588	-0.97	-1.242	-1.427	-1.645	-1.76
+ 1 x H-C=C _ 785cm <sup>-1</sup> :	0.216	0.677	1.057	1.315	1.487	1.684	1.787
Total Increment	-0.087	-0.454	-1.05	-1.637	-2.152	-2.979	-3.603
<i>VINS</i>							
	$S^{\circ}_{\text{int } 298}$	$C_{p300}$	$C_{p400}$	$C_{p500}$	$C_{p600}$	$C_{p800}$	$C_{p1000}$
- 1 x C-H _ 3000cm <sup>-1</sup> :	0	0	-0.005	-0.025	-0.075	-0.26	-0.501
- 1 x H-C-C _ 1150cm <sup>-1</sup> :	-0.049	-0.24	-0.554	-0.849	-1.086	-1.403	-1.586
- 1 x H-C-C _ 1050cm <sup>-1</sup> :	-0.075	-0.326	-0.672	-0.97	-1.195	-1.484	-1.645
- 1 x C=C-C _ 420cm <sup>-1</sup> :	-0.884	-1.427	-1.645	-1.76	-1.826	-1.894	-1.927
+ 1 x C-C=C _ 310cm <sup>-1</sup> :	1.251	1.616	1.767	1.843	1.885	1.929	1.95
Total Increment	0.434	-0.338	-1.206	-1.944	-2.52	-3.34	-3.906

**Table 2.5** Calculation Details of HBI  $\Delta S^{\circ}_{298}$  and  $\Delta C_p(T)$  Values (continued)

<i>ALLPYL_P</i>							
	$S^{\circ}_{int\ 298}$	$C_{p300}$	$C_{p400}$	$C_{p500}$	$C_{p600}$	$C_{p800}$	$C_{p1000}$
- 1 x C-H _ 3000cm <sup>-1</sup> :	0	0	-0.005	-0.025	-0.075	-0.26	-0.501
- 2 x H-C-H _ 1400cm <sup>-1</sup> :	-0.035	-0.212	-0.653	-1.176	-1.66	-2.391	-2.855
- 1 x H-C-C _ 1150cm <sup>-1</sup> :	-0.049	-0.24	-0.554	-0.849	-1.086	-1.403	-1.586
- 1 x H-C-C.TR _ 850cm <sup>-1</sup> :	-0.167	-0.573	-0.954	-1.228	-1.416	-1.638	-1.754
- 1 x C=C _ 1650cm <sup>-1</sup> :	-0.006	-0.044	-0.182	-0.389	-0.611	-0.993	-1.262
- 1 x C-C _ 1000cm <sup>-1</sup> :	-0.091	-0.378	-0.737	-1.033	-1.251	-1.524	-1.674
+ 1 x H-A-H _ 500cm <sup>-1</sup> :	0.651	1.251	1.524	1.674	1.763	1.857	1.903
+ 2 x C=CC.OP _ 770cm <sup>-1</sup> :	0.459	1.405	2.161	2.67	3.005	3.39	3.587
+ 2 x C-C _ 1350cm <sup>-1</sup> :	0.043	0.251	0.729	1.27	1.757	2.474	2.92
- 1 x rotor _ VIN-CH3 :	-4.744	-2.075	-1.887	-1.694	-1.544	-1.351	-1.237
Total Increment	-3.94	-0.616	-0.558	-0.78	-1.119	-1.838	-2.458
<i>ALLYL_S</i>							
	$S^{\circ}_{int\ 298}$	$C_{p300}$	$C_{p400}$	$C_{p500}$	$C_{p600}$	$C_{p800}$	$C_{p1000}$
- 1 x C-H _ 3000cm <sup>-1</sup> :	0	0	-0.005	-0.025	-0.075	-0.26	-0.501
- 1 x H-C-H _ 1400cm <sup>-1</sup> :	-0.017	-0.106	-0.326	-0.588	-0.83	-1.195	-1.427
- 1 x H-C-C _ 1150cm <sup>-1</sup> :	-0.049	-0.24	-0.554	-0.849	-1.086	-1.403	-1.586
- 1 x H-C-C.R _ 750cm <sup>-1</sup> :	-0.248	-0.737	-1.113	-1.361	-1.524	-1.709	-1.803
- 1 x C-C _ 1000cm <sup>-1</sup> :	-0.091	-0.378	-0.737	-1.033	-1.251	-1.524	-1.674
- 1 x C=C _ 1650cm <sup>-1</sup> :	-0.006	-0.044	-0.182	-0.389	-0.611	-0.993	-1.262
+ 1 x C=CC.OP _ 770cm <sup>-1</sup> :	0.229	0.702	1.081	1.335	1.503	1.695	1.794
+ 1 x H-A-C _ 520cm <sup>-1</sup> :	0.603	1.206	1.492	1.651	1.746	1.847	1.896
+ 2 x C-C _ 1350cm <sup>-1</sup> :	0.043	0.251	0.729	1.27	1.757	2.474	2.92
- 1 x rotor _ VIN-CC :	-6.206	-2.152	-1.907	-1.691	-1.531	-1.335	-1.221
- 1 x rotor _ RCH-CH3 :	-4.283	-2.13	-2.19	-2.099	-1.96	-1.7	-1.512
+ 1 x rotor _ RVIN-CH3 :	4.835	2.089	1.894	1.699	1.547	1.352	1.238
Total Increment	-5.19	-1.539	-1.819	-2.081	-2.315	-2.751	-3.139
<i>ALLYL_T</i>							
	$S^{\circ}_{int\ 298}$	$C_{p300}$	$C_{p400}$	$C_{p500}$	$C_{p600}$	$C_{p800}$	$C_{p1000}$
- 1 x C-H _ 3000cm <sup>-1</sup> :	0	0	-0.005	-0.025	-0.075	-0.26	-0.501
- 2 x H-C-C _ 1150cm <sup>-1</sup> :	-0.099	-0.481	-1.108	-1.699	-2.172	-2.805	-3.172
- 1 x C-C _ 1000cm <sup>-1</sup> :	-0.091	-0.378	-0.737	-1.033	-1.251	-1.524	-1.674
- 1 x C=C _ 1650cm <sup>-1</sup> :	-0.006	-0.044	-0.182	-0.389	-0.611	-0.993	-1.262
+ 2 x C-C _ 1350cm <sup>-1</sup> :	0.043	0.251	0.729	1.27	1.757	2.474	2.92
+ 1 x C-A-C _ 540cm <sup>-1</sup> :	0.559	1.162	1.46	1.628	1.729	1.836	1.889
- 1 x rotor _ VIN-CH(ME)2 :	-6.505	-2.201	-1.958	-1.739	-1.574	-1.365	-1.245
- 2 x rotor _ R2CH-CH3 :	-8.642	-4.279	-4.369	-4.153	-3.865	-3.347	-2.976
+ 2 x rotor _ RVIN-CH3 :	9.67	4.178	3.788	3.398	3.094	2.705	2.475
Total Increment	-5.071	-1.792	-2.382	-2.742	-2.967	-3.279	-3.545

**Table 2.5** Calculation Details of HBI  $\Delta S^{\circ}_{298}$  and  $\Delta C_p(T)$  Values (continued)

<i>BENZYL_P</i>							
	$S^{\circ}_{\text{int } 298}$	$C_{p300}$	$C_{p400}$	$C_{p500}$	$C_{p600}$	$C_{p800}$	$C_{p1000}$
- 1 x C-H _ 3000cm <sup>-1</sup> :	0	0	-0.005	-0.025	-0.075	-0.26	-0.501
- 2 x H-C-H _ 1400cm <sup>-1</sup> :	-0.035	-0.212	-0.653	-1.176	-1.66	-2.391	-2.855
- 1 x H-C-C _ 1150cm <sup>-1</sup> :	-0.049	-0.24	-0.554	-0.849	-1.086	-1.403	-1.586
- 1 x H-C-C,TR _ 850cm <sup>-1</sup> :	-0.167	-0.573	-0.954	-1.228	-1.416	-1.638	-1.754
+ 2 x H-C.-C _ 770cm <sup>-1</sup> :	0.459	1.405	2.161	2.67	3.005	3.39	3.587
+ 1 x PH-CH2 _ 450cm <sup>-1</sup> :	0.788	1.361	1.601	1.729	1.803	1.881	1.918
- 1 x rotor _ PH-CH3 :	-5.735	-0.993	-0.993	-0.993	-0.993	-0.993	-0.993
Total Increment	-4.739	0.747	0.604	0.126	-0.422	-1.414	-2.183
<i>BENZYL_S</i>							
	$S^{\circ}_{\text{int } 298}$	$C_{p300}$	$C_{p400}$	$C_{p500}$	$C_{p600}$	$C_{p800}$	$C_{p1000}$
- 1 x C-H _ 3000cm <sup>-1</sup> :	0	0	-0.005	-0.025	-0.075	-0.26	-0.501
- 1 x H-C-H _ 1400cm <sup>-1</sup> :	-0.017	-0.106	-0.326	-0.588	-0.83	-1.195	-1.427
- 1 x H-C-C _ 1150cm <sup>-1</sup> :	-0.049	-0.24	-0.554	-0.849	-1.086	-1.403	-1.586
- 1 x H-C-C,R _ 750cm <sup>-1</sup> :	-0.248	-0.737	-1.113	-1.361	-1.524	-1.709	-1.803
+ 1 x PH-CHC _ 260cm <sup>-1</sup> :	1.652	1.746	1.847	1.896	1.923	1.951	1.964
+ 1 x CH.BEND _ 500cm <sup>-1</sup> :	0.651	1.251	1.524	1.674	1.763	1.857	1.903
- 1 x rotor _ PH-CC :	-7.547	-0.993	-0.993	-0.993	-0.993	-0.993	-0.993
- 1 x rotor _ PHC-C :	-4.321	-2.139	-2.184	-2.076	-1.932	-1.673	-1.488
+ 1 x rotor _ RVIN-CH3 :	4.835	2.089	1.894	1.699	1.547	1.352	1.238
Total Increment	-5.044	0.869	0.089	-0.625	-1.207	-2.073	-2.694
<i>BENZYL_T</i>							
	$S^{\circ}_{\text{int } 298}$	$C_{p300}$	$C_{p400}$	$C_{p500}$	$C_{p600}$	$C_{p800}$	$C_{p1000}$
- 1 x C-H _ 3000cm <sup>-1</sup> :	0	0	-0.005	-0.025	-0.075	-0.26	-0.501
- 2 x H-C-C _ 1150cm <sup>-1</sup> :	-0.099	-0.481	-1.108	-1.699	-2.172	-2.805	-3.172
+ 1 x PH-CC2 _ 200cm <sup>-1</sup> :	2.123	1.84	1.903	1.932	1.949	1.965	1.973
- 1 x rotor _ PH-CC3 :	-8.388	-0.993	-0.993	-0.993	-0.993	-0.993	-0.993
- 2 x rotor _ R2CH-CH3 :	-8.642	-4.279	-4.369	-4.153	-3.865	-3.347	-2.976
+ 2 x rotor _ RVIN-CH3 :	9.67	4.178	3.788	3.398	3.094	2.705	2.475
Total Increment	-5.336	0.265	-0.784	-1.54	-2.061	-2.735	-3.193

**Table 2.6** Standard Entropy and Heat Capacities for Species Used Directly to Calculate HBI Group Values

	$S_{\text{int } 298}^{\circ}$	$C_{p300}$	$C_{p400}$	$C_{p500}$	$C_{p600}$	$C_{p800}$	$C_{p1000}$	$C_{p1500}$
Stable molecules:								
$\text{CH}_2=\text{C}=\text{CH}_2$	58.3	14.16	17.21	19.82	22	25.42	28	32.07
$\text{CH}_3\text{C}\equiv\text{CH}$	59.3	14.55	17.33	19.74	21.8	25.14	27.71	32.8
$\text{CH}_2=\text{C}=\text{CHCH}_3$	70.45	19.41	23.72	27.52	30.79	36.02	39.95	46.08
$\text{CH}_2=\text{CHCH}=\text{CH}_2$	66.62	19.11	24.29	28.52	31.84	36.84	40.52	46.27
$\text{CH}\equiv\text{CCH}_2\text{CH}_3$	69.58	19.55	23.87	27.63	30.83	35.95	39.84	46.98
$\text{CH}_2=\text{CHCH}=\text{CHCH}_3$	76.4	24.9	31.2	36.6	40.9	47.7	52.6	60.32
$\text{CH}_2=\text{CHCH}_2\text{CH}=\text{CH}_2$	79.7	25.2	31.3	36.5	40.8	47.6	52.7	60.57
$\text{CH}_2=\text{C}=\text{C}(\text{CH}_3)_2$	75.82	25.54	31.14	36.1	40.34	47.19	52.35	60.4
$\text{CH}\equiv\text{CCH}_2(\text{CH}_3)_2$	76.31	24.78	30.76	35.95	40.32	47.21	52.32	61.48
$\text{CH}_3\text{CH}=\text{CHC}\equiv\text{CH}$	75.36	22.66	28.19	31.95	36.5	41.83	45.79	51.94
Free radicals:								
$\text{CH}_2=\text{C}=\text{CH}\cdot$	60.97	13.71	16.16	18.18	19.85	22.44	24.4	27.49
$\text{C}\cdot\text{H}_2\text{C}\equiv\text{CH}$	..	..	..	..	..	..	..	..
$\text{CH}_2=\text{C}\cdot\text{CH}=\text{CH}_2$	70.09	19.3	23.53	27.01	29.83	34.14	37.35	42.41
$\text{CH}\equiv\text{C}\cdot\text{HCH}_3$	69.56	18.96	22.67	25.88	28.64	33.04	36.35	41.5
$\text{CH}\cdot=\text{C}=\text{CHCH}_3$	..	..	..	..	..	..	..	..
$\text{CH}_2=\text{CHCH}=\text{CHC}\cdot\text{H}_2$	75.65	23.07	29.34	34.62	38.91	45.4	50.1	57.36
$\text{CH}_2=\text{CHC}\cdot\text{HCH}=\text{CH}_2$	..	..	..	..	..	..	..	..
$\text{CH}\equiv\text{CCH}\cdot(\text{CH}_3)_2$	77.11	25.09	30.09	34.46	38.19	44.21	48.75	55.82
$\text{C}\cdot\text{H}=\text{C}=\text{C}(\text{CH}_3)_2$	..	..	..	..	..	..	..	..
$\text{C}\cdot\text{H}_2\text{CH}=\text{CHC}\equiv\text{CH}$	73.99	21.57	26.57	30.62	33.87	38.76	42.31	47.82

Source of thermodynamic properties:

Molecule:

 $\text{CH}_2=\text{C}=\text{CH}_2$ ,  $\text{CH}_3\text{C}\equiv\text{CH}$ ,  $\text{CH}_2=\text{CHCH}=\text{CH}_2$ ,  $\text{HC}\equiv\text{CCH}_2\text{CH}_3$ , (trans)  $\text{CH}_2=\text{CHCH}=\text{CHCH}_3$ , $\text{CH}_2=\text{CHCH}_2\text{CH}=\text{CH}_2$ , ref. 41 $\text{CH}_2=\text{C}=\text{CHCH}_3$ ,  $\text{CH}=\text{C}=\text{C}(\text{CH}_3)_2$ ,  $\text{CH}\equiv\text{CCH}(\text{CH}_3)_2$ ,  $\text{CH}\equiv\text{CCH}=\text{CHCH}_3$ , ref. 16.

Radical:

(1) this work. MNDO/PM3 molecular orbital calculation, see text and Table 2.7.

 $\text{CH}_2=\text{C}=\text{C}\cdot\text{H}$  (equal to  $\text{C}\cdot\text{H}_2\text{C}\equiv\text{CH}$ ),  $\text{CH}_2=\text{C}\cdot\text{CH}=\text{CH}_2$ ,  $\text{CH}_2=\text{CHCH}=\text{CHC}\cdot\text{H}_2$  (equal to $\text{CH}_2=\text{CHC}\cdot\text{HCH}=\text{CH}_2$ ),  $\text{CH}\equiv\text{CCH}=\text{CHC}\cdot\text{H}_2$ .(2) Use  $\text{C}=\text{C}=\text{CJ}$  HBI Group values derived in this work: $\text{CH}\cdot=\text{C}=\text{CHCH}_3$  (equal to  $\text{CH}\equiv\text{C}\cdot\text{HCH}_3$ ), apply  $\text{C}^*\text{C}^*\text{CJ}$  on  $\text{CH}_2=\text{C}=\text{CHCH}_3$  (data in this Table). $\text{C}\cdot\text{H}=\text{C}=\text{C}(\text{CH}_3)_2$  (equal to  $\text{CH}\equiv\text{C}\cdot(\text{CH}_3)_2$ ), apply  $\text{C}^*\text{C}^*\text{CJ}$  on  $\text{CH}_2=\text{C}=\text{CH}(\text{CH}_3)_2$  (data in this Table).

**Table 2.7** Molecular Weight, Moments of Inertia for External Rotation and Fundamental Vibration Frequencies for the Radicals in Table 2.6

<i>Radical</i>	<i>I</i>	<i>Vibrational Frequency (cm<sup>-1</sup>)</i>
CH <sub>2</sub> =C.CH=CH <sub>2</sub>	1.339, 0.150, 0.139	212, 217, 379, 446, 557, 821, 837, 865, 916, 948, 1048, 1183, 1265, 1324, 1440, 1995, 3000(x5)
CH <sub>2</sub> =CHCH=CHC.H <sub>2</sub> (CH <sub>2</sub> =CHC.HCH=CH <sub>2</sub> )	0.321, 0.136, 0.095	154, 193, 264, 430, 483, 558, 604, 802, 818, 845, 890, 937, 957, 982, 1168, 1218, 1221, 1253, 1263, 1373, 1448, 1513, 1576, 3000(x7)
C.H <sub>2</sub> CH=CHC≡CH	1.319, 0.082, 0.077	133, 186, 416, 420, 476, 574, 751, 803, 835, 860, 910, 930, 1092, 1169, 1232, 1295, 1464, 1494, 2137, 3000(x5)

\*I : Moments of Inertia (cm<sup>-1</sup>)**Table 2.8** Data Base for HBI Group for Hydrocarbon Radicals

	D°(R-H)	ΔS <sup>o</sup> <sub>int 298*</sub>	ΔC <sub>p300</sub>	ΔC <sub>p400</sub>	ΔC <sub>p500</sub>	ΔC <sub>p600</sub>	ΔC <sub>p800</sub>	ΔC <sub>p1000</sub>
<i>CCJ</i>	101.1	2.61	-0.65	-1.21	-1.75	-2.24	-3.02	-3.63
<i>RCCJ</i>	101.1	2.61	-0.77	-1.36	-1.91	-2.4	-3.16	-3.74
<i>ISOBUTYL</i>	101.1	2.91	-0.54	-1.26	-1.92	-2.46	-3.27	-3.84
<i>NEOPENTYL</i>	101.1	3.03	-0.59	-1.32	-2.05	-2.65	-3.5	-4.06
<i>CCJC</i>	98.45	4.51	-1.3	-2.36	-3.02	-3.44	-3.98	-4.36
<i>RCCJC</i>	98.45	5.13	-1.54	-2.77	-3.49	-3.9	-4.35	-4.64
<i>RCCJCC</i>	98.45	4.9	-1.71	-3.14	-3.92	-4.33	-4.71	-4.92
<i>RCJR</i>	98.45	4.44	-1.5	-2.33	-3.1	-3.39	-3.75	-4.45
<i>TERTALKYL</i>	96.3	5.24	-0.78	-2.48	-3.55	-4.15	-4.75	-5.02
<i>VIN</i>	111.2	1.39	-0.19	-0.75	-1.36	-1.92	-2.82	-3.49
<i>VINS</i>	109	1.81	-0.34	-1.21	-1.94	-2.52	-3.34	-3.91
<i>ALLYL_P</i>	88.2	-2.56	-0.62	-0.56	-0.78	-1.12	-1.84	-2.46
<i>ALLYL_S</i>	85.6	-3.81	-1.54	-1.82	-2.08	-2.32	-2.75	-3.14
<i>ALLYL_T</i>	83.4	-3.69	-1.79	-2.38	-2.74	-2.97	-3.28	-3.55
<i>BENZYL_P</i>	88.5	-4.74	0.75	0.60	0.13	-0.42	-1.41	-2.18
<i>BENZYL_S</i>	85.9	-5.04	0.87	0.09	-0.63	-1.21	-2.07	-2.69
<i>BENZYL_T</i>	83.8	-5.34	0.27	-0.78	-1.54	-2.06	-2.74	-3.19
<i>C≡CJ</i>	132.7	2.11	-0.51	-1.56	-2.27	-2.78	-3.47	-3.97
<i>C≡CCJ</i>	89.4	-0.51	-0.84	-1.17	-1.56	-1.95	-2.7	-3.31
<i>C≡CCJC</i>	87	-0.45	-0.59	-1.2	-1.75	-2.19	-2.91	-3.49
<i>C≡CCJC2</i>	84.5	1.48	-0.04	-1.01	-1.74	-2.41	-3.19	-3.65
<i>C=C=CJ</i>	89	1.29	-0.45	-1.05	-1.64	-2.15	-2.98	-3.6
<i>C=CJC=C</i>	99.8	0.71	0.19	-0.76	-1.51	-2.01	-2.7	-3.17
<i>C=CCJC=C</i>	76	-4.05	-2.13	-1.96	-1.88	-1.89	-2.2	-2.6
<i>C=CC=CCJ</i>	80	-1.55	-1.83	-1.86	-1.98	-1.99	-2.3	-2.5
<i>CJC=CC=C</i>	81	-3.55	-1.09	-1.62	-2.01	-2.63	-3.07	-3.48

\* include electronic spin degeneracy

**Table 2.9** Comparison of Calculated Thermodynamic Data from this Study with Literature

	$\Delta H_f^{\circ}{}_{298}$	$S^{\circ}{}_{int, 298}{}^c$	$C_{p300}$	$C_{p400}$	$C_{p500}$	$C_{p600}$	$C_{p800}$	$C_{p1000}$	$C_{p1500}$
<b>HC≡C.</b>									
SANDIA 1990	134.01	49.57	8.92	9.61	10.21	10.72	11.56	12.18	13.29
W. TSANG 1986		49.52	8.89	9.57	10.24	10.7	11.51	12.17	13.27
BURCAT 1993	130.66	50.98	10.04						
J.H.KIFFER'92			9.22	9.93	10.46	10.89	11.61	12.20	13.22
THIS WORK	134.46	51.51	10.05	10.42	10.71	10.96	11.47	11.95	12.92
<b>CH<sub>3</sub>C.H<sub>2</sub></b> (ethyl)									
SANDIA 1990	28.02	60.14	11.32	13.60	15.59	18.29	22.58	25.5	29.56
JACS 1986		59.3	12.11	14.91	17.39	19.58	23.20	25.98	30.41
W. TSANG 1986		59.37	12.13	14.66	17.18	19.22	22.84	25.65	30.24
BURCAT 1993	28.36	59.06	12.07						
N. COHEN 1992		59.23	12.18	14.8	17.24	19.42	23.01	25.82	30.33
THIS WORK	28.6	59.87	11.73	14.47	17.05	19.34	23.02	25.91	30.56
<b>CH<sub>3</sub>CH<sub>2</sub>C.H<sub>2</sub></b> (n-propyl)									
SANDIA 1990	22.60	64.14	18.10	22.27	25.98	29.23	34.37	38.29	44.31
W. TSANG		69.17	17.10		25.37				44.48
BURCAT 1993	24.02	69.18	17.02						
N. COHEN 1992		69.26	17.14	21.62	25.48	28.82	34.17	38.27	44.82
THIS WORK	23.67	69.29	17.11	21.27	25.14	28.53	33.95	38.14	44.7
<b>C.H<sub>2</sub>CH(CH<sub>3</sub>)<sub>2</sub></b> (iso-butyl)									
W. TSANG		76.79	22.99		33.95				58.89
N. COHEN 1992		75.78	22.68	28.51	33.73	38.25	45.28	50.63	59.21
THIS WORK	16.5	76.03	22.34	28.16	33.46	38.02	45.21	50.62	59.26



**Table 2.9** Comparison of Calculated Thermo Data from this Study with Literatures  
(continued)

	$\Delta H_f^\circ_{298}$	$S^\circ_{int, 298}^\circ$	$C_{p300}$	$C_{p400}$	$C_{p500}$	$C_{p600}$	$C_{p800}$	$C_{p1000}$	$C_{p1500}$
<b>CH<sub>3</sub>C.HCH<sub>3</sub></b>									
(iso-propyl)									
JANAF 1986		68.94	16.38	20.42	24.19	27.56	33.19	37.53	44.14
W. TSANG 1988		69.3	15.93	19.91	23.9	27.15	32.88	37.24	44.18
T-ROUX 1990		68.9	16.66	20.47	24.26	27.68	33.33	37.66	44.42
BURCAT 1993	22.30	69.15	15.81						
N. COHEN 1992		69.03	16.59	20.28	24.13	27.51	33.18	37.51	44.44
THIS WORK	21.02	69.01	16.58	20.27	24.03	27.49	33.13	37.52	44.37
<b>CH<sub>3</sub>CH<sub>2</sub>C.HCH<sub>3</sub></b>									
(2-n-butyl)									
T. ROUX 1990		81.65	22.65	28	33.09	37.52	44.52	50.25	58.82
BURCAT 1993	16.97	79.82	20.87						
N. COHEN 1992		80.44	21.82	27.1	32.37	36.92	44.33	49.96	58.94
THIS WORK	16.09	80.42	21.84	26.81	31.81	36.38	43.83	49.58	58.42
<b>(CH<sub>3</sub>)<sub>3</sub>C.</b>									
(tert-butyl)									
JANAF 1986		75.97							
W. TSANG 1990		76.51	18.79		29.77				58.15
BURCAT 1993	12.35	76.37	18.65						
N. COHEN 1992		75.19	22.48	27.42	32.27	36.79	43.91	49.58	58.66
THIS WORK	11.7	75.67	22.33	27.04	31.82	36.27	43.62	49.34	58.53
<b>CH<sub>2</sub>=CHC.H<sub>2</sub></b>									
(allyl)									
W. TSANG 1991		62.2	14.56	18.02	21.48	24.02	28.39	31.6	36.67
BURCAT 1993	40.41	65.62	15.74						
SANDIA	38.65	64.75	16.07	19.55	22.72	25.53	29.99	32.89	37.43
THIS WORK	40.75	62.05	14.83	18.67	21.94	24.67	28.9	32.03	36.9

**Table 3.1** Literature Survey of Standard Enthalpy of Formation (298K) (kcal/mol)

Species	$\Delta H_f^\circ_{298}$	Note	Species	$\Delta H_f^\circ_{298}$	Note
HOOH	-32.6 <sup>a</sup>	1	CH <sub>3</sub> OO.	6.7	13
	-32.53	2		6.1	6
FOOF	15	1		2.70±0.79 <sup>a</sup>	14
ClOOCl	33	1	CH <sub>2</sub> FOO. <sup>b</sup> (G)	-41.34	6
CH <sub>3</sub> OOCH <sub>3</sub>	-30.0	3	(T)	-39.49	6
	-30.1 <sup>a</sup>	4		-40.42 <sup>a</sup>	15
CF <sub>3</sub> OOCF <sub>3</sub>	-360.53±3.11	5	CHF <sub>2</sub> OO. <sup>c</sup> (G)	-95.9	6
C <sub>2</sub> H <sub>5</sub> OOC <sub>2</sub> H <sub>5</sub>	-46.1	4	(T)	-95.5	6
ClOOH	1.0 <sup>a</sup>	1		-95.7 <sup>a</sup>	15
	0.3	6	CF <sub>3</sub> OO.	-161.56	8
	0.2±1	7		-149.9 <sup>a</sup>	6
FOOH	-8.75 <sup>a</sup>	1	CH <sub>2</sub> ClOO. <sup>b</sup> (G)	1.2	6
CH <sub>3</sub> OOH	-31.3	3	(T)	2.2	6
	-31.34±0.19	8		1.7	15
	-33.2 <sup>a</sup>	9		-1.84 <sup>a</sup>	16
CF <sub>3</sub> OOH	-196.53±3.11 <sup>a</sup>	8	CHCl <sub>2</sub> OO. <sup>c</sup> (G)	-1.4	6
	-193	10	(T)	-1.0	6
CH <sub>2</sub> ClOOH	-37.74 <sup>a</sup>	9		-1.2	15
CHCl <sub>2</sub> OOH	-40.88 <sup>a</sup>	9		-4.98 <sup>a</sup>	19
CCl <sub>3</sub> OOH	-36.69 <sup>a</sup>	9	CCl <sub>3</sub> OO.	-0.7	6
C <sub>2</sub> H <sub>5</sub> OOH	-47.6	11		-0.79 <sup>a</sup>	17
	-41.09 <sup>a</sup>	9	C <sub>2</sub> H <sub>5</sub> OO.	-2.3	6
CH <sub>3</sub> CHClOOH	-48.98 <sup>a</sup>	9		-5.19 <sup>a</sup>	18
CH <sub>2</sub> =CHOOH	-7.6 <sup>a</sup>	9	CH <sub>3</sub> CHClOO.	-9.8	6
CH <sub>2</sub> =CClOOH	-16.97 <sup>a</sup>	9		-13.08 <sup>a</sup>	19
CH≡CCH <sub>2</sub> OOH	22.42 <sup>a</sup>	9	C <sub>2</sub> H <sub>2</sub> CH <sub>2</sub> OOH	13.6	6
CH <sub>2</sub> =CHCH <sub>2</sub> OOH	-15.43 <sup>a</sup>	9	CH <sub>2</sub> =CHOO.	28.3 <sup>a</sup>	6
(CH <sub>3</sub> ) <sub>2</sub> CHOOH	-48.58 <sup>a</sup>	9	CH <sub>2</sub> =CClOO.	18.93 <sup>a</sup>	20
(CH <sub>3</sub> ) <sub>3</sub> COOH	-54.83 <sup>a</sup>	9	CH≡CCH <sub>2</sub> OO.	58.32 <sup>a</sup>	21
ClOO.	33.6 <sup>a</sup>	6	CH <sub>2</sub> =CHCH <sub>2</sub> OO.	20.47 <sup>a</sup>	22
FOO.	22.6 <sup>a</sup>	6	(CH <sub>3</sub> ) <sub>2</sub> CHOO.	-12.68 <sup>a</sup>	23
HOO.	3.01±0.41 <sup>a</sup>	12	(CH <sub>3</sub> ) <sub>3</sub> COO.	-18.93 <sup>a</sup>	24
	2.5	13			
	3.6	6			

<sup>a</sup> recommended data adopted into this thermodynamic data base.

<sup>b</sup> (G) = gauche conformation, dihedral angle of HCOO = 60°, (T) = trans conformation, dihedral angle of HCOO = 180°.

<sup>c</sup> (G) = gauche conformation, dihedral angle of ClCOO or FCOO = 60°; (T) = trans conformation, dihedral angle of ClCOO or FCOO = 180°.

- Colussi, A. J.; Grela, M. A. *J. Phys. Chem.* **1993**, *97*, 3775, and reference therein.
- Giguère, P. A.; Liu, I. D. *J. Am. Chem. Soc.* **1955**, *77*, 6477.
- DeMore, W. B. *et al. JPL Publication 92-20*, Jet Propulsion Laboratory, **1992**: Pasadena, CA.
- Baker, G.; Littlefair, J. H.; Shaw, R. and Thynne, J. C. J., *J. Chem. Soc.* **1965**, 6970.
- Levy, J. B.; Kennedy, R. C. *J. Am. Chem. Soc.* **1972**, *94*, 3302.

6. Melius, C. F. "BAC-MP4 Heats of Formation and Free Energies" 1993, Sandia National Laboratories, Livermore, California.
7. Lee, T. J.; Rendell, A. P. *J. Phys. Chem.* **1993**, *97*, 6999.
8. Francisco, J. S.; Williams, I. H. *Int. J. Chem. Kinet.*, **1989**, *20*, 455: TABLE II and reference therein.
9. This work, estimated from  $\Delta H_f^\circ_{298}(\text{ROO}\cdot)$  recommended in this Table.  $\Delta H_f^\circ_{298}(\text{H}\cdot) = 52.1$ , and  $D^\circ(\text{ROO-H}) = 88$ , see text.
10. NIST Standard Reference Database 25, version 1.0, 1991. National Bureau of Standards and Technology. Gaithersburg, MD, USA
11. Kozolov, N. A., and Rabinovich, *Tr. po Knim. i khim. Tekhnol.* **1964**, *2*, 189; *Chem. Abstr.* **1965**, *63*, 6387.
12. Hills, A. J.; Howard, C. J. *J. Chem. Phys.* **1984**, *81*, 4458.
13. Tsang, W.; Hampson, R. F. *J. Phys. Chem. Ref. Data* **1986**, *15*, 1087, and reference therein.
14. Slagle, I. R.; Gutman, D. *J. Am. Chem. Soc.* **1985**, *107*, 5342.
15. Average value of  $\Delta H_f^\circ_{298}$  of (G) and (T) conformers listed above.
16. this work. use  $D^\circ(\text{CH}_2\text{Cl-OO})=28.92$  and  $D^\circ(\text{CHCl}_2\text{-OO})=25.33$  from Russel, J. J. *et al.*, (*J. Phys. Chem.*, **1990**, *94*, 3277). incorporate with  $\Delta H_f^\circ_{298}(\text{CH}_2\text{Cl})=27.08$  and  $\Delta H_f^\circ_{298}(\text{CHCl}_2)=20.35$  (from Kee, R. J. and Miller, J. A., The Chemkin Thermodynamic Data Base, SAND87-8215 UC4, **1987**. Sandia National Lab., Livermore, C.A.), respectively.
17. This work. use  $D^\circ(\text{CCl}_3\text{-OO})=19.04$  from Russel, J. J. *et al.*, (*Symp. (Int'l) Combust., Proc.*, **1990**, *23*, 895). coupled with  $\Delta H_f^\circ_{298}(\text{CCl}_3)=19.04$  (from Kee, R. J. and Miller, J. A., see note 16 of this Table).
18. Wanger, A. F. *et al.*, *J. Phys. Chem.*, **1990**, *94*, 1853.
19. Knyazev, V. D. *et al.*, *J. Phys. Chem.*, **1994**, in press.
20. This work. estimated from  $D^\circ(\text{CH}_2=\text{CCl-OO}\cdot) = 42.5$  incorporated with  $\Delta H_f^\circ_{298}(\text{CH}_2=\text{CHC}\cdot\text{H}_2) = 61.43$  (Melius, C. F. see note 6 of this Table).  $D^\circ(\text{CH}_2=\text{CCl-OO}\cdot)$  estimated from Dean & Bozzelli's  $\Delta H_f^\circ_{298}(\text{R-OH})$  and  $\Delta H_f^\circ_{298}(\text{R-OO}\cdot)$  regressed relationship (Figure 14, ref. 27(b)).
- 21, 22 & 23: This work. estimated from  $D^\circ(\text{HC}\equiv\text{CCH}_2\text{-OO}) = 24.37$ .  $D^\circ((\text{CH}_2=\text{CHCH}_2\text{-OO}) = 19.83$  and  $D^\circ((\text{CH}_3)_2\text{CH-OO}) = 34.18$ . (Benson, S. W., *J. Am. Chem. Soc.*, **1975**, *87*, 972) incorporated with data of  $\Delta H_f^\circ_{298}(\text{HC}\equiv\text{CC}\cdot\text{H}_2)=82.69$  (Tsang, W., *Int. J. Chem. Kin.* **1978**, *10*, 687),  $\Delta H_f^\circ_{298}(\text{CH}_2=\text{CHC}\cdot\text{H}_2)=40.3$  (Tsan, W., *J. Phys. Chem. Ref. Data*, **1991**, *20*, 221) and  $\Delta H_f^\circ_{298}((\text{CH}_3)_2\text{C}\cdot\text{H})=21.5$  (Seakins, P. W. *et al.*, *J. Phys. Chem.*, **1992**, *96*, 9847), respectively.
24. This work. estimated from  $D^\circ((\text{CH}_3)_3\text{C-OO}\cdot) = 31.19$  incorporated with  $\Delta H_f^\circ_{298}((\text{CH}_3)_3\text{C}\cdot) = 12.26$ . (Seakin, P. W. see note 23 of this Table).  $D^\circ((\text{CH}_3)_3\text{C-OO}\cdot)$  estimated from Dean & Bozzelli's  $\Delta H_f^\circ_{298}(\text{R-OH})$  and  $\Delta H_f^\circ_{298}(\text{R-OO}\cdot)$  regressed relationship (ref. 27(b), Figure 14).

**Table 3.2** Bond Energy of (O)O-H Bond in Hydroperoxides ( $D_{298}^{\circ}(\text{ROO-H})$ , kcal/mol)

	$\Delta H_f^{\circ}(\text{ROO}\cdot)$	$\Delta H_f^{\circ}(\text{ROOH})$	$D_{298}^{\circ}(\text{ROO-H})$	comment <sup>a</sup>
CH <sub>3</sub> OO-H	6.1	-29.8	88	BAC/MP4 calculations
HOO-H	3.01	-32.5	87.6	experimental values
	3.6	-32.6	88.3	BAC/MP4 calculations
CF <sub>3</sub> OO-H	-150	-193	95.1	BAC/MP4 calculations
CIOO-H	33.6	0.3	85.4	BAC/MP4 calculations
FOO-H	22.6	-8.75	83.45	BAC/MP4 calculations

a: see notes of Table 3.1 for references of corresponding species.

**Table 3.3** Vibration Frequencies, <sup>a</sup> Barriers of Internal Hindered Rotations <sup>a</sup> and Moments of Inertia ( $I_x, I_y, I_z$ ) <sup>a</sup> for External Rotations of Stable Species

CIOOH.

Frequency: \*112<sup>b</sup>, 355, 710, 819, 1507, 3984. Barrier: 7.5.  $I_x, I_y, I_z$ : 17.49, 135.72, 153.21.

FOOH

Frequency: \*218, 475, 701, 1036, 1541, 3960. Barrier: 7.5.  $I_x, I_y, I_z$ : 16.15, 70.63, 84.42.

CH<sub>3</sub>OOH

Frequency: \*154, \*180, 431, 739, 1024, 1085, 1156, 1334, 1366, 1384, 1471, 3050, 3084, 3141, 3991. Barrier: 6.0, 6.4.  $I_x, I_y, I_z$ : 18.76, 83.65, 97.05.

CH<sub>2</sub>CIOOH

Frequency: \*100, \*158, 336, 471, 645, 731, 948, 1105, 1142, 1241, 1336, 1455, 2984, 3049, 3985. Barrier: 11.9, 7.34.  $I_x, I_y, I_z$ : 58.94, 247.41, 282.13.

CHCl<sub>2</sub>OOH

Frequency: \*97, \*141, 204, 262, 363, 521, 653, 671, 805, 1109, 1110, 1271, 1473, 2973, 3982. Barrier: 11.9, 7.34.  $I_x, I_y, I_z$ : 255.16, 285.66, 451.24.

CCl<sub>3</sub>OOH

Frequency: \*77, \*146, 172, 211, 233, 295, 371, 395, 523, 675, 731, 831, 1196, 1486, 3978. Barrier: 11.9, 7.34.  $I_x, I_y, I_z$ : 426.48, 518.28, 576.79.

CH<sub>2</sub>FOOH

Frequency: \*136, \*156, 379, 528, 732, 963, 1032, 1087, 1182, 1338, 1456, 1499, 2931, 2982, 3987. Barrier: 11.9, 7.34.  $I_x, I_y, I_z$ : 45.39, 149.88, 171.05.

<sup>a</sup> Units : Frequency = cm<sup>-1</sup>, Barrier = kcal/mol, MOI ( $I_x, I_y, I_z$ ) = 10<sup>-40</sup>•g•cm<sup>2</sup>.

<sup>b</sup> Frequencies marked with asterisk represent torsion modes (or hindered internal rotations). These frequencies are not included in the calculations of entropy ( $S_{298}^{\circ}$ ) and heat capacities ( $C_p$ 's). Pitzer and Gwinn's method is used, instead, to calculate contributions of hindered rotors. see text.

**Table 3.3** (continued) Vibration Frequencies, Barriers of Internal Hindered Rotation and Moments of Inertia ( $I_x$ ,  $I_y$ ,  $I_z$ ) for External Rotations of Stable Species

---

**CHF<sub>2</sub>OOH**

Frequency: \*119, \*132, 264, 392, 479, 650, 794, 986, 994, 1182, 1447, 1536, 1559, 2821, 3981. Barrier: 11.9, 7.34.  $I_x$ ,  $I_y$ ,  $I_z$ : 109.10, 182.16, 218.04.

**CF<sub>3</sub>OOH**

Frequency: \*96, \*138, 231, 332, 384, 477, 483, 565, 818, 999, 1431, 1524, 1606, 1646, 3974. Barrier: 11.9, 7.34.  $I_x$ ,  $I_y$ ,  $I_z$ : 154.34, 278.35, 283.22.

**CH<sub>2</sub>=CHOOH**

Frequency: \*69, \*165, 317, 507, 634, 810, 900, 947, 987, 1160, 1275, 1337, 1480, 1818, 3008, 3153, 3158, 3984. Barrier: 8.92, 6.4.  $I_x$ ,  $I_y$ ,  $I_z$ : 18.98, 168.66, 205.65.

**CH<sub>2</sub>=CClOOH**

Frequency: \*42, \*139, 228, 361, 427, 562, 599, 648, 802, 946, 1008, 1236, 1316, 1451, 1805, 3140, 3150, 3984. Barrier: 14.82, 7.34.  $I_x$ ,  $I_y$ ,  $I_z$ : 155.17, 235.78, 360.00.

**CH≡CCH<sub>2</sub>OOH**

Frequency: \*36, \*185, 204, 377, 407, 535, 803, 843, 875, 935, 1047, 1050, 1110, 1334, 1357, 1498, 2322, 2912, 2962, 3353, 3987. Barrier: 6.0, 6.4.  $I_x$ ,  $I_y$ ,  $I_z$ : 26.18, 349.21, 370.0.

**CH<sub>2</sub>=CHCH<sub>2</sub>OOH**

Frequency: \*109, \*168, \*268, 338, 369, 529, 648, 737, 897, 916, 977, 1060, 1140, 1126, 1153, 1208, 1307, 1334, 1373, 1467, 1858, 2937, 3017, 3053, 3136, 3148, 3989. Barrier: 2.0, 6.0, 6.4.  $I_x$ ,  $I_y$ ,  $I_z$ : 52.71, 322.30, 352.73.

**CH<sub>3</sub>CH<sub>2</sub>OOH**

Frequency: \*56, \*142, \*164, 301, 476, 802, 840, 950, 1051, 1112, 1126, 1159, 1326, 1371, 1405, 1407, 1414, 1499, 2933, 2992, 3087, 3088, 3185, 3994. Barrier: 3.77, 6.0, 6.4.  $I_x$ ,  $I_y$ ,  $I_z$ : 26.90, 206.61, 222.81.

**CH<sub>3</sub>CHClOOH**

Frequency: \*66, \*139, \*148, 258, 309, 413, 497, 617, 799, 948, 1013, 1115, 1133, 1179, 1299, 1389, 1391, 1401, 1473, 2883, 3087, 3089, 3181, 3984. Barrier: 3.97, 6.17, 7.34.  $I_x$ ,  $I_y$ ,  $I_z$ : 168.67, 264.56, 401.66.

**(CH<sub>3</sub>)<sub>2</sub>CHOOH**

Frequency: \*62, \*147, \*163, \*169, 294, 365, 464, 516, 801, 927, 953, 962, 972, 1113, 1121, 150, 1285, 1308, 1398, 1400, 1401, 1406, 1408, 1410, 1487, 2844, 3085, 3087, 3090, 3092, 3183, 1385, 3900. Barrier: 4.00, 4.00, 6.0, 6.4.  $I_x$ ,  $I_y$ ,  $I_z$ : 108.64, 230.69, 303.88.

**(CH<sub>3</sub>)<sub>3</sub>COOH**

Frequency: \*94, \*142, \*146, \*185, \*186, 254, 345, 363, 433, 487, 533, 811, 876, 939, 952, 54, 973, 1009, 1010, 1278, 1281, 1400, 1403, 1404, 1405, 1408, 1414, 1414, 1514, 3085, 086, 3087, 3088, 3088, 3089, 3181, 3182, 3183, 3990. Barrier: 4.00, 4.00, 4.00, 6.0, 6.4.  $I_x$ ,  $I_y$ ,  $I_z$ : 187.68, 311.49, 314.45.

**CH<sub>3</sub>OOCH<sub>3</sub>**

Frequency: \*53, \*147, \*179, 295, 454, 741, 1024, 1028, 1055, 1098, 1201, 1203, 1332, 1333, 1366, 1367, 1412, 1415, 3046, 3047, 3078, 3080, 3137, 3137. Barrier: 6.0, 6.4, 6.0.  $I_x$ ,  $I_y$ ,  $I_z$ : 27.40, 192.42, 209.10.

---

**Table 3.4** Potential Barriers for Hindered Internal Rotations (V) about Single Bonds

Rotors	V (kcal/mol)	Rotors	V (kcal/mol)
CH <sub>3</sub> -CH <sub>3</sub>	2.9 <sup>a</sup>	(CH <sub>3</sub> ) <sub>3</sub> C-OH	0.9 <sup>d</sup>
CH <sub>3</sub> -C <sub>2</sub> H <sub>5</sub>	3.3 <sup>a</sup>	CH <sub>3</sub> -C(OH)(CH <sub>3</sub> ) <sub>2</sub>	3.8 <sup>d</sup>
C <sub>2</sub> H <sub>5</sub> -C <sub>2</sub> H <sub>5</sub>	3.5 <sup>a</sup>	CH <sub>3</sub> -CH <sub>2</sub> OOH	3.0 <sup>c</sup>
CH <sub>3</sub> -CH(CH <sub>3</sub> ) <sub>2</sub>	3.8 <sup>a</sup>	CH <sub>3</sub> CH <sub>2</sub> -OOH <sub>(EH)</sub>	2.7 <sup>e</sup>
CH <sub>3</sub> -C(CH <sub>3</sub> ) <sub>3</sub>	4.7 <sup>a</sup>	CH <sub>3</sub> CH <sub>2</sub> -OOH <sub>(EC)</sub>	6.0 <sup>e</sup>
CH <sub>3</sub> -CH <sub>2</sub> Cl	3.7 <sup>b</sup>	CH <sub>3</sub> CH <sub>2</sub> O-OH	6.4 <sup>c</sup>
CH <sub>3</sub> -CH <sub>2</sub> F	3.3 <sup>b</sup>	CH <sub>3</sub> -CHClOOH	3.6 <sup>c</sup>
CH <sub>3</sub> -CH <sub>2</sub> OH	3.33 <sup>c</sup> , 3.3 <sup>d</sup>	CH <sub>3</sub> CHCl-OOH <sub>(EH)</sub>	4.1 <sup>c</sup>
CH <sub>3</sub> -CHCl <sub>2</sub>	4.41 <sup>c</sup>	CH <sub>3</sub> CHCl-OOH <sub>(EC)</sub>	8.7 <sup>c</sup>
CH <sub>3</sub> -CHF <sub>2</sub>	3.18 <sup>c</sup>	CH <sub>3</sub> CHCl-OOH <sub>(EC1)</sub>	11.9 <sup>c</sup>
CH <sub>3</sub> -CCl <sub>3</sub>	5.0 <sup>c</sup>	CH <sub>3</sub> CHClO-OH	7.34 <sup>e</sup>
CH <sub>3</sub> -CF <sub>3</sub>	3.5 <sup>b</sup> , 3.25 <sup>c</sup>	HO-OH	7.0, 9.2 <sup>f</sup>
CH <sub>3</sub> CH <sub>2</sub> -OH	1.13 <sup>d</sup>	(CH <sub>2</sub> =CH)-OH	4.42 <sup>g</sup>
C <sub>3</sub> H <sub>7</sub> -OH	0.8 <sup>d</sup>	(CH <sub>2</sub> =CH)-OOH	8.92 <sup>h</sup>
CH <sub>3</sub> -CH(CH <sub>3</sub> )OH	4.0 <sup>d</sup>	(CH <sub>2</sub> =CCl)-OOH	14.82 <sup>i</sup>
(CH <sub>3</sub> ) <sub>2</sub> CH-OH	1.15 <sup>d</sup>	(CH <sub>2</sub> =CH)-(CH <sub>2</sub> OOH)	2.0 <sup>j</sup>

<sup>a</sup> Cohen, N. J. *J. Phys. Chem.* **1992**, *96*, 9052, and reference therein.

<sup>b</sup> ref. 6, page 306.

<sup>c</sup> Lister, D. G.; MacDonald, J. N.; Owen, N. L. *Internal Rotation and Inversion*, Academic Press, New York, **1978**.

<sup>d</sup> Chao, J. *et al.*, *J. Phys. Ref. Data* **1986**, *15*, 1425.

<sup>e</sup> Using GAUSSIAN92 of MP2/6-31G\*/RHF/6-31G\* level, see Chapter 4. EC indicates the torsion angle of OOC equal to 0. EH denotes the torsion angle OOC equal to 0 and EC1 denotes the torsion angle OOC1 equal to 0.

<sup>f</sup> Hehre, W. J.; Radom, L.; Schleyer, P. R. *Ab initio Molecular Orbital Theory* John Wiley & Sons, New York, **1986**, 267 and literature therein. 7.0 is experimental value, 9.4 is the result of calculations using GAUSSIAN system of programs at MP2/6-31G\*/MP2/6-31G\* level.

<sup>g</sup> H-Gorden, M. and Pople, J. A., *J. Phys. Chem.* **1993**, *97*, 1147.

<sup>h</sup> Estimated from  $V_{\text{CH}_3\text{CH}_2\text{-OOH}} + V_{\text{(CH}_2=\text{CH)-OH}} - V_{\text{CH}_3\text{CH}_2\text{-OH}} = 6.0 + (4.42 - 1.5)$

<sup>i</sup> Estimated from  $V_{\text{CH}_3\text{CHCl-OOH}} + V_{\text{(CH}_2=\text{CH)-OH}} - V_{\text{CH}_3\text{CH}_2\text{-OH}} = 11.9 + (4.42 - 1.5)$

<sup>j</sup> Estimated from  $V_{\text{(CH}_2=\text{CH}_2)\text{-(CH}_2\text{CH}_3)}$  (2.0 kcal/mol, Wiberg, K. B., *Advance in Molecular Modeling*, Vol. 1, p. 101, JAI Press Inc. (1988).

**Table 3.5** Thermodynamic Properties<sup>a</sup> for Stable Molecules and Comparison<sup>b</sup>

Species	$\Delta H_f^\circ_{298}$	$S^\circ_{298}$	$C_p^\circ_{300}$	$C_p^\circ_{400}$	$C_p^\circ_{500}$	$C_p^\circ_{600}$	$C_p^\circ_{800}$	$C_p^\circ_{1000}$	( $\sigma$ , OI) <sup>c</sup>
FOOH	-8.75	62.32	12.41	13.70	14.72	15.50	16.54	17.18	(1,1)
ClOOH	1.00	65.00	12.94	14.19	15.13	15.85	16.77	17.30	(1,1)
CH <sub>3</sub> OOH	-33.2	64.33	15.21	18.13	20.76	22.91	26.04	28.14	(3,1)
<i>ref. 6</i>	-30.88	65.48	15.09	17.34	19.4	21.69	24.42	26.47	
CH <sub>2</sub> FOOH	-77.44	73.63	16.78	19.89	22.59	24.78	28.01	30.18	(1,1)
CH <sub>2</sub> ClOOH	-37.74	76.46	17.77	20.9	23.49	25.56	28.54	30.53	(1,1)
CHF <sub>2</sub> OOH	-132	77.88	19.11	22.23	24.81	26.88	29.83	31.73	(1,1)
CHCl <sub>2</sub> OOH	-40.88	83.39	21.38	24.46	26.81	28.6	31.05	32.58	(1,1)
CF <sub>3</sub> OOH	-196.5	79.64	21.66	24.58	26.92	28.79	31.41	33.03	(3,1)
CCl <sub>3</sub> OOH	-36.8	88.15	25.74	28.57	30.52	31.91	33.7	34.7	(3,1)
C <sub>2</sub> H <sub>5</sub> OOH	-41.09	74.13	20.47	25.07	29.13	32.44	37.27	40.58	(1,1)
<i>ref. 6</i>	-39.1	75.28	20.08	24.19	27.7	31.12	35.53	38.8	
CH <sub>3</sub> CHClOOH	-48.98	82.39	23.9	28.58	32.5	35.59	39.98	42.87	(3,2)
CH <sub>2</sub> =CHOOH	-7.6	71.12	18.4	22.01	25.09	27.58	31.24	33.74	(1,1)
CH <sub>2</sub> =CClOOH	-16.97	80.98	19.66	25.23	28.07	30.31	33.53	35.72	(1,1)
CH≡CCH <sub>2</sub> OOH	22.42	76.33	21.50	25.79	29.32	32.09	36.01	38.63	(1,1)
CH <sub>2</sub> =CHCH <sub>2</sub> OOH	-15.43	81.83	23.38	28.56	33.00	36.62	41.92	45.57	(1,1)
(CH <sub>3</sub> ) <sub>2</sub> CHOOH	-48.58	80.64	26.09	32.42	37.90	42.3	48.72	53.15	(9,1)
<i>ref. 6</i>	-48.4	82.71	26.08	31.82	36.9	41.21	47.25	51.64	
(CH <sub>3</sub> ) <sub>3</sub> COOH	-54.83	83.42	32.09	40.01	46.75	52.14	60.04	65.56	(81,1)
<i>ref. 6</i>	-58.0	86.19	31.8	39.21	45.45	50.97	58.66	64.25	
CCCCOOH <sup>d</sup>	-46.02	83.58	25.97	32.02	37.38	41.79	48.34	52.92	(3,1)
<i>ref. 6</i>	-44.03	84.7	25.58	31.14	35.95	40.47	46.6	51.14	
CCCCOOH <sup>d</sup>	-50.59	93.00	31.47	38.97	45.63	51.14	59.41	65.26	(3,1)
<i>ref. 6</i>	-48.96	94.12	31.08	38.09	44.2	49.82	57.67	63.48	
CCC(C)OOH <sup>d</sup>	-53.51	91.50	31.59	39.37	46.15	51.65	59.79	65.49	(9,2)
<i>ref. 6</i>	-53.33	93.51	31.58	38.77	45.15	50.56	58.32	63.98	
C <sub>2</sub> CCOOH <sup>d</sup>	-53.19	90.31	31.20	38.91	45.70	51.28	59.60	65.40	(9,1)
<i>ref. 6</i>	-51.2	91.44	30.81	38.03	44.27	49.96	57.86	63.62	
CH <sub>3</sub> OOCH <sub>3</sub> <sup>e</sup>	-30.1	72.13	19.91	24.61	28.9	32.46	37.7	41.24	(9,1)
<i>ref. 6</i>	-29.16	75.26	19.78	23.08	26.2	29.98	34.44	37.94	

<sup>a</sup>: Standard state for molecules with optical isomers is an equilibrium mixture of enantiomers at total pressure 1 atm.  $\Delta H_f^\circ_{298}$  in kcal/mol,  $S^\circ_{298}$  and  $C_p^\circ(T)$  in cal/mol-K.

<sup>b</sup>: comparison are performed only where the corresponding GA group values are available in ref. 6. The first line of data without further note are results of this work. The second line (if present) are data calculated from Benson's group values using Benson's GA scheme. (see text).

<sup>c</sup>:  $\sigma$  = symmetry number for external rotations, OI = number of optical isomers. Benson assigned OI equal to 2 for all, di-alkyl peroxides and alkyl hydroperoxides, we assign OI=1 for those species since the contributions to entropies and heat capacities from hindered rotors, RO-OH or RO-OR' have been considered.

<sup>d</sup>: Values are calculated from Scheme II GA approach (see text).

<sup>e</sup>: for deriving the C/H3/OO group values for Scheme II, see text and Table 3.7.

**Table 3.6** Consistence Study of Group Values of General Scheme GA Approach

Calculations <sup>a</sup>	Group Values	$\Delta H_f^\circ_{298}$	$S^\circ_{int, 298}$	$C_p^\circ_{50}$	$C_p^\circ_{100}$
				<sup>b</sup>	<sup>0</sup>
(1/2) HOOH	$\Delta H_f^\circ_{298}(O/H/O)$	-16.27	27.83	6.17	8.425
CH <sub>3</sub> OOH - (1/2)CH <sub>3</sub> OOCH <sub>3</sub>	“	-18.15	28.18	6.31	7.52
C <sub>2</sub> H <sub>5</sub> OOH - (1/2)C <sub>2</sub> H <sub>5</sub> OOC <sub>2</sub> H <sub>5</sub>	“	-18.04			
CH <sub>3</sub> OOH - CH <sub>3</sub> OH	$\Delta H_f^\circ_{298}(O/C/O + O/H/O - O/C/H)$	14.88	6.96	6.54	6.76
C <sub>2</sub> H <sub>5</sub> OOH - C <sub>2</sub> H <sub>5</sub> OH	“	15.03	6.59	6.36	6.75
C <sub>2</sub> CHOOH - C <sub>2</sub> CHOH	“	16.57	6.57	6.01	6.33
C <sub>3</sub> COOH - C <sub>3</sub> COH	“	19.89	5.14	6.48	6.4
CH <sub>2</sub> =CHOOH - CH <sub>2</sub> =CHOH <sup>c</sup>	$\Delta H_f^\circ_{298}(O/C_d/O^d + O/H/O - O/C/H)$	22.4			
CH <sub>2</sub> =CClOOH - CH <sub>2</sub> =CClOH <sup>c</sup>	“	19.97			

<sup>a</sup> Thermodynamic data for hydroperoxides are from Table 3.5, hydroxides are from ref. 23 except as noted below.  $\Delta H_f^\circ_{298}$  in kcal/mol,  $S^\circ_{298}$  and  $C_p^\circ(T)$  in cal/mol-K. <sup>b</sup>  $S^\circ_{int, 298}$  represents “intrinsic entropy”, i.e. entropy without correction for symmetry and number of optical isomers. <sup>c</sup> Melius, C. F. “BAC-MP4 Heats of Formation and Free Energies” 1993, Sandia National Laboratories, Livermore, California.

<sup>d</sup> C<sub>d</sub> represents double-bonded C atom.

**Table 3.7** Group Values<sup>a</sup> of Scheme II

Group <sup>b</sup>	$\Delta H_f^\circ_{298}$	$S^\circ_{int, 298}$ <sup>c</sup>	$C_p^\circ_{300}$	$C_p^\circ_{400}$	$C_p^\circ_{500}$	$C_p^\circ_{600}$	$C_p^\circ_{800}$	$C_p^\circ_{1000}$	note
C/C/H3	-10.2	30.3	6.19	7.84	9.4	10.79	13.02	14.77	1
C <sub>d</sub> /H2	6.26	27.61	5.1	6.36	7.51	8.5	10.07	11.27	2
C <sub>d</sub> /C/H	8.59	7.97	4.16	5.03	5.81	6.5	7.65	8.45	2
C <sub>v</sub> /H	26.93	24.7	5.28	5.99	6.49	6.87	7.47	7.96	2
C <sub>v</sub> /C	27.55	6.35	3.13	3.48	3.81	4.09	4.6	4.92	2
C/H3/OO	-10.2	30.3	6.19	7.84	9.4	10.79	13.02	14.77	3
C <sub>d</sub> /H/OO	2.03	6.2	4.75	6.46	7.64	8.35	9.1	9.56	4
OO/C/H	-23	36.13	9.02	10.29	11.36	12.12	13.02	13.37	5
OO/C2	-9.7	15.9	7.53	8.93	10.1	10.88	11.66	11.7	5
OO/C <sub>d</sub> /H	-15.89	37.31	8.55	9.19	9.94	10.73	12.07	12.91	5
C/C1/H2/OO	-14.74	40.33	8.75	10.61	12.13	13.44	15.52	17.16	5
C/C12/H/OO	-17.88	47.26	12.36	14.17	15.45	16.48	18.03	19.21	5
C/C13/OO	-13.8	54.05	16.72	18.28	19.16	19.79	20.68	21.33	5
C/F/H2/OO	-54.44	37.5	7.76	9.6	11.23	12.66	14.99	16.81	5
C/F2/H/OO	-109	41.75	10.09	11.94	13.45	14.76	16.81	18.36	5
C/F3/OO	-173.5	45.57	12.64	14.29	15.56	16.67	18.39	19.66	5
C <sub>d</sub> /C1/OO	-7.34	16.06	6.01	9.68	10.62	11.08	11.39	11.54	5
C/C/H2/OO	-7.89	9.8	5.26	6.94	8.37	9.53	11.23	12.44	5
C/C/C1/H/OO	-15.78	16.76	8.69	10.45	11.74	12.68	13.94	14.73	5
C/C2/H/OO	-5.18	-11.87	4.69	6.45	7.74	8.6	9.66	10.24	5
C/C3/OO	-1.23	-35.18	4.5	6.2	7.19	7.65	7.96	7.88	5
C/C <sub>v</sub> /H2/OO	-9.06	9.15	4.07	6.03	7.66	9.01	10.92	12.38	5
C/C <sub>d</sub> /H2/OO	-7.28	10.12	5.1	6.88	8.32	9.5	11.18	12.48	5

<sup>a</sup>  $\Delta H_f^\circ_{298}$  in kcal/mol,  $S^\circ_{298}$  and  $C_p^\circ(T)$  in cal/mol-K. <sup>b</sup> C<sub>d</sub> represents double-bonded C atom, C<sub>v</sub> represents triple-bonded C atom. <sup>c</sup>  $S^\circ_{int, 298}$  represent “intrinsic entropy”, i.e. entropy without the correction on symmetry number and number of optical isomers.

1. Cohen, N., *J. Phys. Chem.* **1992**, *96*, 9052. 2. reference 19 (d). 3. assign C/H3/OO = C/C/H3. 4. assign C<sub>d</sub>/H/OO = C<sub>d</sub>/H/O, authors' unpublished results. 5. this work.



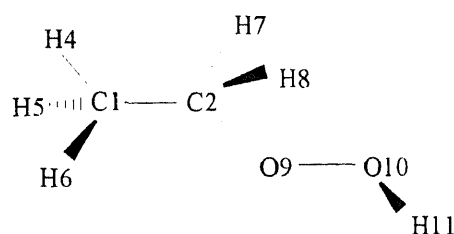
**Table 4.1** Previous studies of geometry and rotational barriers of H<sub>2</sub>O<sub>2</sub> and D<sub>2</sub>O<sub>2</sub> as determined by far IR, microwave spectroscopy and *ab initio* study<sup>a</sup>

<i>Authors</i>	<i>Redington, Olson, Cross 1962</i>	<i>Hunt, et al. 1965</i>	<i>Hunt, Leacock 1966</i>	<i>Oelfke, Grody 1969</i>	<i>Ewing, Harris 1969</i>		<i>Cremer 1978</i>
Method	IR or MW	HR or MW	IR or MW	IR or MW	IR or MW	IR or MW	<i>ab initio</i> <sup>b</sup>
Molecule <sup>c</sup>	H <sub>2</sub> O <sub>2</sub>	H <sub>2</sub> O <sub>2</sub>	D <sub>2</sub> O <sub>2</sub>	H <sub>2</sub> O <sub>2</sub>	H <sub>2</sub> O <sub>2</sub>	D <sub>2</sub> O <sub>2</sub>	H <sub>2</sub> O <sub>2</sub>
R(OH)	0.950						0.967
R(OO)	1.475						1.451
θ(HOOH)	109.5	111.5	110.8	120	112.8	115.3	119.3
V(trans)	0.85	1.10	1.08	1.1	1.10	1.08	1.1
V(cis)	3.71	7.03	7.06	7.0	7.57	8.80	7.4

<sup>a</sup> The data were adapted from the work by D. Cremer. *J. Chem. Phys.* **1978**, *69*, 4440 (and authors were also cited therein.)

<sup>b</sup> Equilibrium structure and barriers to internal rotation of hydrogen peroxide were determined with the Hartree-Fock method and Rayleigh-Schrödinger perturbation theory using a (11s6p2d/6s2p) uncontracted basis set.

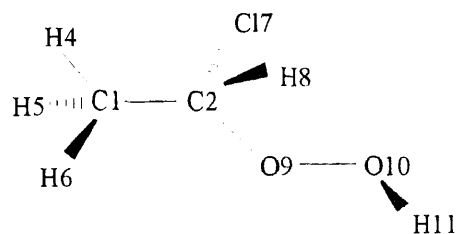
<sup>c</sup> Bond distances (R) in Å, bond angles (θ) in degrees, barriers (V) in kcal/mol.

**Table 4.2** Structure Parameters for CH<sub>3</sub>CH<sub>2</sub>OOH, HF/6-31G\* Basis Set

	aSTS' (3-21G)	aSTS	aETS	aSGS	aSE <sub>H</sub> S	aSE <sub>C</sub> S	aSTT	aSTC
<b>Bond Length</b>								
CC	1.5269	1.5168	1.5314	1.5188	1.5177	1.5183	1.5168	1.5163
C1H3	1.0834	1.0850	1.0834	1.0857	1.0860	1.0859	1.0850	1.0848
C1H4	1.0821	1.0838	1.0834	1.0852	1.0839	1.0816	1.0840	1.0833
C1H5	1.0821	1.0842	1.0836	1.0834	1.0844	1.0824	1.0840	1.0833
C2H6	1.0794	1.0837	1.0827	1.0832	1.0797	1.0837	1.0845	1.0885
C2H7	1.0794	1.0857	1.0848	1.0836	1.0860	1.0853	1.0845	1.0885
CO	1.4509	1.4060	1.4087	1.4068	1.4166	1.4236	1.4030	1.4001
OO	1.4692	1.3932	1.3926	1.3960	1.3930	1.3915	1.4020	1.3987
OH	0.9708	0.9495	0.9495	0.9491	0.9495	0.9492	0.9490	0.9503
<b>Bond Angle</b>								
H3C1C2	110.073	109.921	111.532	110.042	110.273	107.98	109.856	109.966
H4C1C2	110.077	110.621	109.733	110.602	110.488	111.685	110.757	110.431
H5C1C2	110.077	110.845	111.602	110.067	110.697	111.924	110.757	110.447
H6C2C1	111.842	111.39	112.029	110.965	111.52	109.994	111.442	110.823
H7C2C1	111.842	111.383	111.942	111.363	110.925	109.953	111.441	110.822
O8C2C1	105.781	106.973	107.055	113.102	109.494	116.255	107.039	107.2
O9O8C2	104.391	107.704	107.619	107.869	109.771	112.435	106.078	111.535
H10O9O8	99.726	102.15	102.22	102.113	102.128	101.995	100.741	106.26
<b>Dihedral Angle</b>								
H4C1C2H3	120.102	119.82	119.407	119.572	120.223	119.206	119.789	119.912
H5C1C2H3	-120.102	-119.858	-121.508	-119.586	-119.788	-119.063	-119.789	-119.944
H6C2C1H3	-61.559	-60.604	0	-60.227	-62.597	-58.791	-60.653	-60.196
H7C2C1H3	61.559	60.466	121.508	60.678	58.318	59.827	60.652	60.451
O8C2C1H3	-180	-179.862	-119.047	-176.176	-182.777	-179.184	-180.001	-179.874
O9O8C2C1	-180	-182.983	-182.866			0	-180	-179.989
H10O9O8C2	179.997	116.52	115.395	121.784	115.991	245.292	180	0
O9O8C2H6				-191.715	0			

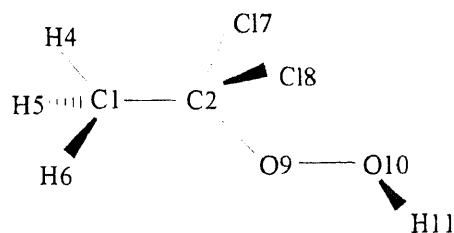
aSTS' optimized at 3-21G level

Unit : bond length in Angstrom, bond angle and dihedral angle in degrees.

**Table 4.3** Structure Parameters for CH<sub>3</sub>CHClOOH, HF/6-31G\* Basis Set

	bSTS	bETS	bSG <sub>C-Cl</sub> S	bSE <sub>H</sub> S	bSE <sub>C</sub> S	bSE <sub>Cl</sub> S	bSTT	bSTC
Bond Length								
CC	1.5112	1.5269	1.5143	1.5102	1.5137	1.5142	1.5128	1.5117
C1H3	1.0817	1.0794	1.0822	1.0820	1.0821	1.0827	1.0816	1.0816
C1H4	1.0821	1.0824	1.0800	1.0824	1.0798	1.0832	1.0823	1.0817
C1H5	1.0839	1.0829	1.0855	1.0842	1.0826	1.0842	1.0840	1.0835
C2C16	1.8191	1.8218	1.8034	1.8176	1.8070	1.7827	1.8090	1.8167
C2H7	1.0760	1.0752	1.0771	1.0736	1.0776	1.0776	1.0768	1.0812
CO	1.3738	1.3753	1.3795	1.3857	1.3955	1.4149	1.3723	1.3682
OO	1.3866	1.3858	1.3933	1.3902	1.3928	1.3821	1.3980	1.3949
OH	0.9518	0.9519	0.9499	0.9512	0.9496	0.9503	0.9498	0.9516
Bond Angle								
H3C1C2	110.23	111.868	109.774	110.682	108.363	110.644	110.135	110.182
H4C1C2	110.35	110.01	111.195	110.216	111.116	110.482	110.264	109.954
H5C1C2	108.766	110.032	108.788	108.512	110.182	108.846	109.027	108.833
C16C2C1	110.342	111.683	110.337	110.184	109.372	110.794	110.261	110.563
H7C2C1	113.534	113.748	111.847	114.466	111.911	111.534	113.135	112.367
O8C2C1	107.707	107.695	114.489	110.04	116.284	108.267	107.427	107.277
O9O8C2	109.551	109.57	110.044	109.733	112.272	115.794	107.659	113.897
H10O9O8	102.721	102.811	101.556	102.27	101.134	102.86	110.622	106.622
Dihedral A								
H4C1C2H3	120.6	120.108	120.586	120.785	120.037	120.872	120.347	120.549
H5C1C2H3	-119.787	-121.097	-118.878	-120.059	-119.06	-119.717	-119.87	-119.909
C16C2C1H3	-58.654	0	-62.027	-57.961	-58.92	-60.525	-57.955	-58.414
H7C2C1H3	58.613	117.381	54.843	58.683	56.154	56.265	59.485	57.83
O8C2C1H3	181.145	239.338	171.974	182.441	179.867	173.154	181.095	180.107
O9O8C2C1	193.776	194.032			0		195.699	186.219
H10O9O8C2	262.105	263.216	234.644	247.202	235.496	261.71	180	0
O9O8C2C16						0		
O9O8C2H7			177.269	0				

Unit : bond length in Angstrom, bond angle and dihedral angle in degrees.

**Table 4.4** Structure Parameters for CH<sub>3</sub>CCl<sub>2</sub>OOH, HF/6-31G\* Basis Set

	cSTS	cETS	cSGS	cSE <sub>C1</sub> S	aSE <sub>C</sub> S	cSTT	cSTC
<b>Bond Length</b>							
CC	1.5164	1.5354	1.5157	1.5171	1.5173	1.5176	1.5150
C1H3	1.08	1.0789	1.0804	1.0804	1.0800	1.0799	1.0800
C1H4	1.0818	1.0816	1.0824	1.0832	1.0801	1.0818	1.0815
C1H5	1.0818	1.0788	1.0794	1.0820	1.0799	1.0818	1.0815
C2C16	1.7978	1.8015	1.7720	1.7721	1.7846	1.7878	1.7883
C2C17	1.7801	1.7828	1.7994	1.7917	1.7968	1.7878	1.7985
CO	1.3678	1.3701	1.3814	1.3979	1.3834	1.3633	1.3567
OO	1.3835	1.3826	1.3880	1.3820	1.3897	1.3954	1.3929
OH	0.9521	0.9521	0.9519	0.9509	0.9512	0.9503	0.9529
<b>Bond Angle</b>							
H3C1C2	110.074	110.891	109.889	110.771	108.355	109.926	110.084
H4C1C2	109.135	108.232	108.396	108.936	109.886	109.018	108.754
H5C1C2	108.756	110.674	109.833	108.837	110.118	109.019	108.758
C16C2C1	110.02	111.09	110.825	110.566	109.942	110.098	110.414
C17C2C1	111.539	111.658	111.062	109.409	109.177	110.101	110.419
O8C2C1	106.011	105.638	113.616	108.183	116.034	105.809	106.429
O9O8C2	112.157	112.288	109.554	115.858	112.462	110.446	116.36
H10O9O8	102.603	102.673	102.293	102.486	101.459	100.041	106.871
<b>Dihedral Angle</b>							
H4C1C2H3	120.386	119.51	119.759	120.459	119.767	120.155	120.32
H5C1C2H3	-120.13	-121.211	-120.634	-120.524	-119.56	-120.156	-120.328
C16C2C1H3	-60.46	0	-59.079	-60.111	-58.444	-60.018	-59.546
C17C2C1H3	59.737	121.777	61.669	59.224	60.143	60.021	59.578
O8C2C1H3	-179.408	241.4	-175.015	-185.503	-179.498	-179.999	-179.989
O9O8C2C1	-178.043	-178.032			0	-179.888	-179.979
H10O9O8C2	-97.539	-96.684	-102.292	-101.829	-118.461	180	0
O9O8C2C16			184.07	0			

Unit : bond length in Angstrom, bond angle and dihedral angle in degrees.

**Table 4.5** Mulliken Charge <sup>a</sup> Distribution, MP2/6-31G\*\* Basis Set

	CH <sub>3</sub> CH <sub>2</sub> OOH	CH <sub>3</sub> CHClOOH	CH <sub>3</sub> CCl <sub>2</sub> OOH
Total atomic charges:			
C1	-0.368514	-0.499311	-0.321850
C2	0.137222	0.088573	0.100081
H3	0.119903	0.196247	0.162869
H4	0.136545	0.204549	0.161416
H5	0.129481	0.197454	0.168088
H6	0.118739		
H7		-0.132724	-0.039159
	Cl6	0.230344	
	Cl7		0.010225
O8	-0.378064	-0.329392	-0.319757
O9	-0.354872	-0.429594	-0.300973
H10	0.360785	0.473855	0.379059
Atomic charges with hydrogens summed into heavy atoms			
C1	0.017415	0.098939	0.170523
C2	0.354736	0.318917	0.100081
O8	-0.378064	-0.329392	-0.319757
O9	0.005913	0.044261	0.078087
Cl6		-0.132724	-0.039159
Cl7			0.010225

<sup>a</sup> For definition and calculation procedure of Mulliken charge distribution, see p. 25-29 in ref. 7.

For discussion of Mulliken charge and Mulliken population analysis, see p. 336-341 in ref. 7.

**Table 4.6** Harmonic Vibration Frequencies ( $\text{cm}^{-1}$ ) of  $\text{CH}_3\text{CH}_2\text{OOH}$  Rotational Conformers, HF/6-31G\* Basis Set

aSTS	IR int.	aETS	aSGS	aSE <sub>H</sub> S	aSE <sub>C</sub> S	aSTT	aSTC
138.46 <sup>b</sup>	6.80	-256.59	165.78 <sup>b</sup>	-141.21	-219.14	-136.76	-486.58
215.09 <sup>c</sup>	138.92	146.58 <sup>b</sup>	225.71 <sup>c</sup>	232.58 <sup>c</sup>	265.93 <sup>c</sup>	136.70 <sup>b</sup>	145.75 <sup>b</sup>
262.16 <sup>a</sup>	8.05	219.23 <sup>c</sup>	267.52 <sup>a</sup>	257.67 <sup>a</sup>	318.65 <sup>a</sup>	259.72 <sup>a</sup>	260.58 <sup>a</sup>
325.54	0.08	340.73	395.33	413.44	342.9	321.58	321.54
534.34	8.35	534.36	551.93	516.48	611.01	516.77	526.17
893.14	0.15	959.22	871.16	858.97	868.73	894.67	909.6
964.57	9.80	998.67	952.27	952.69	917.51	960.08	966.41
1113.29	19.70	1108.96	1074.83	1092.36	1080.45	1113.20	1105.76
1208.06	1.57	1187.71	1189.98	1201.23	1203.81	1213.00	1218.87
1281.28	43.07	1277.5	1252.38	1240.52	1276.21	1262.00	1292.96
1304.46	7.21	1294.78	1315.87	1310.59	1291.99	1307.01	1303.74
1402.85	0.78	1384.2	1446.3	1433.19	1421.85	1405.94	1415.85
1536.83	16.34	1533.26	1530.1	1534.97	1539.19	1531.44	1536.89
1560.94	73.72	1561.68	1561.75	1561.27	1564.46	1562.94	1564.99
1581.51	5.01	1593.64	1573.12	1572.39	1579.05	1613.06	1627.81
1629.08	3.66	1638.9	1630.98	1629.3	1634.67	1629.34	1628.24
1645.00	1.88	1639.76	1639.05	1641.84	1643.17	1646.1	1646.58
1648.57	6.13	1690.34	1652.58	1659.07	1681.89	1686.68	1686.4
3213.17	39.10	3217.95	3209.47	3208.7	3213.83	3215.09	3177.74
3220.03	28.09	3229.72	3239.85	3218.96	3224.49	3225.8	3212.76
3261.77	22.92	3266.89	3271.63	3273.59	3257.34	3261.75	3220.99
3283.45	44.49	3293.14	3280.66	3286.56	3286.3	3283.28	3289.14
3295.56	63.58	3296.88	3301.96	3313.54	3316.26	3295.21	3302.55
4068.11	61.28	4085.49	4094.62	4084.65	4086.04	4108.42	4066.23

<sup>a</sup> The frequency presents torsion motion about  $\text{CH}_3\text{--CH}_2\text{OOH}$  bond.

<sup>b</sup> The frequency presents torsion motion about  $(\text{CH}_3)\text{CH}_2\text{--OOH}$  bond

<sup>c</sup> The frequency presents torsion motion about  $(\text{CH}_3\text{CH}_2)\text{O--OH}$  bond

**Table 4.7** Harmonic Vibration Frequencies ( $\text{cm}^{-1}$ ) of  $\text{CH}_3\text{CHClOOH}$  Rotational Conformers, HF/6-31G\* Basis Set

bSTS	IR int.	bETS	bSG <sub>C-H</sub> S	bSG <sub>C-Cl</sub> S	bSE <sub>H</sub> S	bSE <sub>C</sub> S	bSE <sub>C1</sub> S	bSTT	bSTC
160.52 <sup>b</sup>	-175	-245.19	116.18 <sup>b</sup>	143.54 <sup>b</sup>	-101.11	-147.07	-197.78	-503.05	-491.66
255.85 <sup>a</sup>	-27.5	168.35 <sup>b</sup>	260.68 <sup>a</sup>	201.92 <sup>a</sup>	268.25 <sup>a</sup>	189.28 <sup>a</sup>	269.83 <sup>a</sup>	199.63 <sup>b</sup>	165.23 <sup>b</sup>
285.09 <sup>c</sup>	-0.87	288.17 <sup>c</sup>	270.78 <sup>c</sup>	269.27 <sup>c</sup>	292.16 <sup>c</sup>	327.57 <sup>c</sup>	288.25 <sup>c</sup>	258.62 <sup>a</sup>	255.91 <sup>a</sup>
339.12	-3.48	348.58	308.06	302.69	327.36	333.33	295.19	306.25	289.66
350.66	-15.5	365.51	340.85	372.53	385.03	367.6	349.7	253.76	345.26
477.54	-1.04	481.74	459.69	438.05	412.45	393.32	464.75	475.46	475.10
575.09	-11.4	584.68	508.61	642.97	539.74	631.01	568.67	561.90	571.21
702.23	-18.6	708.17	807.07	752.58	749.35	726.62	767.69	713.22	697.95
989.09	-34.1	1014.86	980.89	968.11	968.38	935.33	977.49	974.84	984.72
1121.52	-22.4	1136.57	1144.36	1081.65	1120.29	1090.73	1087.01	1107.87	1100.31
1187.01	-6.09	1188.54	1158.81	1156.17	1181	1158.53	1183.65	1177.10	1185.09
1247.18	-0.46	1217.07	1230.17	1239.6	1249.75	1244	1220.89	1237.10	1251.63
1296.76	-91.2	1302.14	1265.49	1298.31	1265.94	1292.66	1266.77	1272.81	1311.54
1444.87	-3.81	1444.08	1437.61	1433.33	1431.34	1448.2	1467.73	1445.56	1454.45
1509.95	-8.66	1507.89	1517.15	1515.84	1516.47	1510.57	1498.78	1490.58	1516.39
1572.93	-5.63	1579.21	1567.16	1568.58	1571.02	1574.83	1570.59	1527.75	1569.54
1586.67	-4.87	1586.55	1576.1	1589.49	1575.87	1587.91	1584.69	1574.96	1625.14
1626.23	-5.35	1628.39	1627.49	1628.67	1626.24	1630.19	1628.59	1627.13	1632.34
1632.27	-15	1637.5	1634.67	1639.39	1630.02	1633.18	1630.02	1633.69	1634.55
3232.62	-14.4	3237.11	3231.3	3224.92	3229.17	3241.97	3224.83	3231.34	3235.45
3307.70	-0.05	3309.78	3307	3298.85	3303.7	3311.51	3295.9	3305.34	3280.68
3321.42	-30.1	3336.27	3308.45	3330.63	3318.27	3318.86	3306.08	3320.75	3313.25
3354.45	-58.9	3359.47	3329.49	3348.00	3379.83	3343.99	3328.21	3345.82	3329.06
4058.25	-44.1	4057.24	4082.10	4088.16	4067.62	4090.63	4072.15	4104.48	4057.08

<sup>a</sup> The frequency presents torsion motion about  $\text{CH}_3\text{--CHClOOH}$  bond.<sup>b</sup> The frequency presents torsion motion about  $(\text{CH}_3)\text{CHCl--OOH}$  bond<sup>c</sup> The frequency presents torsion motion about  $(\text{CH}_3\text{CHCl})\text{O--OH}$  bond

**Table 4.8** Harmonic Vibration Frequencies ( $\text{cm}^{-1}$ ) of  $\text{CH}_3\text{CCl}_2\text{OOH}$  Rotational Conformers, HF/6-31G\* Basis Set

cSTS	IR int.	cETS	cSGS	cSE <sub>C1</sub> S	aSE <sub>C</sub> S	cSTT	cSTC
167.27 <sup>b</sup>	-175	-280.0	158.48 <sup>b</sup>	-117.1	-137.03	-255.14	-486.17
240.24 <sup>a</sup>	-27.5	175.82 <sup>b</sup>	247.34 <sup>a</sup>	256.84 <sup>a</sup>	264.73 <sup>a</sup>	163.05 <sup>b</sup>	165.32 <sup>b</sup>
294.89 <sup>c</sup>	-0.87	244.08 <sup>c</sup>	278.73 <sup>c</sup>	276.81 <sup>c</sup>	279.01 <sup>c</sup>	238.43 <sup>a</sup>	244.07 <sup>a</sup>
298.34	-3.48	301.84	290.56	297.32	311.25	297.22	292.83
320.07	-15.5	325.8	335.79	316.45	363.39	316.14	322.62
332.76	-1.04	356.93	359.25	347.87	371.37	328.0	323.9
391.07	-11.4	408.97	394.88	392.99	403.1	392.9	389.9
450.86	-18.6	454.91	463.01	416.12	420.35	445.83	440.93
609.79	-34.1	609.78	501.45	559.33	469.33	603.04	600.11
625.73	-22.4	634.01	660.02	624.82	709.73	617.62	627.6
815.97	0.09	817.57	867.68	848.37	811.21	812.98	794.61
1026.60	-0.46	1036.15	1004.06	1000.37	964.21	1015.53	1007.03
1183.91	-91.2	1172.95	1166.08	1176.8	1175.42	1178.56	1184.82
1220.63	-3.81	1227.3	1214.36	1218.25	1216.83	1221.17	1217.74
1258.16	-8.66	1235.93	1252.35	1250.5	1261.92	1252.22	1256.35
1326.46	-5.63	1321.38	1319.41	1284.43	1314.76	1336.06	1354.71
1570.02	-4.87	1579.07	1571.85	1571.04	1574.45	1568.25	1568.98
1598.70	45.35	1599.12	1590.79	1593.37	1587.93	1615.54	1621.81
1624.07	-15	1626.3	1623.72	1624.27	1625.27	1624.35	1626.13
1627.62	-14.4	1634.27	1631.12	1626.71	1630.9	1632.78	1638.27
3246.99	-0.05	3257.56	3251.49	3237.36	3258.6	3245.78	3248.24
3328.10	-30.1	3338.47	3331.35	3314.97	3345.37	3327.26	3333.33
3343.29	-58.9	3353.39	3349.85	3337.60	3347.97	3343.77	3345.03
4056.56	-44.1	4056.23	4061.29	4067.30	4070.25	4098.33	4044.86

<sup>a</sup> The frequency presents torsion motion about  $\text{CH}_3\text{-CCl}_2\text{OOH}$  bond.<sup>b</sup> The frequency presents torsion motion about  $(\text{CH}_3)\text{CCl}_2\text{-OOH}$  bond<sup>c</sup> The frequency presents torsion motion about  $(\text{CH}_3\text{CCl}_2)\text{O-OH}$  bond



**Table 4.9** Rotational Barriers

<i>conformer</i>	<i>energy</i> <sup>1</sup>		<i>ZPVE</i> <sup>2</sup>	<i>barrier</i> <sup>3</sup>	
	HF/6-31G*	MP2/6-31G**		HF/ 6-31G*	MP2/ 6-31G**
<b>CH<sub>3</sub>CH<sub>2</sub>OOH</b>					
aSTS	-228.8367278	-229.5082360	56.66	0	0
aETS	-228.8315622	-229.5031246	56.41	3.35	3.32
aSGS	-228.8362313	-229.5085202	56.75	0.36	-0.13
aSE <sub>H</sub> S	-228.8320124	-229.5035600	56.46	2.94	2.91
aSE <sub>C</sub> S	-228.8268891	-229.4986688	56.65	6.33	6.15
aSTT	-228.8360071	-229.5075640	56.40	0.49	0.46
aSTC	-228.8249150	-229.4976101	56.36	7.42	6.67
<b>CH<sub>3</sub>CHClOOH</b>					
bSTS	-687.7447739	-688.5390717	50.39	0	0
bETS	-687.7373539	-688.5330887	50.73	5.29	4.39
bSG <sub>C-H</sub> S	-687.7385928	-688.5317279	50.70	4.21	4.94
bSG <sub>C-Cl</sub> S	-687.7385928	-688.5338207	50.80	4.27	3.69
bSE <sub>H</sub> S	-687.7383606	-688.5321130	50.62	4.44	4.78
bSE <sub>C</sub> S	-687.7303011	-688.5246099	50.59	9.47	9.46
bSE <sub>Cl</sub> S	-687.7254932	-688.5194344	50.53	12.43	12.66
bSTT	-687.7407813	-688.5353040	50.44	2.87	2.73
bSTC	-687.7305704	-688.5265874	50.65	9.51	8.43
<b>CH<sub>3</sub>CCl<sub>2</sub>OOH</b>					
cSTS	-1146.6333294	-1147.5563757	44.26	0	0
cETS	-1146.6256585	-1147.5490582	43.98	4.87	4.65
cSGS	-1146.6315638	-1147.5547108	44.21	1.07	1.01
cSE <sub>H</sub> S	-1146.6173271	-1147.5402002	43.81	9.85	9.96
cSE <sub>C</sub> S	-1146.6228546	-1147.5452405	44.00	6.55	6.97
cSTT	-1146.6298992	-1147.5530784	43.85	2.16	2.08
cSTC	-1146.6230935	-1147.5478277	43.82	6.41	5.35

<sup>1</sup> Unit in hartrees.<sup>2</sup> Unscaled zero-pointed vibrational energy, in kcal/mol<sup>3</sup> The scaled (x0.9) zero-point vibrational energies were included in the calculation of barriers. unit in kcal/mol.

**Table 4.10** Coefficients <sup>a</sup> of Fourier Expansions for Internal Rotations

<i>Rotors</i>	$V_1$	$V_2$	$V_3$	$V'_1$	$V'_2$		
C-C bond							
CH <sub>3</sub> -CH <sub>2</sub> OOH			-3.32				
CH <sub>3</sub> -CHClOOH			-4.39				
CH <sub>3</sub> -CCl <sub>2</sub> OOH			-4.65				
C-O bond							
CH <sub>3</sub> CH <sub>2</sub> -OOH	-2.308	-2.039	-3.842				
CH <sub>3</sub> CHCl-OOH	-1.986	-5.401	-5.734	4.537	-0.8673		
CH <sub>3</sub> CCl <sub>2</sub> -OOH	1.987	2.147	-8.957				
O-O bond							
CH <sub>3</sub> CH <sub>2</sub> O-OH	-6.210	-2.658					
CH <sub>3</sub> CHClO-OH	-5.700	-5.190					
CH <sub>3</sub> CCl <sub>2</sub> O-OH	-3.270	-3.528					
	$a_0$	$a_1$	$a_2$	$a_3$	$b_1$	$b_2$	
C-C bond							
CH <sub>3</sub> -CH <sub>2</sub> OOH	1.66			1.66			
CH <sub>3</sub> -CHClOOH	2.195			2.195			
CH <sub>3</sub> -CCl <sub>2</sub> OOH	2.325			2.325			
C-O bond							
CH <sub>3</sub> CH <sub>2</sub> -OOH	2.056	1.154	1.019	1.921			
CH <sub>3</sub> CHCl-OOH	6.053	1.063	2.747	2.797	2.282	-0.466	
CH <sub>3</sub> CCl <sub>2</sub> -OOH	4.559	-0.9936	-1.074	4.479			
O-O bond							
CH <sub>3</sub> CH <sub>2</sub> O-OH	2.236	3.105	1.329				
CH <sub>3</sub> CHClO-OH	2.985	2.850	2.595				
CH <sub>3</sub> CCl <sub>2</sub> O-OH	1.951	1.635	1.764				

<sup>a</sup> Unit of kcal/mol

**Table 4.11** Total Energy and Enthalpies of Formation for Species in Isodesmic Reactions and the Reaction Energies

	HF/6-31G* (Hartree)	MP2/6-31G** (Hartree)	ZPVE (kcal/mol)	$\Delta H_f^\circ_{298}$ (kcal/mol)
CH <sub>4</sub>	-40.1915717	-40.3646486	29.97	-17.89 <sup>a</sup>
C <sub>2</sub> H <sub>6</sub>	-79.2287550	-79.5433489	50.05	-20.24 <sup>a</sup>
C <sub>2</sub> H <sub>5</sub> Cl	-538.1315203	-538.5639110	44.90	-26.70 <sup>a</sup>
1,1C <sub>2</sub> H <sub>4</sub> Cl <sub>2</sub>	-997.0254869	-997.5817817	38.92	-31.05 <sup>a</sup>
CH <sub>3</sub> OH	-115.035418	-115.3812742	34.72	-48.08 <sup>a</sup>
CH <sub>3</sub> OOH	-189.7967191	-190.3213230	37.55	-31.30 <sup>b</sup> , -33.2 <sup>c</sup> , -33 <sup>d</sup>
CH <sub>3</sub> CH <sub>2</sub> OH	-154.0757446	-154.5682726	53.98	-56.12 <sup>a</sup>
CH <sub>3</sub> CHClOH	-612.9773607	-613.5875823	48.57	-64.2 <sup>c</sup>
CH <sub>3</sub> CCl <sub>2</sub> OH	-1071.8820169	-1072.6232440	41.72	-71.8 <sup>f</sup>
CH <sub>3</sub> CH <sub>2</sub> OOH	-228.8367278	-229.5082360	56.66	
CH <sub>3</sub> CHClOOH	-687.7447739	-688.5390717	50.39	
CH <sub>3</sub> CCl <sub>2</sub> OOH	-1146.633329	-1147.5563757	44.26	

<sup>a</sup> Stull, D. R.; Westrum, E. F., Jr.; Sinke, G. C. *The Chemical Thermodynamics of Organic Compounds*. Robert E. Krieger Publishing Co., Inc., Malabar (1987). <sup>b</sup> DeMore, W. B. *et al.*, 'Chemical Kinetics and Photochemical Data for Use in Stratospheric Modeling', NASA Jet Propulsion Laboratory, (1990). <sup>c</sup> Estimated from  $\Delta H_f^\circ_{298}$  (CH<sub>3</sub>OOH) equal to 2.70 kcal/mol with  $\Delta H_f^\circ_{298}$  (H) equal to 52.1 kcal/mol and  $DH^\circ$ (CH<sub>3</sub>OO-H) equal to 88.0 kcal/mol (see Chapter 3). <sup>d</sup> Ref. 1. <sup>e</sup> Estimated in this work. The  $\Delta H_f^\circ_{298}$  (CH<sub>3</sub>CHClOH) was estimated from  $\Delta H_f^\circ_{298}$  of (C<sub>2</sub>H<sub>5</sub>CHClOH) equal to -15.2 kcal/mol. (results of BAC/MP4 by Melius, ref. 27), with  $\Delta H_f^\circ_{298}$  (H) equal to 52.1 kcal/mol and the average bond dissociation energy of primary C-H bond as 101.1 kcal/mol (ref. 28). <sup>f</sup> Estimated in this work. The  $\Delta H_f^\circ_{298}$  (CH<sub>3</sub>CCl<sub>2</sub>OH) was estimated from  $\Delta H_f^\circ_{298}$  of (C<sub>2</sub>H<sub>5</sub>CCl<sub>2</sub>OH) equal to -22.8 kcal/mol. (results of BAC/MP4 by Melius, ref. 27), with  $\Delta H_f^\circ_{298}$  (H) equal to 52.1 kcal/mol and the average bond dissociation energy of primary C-H bond as 101.1 kcal/mol (ref.28).

**Table 4.12** Reaction Energies (kcal/mol) and Enthalpies of Formation (kcal/mol) for CH<sub>3</sub>CH<sub>2</sub>OOH, CH<sub>3</sub>CHClOOH and CH<sub>3</sub>CCl<sub>2</sub>OOH

	$\Delta H_{rxn}^\circ$ (HF/6-31G*)	$\Delta H_{rxn}^\circ$ (MP2/6-31G**)	$\Delta H_f^\circ_{298}$ <sup>a</sup>	$\Delta H_f^\circ_{298}$ <sup>b</sup>	$\Delta H_f^\circ_{298}$ (literature)
CH <sub>3</sub> CH <sub>2</sub> OOH					-40.2 <sup>c</sup> , -41.09 <sup>d</sup>
Scheme I	-2.65	-6.02	-39.68	-41.58	
Scheme II	0.06	-0.08	-39.42	<b>-41.32</b>	
CH <sub>3</sub> CHClOOH					-48.98 <sup>d</sup>
Scheme I	-6.97	-13.48	-53.59	-55.49	
Scheme II	1.00	-0.04	-47.36	<b>-49.36</b>	
CH <sub>3</sub> CCl <sub>2</sub> OOH					
Scheme I	-3.71	-13.26	-57.72	-59.62	
Scheme II	6.01	4.08	-50.84	<b>-52.84</b>	

<sup>a</sup> use MP2/6-31G\*\* energy and  $\Delta H_f^\circ_{298}$  (CH<sub>3</sub>OOH) = 31.3 kcal/mol. <sup>b</sup> use MP2/6-31G\*\* energy and  $\Delta H_f^\circ_{298}$  (CH<sub>3</sub>OOH) = 33.2 kcal/mol. <sup>c</sup> Ref. 1. <sup>d</sup> See Chapter 3 of this dissertation.

**Table 4.13** Comparison of difference of bond dissociation energies for  $DH^\circ(R-OH) - DH^\circ(R-OOH)$ 

	$\Delta D^\circ$ (kcal/mol) <sup>a</sup>
$DH^\circ(CH_3-OH) - DH^\circ(CH_3-OOH)$	21.70 <sup>b</sup>
$DH^\circ(CH_3CH_2-OH) - DH^\circ(CH_3CH_2-OOH)$	21.62
$DH^\circ(CH_3CHCl-OH) - DH^\circ(CH_3CHCl-OOH)$	21.66
$DH^\circ(CH_3CCl_2-OH) - DH^\circ(CH_3CCl_2-OOH)$	25.78

<sup>a</sup> All values were calculated from the  $\Delta H^\circ_{rxn}$  of reactions in Scheme II at MP2/6-31G\*\* level, see text. <sup>b</sup> Calculated from the following values, (unit in kcal/mol):  $\Delta H_f^\circ_{298}(OH) = 9.32$  kcal/mol,  $\Delta H_f^\circ_{298}(HO_2) = 2.50$ ,  $\Delta H_f^\circ_{298}(CH_3OH) = -48.08$  and  $\Delta H_f^\circ_{298}(CH_3OOH) = 33.2$ , see Table 4.11 for reference.

**Table 4.14** Ideal Gas Phase Thermodynamic Properties for  $CH_3CH_2OOH$ ,  $CH_3CHClOOH$  and  $CH_3CCl_2OOH$ 

	$\Delta H_f^\circ_{298}$ <sup>a</sup>	$S^\circ_{298}$ <sup>b</sup>	$C_{p300}$ <sup>c</sup>	$C_{p400}$	$C_{p500}$	$C_{p600}$	$C_{p800}$	$C_{p1000}$	$C_{p1500}$
$CH_3CH_2OOH$ ( $\sigma^d = 3$ )									
vib. <sup>e</sup>		2.906	6.098	10.117	13.986	17.377	22.783	26.800	33.023
ext.-rot. <sup>f</sup>		21.569	2.981	2.981	2.981	2.981	2.981	2.981	2.981
tra. <sup>g</sup>		38.276	4.968	4.968	4.968	4.968	4.968	4.968	4.968
C--C <sup>h</sup>		4.233	2.122	2.186	2.102	1.967	1.707	1.516	1.262
C--O <sup>i</sup>		5.763	2.243	2.216	2.104	1.960	1.660	1.388	0.893
O--O <sup>j</sup>		3.233	1.377	1.447	1.510	1.562	1.616	1.609	1.489
total	-41.32	75.980	19.789	23.915	27.651	30.816	35.714	39.262	44.616
$CH_3CHClOOH$ ( $\sigma = 3$ )									
vib.		5.113	9.286	13.469	17.213	20.370	25.234	28.760	34.163
ext.-rot.		24.314	2.981	2.981	2.981	2.981	2.981	2.981	2.981
tra.		39.592	4.968	4.968	4.968	4.968	4.968	4.968	4.968
C--C		3.932	1.987	2.179	2.226	2.179	1.976	1.768	1.427
C--O		3.292	2.308	2.827	3.289	3.528	3.412	2.948	1.857
O--O		2.723	1.802	1.915	1.915	1.885	1.813	1.741	1.569
total	-49.36	78.966	23.331	28.339	32.592	35.911	40.383	43.167	46.965
$CH_3CCl_2OOH$ ( $\sigma = 3$ )									
vib.		8.360	13.126	17.350	20.865	23.711	27.948	30.940	35.451
ext.-rot.		25.675	2.981	2.981	2.981	2.981	2.981	2.981	2.981
tra.		40.501	4.968	4.968	4.968	4.968	4.968	4.968	4.968
C--C		3.877	1.955	2.161	2.232	2.208	2.029	1.825	1.469
C--O		5.133	1.992	2.027	2.033	2.023	1.952	1.821	1.386
O--O		3.087	1.885	1.910	1.871	1.814	1.685	1.566	1.354
total	-52.84	86.633	26.907	31.396	34.951	37.704	41.563	44.100	47.609

<sup>a</sup> Unit in kcal/mol, <sup>b,c</sup> Unit in cal/mol-K, <sup>d</sup>  $\sigma$ : symmetry, <sup>e</sup> vib.: Contribution from vibrational frequencies <sup>f</sup> ext.-rot.: Contribution from external rotations, <sup>g</sup> tra.: Contribution from translations, <sup>h</sup> C--C: Contribution from internal rotation about C-C bond, <sup>i</sup> C--O: Contribution from internal rotation about C-O bond, <sup>j</sup> O--O: Contribution from internal rotation about O-O bond

**Table 4.15** Comparison of Pitzer & Gwinn's Method and the Method Used in this Study for Calculation of Thermodynamic Properties of Molecules with Hindered Rotors

		$I_r^a$ (amu-Å <sup>2</sup> )	$V_{\text{mean}}^b$ (kcal/mol)	$n^c$	$S_{298}^\circ$ (cal/mol-K)	$C_{p,300}$ (cal/mol-K)	$C_{p,500}$
<b>CH<sub>3</sub>CH<sub>2</sub>OOH</b>							
C--O <sup>d</sup>	Pitzer	17.22	4.53	3	5.494	2.183	2.317
	this				5.763	2.243	2.104
O--O <sup>e</sup>	Pitzer	0.86	6.67	2	2.350	1.576	2.054
	this				3.233	1.377	1.510
<b>CH<sub>3</sub>CHClOOH</b>							
C--O	Pitzer	24.95	8.97	3	5.089	2.002	2.147
	this				3.292	2.308	3.289
O--O	Pitzer	0.87	8.43	2	2.167	1.425	1.921
	this				2.723	1.802	1.915
<b>CH<sub>3</sub>CCl<sub>2</sub>OOH</b>							
C--O	Pitzer	25.96	8.465	3	5.187	2.014	2.17
	this				5.133	1.992	2.033
O--O	Pitzer	0.87	5.35	2	2.551	1.725	2.148
	this				3.087	1.885	1.871

<sup>a</sup> Reduced moment of inertia. <sup>b</sup> Mean Rotational Barrier. <sup>c</sup> Number of potential maximum.

<sup>d</sup> C--O : Contribution from internal rotation about C-O bond. <sup>e</sup> O--O : Contribution from internal rotation about O-O bond.

**Table 4.16** Comparison of Bond Lengths (Angstrom) between Different Calculation Levels

	<i>6-31G*</i>	<i>AMI</i>	$(r_{AMI}-r_{6-31G*})$ $/r_{6-31G*}$	<i>PM3</i>	$(r_{PM3}-r_{6-31G*})$ $/r_{6-31G*}$
<b>a</b>					
CC	1.5168	1.5072	-0.63%	1.5196	0.18%
C1H3	1.0850	1.1155	2.81%	1.0972	1.12%
C1H4	1.0838	1.1164	3.01%	1.0979	1.30%
C1H5	1.0842	1.1162	2.95%	1.098	1.27%
C2H6	1.0837	1.119	3.26%	1.107	2.15%
C2H7	1.0857	1.1201	3.17%	1.1069	1.95%
CO	1.4060	1.4525	3.31%	1.4114	0.38%
OO	1.3932	1.2895	-7.44%	1.5144	8.70%
OH	0.9495	0.9842	3.65%	0.9429	-0.70%
<b>b</b>					
CC	1.5112	1.5117	0.03%	1.5163	0.34%
C1H3	1.0817	1.1158	3.15%	1.0973	1.44%
C1H4	1.0821	1.1167	3.20%	1.0982	1.49%
C1H5	1.0839	1.1171	3.06%	1.0979	1.29%
C2Cl6	1.8191	1.7748	-2.44%	1.8231	0.22%
C2H7	1.0760	1.1189	3.99%	1.1144	3.57%
CO	1.3738	1.4453	5.20%	1.3953	1.57%
OO	1.3866	1.2897	-6.99%	1.5151	9.27%
OH	0.9518	0.9852	3.51%	0.9431	-0.91%
<b>c</b>					
CC	1.5164	1.5194	0.20%	1.515	-0.09%
C1H3	1.0800	1.1159	3.32%	1.0977	1.64%
C1H4	1.0818	1.1175	3.30%	1.098	1.50%
C1H5	1.0818	1.1171	3.26%	1.098	1.50%
C2Cl6	1.7978	1.7708	-1.50%	1.7937	-0.23%
C2Cl7	1.7801	1.7844	0.24%	1.7935	0.75%
CO	1.3678	1.4466	5.76%	1.393	1.84%
OO	1.3835	1.2823	-7.31%	1.5166	9.62%
OH	0.9521	0.9873	3.70%	0.9433	-0.92%

**Table 4.17** Comparison of Bond Angles (degree) between Different Calculation Levels

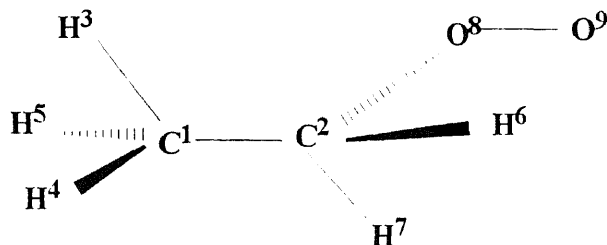
	<i>6-31G*</i>	<i>AMI</i>	$(a_{AMI}-a_{6-31G*})$ $/a_{6-31G*}$	<i>PM3</i>	$(a_{PM3}-a_{6-31G*})$ $/a_{6-31G*}$
<b>a</b>					
H3C1C2	109.921	109.287	-0.58%	109.914	-0.01%
H4C1C2	110.621	110.427	-0.18%	112.134	1.37%
H5C1C2	110.845	110.579	-0.24%	112.141	1.17%
H6C2C1	111.390	112.132	0.67%	111.349	-0.04%
H7C2C1	111.383	112.037	0.59%	111.39	0.01%
O8C2C1	106.973	106.015	-0.90%	106.388	-0.55%
O9O8C2	107.704	111.264	3.31%	106.276	-1.33%
H10O9O8	102.150	107.491	5.23%	94.762	-7.23%
<b>b</b>					
H3C1C2	110.230	109.673	-0.51%	109.939	-0.26%
H4C1C2	110.350	110.688	0.31%	112.147	1.63%
H5C1C2	108.766	109.46	0.64%	111.531	2.54%
C1C2C1	110.342	110.792	0.41%	107.657	-2.43%
H7C2C1	113.534	113.584	0.04%	112.779	-0.66%
O8C2C1	107.707	105.957	-1.62%	107.986	0.26%
O9O8C2	109.551	112.323	2.53%	106.783	-2.53%
<b>c</b>					
H3C1C2	110.074	109.892	-0.17%	109.828	-0.22%
H4C1C2	109.135	109.52	0.35%	111.712	2.36%
H5C1C2	108.756	109.768	0.93%	111.672	2.68%
C16C2C1	110.020	110.747	0.66%	109.685	-0.30%
C17C2C1	111.539	110.403	-1.02%	109.651	-1.69%
O8C2C1	106.011	104.752	-1.19%	108.187	2.05%
O9O8C2	112.157	115.49	2.97%	106.773	-4.80%
H10O9O8	102.603	108.25	5.50%	94.725	-7.68%

**Table 4.18** Comparison of Dihedral Angles (degree) between Different Calculation Levels

	<i>6-31G*</i>	<i>AM1</i>	$(d_{AM1}-d_{6-31G*})$ $/d_{6-31G*}$	<i>PM3</i>	$(d_{PM3}-d_{6-31G*})$ $/d_{6-31G*}$
<b>a</b>					
H4C1C2H3	119.820	120.035	0.18%	119.553	-0.22%
H5C1C2H3	-119.858	-120.121	0.22%	-119.539	-0.27%
H6C2C1H3	-60.604	-61.204	0.99%	-60.079	-0.87%
H7C2C1H3	60.466	62.218	2.90%	59.754	-1.18%
O8C2C1H3	-179.862	-179.738	-0.07%	-179.769	-0.05%
O9O8C2C1	-182.983	-173.687	-5.08%	-179.071	-2.14%
H10O9O8C2	116.520	99.761	-14.38%	179.316	53.89%
<b>b</b>					
H4C1C2H3	120.600	120.559	-0.03%	119.667	-0.77%
H5C1C2H3	-119.787	-119.817	0.03%	-119.48	-0.26%
C16C2C1H3	-58.654	-59.77	1.90%	-60.88	3.80%
H7C2C1H3	58.613	58.782	0.29%	56.658	-3.34%
O8C2C1H3	181.145	179.456	-0.93%	178.236	-1.61%
O9O8C2C1	193.776	160.31	-17.27%	160.748	-17.04%
H10O9O8C2	97.895	101.986	4.18%	160.925	64.39%
<b>c</b>					
H4C1C2H3	120.386	120.26	-0.10%	119.528	-0.71%
H5C1C2H3	-120.130	-120.376	0.20%	-119.55	-0.48%
C16C2C1H3	-60.460	-59.73	-1.21%	-57.3	-5.23%
C17C2C1H3	59.737	60.394	1.10%	58.646	-1.83%
O8C2C1H3	-179.408	-179.029	-0.21%	-179.323	-0.05%
O9O8C2C1	-178.043	-176.39	-0.93%	-179.948	1.07%
H10O9O8C2	-97.539	-88.333	-9.44%	-179.912	84.45%

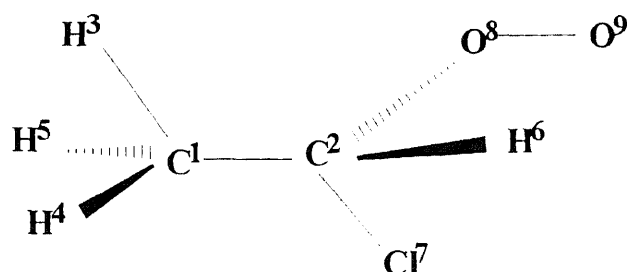


**Table 5.1** Optimized Molecular Geometry Parameters of CH<sub>3</sub>CH<sub>2</sub>OO Rotational Conformers



<i>Parameter</i> <sup>#</sup>	<i>aTrans</i>	<i>aGauche</i>	<i>aCis<sub>H</sub></i>	<i>aCis<sub>C</sub></i>
r21	1.51433	1.51614	1.516	1.51536
r31	1.08472	1.08532	1.08532	1.08537
r41	1.08378	1.08341	1.084	1.08211
r51	1.08377	1.0842	1.08397	1.08209
r62	1.08220	1.08175	1.0795	1.08229
r72	1.08220	1.08133	1.0827	1.08231
r82	1.42490	1.42517	1.42917	1.43575
r92	1.30079	1.30114	1.29754	1.29428
a312	109.800	109.896	109.971	107.942
a412	110.762	110.802	110.689	111.725
a512	110.766	110.624	110.746	111.712
a621	111.907	111.972	112.231	111.061
a721	111.907	111.604	111.411	111.065
a821	107.132	111.75	109.315	115.086
a982	111.238	111.314	112.718	114.739
d4123	119.781	119.657	119.991	119.150
d5123	-119.79	-119.763	-119.689	-119.139
d6213	-61.269	-60.765	-63.303	-60.270
d7213	61.339	61.764	59.507	60.256
d8213	-179.965	-182.368	-182.728	-180.006
d9821	-179.996			0
d9826		193.398	0	

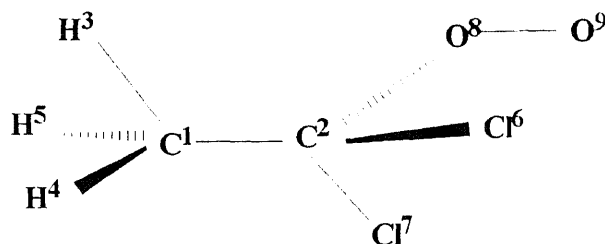
<sup>a</sup> “r” represent bond length, r12 represents the bond length of a C-C bond, where 1 and 2 are the index of atom. “a” represent a bond angle, a312 represents the angle between bond C1-H3 and C1-H2. “d” represents a dihedral angle, d4123 represents the dihedral angle constructed by H4-C1-C2-H3.

**Table 5.2** Optimized Molecular Geometry Parameters of CH<sub>3</sub>CHClOO Rotational Conformers

<i>Parameter<sup>#</sup></i>	<i>bTrans</i>	<i>bG<sub>C-Cl</sub></i>	<i>bG<sub>C-H</sub></i>	<i>bCis<sub>C</sub></i>	<i>bCis<sub>H</sub></i>	<i>bCis<sub>Cl</sub></i>
r21	1.51090	1.51261	1.15113	1.51212	1.50176	1.51233
r31	1.08174	1.08212	1.08251	1.08206	1.08205	1.08242
r41	1.08217	1.08056	1.08242	1.08032	1.08229	1.08249
r51	1.08389	1.08453	1.08394	1.08250	1.08425	1.08398
r62	1.07590	1.07588	1.07611	1.07609	1.07458	1.07691
r72	1.79110	1.78893	1.77500	1.79077	1.79018	1.77063
r82	1.40095	1.40482	1.41981	1.41634	1.40904	1.42885
r92	1.30666	1.30362	1.30252	1.29914	1.30240	1.29462
a312	110.098	109.701	110.288	108.241	110.358	110.305
a412	110.301	110.995	110.232	111.246	110.295	110.248
a512	109.058	108.866	109.069	110.199	108.897	109.006
a621	111.216	111.348	111.701	110.598	111.050	111.672
a721	113.339	112.278	112.794	112.366	113.958	111.996
a821	107.173	113.053	111.114	115.181	109.259	107.502
a982	111.939	112.717	109.933	114.546	112.079	117.480
d4123	120.418	120.501	120.652	119.869	120.599	120.781
d5123	-119.821	-119.161	-119.472	-199.021	-119.852	-119.650
d6213	-58.356	-61.502	-61.831	-60.078	-59.246	-61.166
d7213	60.104	57.449	59.220	57.556	60.507	57.890
d8213	180.388	173.850	180.774	178.959	181.560	173.603
d9821	197.298			0		
d9826		176.127			0	
d9827			160.035			0

# : see note for parameters of Table 5.1.

**Table 5.3** Optimized Molecular Geometry Parameters of CH<sub>3</sub>CCl<sub>2</sub>OO. Rotational Conformers



Parameter <sup>#</sup>	<i>cTrans</i>	<i>cGauche</i>	<i>cCisC</i>	<i>cCisCl</i>	<i>cE<sub>MeT</sub>*</i>
r21	1.51515	1.51565	1.51613	1.51531	1.53441
r31	1.08005	1.08032	1.08115	1.08037	1.07887
r41	1.08184	1.08245	1.08030	1.08244	1.08156
r51	1.08183	1.08045	1.08030	1.08190	1.07893
r62	1.77686	1.76797	1.77772	1.76386	1.78002
r72	1.77680	1.77776	1.77772	1.78154	1.77928
r82	1.39605	1.40906	1.41015	1.41815	1.33880
r92	1.30837	1.30620	1.30057	1.29710	1.30792
a312	109.957	109.713	108.171	110.378	110.731
a412	109.043	108.847	110.121	108.862	108.417
a512	109.046	109.729	110.120	108.965	110.713
a621	110.868	111.022	110.405	111.218	111.854
a721	110.875	110.839	110.405	110.309	111.886
a821	105.495	112.192	114.739	107.146	105.358
a982	113.841	111.830	114.253	117.272	113.853
d4123	120.208	119.762	119.531	120.436	119.533
d5123	-120.215	-120.125	-119.529	-120.371	-121.038
d6213	-60.981	-60.361	-60.428	-61.142	0
d7213	61.012	62.100	61.414	60.367	122.613
d8213	-179.986	-175.370	-180.007	-185.066	-118.688
d9821	-180.027		0.000		-180.096
d9826		184.261		0.000	

# : See note for parameters of Table 5.1.

\* : The conformer for study of rotational barrier of methyl rotor. The methyl group is eclipsed with the atoms at C2, and CCOO is in *trans* conformation with dihedral angle  $\approx 180^\circ$ .

**Table 5.4** Mulliken Charge <sup>a</sup> Distribution Calculated at the UHF/6-31G\* Level

	CH <sub>3</sub> CH <sub>2</sub> OO	CH <sub>3</sub> CHClOO	CH <sub>3</sub> CCl <sub>2</sub> OO
Total atomic charges:			
C1	-0.516313	-0.500571	-0.480426
C2	0.004983	0.055879	0.079006
H3	0.175019	0.199940	0.215662
H4	0.186456	0.209587	0.216466
H5	0.186444	0.196803	0.216464
H6	0.176521		
Cl6		-0.066784	0.018588
H7	0.176524	0.233936	
Cl7			0.018613
O8	-0.314097	-0.290074	-0.280240
O9	-0.075538	-0.038715	-0.004135
Atomic charges with hydrogens summed into heavy atoms			
C1	0.031607	0.105759	0.168168
C2	0.358028	0.289814	0.079006
O8	-0.314097	-0.290074	-0.280240
O9	-0.075538	-0.038715	-0.004135
Cl6		-0.066784	0.018588
Cl7			0.018613

<sup>a</sup> For definition and calculation procedure of Mulliken charge distribution, see p. 25-29 in ref. 22.  
 For discussion of Mulliken charge and Mulliken population analysis, see p. 336-341 in ref. 22.

**Table 5.5** Harmonic Vibration Frequencies ( $\text{cm}^{-1}$ )

	Frequencies (the ones with negative values are imaginary frequencies)											
<i>aTrans</i>	103.5 <sup>a</sup>	258.5 <sup>b</sup>	336.5	550.2	880.7	962.4	1126.4	1264.8	1281.8	1290.6	1409.7	
	1535.8	1579.6	1628.6	1643.5	1671.6	3219.1	3249.2	3285.4	3288.3	3310.0		
<i>aGauche</i>	133.5 <sup>a</sup>	254.1 <sup>b</sup>	401.1	575.8	872.2	949.8	1110.1	1204.7	1275.3	1322.6	1443.4	
	1530.9	1572.1	1629.9	1639.5	1652	3216	3259.7	3283.3	3290.9	3320.2		
<i>aCis<sub>H</sub></i>	-101.6	252.2 <sup>b</sup>	411.9	553.4	867.6	951.1	1113.7	1211.6	1276.3	1342.4	1433.5	
	1529.2	1571.6	1629.1	1640.9	1655.3	3214.9	3253.9	3282.8	3289.1	3327.7		
<i>aCis<sub>C</sub></i>	-161.6	308.8 <sup>b</sup>	349	649.5	867.6	917.6	1111.4	1216.6	1272	1330.8	1414.3	
	1546.2	1582.3	1632.4	1642.3	1672.9	3223.3	3250.2	3288.1	3291.6	3318.8		
<i>bTrans</i>	122.5 <sup>a</sup>	256.7 <sup>b</sup>	308.3	351.6	470.5	591	741.1	989.2	1119.9	1216.2	1260.4	
	1281.3	1448.7	1507.6	1574.4	1626.1	1630.9	3234.6	3310.3	3322.2	3355		
<i>bG<sub>C-H</sub></i>	134.7 <sup>a</sup>	272.5 <sup>b</sup>	324.5	374.4	428.6	661.6	771.7	972.0	1106.8	1189.9	1244.2	
	1271.0	1441.6	1522.9	1573.3	1627.1	1636.1	3231.7	3305.7	3330.9	3360.9		
<i>bG<sub>C-H</sub></i>	87.1 <sup>a</sup>	275.3 <sup>b</sup>	318.9	340.9	485.3	498.2	827.7	973.9	1154.6	1208.1	1234.4	
	1267.7	1444.6	1507	1572	1627.9	1631.6	3229.7	3304.7	3315.7	3353.2		
<i>bCis<sub>C</sub></i>	-114.3	321.1 <sup>b</sup>	342.2	362.4	408	658.7	746.7	940.1	1111.8	1195.4	1245.9	
	1309.3	1449.4	1512.6	1577	1628.9	1631.5	3242.3	3315.4	3331.3	3351.7		
<i>bG<sub>C-H</sub></i>	-75.4	267.2 <sup>b</sup>	331	390.5	413.7	552.5	795.1	971.8	1129.9	1212.4	1248.9	
	1295.2	1441.7	1505.9	1573.6	1626.1	1629.6	3329.3	3304.1	3319.9	3372.4		
<i>bCis<sub>Cl</sub></i>	-168.5	278.1 <sup>b</sup>	293.3	350.5	461.8	603.6	777.4	974.3	1101.3	1201.8	1224.3	
	1311.4	1469.6	1501.7	1571.7	1627.6	1629.8	3229.2	3303.4	3314.2	3339.4		
<i>cTrans</i>	149.9 <sup>a</sup>	244.3 <sup>b</sup>	294.9	322.6	326	392.7	436.2	618.2	646.8	834.2	1021.7	
	1120.1	1224.8	1269.5	1289.7	1572.3	1623.1	1626.2	3246	3328.5	3343.7		
<i>cGauche</i>	135.9 <sup>a</sup>	256.7 <sup>b</sup>	287	308.8	359.8	409.2	450.4	513.6	678.9	887.9	998.9	
	1217.3	1238.6	1260.3	1272.5	1570.6	1624.5	1631.4	3247.3	3331.2	3344.3		
<i>cCis<sub>C</sub></i>	-112.3	279.2 <sup>b</sup>	306.8	357.6	375.7	403.7	416.3	493.7	727	834.1	966.5	
	1223	1242.4	1273.2	1300.5	1575	1624.3	1629.4	3256.5	3345.1	3345.4		
<i>cCis<sub>Cl</sub></i>	-148.8	276.9 <sup>b</sup>	286.5	310.5	353.2	392.6	413.8	583.4	632.8	868.6	996.3	
	1205.5	1232.9	1253.5	1318.9	1572.2	1623.6	1624.8	3242.2	3323.4	3339.7		

a : Frequencies corresponded to torsion motion about C-O bond.

b : Frequencies corresponded to torsion motion about C-C bond

**Table 5.6** Rotation Barriers<sup>a</sup>

	UHF/6-31G* (Hartree)	MP2/6-31G** (Hartree)	ZPVE (kcal/mol)	BAR/UHF (kcal/mol)	BAR/MP2 (kcal/mol)	S <sup>2</sup>
<i>aTrans</i>	-228.2427062	-228.8686401	48.43	-0.10	0.42	0.76
<i>aGauche</i>	-228.2426116	-228.8693803	48.52	0.00	0.00	0.76
<i>aCis<sub>H</sub></i>	-228.2406562	-228.8677986	48.33	1.23	0.99	0.76
<i>aCis<sub>C</sub></i>	-228.2372527	-228.8655090	48.44	3.46	2.53	0.76
<i>bTrans</i>	-687.1440692	-687.8907096	42.48	0.00	0.00	0.76
<i>bG<sub>C-Cl</sub></i>	-687.1424627	-687.8899762	42.54	1.05(1.06)	0.56(0.54)	0.76
<i>bG<sub>C-H</sub></i>	-687.1408767	-687.8898488	42.40	1.98(1.97)	0.51(0.55)	0.76
<i>bCis<sub>C</sub></i>	-687.1372023	-687.8862882	42.43	4.42(4.70)	2.89(2.96)	0.76
<i>bCis<sub>H</sub></i>	-687.1414377	-687.8895587	42.33	1.68(2.15)	0.75(0.87)	0.76
<i>bCis<sub>Cl</sub></i>	-687.1368330	-687.8836404	42.26	4.50(3.87)	4.40(4.46)	0.76
<i>cTrans</i>	-1146.032266	-1146.9062635	35.78	0.00	0.00	0.76
<i>cGauche</i>	-1146.030008	-1146.9060895	35.76	1.42	0.11	0.76
<i>cCis<sub>C</sub></i>	-1146.026087	-1146.9027171	35.70	4.00	2.35	0.76
<i>cCis<sub>Cl</sub></i>	-1146.023427	-1146.9006238	35.52	5.51	3.50	0.76
<i>cE<sub>Me</sub>T<sup>b</sup></i>	-1146.024542	-1146.8989171	35.51	4.92	4.68	0.76

<sup>a</sup> Data in parentheses are from ref. 15. <sup>b</sup> The conformer for study of rotational barrier of methyl rotor. The methyl group is eclipsed with the atoms at C2, and CCOO is in *trans* conformation with dihedral angle  $\approx 180^\circ$ . Harmonic vibrational frequencies (unscaled): -280 (imaginary), 158, 249, 329, 346, 413, 440, 621, 652, 835, 1025, 1204, 1232, 1257, 1280, 1581, 1625, 1633, 3257, 3339, 3353.

**Table 5.7** Potential Constants (kcal/mol) of Fourier Expansions for Internal Rotations

<i>Rotors</i>	V <sub>1</sub>	V <sub>2</sub>	V <sub>3</sub>	V' <sub>1</sub>	V' <sub>2</sub>
C-C bond					
CH <sub>3</sub> -CH <sub>2</sub> OO			-2.90		
CH <sub>3</sub> -CHClOO			-4.51		
CH <sub>3</sub> -CCl <sub>2</sub> OO			-4.68		
C-O bond					
CH <sub>3</sub> CH <sub>2</sub> -OO	-2.308	-2.039	-3.842		
CH <sub>3</sub> CHCl-OO	-1.986	-5.401	-5.734	4.537	-0.8673
CH <sub>3</sub> CCl <sub>2</sub> -OO	1.987	2.147	-8.957		
	a <sub>0</sub>	a <sub>1</sub>	a <sub>2</sub>	a <sub>3</sub>	b <sub>1</sub> b <sub>2</sub>
C-C bond					
CH <sub>3</sub> -CH <sub>2</sub> OO	1.45			1.45	
CH <sub>3</sub> -CHClOO	2.255			2.255	
CH <sub>3</sub> -CCl <sub>2</sub> OO	2.34			2.34	
C-O bond					
CH <sub>3</sub> CH <sub>2</sub> -OO	0.9260	0.3377	0.5490	0.7173	
CH <sub>3</sub> CHCl-OO	1.658	0.05745	1.022	-1.014	1.093
CH <sub>3</sub> CCl <sub>2</sub> -OO	1.608	-0.3340	-0.4327	1.509	

**Table 5.8** Total Energy and Enthalpies of Formation for Species in Isodesmic Reactions and the Reaction Energies

	(U)HF/6-31G* (Hartree)	MP2/6-31G** (Hartree)	ZPVE (kcal/mol)	$\Delta H_f^{\circ}_{298}$ (kcal/mol)
CH <sub>3</sub> OH	-115.035418	-115.3812742	34.72	-48.08 <sup>a</sup>
CH <sub>3</sub> CH <sub>2</sub> OH	-154.0757446	-154.5682726	53.98	-56.12 <sup>a</sup>
CH <sub>3</sub> CHClOH	-612.9773607	-613.5875823	48.57	-64.2 <sup>b</sup>
CH <sub>3</sub> CCl <sub>2</sub> OH	-1071.8820169	-1072.6232440	41.72	-71.8 <sup>b</sup>
CH <sub>3</sub> O	-114.4207495	-114.7096743	25.27	3.9 <sup>c</sup>
CH <sub>3</sub> OO	-189.2022799	-189.6814057	29.29	2.7 <sup>d</sup>
CH <sub>3</sub> CH <sub>2</sub> O	-153.4598496	-153.8950472	44.34	-4 <sup>e</sup>
CH <sub>3</sub> CHClO	-612.366816	-612.9242882	39.24	-12.3 <sup>f</sup>
CH <sub>3</sub> CCl <sub>2</sub> O	-1071.256744	-1071.9412362	32.86	-19.9 <sup>g</sup>
CH <sub>3</sub> CH <sub>2</sub> OO	-228.2426116	-228.8693803	48.52	
CH <sub>3</sub> CHClOO	-687.1440692	-687.8907096	42.48	
CH <sub>3</sub> CCl <sub>2</sub> OO	-1146.032266	-1146.9062635	35.78	

<sup>a</sup> Stull, D. R.; Westrum, E. F., Jr.; Sinke, G. C. *The Chemical Thermodynamics of Organic Compounds*. Robert E. Krieger Publishing Co., Inc., Malabar (1987). <sup>b</sup> see Chapter 4. <sup>c</sup> JANAF Thermochemical Tables (1986) Edited by Chase et al., *J. Phys. Chem. Ref. Data* **1986**, Supplement No.1. <sup>d</sup> ref. 12.

<sup>e</sup> ref. 36. <sup>f</sup> Estimated in this work. The  $\Delta H_f^{\circ}_{298}$  (CH<sub>3</sub>CHClOH) is estimated to be -64.2 kcal/mol, and the O-H bond energy is assumed to be 104 kcal/mol. <sup>g</sup> Estimated in this work. The  $\Delta H_f^{\circ}_{298}$  (CH<sub>3</sub>CCl<sub>2</sub>OH) is estimated to be -71.8 kcal/mol, and the O-H bond energy is assumed to be 104 kcal/mol.

**Table 5.9** Reaction Energies (kcal/mol) and Enthalpies of Formation (kcal/mol) for CH<sub>3</sub>CH<sub>2</sub>OO, CH<sub>3</sub>CHClOO and CH<sub>3</sub>CCl<sub>2</sub>OO

	$\Delta H^{\circ}_{rxn}$ (HF 6-31G*)	$\Delta H^{\circ}_{rxn}$ (MP2/6-31G**)	$\Delta H_f^{\circ}_{298}$ <sup>*</sup> (kcal/mol)	$\Delta H_f^{\circ}_{298}$ (expt.)
CH <sub>3</sub> CH <sub>2</sub> OO				-5.19 <sup>a</sup>
Scheme I	-0.03	-0.03	<b>-5.37</b>	
Scheme II	-0.63	-1.49	-6.69	
CH <sub>3</sub> CHClOO				-13.07 <sup>b</sup>
Scheme I	-0.59	-0.60	-14.01	
Scheme II	1.98	2.63	-10.87	
Scheme III	2.61	4.12	-9.27	
CH <sub>3</sub> CCl <sub>2</sub> OO				(16.94) <sup>c</sup>
Scheme I	-0.44	-0.44	-21.46	
Scheme II	2.78	3.34	-17.76	
Scheme III	3.41	4.83	<b>-16.16</b>	

\* Using the energies calculated at MP2/6-31G\*\* level of theory.

<sup>a</sup> Ref. 8. <sup>b</sup> Ref. 15. <sup>c</sup> Estimated from  $\Delta H_f^{\circ}_{298}$  (CH<sub>3</sub>CCl<sub>2</sub>OOH) = -52.84 kcal/mol (see Chapter 4) with  $\Delta H_f^{\circ}_{298}$  (H.) = 52.1 kcal/mol and the average bond energy D<sup>o</sup>(ROO-H) = 88 kcal/mol.

**Table 5.10** Ideal Gas Phase Thermodynamic Properties for CH<sub>3</sub>CH<sub>2</sub>OO, CH<sub>3</sub>CHClOO and CH<sub>3</sub>CCl<sub>2</sub>OO

	$\Delta H_f^\circ_{298}$ <sup>a</sup>	$S^\circ_{298}$ <sup>b</sup>	$C_{p300}$ <sup>c</sup>	$C_{p400}$	$C_{p500}$	$C_{p600}$	$C_{p800}$	$C_{p1000}$	$C_{p1500}$
CH <sub>3</sub> CH <sub>2</sub> OO ( $\sigma^d = 3$ )									
vib. <sup>e</sup>		2.790	5.907	9.696	13.297	16.431	21.383	25.008	30.480
ext.-rot. <sup>f</sup>		21.488	2.981	2.981	2.981	2.981	2.981	2.981	2.981
tra. <sup>g</sup>		38.228	4.968	4.968	4.968	4.968	4.968	4.968	4.968
C--C <sup>h</sup>		4.402	2.154	2.134	1.997	1.841	1.585	1.415	1.204
C--O <sup>i</sup>		6.603	1.950	1.674	1.494	1.364	1.168	1.006	0.692
spin <sup>j</sup>		1.377							
total	-5.19	74.888	17.960	21.453	24.737	27.585	32.084	35.379	40.325
CH <sub>3</sub> CHClOO ( $\sigma = 3$ )									
vib.		5.185	9.125	13.084	16.573	19.480	23.895	27.027	31.663
ext.-rot.		24.244	2.981	2.981	2.981	2.981	2.981	2.981	2.981
tra.		39.560	4.968	4.968	4.968	4.968	4.968	4.968	4.968
C--C		3.902	1.970	2.170	2.229	2.193	2.001	1.795	1.446
C--O		4.566	3.612	3.796	3.463	2.987	2.150	1.579	0.836
spin		1.377							
total	-13.07	78.833	22.657	26.999	30.214	32.609	35.995	38.349	41.894
CH <sub>3</sub> CCl <sub>2</sub> OO ( $\sigma = 3$ )									
vib.		8.384	13.057	17.099	20.360	22.945	26.703	29.277	32.988
ext.-rot.		25.581	2.981	2.981	2.981	2.981	2.981	2.981	2.981
tra.		40.478	4.968	4.968	4.968	4.968	4.968	4.968	4.968
C--C		3.870	1.951	2.158	2.232	2.210	2.035	1.831	1.474
C--O		6.207	2.290	2.200	2.018	1.810	1.420	1.114	0.645
spin		1.377							
total	-16.16	85.897	25.247	29.406	32.559	34.914	38.107	40.171	43.056

<sup>a</sup> Unit in kcal/mol. <sup>b,c</sup> Unit in cal/mol-K. <sup>d</sup>  $\sigma$  : symmetry. <sup>e</sup> vib. : Contribution from vibrational frequencies

<sup>f</sup> ext.-rot. : Contribution from external rotations. <sup>g</sup> tra. : Contribution from translations.

<sup>h</sup> C--C : Contribution from internal rotation about C-C bond

<sup>i</sup> C--O : Contribution from internal rotation about C-O bond

<sup>j</sup> spin : Spin degeneracy



**Table 5.11** Comparison of Pitzer & Gwinn's Method and the Method Used in this Study for Calculation of Thermodynamic Properties of Molecules with Hindered Rotors

		$I_r^a$	$V_{\text{mean}}^b$	$n^c$	$S_{298}^{\circ d}$	$C_{p300}^e$	$C_{p500}$
<b>CH<sub>3</sub>CH<sub>2</sub>OO</b>							
C--O <sup>f</sup>	Pitzer	14.65	1.76	3	6.529	2.056	1.577
	this				6.603	1.950	1.494
<b>CH<sub>3</sub>CHClOO</b>							
C--O	Pitzer	20.06	3.645	2	5.904	2.291	2.243
	Pitzer		2.68	3	6.319	2.308	1.981
	this				4.566	3.612	3.463
<b>CH<sub>3</sub>CCl<sub>2</sub>OO</b>							
C--O	Pitzer	20.88	2.925	3	6.241	2.315	2.068
	this				6.207	2.290	2.018

<sup>a</sup> Reduced moment of inertia, amu-Å<sup>2</sup>. <sup>b</sup> Mean Rotational Barrier, kcal/mol. <sup>c</sup> Number of potential maximum. <sup>d,e</sup> unit in cal/mol-K. <sup>f</sup> C--O : Contribution from internal rotation about C-O bond

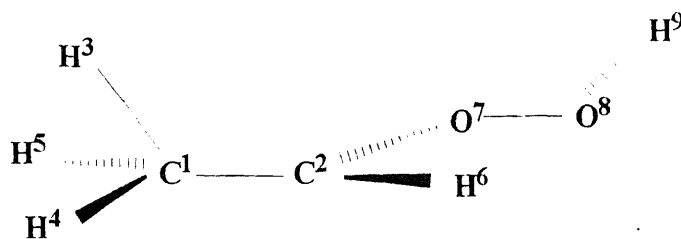
**Table 5.12** Comparison of Bond Lengths at Different Calculation Levels

	6-31G*	AMI	$(r_{\text{AMI}} - r_{6-31G^*}) / r_{6-31G^*}$	PM3	$(r_{\text{PM3}} - r_{6-31G^*}) / r_{6-31G^*}$
<b>a</b>					
CC	1.5143	1.5015	-0.85%	1.5127	-0.11%
C1H3	1.0847	1.1166	2.94%	1.0975	1.18%
C1H4	1.0838	1.1169	3.05%	1.0982	1.33%
C1H5	1.0838	1.1169	3.06%	1.0982	1.33%
C2H6	1.0822	1.1168	3.19%	1.1059	2.19%
C2H7	1.0822	1.1166	3.18%	1.1060	2.20%
CO	1.4249	1.4959	4.98%	1.4609	2.53%
OO	1.3008	1.1161	-14.20%	1.2583	-3.26%
<b>b</b>					
CC	1.5109	1.5048	-0.41%	1.5104	-0.03%
C1H3	1.0817	1.1167	3.23%	1.0976	1.47%
C1H4	1.0822	1.1180	3.31%	1.0981	1.47%
C1H5	1.0839	1.1172	3.08%	1.0985	1.35%
C2Cl6	1.0759	1.1171	3.83%	1.1145	3.59%
C2H7	1.7911	1.7556	-1.98%	1.7931	0.11%
CO	1.4010	1.5070	7.57%	1.4580	4.07%
OO	1.3067	1.1625	-11.03%	1.2599	-3.58%
<b>c</b>					
CC	1.5152	1.5126	-0.17%	1.5091	-0.40%
C1H3	1.0801	1.1168	3.40%	1.0979	1.66%
C1H4	1.0818	1.1177	3.32%	1.0984	1.53%
C1H5	1.0818	1.1179	3.33%	1.0983	1.53%
C2Cl6	1.7769	1.7580	-1.06%	1.7726	-0.24%
C2Cl7	1.7768	1.7579	-1.06%	1.7729	-0.22%
CO	1.3961	1.5275	9.42%	1.4601	4.59%
OO	1.3084	1.1539	-11.80%	1.2592	-3.76%

**Table 5.13** Comparison of Bond Angles and Dihedral Angles at Different Calculation Levels

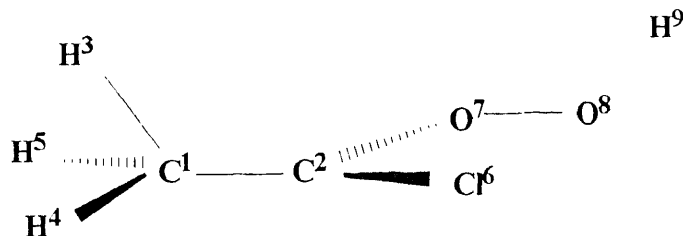
	6-31G*	AM1	$(a_{AM1}-a_{6-31G*})$ % $a_{6-31G*}$	PM3	$(a_{PM3}-a_{6-31G*})$ % $a_{6-31G*}$
<b>a</b>					
H3C1C2	109.8	109.3	-0.43%	110.1	0.23%
H4C1C2	110.8	110.7	-0.09%	112.1	1.22%
H6C2C1	111.9	112.9	0.89%	111.9	0.03%
H7C2C1	111.9	112.9	0.92%	111.9	0.02%
O8C2C1	107.1	105.8	-1.26%	106.3	-0.79%
O9O8C2	111.2	115.9	4.16%	114.2	2.64%
H4C1C2H3	119.8	120.0	0.17%	119.6	-0.18%
H6C2C1H3	-61.3	-63.3	3.38%	-60.3	-1.63%
H7C2C1H3	61.3	62.6	2.10%	60.6	-1.25%
O8C2C1H3	-180.0	-179.8	-0.07%	-179.7	-0.15%
O9O8C2C1	-180.0	-177.3	-1.50%	-178.6	-0.79%
<b>b</b>					
H3C1C2	110.1	109.8	-0.24%	110.1	0.02%
H4C1C2	110.3	109.4	-0.80%	111.5	1.11%
H5C1C2	109.1	110.9	1.70%	112.1	2.81%
C1C2C1	111.2	114.2	2.65%	112.8	1.46%
H7C2C1	113.3	112.5	-0.75%	108.9	-3.88%
O8C2C1	107.2	105.3	-1.71%	107.3	0.15%
O9O8C2	111.9	116.1	3.73%	114.1	1.97%
H4C1C2H3	120.4	119.7	-0.62%	119.4	-0.82%
H5C1C2H3	-119.8	-120.6	0.66%	-119.8	-0.04%
C16C2C1H3	-58.4	-61.0	4.45%	-57.9	-0.71%
H7C2C1H3	60.1	61.7	2.61%	62.2	3.54%
O8C2C1H3	180.4	179.5	-0.50%	178.2	-1.20%
O9O8C2C1	197.3	147.8	-25.10%	153.8	-22.03%
<b>c</b>					
H3C1C2	110.0	110.1	0.09%	110.1	0.10%
H4C1C2	109.0	109.8	0.73%	111.6	2.36%
C16C2C1	110.9	111.7	0.74%	110.7	-0.16%
C17C2C1	110.9	111.7	0.74%	110.7	-0.18%
O8C2C1	105.5	103.4	-2.02%	107.3	1.68%
O9O8C2	113.8	118.8	4.31%	114.4	0.50%
H4C1C2H3	120.2	120.3	0.10%	119.6	-0.53%
C16C2C1H3	-61.0	-62.8	2.97%	-59.4	-2.53%
C17C2C1H3	61.0	61.2	0.29%	59.5	-2.49%
O8C2C1H3	-180.0	-179.2	-0.43%	-180.0	-0.01%
O9O8C2C1	-180.0	-179.8	-0.11%	-179.6	-0.22%

**Table 6.1** Optimized Molecular Geometry Parameters <sup>a</sup> of CH<sub>3</sub>C.HOOH Rotational Conformers



	<i>a</i> <sub>STS</sub>	<i>a</i> <sub>E<sub>H</sub>TS</sub>	<i>a</i> <sub>E<sub>O</sub>TS</sub>	<i>a</i> <sub>SE<sub>H</sub>S</sub>	<i>a</i> <sub>SE<sub>C</sub>S</sub>	<i>a</i> <sub>STC</sub>	<i>a</i> <sub>STT</sub>
r21	1.49391	1.4973	1.4991	1.4927	1.4917	1.4934	1.4937
r31	1.0888	1.0841	1.0839	1.0891	1.0887	1.0883	1.0891
r41	1.08482	1.0861	1.0862	1.0851	1.0830	1.0840	1.0847
r51	1.08408	1.0867	1.0863	1.0842	1.0843	1.0839	1.0840
r62	1.07555	1.0738	1.0749	1.0724	1.0750	1.0822	1.0760
r72	1.36949	1.3692	1.3685	1.3708	1.3730	1.3590	1.3655
r87	1.38951	1.3893	1.3937	1.3927	1.3927	1.3978	1.3991
r98	0.95015	0.9502	0.9496	0.9498	0.9497	0.9511	0.9493
a312	111.649	110.560	110.231	111.642	112.731	111.547	111.874
a412	110.775	110.502	111.543	110.831	111.425	110.360	110.681
a512	109.864	111.881	111.274	109.959	108.491	109.922	109.754
a621	121.170	122.986	122.462	122.668	121.625	119.889	121.155
a721	112.037	112.873	112.821	113.623	121.631	112.647	112.116
a872	109.431	109.402	108.647	109.818	111.878	112.641	107.743
a987	102.369	102.417	101.472	101.881	101.632	105.579	100.562
d4123	120.201	119.199	120.044	120.114	121.048	120.035	120.379
d5123	-120.030	-120.830	-119.746	-120.241	-119.509	-120.039	-120.013
d6123	73.130	0	-143.419	75.295	82.838	75.311	72.922
d7213	-66.460	-145.020	0	-69.532	-65.065	-64.478	-66.672
d8721	174.852	179.675	175.972		0	190.341	177.758
d8726				0		0	
d9872	-254.590	-255.987	-231.205	-239.527	-241.503		180.0

<sup>a</sup> "r" represent bond length, r12 represents the bond length of a C-C bond, where 1 and 2 are the index of atom. "a" represent a bond angle, a312 represents the angle between bond C1-H3 and C1-H2. "d" represents a dihedral angle, d4123 represents the dihedral angle constructed by H4-C1-C2-H3.

**Table 6.2** Optimized Molecular Geometry Parameters<sup>a</sup> of CH<sub>3</sub>C.ClOOH Rotational Conformers

	<i>bSTS</i>	<i>bE<sub>C1</sub>TS</i>	<i>bE<sub>O</sub>TS</i>	<i>bSE<sub>C</sub>S</i>	<i>bSE<sub>C</sub>S</i>	<i>bSTC</i>	<i>bSTT</i>
r21	1.49531	1.50231	1.50293	1.49582	1.49597	1.49548	1.49616
r31	1.08156	1.08049	1.08287	1.08152	1.08181	1.08147	1.08151
r41	1.08300	1.08481	1.08215	1.08152	1.0835	1.08275	1.08314
r51	1.08692	1.0846	1.08475	1.08595	1.08823	1.08628	1.08704
r62	1.75916	1.75611	1.75575	1.74628	1.72884	1.76776	1.75239
r72	1.34807	1.34808	1.34852	1.36178	1.3718	1.33904	1.34527
r87	1.39333	1.39364	1.39381	1.39605	1.38428	1.39853	1.40381
r98	0.95144	0.95141	0.9514	0.5903	0.95088	0.95253	0.95024
a312	110.143	111.338	109.383	108.745	110.256	110.146	110.057
a412	108.874	109.864	111.491	110.285	109.143	108.885	109.111
a512	111.094	109.755	110.092	111.464	111.344	110.797	111.069
a621	116.656	118.497	118.009	116.617	118.121	116.373	116.659
a721	112.712	113.11	113.543	120.900	112.632	112.587	112.477
a872	110.496	110.496	110.455	111.596	115.258	114.576	109.13
a987	102.36	102.369	102.38	101.093	102.324	105.873	100.056
d4123	119.928	120.855	120.428	119.564	119.638	120.03	119.97
d5123	-120.449	-120.384	-119.363	-120.002	-120.707	-120.433	-120.265
d6123	51.079	0	-138.798	47.548	52.195	51.024	50.098
d7213	-173.131	-221.107	0	-174.583	-163.495	-172.505	-173.226
d8721	158.56	154.61	155.391	0		163.949	158.876
d8726					0		
d9872	-256.542	-256.548	-256.626	-233.56	-256.885	0	180

<sup>a</sup> see note for parameters of Table 6.1.**Table 6.3** Mulliken Charge<sup>a</sup> Distribution Calculated at UHF/6-31G\*

	CH <sub>3</sub> C.HOOH	CH <sub>3</sub> C.ClOOH
Total atomic charges:		
C1	-0.53235	-0.52421
C2	0.13091	0.27129
H3	0.18152	0.20242
H4	0.18371	0.20593
H5	0.17599	0.19762
H6	0.17517	
Cl6		-0.07860
O7	-0.33904	-0.33195
O8	-0.43723	-0.41468
H9	0.46132	0.47219

<sup>a</sup> See note of Table 5.4.

**Table 6.4** The Out-of-plane Angle <sup>a</sup> ( $\gamma$ , in degrees) for All Rotational Conformers

	<i>aSTS</i>	<i>aE<sub>H</sub>TS</i>	<i>aE<sub>O</sub>TS</i>	<i>aSE<sub>H</sub>S</i>	<i>aSE<sub>C</sub>S</i>	<i>aSTC</i>	<i>aSTT</i>
$\gamma$	41.3	35.6	37.2	35.4	28.8	41.0	41.2
	<i>bSTS</i>	<i>bE<sub>C</sub>TS</i>	<i>bE<sub>O</sub>TS</i>	<i>bSE<sub>C</sub>S</i>	<i>bSE<sub>C</sub>'S</i>	<i>bSTC</i>	<i>bSTT</i>
$\gamma$	45.1	41.8	37.9	37.7	37.9	44.8	44.6

<sup>a</sup> For definition of out-of-plane angle, see Figure 6.2.

**Table 6.5** Harmonic Vibration Frequencies (cm<sup>-1</sup>) for Rotational Conformers of CH<sub>3</sub>C.HOOH

<i>aSTS</i>	<i>aE<sub>H</sub>TS</i>	<i>aE<sub>O</sub>TS</i>	<i>aSE<sub>H</sub>S</i>	<i>aSE<sub>C</sub>S</i>	<i>aSTC</i>	<i>aSTT</i>
118.9 <sup>a</sup>	-136.7	-184.5	-71.8	-150.9	-430.8	-160.2
189.5 <sup>b</sup>	117 <sup>a</sup>	113.5 <sup>a</sup>	186.6 <sup>b</sup>	210.6 <sup>b</sup>	115.1 <sup>a</sup>	118.1 <sup>a</sup>
260.2 <sup>c</sup>	261.1 <sup>c</sup>	195.5 <sup>b</sup>	233.6 <sup>c</sup>	235.4 <sup>c</sup>	185.1 <sup>b</sup>	193.5 <sup>b</sup>
327.3	328.3	331.1	352.2	317.6	327.9	318.7
537.2	537.3	539.2	500.9	563.1	536.1	526.5
756.9	662.7	702.1	618.7	663.2	804.0	753.8
977.3	985.7	988.8	969.4	941.8	974.5	971.0
1141.4	1108.8	1113.8	1126.3	1089.3	1128.8	1139.8
1156.8	1155.2	1149.1	1146.0	1118.2	1155.8	1154.9
1237.7	1223.1	1217.8	1240.0	1241.2	1240.2	1239.9
1321.2	1324.5	1305.6	1300.6	1326.0	1326.9	1299.6
1487.2	1481.6	1487.5	1491.9	1495.0	1500.0	1495.0
1568.8	1568.6	1572.6	1571.0	1566.3	1566.1	1569.8
1570.6	1573.9	1586.5	1577.0	1581.7	1613.1	1606.8
1618.2	1621.1	1620.8	1618.1	1620.1	1616.8	1618.6
1636.0	1635.7	1638.6	1635.1	1634.7	1635.6	1639.0
3182.9	3196.1	3197.4	3178.1	3180.7	3188.6	3179.6
3251.0	3249.7	3246.5	3247.5	3254.6	3258.5	3250.6
3284.6	3277.8	3283.7	3282.4	3292.5	3268.2	3285.4
3357.8	3377	3361.5	3394.5	3361.6	3294.6	3352.1
4077.2	4075.4	4091.1	4086.6	4084.7	4058.1	4105.8

<sup>a</sup> Frequencies corresponded to torsion motion about C-O bond. <sup>b</sup> Frequencies corresponded to torsion motion about C-C bond. <sup>c</sup> Frequencies corresponded to torsion motion about O-O bond

**Table 6.6** Vibration Frequencies ( $\text{cm}^{-1}$ ) for Rotational Conformers of  $\text{CH}_3\text{C}\cdot\text{ClOOH}$ 

<i>bSTS</i>	<i>bE<sub>C</sub>TS</i>	<i>bE<sub>O</sub>TS</i>	<i>bSE<sub>C</sub>S</i>	<i>bSE<sub>C</sub>TS</i>	<i>bSTC</i>	<i>bSTT</i>
133.1 <sup>a</sup>	-173.5	-184.0	-127.7	-176.4	-421.1	-192.4
189.8 <sup>b</sup>	127.4 <sup>a</sup>	126.0 <sup>a</sup>	209.9 <sup>b</sup>	203.3 <sup>b</sup>	133.1 <sup>a</sup>	123.3 <sup>a</sup>
250.5 <sup>c</sup>	249.6 <sup>c</sup>	251.0 <sup>c</sup>	241.5 <sup>c</sup>	243.3 <sup>c</sup>	186.6 <sup>b</sup>	188.2 <sup>b</sup>
279.8	276.5	278.4	315.2	285.3	265.2	255.8
346.7	357.0	356.9	361.6	336.3	345.0	349.9
469.4	463.2	464.9	389.1	364.4	462.5	460.8
569.4	574.1	574.4	526.5	586.5	570.7	557.2
681.2	671.2	673.6	737.5	680.6	660.6	686.7
1060.3	1018.7	1023.0	982.2	1020.4	999.8	1006.8
1134.7	1124.0	1120.7	1142.5	1145.3	1146.0	1130.7
1156.0	1135.1	1138.6	1144.0	1175.8	1162.0	1153.7
1250.7	1251.1	1238.6	1265.7	1267.1	1249.7	1246.7
1356.6	1355.8	1359.6	1354.5	1359.1	1379.5	1356.5
1562.9	1565.9	1565.4	1565.5	1564.5	1562.0	1562.8
1586.8	1585.3	1584.8	1591.0	1583.1	1615.8	1603.8
1616.6	1619.0	1617.6	1620.2	1618.9	1619.6	1618.6
1624.6	1626.7	1629.2	1624.7	1624.5	1625.8	1627.8
3205.3	3217.6	3220.5	3214.8	3190.3	3211.7	3204.0
3282.2	3278.8	3288.1	3291.7	3272.6	3287.5	3280.0
3319.4	3322.8	3311.7	3322.3	3313.8	3321.4	3318.4
4066.7	4067.1	4067.2	4085.9	4066.9	4047.8	4097.0

<sup>a</sup>: Frequencies corresponded to torsion motion about C-O bond. <sup>b</sup>: Frequencies corresponded to torsion motion about C-C bond. <sup>c</sup>: Frequencies corresponded to torsion motion about O-O bond

**Table 6.7** Rotation Barriers

	UHF/6-31G*	MP2/6-31G**	ZPVE	BAR/UHF	BAR/MP2	S <sup>2</sup>
<b>CH<sub>3</sub>C·HOOH</b>						
<i>aSTS</i>	-228.2095491	-228.8487100	47.26	0.00	0.00	0.76
<i>aE<sub>H</sub>TS</i>	-228.2073828	-228.8465643	46.83	1.22	1.20	0.76
<i>aE<sub>O</sub>TS</i>	-228.2062409	-228.8455411	46.81	1.91	1.83	0.76
<i>aSE<sub>H</sub>S</i>	-228.2080650	-228.8475386	46.83	0.70	0.50	0.76
<i>aSE<sub>C</sub>S</i>	-228.2041587	-228.8441302	46.86	3.18	2.67	0.76
<i>aSTC</i>	-228.1990916	-228.8403632	46.88	6.55	5.23	0.76
<i>aSTT</i>	-228.2082148	-228.8475259	46.92	0.87	0.77	0.76
<b>CH<sub>3</sub>C·ClOOH</b>						
<i>bSTS</i>	-687.1152872	-687.8771493	41.61	0.00	0.00	0.76
<i>bE<sub>H</sub>TS</i>	-687.1121587	-687.8740373	41.32	1.95	1.94	0.76
<i>bE<sub>O</sub>TS</i>	-687.1120222	-687.8738839	41.31	2.02	2.02	0.76
<i>bSE<sub>C</sub>S</i>	-687.1085159	-687.8715664	41.44	4.27	3.52	0.76
<i>bSE<sub>C</sub>TS</i>	-687.1043415	-687.8670967	41.32	6.78	6.22	0.76
<i>bSTC</i>	-687.1057837	-687.8704318	41.25	5.96	4.21	0.76
<i>bSTT</i>	-687.1120167	-687.8744774	41.21	2.01	1.64	0.76

**Table 6.8** Potential Constants (kcal/mol) of Fourier Expansions for Internal Rotations

<i>Rotors</i>	$V_1$	$V_2$	$V_3$	$V'_1$	$V'_2$
C-C bond					
CH <sub>3</sub> -C.HOOH			-1.83		
CH <sub>3</sub> -C.ClOOH			-2.02		
C-O bond					
CH <sub>3</sub> C.H-OOH	-2.170	-1.370			
CH <sub>3</sub> C.Cl-OOH	-2.700	-4.776			
O-O bond					
CH <sub>3</sub> C.HO-OH	-4.460	-2.504			
CH <sub>3</sub> C.ClO-OH	-2.570	-2.778			
	$a_0$	$a_1$	$a_2$	$a_3$	$b_1$
C-C bond					
CH <sub>3</sub> -C.HOOH	0.915			0.915	
CH <sub>3</sub> -C.ClOOH	1.01			1.01	
C-O bond					
CH <sub>3</sub> C.H-OOH	0.8998	1.085	0.6852		
CH <sub>3</sub> C.Cl-OOH	2.482	1.350	2.388		
O-O bond					
CH <sub>3</sub> C.HO-OH	1.748	1.230	1.252		
CH <sub>3</sub> C.ClO-OH	1.536	1.285	1.389		

**Table 6.9** Total Energy and Enthalpies of Formation for Species in Isodesmic Reactions and the Reaction Energies

	(U)HF/6-31G* (Hartree)	MP2/6-31G** (Hartree)	ZPVE (kcal/mol)	$\Delta H_f^{\circ}_{298}$ (kcal/mol)
CH <sub>3</sub> CH <sub>2</sub> OH	-154.0757446	-154.5682726	53.98	-56.12 <sup>a</sup>
CH <sub>3</sub> CHClOH	-612.9773607	-613.5875823	48.57	-64.2 <sup>b</sup>
CH <sub>3</sub> C.HOH	-153.4513227	-153.9120555	44.58	-14.3 <sup>c</sup> , -11.9 <sup>d</sup>
CH <sub>3</sub> C.ClOH	-612.3627070	-612.9448540	39.22	
CH <sub>3</sub> CH <sub>2</sub> OOH	-228.8367278	-229.5082360	56.66	-41.32 <sup>a</sup>
CH <sub>3</sub> CHClOOH	-687.7447739	-688.5390717	50.39	-49.36 <sup>a</sup>
CH <sub>3</sub> C.HOOH	-228.2095491	-228.8487100	47.26	
CH <sub>3</sub> C.ClOOH	-687.1152872	-687.8771493	41.61	

<sup>a</sup> ref. 3. <sup>b</sup> Chapter 4. <sup>c</sup> ref. 3. <sup>d</sup> Estimation from D(H-C(CH<sub>3</sub>)HOH) = 96.3 kcal/mol, see text for the evaluation of D(H-C(CH<sub>3</sub>)HOH).

**Table 6.10** Reaction Energies (kcal/mol) and Enthalpies of Formation (kcal/mol) for CH<sub>3</sub>C.HOOH and CH<sub>3</sub>C.CIOOH

	$\Delta H_{rxn}^{\circ}$ (HF/6-31G*)	$\Delta H_{rxn}^{\circ}$ (MP2/6-31G**)	$\Delta H_f^{\circ}_{298}$
CH <sub>3</sub> C.HOOH reaction (1)	1.73	2.08	5.0
CH <sub>3</sub> C.CIOOH reaction (2)	3.74	4.14	-1.0
reaction (7)	0.53	0.53	

**Table 6.11** Ideal Gas Phase Thermodynamic Properties for CH<sub>3</sub>C.HOOH and CH<sub>3</sub>C.CIOOH

	$\Delta H_f^{\circ}_{298}$ <sup>a</sup>	$S^{\circ}_{298}$ <sup>b</sup>	$C_{p300}$ <sup>c</sup>	$C_{p400}$	$C_{p500}$	$C_{p600}$	$C_{p800}$	$C_{p1000}$	$C_{p1500}$
CH <sub>3</sub> C.HOOH ( $\sigma^d = 3$ )									
vib. <sup>e</sup>		2.979	6.101	9.666	12.954	15.771	20.191	23.458	28.543
ext.-rot. <sup>f</sup>		21.534	2.981	2.981	2.981	2.981	2.981	2.981	2.981
tra. <sup>g</sup>		38.228	4.968	4.968	4.968	4.968	4.968	4.968	4.968
C--C <sup>h</sup>		4.938	1.986	1.764	1.576	1.440	1.272	1.181	1.082
C--O <sup>i</sup>		6.660	1.645	1.591	1.511	1.417	1.219	1.033	0.680
O--O <sup>j</sup>		3.418	1.814	1.778	1.712	1.636	1.496	1.386	1.219
spin <sup>k</sup>		1.377							
total	5.86	79.133	19.495	22.748	25.702	28.213	32.128	35.008	39.472
CH <sub>3</sub> C.CIOOH ( $\sigma = 3$ )									
vib.		5.442	9.076	12.684	15.835	18.454	22.440	25.301	29.661
ext.-rot.		24.336	2.981	2.981	2.981	2.981	2.981	2.981	2.981
tra.		39.560	4.968	4.968	4.968	4.968	4.968	4.968	4.968
C--C		4.868	2.060	1.858	1.665	1.516	1.325	1.219	1.100
C--O		5.789	2.211	2.237	2.168	2.036	1.708	1.395	0.847
O--O		3.329	1.863	1.838	1.773	1.697	1.551	1.433	1.249
spin		1.377							
total	-0.12	79.133	19.495	22.748	25.702	28.213	32.128	35.008	39.472

<sup>a</sup> Unit in kcal/mol. <sup>b,c</sup> Unit in cal/mol-K. <sup>d</sup>  $\sigma$  : symmetry. <sup>e</sup> vib. : Contribution from vibrational frequencies  
<sup>f</sup> ext.-rot. : Contribution from external rotations. <sup>g</sup> tra. : Contribution from translations.

<sup>h</sup> C--C : Contribution from internal rotation about C-C bond. <sup>i</sup> C--O : Contribution from internal rotation about C-O bond. <sup>j</sup> O--O : Contribution from internal rotation about O-O bond. <sup>k</sup> spin : Spin degeneracy



**Table 6.12** Comparison of Pitzer & Gwinn's and the Method Used in this Study for Calculation of Thermodynamic Properties of Molecules with Hindered Rotors

		$I_r^a$ (amu-Å <sup>2</sup> )	$V_{\text{mean}}^b$ (kcal/mol)	$n^c$	$S_{298}^\circ$ (cal/mol-K)	$C_{p300}$ (cal/mol-K)	$C_{p500}$
CH <sub>3</sub> C.HOOH							
C--O <sup>d</sup>	Pitzer	16.23	2.67	2	6.107	2.319	1.982
	this				6.660	1.645	1.511
O--O <sup>e</sup>	Pitzer	0.85	5.23	2	2.564	1.738	2.152
	this				3.418	1.814	1.712
CH <sub>3</sub> C.CIOOH							
C--O	Pitzer	24.23	4.87	3	5.736	2.169	2.327
	this				5.789	2.211	2.168
O--O	Pitzer	0.87	4.21	2	2.795	1.897	2.164
	this				3.329	1.863	1.773

<sup>a</sup> Reduced moment of inertia. <sup>b</sup> Mean Rotational Barrier. <sup>c</sup> Number of potential maximum.

<sup>d</sup> C--O : Contribution from internal rotation about C-O bond. <sup>e</sup> O--O : Contribution from internal rotation about O-O bond.

**Table 6.13** Comparison of Bond Lengths (Å) among Different Calculation Levels

	<i>6-31G*</i>	<i>AMI</i> ( $r_{\text{AMI}}-r_{6-31G^*}$ ) / $r_{6-31G^*}$	<i>PM3</i> ( $r_{\text{PM3}}-r_{6-31G^*}$ ) / $r_{6-31G^*}$
<b>a</b>			
CC	1.49391	1.46096	-2.21%
C1H3	1.0888	1.12031	2.89%
C1H4	1.08482	1.11822	3.08%
C1H5	1.08408	1.11925	3.24%
C2H6	1.07555	1.08793	1.15%
C2O7	1.36949	1.38538	1.16%
OO	1.38951	<b>1.29939</b>	-6.49%
OH	0.95015	0.98340	3.50%
<b>b</b>			
CC	1.49531	1.47198	-1.56%
C1H3	1.08156	1.11898	3.46%
C1H4	1.08300	1.11891	3.32%
C1H5	1.08692	1.11904	2.96%
C2Cl6	1.75916	1.67760	-4.64%
C2O7	1.34807	1.39246	3.29%
OO	1.39333	<b>1.29073</b>	-7.36%
OH	0.95144	0.98501	3.53%

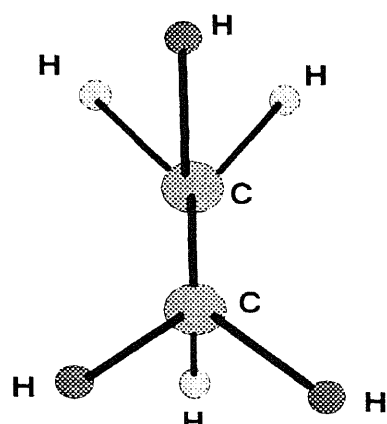
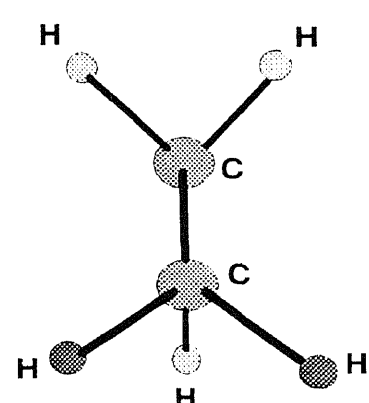
**Table 6.14** Comparison of Bond Angles and Dihedral Angles (in degrees) among Different Calculation Levels

	<i>6-31G*</i>	<i>AM1</i>	$(a_{AM1}-a_{6-31G*})$ $/a_{6-31G*}$	<i>PM3</i>	$(a_{PM3}-a_{6-31G*})$ $/a_{6-31G*}$
<b>a</b>					
H3C1C2	111.649	109.836	-1.62%	110.080	-1.41%
H4C1C2	110.775	111.557	0.71%	113.714	2.65%
H5C1C2	109.864	109.451	-0.38%	109.823	-0.04%
H6C2C1	121.170	126.238	4.18%	117.112	-3.35%
O7C2C1	112.037	114.398	2.11%	122.155	9.03%
O8O2C2	109.431	112.463	2.77%	112.725	3.01%
H9O8O7	102.369	107.095	4.62%	100.943	-1.39%
H4C1C2H3	120.201	120.440	0.20%	121.128	0.77%
H5C1C2H3	-120.030	-119.019	-0.84%	-118.117	-1.59%
H6C2C1H3	73.130	59.073	-19.22%	53.036	-27.48%
O7C2C1H3	-66.460	<b>-113.503</b>	70.78%	<b>-126.894</b>	90.93%
O8O7C2C1	174.852	173.619	-0.71%	169.638	-2.98%
H9O8C7C2	-254.590	-257.575	1.17%	<b>-189.756</b>	-25.47%
<b>b</b>					
H3C1C2	110.143	110.880	0.67%	110.043	-0.09%
H4C1C2	108.874	110.462	1.46%	112.732	3.54%
H5C1C2	111.094	108.914	-1.96%	110.335	-0.68%
C1C2C1	116.656	121.771	4.38%	112.950	-3.18%
O7C2C1	112.712	112.390	-0.29%	125.586	11.42%
O8O7C2	110.496	115.994	4.98%	116.430	5.37%
O9O8C2	102.36	108.133	5.64%	102.184	-0.17%
H4C1C2H3	119.928	120.583	0.55%	120.414	0.41%
H5C1C2H3	-120.449	-119.669	-0.65%	-118.845	-1.33%
C16C2C1H3	51.079	52.693	3.16%	62.556	22.47%
H7C2C1H3	-173.131	<b>-107.850</b>	-37.71%	<b>-117.424</b>	-32.18%
O8O7C2C1	158.56	177.331	11.84%	178.270	12.43%
H9O8O7C2	-256.542	-274.993	7.19%	<b>-181.515</b>	-29.25%

## APPENDIX B

### FIGURES FOR SECTION I

#### Vibration Frequency Analysis

CH <sub>3</sub> CH <sub>3</sub>	vs	C.H <sub>2</sub> CH <sub>3</sub>
		
Frequencies (cm <sup>-1</sup> )	Vibration Mode	Frequencies (cm <sup>-1</sup> )
3000 (x6)	C-H stretch	3000 (x5)
1400 (x6)	CH <sub>3</sub> bend	1400 (x4)
1150 (x2)	CH <sub>2</sub> twist, wag	1150 (x2)
993 (x1)	C-C stretch	975 (x1)
822 (x2)	C-CH <sub>3</sub> rock C-C.H <sub>2</sub> inversion	784 (x1) 540 (x1)

Compare C.H<sub>2</sub>CH<sub>3</sub> to CH<sub>3</sub>CH<sub>3</sub> :

lose one C-H stretching, two H-C-H bending, one H-C-C rocking,  
gain one C.H<sub>2</sub> inversion, also,  
the barrier of internal rotation along C-C axis changes

**Conclusion :** C.H<sub>2</sub>CH<sub>3</sub> = C<sub>2</sub>H<sub>6</sub> - v/C-H/ - 2v/H-C-H/  
- v/H-C-C/ + v/inv-CH<sub>2</sub>/ - ir/CH<sub>3</sub>-CH<sub>3</sub>/ + ir/CH<sub>2</sub>-CH<sub>3</sub>/

Figure 2.1 Example of HBI Approach

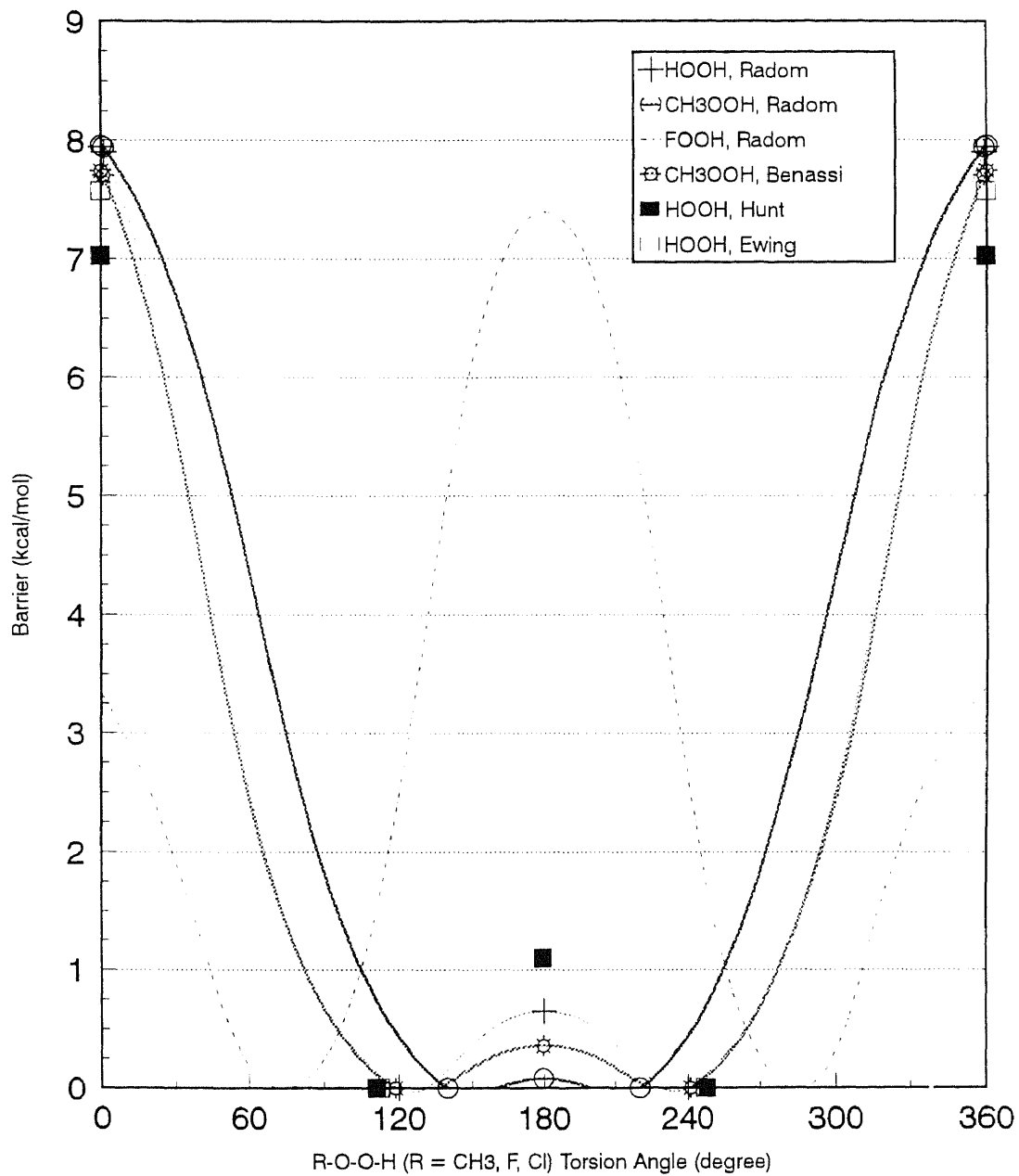
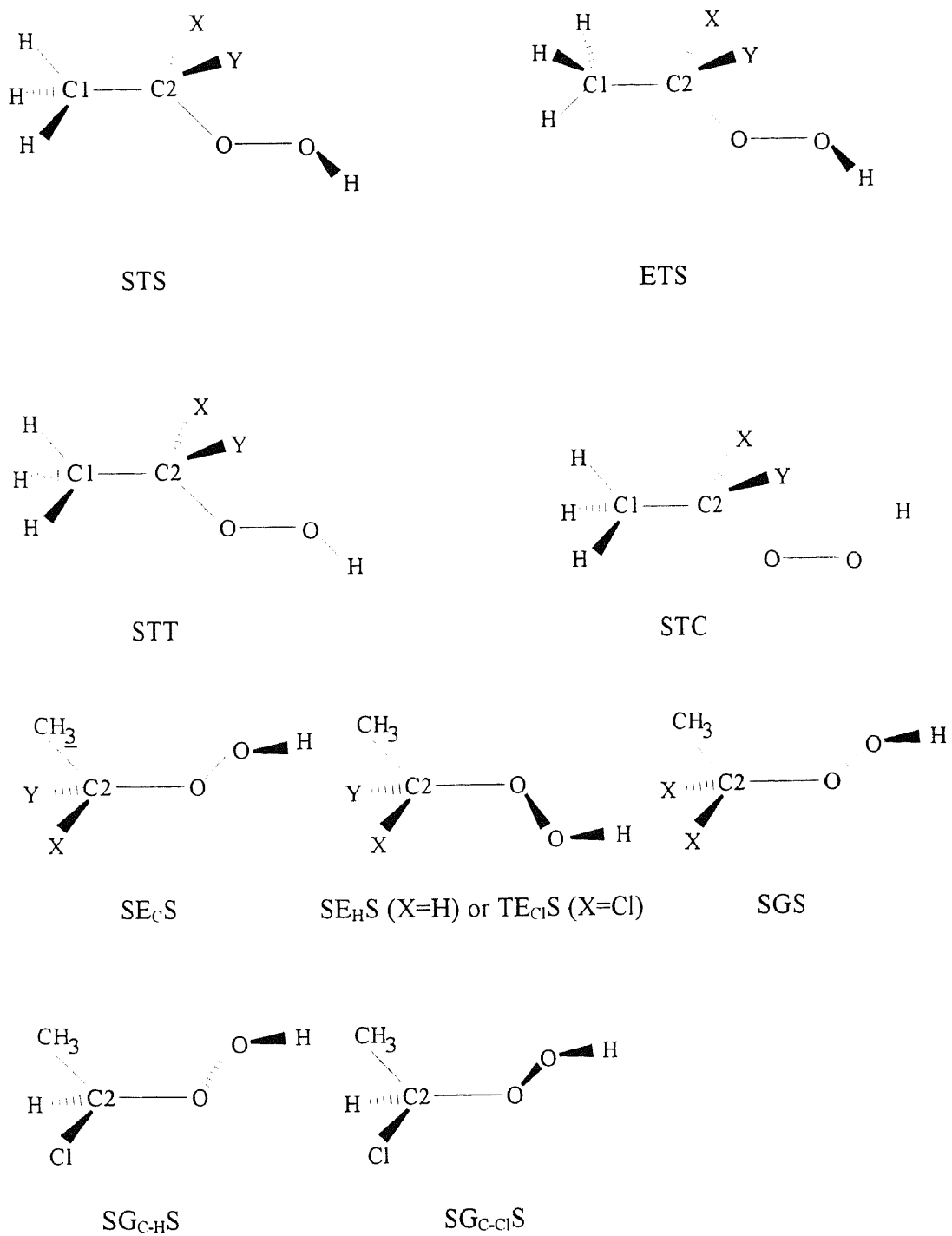


Figure 4.1 Previous Studies of Rotational Barriers for RO--OH



**Figure 4.2** Definitions of Nomenclature Used in this Work

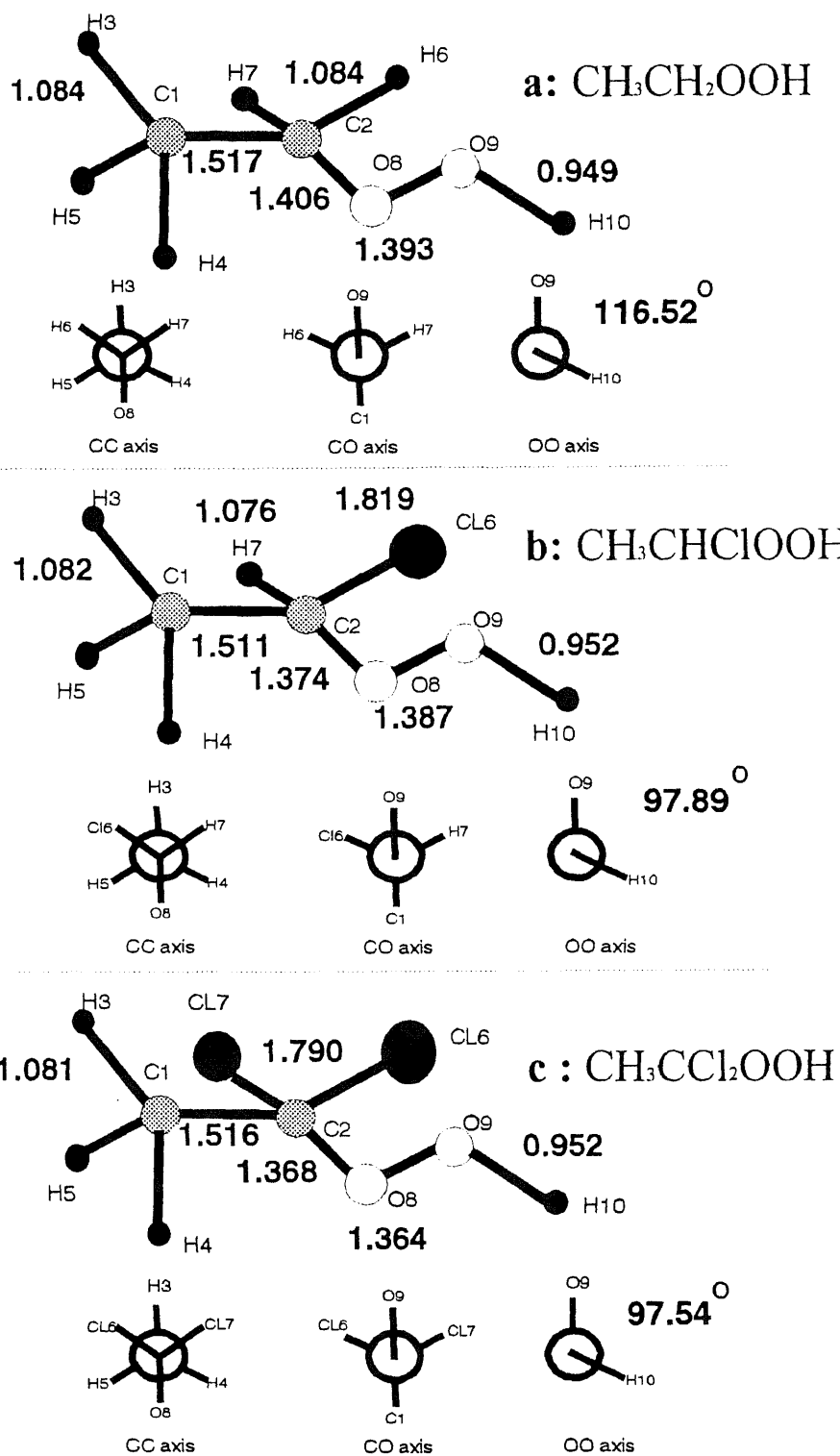


Figure 4.3 Optimized Geometries at HF/6-31G\*

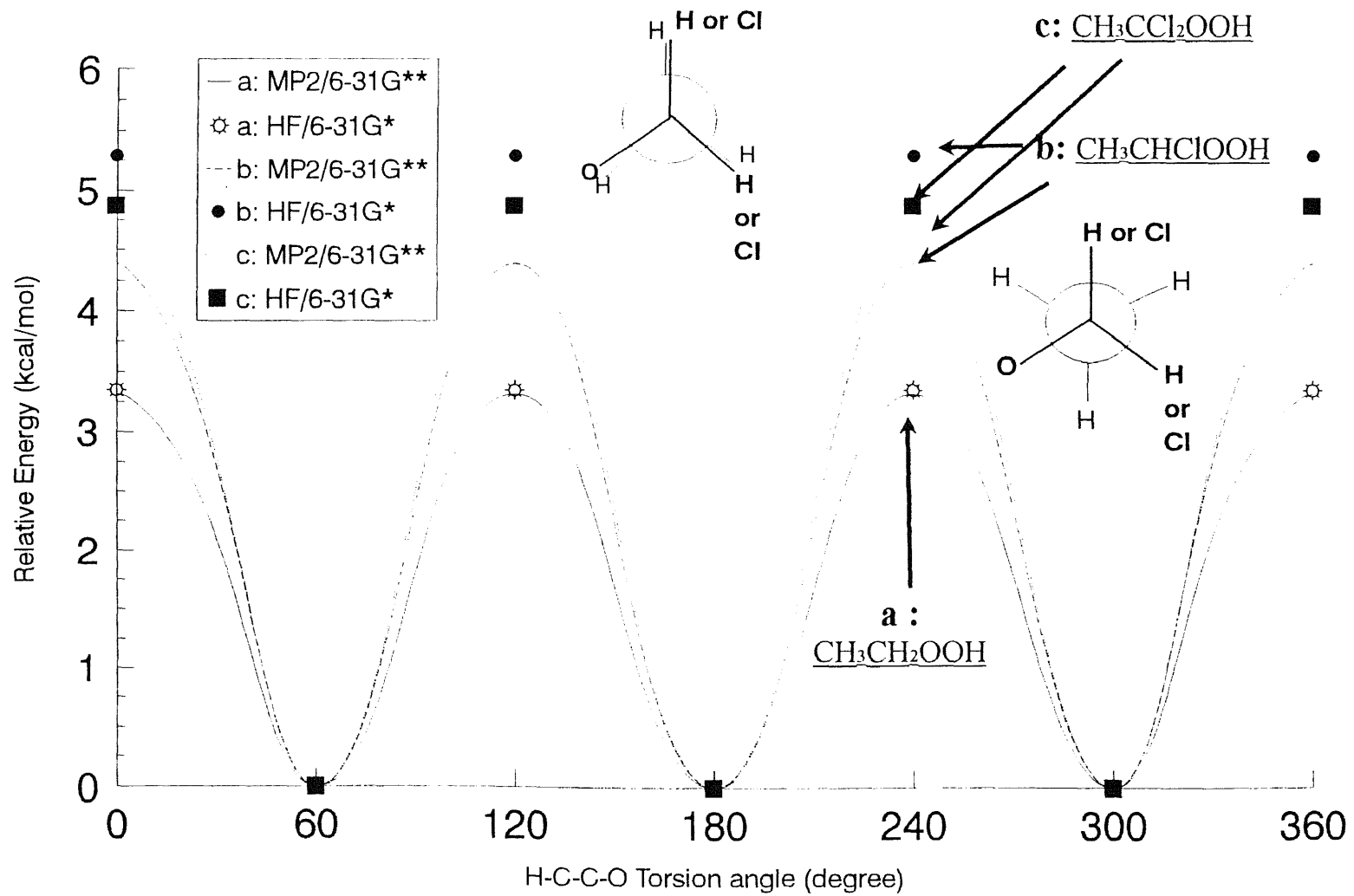


Figure 4.4 Calculated Potential Barriers for Internal Rotation about C-C Bond

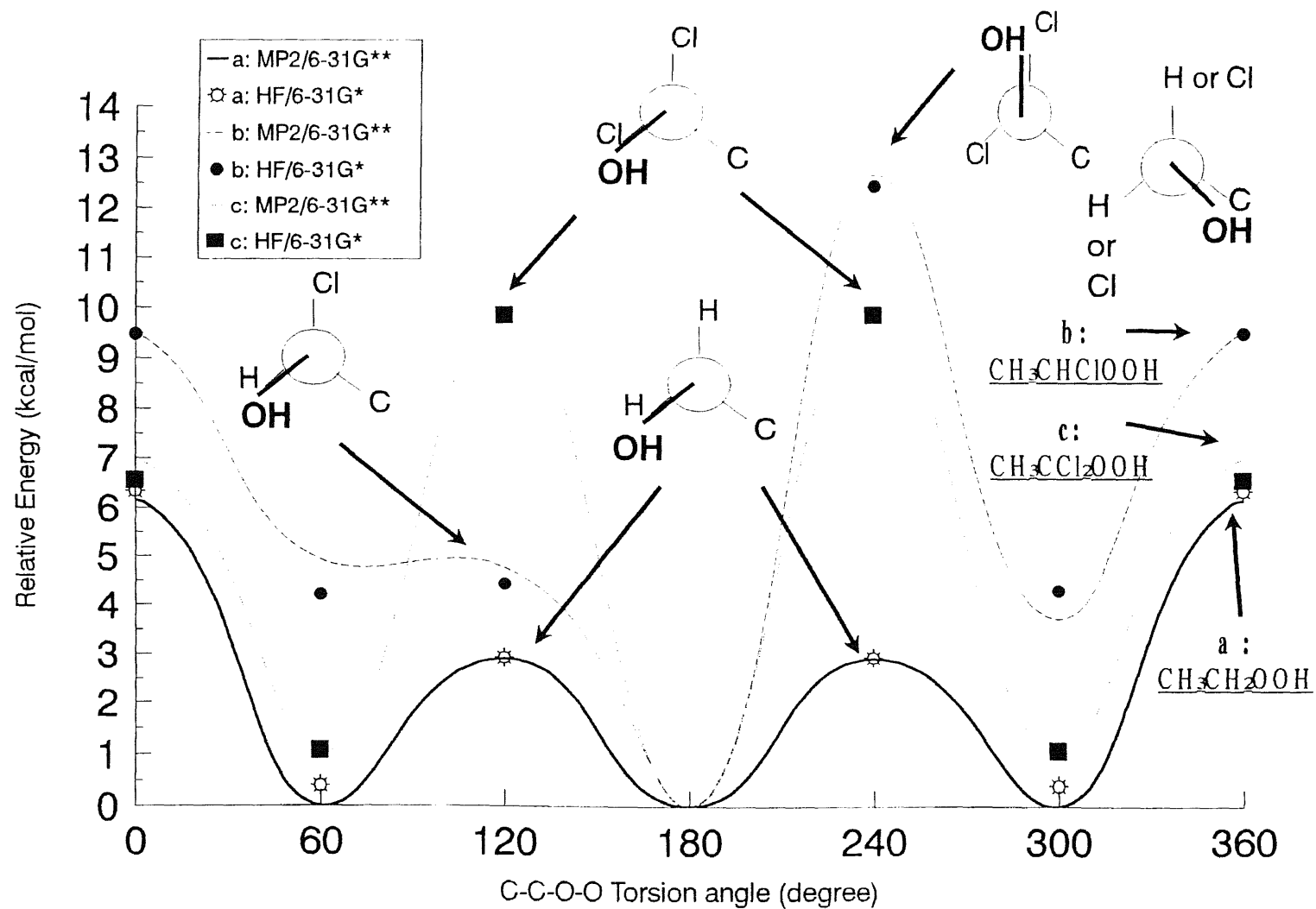


Figure 4.5 Calculated Potential Barriers for Internal Rotation about C-O Bond



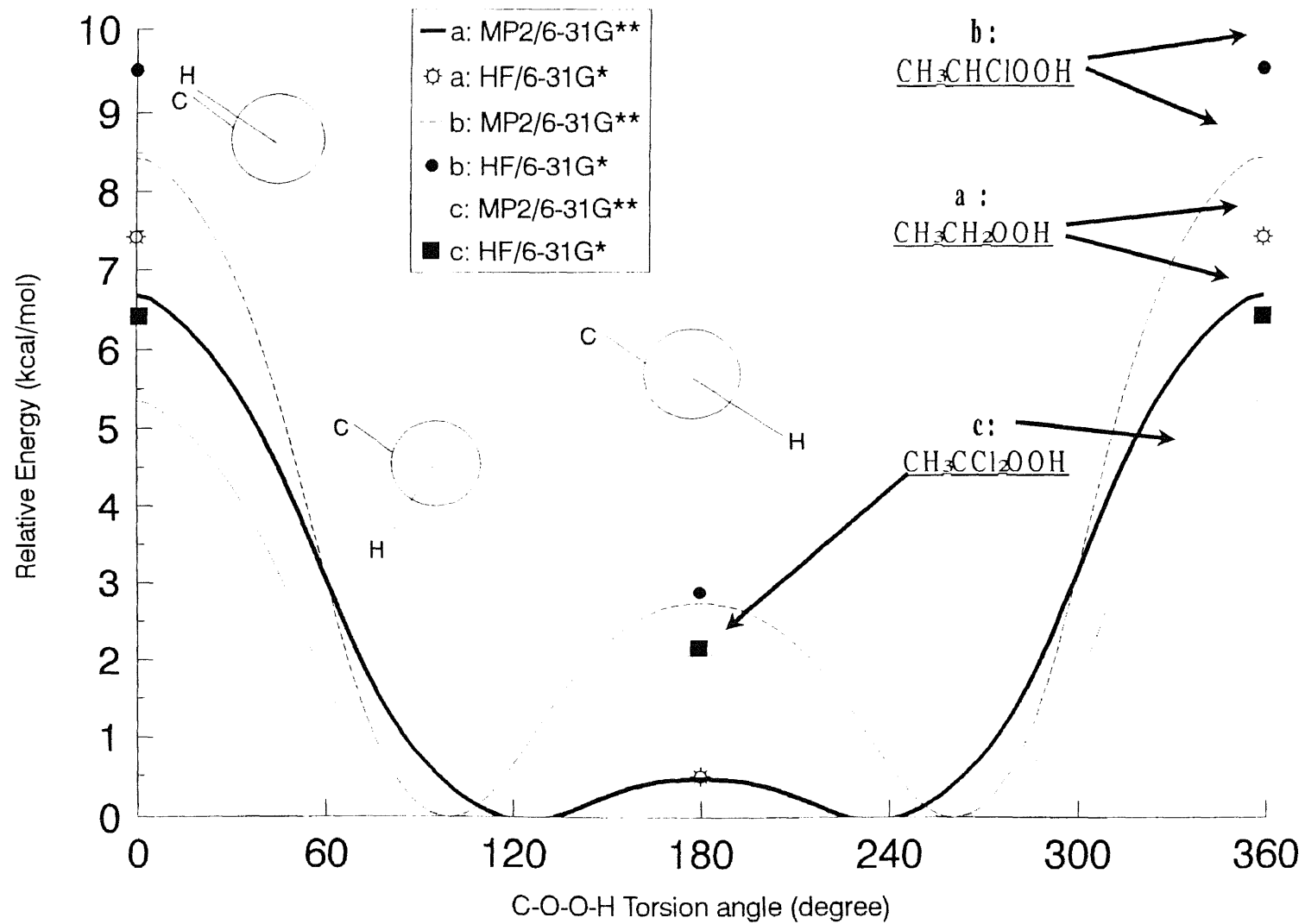
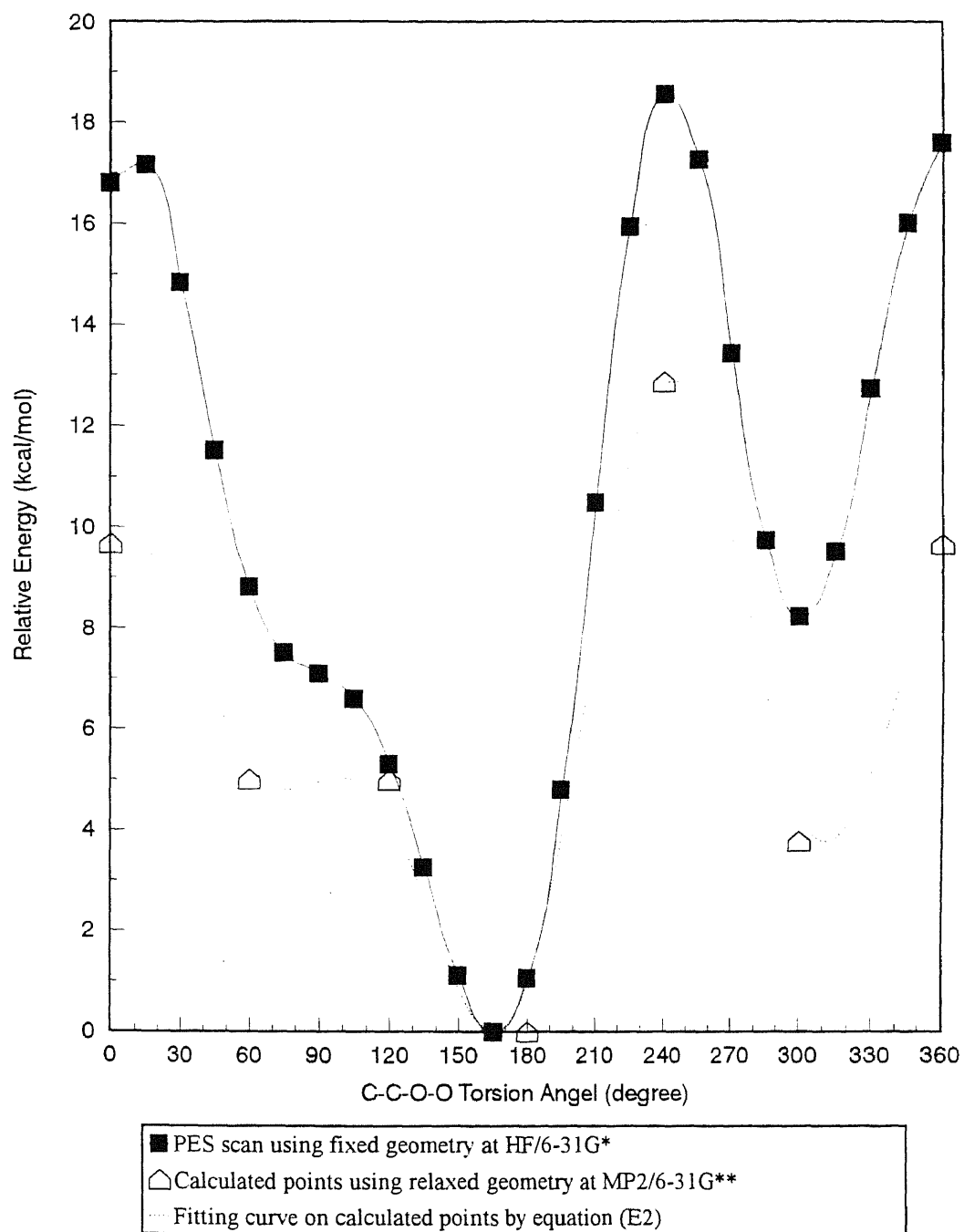


Figure 4.6 Calculated Potential Barriers for Internal Rotation about O-O Bond



**Figure 4.7** Investigation of Potential Energy Surface for Rotation about C-O Bond in CH<sub>3</sub>CHClOOH

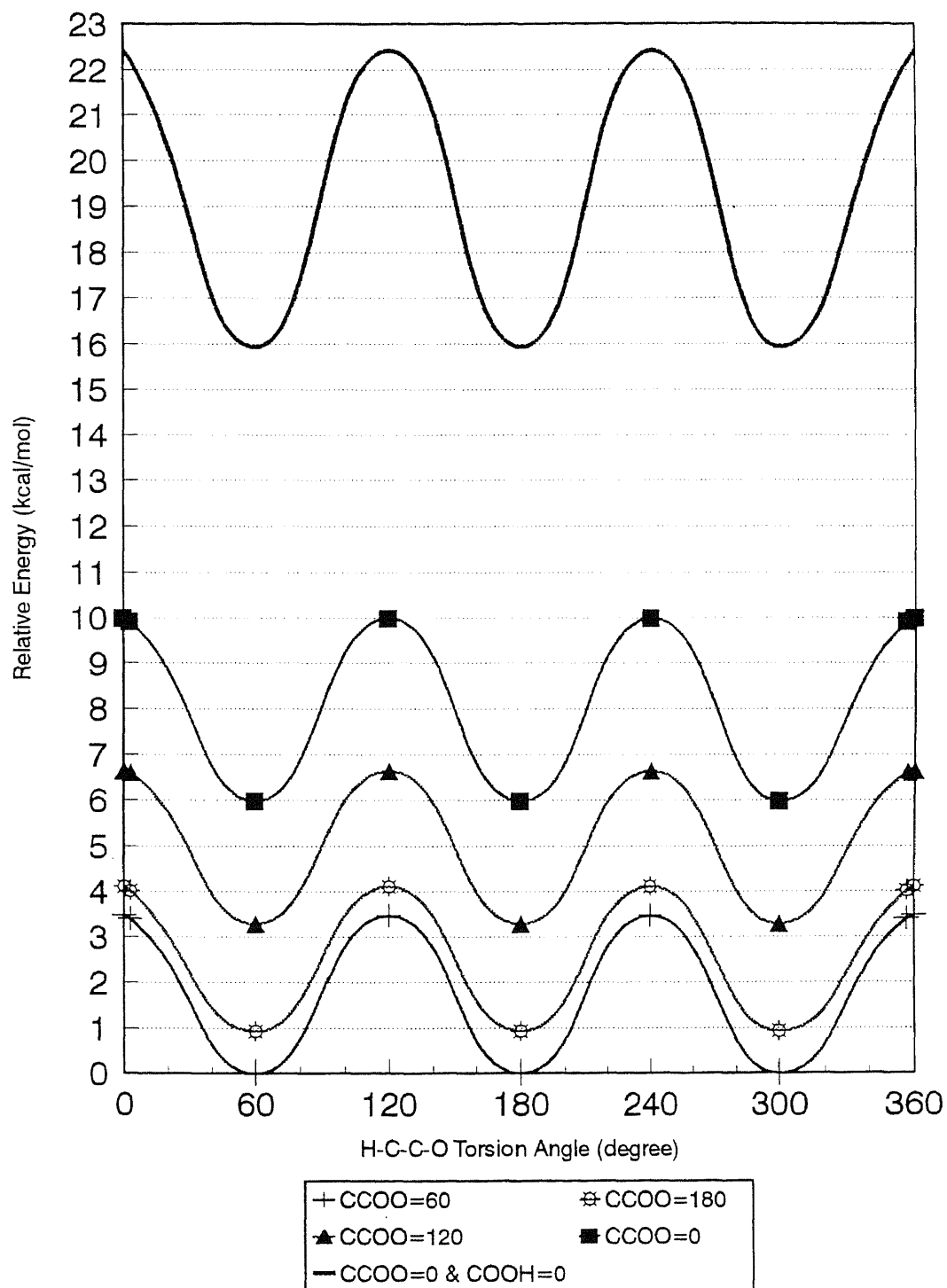


Figure 4.8 Coupling Effects for Rotational Barriers of CH<sub>3</sub>--CH<sub>2</sub>OOH

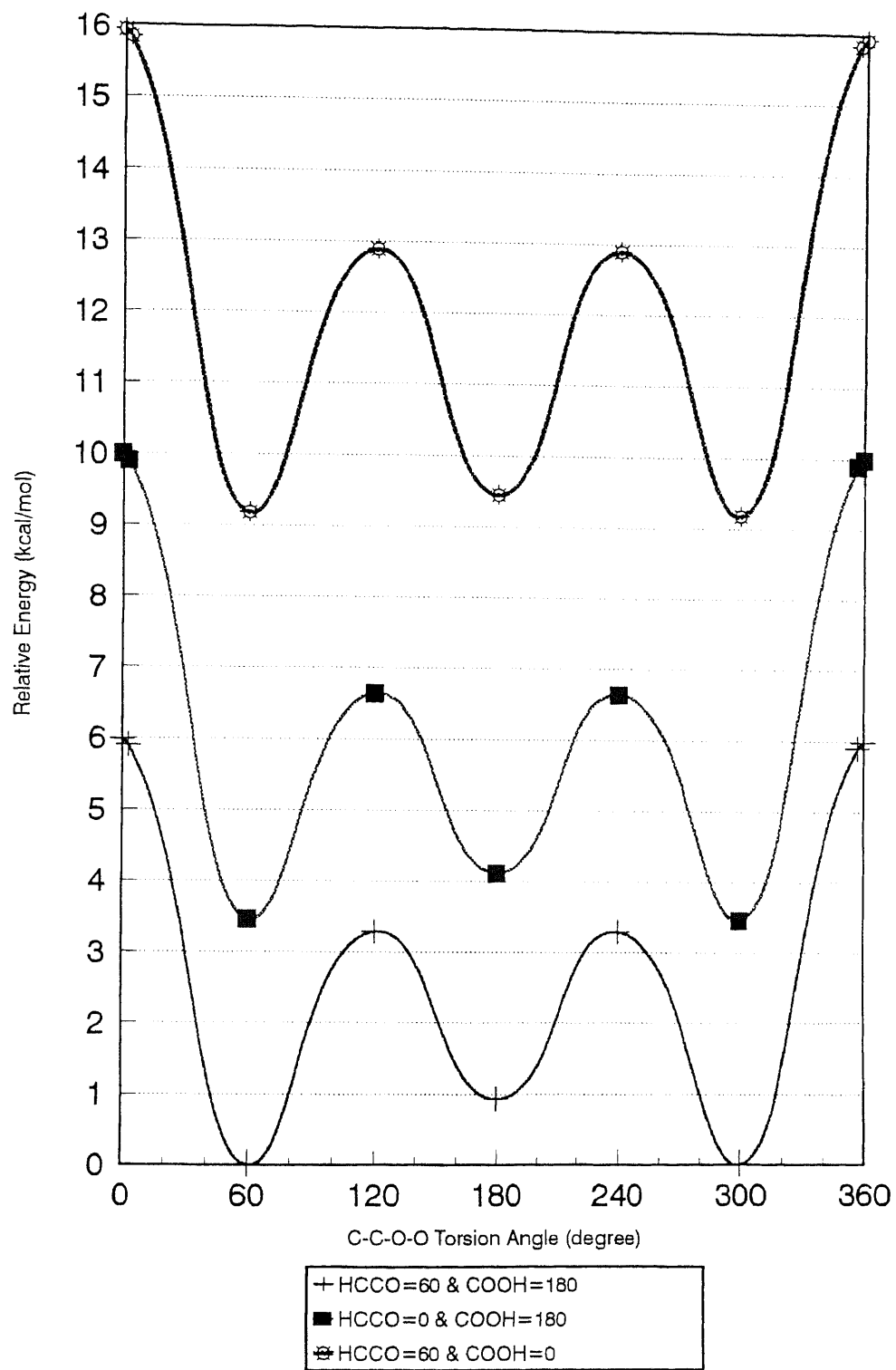


Figure 4.9 Coupling Effects for Rotational Barriers of CH<sub>3</sub>CH<sub>2</sub>--OOH

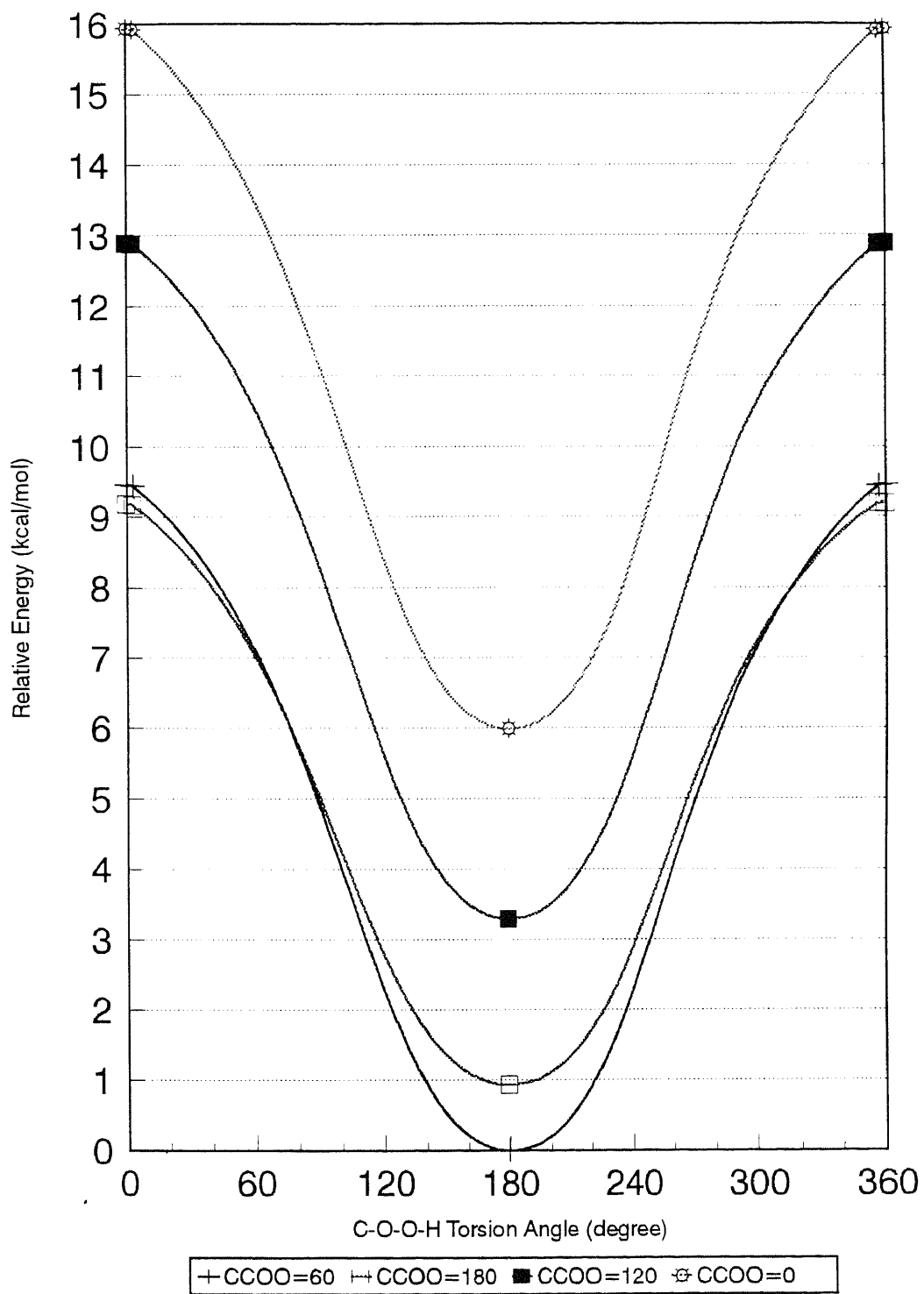


Figure 4.10 Coupling Effects for Rotational Barriers of CH<sub>3</sub>CH<sub>2</sub>O--OH

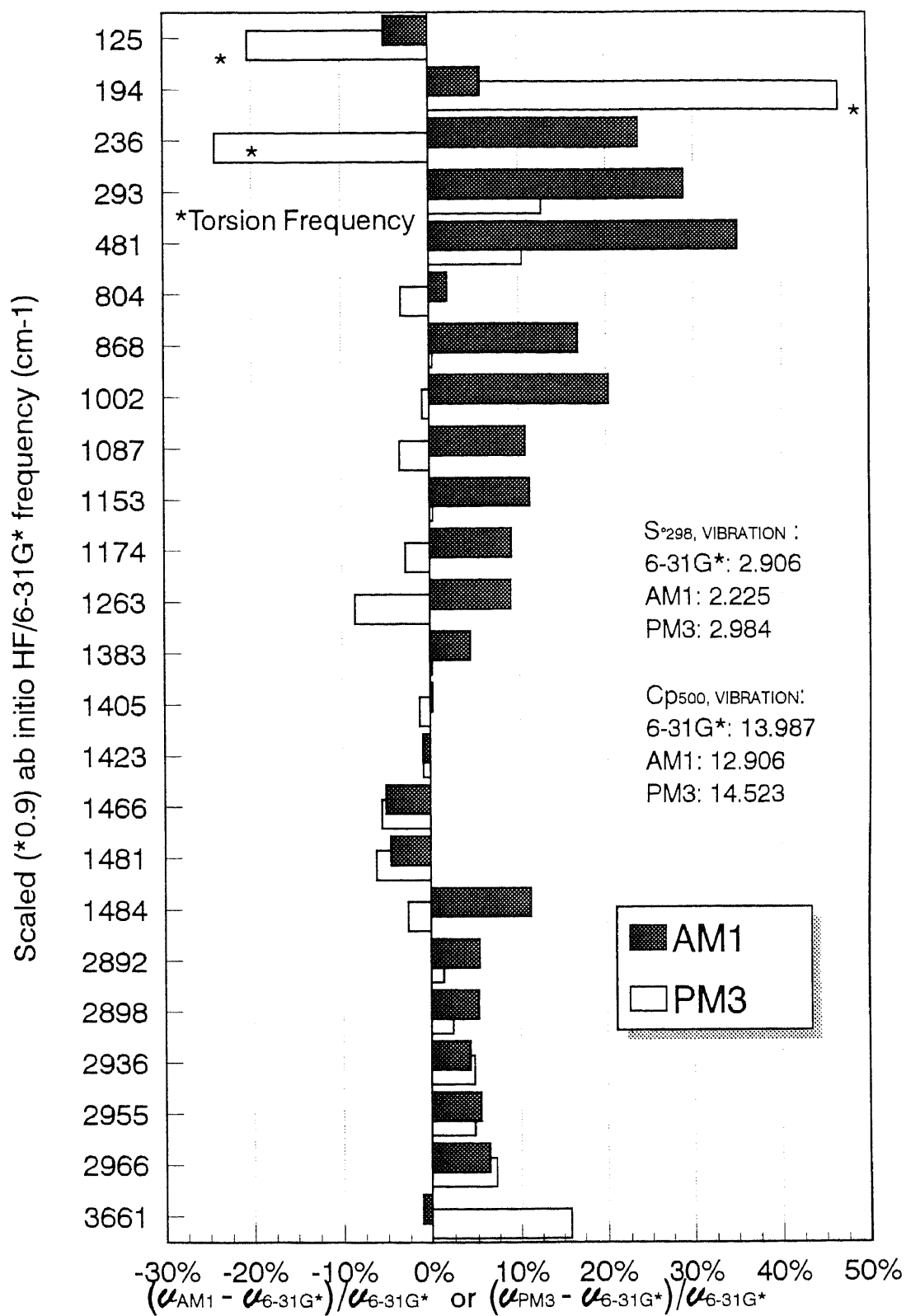


Figure 4.11 Comparison of Harmonic Vibrational Frequencies Calculated using Semiempirical and *ab initio* MO for CH<sub>3</sub>CH<sub>2</sub>OOH

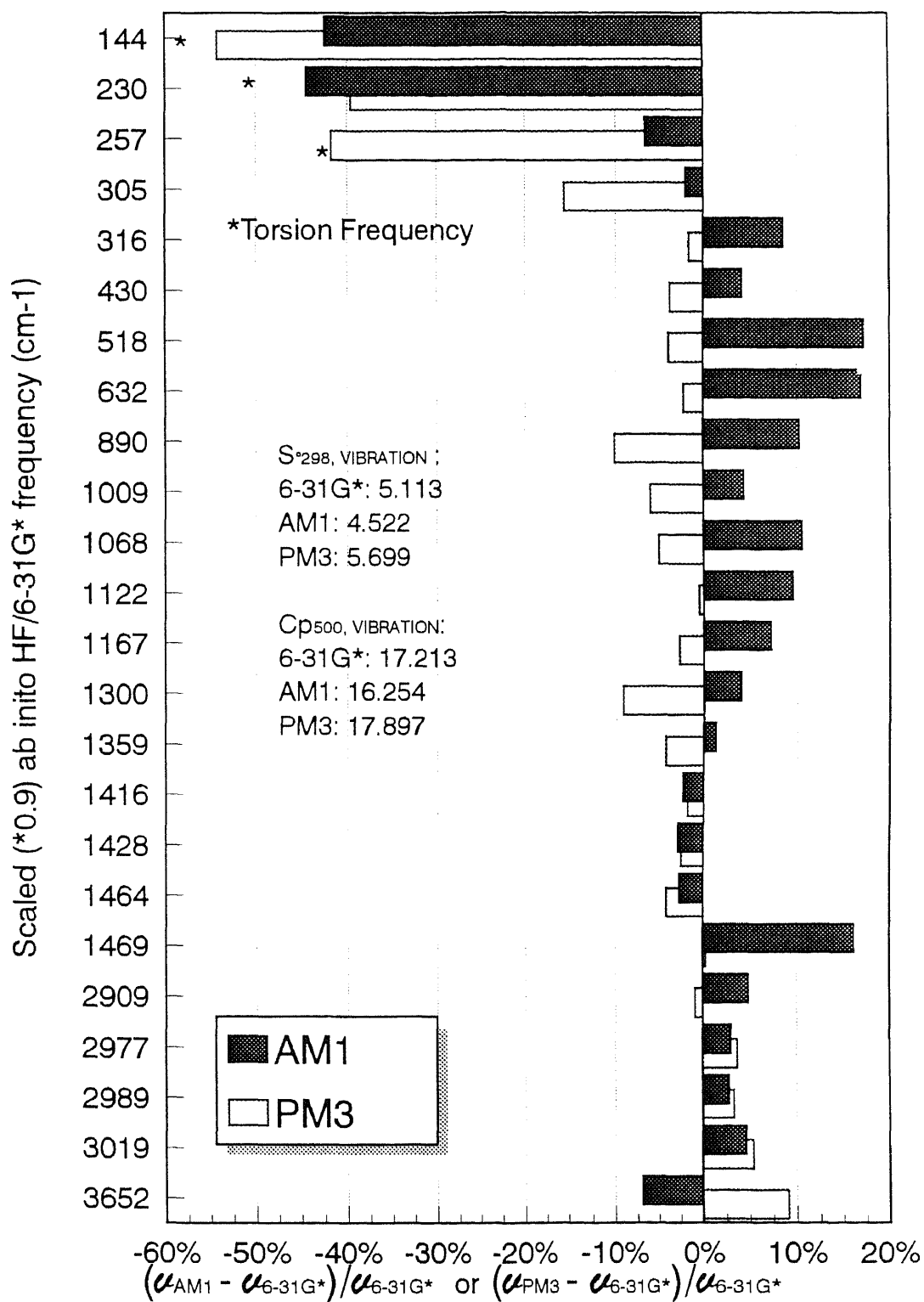
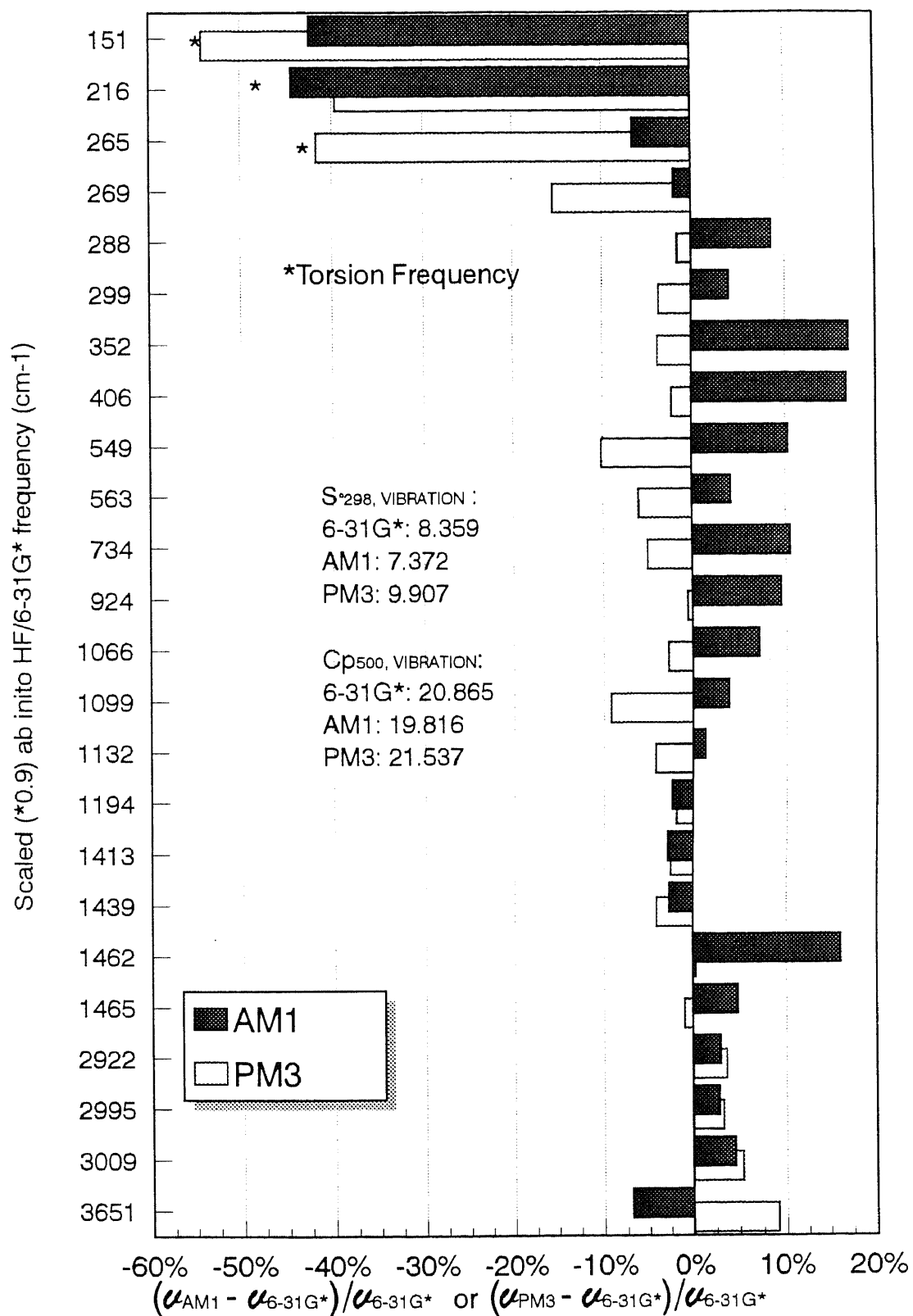
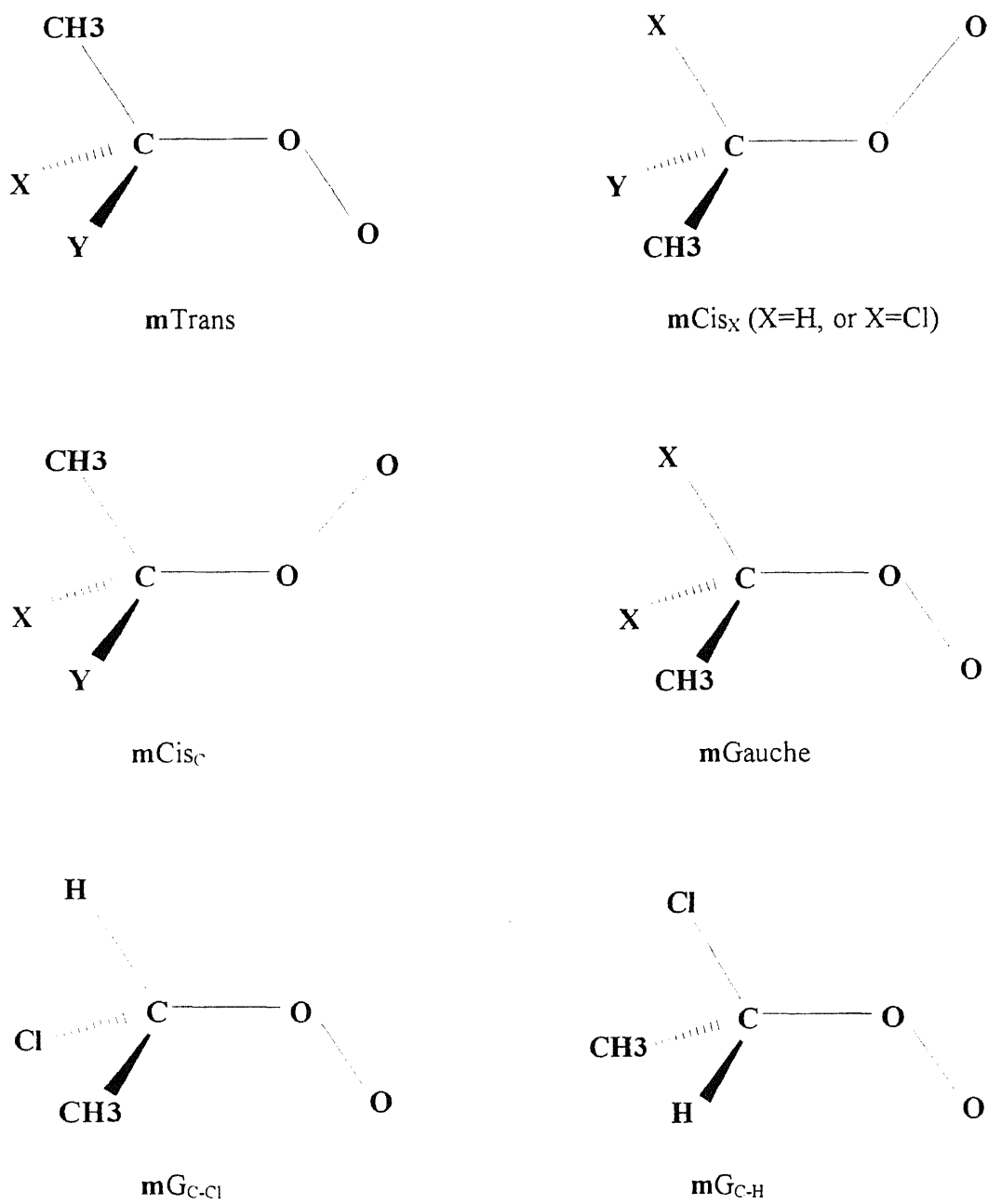


Figure 4.12 Comparison of Harmonic Vibrational Frequencies Calculated using Semiempirical and *ab initio* MO for CH<sub>3</sub>CHClOOH



**Figure 4.13** Comparison of Harmonic Vibrational Frequencies Calculated using Semiempirical and *ab initio* MO for CH<sub>3</sub>CHClOOH





$\text{X}, \text{Y} = \text{H}$  or  $\text{Cl}$

**m=a** where  $\text{X}=\text{Y}=\text{H}$ , **m=b** where  $\text{X}=\text{H}$  and  $\text{Y}=\text{Cl}$ , **m=c** where  $\text{X}=\text{Y}=\text{Cl}$

**Figure 5.1** Definitions of Nomenclature Used in this Work

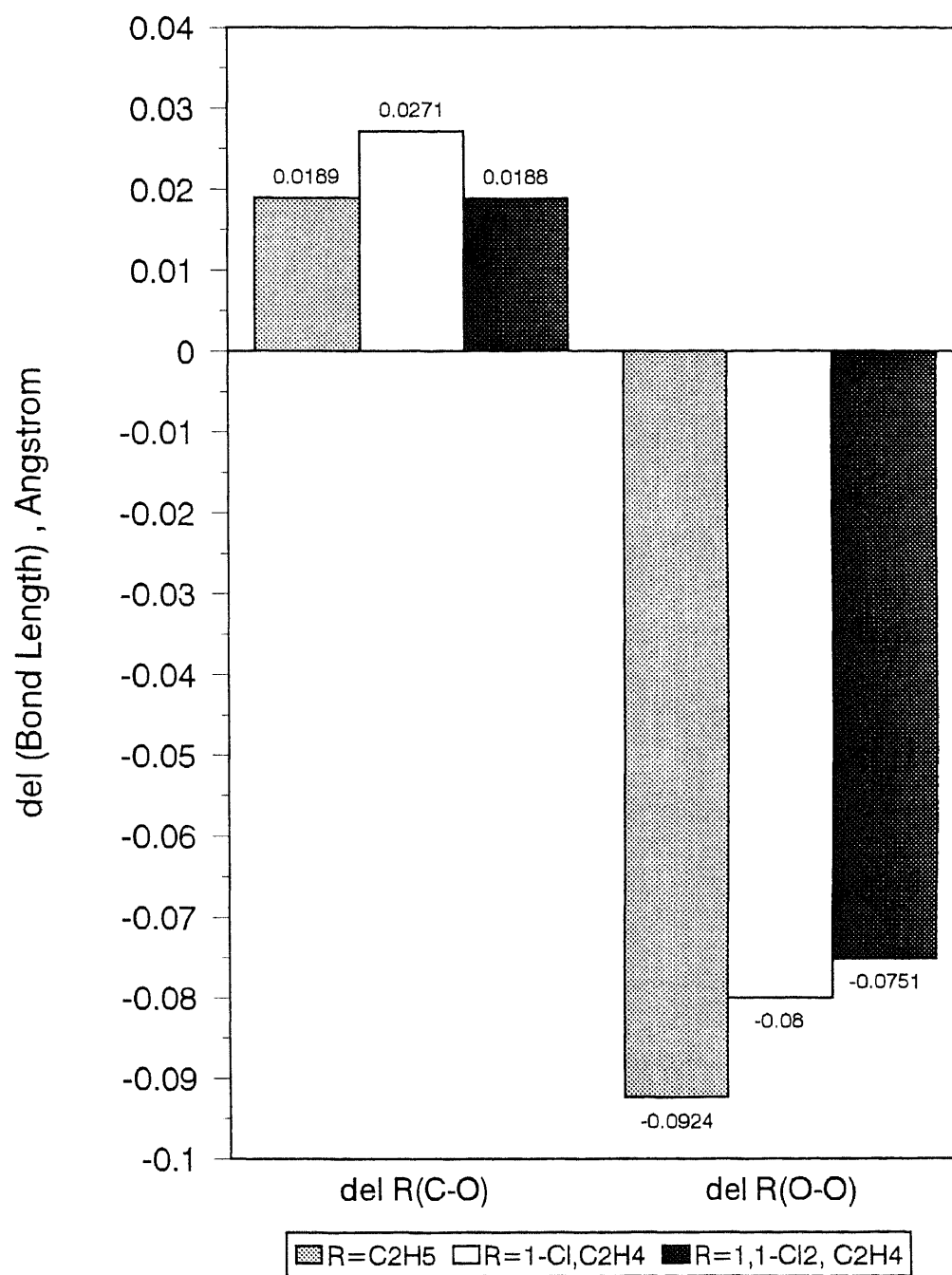


**Figure 5.2** Comparison of C-O and O-O Bond Lengths between ROO and ROOH

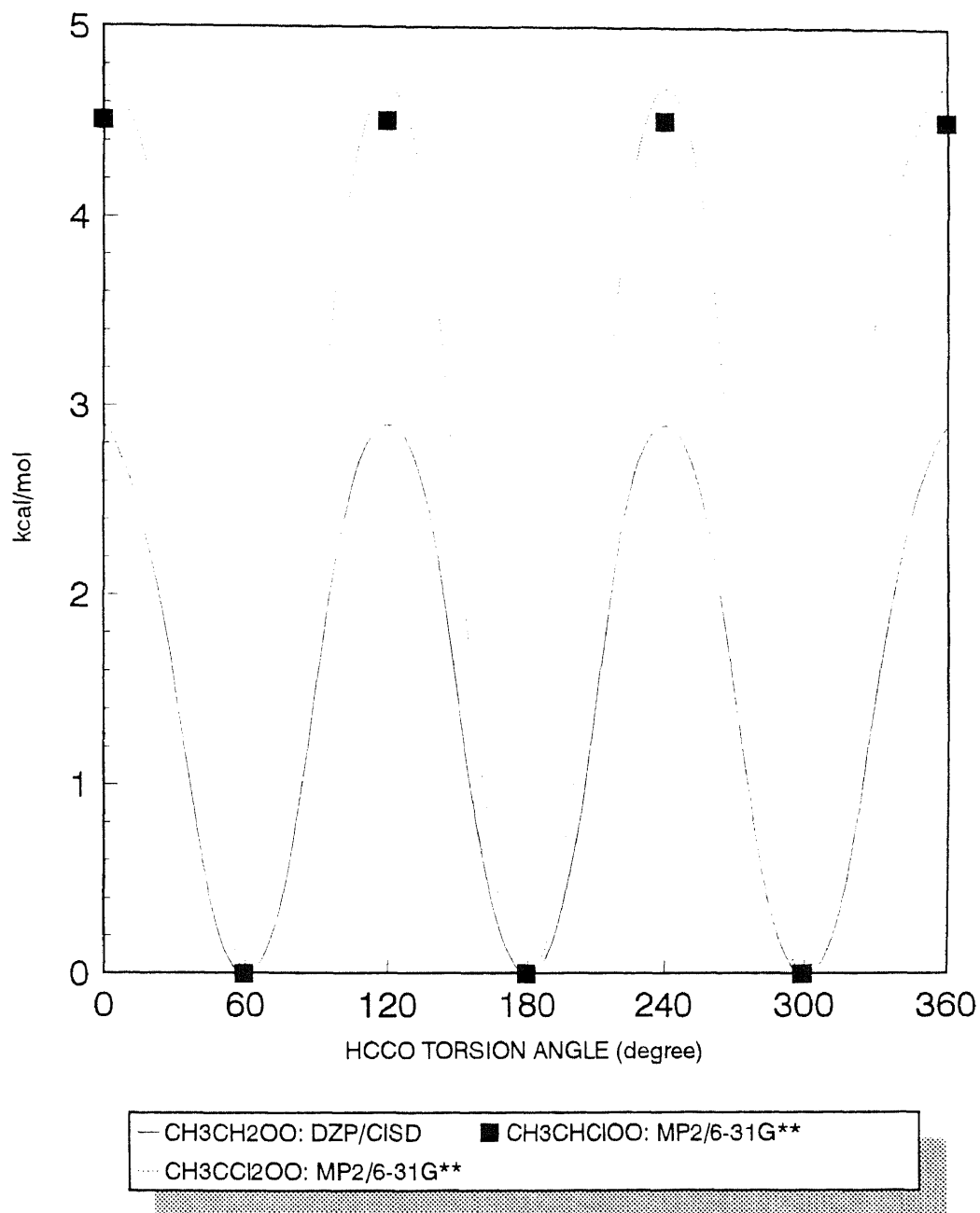


Figure 5.3 Rotational Barrier for CH3--CXYOO

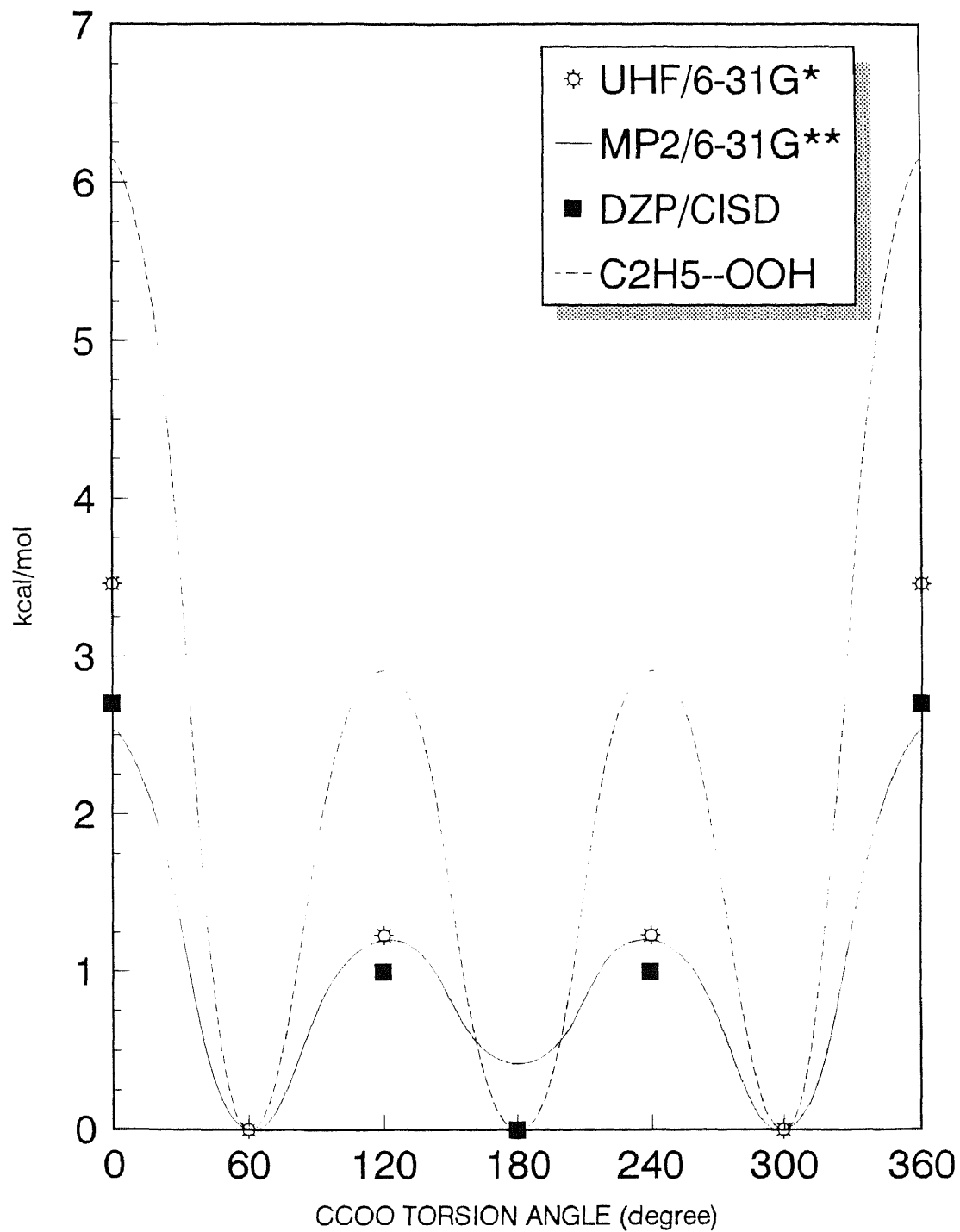


Figure 5.4 Rotational Barrier for CH<sub>3</sub>CH<sub>2</sub>-OO

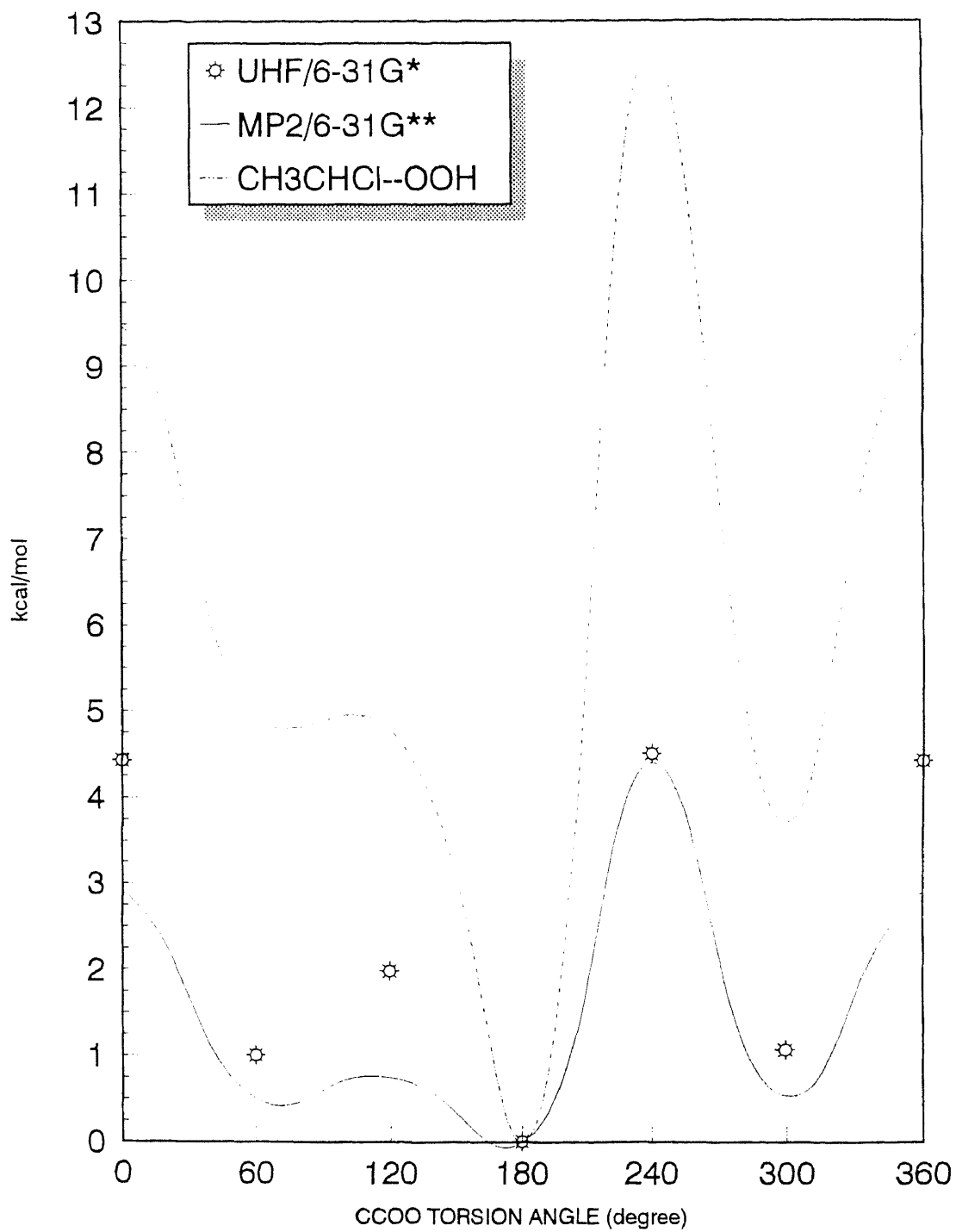


Figure 5.5 Rotational Barrier for CH<sub>3</sub>CHCl-OO

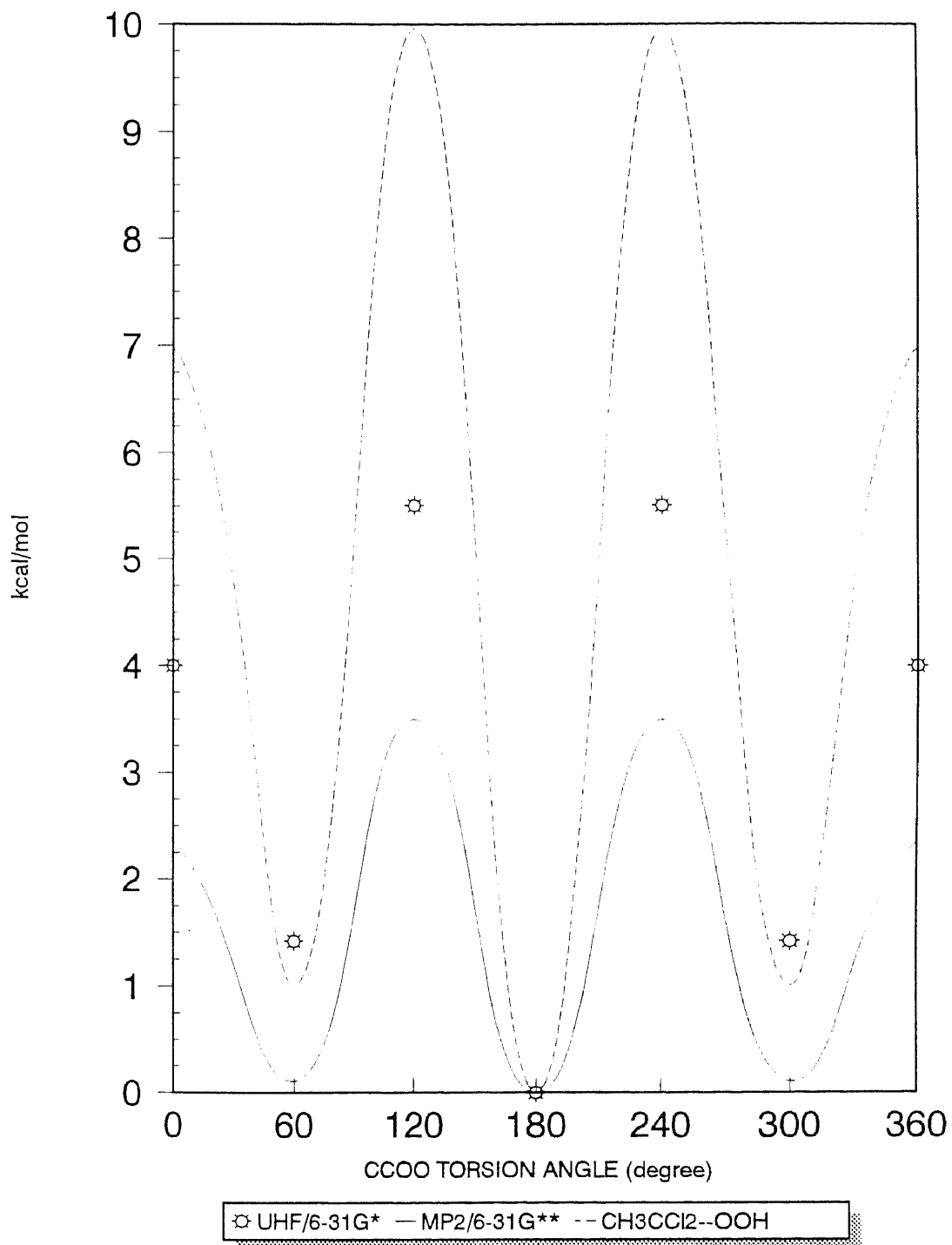


Figure 5.6 Rotational Barrier for CH<sub>3</sub>CCl<sub>2</sub>-OO

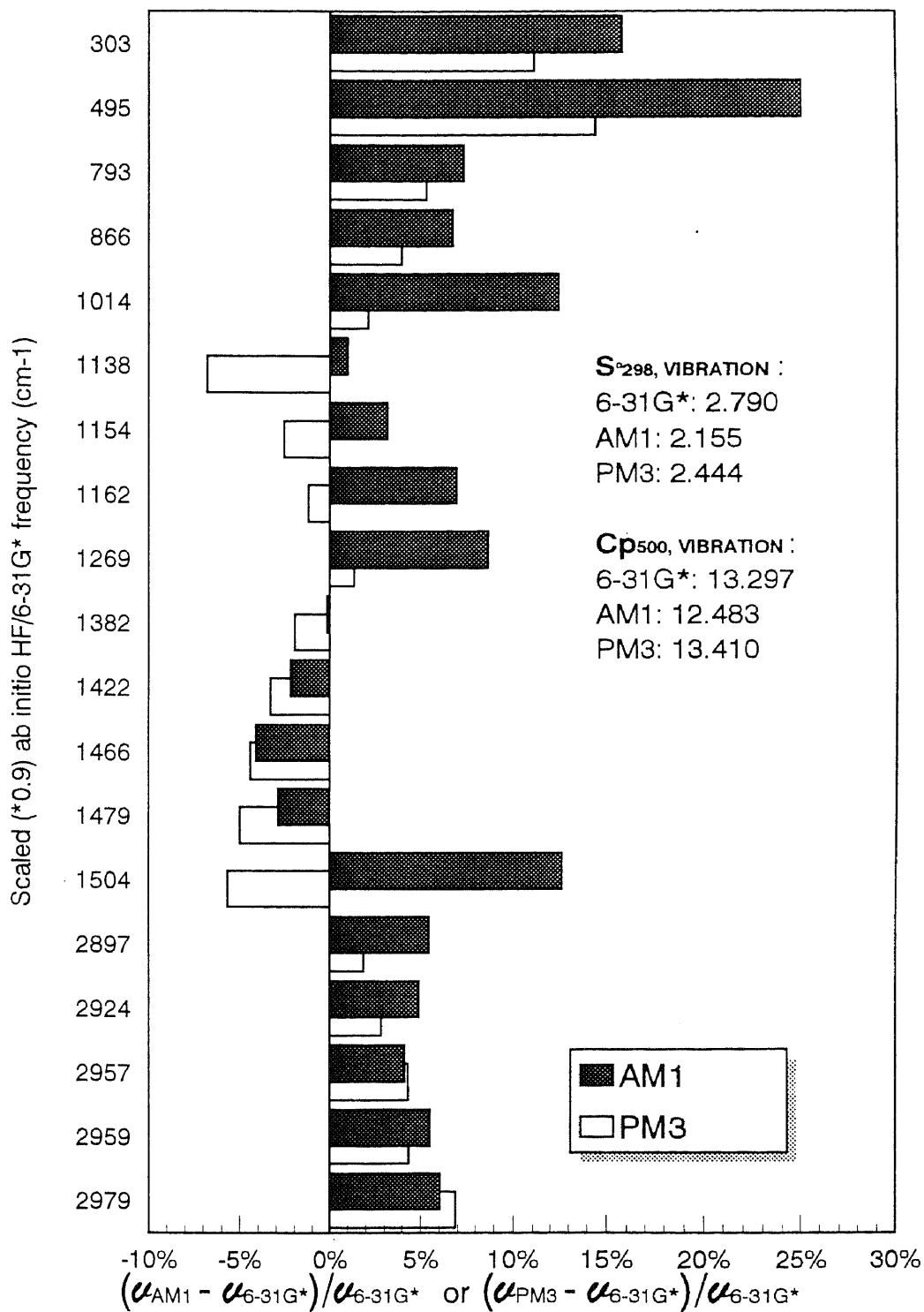
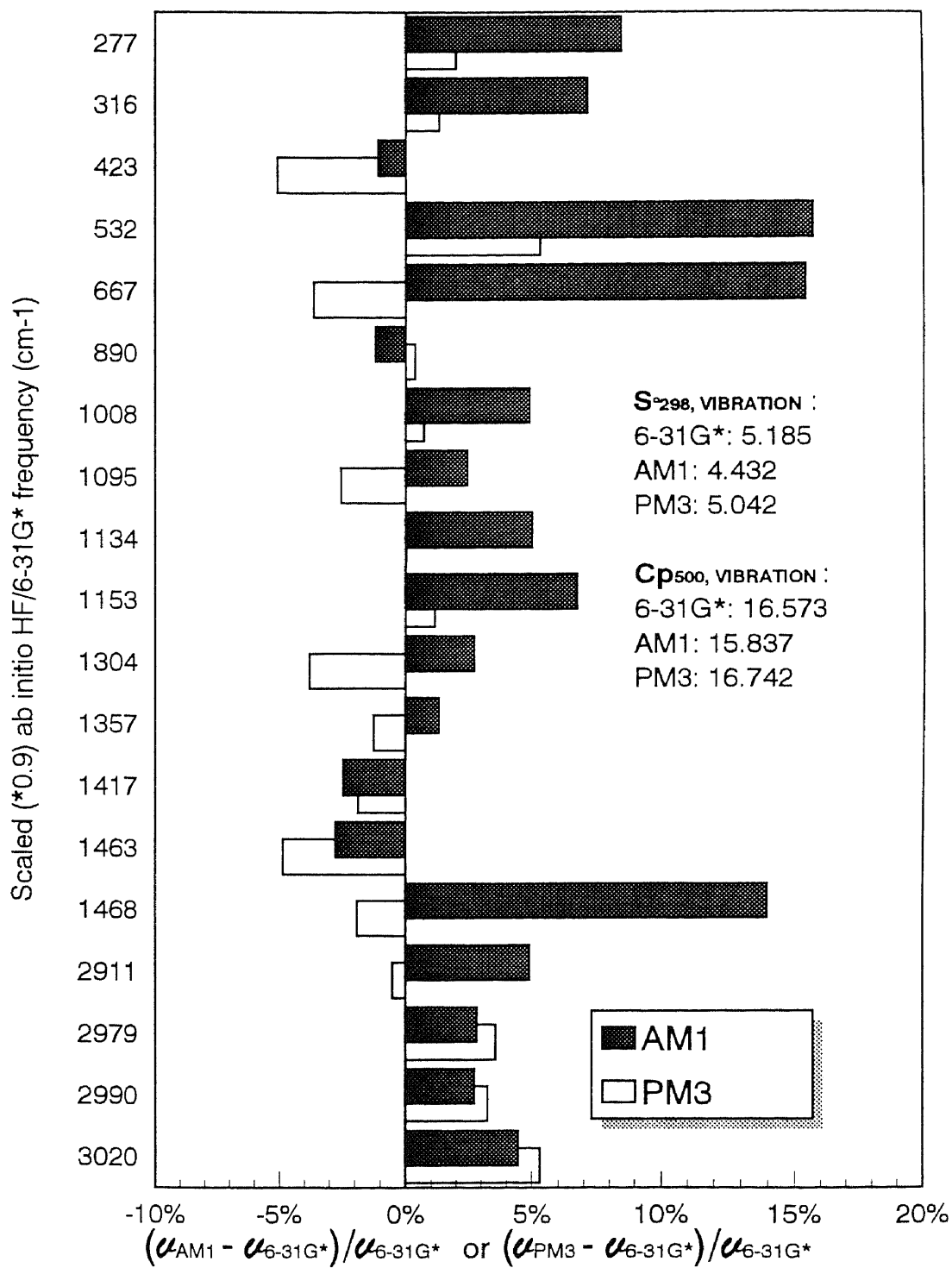


Figure 5.7 Comparison of Harmonic Vibrational Frequencies Calculated using Semiempirical and *ab initio* MO for CH<sub>3</sub>CH<sub>2</sub>OO



**Figure 5.8** Comparison of Harmonic Vibrational Frequencies Calculated using Semiempirical and *ab initio* MO for CH<sub>3</sub>CHClOO



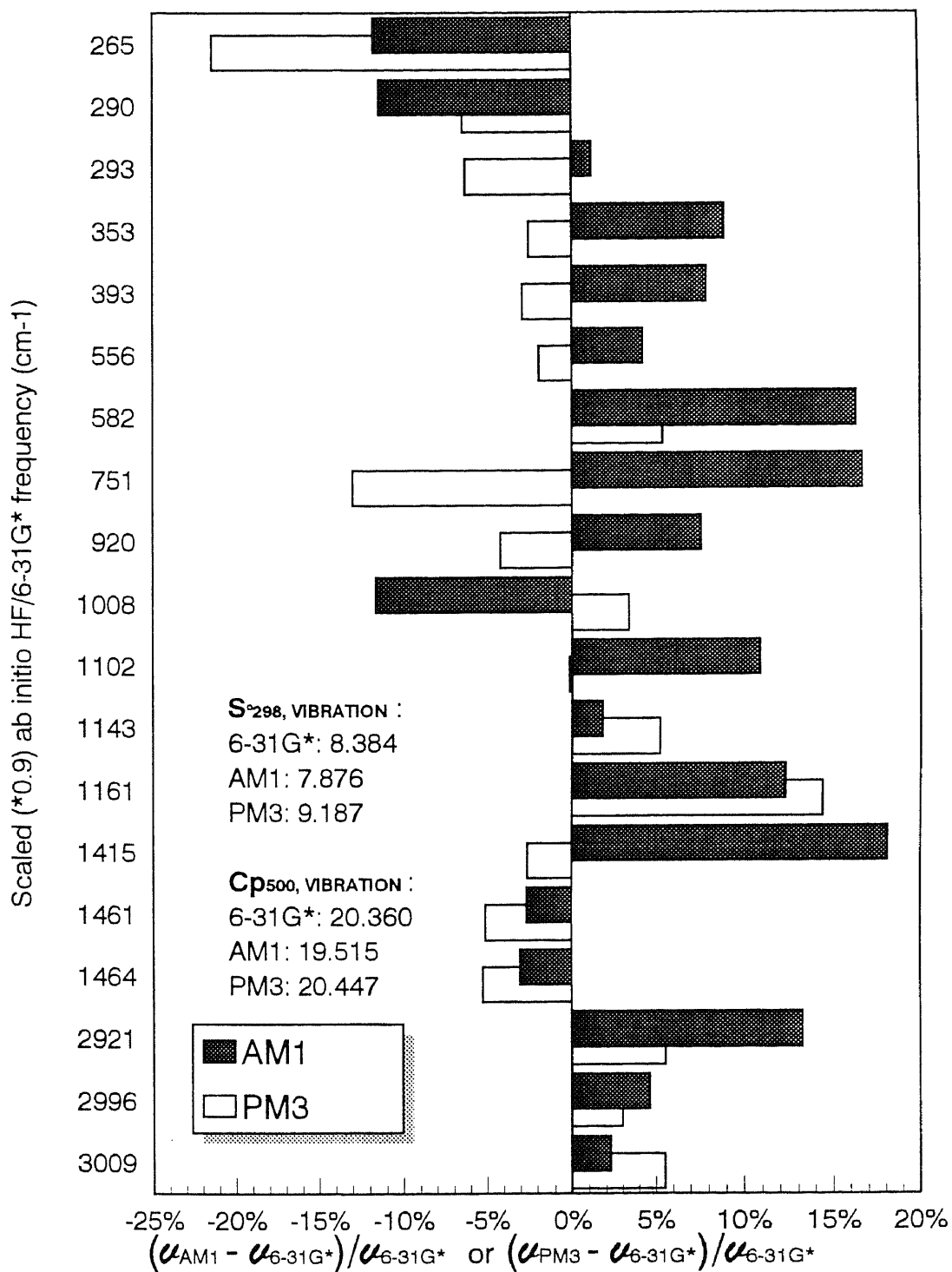
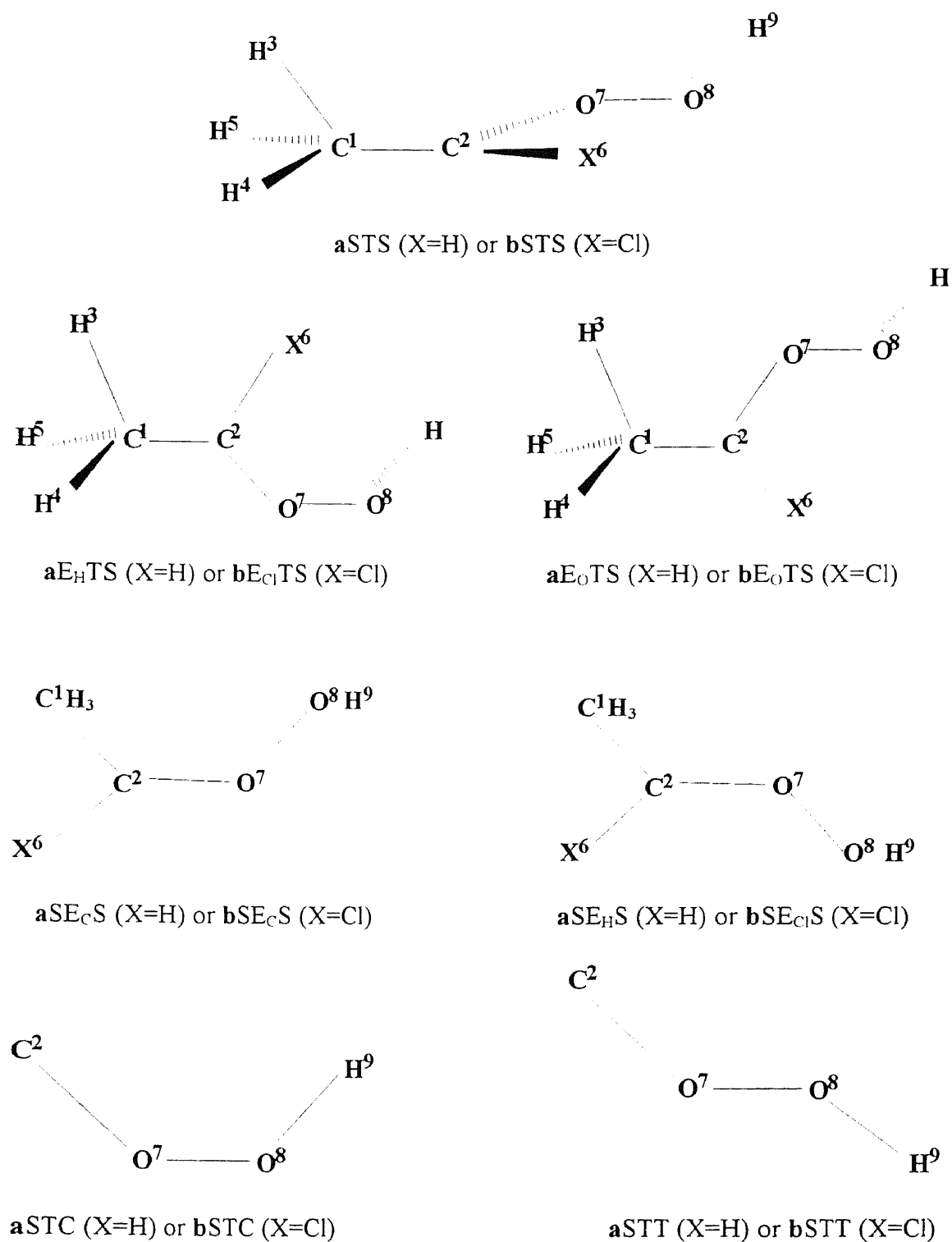
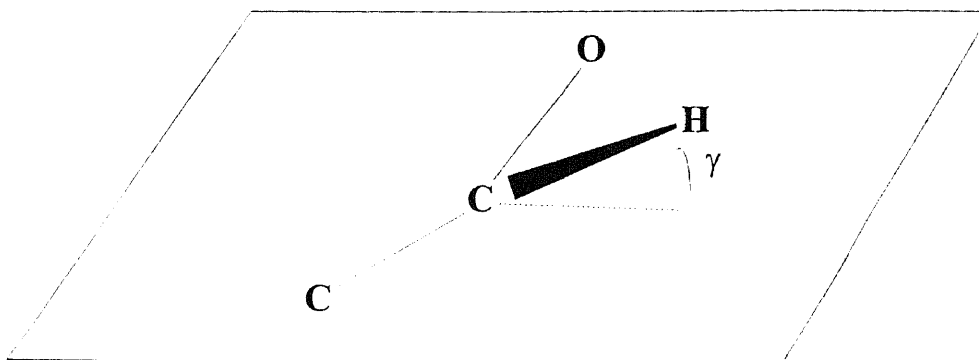


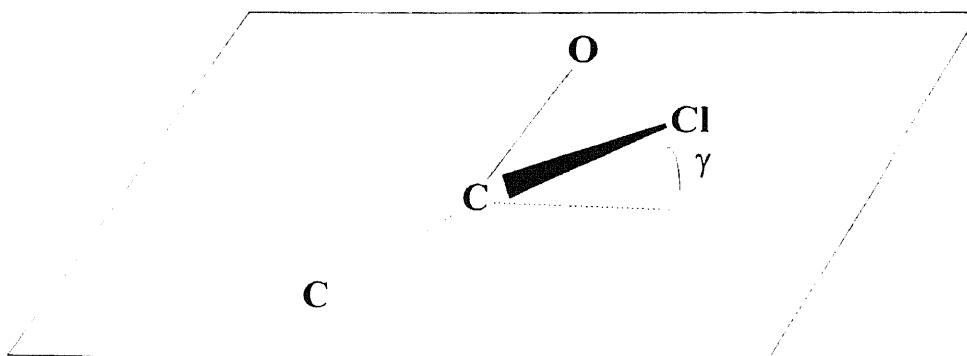
Figure 5.9 Comparison of Harmonic Vibrational Frequencies Calculated using Semiempirical and *ab initio* MO for CH<sub>3</sub>CCl<sub>2</sub>OO



**Figure 6.1** Definitions of Nomenclature Used in this Work



a:  $\text{CH}_3\text{C.HOOH}$



b:  $\text{CH}_3\text{C.ClOOH}$

Figure 6.2 Definition of Out-of-plane Angle

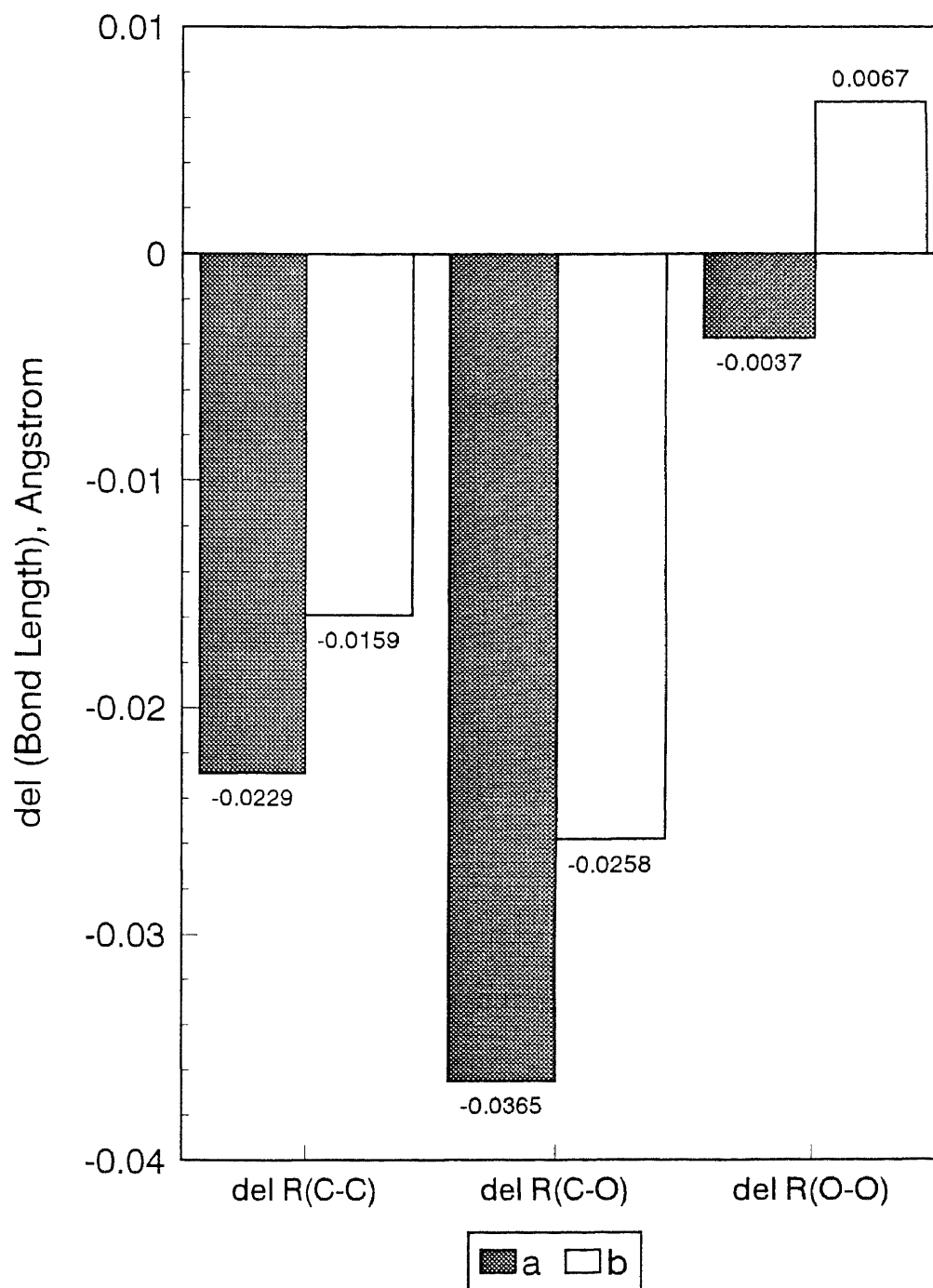


**Figure 6.3** Comparison of C-C, C-O and O-O Bond Lengths Between  
(a) CH<sub>3</sub>C.HOOH and CH<sub>3</sub>CH<sub>2</sub>OOH;  
(b) CH<sub>3</sub>C.ClOOH and CH<sub>3</sub>CHClOOH

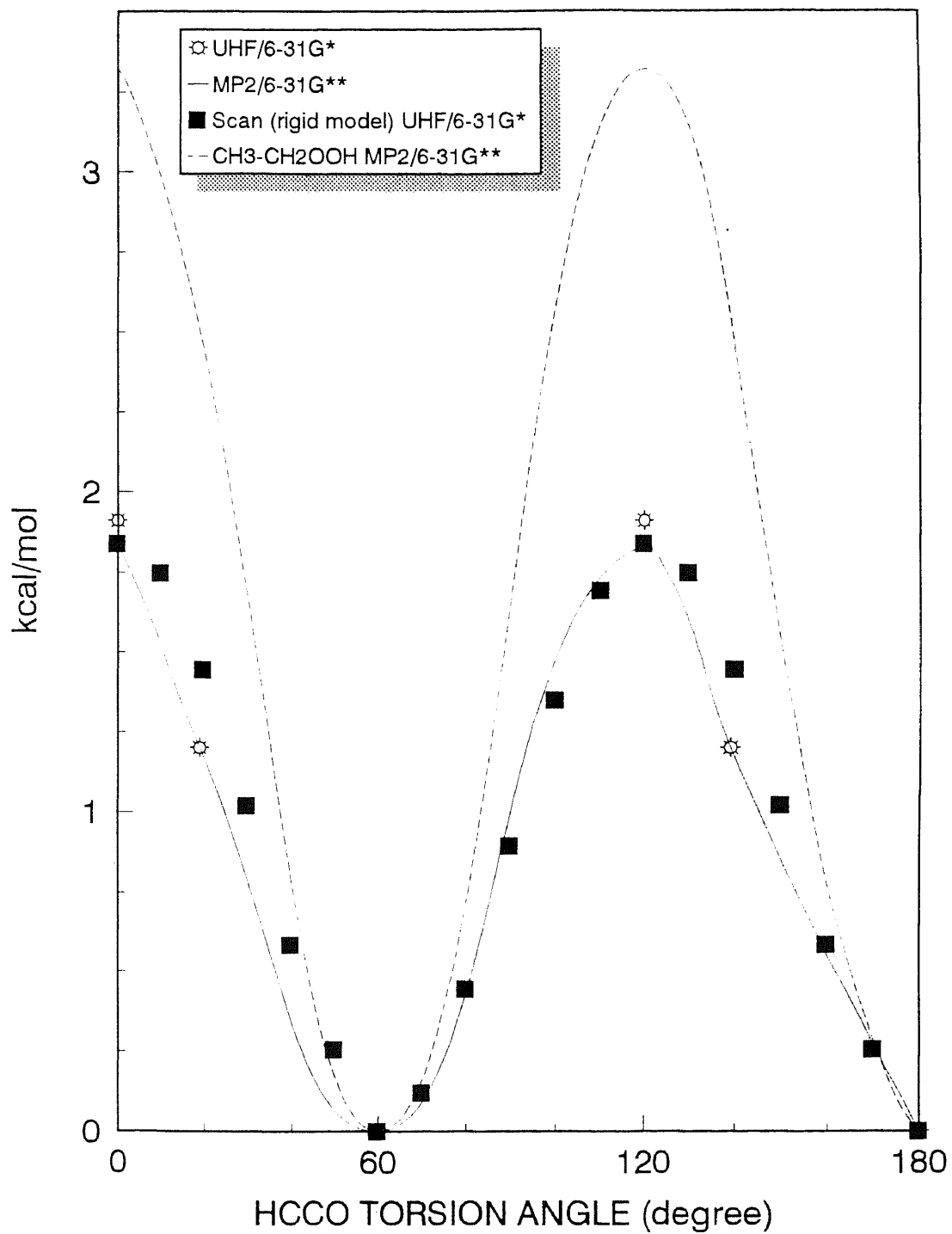


**Figure 6.4** Comparison of Rotation Barrier for CH<sub>3</sub>-C.HOOH and CH<sub>3</sub>-CH<sub>2</sub>OOH

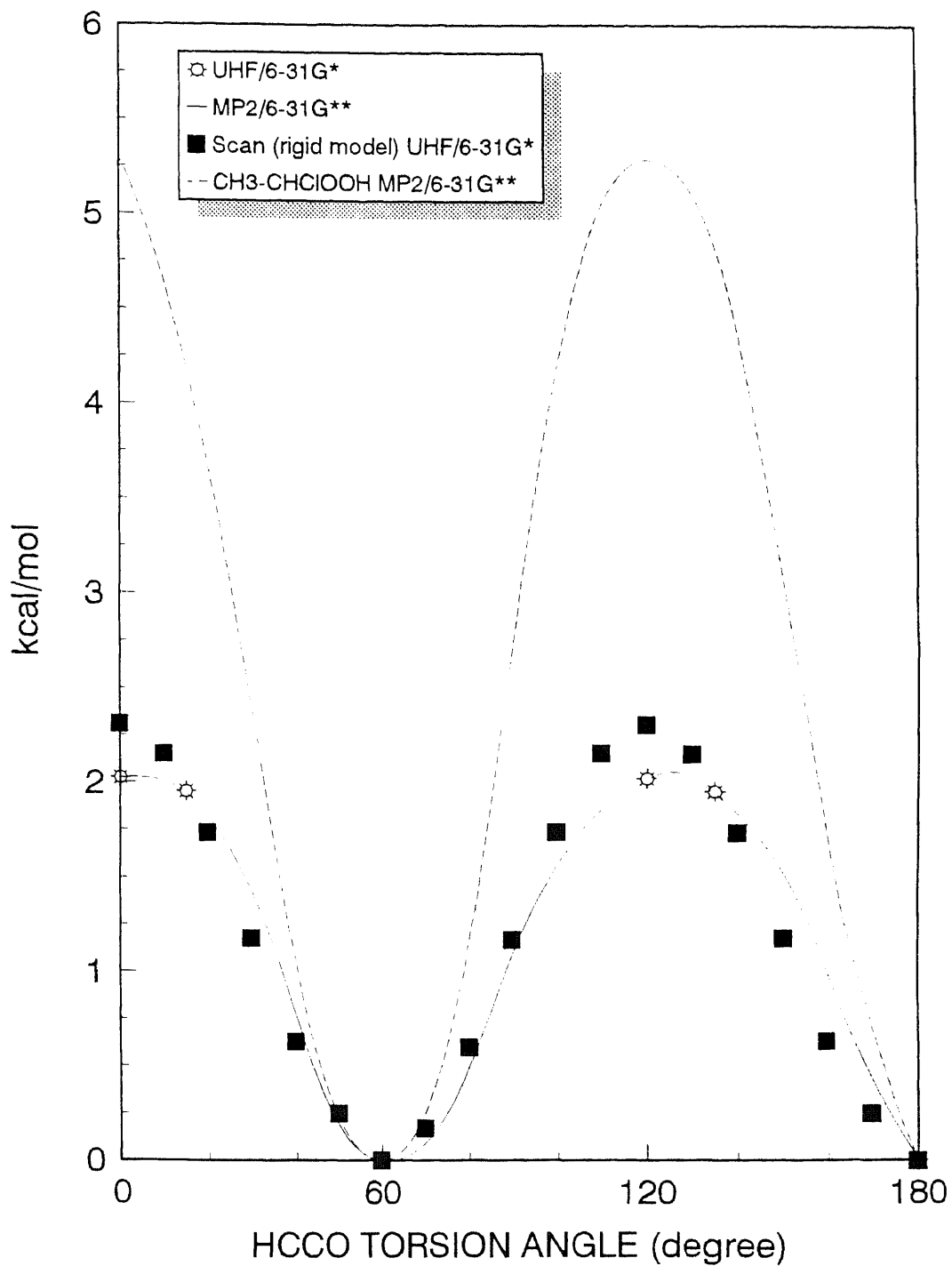


Figure 6.5 Comparison of Rotational Barrier for  $\text{CH}_3\text{-C(=O)OOH}$  and  $\text{CH}_3\text{-CH(Cl)OOH}$

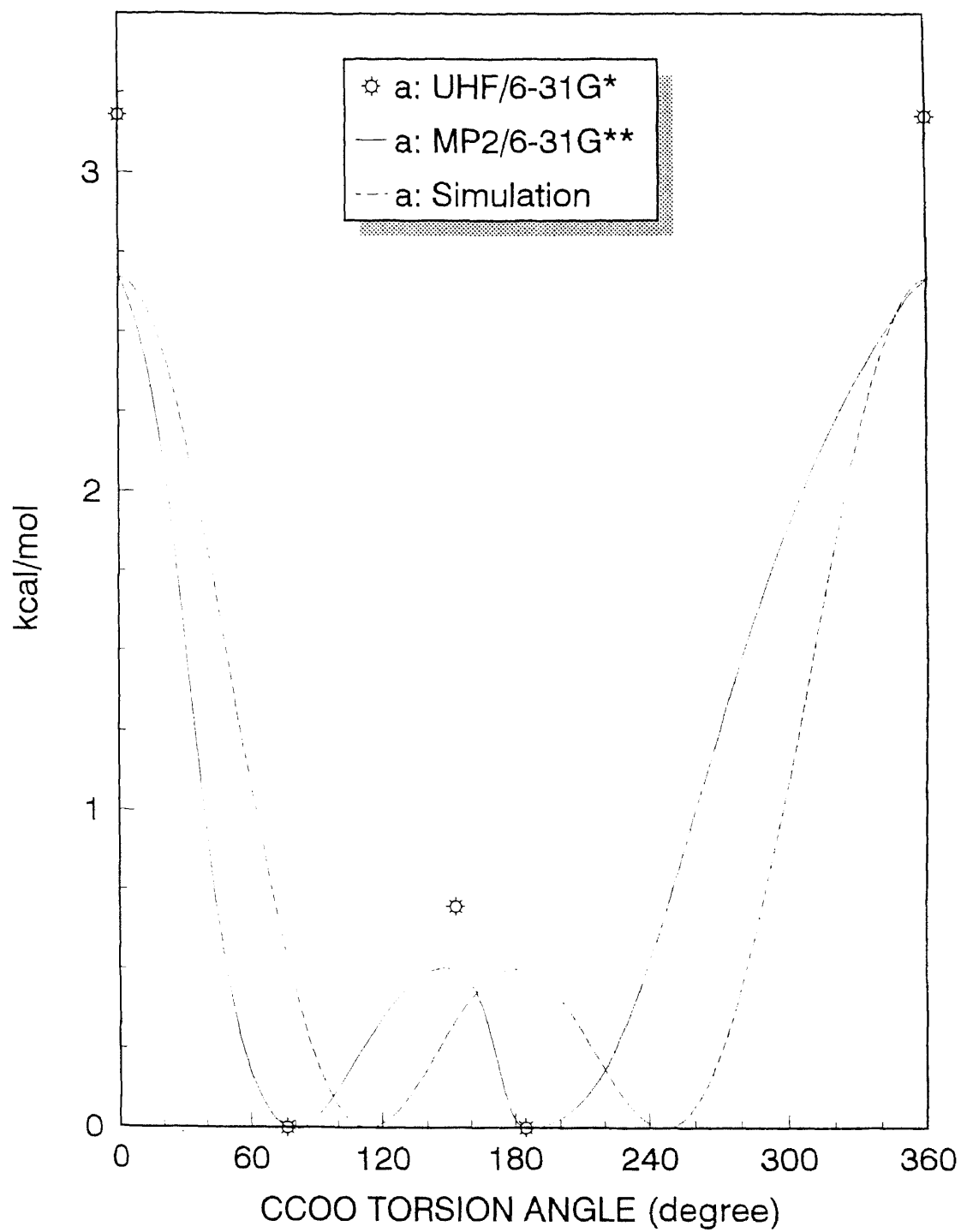


Figure 6.6 Rotational Barrier for CH<sub>3</sub>C.H--OOH

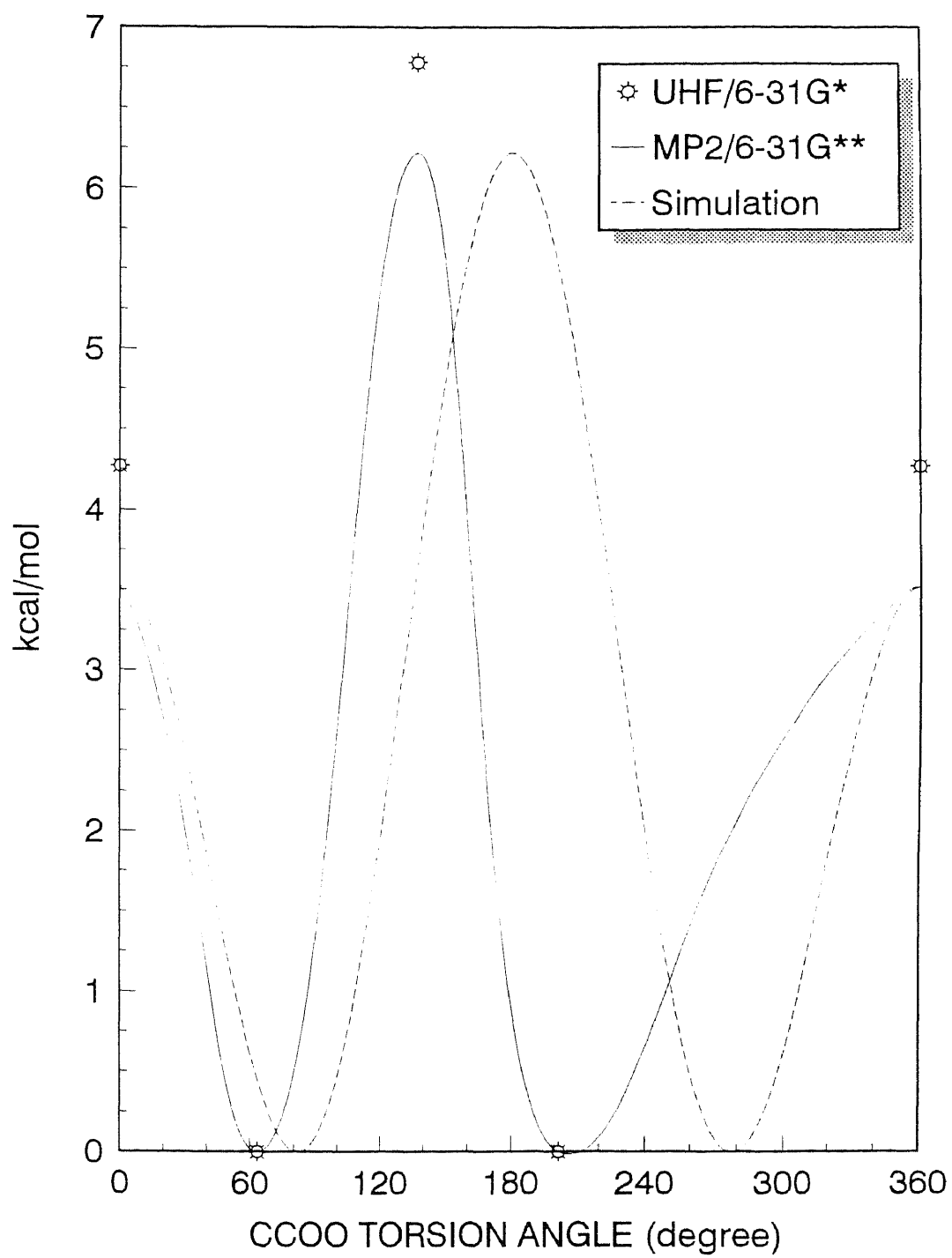
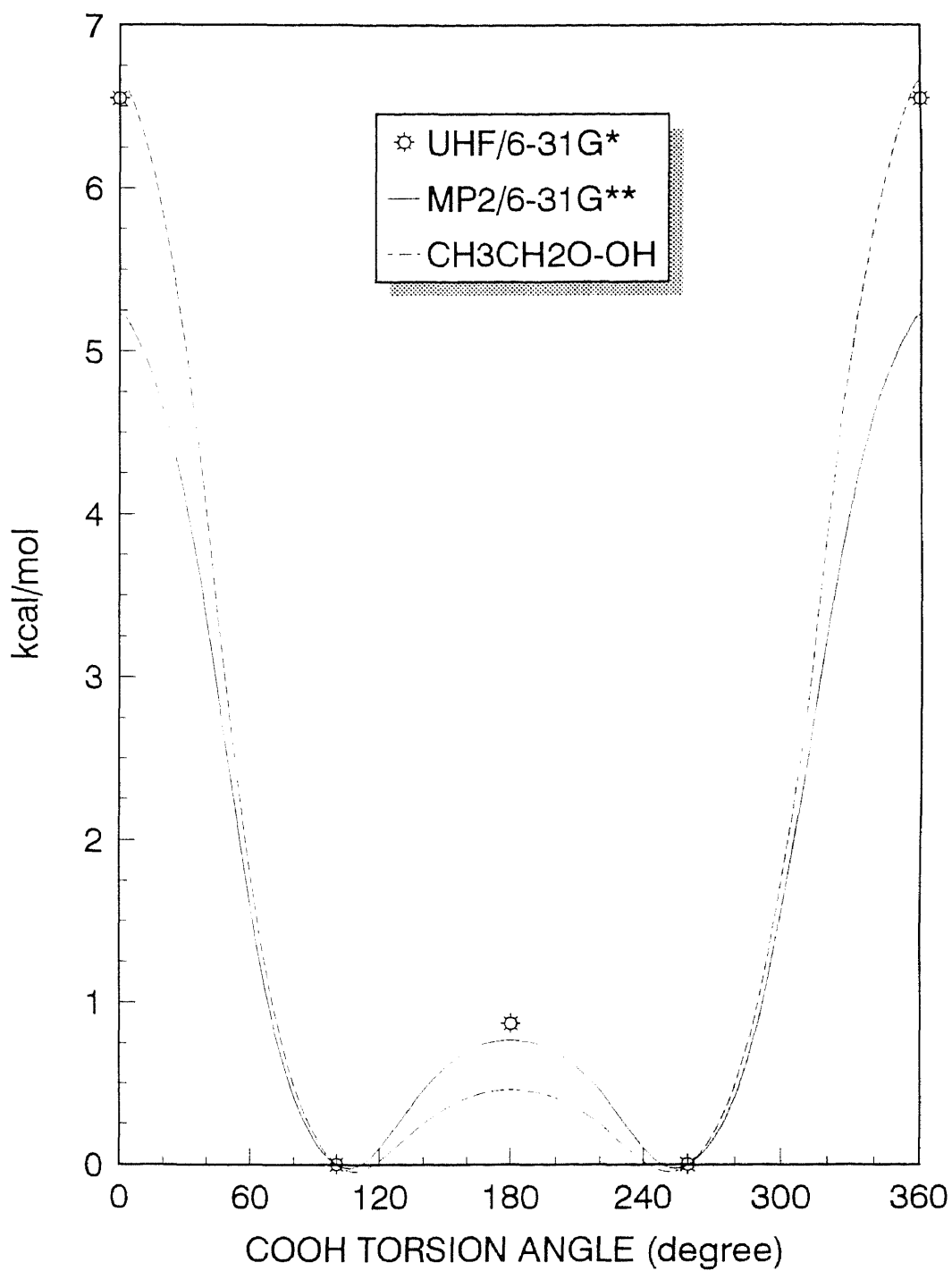
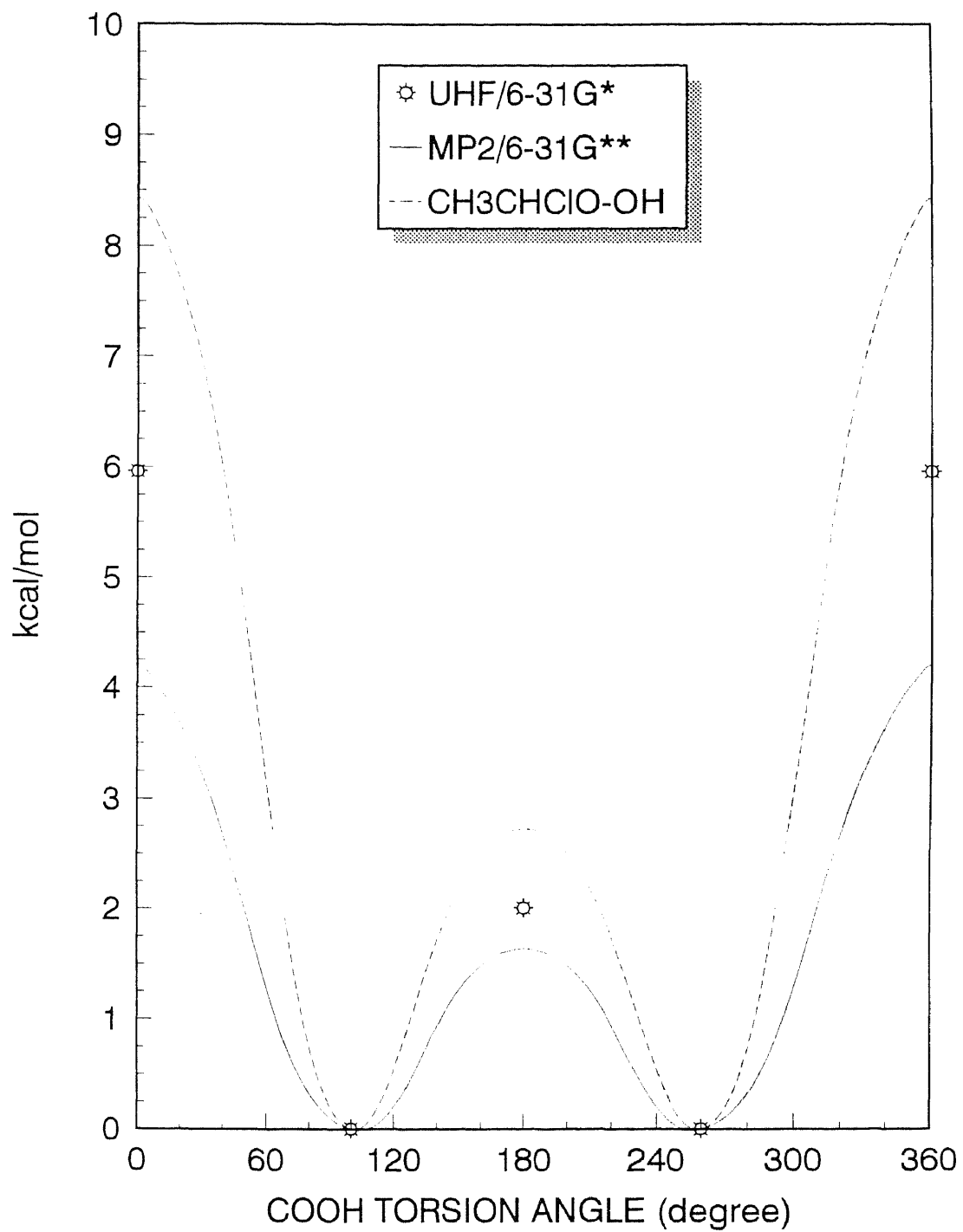


Figure 6.7 Rotational Barrier for CH<sub>3</sub>C.Cl--OOH





**Figure 6.8** Comparison of Rotational Barrier for CH3C.HO--OH and CH3CH2O--OH



**Figure 6.9** Comparison of Rotational Barrier for CH<sub>3</sub>C(Cl)O-OH and CH<sub>3</sub>CH(Cl)O-OH

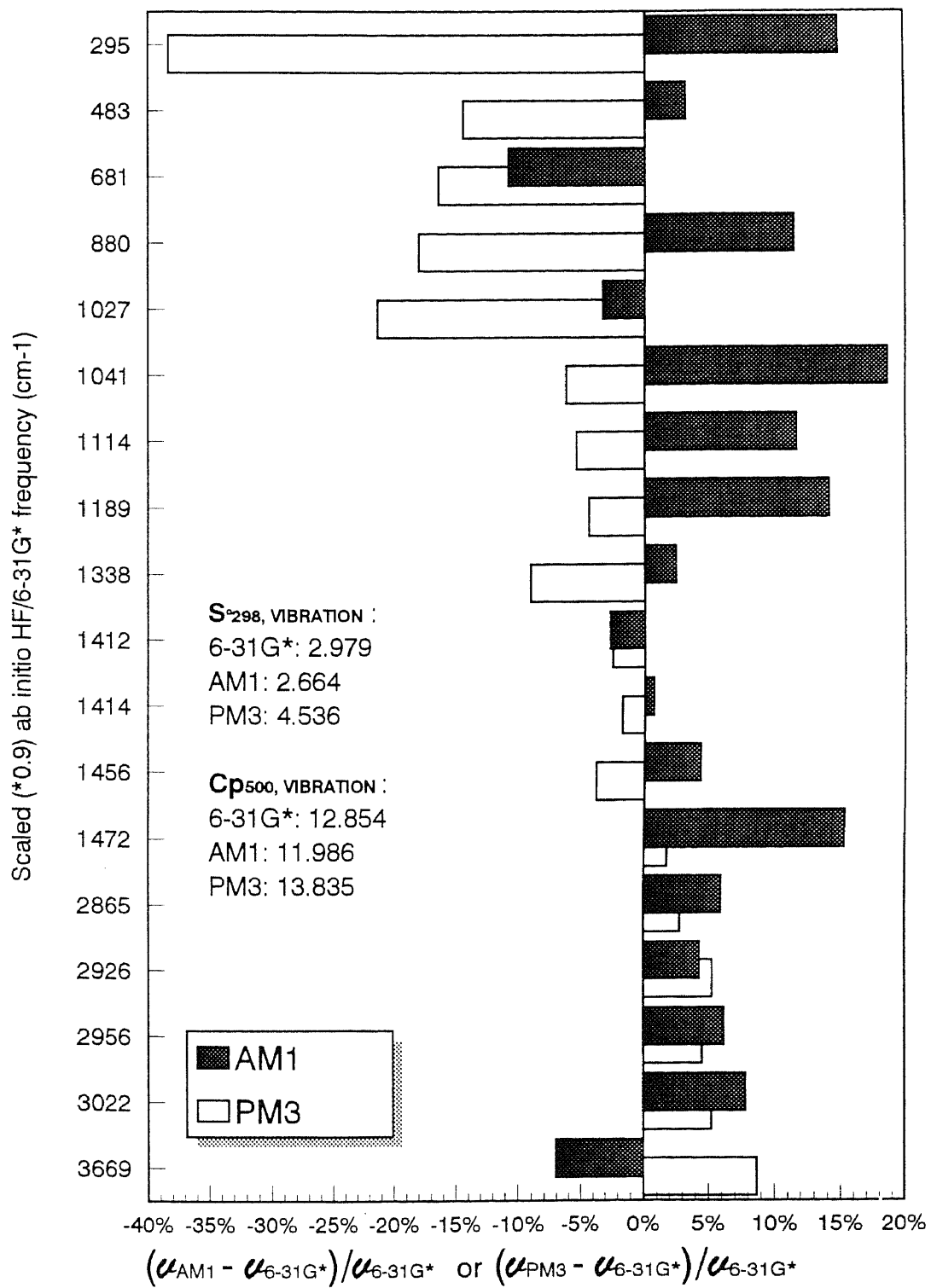
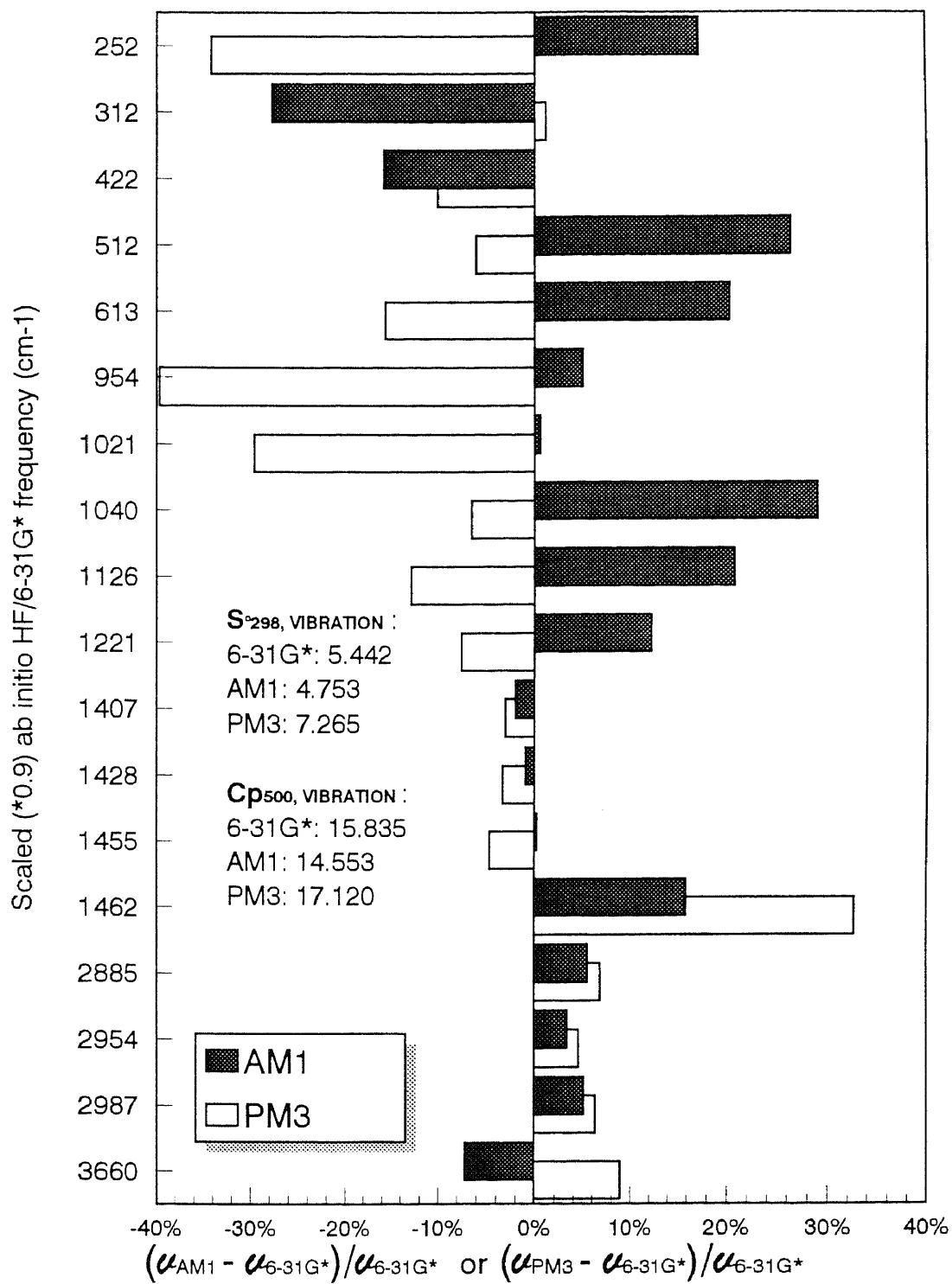


Figure 6.10 Comparison of Harmonic Vibrational Frequencies Calculated using Semiempirical and *ab initio* MO for CH<sub>3</sub>C.HOOH



**Figure 6.11** Comparison of Harmonic Vibrational Frequencies Calculated using Semiempirical and *ab initio* MO for CH<sub>3</sub>C<sub>1</sub>OOH

## APPENDIX C

### TABLES FOR SECTION II

**Table 7.1** Detailed mechanism for Chloroform Pyrolysis in Ar Bath (Model A)

<i>REACTIONS CONSIDERED*</i>	<i>A</i> <i>(cc-mol-sec)</i>	<i>n</i>	<i>Ea</i> <i>(cal/mol)</i>	<i>Source</i>
1. $\text{CHCl}_3 = \text{CCl}_2 + \text{HCl}$	6.11E+38	-7.8	63549	DISSOC
2. $\text{CHCl}_3 = \text{CHCl}_2 + \text{Cl}$	3.90E+38	-8	78754	DISSOC
3. $\text{CHCl}_3 = \text{CCl}_3 + \text{H}$	4.53E+30	-6.1	98582	DISSOC
4. $\text{CHCl}_3 + \text{Cl} = \text{CCl}_3 + \text{HCl}$	2.00E+13	0	2800	Kerr
5. $\text{CHCl}_3 + \text{Cl} = \text{CHCl}_2 + \text{Cl}_2$	1.00E+14	0	21000	Chiang
6. $\text{CHCl}_3 + \text{CHCl}_2 = \text{CCl}_3 + \text{CH}_2\text{Cl}_2$	1.81E+09	0	6399	Chiang
7. $\text{CHCl}_3 + \text{CCl}_2 = \text{C}_2\text{HCl}_5$	3.08E+27	-5.4	7810	QRRK
8. $\text{CHCl}_3 + \text{CCl}_2 = \text{HCl} + \text{C}_2\text{Cl}_4$	1.69E+08	1	7310	QRRK
9. $\text{CHCl}_3 + \text{CCl}_2 = \text{CHCl}_2\text{CCl}_2 + \text{Cl}$	1.38E+05	2.1	11590	QRRK
10. $\text{CHCl}_3 + \text{CCl}_2 = \text{CCl}_3 + \text{CHCl}_2$	2.00E+12	0	29700	Won
11. $\text{CHCl}_3 + \text{H} = \text{CHCl}_2 + \text{HCl}$	3.60E+12	0	6200	Won
12. $\text{C}_2\text{HCl}_5 = \text{HCl} + \text{C}_2\text{Cl}_4$	1.02E+27	-4.4	52070	DISSOC
13. $\text{C}_2\text{HCl}_5 = \text{CHCl}_2\text{CCl}_2 + \text{Cl}$	7.28E+42	-9	72720	DISSOC
14. $\text{CCl}_2 + \text{CCl}_2 = \text{C}_2\text{Cl}_4$	2.70E+40	-10	8410	QRRK
15. $\text{CCl}_2 + \text{CCl}_2 = \text{C}_2\text{Cl}_3 + \text{Cl}$	2.94E+11	0	1750	QRRK
16. $\text{C}_2\text{Cl}_4 = \text{Cl} + \text{C}_2\text{Cl}_3$	8.97E+27	-4.1	85550	DISSOC
17. $\text{CCl}_2 + \text{CCl}_3 = \text{C}_2\text{Cl}_5$	1.69E+07	0.4	-1960	QRRK
18. $\text{CCl}_2 + \text{CCl}_3 = \text{C}_2\text{Cl}_4 + \text{Cl}$	5.06E+12	-0.1	60	QRRK
19. $\text{C}_2\text{Cl}_5 = \text{Cl} + \text{C}_2\text{Cl}_4$	7.88E+32	-6.8	20960	DISSOC
20. $\text{CCl}_3 + \text{CCl}_3 = \text{C}_2\text{Cl}_6$	8.62E+33	-7	5520	QRRK
21. $\text{CCl}_3 + \text{CCl}_3 = \text{C}_2\text{Cl}_4 + \text{Cl}_2$	7.98E+15	-1.4	6570	QRRK
22. $\text{CCl}_3 + \text{CCl}_3 = \text{C}_2\text{Cl}_5 + \text{Cl}$	3.50E+18	-1.7	9880	QRRK
23. $\text{C}_2\text{Cl}_6 = \text{C}_2\text{Cl}_4 + \text{Cl}_2$	1.68E+23	-3.4	56700	DISSOC
24. $\text{C}_2\text{Cl}_6 = \text{C}_2\text{Cl}_5 + \text{Cl}$	1.91E+40	-8	73490	DISSOC
25. $\text{Cl} + \text{C}_2\text{Cl}_5 = \text{C}_2\text{Cl}_4 + \text{Cl}_2$	6.10E+11	0.2	6210	QRRK
26. $\text{C}_2\text{HCl}_5 + \text{Cl} = \text{C}_2\text{Cl}_5 + \text{HCl}$	6.30E+12	0	3300	Won
27. $\text{C}_2\text{HCl}_5 + \text{H} = \text{CHCl}_2\text{CCl}_2 + \text{HCl}$	3.60E+12	0	4300	Won

**Table 7.1** (continued) Detailed mechanism for Chloroform Pyrolysis in Ar Bath (Model A)

<i>REACTIONS CONSIDERED</i>	<i>A</i> ( <i>cc-mol-sec</i> )	<i>n</i>	<i>Ea</i> ( <i>cal/mol</i> )	<i>Source</i>
28. $\text{CCl}_4 + \text{H} = \text{CCl}_3 + \text{HCl}$	5.00E+13	0	5000	Won
29. $\text{CHCl}_2 + \text{CCl}_3 = \text{C}_2\text{HCl}_5$	1.94E+47	-11.1	9960	Chiang
30. $\text{CHCl}_2 + \text{CCl}_3 = \text{C}_2\text{Cl}_4 + \text{HCl}$	2.52E+27	-4.9	8930	Chiang
31. $\text{CHCl}_2 + \text{CCl}_3 = \text{CHCl}_2\text{CCl}_2 + \text{Cl}$	5.48E+25	-4.1	9230	Chiang
32. $\text{CHCl}_2\text{CCl}_2 + \text{Cl} = \text{C}_2\text{Cl}_4 + \text{HCl}$	5.34E+18	-1.2	8640	Chiang
33. $\text{C}_2\text{HCl}_3 + \text{Cl} = \text{C}_2\text{Cl}_3 + \text{HCl}$	1.70E+13	0	7000	Won
34. $\text{C}_2\text{Cl}_4 + \text{H} = \text{C}_2\text{Cl}_3 + \text{HCl}$	1.20E+12	0	15000	Won
35. $\text{C}_2\text{Cl}_4 + \text{Cl} = \text{C}_2\text{Cl}_3 + \text{Cl}_2$	6.75E+09	1.2	52580	QRRK
36. $\text{C}_2\text{Cl}_5 = \text{C}_2\text{Cl}_3 + \text{Cl}_2$	7.19E+07	0.8	68100	QRRK
37. $\text{CCl}_2 + \text{CHCl}_2 = \text{CHCl}_2\text{CCl}_2$	1.00E+14	-2	-830	QRRK
38. $\text{CCl}_2 + \text{CHCl}_2 = \text{C}_2\text{HCl}_3 + \text{Cl}$	1.37E+13	-0.1	90	QRRK
39. $\text{CHCl}_2\text{CCl}_2 = \text{C}_2\text{HCl}_3 + \text{Cl}$	5.13E+41	-9.5	27200	DISSOC
40. $\text{C}_2\text{HCl}_3 = \text{CHClCCl} + \text{Cl}$	9.30E+40	-8.3	91260	DISSOC
41. $\text{C}_2\text{HCl}_3 = \text{CHCCl}_2 + \text{Cl}$	1.10E+41	-8.5	93960	DISSOC
42. $\text{C}_2\text{HCl}_3 = \text{C}_2\text{Cl}_2 + \text{HCl}$	1.76E+31	-5.5	74360	DISSOC
43. $\text{CHCl}_2 + \text{CHCl}_2 = \text{CHCl}_2\text{CHCl}_2$	7.62E+48	-11.5	10570	Chiang
44. $\text{CHCl}_2 + \text{CHCl}_2 = \text{C}_2\text{HCl}_3 + \text{HCl}$	2.17E+31	-5.8	10040	Chiang
45. $\text{CHCl}_2 + \text{CHCl}_2 = \text{CHCl}_2\text{CHCl} + \text{Cl}$	1.48E+26	-4	10790	Chiang
46. $\text{CHCl}_2\text{CHCl}_2 = \text{C}_2\text{HCl}_3 + \text{HCl}$	6.14E+33	-6.3	65300	Chiang
47. $\text{CHCl}_2\text{CHCl}_2 = \text{CHCl}_2\text{CHCl} + \text{Cl}$	1.24E+47	-9.9	82660	Chiang
48. $\text{CCl}_4 = \text{CCl}_3 + \text{Cl}$	1.89E+50	-11.1	77110	Won
49. $\text{Cl} + \text{Cl} + \text{M} = \text{Cl}_2 + \text{M}$	2.34E+14	0	-1800	Kerr
50. $\text{H} + \text{Cl} + \text{M} = \text{HCl} + \text{M}$	7.20E+21	-2	0	Pitz
51. $\text{H} + \text{H} + \text{M} = \text{H}_2 + \text{M}$	5.44E+18	-1.3	-2000	Tsan
52. $\text{HCl} + \text{H} = \text{Cl} + \text{H}_2$	2.30E+13	0	3500	Kerr
53. $\text{Cl} + \text{CCl}_2 = \text{CCl}_3$	1.58E+13	0	0	Won
54. $\text{H} + \text{CCl}_2 = \text{CHCl}_2$	1.00E+14	0	0	Won
55. $\text{CCl}_3 + \text{Cl}_2 = \text{CCl}_4 + \text{Cl}$	4.80E+11	0	2500	Kerr
56. $\text{C}_2\text{Cl}_3 = \text{C}_2\text{Cl}_2 + \text{Cl}$	5.08E+13	0	28000	est.
57. $\text{C}_2\text{Cl}_4 + \text{H} = \text{CHCl}_2\text{CCl}_2$	9.07E+07	0	2700	Won
58. $\text{C}_2\text{Cl}_4 + \text{H} = \text{C}_2\text{HCl}_3 + \text{Cl}$	1.40E+13	0	9200	Won
59. $\text{CHClCCl} = \text{C}_2\text{HCl} + \text{Cl}$	2.35E+14	0	19200	Won
60. $\text{CHCCl}_2 = \text{C}_2\text{HCl} + \text{Cl}$	5.72E+14	0	19600	Won

\* rate constant  $k = A T^n \exp(-E_a/RT)$

Note:

- DISSOC Apparent rate constant calculated using DISSOCIATION computer code. (Dean, A. M., Bozzelli, J. W. and Ritter, E. R., *J. Phys. Chem.* **1985**, *89*, 4600).  
For reaction (1), (2), (3), see Table 7.A.1.
- QRRK Apparent rate constant calculated using CHEMAT computer code. (Dean, A. M., Bozzelli, J. W. and Ritter, E. R., *Comb. Sci. and Tech.* **1991**, *84*, 63).  
For (7), (8), (9), see Table 7.A.2; for (14), (15), see Table 7.A.3; for (17), (18), see Table 7.A.4; for (20), (21), see Table 7.A.5.
- Kerr Kerr, J. A. and Moss, S. J., 'Handbook of Bimolecular and Termolecular Gas Reaction', Vol. I and II, CRC Press Inc., 1981.
- Chiang Hong-Ming Chiang's work (estimation of Arrhenius A factors and QRRK calculations) at NJIT on the systematic study of pyrolysis and combustion of chlorohydrocarbon species.
- Won Won, Y. S. and Bozzelli, J. W., 'Chloroform Pyrolysis: Experimental and Detailed Model', *Comb. Sci. and Tech.* **1992**, *85*, 345
- Tsan Tsan, W. and Hampson, R. F., *J. Phys. Chem. Ref. Data.* **1986**, *15*, 1087.
- Pitz  
est. Rate constant estimated in this study, based on thermodynamic properties of the reactants and products.

**Table 7.2** Detailed mechanism for Chloroform Oxidation in Ar Bath (Model B)

<i>REACTIONS CONSIDERED</i>		<i>A</i>	<i>n</i>	<i>Ea</i>	<i>Source</i>
		<i>(cc-mol-sec)</i>		<i>(cal-mol)</i>	
61.	$\text{CHCl}_3 + \text{OH} = \text{CCl}_3 + \text{H}_2\text{O}$	1.02E+04	2.8	199	Cohen
62.	$\text{CHCl}_3 + \text{O}_2 = \text{CCl}_3 + \text{HO}_2$	1.00E+13	0	47200	Won
63.	$\text{CHCl}_3 + \text{HO}_2 = \text{CCl}_3 + \text{H}_2\text{O}_2$	4.50E+10	0	14200	Won
64.	$\text{CHCl}_3 + \text{O} = \text{CCl}_3 + \text{OH}$	3.00E+12	0	4968	Herron
65.	$\text{CHCl}_3 + \text{ClO} = \text{CCl}_3 + \text{HOCl}$	5.00E+11	0	7600	est.
66.	$\text{CCl}_4 + \text{OH} = \text{CCl}_3 + \text{HOCl}$	6.00E+11	0	4600	Atkinson
67.	$\text{CCl}_4 + \text{O} = \text{CCl}_3 + \text{ClO}$	3.00E+11	0	4400	Herron
68.	$\text{C}_2\text{HCl}_5 + \text{OH} = \text{C}_2\text{Cl}_5 + \text{H}_2\text{O}$	4.00E+11	0	600	Won
69.	$\text{C}_2\text{HCl}_5 + \text{O} = \text{C}_2\text{Cl}_5 + \text{OH}$	1.20E+12	0	2500	Won
70.	$\text{C}_2\text{HCl}_5 + \text{O}_2 = \text{C}_2\text{Cl}_5 + \text{HO}_2$	1.00E+12	0	45500	Won
71.	$\text{C}_2\text{HCl}_5 + \text{HO}_2 = \text{C}_2\text{Cl}_5 + \text{H}_2\text{O}_2$	7.40E+09	0	10500	Won
72.	$\text{C}_2\text{HCl}_3 + \text{OH} = \text{C}_2\text{Cl}_3 + \text{H}_2\text{O}$	3.30E+12	0	5800	Won
73.	$\text{C}_2\text{HCl}_3 + \text{O}_2 = \text{C}_2\text{Cl}_3 + \text{HO}_2$	2.30E+12	0	61900	Won
74.	$\text{CHClO} = \text{CHO} + \text{Cl}$	8.86E+29	-5.1	92920	Ho
75.	$\text{CHClO} = \text{CO} + \text{HCl}$	1.10E+30	-5.2	92960	Ho
76.	$\text{CHClO} + \text{OH} = \text{CClO} + \text{H}_2\text{O}$	7.50E+12	0	1200	Won
77.	$\text{CHClO} + \text{O} = \text{CClO} + \text{OH}$	8.80E+12	0	3500	Won
78.	$\text{CHClO} + \text{O}_2 = \text{CClO} + \text{HO}_2$	4.50E+12	0	41800	Won
79.	$\text{CHClO} + \text{Cl} = \text{CClO} + \text{HCl}$	2.40E+13	0	500	Won
80.	$\text{CHClO} + \text{ClO} = \text{CClO} + \text{HOCl}$	3.00E+11	0	7000	DeMore
81.	$\text{CCl}_2\text{O} + \text{OH} = \text{CClO} + \text{HOCl}$	1.00E+13	0	15000	Chang
82.	$\text{CCl}_2\text{O} + \text{O} = \text{CClO} + \text{ClO}$	2.00E+13	0	17000	Won
83.	$\text{CCl}_2\text{O} + \text{H} = \text{CClO} + \text{HCl}$	5.00E+13	0	6350	Won
84.	$\text{CClO} + \text{Cl}_2 = \text{CCl}_2\text{O} + \text{Cl}$	7.00E+12	0	2960	est.
85.	$\text{CHO} = \text{CO} + \text{H}$	2.50E+14	0	16700	Warnatz
86.	$\text{CHO} + \text{OH} = \text{CO} + \text{H}_2\text{O}$	5.00E+13	0	0	Warnatz
87.	$\text{CHO} + \text{O} = \text{CO} + \text{OH}$	3.00E+13	0	0	Warnatz
88.	$\text{CHO} + \text{O}_2 = \text{CO} + \text{HO}_2$	3.00E+13	0	0	Warnatz
89.	$\text{CHO} + \text{HO}_2 = \text{CO} + \text{H}_2\text{O}_2$	5.00E+12	0	0	Won
90.	$\text{CHO} + \text{Cl} = \text{CO} + \text{HCl}$	1.50E+13	0	0	Won



**Table 7.2 (cont.)** Detailed mechanism for Chloroform Oxidation in Ar Bath (Model B)

<i>REACTIONS CONSIDERED</i>		<i>A</i>	<i>n</i>	<i>Ea</i>	<i>Source</i>
		<i>(cc-mol-sec)</i>		<i>(cal/mol)</i>	
91.	CClO=CO+Cl	2.56E+17	-2.6	8560	DISSOC
92.	CClO+OH=CO+HOCl	3.30E+12	0	0	Won
93.	CClO+Cl=CO+Cl <sub>2</sub>	1.50E+19	-2.2	1500	Baulch
94.	CO+OH=CO <sub>2</sub> +H	4.40E+06	1.5	-497	Baulch
95.	CO+O+M=CO <sub>2</sub> +M	6.17E+14	0	3001	Tsang
96.	CO+HO <sub>2</sub> =CO <sub>2</sub> +OH	1.50E+14	0	23500	Warnatz
97.	CO+O <sub>2</sub> =CO <sub>2</sub> +O	2.53E+13	0	47693	Warnatz
98.	CHCl <sub>2</sub> +OH=CHCl <sub>2</sub> OH	7.62E+17	-3	290	Chiang
99.	CHCl <sub>2</sub> +OH=CHClO+HCl	7.84E+15	-0.9	822	Chiang
100.	CHCl <sub>2</sub> +OH=CHClOH+Cl	3.57E+03	2.7	-920	Chiang
101.	CHCl <sub>2</sub> +O <sub>2</sub> =CHCl <sub>2</sub> OO	4.54E+29	-6.3	2450	Chiang
102.	CHCl <sub>2</sub> +O <sub>2</sub> =CHCl <sub>2</sub> O+O	5.82E+00	1.8	31800	Chiang
103.	CHCl <sub>2</sub> +O <sub>2</sub> =CCl <sub>2</sub> O+OH	7.07E+02	2.6	16260	Chiang
104.	CHCl <sub>2</sub> +O <sub>2</sub> =CHClO+ClO	4.77E+02	2.7	1650	Chiang
105.	CHCl <sub>2</sub> OO=CHCl <sub>2</sub> O+O	1.30E+11	-2.4	56890	Chiang
106.	CHCl <sub>2</sub> OO=CHClO+ClO	4.63E+25	-5	27550	Chiang
107.	CHCl <sub>2</sub> OO=CCl <sub>2</sub> O+OH	3.38E+14	-1.9	41080	Chiang
108.	CCl <sub>2</sub> OOH=CCl <sub>2</sub> O+OH	7.37E+12	-1.1	1730	Chiang
109.	CHCl <sub>2</sub> +O=CHCl <sub>2</sub> O	5.76E+09	-0.6	-220	Chiang
110.	CHCl <sub>2</sub> +O=CHClO+Cl	1.76E+13	0	20	Chiang
111.	CHCl <sub>2</sub> +O=CClO+HCl	3.54E+11	0.2	-130	Chiang
112.	CHCl <sub>2</sub> O=CHClO+Cl	4.61E+13	-1.3	1140	Chiang
113.	CHCl <sub>2</sub> +HO <sub>2</sub> =CHCl <sub>2</sub> OOH	5.29E+16	-6.2	2300	Chiang
114.	CHCl <sub>2</sub> +HO <sub>2</sub> =CHCl <sub>2</sub> O+OH	2.40E+01	-0.2	290	Chiang
115.	CHCl <sub>2</sub> +HO <sub>2</sub> =CCl <sub>2</sub> O+H <sub>2</sub> O	3.50E+01	-1	690	Chiang
116.	CHCl <sub>2</sub> +ClO=CHCl <sub>2</sub> OCl	1.27E+19	-3.4	120	Chiang
117.	CHCl <sub>2</sub> +ClO=CHCl <sub>2</sub> O+Cl	7.77E+11	0.2	370	Chiang
118.	CHCl <sub>2</sub> +ClO=CCl <sub>2</sub> O+HCl	7.07E+17	-1.8	1380	Chiang
119.	CCl <sub>2</sub> +OH=CCl <sub>2</sub> OH	1.41E+04	1.4	-1590	QRRK
120.	CCl <sub>2</sub> +OH=CCl <sub>2</sub> O+H	2.35E+13	-0.2	110	QRRK

**Table 7.2** (cont.) Detailed mechanism for Chloroform Oxidation in Ar Bath (Model B)

<i>REACTIONS CONSIDERED</i>	<i>A</i> ( <i>cc-mol-sec</i> )	<i>n</i>	<i>Ea</i> ( <i>cal/mol</i> )	<i>Source</i>
121. $\text{CCl}_2 + \text{OH} = \text{CClO} + \text{HCl}$	1.35E+15	2	-1100	QRRK
122. $\text{CCl}_2 + \text{OH} = \text{CHCl}_2\text{O}$	4.47E-11	4.6	-2950	QRRK
123. $\text{CCl}_2 + \text{OH} = \text{CHClO} + \text{Cl}$	8.73E-03	3.8	-2040	QRRK
124. $\text{CCl}_2\text{OH} = \text{CCl}_2\text{O} + \text{H}$	2.26E+13	-1.3	2200	DISSOC
125. $\text{CCl}_2\text{OH} = \text{CClO} + \text{HCl}$	1.17E+05	1.2	19420	DISSOC
126. $\text{CCl}_2\text{OH} = \text{CHClO} + \text{Cl}$	6.18E+04	1.2	43220	DISSOC
127. $\text{CCl}_2 + \text{O}_2 = \text{CCl}_2\text{OO}$	1.23E+05	1.1	23799	QRRK
128. $\text{CCl}_2 + \text{O}_2 = \text{CCl}_2\text{O} + \text{O}$	1.11E+14	-0.7	25548	QRRK
129. $\text{CCl}_2 + \text{O}_2 = \text{CClO} + \text{ClO}$	5.45E-01	3.5	30581	QRRK
130. $\text{CCl}_2\text{OO} = \text{CCl}_2\text{O} + \text{O}$	6.84E+13	-1.4	2552	DISSOC
131. $\text{CCl}_2\text{OO} = \text{CClO} + \text{ClO}$	4.36E+06	1	27439	DISSOC
132. $\text{CCl}_2 + \text{O} = \text{CCl}_2\text{O}$	2.34E+17	-3	860	QRRK
133. $\text{CCl}_2 + \text{O} = \text{CClO} + \text{Cl}$	1.37E+14	-1.3	510	QRRK
134. $\text{CCl}_2\text{O} = \text{CClO} + \text{Cl}$	1.09E+28	-6.3	78520	DISSOC
135. $\text{CCl}_2 + \text{HO}_2 = \text{CCl}_2\text{OOH}$	4.89E-01	3	-1290	QRRK
136. $\text{CCl}_2 + \text{HO}_2 = \text{CCl}_2\text{O} + \text{OH}$	2.87E+13	-0.2	140	QRRK
137. $\text{CCl}_3 + \text{OH} = \text{CCl}_3\text{OH}$	9.13E+09	0	-5500	QRRK
138. $\text{CCl}_3 + \text{OH} = \text{CCl}_2\text{O} + \text{HCl}$	1.62E+13	0	-300	QRRK
139. $\text{CCl}_3 + \text{OH} = \text{CCl}_2\text{OH} + \text{Cl}$	8.65E+12	0	4300	QRRK
140. $\text{CHClOCCl}_2 = \text{CCl}_2 + \text{CHClO}$	1.72E+17	-2.4	5320	DISSOC
141. $\text{CHClCCl}_2\text{O} = \text{CCl}_2\text{O} + \text{CHCl}$	1.92E+17	-2.4	5380	DISSOC
142. $\text{CCl}_2\text{CCl}_2\text{O} = \text{CCl}_2\text{O} + \text{CCl}_2$	2.54E+16	-2.1	4780	DISSOC
143. $\text{CCl}_3 + \text{O}_2 = \text{CCl}_3\text{OO}$	1.31E+24	-4.6	1283	QRRK
144. $\text{CCl}_3 + \text{O}_2 = \text{CCl}_3\text{O} + \text{O}$	4.36E+06	1	38050	QRRK
145. $\text{CCl}_3 + \text{O}_2 = \text{CCl}_2\text{O} + \text{ClO}$	2.80E+03	2.5	9009	QRRK
146. $\text{CCl}_3\text{OO} = \text{CCl}_3\text{O} + \text{O}$	1.62E+09	-0.8	55877	DISSOC
147. $\text{CCl}_3\text{OO} = \text{CCl}_2\text{O} + \text{ClO}$	1.99E+14	-1.6	27674	DISSOC
148. $\text{CCl}_3 + \text{O} = \text{CCl}_3\text{O}$	6.07E+06	1.2	-470	QRRK
149. $\text{CCl}_3 + \text{O} = \text{CCl}_2\text{O} + \text{Cl}$	6.19E+13	-0.2	130	QRRK
150. $\text{CCl}_3\text{O} = \text{CCl}_2\text{O} + \text{Cl}$	8.09E12	-1.06	1510	DISSOC

**Table 7.2** (cont.) Detailed mechanism for Chloroform Oxidation in Ar Bath (Model B)

<i>REACTIONS CONSIDERED</i>	<i>A</i> ( <i>cc-mol-sec</i> )	<i>n</i>	<i>Ea</i> ( <i>cal/mol</i> )	<i>Source</i>
151. $\text{CCl}_3 + \text{HO}_2 = \text{CCl}_3\text{OOH}$	5.50E+07	0	-8600	Won
152. $\text{CCl}_3 + \text{HO}_2 = \text{CCl}_3\text{O} + \text{OH}$	5.81E+12	0	-100	Won
153. $\text{C}_2\text{HCl}_3 + \text{OH} = \text{CHClCCl}_2\text{OH}$	1.24E+09	0	-7800	Won
154. $\text{C}_2\text{HCl}_3 + \text{OH} = \text{CHClCClOH} + \text{Cl}$	4.69E+11	0	800	Won
155. $\text{C}_2\text{HCl}_3 + \text{OH} = \text{CH}_2\text{ClCCl}_2\text{O}$	4.09E+04	0	6900	Won
156. $\text{C}_2\text{HCl}_3 + \text{OH} = \text{CH}_2\text{ClCClO} + \text{Cl}$	2.01E+09	0	10300	Won
157. $\text{C}_2\text{HCl}_3 + \text{OH} = \text{CH}_2\text{Cl} + \text{CCl}_2\text{O}$	2.43E+10	0	11400	Won
158. $\text{C}_2\text{HCl}_3 + \text{O} = \text{C}_2\text{Cl}_3 + \text{OH}$	6.02E+07	0	7190	est.
159. $\text{C}_2\text{Cl}_4 + \text{ClO} = \text{CCl}_2\text{CClO} + \text{Cl}_2$	4.00E+13	0	21000	est.
160. $\text{C}_2\text{Cl}_4 + \text{O}_2 = \text{C}_2\text{Cl}_3 + \text{ClOO}$	4.22E+13	0	81400	est.
161. $\text{ClOO} = \text{Cl} + \text{O}_2$	1.26E+13	-1.3	3130	DISSOC
162. $\text{C}_2\text{Cl}_4 + \text{OH} = \text{CCl}_2\text{CCl}_2\text{OH}$	2.17E+09	0	-5800	Won
163. $\text{C}_2\text{Cl}_4 + \text{OH} = \text{CCl}_2\text{CClOH} + \text{Cl}$	5.70E+12	0	2500	Won
164. $\text{C}_2\text{Cl}_4 + \text{OH} = \text{CHCl}_2\text{CCl}_2\text{O}$	8.84E+04	0	9300	Won
165. $\text{C}_2\text{Cl}_4 + \text{OH} = \text{CHCl}_2 + \text{CCl}_2\text{O}$	9.18E+10	0	13800	Won
166. $\text{C}_2\text{Cl}_4 + \text{OH} = \text{CHCl}_2\text{CClO} + \text{Cl}$	1.88E+09	0	12700	Won
167. $\text{C}_2\text{Cl}_4 + \text{OH} = \text{C}_2\text{Cl}_3 + \text{HOCl}$	3.00E+11	0	6400	Won
168. $\text{C}_2\text{Cl}_4 + \text{O} = \text{CCl}_2\text{CCl}_2\text{O}$	5.36E+11	-1.9	3999	QRRK.
169. $\text{C}_2\text{Cl}_4 + \text{O} = \text{CCl}_2 + \text{CCl}_2\text{O}$	4.74E+29	-6.3	8077	QRRK
170. $\text{C}_2\text{Cl}_4 + \text{O} = \text{CCl}_2\text{CClO} + \text{Cl}$	4.78E+12	-0.25	5276	QRRK
171. $\text{CCl}_2\text{CCl}_2\text{O} = \text{CCl}_2 + \text{CCl}_2\text{O}$	5.76E+29	-6.5	8351	DISSOC
172. $\text{CCl}_2\text{CCl}_2\text{O} = \text{CCl}_2\text{CClO} + \text{Cl}$	8.05E+25	-4.4	21814	DISSOC
173. $\text{CCl}_2\text{CClOH} + \text{OH} = \text{CCl}_2\text{CClO} + \text{H}_2\text{O}$	1.00E+13	0	1697	est.
174. $\text{CCl}_2\text{CClOH} + \text{Cl} = \text{CCl}_2\text{CClO} + \text{HCl}$	1.25E+13	0	3900	est.
175. $\text{CCl}_2\text{CClO} = \text{CCl}_2\text{CO} + \text{Cl}$	2.86E+13	0	1000	est.
176. $\text{CCl}_2\text{CO} + \text{OH} = \text{CCl}_2\text{O} + \text{CHO}$	6.00E+12	0	2300	est.
177. $\text{CCl}_2\text{CO} + \text{O} = \text{CClO} + \text{CClO}$	3.00E+11	0	0	est.
178. $\text{CCl}_2\text{CO} = \text{CCl}_2 + \text{CO}$	3.00E+14	0	47230	est.
179. $\text{C}_2\text{Cl}_3 + \text{O}_2 = \text{CCl}_2\text{O} + \text{CClO}$	1.21E+12	0	-829	Russel
180. $\text{CHCCl}_2 + \text{O}_2 = \text{CCl}_2\text{O} + \text{CHO}$	3.06E+12	0	-600	Russel

**Table 7.2** (cont.) Detailed mechanism for Chloroform Oxidation in Ar Bath (Model B)

<i>REACTIONS CONSIDERED</i>		<i>A</i>	<i>n</i>	<i>Ea</i>	<i>Source</i>
		<i>(cc-mol-sec)</i>		<i>(cal/mol)</i>	
181.	CHCl <sub>3</sub> +O <sub>2</sub> =CHClO+CClO	3.06E+12	0	-600	Russel
182.	CHCl <sub>2</sub> O+M=CHClO+Cl+M	1.59E+15	0	1500	Won
183.	O <sub>2</sub> +M=O+O+M	1.20E+14	0	107552	Tsang
184.	H+O <sub>2</sub> +M=HO <sub>2</sub> +M	6.42E+18	-1	0	Tsang
185.	H+O <sub>2</sub> =OH+O	1.69E+17	-0.9	17388	Tsang
186.	O+H <sub>2</sub> O=OH+OH	4.58E+09	1.3	17100	Tsang
187.	H+OH+M=H <sub>2</sub> O+M	7.50E+23	-2.6	0	Miller
188.	O+HO <sub>2</sub> =OH+O <sub>2</sub>	1.75E+13	0	-397	Tsang
189.	OH+HO <sub>2</sub> =H <sub>2</sub> O+O <sub>2</sub>	1.45E+16	-1	0	Tsang
190.	H+O+M=OH+M	4.71E+18	-1	0	Tsang
191.	H <sub>2</sub> O <sub>2</sub> =2OH	1.20E+17	0	45200	Warnatz
192.	HCl+O=OH+Cl	6.03E+12	0	6600	DeMore
193.	OH+HCl=H <sub>2</sub> O+Cl	1.45E+12	0	656	Atkinson
194.	HOCl+O=OH+ClO	6.03E+12	0	4400	DeMore
195.	Cl <sub>2</sub> +OH=Cl+HOCl	8.43E+11	0	1788	DeMore
196.	Cl+HO <sub>2</sub> =HCl+O <sub>2</sub>	1.08E+13	0	100	DeMore
197.	Cl+HO <sub>2</sub> =OH+ClO	2.42E+13	0	2300	DeMore
198.	Cl+O <sub>2</sub> =ClO+O	8.77E+14	0	55000	Baulch
199.	ClO+Cl=O+Cl <sub>2</sub>	1.05E+12	0	9200	DeMore
200.	OH+HOCl=H <sub>2</sub> O+ClO	1.81E+12	0	990	DeMore
201.	HOCl+M=OH+Cl+M	1.76E+20	-3	56720	Ho
202.	ClO+M=Cl+O+M	1.07E+16	0	63460	est.

\* rate constant  $k = A T^n \exp(-E_a/RT)$

Note:

Cohen Cohen, N. and Westberg, K. R., *J. Phys. Chem. Ref. Data* **1991**, *20*, 1211.

Herron Herron, J. T., *J. Phys. Chem. Ref. Data* **1988**, *17*, 967.

Atkinson Atkinson *et al.*, *J. Phys. Chem. Ref. Data* **1989**, *18*, 881.

Ho Ho, W. P., Barat, R. B. and Bozzelli, J. W., *24th Symposium (International) on Combustion (Proc.)* **1992**, 743, The Combustion Institute, PA.

DeMore DeMore, W. B. *et al.*, 'Chemical Kinetics and Photochemical Data for Use in Stratospheric Modeling', NASA Jet Propulsion Laboratory, 1990.

Chang Chang, M. D., Kara, S. B. and Senken, S. M., *Combustion and Flame* **1986**, *49*, 107.

Warnatz Warnatz, J. in 'Combustion Chemistry' (Ed. Gardiner, Jr., W. C.), Springer-Verlag, New York, 1984.

Baulch Baulch *et al.*, *J. Phys. Chem. Ref. Data* **1992**, *21*, 411.

Russel Russell *et al.*, *J. Phys. Chem.* **1989**, *93*, 1934.

Tsang Tsan, W. and Hampson, R. F., *J. Phys. Chem. Ref. Data*, **1986**, *15*, 1087.

Won, DISSOC, QRRK, Chiang, est. : see note of Table 7.1.

**Table 7.A.1** Input Parameters for QRRK Calculation:  $\text{CHCl}_3$  Decomposition  
(Temperature = 250-2000 K)

	<i>reaction</i>	<i>A</i> ( <i>s<sup>-1</sup></i> )	<i>Ea</i> ( <i>kcal/mol</i> )
$k_1$	$\text{CHCl}_3 \rightarrow \text{CCl}_2 + \text{HCl}$	7.18E14	57.51
$k_2$	$\text{CHCl}_3 \rightarrow \text{CHCl}_2 + \text{Cl}$	4.47E16	74.92
$k_3$	$\text{CHCl}_3 \rightarrow \text{CCl}_3 + \text{H}$	3.22E15	94.69

Geometric mean frequency (from CPFIT, ref. A1):

$\langle \nu \rangle$  293.5  $\text{cm}^{-1}$  (x 3.57), 994.8  $\text{cm}^{-1}$  (x 4.42), 3050.2  $\text{cm}^{-1}$  (x 1.01).

Lennard-Jones parameters:  $\sigma = 5.176 \text{ \AA}$ ,  $e/k = 357.0 \text{ K}$

- $k_1$   $A_1$  from transition state study (TST) using PM3 MO calculations.  $E_a$ , best fit of experimental data.
- $k_2$  Via  $k_2$  and Microscopic Reversibility (MR),  $E_a = \Delta H_{\text{rxn}} - RT_m$
- $k_{-2}$   $A_{-2} = 1.05\text{E}14$  from trend of Arrhenius parameters for Cl + methyl and chloromethyl radical recombination (literature review) (literature review, ref. A2).  $E_{a,2} = 0$ .
- $k_3$  Via  $k_3$  and MR,  $E_a = \Delta H_{\text{rxn}} - RT_m$
- $k_{-3}$   $A_{-3} = 1.20\text{E}14$ , estimated from trend of Arrhenius parameters for H + methyl and chloromethyl radical recombination (literature review). (literature review, ref. A2)  $E_{a,3} = 0$ .
- $\sigma$ ,  $e/k$  Calculated from critical properties (ref. A3)

**Table 7.A.2** Input Parameters for QRRK Calculation:  $\text{CCl}_2 + \text{CHCl}_3 \rightarrow \text{Products}$   
(Temperature = 250-2000 K)

	<i>reaction</i>	<i>A</i> ( <i>s<sup>-1</sup> or cc·mol<sup>-1</sup>·s</i> )	<i>Ea</i> ( <i>kcal/mol</i> )
$k_1$	$\text{CCl}_2 + \text{CHCl}_3 \rightarrow \text{C}_2\text{HCl}_5$	3.03E10	1.80
$k_{-1}$	$\text{C}_2\text{HCl}_5 \rightarrow \text{CCl}_2 + \text{CHCl}_3$	1.60E14	63.6
$k_2$	$\text{C}_2\text{HCl}_5 \rightarrow \text{HCl} + \text{C}_2\text{Cl}_4$	3.00E13	48.6
$k_3$	$\text{C}_2\text{HCl}_5 \rightarrow \text{Cl} + \text{C}_2\text{HCl}_4$	2.51E16	66.62

Geometric mean frequency (from CPFIT, ref. A1):

$\langle \nu \rangle$  394.7  $\text{cm}^{-1}$  (x 8.74), 401.5  $\text{cm}^{-1}$  (x 3.66), 1298.4  $\text{cm}^{-1}$  (x 5.10).

Lennard-Jones parameters:  $\sigma = 6.14 \text{ \AA}$ ,  $e/k = 556.0 \text{ K}$

- $k_1$  Via  $k_1$  and MR,  $E_{a,1}$ , estimated in this work.
- $k_{-1}$   $A_{-1}$  from transition state (TS) study using PM3.  $E_{a,1} = \Delta H_{\text{rxn}} + E_{a,1}$
- $k_2$   $A_2$  from TS study using PM3.  $E_{a,2}$  estimated from  $\Delta H_{\text{rxn}} + 40$ .
- $k_3$  Via  $k_3$  and MR,  $E_a = \Delta H_{\text{rxn}} - RT_m$
- $k_{-3}$   $A_{-3} = 6.5\text{E}13$ , estimated from trend of Arrhenius parameters for Cl + chloroalkene additions (literature review, ref. A2).  $E_{a,3} = 0$ .
- $\sigma$ ,  $e/k$  Calculated from critical properties (ref. A3)

**Table 7.A.3** Input Parameters for QRRK Calculation:  $\text{CCl}_2 + \text{CCl}_2 \rightarrow \text{Products}$   
(Temperature = 250-2000 K)

	<i>reaction</i>	<i>A</i> ( <i>s<sup>-1</sup> or cc/mol-s</i> )	<i>Ea</i> ( <i>kcal/mol</i> )
$k_1$	$\text{CCl}_2 + \text{CCl}_2 \rightarrow \text{C}_2\text{Cl}_4$	2.50E11	1.60
$k_{-1}$	$\text{C}_2\text{Cl}_4 \rightarrow \text{CCl}_2 + \text{CCl}_2$	8.25E15	109.0
$k_2$	$\text{C}_2\text{Cl}_4 \rightarrow \text{Cl} + \text{C}_2\text{Cl}_3$	5.70E15	83.74

Geometric mean frequency (from CPFIT, ref. A1):

$\langle \nu \rangle$  250.1  $\text{cm}^{-1}$  (x 7.19), 1033.6  $\text{cm}^{-1}$  (x 3.66), 1296.0  $\text{cm}^{-1}$  (x 1.15).

Lennard-Jones parameters:  $\sigma = 5.64 \text{ \AA}$ ,  $e/k = 541.9 \text{ K}$

$k_1$  Taken from  $\text{CF}_2 + \text{CF}_2 = \text{C}_2\text{F}_4$ , (ref. A4)

$k_{-1}$  Via  $k_1$  and MR.  $E_{a,1} = \Delta H_{\text{rxn}} + E_{a1}$

$k_2$  Via  $k_{-2}$  and MR.  $E_a = \Delta H_{\text{rxn}} - RT_m$

$k_{-2}$   $A_{-2} = 7.29\text{E}12$ , estimated from trend of Arrhenius parameters for Cl + chloroalkyl radical recombination (literature review, ref. A2).  $E_{a,3} = 0$ .

$\sigma$ ,  $e/k$  Calculated from critical properties (ref. A3)

**Table 7.A.4** Input Parameters for QRRK Calculation:  $\text{CCl}_2 + \text{CCl}_3 \rightarrow \text{Products}$   
(Temperature = 250-2000 K)

	<i>reaction</i>	<i>A</i> ( <i>s<sup>-1</sup> or cc/mol-s</i> )	<i>Ea</i> ( <i>kcal/mol</i> )
$k_1$	$\text{CCl}_2 + \text{CCl}_3 \rightarrow \text{C}_2\text{Cl}_5$	3.20E12	0.00
$k_{-1}$	$\text{C}_2\text{Cl}_5 \rightarrow \text{CCl}_2 + \text{CCl}_3$	5.76E15	60.59
$k_2$	$\text{C}_2\text{Cl}_5 \rightarrow \text{Cl} + \text{C}_2\text{Cl}_4$	6.21E12	18.50

Geometric mean frequency (from CPFIT, ref. A1):

$\langle \nu \rangle$  250.0  $\text{cm}^{-1}$  (x 9.62), 943.7  $\text{cm}^{-1}$  (x 4.57), 2218.6  $\text{cm}^{-1}$  (x 0.81).

Lennard-Jones parameters:  $\sigma = 6.14 \text{ \AA}$ ,  $e/k = 556.0 \text{ K}$

$k_1$   $A_1$  estimated from the trend of Arrhenius parameters for  $\text{CCl}_3 + \text{radicals}$  (literature review).  $E_{a1} = 0$ .

$k_{-1}$  Via  $k_1$  and MR.  $E_a = \Delta H_{\text{rxn}} - RT_m$

$k_2$  Via  $k_{-2}$  and MR.  $E_a = \Delta H_{\text{rxn}} - RT_m$

$k_{-2}$   $A_{-2} = 3.16\text{E}12$ ,  $E_{a,2} = 0.5$ , taken from Kerr and Moss (ref. A5).

$\sigma$ ,  $e/k$  Calculated from critical properties for  $\text{C}_2\text{HCl}_5$  (ref. A3)

**Table 7.A.5** Input Parameters for QRRK Calculation:  $\text{CCl}_3 + \text{CCl}_3 \rightarrow \text{Products}$   
(Temperature = 250-2000 K)

	<i>reaction</i>	<i>A</i> ( <i>s<sup>-1</sup> or cc/mol-s</i> )	<i>Ea</i> ( <i>kcal/mol</i> )
$k_1$	$\text{CCl}_3 + \text{CCl}_3 \rightarrow \text{C}_2\text{Cl}_6$	2.90E12	0.00
$k_{-1}$	$\text{C}_2\text{Cl}_6 \rightarrow \text{CCl}_3 + \text{CCl}_3$	2.37E17	69.97
$k_2$	$\text{C}_2\text{Cl}_6 \rightarrow \text{Cl}_2 + \text{C}_2\text{Cl}_4$	5.35E12	64.00
$k_3$	$\text{C}_2\text{Cl}_6 \rightarrow \text{Cl} + \text{C}_2\text{Cl}_5$	1.00E16	68.12

Geometric mean frequency (from CPFIT, ref. A1):

$\langle \nu \rangle$  250.0  $\text{cm}^{-1}$  (x 9.63), 1186.1  $\text{cm}^{-1}$  (x 6.62), 1604.2  $\text{cm}^{-1}$  (x 1.75).

Lennard-Jones parameters:  $\sigma = 6.45 \text{ \AA}$ ,  $e/k = 554.4 \text{ K}$

- $k_1$   $A_1$  estimated from the trend of Arrhenius parameters for  $\text{CCl}_3 + \text{radicals}$  (literature review).  $E_{a1}=0$ .
- $k_{-1}$  Via  $k_1$  and MR.  $E_a = \Delta H_{\text{rxn}} - RT_m$
- $k_2$   $A_2$ , estimated using TST.  $E_{a2}$ , evaluated from  $\text{H}_2$  and  $\text{HCl}$  elimination of chloroethane species (literature review).
- $k_3$  Via  $k_3$  and MR.  $E_a = \Delta H_{\text{rxn}} - RT_m$
- $k_{-3}$   $A_{-3} = 6.5\text{E}12$ , estimated from trend of Arrhenius parameters for  $\text{Cl} + \text{chloroethyl radical}$  recombination (literature review, ref. A2).  $E_{a,-3}=0$ .
- $\sigma$ ,  $e/k$  Calculated from critical properties. (ref. A3)

**Table 7.A.6** Input Parameters for QRRK Calculation:  $\text{CCl}_2 + \text{O}_2 \rightarrow \text{Products}$   
(Temperature = 250-2000 K)

	<i>reaction</i>	<i>A</i> ( <i>s<sup>-1</sup> or cc/mol-s</i> )	<i>Ea</i> ( <i>kcal/mol</i> )
$k_1$	$\text{CCl}_2 + \text{O}_2 \rightarrow \text{CCl}_2\text{OO}$	1.00E12	14.0
$k_{-1}$	$\text{CCl}_2\text{OO} \rightarrow \text{CCl}_2 + \text{O}_2$	2.48E14	28.4
$k_2$	$\text{CCl}_2\text{OO} \rightarrow \text{CCl}_2\text{O} + \text{O}$	6.75E13	3.5
$k_3$	$\text{CCl}_2\text{OO} \rightarrow \text{CClO} + \text{ClO}$	2.10E13	28.6

Geometric mean frequency (from CPFIT, ref. A1):

$\langle \nu \rangle$  313.7  $\text{cm}^{-1}$  (x 5.38), 998.9  $\text{cm}^{-1}$  (x 3.41), 1835.8  $\text{cm}^{-1}$  (x 0.21).

Lennard-Jones parameters:  $\sigma = 5.486 \text{ \AA}$ ,  $e/k = 677.3 \text{ K}$

- $k_1$   $A_1$  estimated from the trend of Arrhenius parameters for  $\text{O}_2 + \text{radical additions}$  (literature review).  $E_{a1}=14$ , best fit of experimental data in this study.
- $k_{-1}$  Via  $k_1$  and MR.  $E_a = \Delta H_{\text{rxn}} + E_{a1}$
- $k_2$   $A_2$  via  $A_{-2}$  and MR.  $E_{a2}$  estimated in this work.
- $k_{-2}$   $A_{-2}=3.50\text{E}12$  taken from  $\text{CH}_2\text{O} + \text{O}$  (ref. A6)
- $k_3$   $A_3$  estimated using TST,  $E_{a3}$  estimated in this study.
- $\sigma$ ,  $e/k$  Calculated from critical properties for  $\text{CHCl}_2\text{OOH}$  (Lydersen method by Won, ref. A7)

**Table 7.A.7** Input Parameters for QRRK Calculation:  $\text{CCl}_2 + \text{O} \rightarrow \text{Products}$   
(Temperature = 250-2000 K)

	<i>reaction</i>	<i>A</i> ( <i>s<sup>-1</sup> or cc/mol-s</i> )	<i>Ea</i> ( <i>kcal/mol</i> )
$k_1$	$\text{CCl}_2 + \text{O} \rightarrow \text{CCl}_2\text{O}$	1.00E13	0.0
$k_{-1}$	$\text{CCl}_2\text{O} \rightarrow \text{CCl}_2 + \text{O}$	1.15E16	163.1
$k_2$	$\text{CCl}_2\text{O} \rightarrow \text{CClO} + \text{Cl}$	2.00E14	75.7
$k_3$	$\text{CCl}_2\text{O} \rightarrow \text{CO} + \text{Cl}_2$	2.07E14	60.7

Geometric mean frequency (from CPFIT, A1):

$\langle \nu \rangle$  480.9  $\text{cm}^{-1}$  (x 4.96), 1899.0  $\text{cm}^{-1}$  (x 0.68), 2029.3  $\text{cm}^{-1}$  (x 0.36).

Lennard-Jones parameters:  $\sigma = 4.70 \text{ \AA}$ ,  $\epsilon/k = 376.0 \text{ K}$

$k_1$   $A_1$  estimated from  $\text{CF}_2 + \text{O}$  recombination (ref. A8).

$k_{-1}$  Via  $k_1$  and MR.  $E_a = \Delta H_{\text{rxn}} - RT_m$

$k_2$  Via  $k_{-2}$  and MR.  $E_a = \Delta H_{\text{rxn}} - RT_m$ .

$k_{-2}$   $A_{-2} = 1.0\text{E}14$  estimated in this work.  $E_{a,-2} = 0$ .

$k_3$   $A_3$  estimated using TST.  $E_{a3}$  evaluated from enthalpy of TS using PM3 MO calculations.

$\sigma$ ,  $\epsilon/k$  Calculated from critical properties (Won, ref. A7)

**Table 7.A.8** Input Parameters for QRRK Calculation:  $\text{CCl}_2 + \text{OH} \rightarrow \text{Products}$   
(Temperature = 250-2000 K)

	<i>reaction</i>	<i>A</i> ( <i>s<sup>-1</sup> or cc/mol-s</i> )	<i>Ea</i> ( <i>kcal/mol</i> )
$k_1$	$\text{CCl}_2 + \text{OH} \rightarrow \text{CCl}_2\text{OH}$	8.17E12	0.0
$k_{-1}$	$\text{CCl}_2\text{OH} \rightarrow \text{CCl}_2 + \text{OH}$	3.41E15	66.6
$k_2$	$\text{CCl}_2\text{OH} \rightarrow \text{CCl}_2\text{O} + \text{H}$	2.46E13	2.4
$k_3$	$\text{CCl}_2\text{OH} \rightarrow \text{CClO} + \text{HCl}$	6.10E12	20.8
$k_4$	$\text{CCl}_2\text{OH} \rightarrow \text{CHCl}_2\text{O}$	6.10E12	44.6
$k_5$	$\text{CHCl}_2\text{O} \rightarrow \text{CHClO} + \text{Cl}$	1.10E15	0.5

Geometric mean frequency (from CPFIT, ref. A1):

$\langle \nu \rangle$  391.6  $\text{cm}^{-1}$  (x 4.41), 944.9  $\text{cm}^{-1}$  (x 4.08), 3989.9  $\text{cm}^{-1}$  (x 0.51).

Lennard-Jones parameters:  $\sigma = 4.70 \text{ \AA}$ ,  $\epsilon/k = 376.0 \text{ K}$

$k_1$   $A_1$  estimated from  $\text{CH}_2 + \text{OH}$  recombination (ref. A9).

$k_{-1}$  Via  $k_1$  and MR.  $E_a = \Delta H_{\text{rxn}} - RT_m$

$k_2$   $A_2$  via  $A_{-2}$  and MR.  $E_{a2} = 2.4$  estimated in this work.

$k_{-2}$   $A_{-2} = 1.23\text{E}13$  taken from  $\text{H} + \text{CH}_3\text{CHO}$  addition (ref. A10)

$k_3$   $A_3$  estimated using TST (loss of one rotor),  $E_{a3}$  evaluated from enthalpy of TS using PM3 MO calculations.

$k_4$   $A_4$  estimated using TST (loss of one rotor),  $E_{a4}$  evaluated from ring strain (27.7) +  $\Delta H_{\text{rxn}}$  (6.6) +  $E_{a\text{abstraction}}$  (10.3) = 44.6 (unit in kcal/mol).

$k_5$   $A_5$  via  $A_{-5}$  and MR.  $E_a = 0.5$  estimated in this work.

$k_{-5}$   $A_{-5} = 2.8\text{E}13$  estimated from  $\text{Cl} + \text{C}_2\text{H}_4$  addition ( $A = 5.6\text{E}13$ , ref. A5).

$\sigma$ ,  $\epsilon/k$  Calculated from critical properties for  $\text{CCl}_2\text{O}$  (Won, ref. A7)



**Table 7.A.9** Input Parameters for QRRK Calculation:  $\text{CCl}_3 + \text{O}_2 \rightarrow \text{Products}$   
(Temperature = 250-2000 K)

	<i>reaction</i>	<i>A</i> ( <i>s</i> <sup>-1</sup> or <i>cc/mol-s</i> )	<i>Ea</i> ( <i>kcal/mol</i> )
$k_1$	$\text{CCl}_3 + \text{O}_2 \rightarrow \text{CCl}_3\text{OO}$	2.17E12	0.0
$k_{-1}$	$\text{CCl}_3\text{OO} \rightarrow \text{CCl}_3 + \text{O}_2$	4.80E14	19.0
$k_2$	$\text{CCl}_3\text{OO} \rightarrow \text{CCl}_3\text{O} + \text{O}$	7.57E14	57.1
$k_3$	$\text{CCl}_3\text{OO} \rightarrow \text{CCl}_2\text{O} + \text{ClO}$	1.10E13	27.8

Geometric mean frequency (from CPFIT, ref. A1):

$\langle \nu \rangle$  287.3  $\text{cm}^{-1}$  (x 5.85), 524.9  $\text{cm}^{-1}$  (x 4.56), 601.3  $\text{cm}^{-1}$  (x 1.59).

Lennard-Jones parameters:  $\sigma = 5.842 \text{ \AA}$ ,  $e/k = 697.2 \text{ K}$

$k_1$   $A_1$  taken from the work of Atkinson *et al.* (ref. A11)

$k_{-1}$  Via  $k_1$  and MR.  $E_a = \Delta H_{\text{rxn}} - RT_m$

$k_2$   $A_2$  via  $A_{-2}$  and MR.  $E_{a2}$  estimated in this work.

$k_{-2}$   $A_{-2} = 1.27\text{E}13$  evaluated from  $\text{CH}_3\text{O} + \text{O}$  ( $A = 1.51\text{E}13$ , ref. A10)

$k_3$   $A_3$  estimated using TST (loss of one rotor).  $E_{a3}$  evaluated from ring strain (17) +  $\Delta H_{\text{rxn}}$  (4.6) +  $E_{a\text{abstraction}}$  (6.2) = 27.8 (unit in kcal/mol).

$\sigma$ ,  $e/k$  Calculated from critical properties for  $\text{CCl}_3\text{OOH}$  (Lydersen method by Won, ref. A7)

**Table 7.A.10** Input Parameters for QRRK Calculation:  $\text{CCl}_3 + \text{O} \rightarrow \text{Products}$   
(Temperature = 250-2000 K)

	<i>reaction</i>	<i>A</i> ( <i>s</i> <sup>-1</sup> or <i>cc/mol-s</i> )	<i>Ea</i> ( <i>kcal/mol</i> )
$k_1$	$\text{CCl}_3 + \text{O} \rightarrow \text{CCl}_3\text{O}$	2.00E13	0.0
$k_{-1}$	$\text{CCl}_3\text{O} \rightarrow \text{CCl}_3 + \text{O}$	1.11E15	77.4
$k_2$	$\text{CCl}_3\text{O} \rightarrow \text{CCl}_2\text{O} + \text{Cl}$	1.04E15	2.0

Geometric mean frequency (from CPFIT, ref. A1):

$\langle \nu \rangle$  100.1  $\text{cm}^{-1}$  (x 3.95), 641.3  $\text{cm}^{-1}$  (x 2.09), 893.7  $\text{cm}^{-1}$  (x 2.96).

Lennard-Jones parameters:  $\sigma = 5.257 \text{ \AA}$ ,  $e/k = 733.8 \text{ K}$

$k_1$   $A_1$  estimated from  $(\text{CH}_3)_3\text{C} + \text{O}$  recombination (ref. A12).

$k_{-1}$  Via  $k_1$  and MR.  $E_a = \Delta H_{\text{rxn}} - RT_m$

$k_2$   $A_2$  via  $A_{-2}$  and MR.  $E_{a2}$  estimated in this work.

$k_{-2}$   $A_{-2} = 1.0\text{E}14$  evaluated from  $(\text{CH}_3)_2\text{C}=\text{CH}_2 + \text{CH}_3$  addition ( $A = 2.23\text{E}11$ , ref. A13).

$\sigma$ ,  $e/k$  Calculated from critical properties for  $\text{CCl}_3\text{OH}$  (Lydersen method by Won, ref. A7)

**Table 7.A.11** Input Parameters for QRRK Calculation:  $C_2Cl_4 + O \rightarrow$  Products  
(Temperature = 250-2000 K)

	<i>reaction</i>	<i>A</i> ( <i>s<sup>-1</sup> or cc/mol-s</i> )	<i>Ea</i> ( <i>kcal/mol</i> )
$k_1$	$C_2Cl_4 + O \rightarrow C_2Cl_4O$	5.90E11	4.5
$k_{-1}$	$C_2Cl_4O \rightarrow C_2Cl_4 + O$	5.49E12	33.6
$k_2$	$C_2Cl_4O \rightarrow CCl_2O + CCl_2$	6.40E13	6.9
$k_3$	$C_2Cl_4O \rightarrow CCl_2CClO + Cl$	1.32E16	20.2

Geometric mean frequency (from CPFIT, ref. A1):

$\langle \nu \rangle$  317.5  $cm^{-1}$  (x 8.05), 510.4  $cm^{-1}$  (x 5.37), 1999.7  $cm^{-1}$  (x 1.58).

Lennard-Jones parameters:  $\sigma = 5.997 \text{ \AA}$ ,  $\epsilon/k = 751.3 \text{ K}$

$k_1$   $A_1$  and  $E_{a1}$  estimated from  $CH_2CCl_2 + O$  addition. (ref. A14)

**Table 8.1** Ideal Gas Phase Thermodynamic Properties  $\Delta H_f^\circ_{298}$  ( kcal/mol),  $S^\circ_{298}$ (cal/mol-K) and  $C_p(T)$ 's (cal/mol-K,  $300 \leq T/K \leq 1000$ )

No.	Species	$\Delta H_f^\circ_{298}$	$S^\circ_{298}$	$C_{p300}$	$C_{p400}$	$C_{p500}$	$C_{p600}$	$C_{p800}$	$C_{p1000}$	Formula
1	Hexadienyl (Tsang)	49.93	73.39	21.51	28.43	35.12	40.55	48.71	54.41	C6 H7
2	Hexadienyl (This)	49.93	73.19	21.86	29.48	35.99	41.26	49.09	54.57	C6 H7
3	1,3-Hexadiene	3.89	72.49	22.66	30.72	37.76	43.56	52.27	58.42	C6 H8
4	Benzene	19.81	64.37	19.92	27.09	33.25	38.38	45.87	51.05	C6 H6
5	Toluene	11.81	76.81	25.06	33.18	40.38	46.44	55.68	62.26	C7 H8
6	I (Benzene-OH)	10.79	84.11	25.51	33.94	40.94	46.17	54.13	59.52	C6 H7 O1
7	II(I <sub>+H</sub> )	-13.73	84.79	26.31	35.18	42.71	48.47	57.31	63.37	C6 H8 O1
8	III (Benzene--OH-O <sub>2</sub> )	-1.2	100.65	32.72	42.33	50.06	55.56	64.08	70.13	C6 H7 O3
9	VI (III <sub>+H</sub> )	-37.3	100.43	34.77	45.17	53.61	59.65	68.8	75.1	C6 H8 O3
10	V	-13.2	87.17	30	40.16	48.58	54.74	63.75	69.65	C6 H7 O3
11	V <sub>-H</sub>	-44.93	87.11	30.36	40.93	49.88	56.6	66.65	73.35	C6 H8 O3
12	VI	3.86	90.28	30.23	40.24	48.53	54.63	63.58	69.49	C6 H7 O3
13	VI <sub>-H</sub>	-42.14	88.1	30.2	40.79	49.75	56.5	66.56	73.27	C6 H8 O3
14	VII	2.1	88.81	30.44	40.65	48.94	55.03	63.95	69.83	C6 H7 O3
15	VII <sub>-H</sub>	-43.9	86.63	30.41	41.2	50.16	56.9	66.93	73.61	C6 H8 O3
16	VIII	12.59	89.55	30.66	40.72	48.97	55.08	64.06	69.98	C7 H7 O3
17	VIII <sub>+H</sub>	-19.14	89.49	31.02	41.49	50.27	56.94	66.96	73.68	C6 H8 O3
18	IX	-32.11	94.19	32.9	44.1	53.27	59.68	69.36	75.52	C6 H7 O4
19	IX <sub>-H</sub>	-84.07	96.65	34.01	45.39	54.83	61.51	71.69	78.28	C6 H8 O4
20	IX <sub>-O</sub>	-32.4	102.97	36.77	48.08	57.23	63.69	73.42	80.11	C6 H7 O5
21	IX <sub>-OH</sub>	-68.5	102.75	38.82	50.92	60.78	67.78	78.14	85.08	C6 H8 O5
22	X	-30.35	94.29	32.69	43.69	52.86	59.28	68.99	75.18	C6 H7 O4
23	X <sub>+H</sub>	-82.31	96.75	33.8	44.98	54.42	61.11	71.32	77.94	C6 H8 O4
24	X <sub>-O</sub>	-30.64	103.07	36.56	47.67	56.82	63.29	73.05	79.77	C6 H7 O5
25	X <sub>+OH</sub>	-66.74	102.85	38.61	50.51	60.37	67.38	77.77	84.74	C6 H8 O5
26	XI	-29.84	114.61	33.6	44.41	53.42	60.3	70.62	77.46	C6 H7 O4
27	XI <sub>+H</sub>	-81.8	117.07	34.71	45.7	54.98	62.13	72.95	80.22	C6 H8 O4
28	XI <sub>-O</sub>	-30.13	123.39	37.47	48.39	57.38	64.31	74.68	82.05	C6 H7 O5
29	XI <sub>-OH</sub>	-66.23	123.17	39.52	51.23	60.93	68.4	79.4	87.02	C6 H8 O5
30	XII (Toluene-OH)	2.34	91.67	31.64	41.36	49.52	55.72	65.3	71.92	C7 H9 O1
31	XII <sub>-H</sub>	-22.18	92.35	32.44	42.60	51.29	58.02	68.48	75.77	C7 H10 O1
32	XIII (Toluene-OH-O <sub>2</sub> )	-9.55	108.37	39.68	49.62	58.23	64.75	73.87	81.72	C7 H9 O3
33	XIII <sub>+H</sub>	-45.65	108.15	41.73	52.46	61.78	68.84	78.59	86.69	C7 H10 O3
34	XIV	-22.8	94.21	35.72	47.55	57.13	64.5	75.16	82.26	C7 H9 O3
35	XIV <sub>+H</sub>	-54.53	94.15	36.08	48.32	58.43	66.36	78.06	85.96	C7 H10 O3
36	XV	-8.73	96.13	35.71	47.94	57.91	65.2	75.78	83.08	C7 H9 O3
37	XV <sub>+H</sub>	-52.93	93.04	36.03	49.2	59.95	67.83	79.22	87.07	C7 H10 O3
38	XVI	-6.35	97.74	36.57	48.07	57.52	64.58	75.12	82.23	C7 H9 O3
39	XVI <sub>+H</sub>	-52.35	95.56	36.54	48.62	58.74	66.45	78.1	86.01	C7 H10 O3
40	XVII	4.14	97.11	36.79	48.14	57.55	64.63	75.23	82.38	C7 H9 O3
41	XVII <sub>+H</sub>	-27.59	97.05	37.15	48.91	58.85	66.49	78.13	86.08	C7 H10 O3
42	XVIII	-41.71	99.86	38.62	51.49	61.82	69.44	80.77	88.13	C7 H9 O4
43	XVIII <sub>-H</sub>	-93.67	102.32	39.73	52.78	63.38	71.27	83.1	90.89	C7 H10 O4

**Table 8.1** (Continued) Ideal Gas Phase Thermodynamic Properties  $\Delta H_f^\circ$  (kcal/mol),  $S^\circ$  (cal/mol-K) and  $C_p(T)$ 's (cal/mol-K,  $300 \leq T/K \leq 1000$ )

No. Species	$\Delta H_f^\circ$ <sub>298</sub>	$S^\circ$ <sub>298</sub>	$C_{p300}$	$C_{p400}$	$C_{p500}$	$C_{p600}$	$C_{p800}$	$C_{p1000}$	Formula
44 XVIII <sub>+O</sub>	-55.01	59.29	51.74	64.68	74.51	80.88	91.22	98.56	C7 H9 O5
45 XVIII <sub>+OH</sub>	-91.11	59.07	53.79	67.52	78.06	84.97	95.94	103.53	C7 H10 O5
46 XIX	-43.57	98.16	39.01	52.6	63.29	70.88	81.8	89.11	C7 H9 O4
47 XIX <sub>+H</sub>	-95.53	100.62	40.12	53.89	64.85	72.71	84.13	91.87	C7 H10 O4
48 XIX <sub>+O</sub>	-43.86	106.94	42.88	56.58	67.25	74.89	85.86	93.7	C7 H9 O5
49 XIX <sub>+OH</sub>	-79.96	106.72	44.93	59.42	70.8	78.98	90.58	98.67	C7 H10 O5
50 XX	-40.56	101.75	39.03	51.52	61.85	69.23	80.53	87.92	C7 H9 O4
51 XX <sub>+H</sub>	-92.52	104.21	40.14	52.81	63.41	71.06	82.86	90.68	C7 H10 O4
52 XX <sub>+O</sub>	-78.75	139.6	47.2	60	70.63	78.47	90.61	99.12	C7 H9 O5
53 XX <sub>+OH</sub>	-114.85	139.38	49.25	62.84	74.18	82.56	95.33	104.09	C7 H10 O5
54 Glyoxal	-50.6	65.42	14.9	17.54	19.64	21.4	24.28	25.8	C2 H2 O2
55 CHOCHOH	-34.6	67.38	15.54	18.62	21.25	23.4	26.66	29	C2 H3 O2
56 CHOCH <sub>2</sub> OH	-73.5	73.57	17.53	20.07	22.34	24.41	28.32	31.01	C2 H4 O2
57 Methylglyoxal	-64.48	76.23	19.1	22.93	26.39	29.37	34.16	37.44	C3 H4 O2
58 CH <sub>3</sub> COCHOH	-46.98	75.72	20.29	24.91	28.92	32.27	37.37	41.18	C3 H5 O2
59 CH <sub>3</sub> COCH <sub>2</sub> OH	-85.88	81.91	22.28	26.36	30.01	33.28	39.03	43.19	C3 H6 O2
60 Butenedial	-53.16	78.18	23.82	29.12	33.14	36.24	40.98	44.02	C4 H4 O2
61 CHOCHCHCHOH	-32.6	82.27	25.01	30.91	35.48	38.96	44.03	47.4	C4 H5 O2
62 CHOCHCHCH <sub>2</sub> OH	-62.65	86.62	25.49	30.95	35.52	39.34	45.38	49.55	C4 H6 O2
63 Methylbutenedial	-63.24	88.99	28.02	34.51	39.89	44.21	50.86	55.66	C5 H6 O2
64 PhOO	37.04	85.62	26.76	34.25	40.07	44.82	51.76	56.48	C6 H5 O2
65 Benzaldehyde	-8.91	84.75	26.82	34.04	40.5	45.9	54.18	59.86	C7 H6 O1
66 PhOOH	0.94	85.4	28.81	37.09	43.62	48.91	56.48	61.45	C6 H6 O2
67 Hexadienedial	-37.6	92.32	30.06	38.52	45.02	49.86	56.98	61.72	C6 H6 O2
68 PHENOH	-28.35	92.28	29.16	38.4	45.89	51.08	59.17	64.45	C6 H7 O2
69 OCHDQH	14.66	97.97	33.66	43.88	52.05	57.82	66.47	72.34	C6 H7 O3
70 OHCHDRQH	-12.78	99.75	33.97	43.93	51.84	57.35	65.62	71.25	C6 H7 O3
71 HDEA1HQH	-5.74	100.92	36.36	46.6	54.25	59.77	67.18	72.56	C6 H7 O3
72 PHENHOH	-52.87	92.96	29.96	39.64	47.66	53.38	62.35	68.3	C6 H8 O2
73 HDEA1H2QH	-35.79	103.89	36.84	46.64	54.29	60.15	68.53	74.71	C6 H8 O3
74 PhCH <sub>2</sub>	48.21	75.63	25.81	33.78	40.51	46.02	54.27	60.08	C7 H7
75 PhCH <sub>2</sub> O	27.97	86.37	27.05	35.4	42.54	48.48	57.46	63.67	C7 H7 O1
76 OMPHOX	4.11	86.86	28.44	36.3	43.27	49.04	57.85	63.95	C7 H7 O1
77 PhCH <sub>2</sub> OO	29.91	96.1	31.29	39.81	47.16	53.17	62.19	68.43	C7 H7 O2
78 PhCH <sub>2</sub> OH	-23.99	88.83	28.16	36.69	44.1	50.31	59.79	66.43	C7 H8 O1
79 o-Cresol	-30.29	85.56	30.02	38.54	45.94	51.97	61.06	67.36	C7 H8 O1
80 PhCH <sub>2</sub> OOH	-6.19	95.88	33.34	42.65	50.71	57.26	66.91	73.4	C7 H8 O2
81 Methylhexadiene- dial	-44.62	100.95	36.19	45.94	53.6	59.41	68.15	74	C7 H8 O2
82 HDEDA1OH	-96.9	98.2	32.38	41.45	48.4	53.48	60.91	65.98	C6 H6 O3

**Table 8.2** Selected HBI Group Values,  $\Delta S^\circ_{298}$  and  $\Delta C_p(T)$  (cal/mol-K) in Use for Thermodynamic Properties of Radicals

	$\Delta S^\circ_{int,298}$	$\Delta C_p^\circ_{300}$	$\Delta C_p^\circ_{400}$	$\Delta C_p^\circ_{500}$	$\Delta C_p^\circ_{600}$	$\Delta C_p^\circ_{800}$	$\Delta C_p^\circ_{1000}$
<i>CHD,</i>	-0.68	-0.8	-1.24	-1.77	-2.3	-3.18	-3.85
<i>CHENE,</i>	2.18	0.03	-0.55	-1.22	-1.87	-2.98	-3.78
<i>CHENEA,</i>	0.06	-0.36	-0.77	-1.3	-1.86	-2.9	-3.7
<i>ALPEROX,</i>	0.22	-2.05	-2.84	-3.55	-4.09	-4.72	-4.97
<i>ALKOXY,</i>	-1.46	-0.98	-1.3	-1.61	-1.89	-2.38	-2.8

**Table 8.3** Input Parameters for QRRK Calculation and the Results of Apparent Rate Constants: Benzene + OH (Temperature=298K)

	<i>reaction</i>	<i>A</i> ( <i>s<sup>-1</sup> or cc.mol-s</i> )	<i>Ea</i> ( <i>kcal mol</i> )
1	Benzene + OH => Benzene-OH	2.29E12	0.68
-1	Benzene-OH => Benzene + OH	7.78E13	17.7
2	Benzene-OH => Phenol + H	3.28E10	18.1

geometric mean frequency (from CPFIT<sup>40</sup>): 741.6 cm<sup>-1</sup> (21.6), 1859.0 cm<sup>-1</sup> (1.63), 2523.0 cm<sup>-1</sup> (12.77).  
Lennard-Jones parameters:  $\sigma = 5.50$  Å,  $\epsilon/k = 450$  K (estimated from Phenol)

$k_1$  Baulch *et al.*, ref. 32.

$k_{-1}$  microscopic reversibility (MR)

$k_2$  The rate constant of reverse reaction:  $A_{-2}$  and  $E_{a,-2}$  is estimated from ref. 33 for  $H + C_6H_6 \rightarrow C_6H_7$ .  $A_{-2} = 3.98E13$  cm<sup>3</sup>/mol.s.  $E_{a,-2} = 4.00$  kcal/mol.  $k_2$  is from MR.

Calculated Apparent Reaction Parameters at  $P = 1$ atm,  $k = AT^n(-Ea RT)$   
(Temperature range: 200K to 2000K)

	<i>reaction</i>	<i>A</i> ( <i>cc mol-s</i> )	<i>n</i>	<i>Ea</i> ( <i>kcal mol</i> )	<i>k<sub>298</sub></i> ( <i>cc mol-s</i> )
1	Benzene + OH => Benzene-OH	3.03E37	-8.42	6.45	7.24E11
2	Benzene + OH => Phenol + H	1.08E17	-1.25	6.59	1.06E09

**Table 8.4** Input Parameters for QRRK Calculation and the Results of Apparent Rate Constants: Benzene-OH + O<sub>2</sub> (Temperature=298K)

	<i>reaction</i>	<i>A</i> ( <i>s<sup>-1</sup> or cc/mol-s</i> )	<i>Ea</i> ( <i>kcal/mol</i> )
1	Benzene-OH + O <sub>2</sub> => Benz-OH-O <sub>2</sub>	1.21E12	0.0
-1	Benz-OH-O <sub>2</sub> => Benzene-OH + O <sub>2</sub>	2.27E14	11.4
2(BA)	Benz-OH-O <sub>2</sub> => 2,4-Hexadien-1,6-dial + OH	4.77E11	19.4
3(BB)	Benz-OH-O <sub>2</sub> => Phenol + HO <sub>2</sub>	2.62E11	15.0
4(BC)	Benz-OH-O <sub>2</sub> => Adduct IX	1.41E11	14.0
5(BD)	Benz-OH-O <sub>2</sub> => Adduct XI	1.76E11	14.0
6(BE)	Benz-OH-O <sub>2</sub> => Adduct X	2.49E11	15.6
7(BF)	Benz-OH-O <sub>2</sub> => Adduct XII	1.69E11	39.6

geometric mean frequency (from CPFIT<sup>40</sup>): 421.8 cm<sup>-1</sup> (13.7), 1261.0 cm<sup>-1</sup> (20.1), 3347.0 cm<sup>-1</sup> (8.2),  
Lennard-Jones parameters:  $\sigma = 5.50 \text{ \AA}$ ,  $\epsilon/k = 450 \text{ K}$  (estimated from Phenol)

$k_1$ : Estimated from regression plot: R. + O<sub>2</sub> by assuming activation energy equal 0.

$k_{-1}$ : MR.

$k_2$ : First step of the H transfer from the OH group to the peroxy group is the rate determining step). see Fig. 8.  $A_2$  is calculated by Transition State at T=298K for H transfer step using PM3/UHF method. and standard parameters in MOPAC 6.0 program package.  $\Delta S^\ddagger_{298} = -10.14 \text{ cal/mol-K}$ .  $Ea_2 = (Ea_{\text{abstraction}}, 7.05) + (\Delta H_{\text{rxn}}, 16.36) - (\Delta H_{\text{hydrogen-bonding}}, 4) = 19.41 \text{ kcal/mol-K}$ .  $Ea_{\text{abstraction}}$  estimated from  $12.5 \text{ kcal/mol} - \Delta H_{\text{rxn}} * 1/3$ . Evans' Polanyi plot. 4 kcal/mol is adapted as an average value of  $\Delta H_{\text{hydrogen-bonding}}$

$k_3$ :  $A_3$ . TS of the H transfer first step, rate determining. see Fig. 9, similar procedure to  $A_2$ .  $Ea_3$ , estimated from  $(Ea_{\text{abstraction}}, 9.4 \text{ kcal/mol}) + (\text{ring strain}, 5.6 \text{ kcal/mol}) = 16.6 \text{ kcal/mol}$ .

$k_4$ ,  $k_5$ ,  $k_6$  &  $k_7$ : The entropies of Transition States of reaction channel 3, 4, 5 & 6 are assumed to be the same as products (from TS study by PM3/UHF,  $S_{\text{vibration}}$  of TS's  $\approx S_{\text{vibration}}$  of product), plus one optical isomer gained at TS's.  $\Delta S^\ddagger_{298} = S_{\text{product}} - S_{\text{reactant}} + R \ln 2$ .  $Ea = (Ea_{\text{addition}}, 5 \text{ kcal/mol}) + (\text{Bicyclic ring strain}) - (1.3 \text{ cyclohexadiene ring strain}, 4.19 \text{ kcal/mol})$ . For ring strain energy of bicyclic adducts, see text.

Calculated Apparent Reaction Parameters at P = 1atm,  $k = AT^n(-Ea/RT)$   
(Temperature range: 200K to 2000K)

	<i>reaction</i>	<i>A</i> ( <i>cc/mol-s</i> )	<i>n</i>	<i>Ea</i> ( <i>kcal/mol</i> )	<i>k<sub>298</sub></i> ( <i>cc/mol-s</i> )
1	Benz-OH + O <sub>2</sub> => Benz-OH-O <sub>2</sub>	3.64E27	-6.25	0.37	6.59E11
2	Benz-OH + O <sub>2</sub> => Hexadienedial + OH	1.03E10	-0.18	8.30	3.09E03
3	Benz-OH + O <sub>2</sub> => Phenol + HO <sub>2</sub>	1.13E09	-0.26	4.05	2.71E06
4	Benz-OH + O <sub>2</sub> => Adduct IX	1.32E10	-0.36	3.22	7.32E06
5	Benz-OH + O <sub>2</sub> => Adduct XI	1.65E10	-0.36	3.22	9.14E06
6	Benz-OH + O <sub>2</sub> => Adduct X	3.91E09	-0.14	4.41	1.05E05
7	Benz-OH + O <sub>2</sub> => Adduct XII	4.99E08	-0.07	28.1	2.00E-12

**Table 8.5** Input Parameters for QRRK Calculation and the Results of Apparent Rate Constants: Toluene + OH (Temperature=298K)

	<i>reaction</i>	<i>A</i> ( <i>s<sup>-1</sup> or cc/mol-s</i> )	<i>Ea</i> ( <i>kcal/mol</i> )
1	Toluene + OH => Toluene-OH	2.29E12	-0.36
-1	Toluene-OH => Toluene + OH	7.58E13	18.96
2	Toluene-OH => <i>o</i> -Cresol + H	2.46E13	23.47

geometric mean frequency (from CPFIT<sup>40</sup>): 584.7 cm<sup>-1</sup> (20.8), 1511.0 cm<sup>-1</sup> (17.8), 3999.0 cm<sup>-1</sup> (5.4).

Lennard-Jones parameters:  $\sigma = 5.50 \text{ \AA}$ ,  $\epsilon/k = 450 \text{ K}$  (estimated from Phenol)

$k_1$  Baulch *et al.*, ref. 32.

$k_1$  microscopic reversibility (MR)

$k_2$  The rate constant of reverse reaction:  $A_{-2}$  and  $Ea_{-2}$  is estimated from ref. 33 for  $H + C_6H_6 \rightarrow C_6H_7$ ,  $A_{-2} = 3.98E13 \text{ cm}^3/\text{mol.s}$ ,  $Ea_{-2} = 4.00 \text{ kcal/mol}$ .  $k_2$  is from MR.

Calculated Apparent Reaction Parameters at  $P = 1 \text{ atm}$ ,  $k = AT^n(-Ea/RT)$

(Temperature range: 200K to 2000K)

	<i>reaction</i>	<i>A</i> ( <i>cc/mol-s</i> )	<i>n</i>	<i>Ea</i> ( <i>kcal/mol</i> )	<i>k</i> <sub>298</sub> ( <i>cc/mol-s</i> )
1	Toluene + OH => Toluene-OH	2.50E39	-9.19	5.42	4.18E12
2	Toluene + OH => <i>o</i> -Cresol + H	4.73E19	-2.21	9.41	1.75E07

**Table 8.6** Input Parameters for QRRK Calculation and the Results of Apparent Rate Constants: Toluene-OH + O<sub>2</sub> (Temperature=298K)

	<i>reaction</i>	<i>A (s<sup>-1</sup> or cc/mol-s)</i>	<i>Ea (kcal/mol)</i>
1	Toluene-OH + O <sub>2</sub> => Tolu-OH-O <sub>2</sub>	1.21E12	0.0
-1	Tolu-OH-O <sub>2</sub> => Toluene-OH + O <sub>2</sub>	2.10E14	11.4
2(TA)	Tolu-OH-O <sub>2</sub> => 2-Methylhexadien-1,6-dial + OH	4.77E11	19.4
3(TB)	Tolu-OH-O <sub>2</sub> => o-Cresol + HO <sub>2</sub>	2.62E11	15.0
4(TC)	Tolu-OH-O <sub>2</sub> => Adduct XIII	1.41E11	14.0
5(TD)	Tolu-OH-O <sub>2</sub> => Adduct XV	1.76E11	14.0
6(TE)	Tolu-OH-O <sub>2</sub> => Adduct XIV	2.49E11	15.6
7(TF)	Tolu-OH-O <sub>2</sub> => Adduct XVI	1.69E11	39.6

geometric mean frequency (from CPFIT<sup>(b)</sup>): 250.3 cm<sup>-1</sup> (12.14), 974.2 cm<sup>-1</sup> (24.61), 2723.9 cm<sup>-1</sup> (12.75).  
Lennard-Jones parameters:  $\sigma = 5.50$  Å,  $\epsilon/k = 450$  K (estimated from Phenol)

$k_1$ : Estimated from regression plot: R. + O<sub>2</sub> by assuming activation energy equal 0.

$k_{-1}$ : MR.

$k_2, k_3, k_4, k_5, k_6$  &  $k_7$ : the same as those in Benzene-OH + O<sub>2</sub>, reaction 2, 3, 4, 5, 6 and 7. see Table 8.4.

Calculated Apparent Reaction Parameters at P = 1atm,  $k = AT^n(-Ea/RT)$   
(Temperature range: 200K to 2000K)

	<i>reaction</i>	<i>A (cc·mol-s)</i>	<i>n</i>	<i>Ea (kcal/mol)</i>	<i>k<sub>298</sub> (cc·mol-s)</i>
1	Toluene-OH + O <sub>2</sub> => Tolu-OH-O <sub>2</sub>	3.33E27	-6.20	0.33	8.76E11
2	Toluene-OH + O <sub>2</sub> => 2-Methyl-2,4-hexadien-1,6-dial +OH	1.49E10	-0.21	8.47	2.74E03
3	Toluene-OH + O <sub>2</sub> => o-Cresol + HO <sub>2</sub>	3.63E11	-0.69	4.89	1.87E06
4	Toluene-OH + O <sub>2</sub> => Adduct XIII	1.14E12	-0.91	4.27	4.64E06
5	Toluene-OH + O <sub>2</sub> => Adduct XV	1.42E12	-0.92	4.27	5.79E06
6	Toluene-OH + O <sub>2</sub> => Adduct XIV	1.50E12	-0.59	5.28	7.19E05
7	Toluene-OH + O <sub>2</sub> => Adduct XVI	1.29E09	-0.04	28.4	1.70E-12



**Table 8.7** Reaction Mechanism of Benzene Photooxidation

	<i>REACTIONS</i>	<i>A(mol-cm<sup>3</sup>-s)</i>	<i>n</i>	<i>Ea(cal mol)</i>
1.	AA + HV => BB+OH	1.60E-04	0	0
2.	BB + OH => AA	2.00E+11	0	0
3.	C6H6+OH=Ph+H2O	6.03E+11	0	4948
4.	C6H6+OH=Benzene-OH	3.04E+37	-8.42	6450
5.	C6H6 + OH = PhOH + H	1.08E+17	-1.25	6590
6.	Benzene-OH = PhOH + H	2.31E+39	-8.75	26570
7.	Benzene-OH + O <sub>2</sub> = Benzene-OH-O <sub>2</sub>	3.64E+27	-6.25	370
8.	Benzene-OH + O <sub>2</sub> = HDEDA+OH	1.03E+10	-0.18	8300
9.	Benzene-OH-O <sub>2</sub> = HDEDA+OH	5.69E+18	-3.73	18460
10.	Benzene-OH + O <sub>2</sub> = PhOH+HO <sub>2</sub>	1.13E+10	-0.26	4050
11.	Benzene-OH-O <sub>2</sub> = PhOH+HO <sub>2</sub>	1.50E+21	-4.54	14010
12.	Benzene-OH + O <sub>2</sub> = Adduct-IX	1.32E+10	-0.36	3220
13.	Benzene-OH-O <sub>2</sub> = Adduct-IX	8.27E+21	-4.85	13200
14.	Benzene-OH + O <sub>2</sub> = Adduct-XI	1.65E+10	-0.36	3220
15.	Benzene-OH-O <sub>2</sub> = Adduct-XI	1.03E+22	-4.85	13200
16.	Benzene-OH + O <sub>2</sub> = Adduct-X	3.91E+09	-0.14	4410
17.	Benzene-OH-O <sub>2</sub> = Adduct-X	1.08E+20	-4.21	14300
18.	Benzene-OH + O <sub>2</sub> = Adduct-XII	4.99E+08	0.07	28070
19.	Adduct-IX + O <sub>2</sub> = Adduct-IXO	1.20E+12	0	0
20.	Adduct-IXO + NO = Adduct-XIX + NO <sub>2</sub>	5.36E+12	0	0
21.	Adduct-XIX = BDA + CHOCHOH	3.07E+13	0	10260
22.	Adduct-X + O <sub>2</sub> = Adduct-XXO	1.20E+12	0	0
23.	Adduct-XXO + NO = Adduct-XX + NO <sub>2</sub>	5.36E+12	0	0
24.	Adduct-XIX = BDA + CHOCHOH	3.07E+13	0	10260
25.	Adduct-XXI + O <sub>2</sub> = Adduct-XXIO	1.20E+12	0	0
26.	Adduct-XXIO + NO = Adduct-XIX + NO <sub>2</sub>	5.36E+12	0	0
27.	Adduct-XXI = BDAH + GLY	3.07E+13	0	10260
28.	CHOCHOH + O <sub>2</sub> = GLY+HO <sub>2</sub>	5.66E+12	0	0
29.	BDAH + O <sub>2</sub> = BDA+HO <sub>2</sub>	5.66E+12	0	0

$k = AT^n \exp(-E_a/RT)$ , all reactions in the mechanisms are considered by the integrator in both forward and reverse directions via principles of Microscopic Reversibility (MR).

Symbols in used for species:

Ph = C6H5- (phenyl group), HDEDA = 2,4-hexadiene-1,6-dial

BDA = 2-Butene-1,4-dial, GLY = Glyoxal, BDAH = 2-Butene-1-al-4-hydroxy-4-yl.

Adduct-XIXO = the peroxy radical with one more oxygen than adduct-XIX (oxy radical), so are the Adduct-XXO and Adduct-XXIO.

**Table 8.8** Reaction Mechanism of Toluene Photo-Oxidation

	<i>REACTIONS</i>	<i>A(mol-cm<sup>3</sup>-s)</i>	<i>n</i>	<i>Ea(cal/mol)</i>
1.	AA + HV => BB+OH	7.00E-04	0	0
2.	BB + OH => AA	2.50E+11	0	0
3.	PhCH <sub>3</sub> + OH = PhCH <sub>2</sub> + H <sub>2</sub> O	6.45E+06	2	477
4.	PhCH <sub>2</sub> +O <sub>2</sub> = PhCH <sub>2</sub> OO	6.32E+11	0	0
5.	PhCH <sub>2</sub> OO + NO = PhCH <sub>2</sub> O + NO <sub>2</sub>	5.36E+12	0	0
6.	PhCH <sub>2</sub> O + O <sub>2</sub> = PhCHO + HO <sub>2</sub>	4.08E+09	0	0
7.	PhCH <sub>3</sub> + OH = Toluene-OH	2.50E+39	-9.19	5420
8.	PhCH <sub>3</sub> + OH = o-Cresol + H	4.73E+19	-2.21	9410
9.	Toluene-OH = o-Cresol + H	5.10E+39	-9.03	29030
10.	Toluene-OH + O <sub>2</sub> = Toluene-OH-O <sub>2</sub>	3.33E+27	-6.2	330
11.	Toluene-OH + O <sub>2</sub> = MHDEDA + OH	1.49E+10	-0.21	8470
12.	Toluene-OH-O <sub>2</sub> = MHDEDA+ OH	1.25E+17	-3.21	17320
13.	Toluene-OH + O <sub>2</sub> = o-Cresol + HO <sub>2</sub>	3.63E+11	-0.69	4890
14.	Toluene-OH-O <sub>2</sub> = o-Cresol + HO <sub>2</sub>	4.00E+20	-4.34	13520
15.	Toluene-OH + O <sub>2</sub> = Adduct-XIII	1.14E+12	-0.92	4270
16.	Toluene-OH-O <sub>2</sub> = Adduct-XIII	6.25E+21	-4.77	12910
17.	Toluene-OH + O <sub>2</sub> = Adduct-XV	1.42E+12	-0.92	4270
18.	Toluene-OH-O <sub>2</sub> = Adduct-XV	7.80E+21	-4.77	12910
19.	Toluene-OH + O <sub>2</sub> = Adduct-XIV	1.50E+12	-0.59	5280
20.	Toluene-OH-O <sub>2</sub> = Adduct-XIV	7.38E+19	-4.13	13940
21.	Toluene-OH + O <sub>2</sub> = Adduct-XVI	1.29E+09	-0.04	28350
22.	Adduct-XIII + O <sub>2</sub> = Adduct-XXIIO	1.20E+12	0	0
23.	Adduct-XXIIO + NO = Adduct-XXII + NO <sub>2</sub>	5.36E+12	0	0
24.	Adduct-XXII = BDA + MGLYH	3.07E+13	0	10260
25.	MGLYH + O <sub>2</sub> = MGLY + HO <sub>2</sub>	5.66E+12	0	0

$k = AT^n \exp(-E_a/RT)$ . all reactions in the mechanisms are considered by the integrator in both forward and reverse directions via principles of Microscopic Reversibility (MR).

Symbols in used for species:

Ph = C<sub>6</sub>H<sub>5</sub>- (phenyl group), MHDEDA = 2-Methyl-2,4-hexadiene-1,6-dial

BDA = 2-Butene-1,4-dial, MGLY = Methylglyoxal (Propanal-2-al), MGLYH = Propanal-2-hydroxy-2-yl.

Adduct-XXIIO = the peroxy radical with one more oxygen than adduct-XXII (oxy radical).

**Table 8.9** Forward Rate constants, Concentration Equilibrium Constants and Backward Rate Constants for *Benzene-OH + O<sub>2</sub>* System of Reactions

<i>Rxn.</i>	<i>Reactions</i>	$k_f$ ( $s^{-1}$ or $cc/mol-s$ )	$K_{eq}$	$k_r$ ( $s^{-1}$ or $cc/mol-s$ )
	Addition-(elimination or isomerization)			
1(A)	Benz-OH + O <sub>2</sub> => Benz-OH-O <sub>2</sub>	6.585E11	1.206E3	5.46E8
2(BA)	Benz-OH + O <sub>2</sub> => Hexadienedial + OH	3.09E3	1.56E29	
3(BB)	Benz-OH + O <sub>2</sub> => Phenol + HO <sub>2</sub>	2.70E6	2.311E23	
4(BC)	Benz-OH + O <sub>2</sub> => Adduct IX	7.32E6	8.55E8	
5(BD)	Benz-OH + O <sub>2</sub> => Adduct XI	9.14E6	1.187E-2	7.70E8
6(BE)	Benz-OH + O <sub>2</sub> => Adduct X	1.05E6	1.275E-3	8.23E8
7(BF)	Benz-OH + O <sub>2</sub> => Adduct XII	2.00E-12	3.517E-10	
	Dissociation			
8(C1)	Benz-OH-O <sub>2</sub> = PhOH + H O <sub>2</sub>	4.136E-1	1.915E20	
9(C2)	Benz-OH-O <sub>2</sub> = adduct IX	1.818	7.09E5	
10(C3)	Benz-OH-O <sub>2</sub> = adduct XI	2.269	9.84E-6	2.31E5
11(C4)	Benz-OH-O <sub>2</sub> = adduct X	1.387E-1	1.057E-6	1.31E5

**APPENDIX D**

**FIGURES FOR SECTION II**

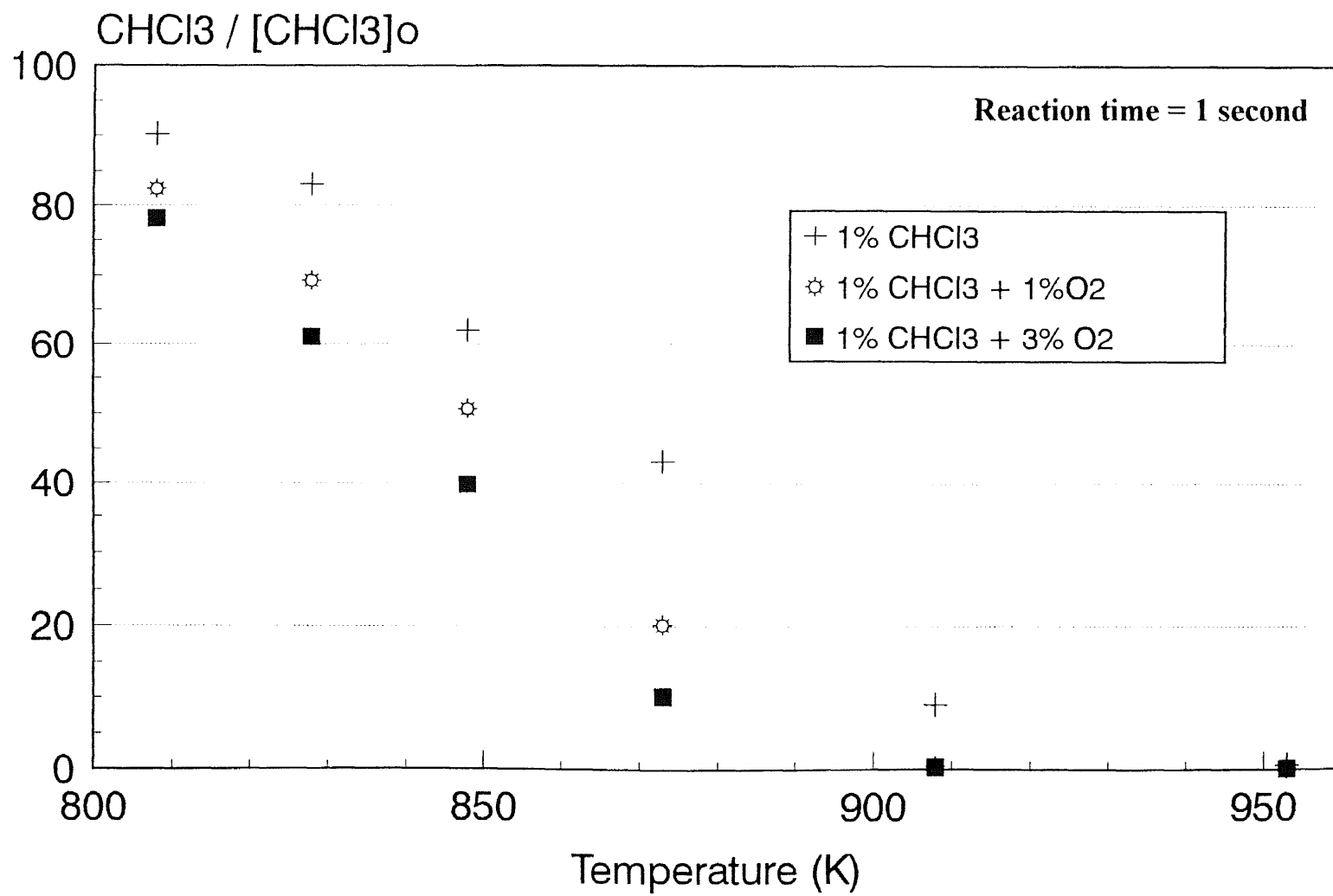


Figure 7.1 Comparison of CHCl<sub>3</sub> Decay vs Temperature at Pyrolytic and Oxidative Environments

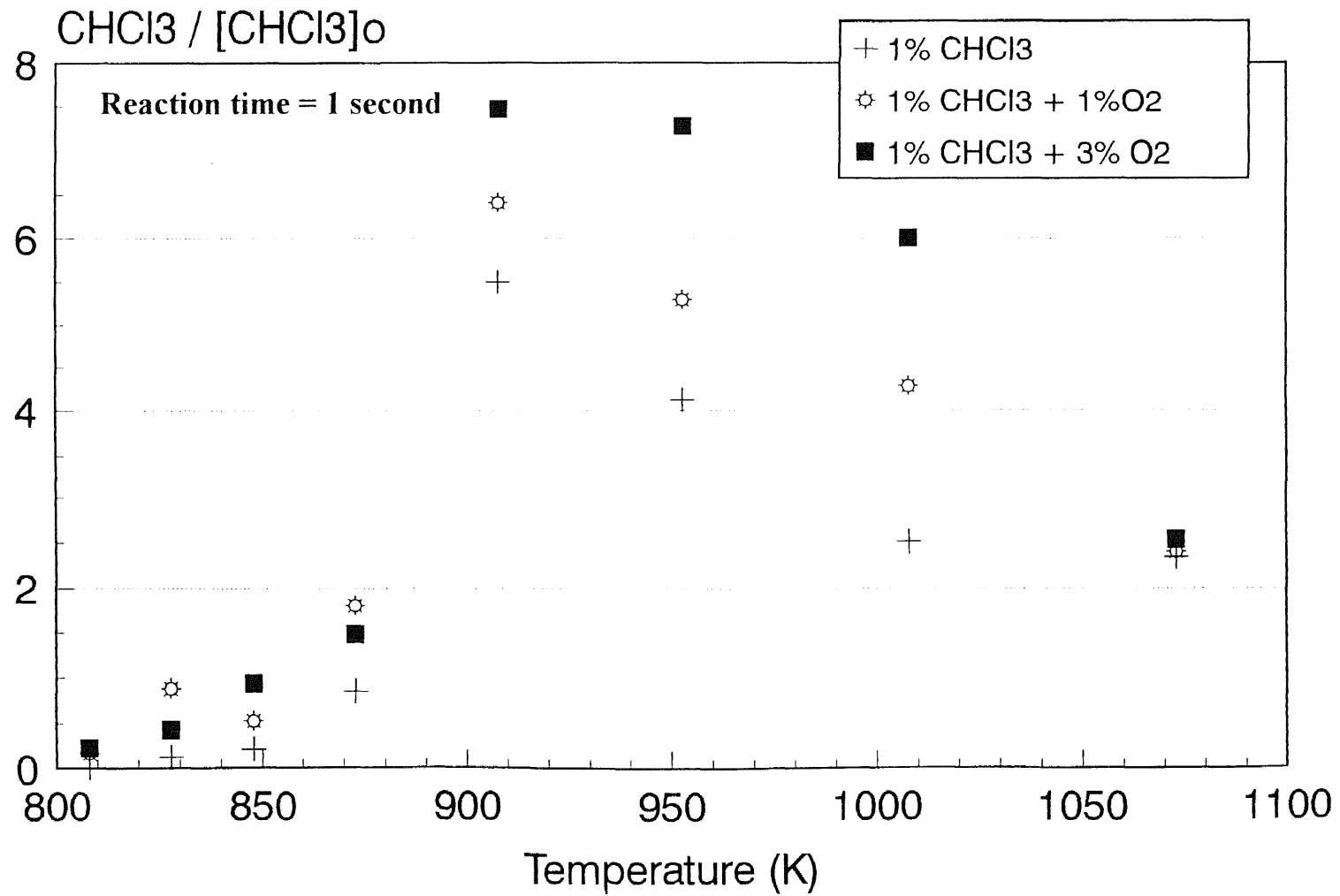
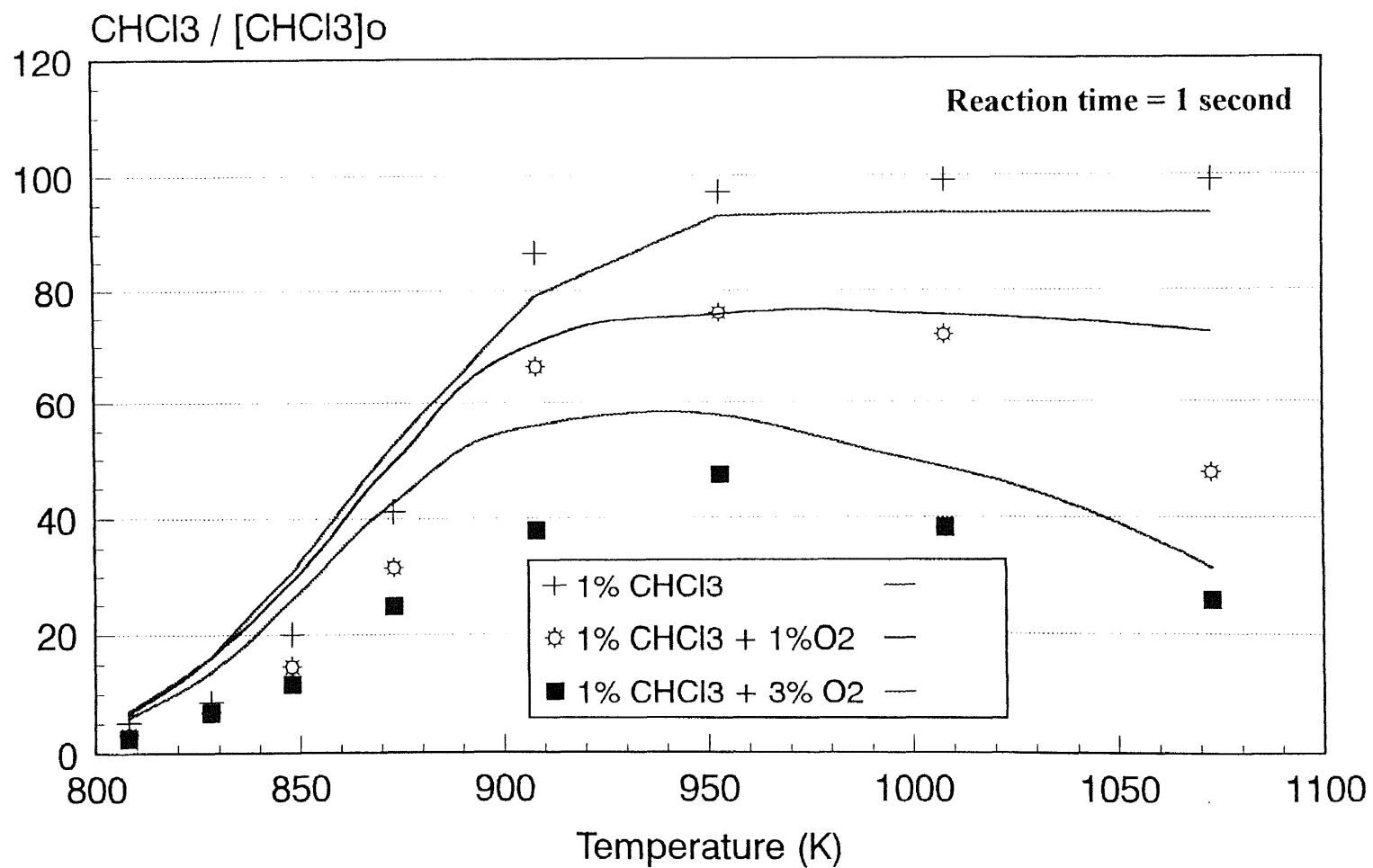
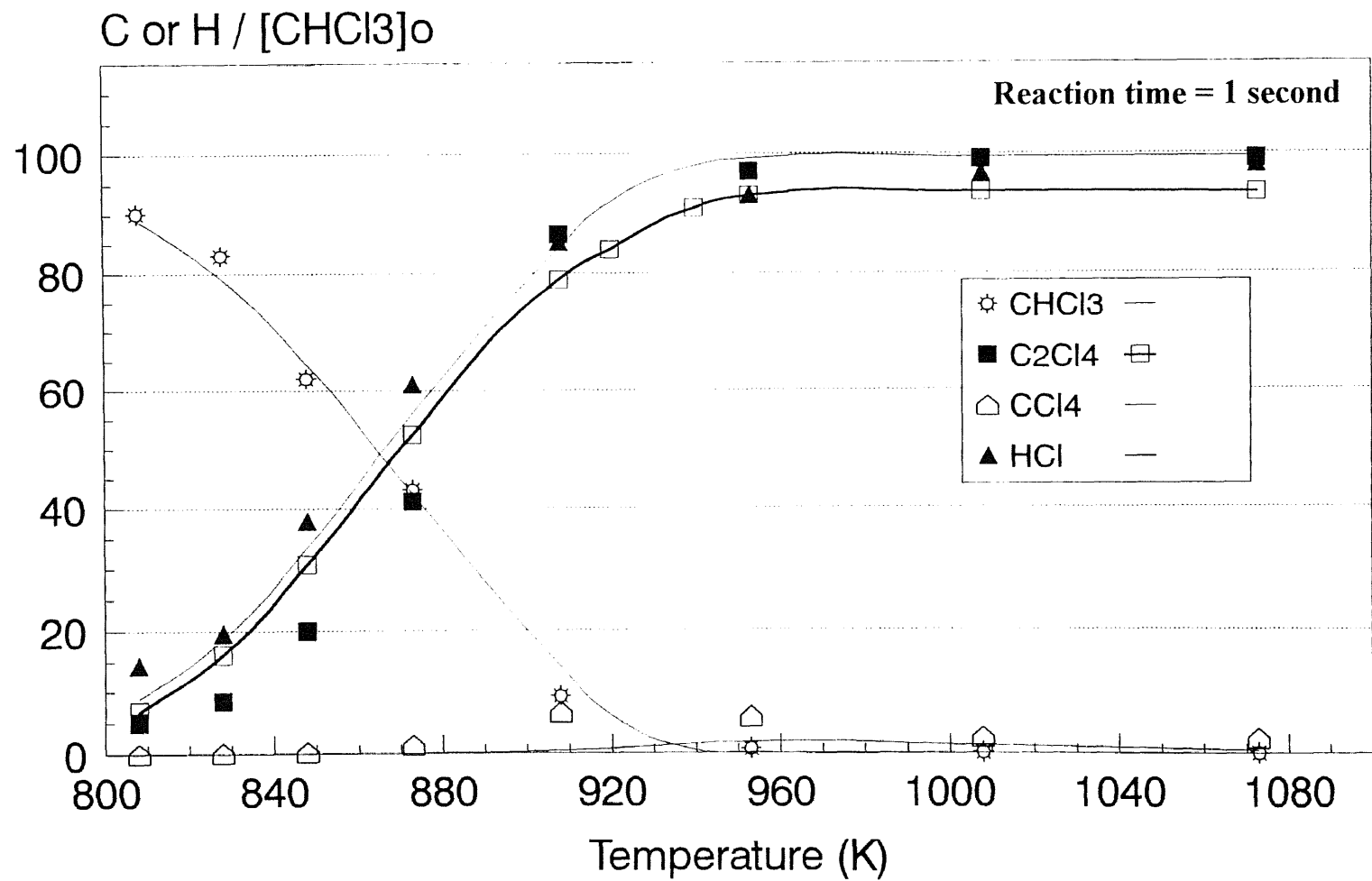


Figure 7.2 CCl<sub>4</sub> Formed per mole of CHCl<sub>3</sub> in Presence and Absence of Added O<sub>2</sub>



**Figure 7.3**  $\text{C}_2\text{Cl}_4$  Formed per mole of  $\text{CHCl}_3$  in Presence and Absence of Added  $\text{O}_2$   
 (point : experimental data, line: model prediction)



**Figure 7.4** CHCl<sub>3</sub> Pyrolysis Product Distribution vs Temperature (CHCl<sub>3</sub>/Ar)  
 (point : experimental data, line: model prediction)



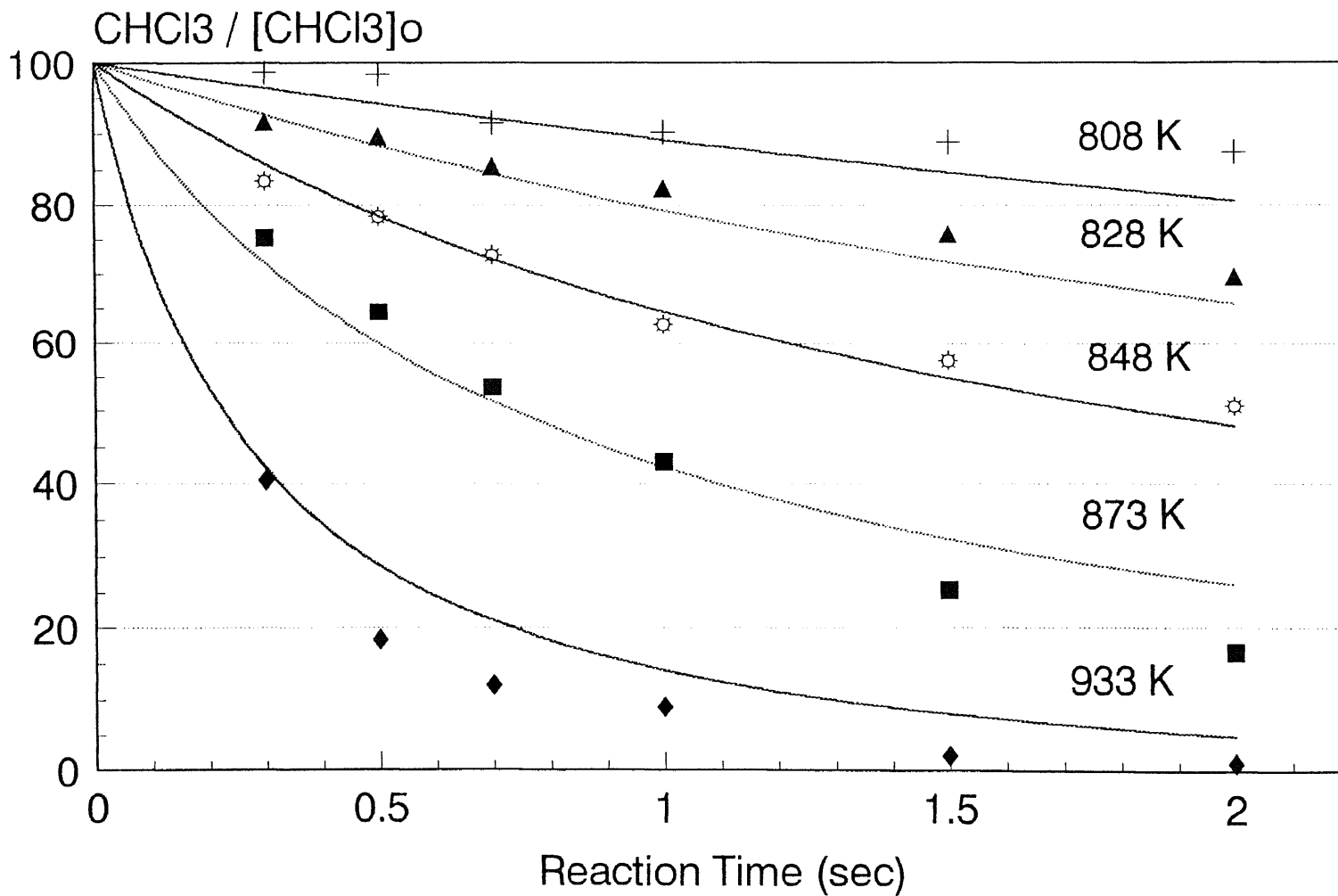


**Figure 7.5** Decay of CHCl<sub>3</sub> in Chloroform Pyrolysis (CHCl<sub>3</sub>/Ar)  
(point : experimental data, line: model prediction)

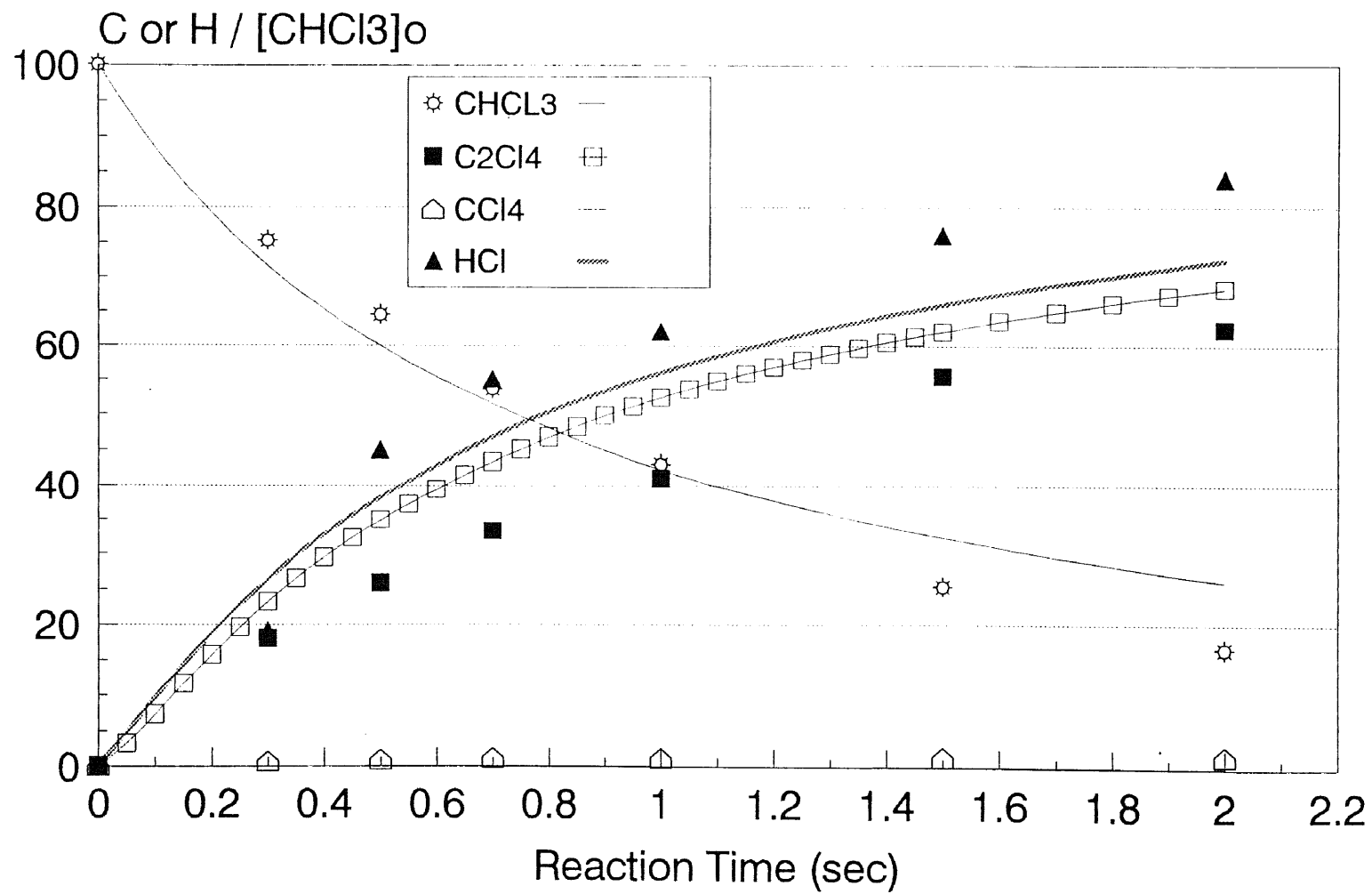
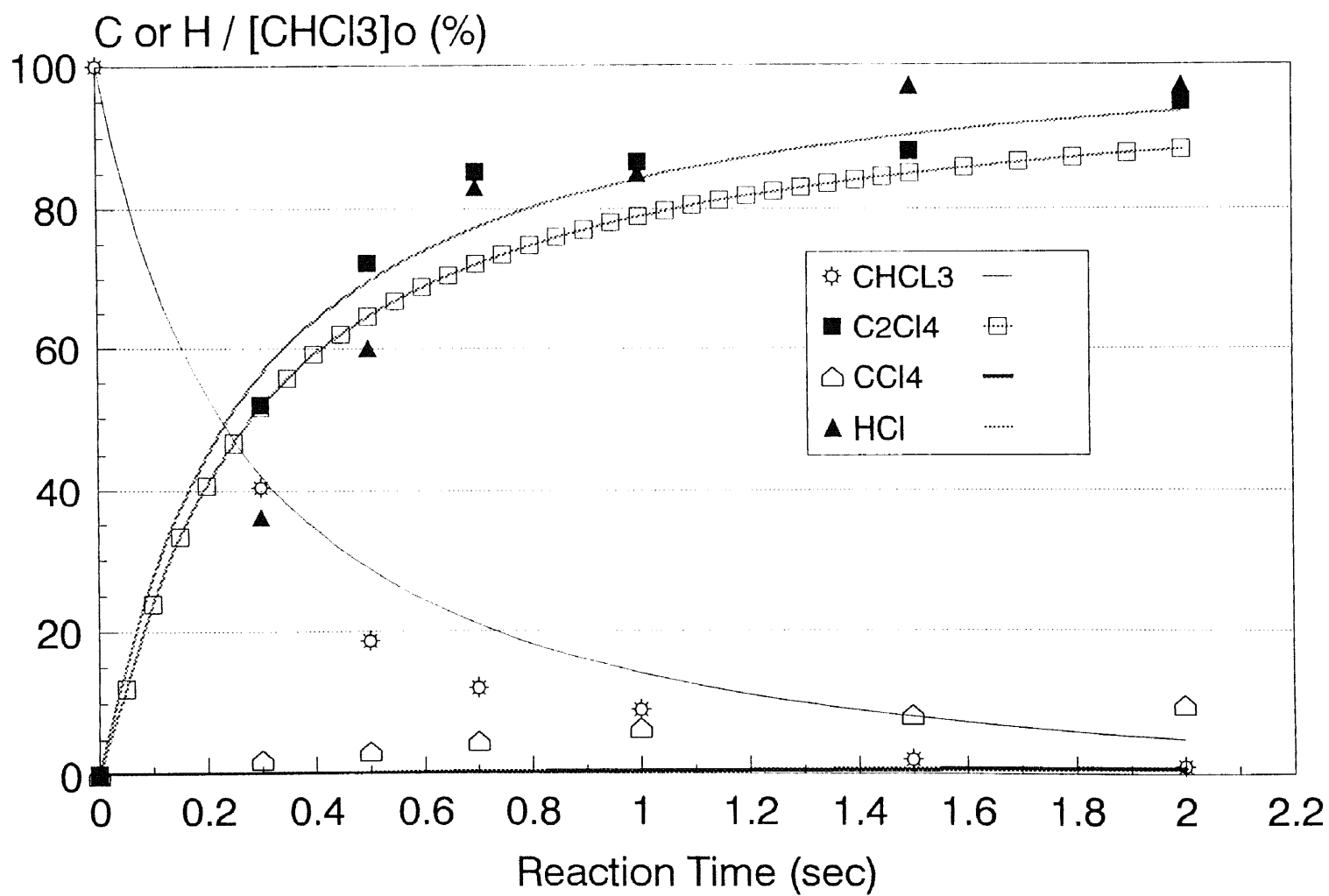
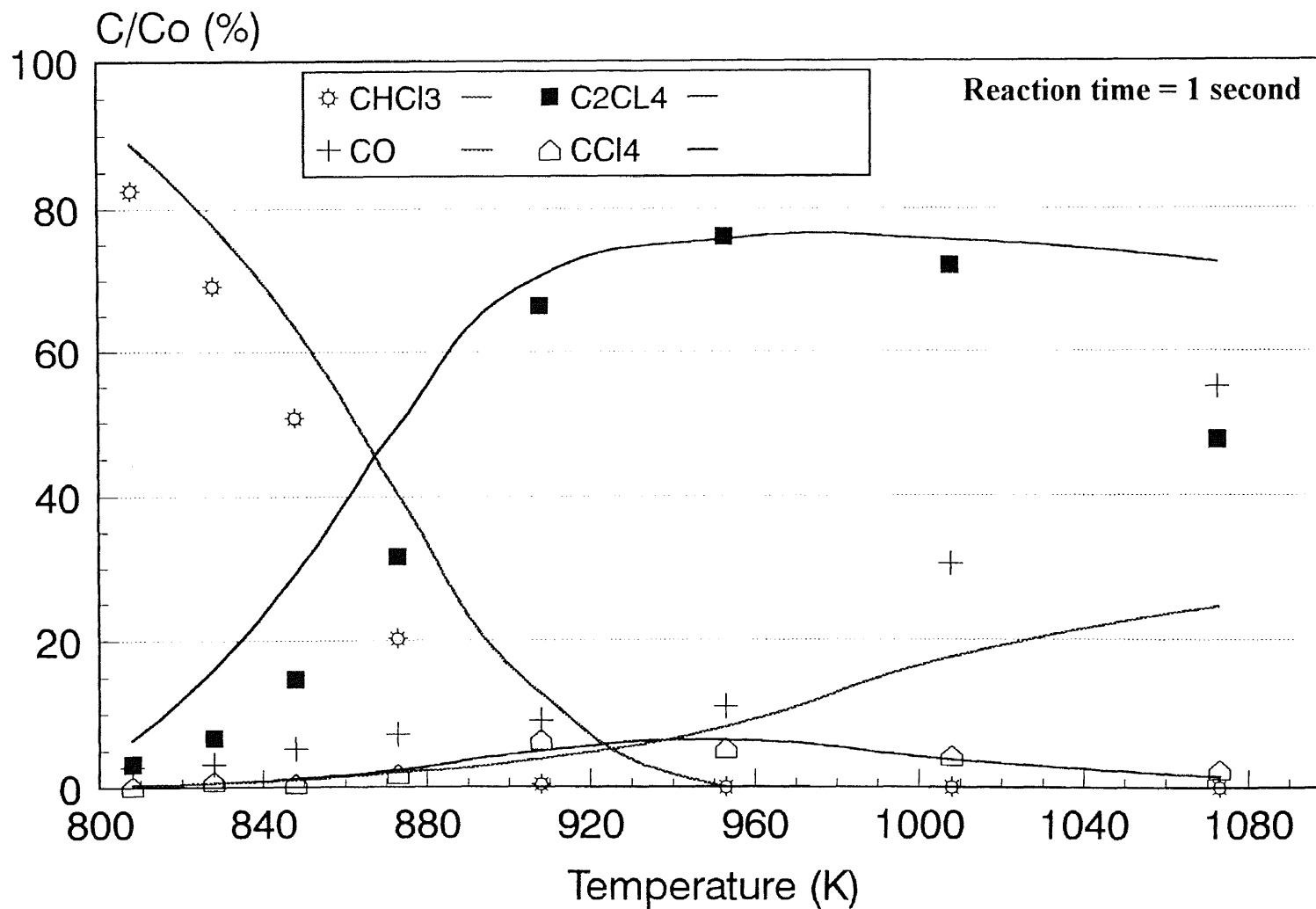


Figure 7.6 CHCl<sub>3</sub> Pyrolysis at 873 K (CHCl<sub>3</sub>/Ar)  
 (point : experimental data, line: model prediction)



**Figure 7.7**  $\text{CHCl}_3$  Pyrolysis at 908 K ( $\text{CHCl}_3/\text{Ar}$ )  
 (point : experimental data, line: model prediction)



**Figure 7.8** CHCl<sub>3</sub> Oxidation Product Distribution vs Temperature (1% CHCl<sub>3</sub> + 1% O<sub>2</sub>)  
 (point : experimental data, line: model prediction)

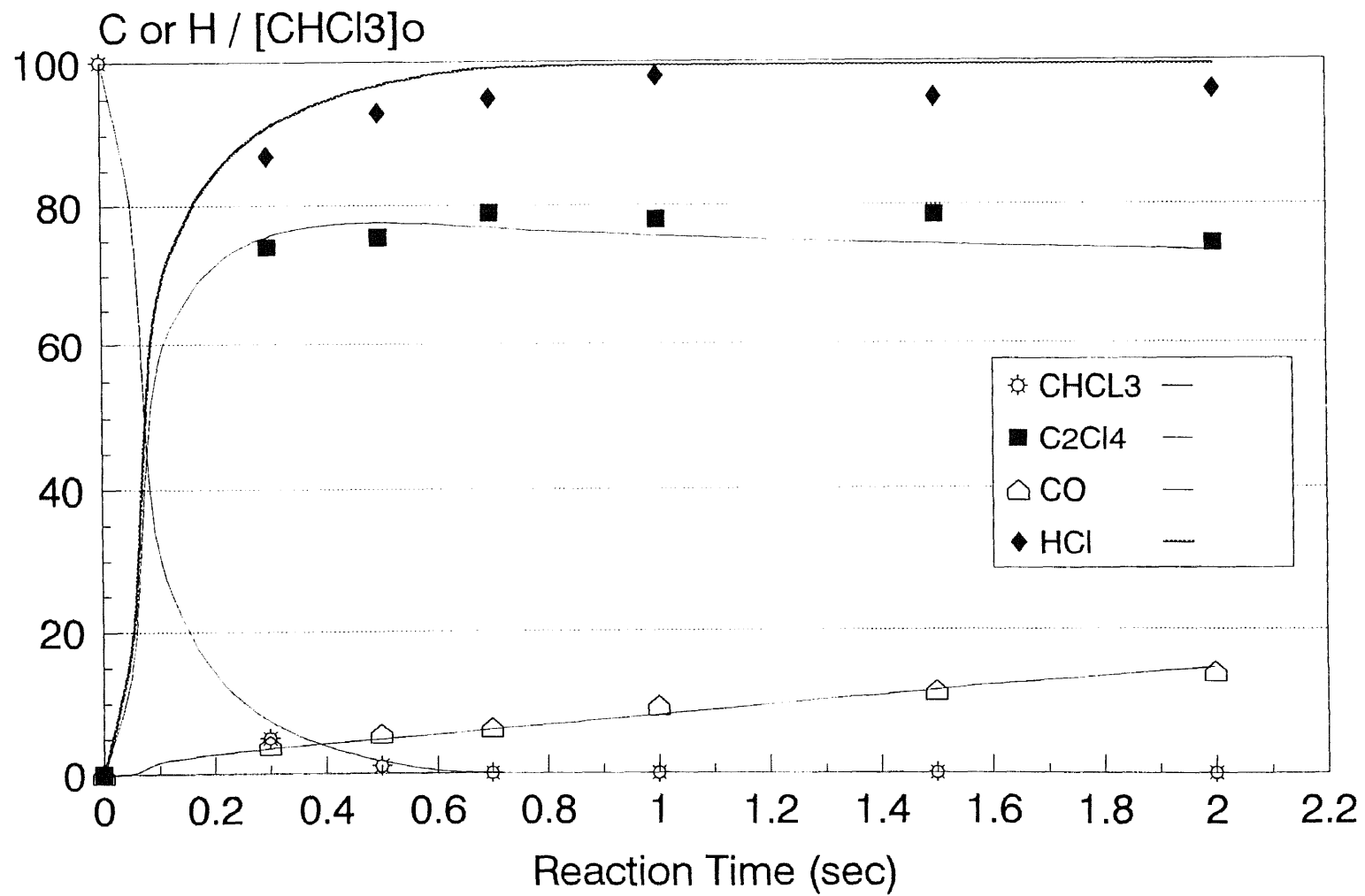


**Figure 7.9**  $\text{CHCl}_3$  Oxidation at 953 K ( 1%  $\text{CHCl}_3$  + 1%  $\text{O}_2$ )  
 (point : experimental data, line: model prediction)

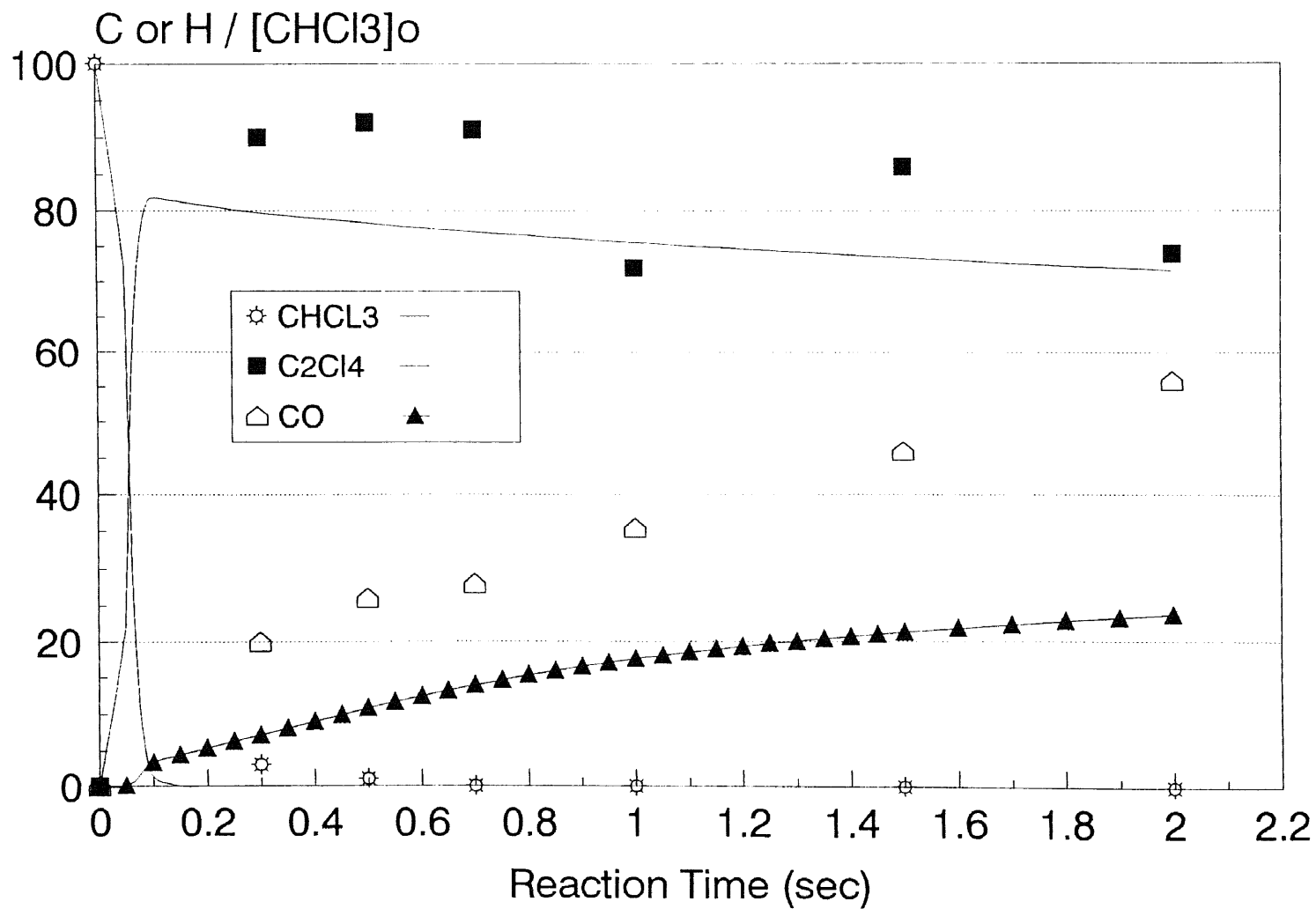


**Figure 7.10**  $\text{CHCl}_3$  Oxidation at 1008 K ( 1%  $\text{CHCl}_3$  + 1%  $\text{O}_2$ )  
 (point : experimental data, line: model prediction)

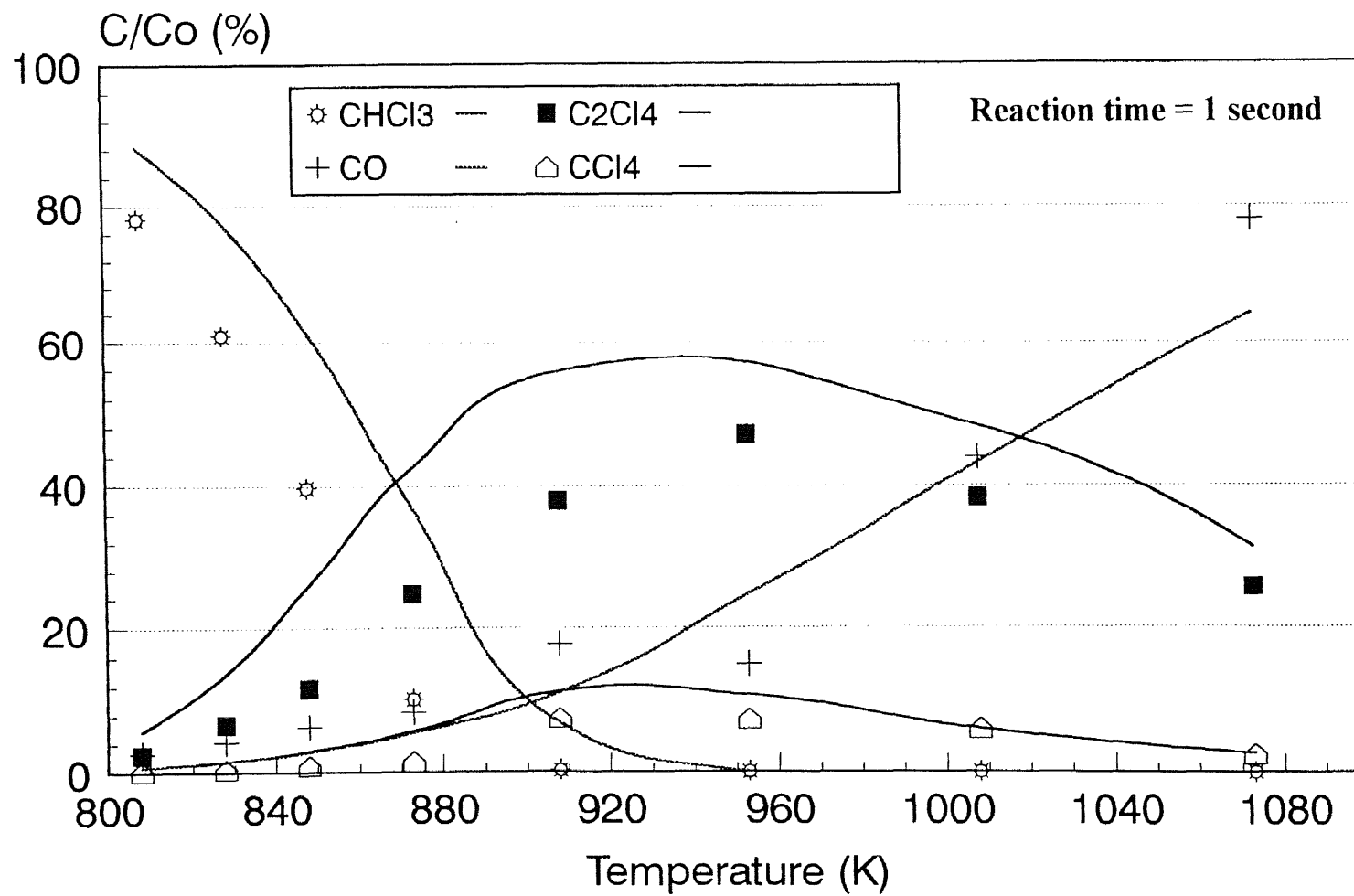
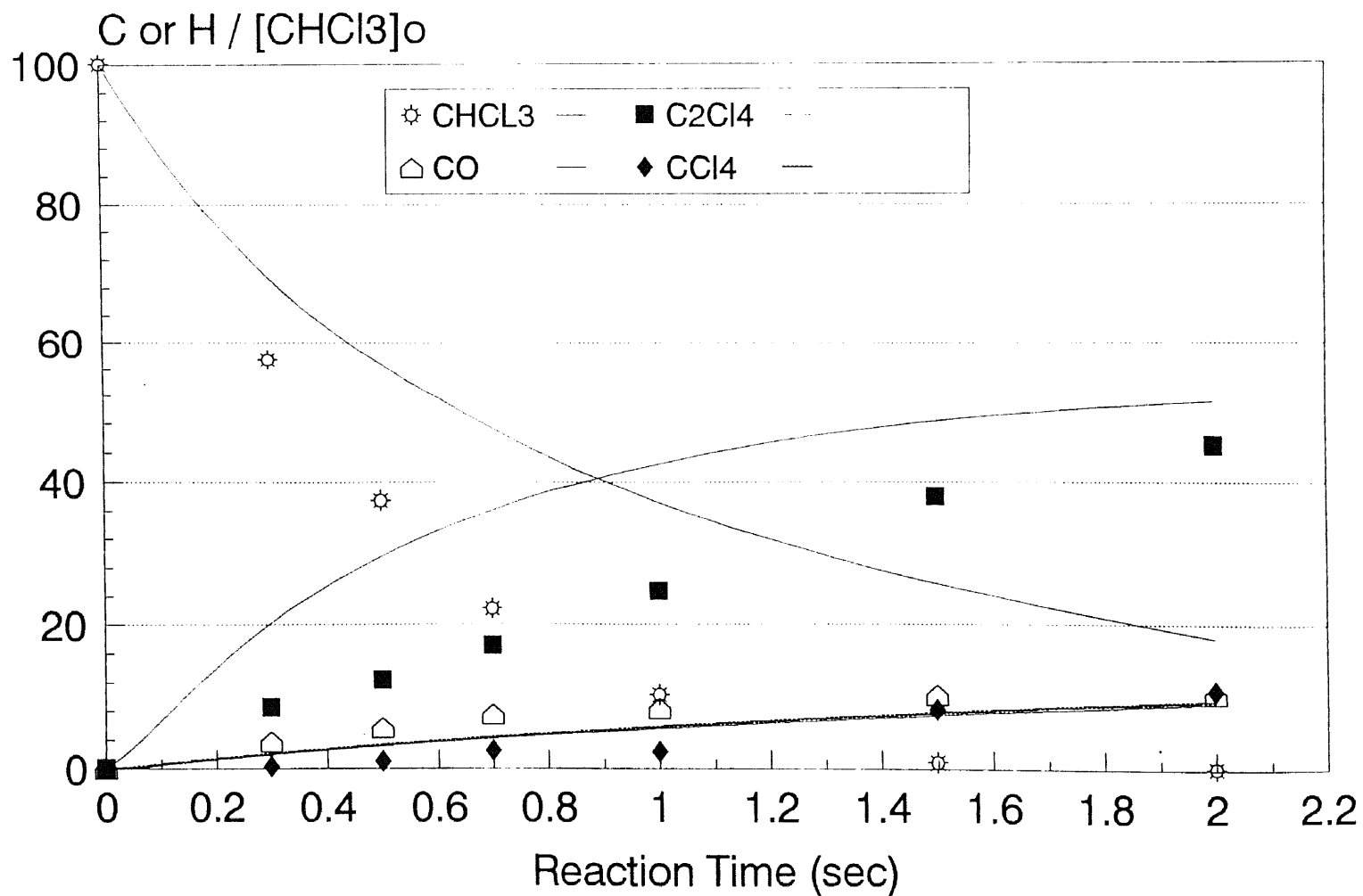
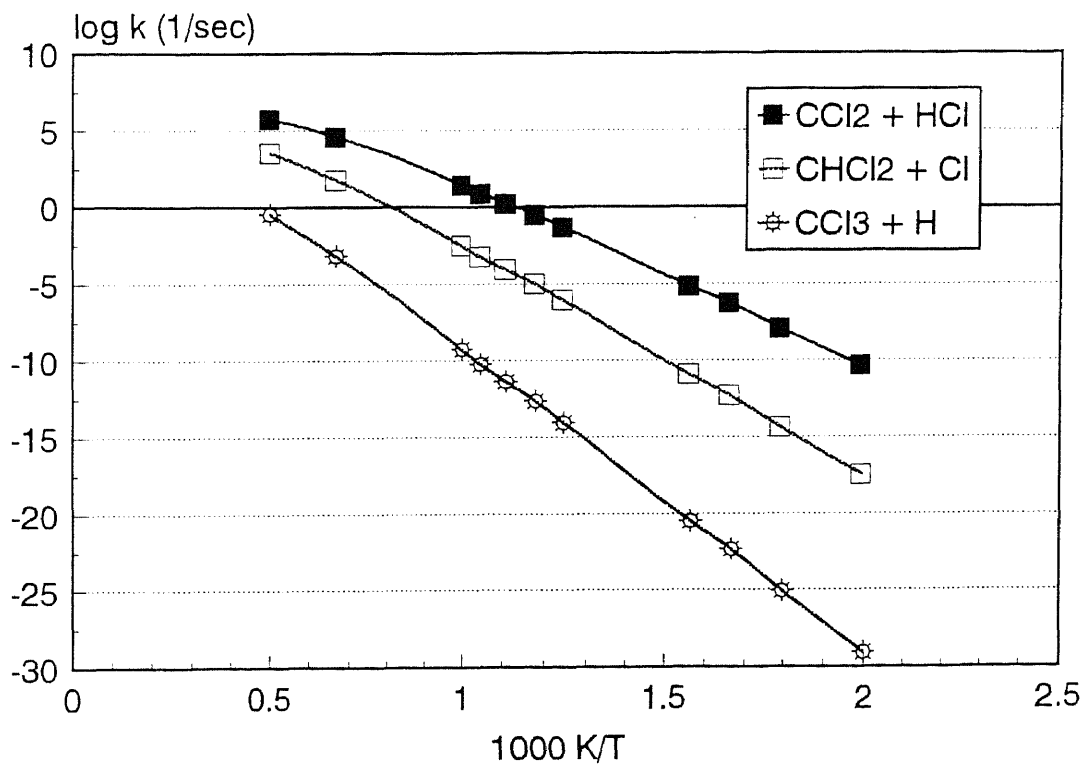
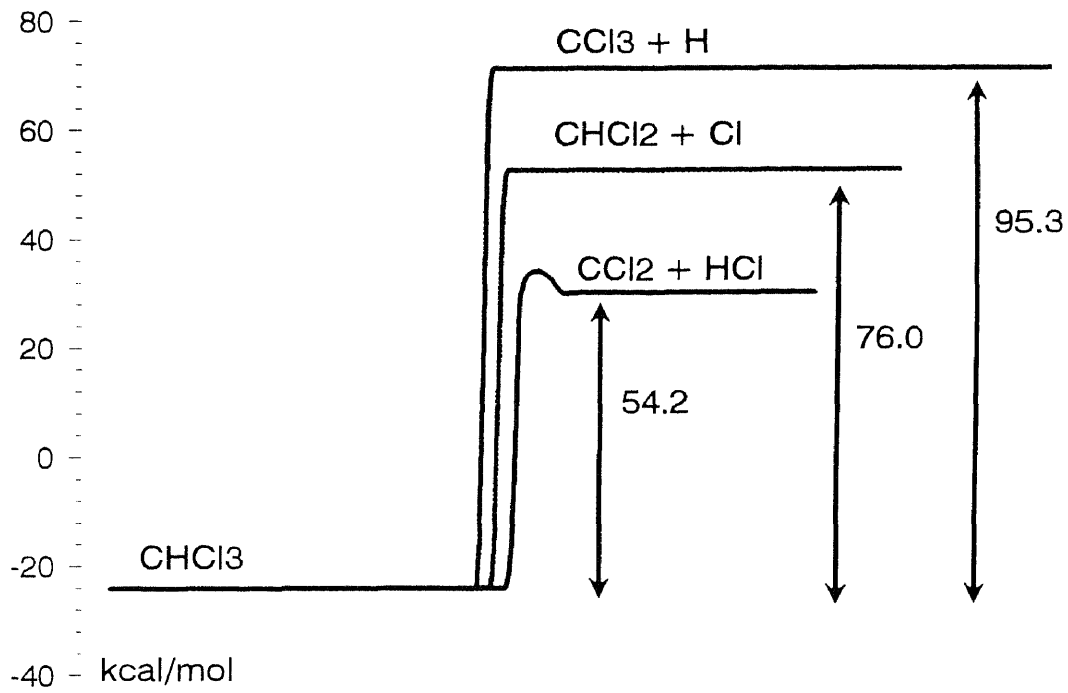


Figure 7.11 CHCl<sub>3</sub> Oxidation Product Distribution vs Temperature (1% CHCl<sub>3</sub> + 3% O<sub>2</sub>)  
 (point : experimental data, line: model prediction)



**Figure 7.12**  $\text{CHCl}_3$  Oxidation at 873 K ( 1%  $\text{CHCl}_3$  + 3%  $\text{O}_2$ )  
 (point : experimental data, line: model prediction)





**Figure 7.A.1** Potential Energy Diagram and Arrhenius Plot for Reactions:  $\text{CHCl}_3 \Rightarrow \text{Products}$

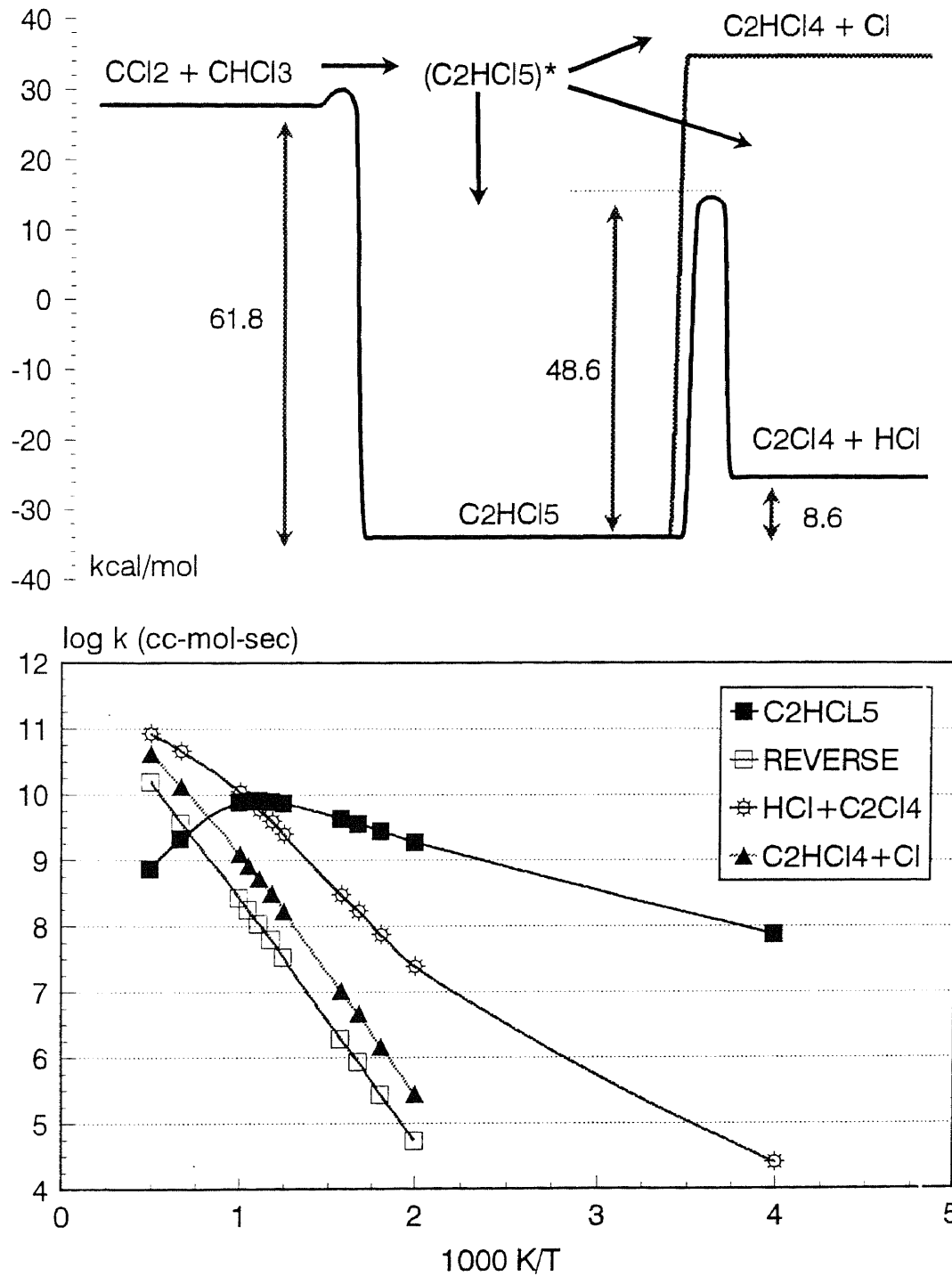


**Figure 7.A.2** Potential Energy Diagram and Arrhenius Plot for Reactions:  
 $\text{CCl}_2 + \text{CHCl}_3 \Rightarrow \text{Products}$

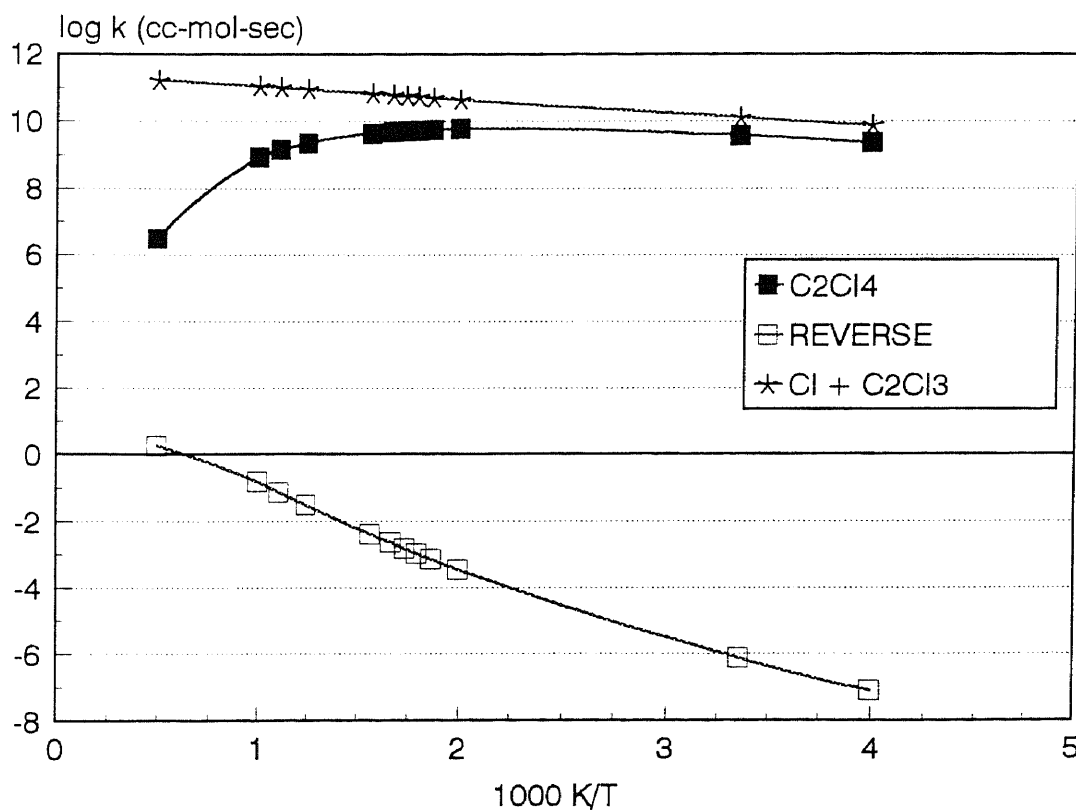
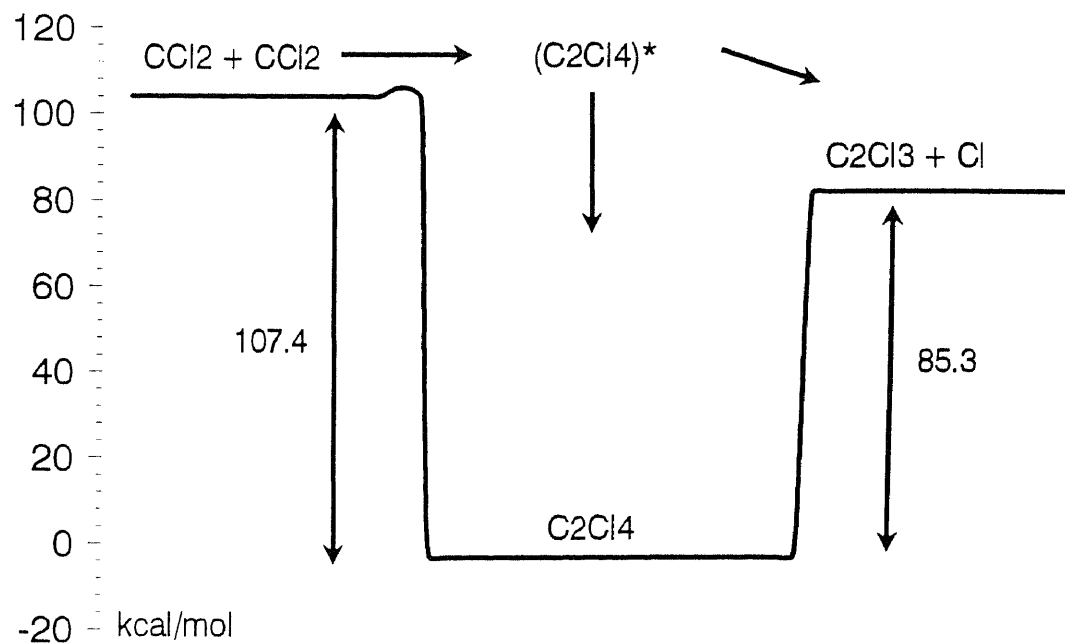


Figure 7.A.3 Potential Energy Diagram and Arrhenius Plot for Reactions:  
 $\text{CCl}_2 + \text{CCl}_2 \Rightarrow \text{Products}$

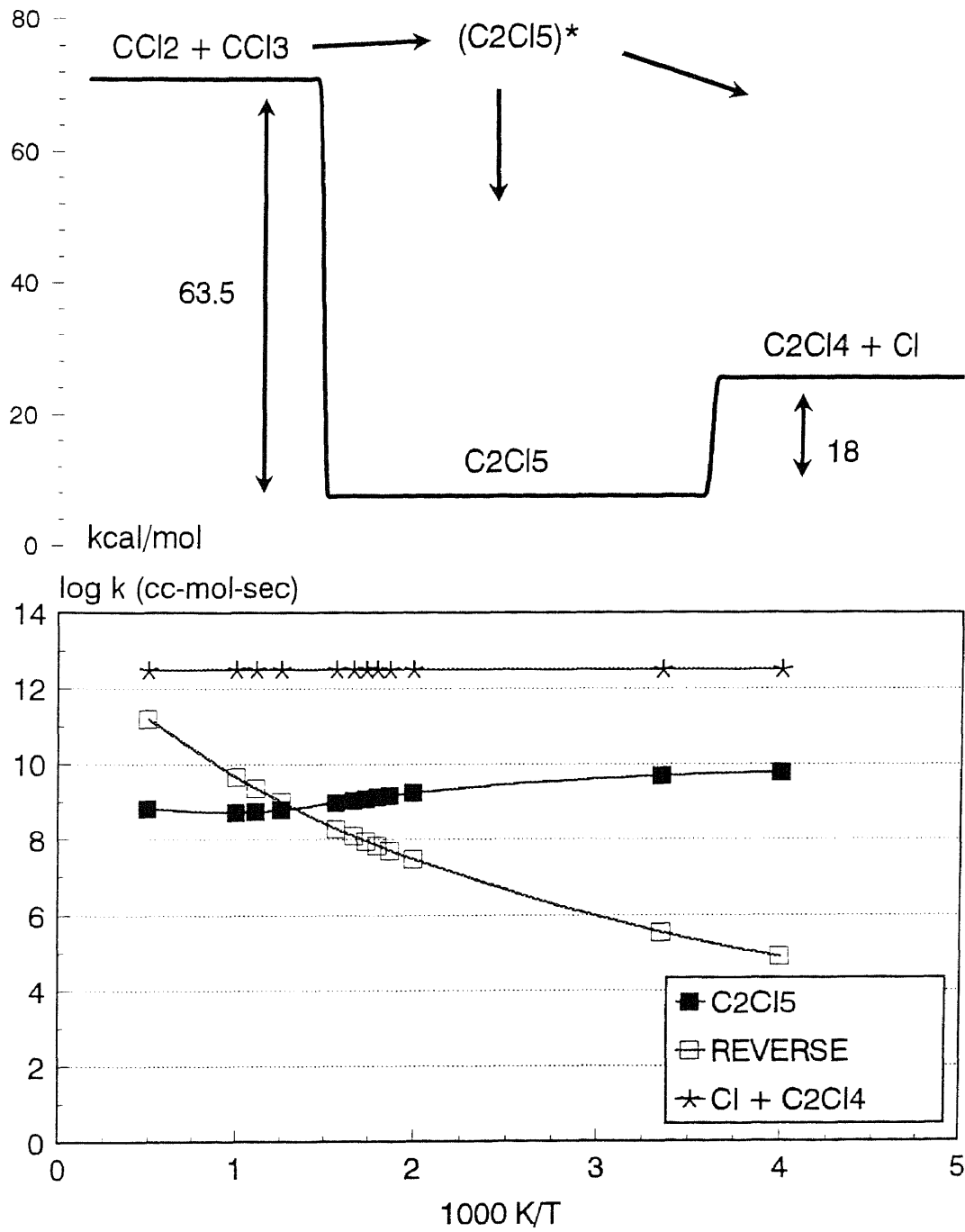
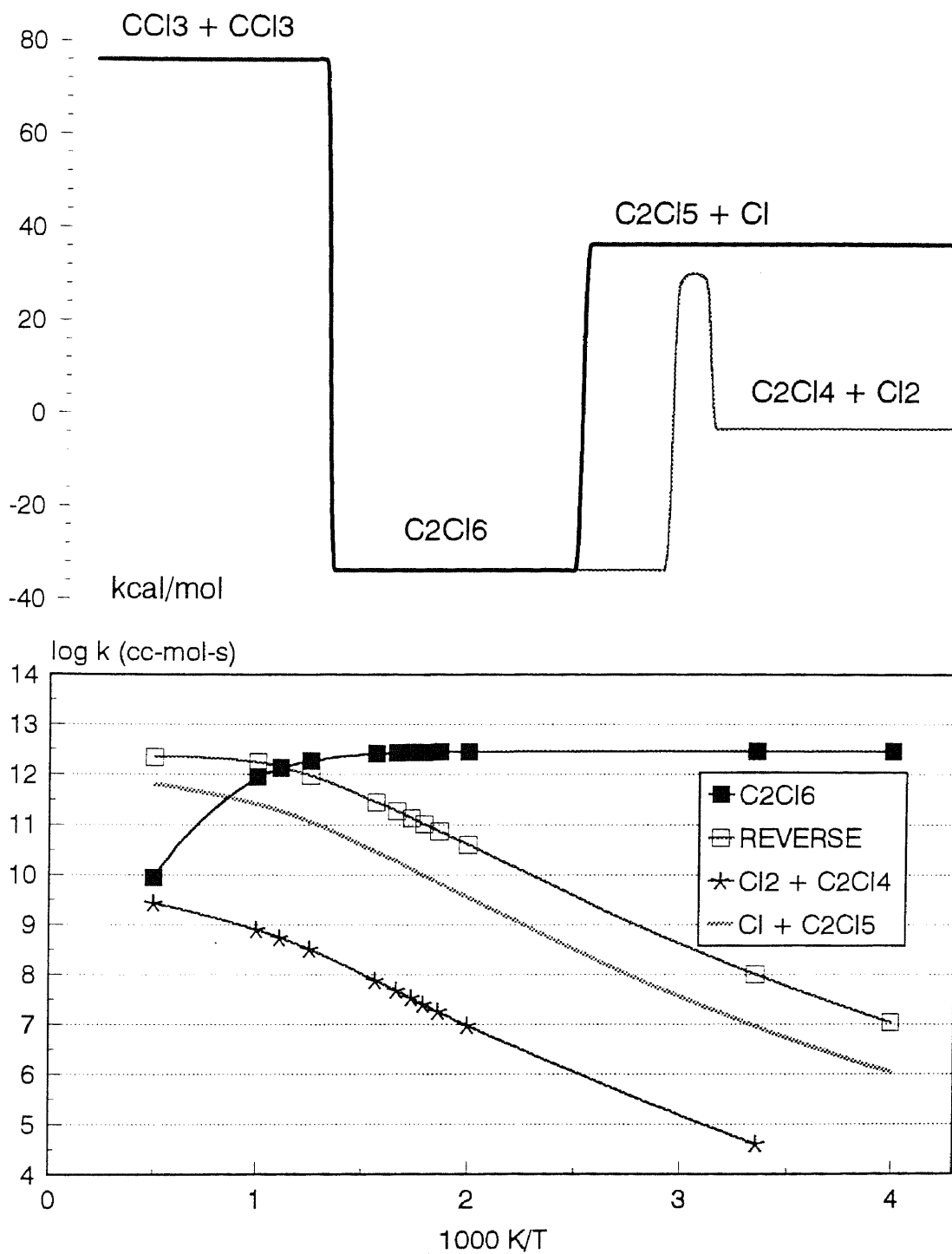


Figure 7.A.4 Potential Energy Diagram and Arrhenius Plot for Reactions:  
 $\text{CCl}_2 + \text{CCl}_3 \Rightarrow \text{Products}$



**Figure 7.A.5** Potential Energy Diagram and Arrhenius Plot for Reactions:  
 $\text{CCl}_3 + \text{CCl}_3 \Rightarrow \text{Products}$

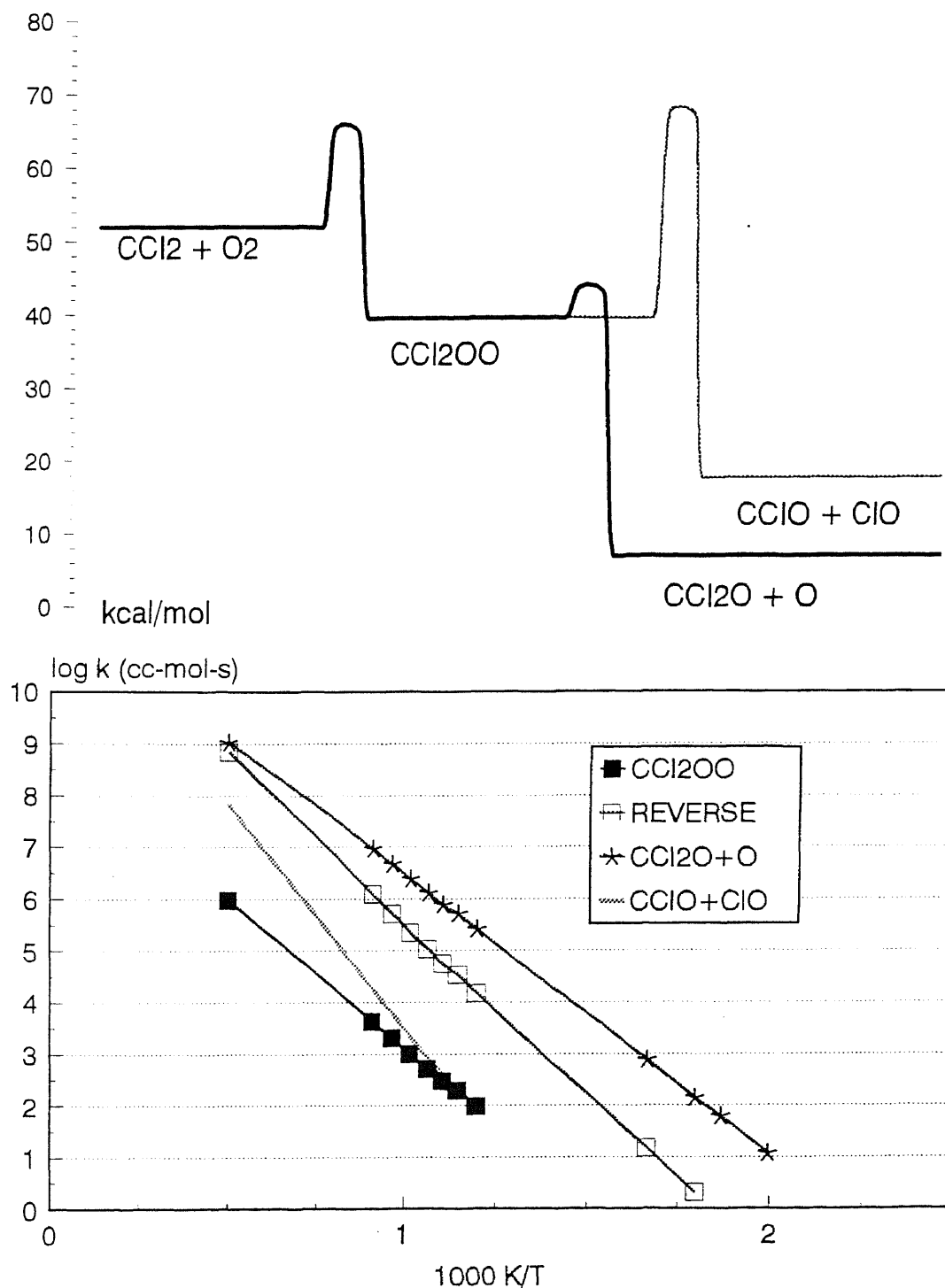
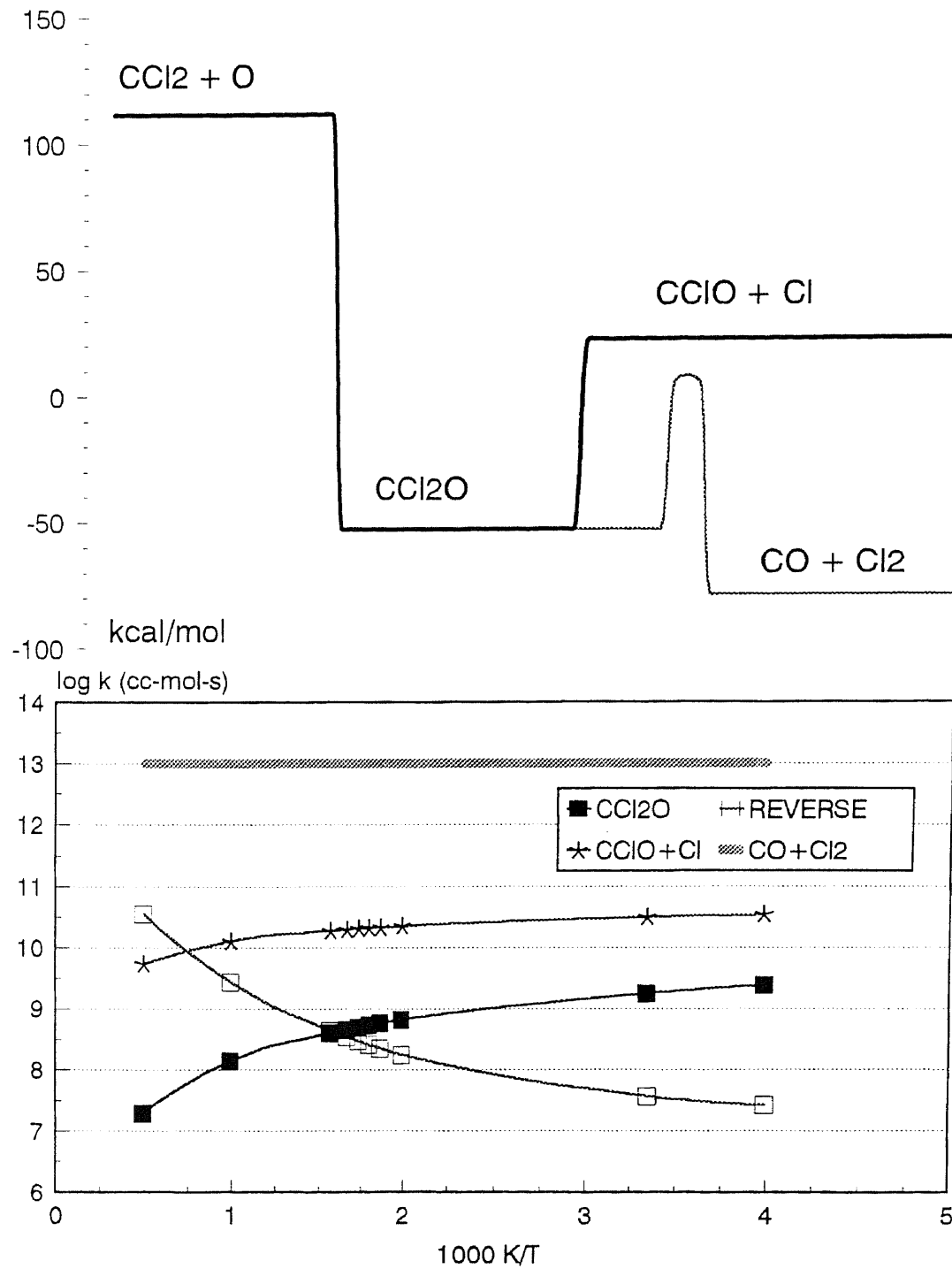


Figure 7.A.6 Potential Energy Diagram and Arrhenius Plot for Reactions:  
 $\text{CCl}_2 + \text{O}_2 \Rightarrow \text{Products}$



**Figure 7.A.7** Potential Energy Diagram and Arrhenius Plot for Reactions:  
 $CCl_2 + O \Rightarrow$  Products

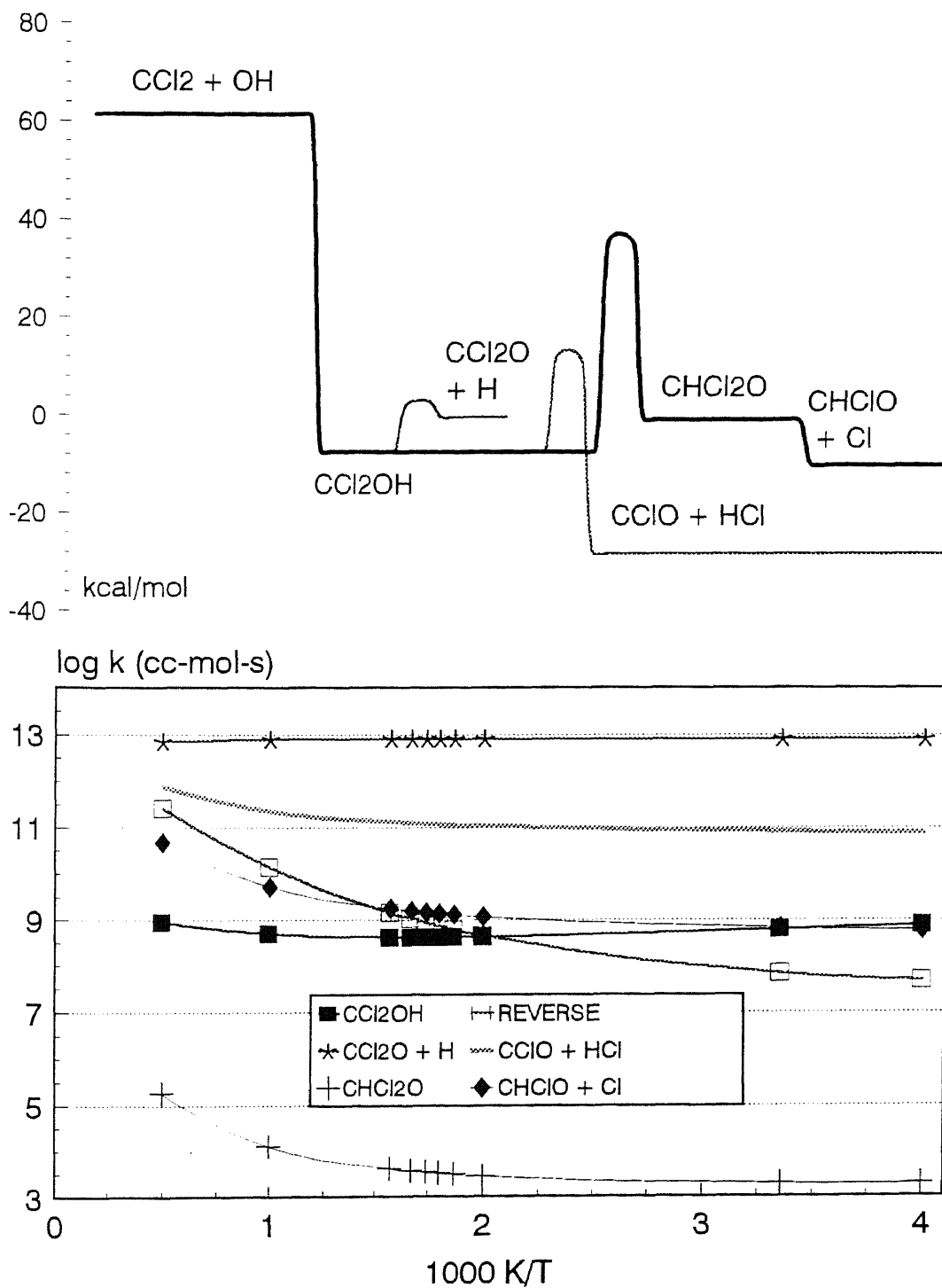


Figure 7.A.8 Potential Energy Diagram and Arrhenius Plot for Reactions:  
 $\text{CCl}_2 + \text{OH} \Rightarrow \text{Products}$



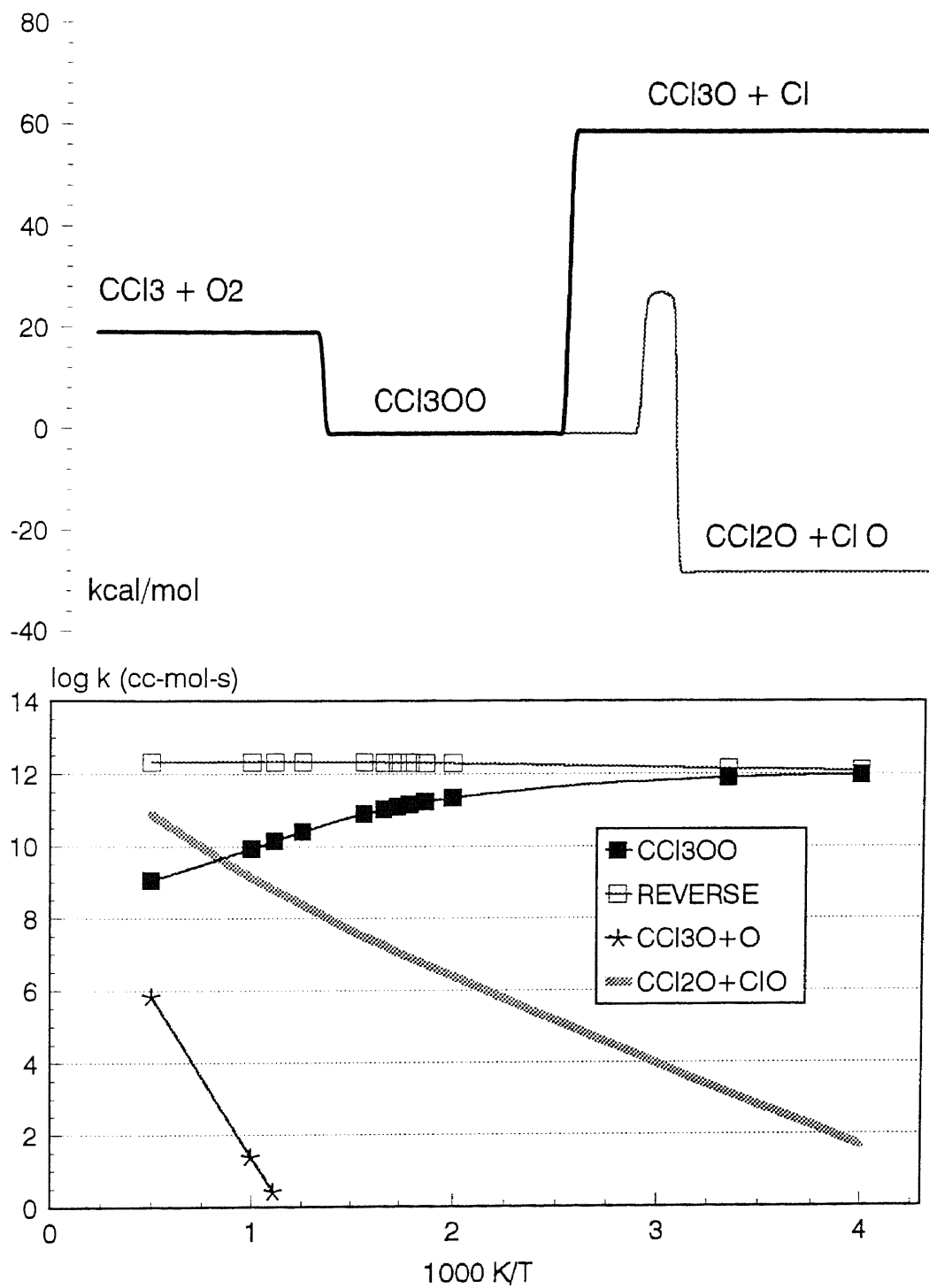


Figure 7.A.9 Potential Energy Diagram and Arrhenius Plot for Reactions:  
 $\text{CCl}_3 + \text{O}_2 \Rightarrow \text{Products}$

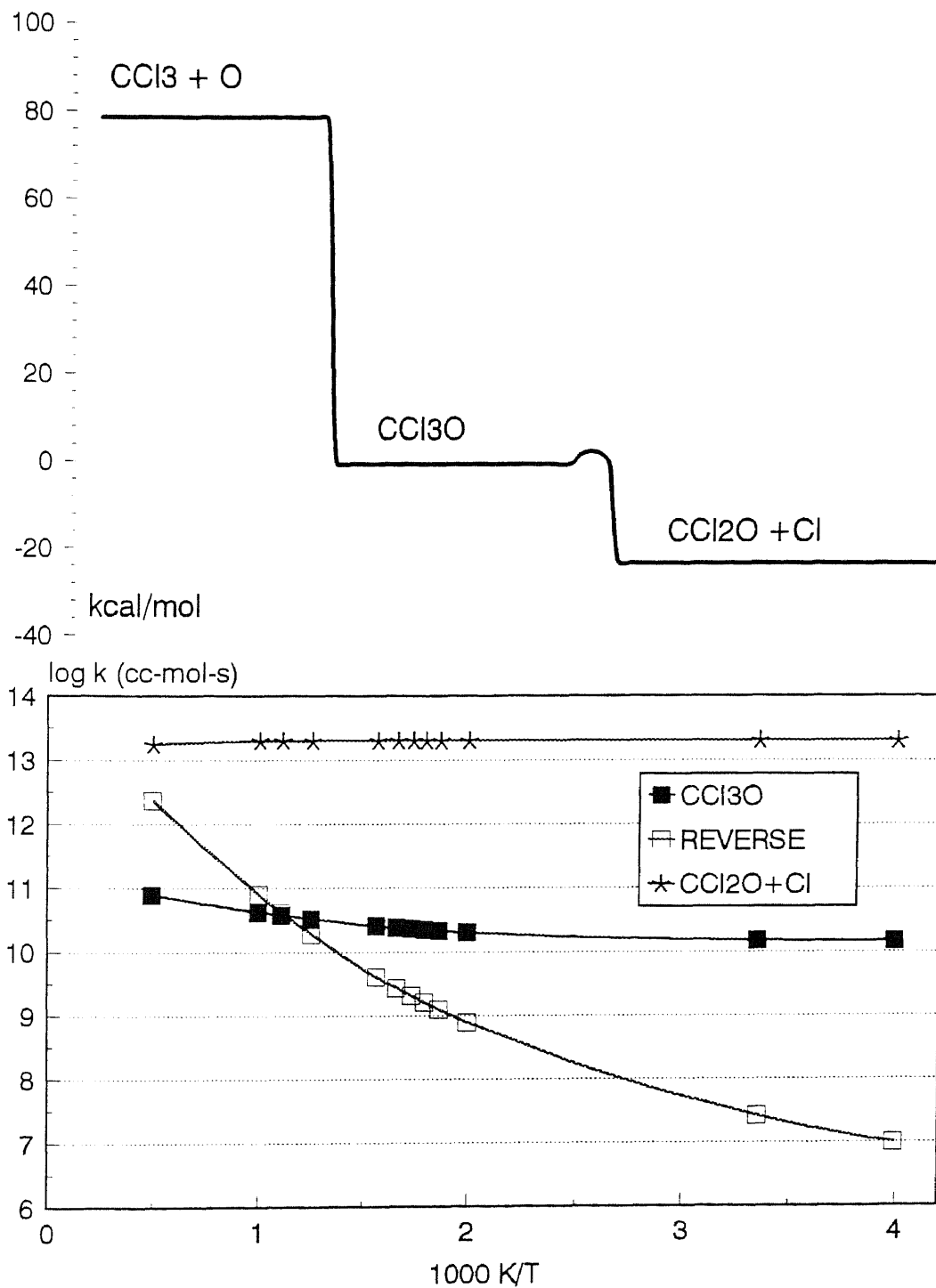


Figure 7.A.10 Potential Energy Diagram and Arrhenius Plot for Reactions:  
 $\text{CCl}_3 + \text{O} \Rightarrow \text{Products}$

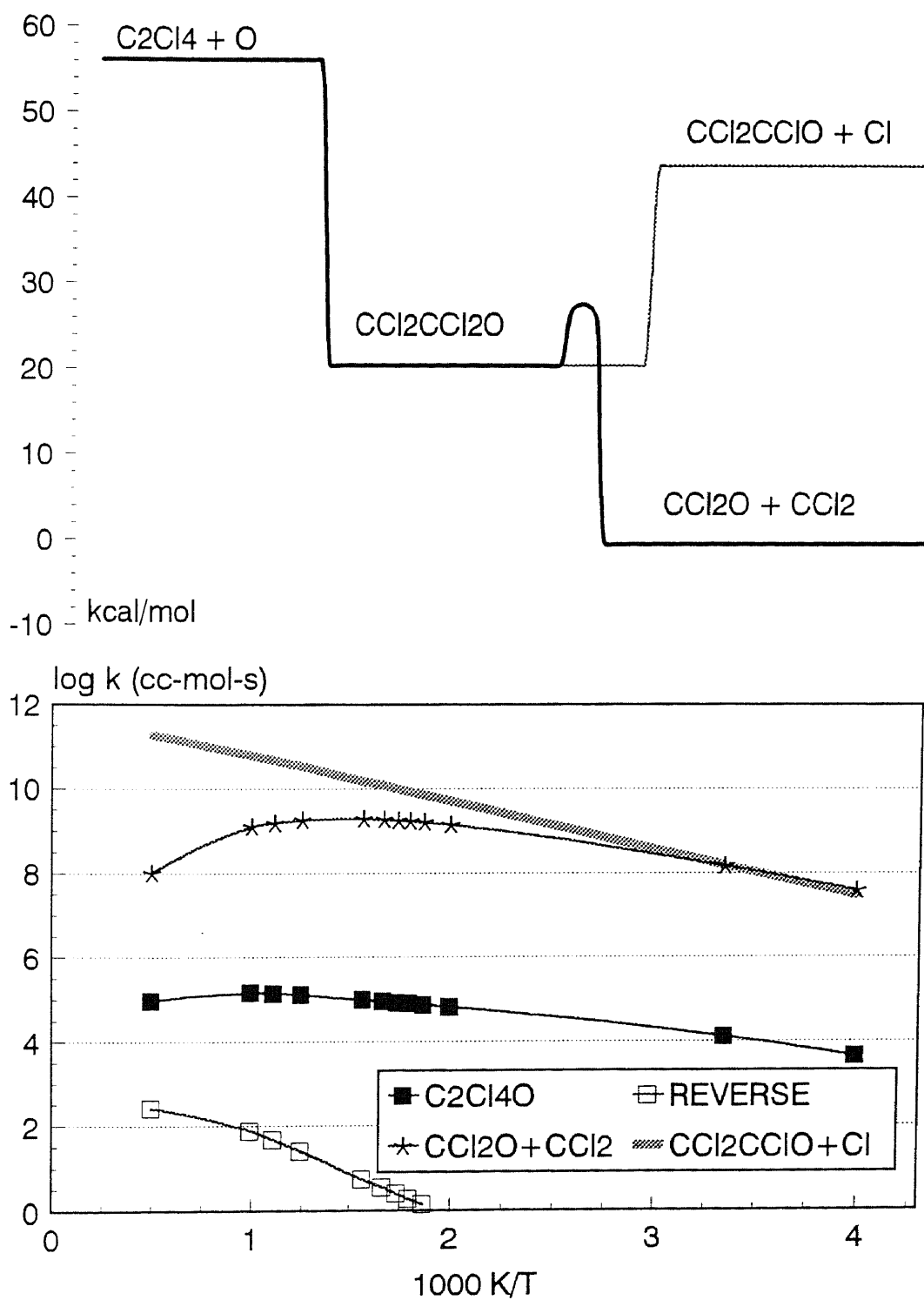


Figure 7.A.11 Potential Energy Diagram and Arrhenius Plot for Reactions:  
 $C_2Cl_4 + O \Rightarrow$  Products

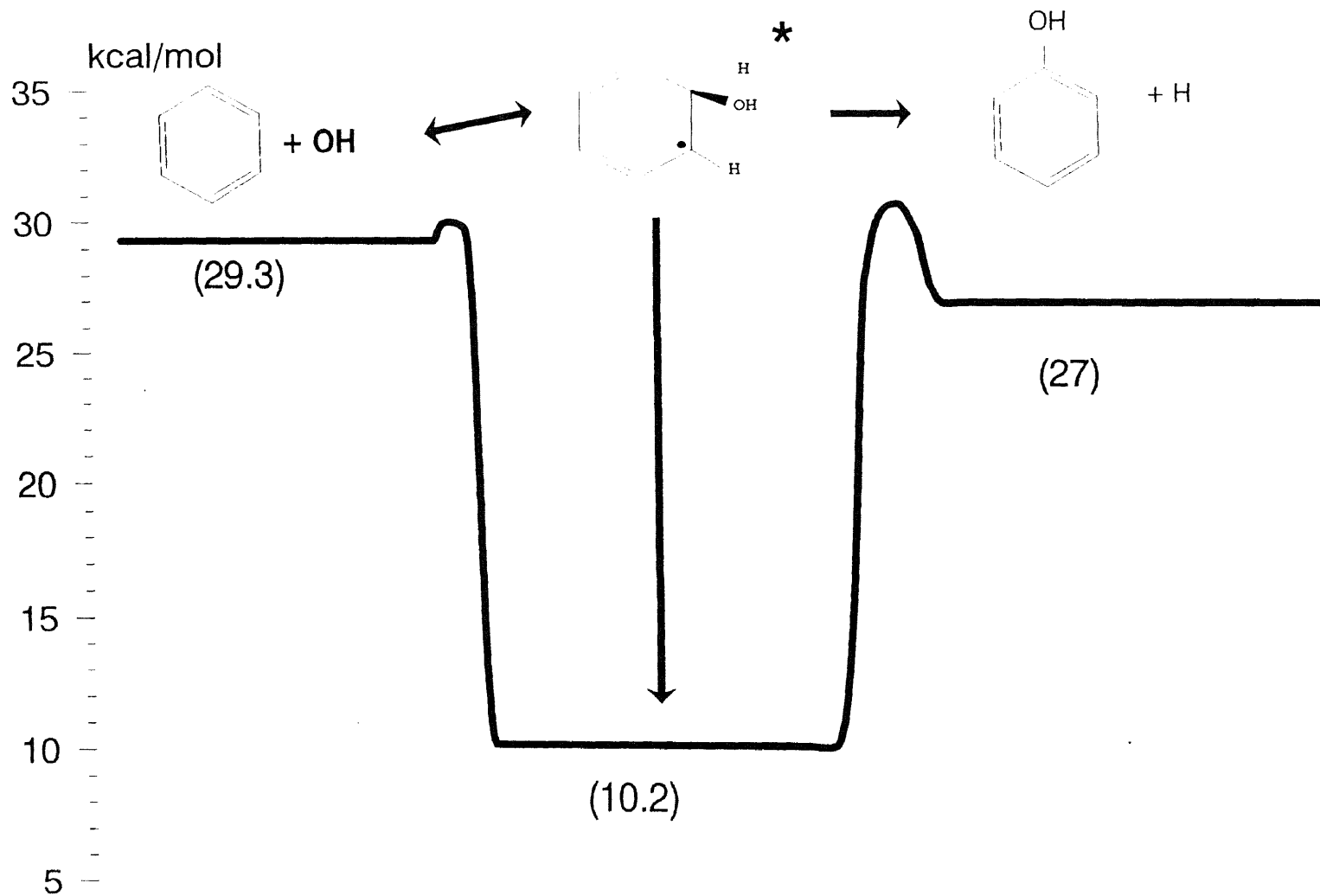


Figure 8.1 Potential Energy Diagram for Benzene + OH

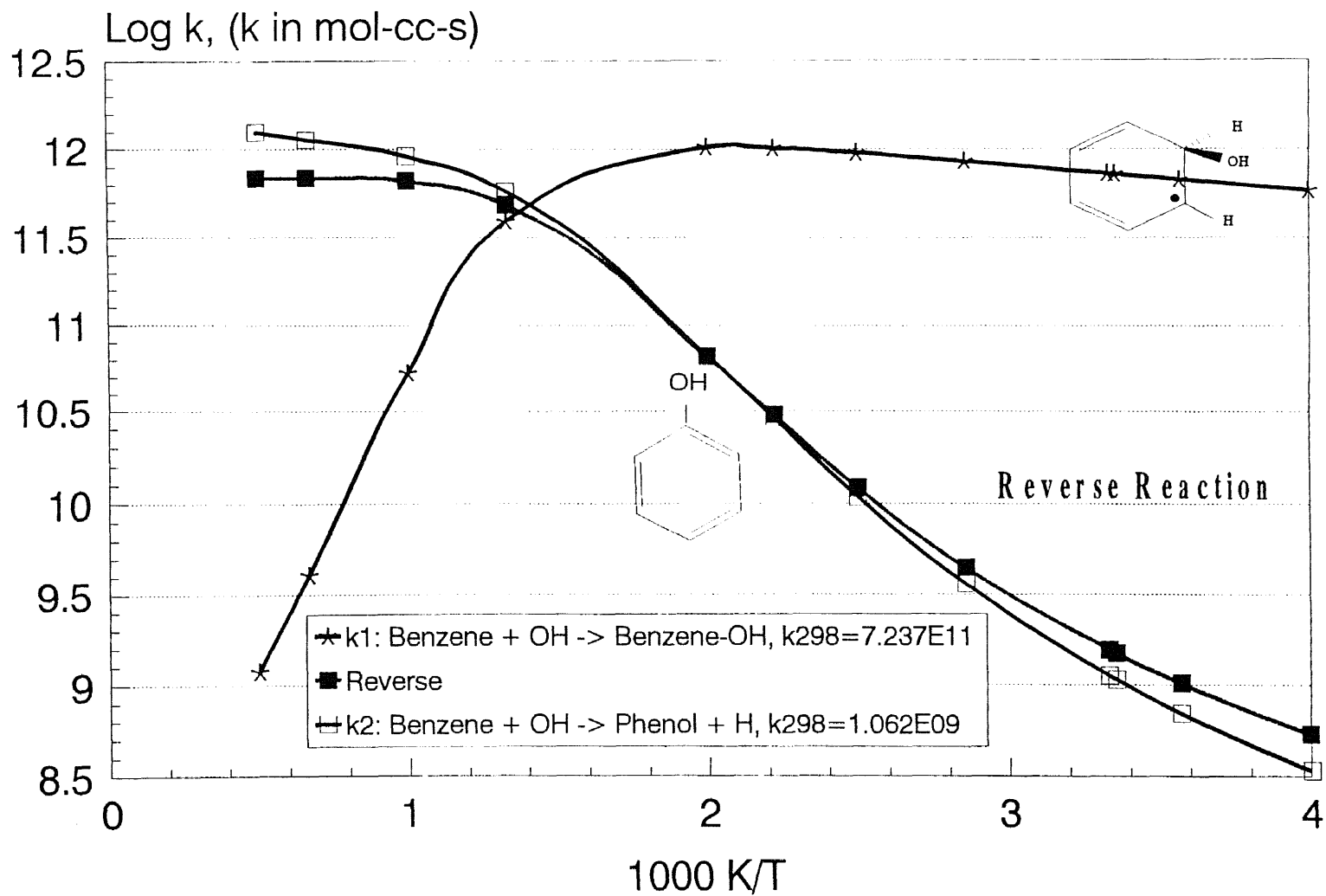


Figure 8.2 Arrhenius Plot of Benzene + OH => Products

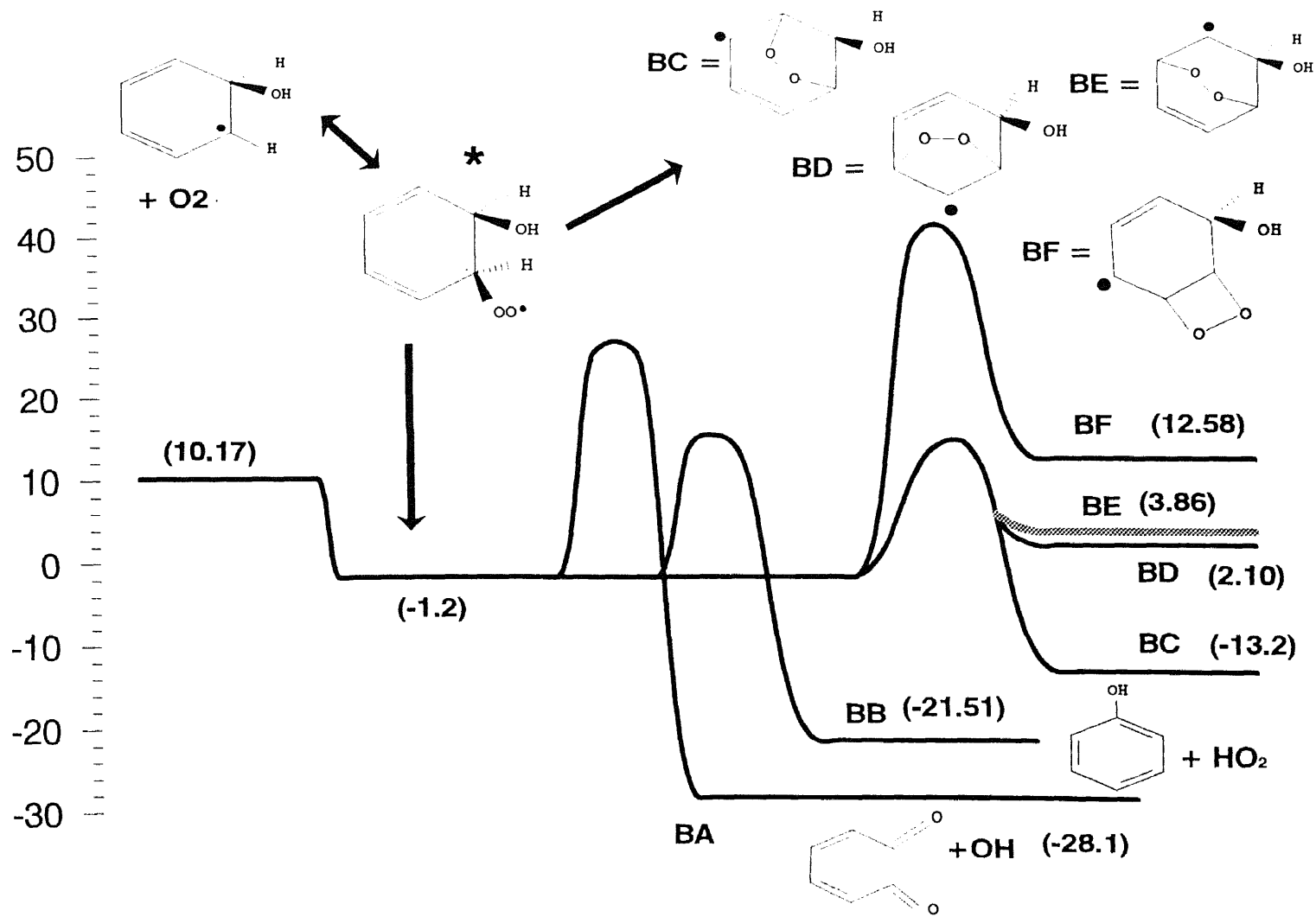


Figure 8.3 Potential Energy Diagram for Benzene-OH adduct + O<sub>2</sub>

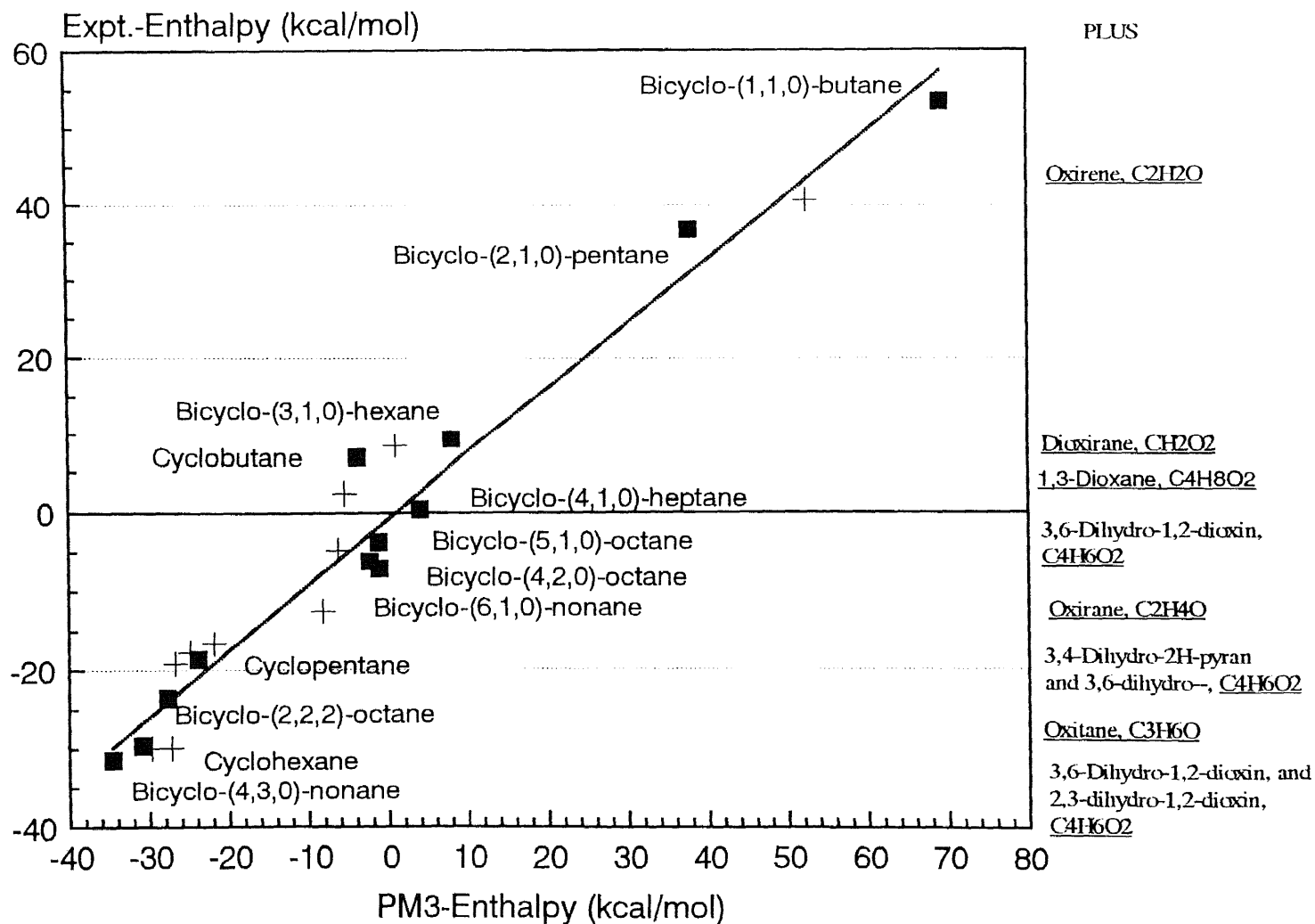


Figure 8.4 Analysis of Correlation Factor for PM3 Enthalpy to Expt. Enthalpy

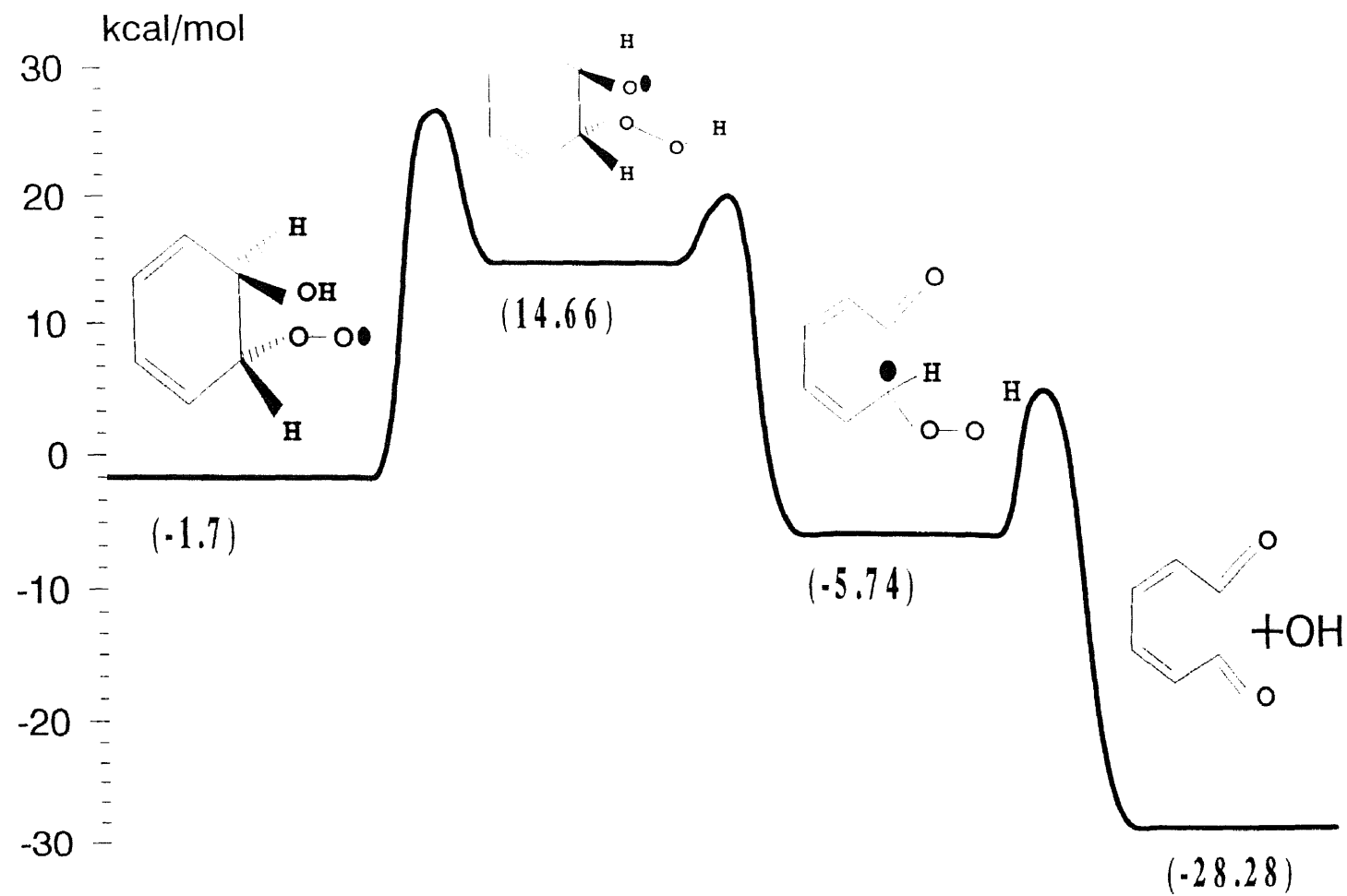


Figure 8.5 Potential Energy Diagram for Channel BA: Benzene-OH-O<sub>2</sub> ⇒ 2,4-hexadiene-1,6-dial + OH



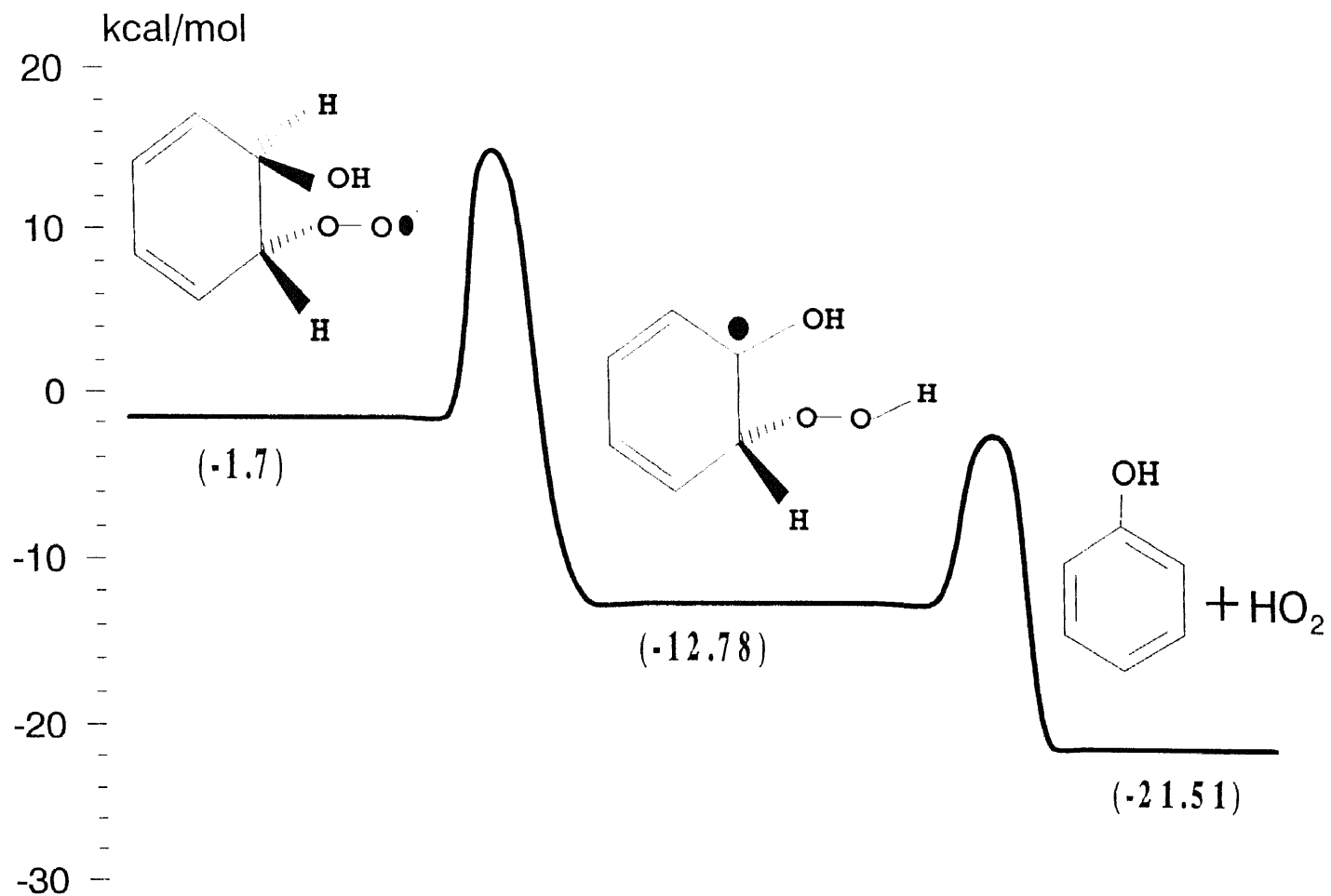


Figure 8.6 Potential Energy Diagram for Channel BB: Benzene-OH-O<sub>2</sub> ⇒ Phenol + HO<sub>2</sub>

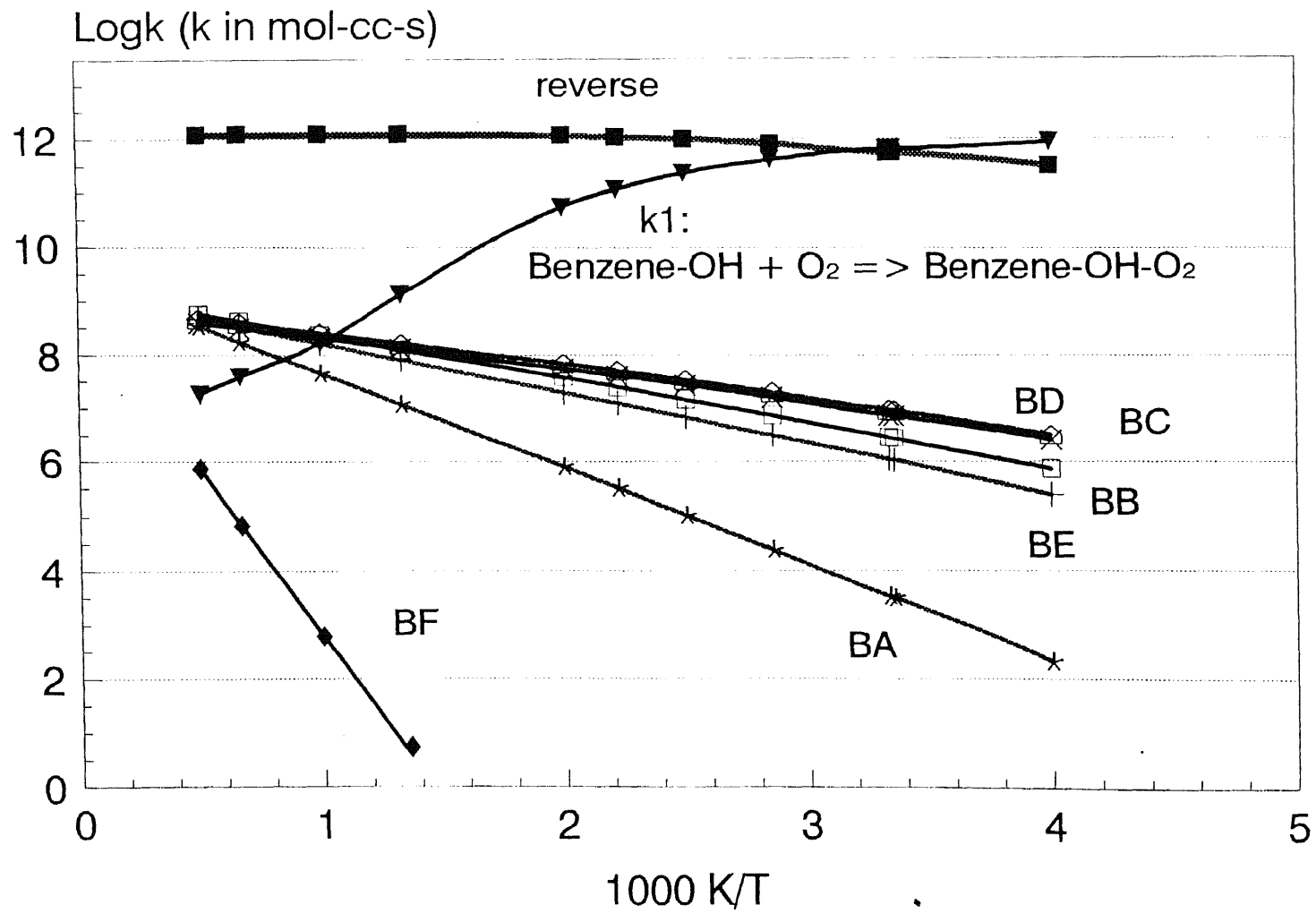


Figure 8.7 Arrhenius Plot of Benzene-OH + O<sub>2</sub> => Products

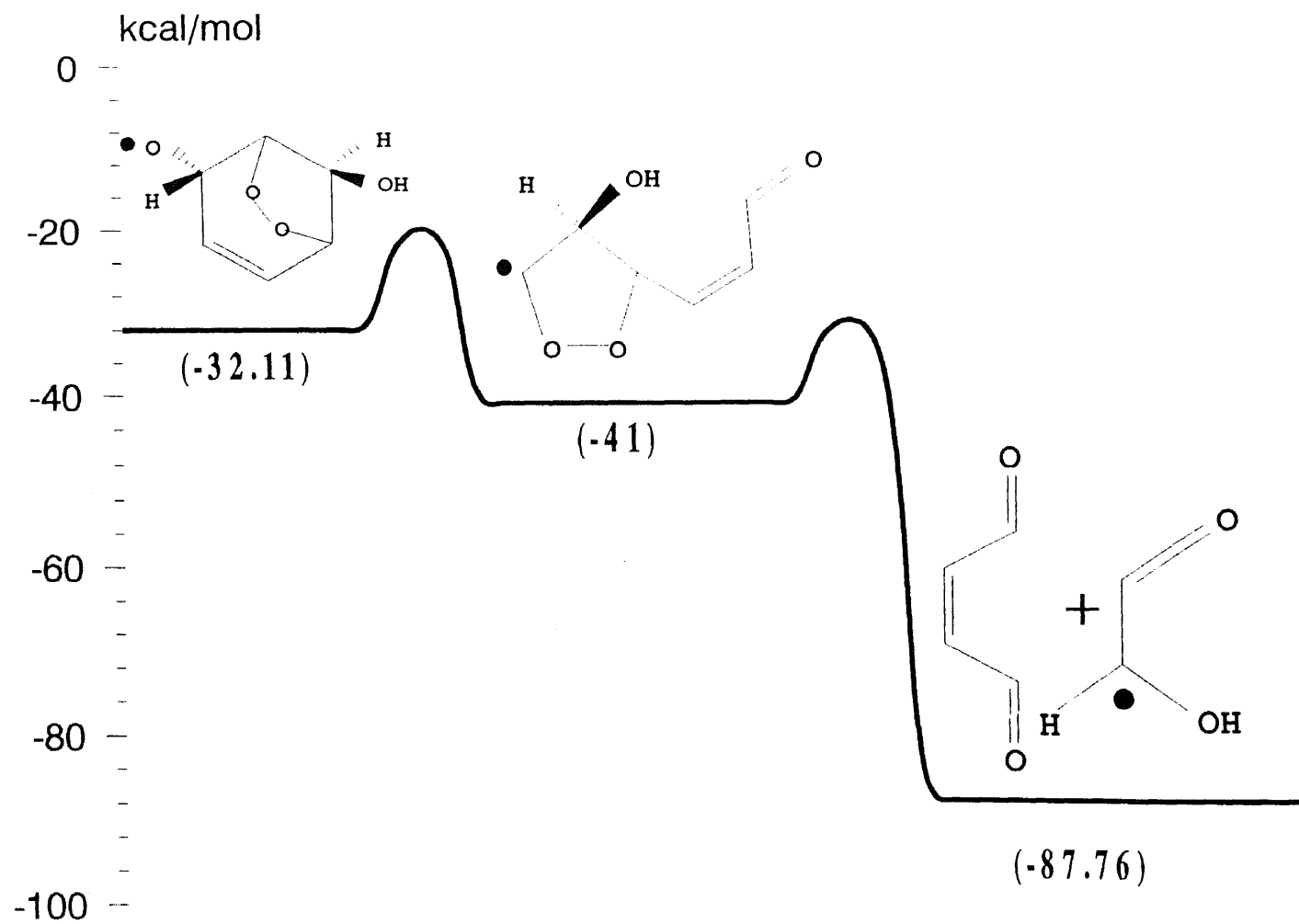


Figure 8.8 Potential Energy Diagram for Adduct IX  $\beta$ -Scission

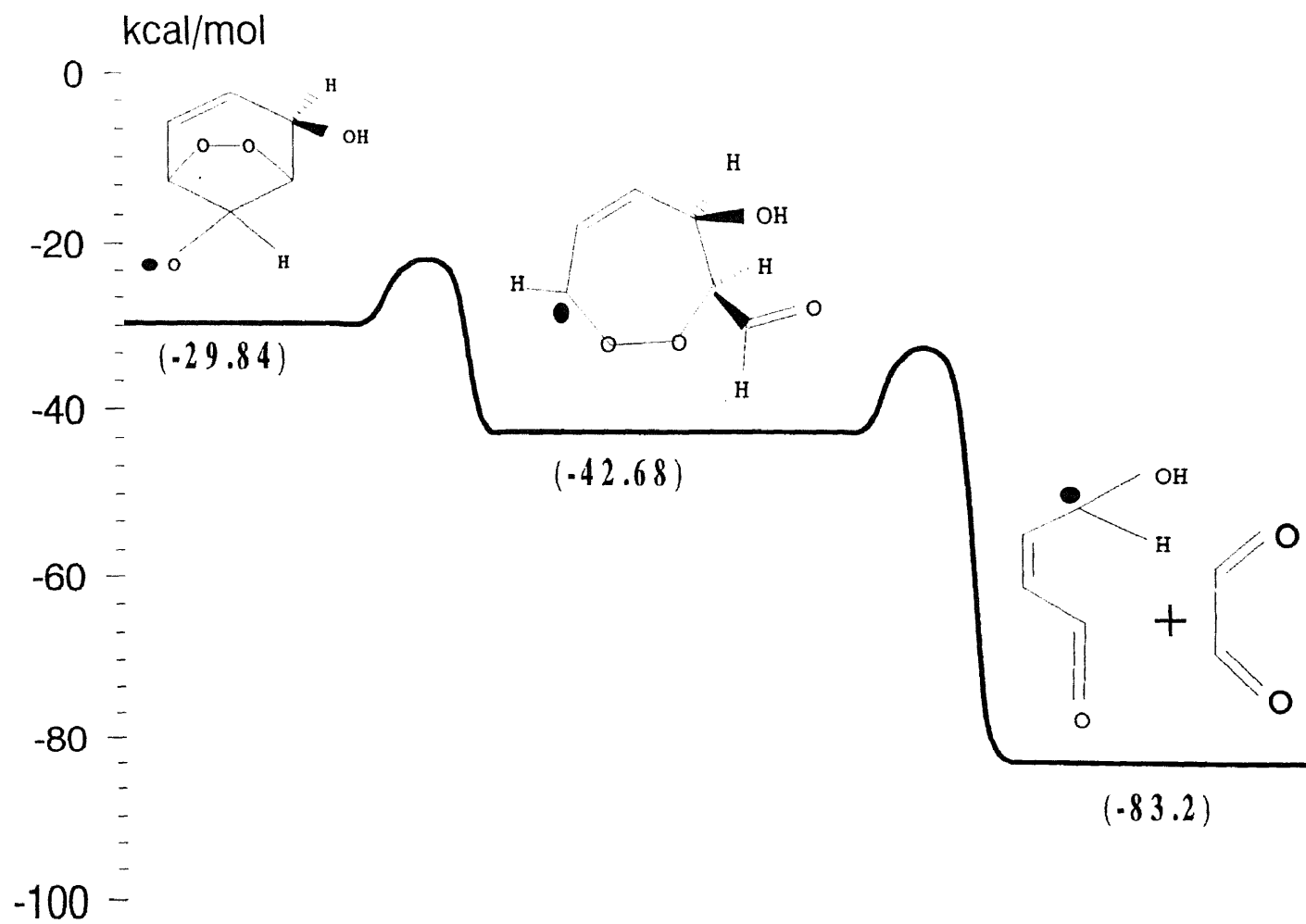


Figure 8.9 Potential Energy Diagram for Adduct X  $\beta$ -Scission

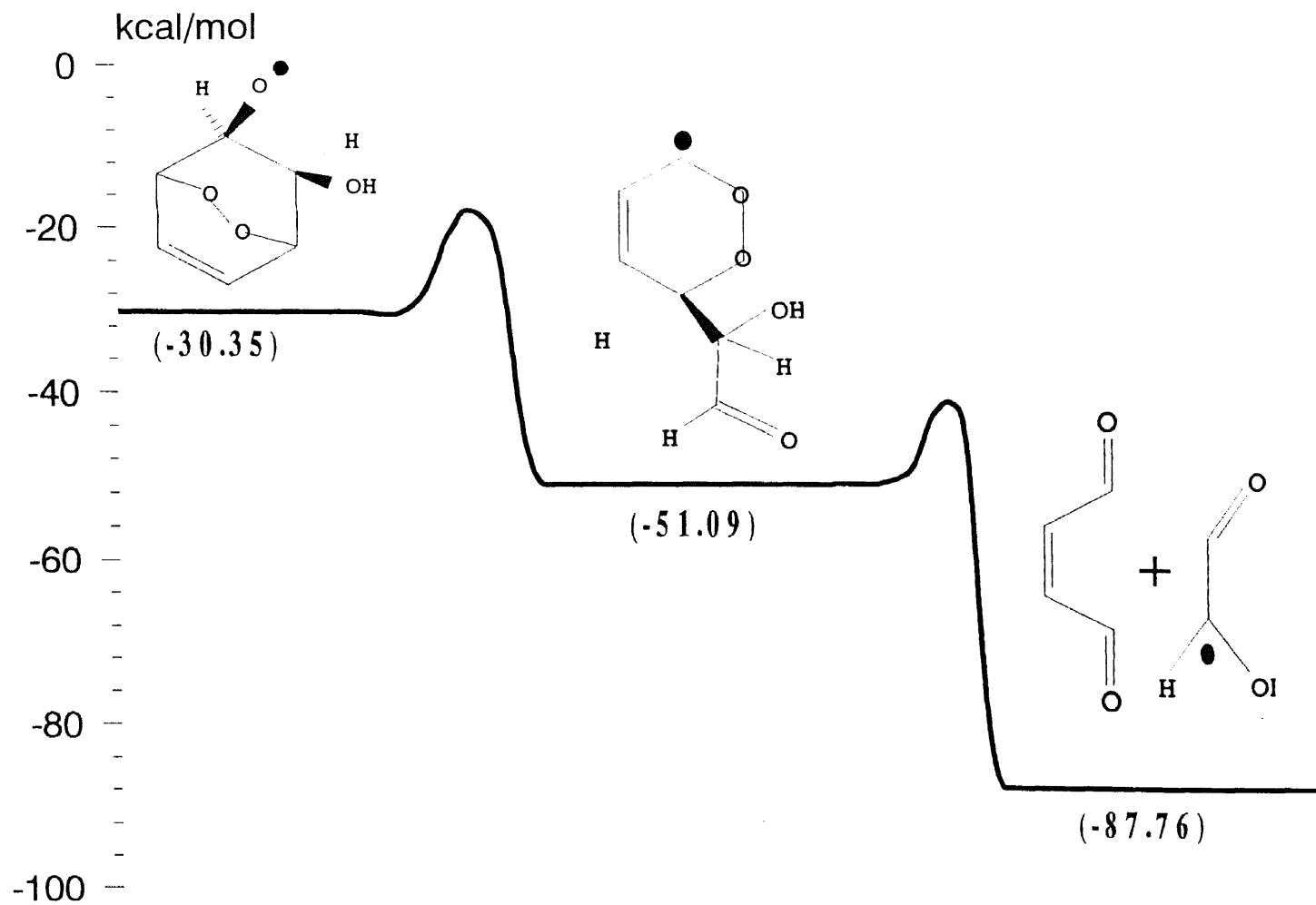


Figure 8.10 Potential Energy Diagram for Adduct XI  $\beta$ -Scission

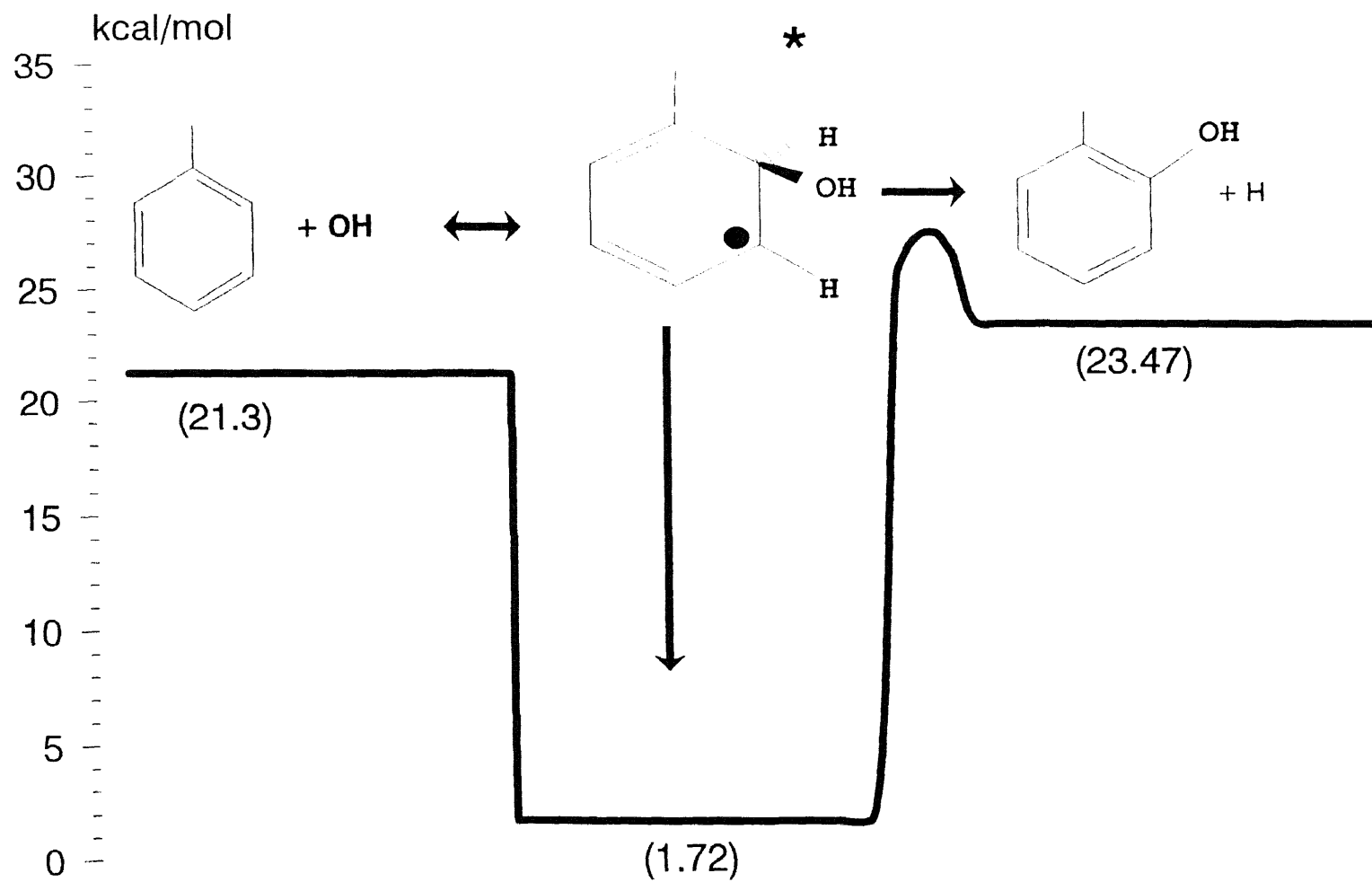


Figure 8.11 Potential Energy Diagram for Toluene + OH

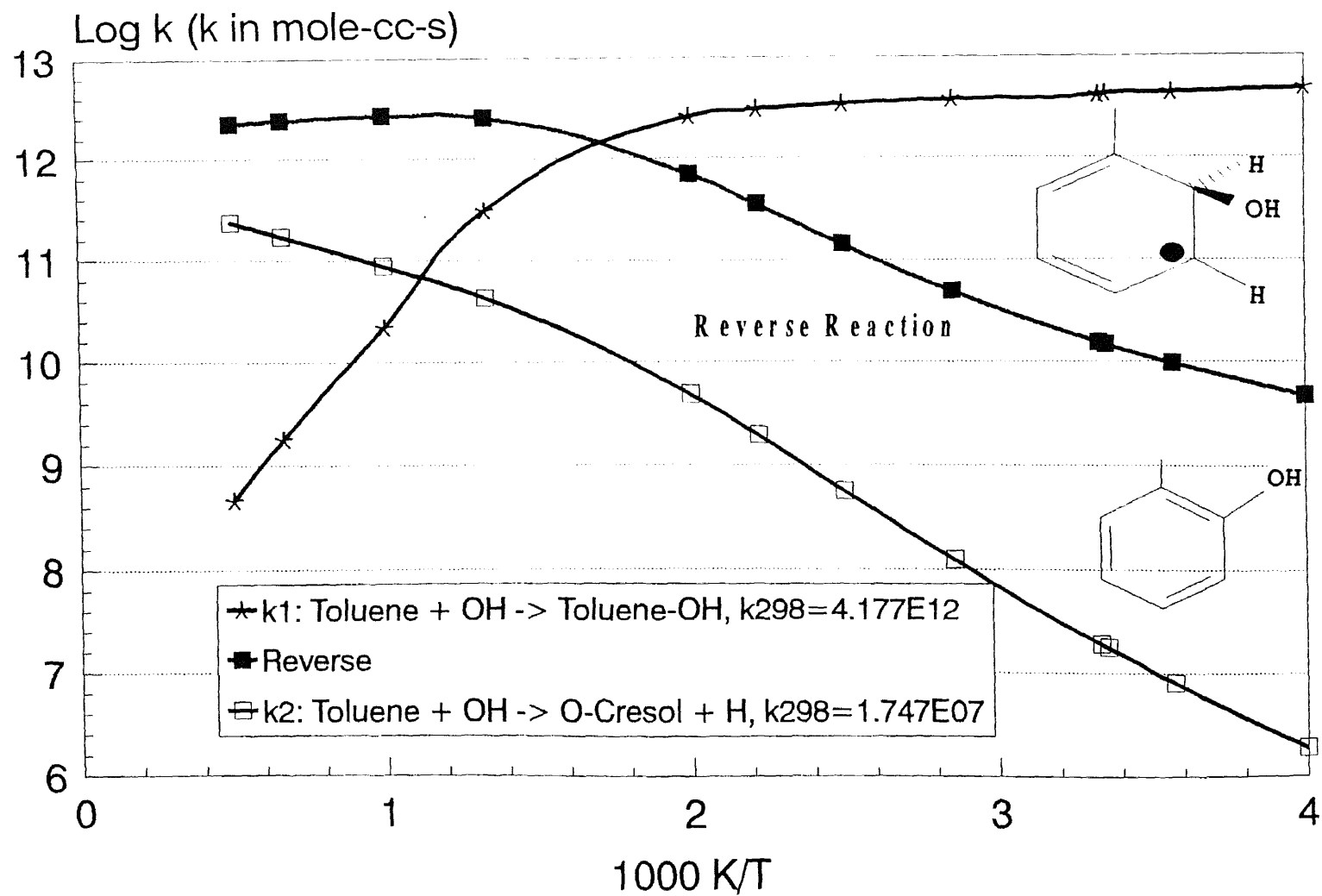


Figure 8.12 Arrhenius Plot of Toluene + OH  $\Rightarrow$  Products

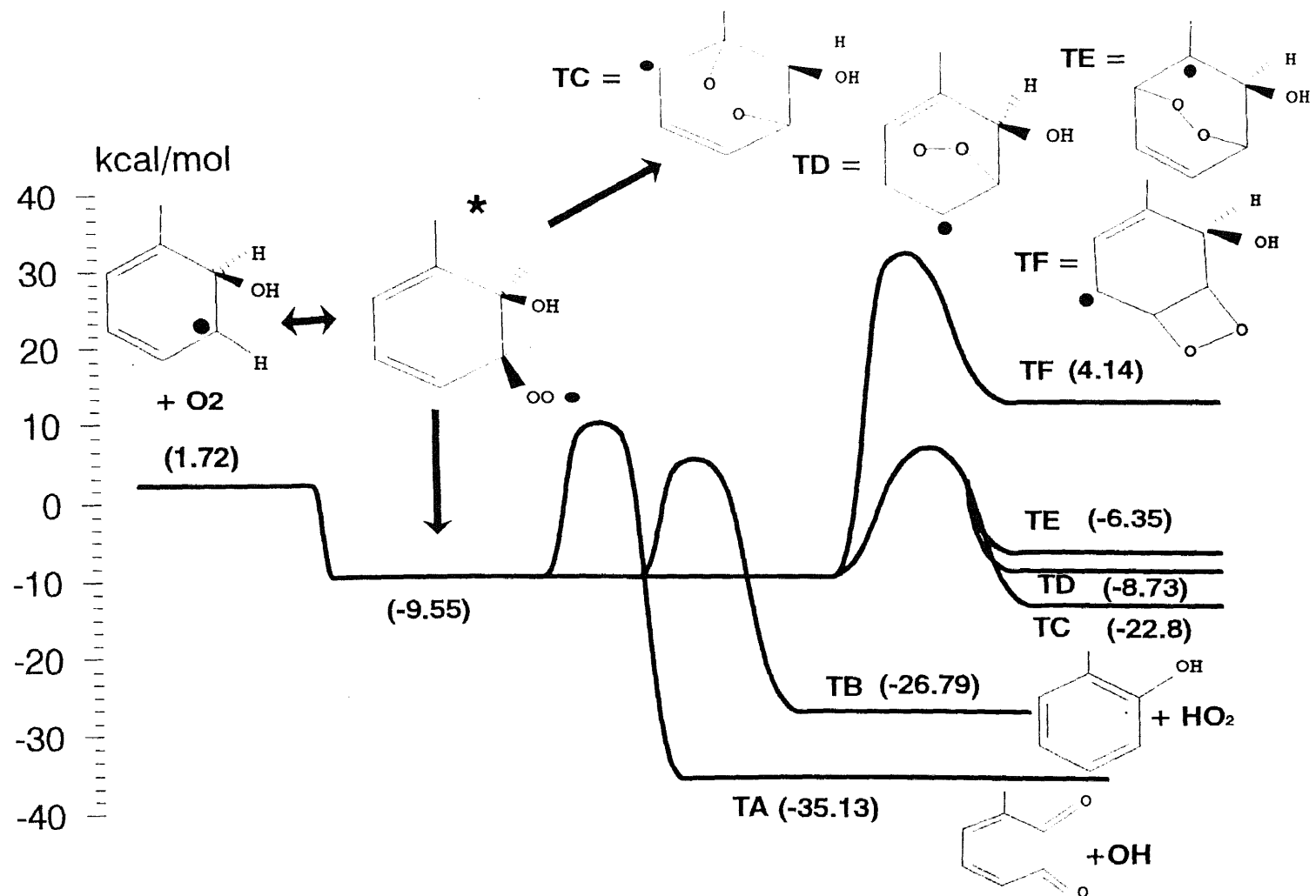


Figure 8.13 Potential Energy Diagram for Toluene-OH Adduct + O<sub>2</sub>



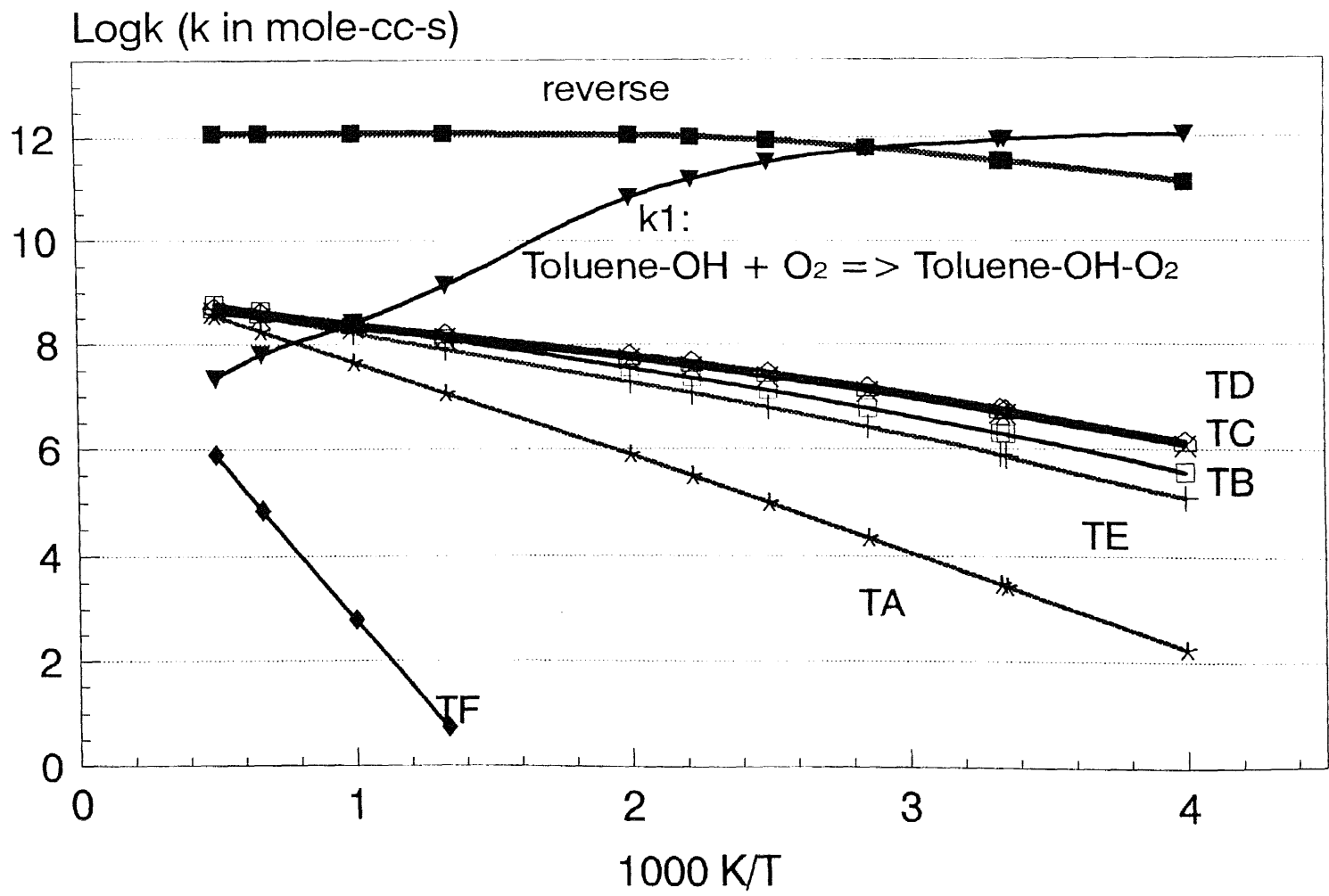


Figure 8.14 Arrhenius Plot of Toluene-OH + O<sub>2</sub> => Products

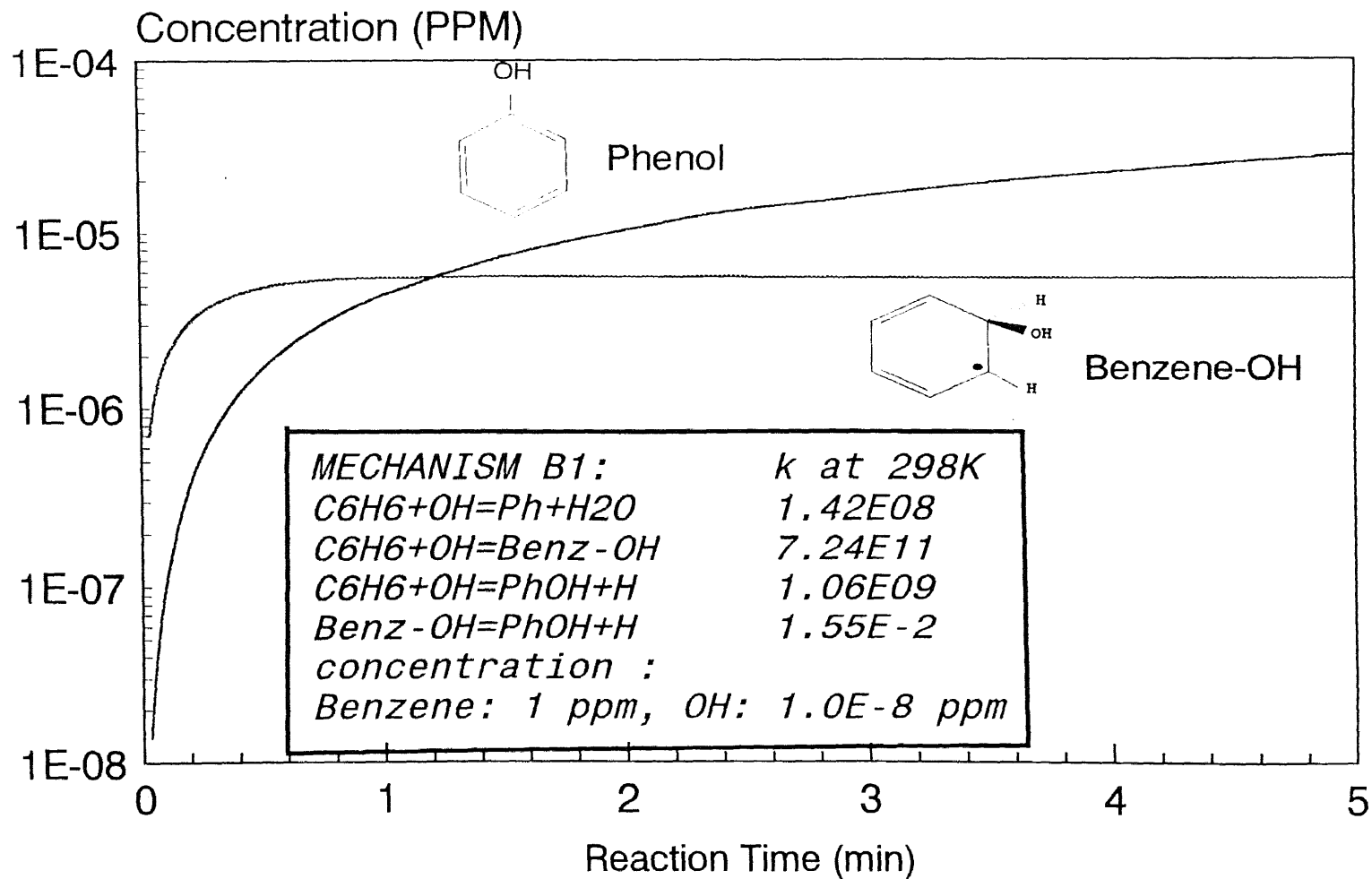


Figure 8.15 Selected Species Profiles of Modeling BM1 (Benzene + OH Initial Steps, Reversible Reactions)

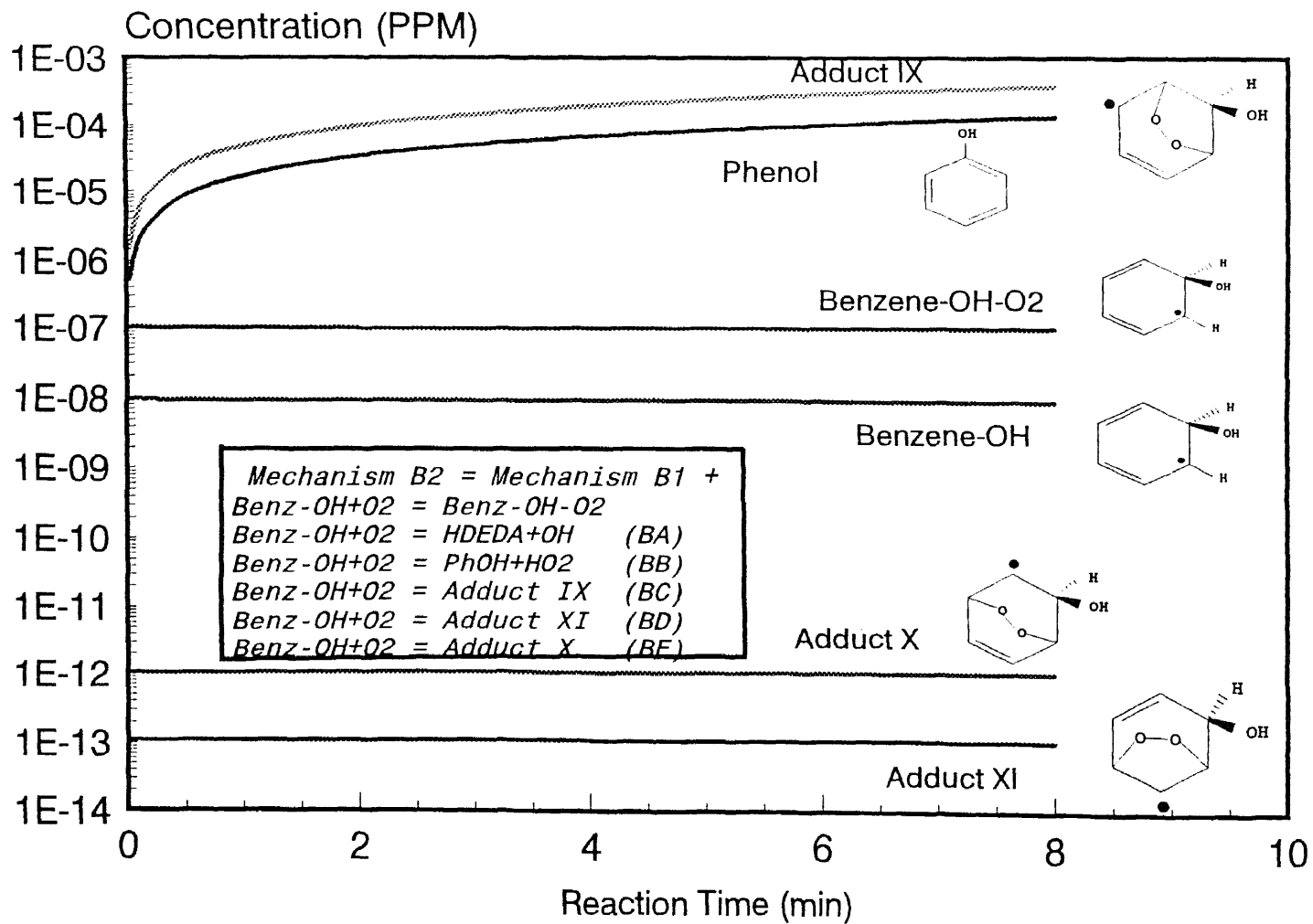


Figure 8.16 Selected Species Profiles of Modeling BM2 (Reactions of Benzene-OH + O2 => products Added)

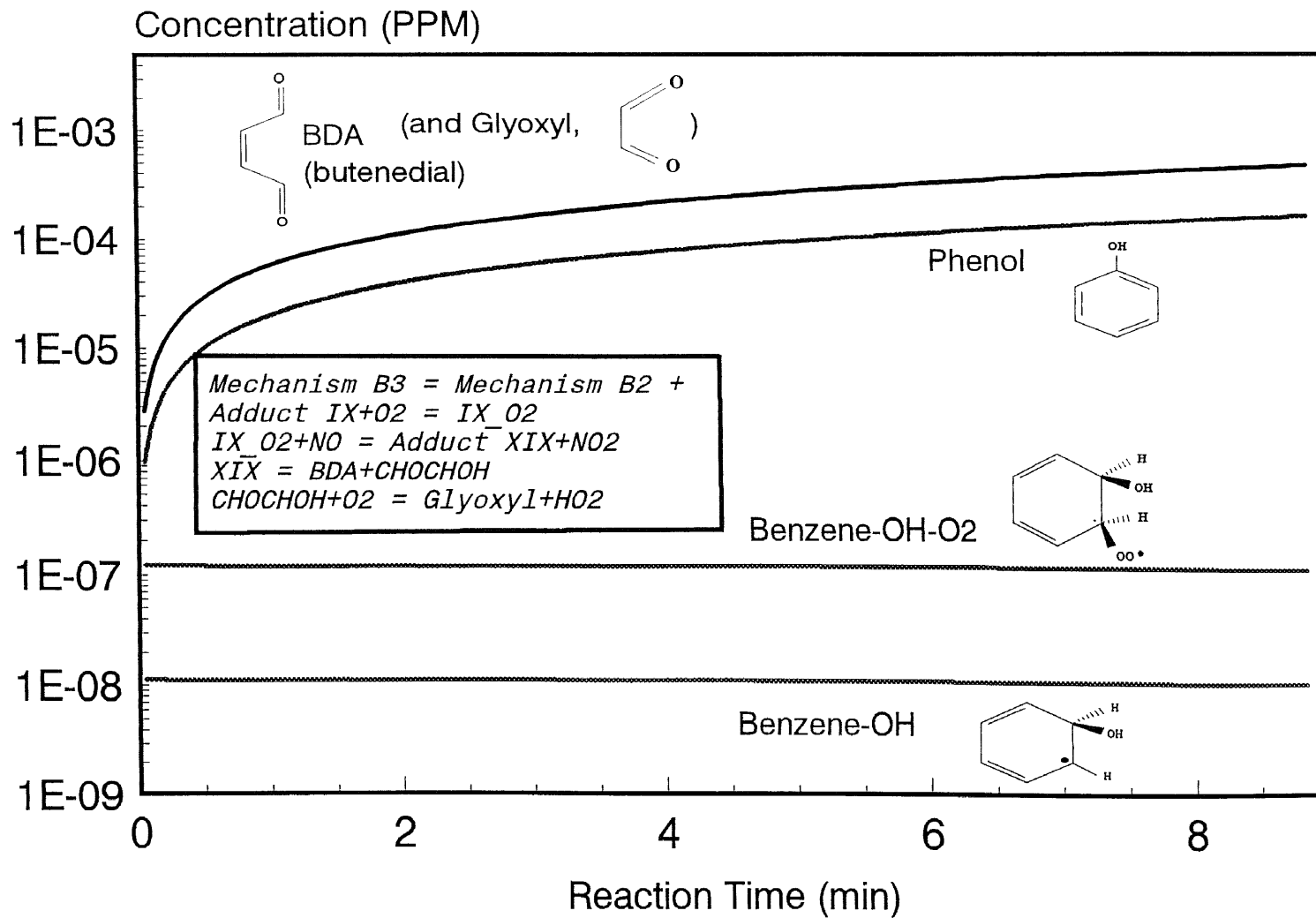


Figure 8.17 Selected Species Profiles of Modeling BM3 (Ring Opening Reactions Included)

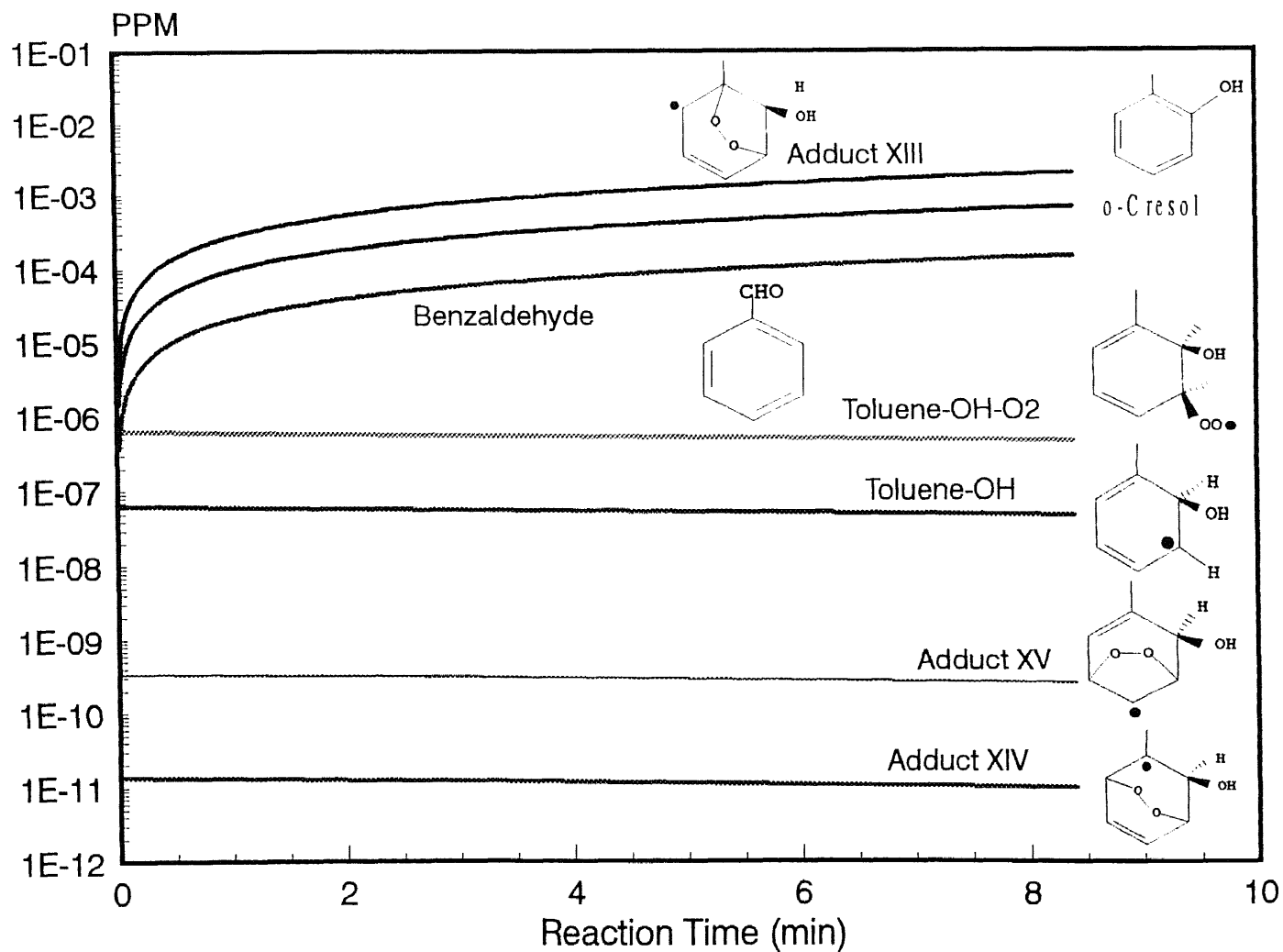


Figure 8.18 Selected Species Profiles of Model TM1 (Ring Opening Reactions Not Included)

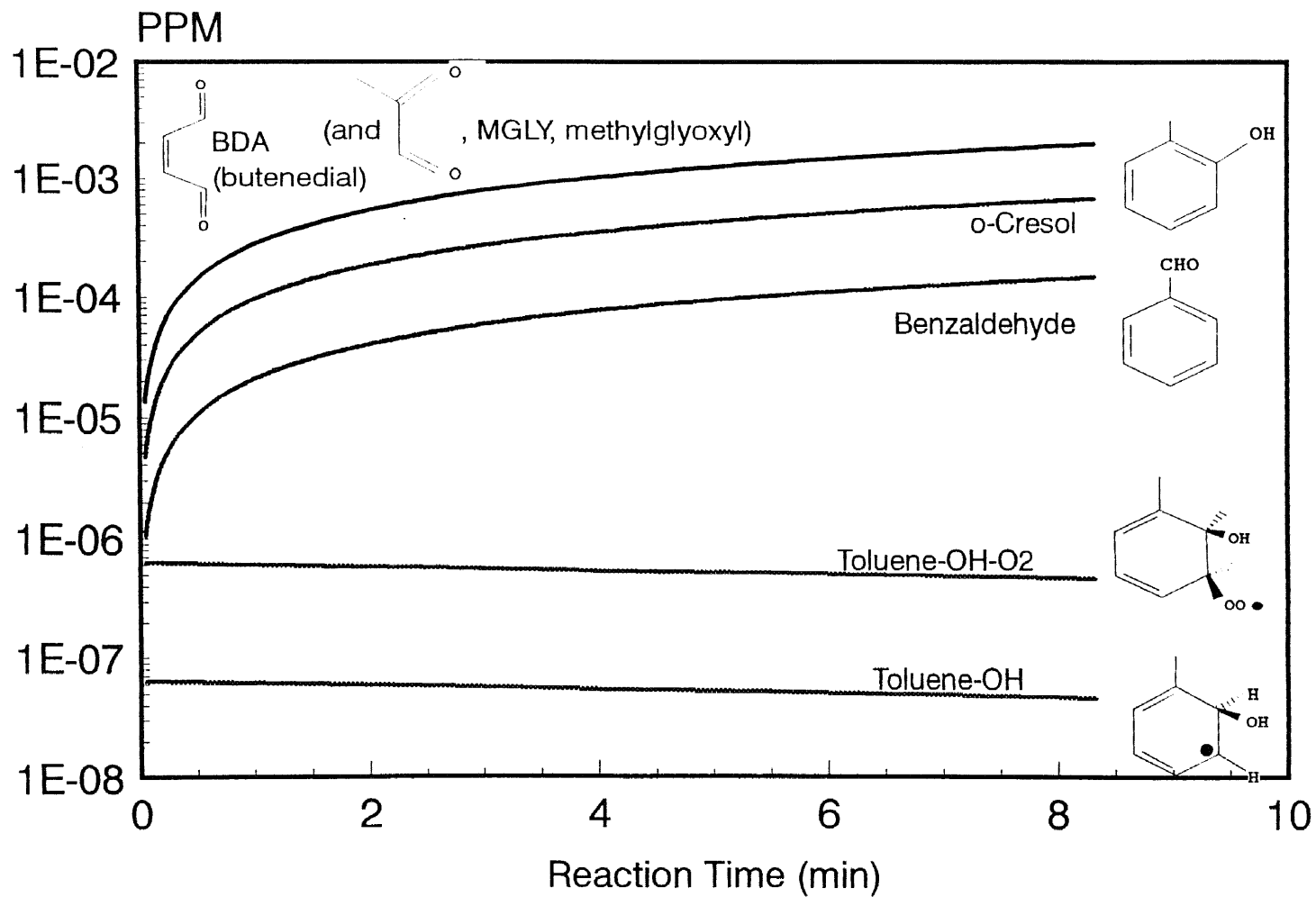


Figure 8.19 Selected Species Profiles of Model TM2 (Ring Opening Reactions Included)

## REFERENCES

### REFERENCES FOR SECTION I

1. Chen, Y., Rauk, A. and Tschuikow-Roux, E., *J. Phys. Chem.* **1990**, *94*, 2775.
2. (a) Bozzelli, J. W.; and Dean, A. M. *J. Phys. Chem.* **1990**, *94*, 3313, (b) *ibid.* **1993**, *97*, 4427, and reference therein.
3. Niki, H., Maker, P. D., Savage, C. M. and Breitenbach, L. P., *J. Phys. Chem.* **1982**, *86*, 3825.
4. Wallington, T. J., Gierzak, C. A., Ball, J. C. and Japar, S. M., *Int. J. Chem. Kinet.* **1989**, *21*, 1077.
5. (1) Wallington, T. J. and Japar, S. M., *Chem. Phys. Letters* **1990**, *166*, 495.  
(2) *ibid.* **1990**, *167*, 513.
6. Fenter, F. F., Catoire, V., Lesclaux, R. & Lightfoot, P. D., *J. Phys. Chem.* **1993**, *97*, 3530.
7. Sahetchian, K. A., Rigny, R. and Tardieu de Maleissye, (*Int'l*) *Combust., Proc.* **1992**, *24*, 637.
8. McQuarrie, D. A., *Statistical Mechanics*, Harper & Row **1976**.
9. (1) Stewart, J. J. P. *J. Comput. Chem.* **1989**, *10*, 209, (2) *ibid.* *10*, 221.
10. Stewart, J. J. P. *MOPAC 6.0 : A General Molecular Orbital Package*, **1990**.  
Frank J. Seiler Research Lab., US Air Force Academy, CO 80840.
11. (1) Pitzer, K. S. *J. Chem. Phys.* **1937**, *5*, 469, (2) *ibid.* **1946**, *14*, 239. (3) Pitzer, K. S.,  
Gwinn, W. D. *J. Chem. Phys.* **1942**, *10*, 428.
12. Gaussian 92, Revision C, M. J. Frisch, G. W. Trucks, M. Head-Gordon, P. M. W.  
Gill, M. W. Wong, J. B. Foresman, B. G. Johnson, H. B. Schlegel, M. A. Robb, E.  
S. Replogle, R. Gomperts, J. L. Andres, K. Raghavachari, J. S. Binkley, C.  
Gonzalez, R. L. Martin, D. J. Fox, D. J. Defrees, J. Baker, J. J. P. Stewart, and J.  
A. Pople, Gaussian Inc., Pittsburgh PA, **1992**.
13. Hehre, W. J., Ditchfield, R. and Pople, J. A., *J. Chem. Phys.* **1982**, *56*, 2257.

14. Harriharan, P. C. and Pople, J. A., *Theor. Chim. Phys. Acta* **1973**, *28*, 213.
15. Frisch, M. J., Pople, J. A. and Binkley, J. S. *J. Chem. Phys.* **1984**, *80*, 3265.
16. Hehre, W. J.; Radom, L.; Schleyer, P. R. and Pople, J. A., *Ab Initio Molecular Orbital Theory* John Wiley & Sons, New York, **1986**, and references therein.
17. (1) Dewar, M. J. S. and Thiel, W., *J. Am. Chem. Soc.* **1977**, *99*, 4899. (2) Dewar, M. J. S., Zoebisch, E. G., Healy, E. F. and Stewart, J. J. P., *J. Am. Chem. Soc.* **1985**, *107*, 3902.
18. Krasnoperov, L. N., Lay, T. H. and Shokhirev, N. V., *Thermodynamic Properties of Hindered rotor by Diagonalization of Hamiltonian Matrix*, to be published.
19. Mizushima, S., *Structure of Molecules and Internal Rotation*, Academic Press, New York, N. Y., **1954**.
20. Lister, D. G., McDonald, J. N. and Owen, N. L., *Internal Rotation and Inversion*, Academic Press, New York, N. Y., **1978**.
21. Radom, L., Hehre, W. J. and Pople, J. A., *J. Am. Soc. Chem.* **1972**, *94*, 2371.
22. Won, Y. S., Ph.D. Dissertation, New Jersey Institute of Technology, Newark, New Jersey, **1991**.
23. Chevalier, C.; Pitz W. J.; Warnatz, J.; Westbrook, C. K.; Melenk, H. *Twenty Fourth Symposium (International) on Combustion*, The Combustion Institute, **1992**, 93.
24. Paulson, S. E.; Seinfeld, J. H. *J. Geophysical Research* **1992**, *97*, 20703.
25. Carter, W. P.; and Atkinson, R. *Environ. Science and Technol.* **1989**, *23*, 864.
26. (a) Washington, W. M.; and Meehl, G. A. *Climate Dynamics* **1989**, *1*, 39; (b) Stauffer, R. J.; Manabe, S.; Byron, K. *Nature* **1989**, 342, 660.
27. Ho, W. P.; Wu, Y. P.; Bozzelli, J. W. *Combustion Science and Technology* **1992**, *83*, 23.
28. Hu, H.; Keck, J., *SAE Paper* **1987**, 872110.
29. Morley C. *Combust. Sci. and Tech.* **1987**, *55*, 115.
30. Griffiths, J.F. *Combust. Flame* **1991**, *93*, 202.



31. Summerfield, M and Kuo, K., (Ed.) *Fundamentals of Solid Propellant Combustion* (1984).
32. Benson, S. W., *Thermodynamic Kinetics* ( 2nd ed.) Wiley-Interscience, New York, 1976.
33. Reid, R. C.; Prausnitz, J. M.; Sherwood, T. K., *The Properties of Gases and Liquids*, McGraw-Hill Co., New York, 1979.
34. Cohen, N., *J. Phys. Chem.* 1992, 96, 9052.
35. Pedley, J. B., Naylor, R. D. and Kirby, S. P., *Thermochemical Data of Organic Compounds*, (2nd Ed.), Chapman and Hall, 1986.
36. (a) Freedman, E. and Seaton, W. H., USA Ballistic Research Lab. Memorandum Report No. 2320, Aberdeen Proving Ground, Maryland, 1973.  
(b) Frurip, D. J., Freedman, E. and Hertel, G. R., *Int'l Symp. on Runway Reactions* (Proc.), Cambridge, Massachusetts, 1989.  
(c) Muller, C., Scacchi, G. and Come, G. M., AICHE 77th Annual Meeting, San Francisco, California, 1984.
37. Ritter, E. R. and Bozzelli, J. W., *Int. J. Chem. Kinet.* 1991, 23, 767.
38. Shaw, R. and Benson, S. W., *Organic Peroxides*, Vol. 1 (Edited by Sween, D.), Wiley-Interscience, New York-London, 1970.
39. Cohen, N. and Benson, S. W., *Chem. Rev.* 1993, 93, 2419.
40. Pacansky, J. and Schrader, B., *J. Chem. Phys.* 1983, 78, 1033.
41. Chen, Y., Rauk, A. and Tschuikow-Roux, E., *J. Chem. Phys.* 1990, 93, 1187.
42. (a) Mizushima, S., *Structure of Molecules and Internal Rotation*, Academic Press, New York, N. Y., 1954.  
(b) Lister, D. G., McDonald, J. N. and Owen, N. L., *Internal Rotation and Inversion*, Academic Press, New York, N. Y., 1978.
43. Schimanouchi, T., *Tables of Molecular Vibrational Frequencies*, Consolidated Vol. I., NSRDS-NBS39, 1977.
44. Pacansky, J. and Coufal, H., *J. Chem. Phys.* 1980, 72, 3298.
45. Schrader, B., Pacansky, J. and Pfeiffer, U., *J. Phys. Chem.* 1984, 88, 4069.
46. Chen, Y., Rauk, A. and Tschuikow-Roux, E., *J. Phys. Chem.* 1990, 94, 6250.

47. Kiefer, J. H., Sidhu, S. S., Kern, R. D., Xie, K., Chen, H. and Harding, L. B., *Combust. Sci. and Tech.* **1992**, *82*, 101.
48. HyperChem computer package, Release 3 (a molecular modeling and simulation program), Autodesk, Inc., Publication 102836, **1993**.
49. Wu, C. J. and Carter, E. A., *J. Phys. Chem.* **1991**, *95*, 8352.
50. (a) Ervin, K. M., Gronert, S., Barlow, S. E., Gilles, M. K., Harrison, A. G., Bierbaum, V. M., Depuy, C. H., Lineberger c., Ellison, B., *J. Am. Chem. Soc.* **1990**, *112*, 5750;  
(b) Curtiss, L. A., and Pople, J. A., *J. Chem. Phys.* **1988**, *88*, 7405;  
(c) Defrees, D. J., McIver Jr, R. T., Hehre, W. J., *J. Am. Chem. Soc.* **1980**, *102*, 3334.
51. Miller, J. A. and Melius, K. F., *Twenty Fourth Symposium (International) on Combustion*, The Combustion Institute, **1992**, 93.
52. Wilberg, K. B., *Advance in Molecular Modeling*, Volume 1, pages 101-134, JAI Press Inc., **1988**.
53. Kee, R. J., Miller, J. A. and Jefferson, T. H., *CHEMKIN: Fortran Chemical Kinetics Code Package*, Sandia Report, SAND80-8003. UC-4 (1980)
54. (a) McBride, B. J. and Gordon, S., *Fortran IV Program for Calculation of Thermodynamic Data*, NASA Report TN-D 4097.  
(b) McBride, B. J., *Computer Program for Calculating and Fitting Thermodynamic Functions*, NASA Report RP 1271.
55. Stull, D. R.; Westrum, E. F., Jr.; Sinke, G. C. *The Chemical Thermodynamics of Organic Compounds*, Robert E. Krieger Publishing Co., Inc., Malabar, **1987**.
56. Coolidge, M. B.; Marlin, J. E.; Stewart, J. J. P. *J. Comp. Chem.* **1991**, *112*, 948.
57. Hu, H.; Keck, J., SAE Paper **1987**, 872110.
58. Morley C., *Combust. Sci. and Tech.* **1987**, *55*, 115.
59. Griffiths, J.F., *Combust. Flame* **1991**, *93*, 202.
60. Baldwin, A. C., 'Thermochemistry of Peroxides' (Ch.3) in *The Chemistry of Functional Groups, Peroxides*, Patai, S.(ed.), John Wiley & Sons Ltd., New York, **1983**.

61. (a) Freedman, E. and Seaton, W. H., USA Ballistic Research Lab. *Memorandum Report No. 2320*, Aberdeen Proving Ground, Maryland 1973. (b) Frurip, D. J., Freedman, E. and Hertel, G. R., *Int'l Symp. on Runway Reactions (Proc.)*, Cambridge, Mass, 1989. (c) Muller, C., Scacchi, G. and Come, G. M., AICHE 77th Annual Meeting, San Francisco, 1984. (d) Ritter, E. R. and Bozzelli, J. W., *Int'l J. Chem. Kin.* **1991**, *23*, 767.
62. Benson, S. W., *J. Am. Chem. Soc.*, **1965**, *87*, 972.
63. Batt, L., *Int. Rev. Phys. Chem.* **1987**, *6*, 53.
64. Francisco, J. S., Williams, I. H., *Int. J. Chem. Kinet.*, **1989**, *20*, 455; TABLE II and references therein.
65. Slagle, I. R., Feng, Q. and Gutman, D., *J. Phys. Chem.* **1984**, *88*, 3648.
66. Wagner, A. F., Slagle, I. R., Dariusz Sarzynski, D. and Gutman D., *J. Phys. Chem.* **1990**, *94*, 1853.
67. Slagle, I. R., Bensburg, A., Xing, S.-B. and Gutman, D., *Symp. (Int'l) Combust., Proc.* **1992**, *24*, 653.
68. Boyd, S. L., Boyd, R. J. and Barclay, R. C., *J. Am. Chem. Soc.*, **1990**, *112*, 5724. and refernce therein.
69. Melius, C. F., *BAC-MP4 Heats of Formation and Free Energies 1993*, Sandia National Laboratories, Livermore, California.
70. Silo, B. J., *J. Chim. Phys.* **1979**, *76*, 21.
71. Dewar, M. J. S., Ford, G. P., *J. Am. Chem. Soc.* **1977**, *99*, 1685.
72. Dewar, M. J. S., Ford G. P., Mckee, M., Rzepa, H. S., Yamaguchi, Y., *J. Mol. Struct.* **1978**, *43*, 135.
73. Benassi, R., Folli, U., Sbardellati, S. and Taddei, F., *J. Comp. Chem.* **1993**, *4*, 379, and references therein.
74. Cremer, D., *J. Chem. Phys.* **1978**, *69*, 440.
75. Hunt, R. H., Leacock, R. A., Peters, C. W. and Hecht, K. T., *J. Chem. Phys.* **1965**, *42*, 1931.
76. Redington, R. L., Olson, W. B. and Cross, P. C., *J. Phys. Chem.* **1962**, *36*, 1311.

77. Khachkuruzov, G. A. and Przhevalskii, I. N., *Spectrosk.* **1974**, *36*, 172.
78. Francisco, J. S., Sander, S. P., Lee, T. J. and Redell, A. P., *J. Phys. Chem.* **1994**, *98*, 5644.
79. Tyblewsky, M., Meyer, R. and Bauder, A., *8th Colloquium on High Resolution Molecular Spectroscopy*, Tours, France, **1983**.
80. Chen, K. and Allinger, M. L., *J. Comp. Chem.* **1993**, *7*, 755, and references therein
81. Christen, D., Mack, H.-G. and Oberhammer, H., *Tetrahedron*, **1988**, *44*, 7363.
82. Stathis, E. C. and Egerton, *Trans. Faraday Soc.* **1940**, *36*, 606.
83. Benson, S. W., *J. Chem. Phys.* **1964**, *40*, 1007.
84. Pople, J. A. and Beveridge, D. L., *Approximate Molecular Orbital Theory*, McGraw-Hill, New York (1970).
85. Ohkubo, K., Fujita, T. and Sato, H., *J. Mol. Struct.* **1977**, *36*, 101.
86. Pulay, P. In *Applications of Electronic Structure Theory*; Schaefer, H. F.; III, Ed.; Plenum Press: New York, **1977**; p 153.
87. Schlegel, H. B., "Geometry Optimization on Potential Energy Surfaces", in *Modern Electronic Structure Theory*, Yakony, D. R. (ed.), Word Scientific Publishing, **1993**.
88. Seakins, P. W., Pilling, M. J., Nitranen, J. T., Gutman, D., Krasnoperov, L. N., *J. Phys. Chem.* **1992**, *96*, 9847,
89. Chapter 3 of this dissertation for  $\Delta H_f^\circ_{298}$  of  $\text{CH}_3\text{OOH}$  and  $\text{D}^\circ\text{H}(\text{ROO-H})$ .
90. Knyazev, V. D., Bencsura, Á., Dubinsky, I. A., Gutman, D., Melius, C. and Senkan, S. M., 'Kinetics and Thermochemistry of the Reaction of 1-Chloroethyl Radical With Molecular Oxygen', *J. Phys. Chem.* **1994**. in press.
91. Alfassi, Z. B., Huie, R. E. and Neta, P., *J. Phys. Chem.* **1993**, *97*, 6835.
92. Hughes, K. J., Halford-Maw, P. A., Lightfoot, P. D., Turányi, T. and Pilling, M. J., *(Int'l) Combust., Proc.* **1992**, *24*, 645.
93. (1) Fenter, F. F., Catorie, V., Lesclaus, R. and Lightfoot, P., *J. Phys. Chem.* **1993**, *97*, 3530. (2) Fenter, F. F., Lightfoot, P. D., *J. Phys. Chem.* **1993**, *97*, 5313.

94. Munk, J., Pagsberg, P., Ratajczak, E. and Sillesen, A., *J. Phys. Chem.* **1986**, *90*, 2752.
95. Westmoreland, P. R., *Combust. Sci. and Tech.* **1992**, *82*, 151.
96. Wallington, T. J. and Gagaut, P., *Chem. Rev.* **1992**, *92*, 667.
97. Wu, F. and Carr, R. W., *J. Phys. Chem.* **1992**, *96*, 1743.
98. Slagle, I. R.; Gutman, D. *J. Am. Chem. Soc.* **1985**, *107*, 5342.
99. (1) Fenter, F. F., Lightfoot, P. D., Caralp, F., Lesclaux, R., Niiranen, J. T. and Gutman, D, *J. Phys. Chem.* **1993**, *97*, 4695. (2) . Russel, J. J. *et al.*, *J. Phys. Chem.* **1990**, *94*, 3277
100. Russel, J. J. *et al.*, *Symp. (Int'l) Combust., Proc.* **1990**, *23*, 895
101. Chettur, G. and Snelson, A., *J. Phys. Chem.* **1987**, *91*, 3483.
102. Quelch, G. E., Gallo, M. M. and Schaefer III, H. F., *J. Am. Chem. Soc.* **1992**, *114*, 8239.
103. Besler, B. H., Sevilla, M. D. and MacNeille, *J. Phys. Chem.* **1986**, *90*, 6446.
104. For the approach using fixed dihedral angle to study rotational barriers, see ref. 21 and (2) Yoshimine, M. and Pacansky, J., *J. Chem. Phys.* **1981**, *74*, 5168.  
(3) Dixon, D. A. *et al.*, *J. Phys. Chem.* **1992**, *96*, 10740.  
(4) Franciscon, J. S. *et al.*, *J. Phys. Chem.* **1994**, *98*, 5644.
105. Chapter 4 of this dissertation and reference therein.
106. CO-H bond energy = 104 kcal/mol, evaluated from  $\Delta H_f^\circ_{298}(\text{CH}_3\text{OH})$  and  $\Delta H_f^\circ_{298}(\text{CH}_3\text{O})$ , see Table 4.9 for reference sources.
107. Golden, D. M. and Benson, S. W., *Chem. Rev.* **1969**, *69*, 125.
108. Seetula, J. A. and Gutman, D., *J. Phys. Chem.* **1992**, *96*, 5401.
109. Pardo, L., Banfelder, J. R. and Osman, R., *J. Am. Chem. Soc.* **1992**, *114*, 2382.  
Based on the data provided in this article, one isodesmic reaction can be set up to calculate the value of  $D^\circ(\text{H--C}(\text{CH}_3)\text{HOOH}) - D^\circ(\text{H--CH}_2\text{OH})$  :  
 $\text{C}_2\text{H}_5\text{OH} + \text{CH}_3\text{CH}_2\text{OH} \Rightarrow \text{CH}_3\text{OH} + \text{CH}_3\text{C}_2\text{HOH}$ .  
The value of  $D^\circ(\text{H--C}(\text{CH}_3)\text{HOOH}) - D^\circ(\text{H--CH}_2\text{OH})$  is thus determined as -1.63 kcal/mol, based on the energies calculated at MP2/6-31G\*\*/UHF/6-31 level of theory for the species involved in the above reaction.

## REFERENCES FOR SECTION II

1. Ho, W.P., Barat, R.B. and Bozzelli, J.W., *Combustion and Flame* **1992**, 88, 265.
2. (1) Semeluk, G.P. and Bernstein, R.B., *J. Am. Chem. Soc.* **1954**, 76, 3793,  
(2) Semeluk, G.P. and Bernstein, R.B., *J. Am. Chem. Soc.* **1957**, 79, 46.
3. Kung, F.E. and Bissinger, W.E., *J. Org. Chem.* **1964**, 29, 2739.
4. Benson, S.W. and Spokes, G.N., *11th Symposium (International) on Combustion* **1966**, 11, 95.
5. Schug, K.P., Wagner, H.G. and Zabel, F., *Ber. Bunsenges Phys. Chem.* **1979**, 83, 167.
6. Herman, I.P., Magnotta, F., Buss, R.J. and Lee, Y.T., *J. Chem. Phys.* **1983**, 79, 1789.
7. Taylor, P.H. and Dellinger, B., *Environ. Sci. and Tech.* **1988**, 22, 438.
8. Chuang, S.C. and Bozzelli, J.W., *Environ. Sci. and Tech.* **1986**, 20, 568.
9. Won, Y. S., Ph.D. Dissertation, New Jersey Institute of Technology, Newark, New Jersey, **1991**.
10. Ritter, E.R. and Bozzelli, J.W., *Combust. Sci. and Tech.* **1990**, 74, 117.
11. Tirey, D.A., Taylor, P.H., Kasner, J. and Dellinger, B., *Combust. Sci. and Tech.* **1990**, 74, 137.
12. Won, Y.S. and Bozzelli, "Chloroform Pyrolysis: Experiment and Detailed Reaction Model", *Comb. Sci. and Tech.* **1992**, 85, 345.
13. (1) Dean, A. M., Bozzelli, J. W. and Ritter, E. R., *Combust. Sci. Technol.* **1991**, 80, 63. (2) Dean, A. M., *J. Phys. Chem.* **1985**, 89, 4600.
14. (1) Steward, J. J. P. *J. Comput. Chem.* **1989**, 10, 209, (2) *ibid.* 10, 221.
15. The results of PM3 calculation:  
For **CHCl<sub>3</sub>** (symmetry = 3), frequencies (cm<sup>-1</sup>): 240, 240, 346, 636, 660, 661, 1146, 1146, 2966. Moments of inertia (cm<sup>-1</sup>): 0.112, 0.112, 0.059.  
For **TS1** (symmetry = 1), frequencies (cm<sup>-1</sup>): (649, imaginary), 110, 208, 331, 537, 580, 686, 913, 1643. Moments of inertia (cm<sup>-1</sup>): 0.112, 0.080, 0.048.

16. (1) Russell, J.J., Seetula, J.A., Gutman, D. and Senken, S.M., *J. Phys. Chem.* **1989**, *93*, 1934. (2) Russell, J.J., Seetula, J.A., Gutman, D. and Melius, C.F., *23rd Symposium (International) on Combustion* **1991**, 217, The Combustion Institute.
17. Benson, S.W., *Thermochemical Kinetics*, John Wiley and Son, NY, **1976**.
18. Dean, A. M., Westmoreland, P. W. Longwell, J., Howard, J. and Sarofim, A. *AICHE Journal* **1986**, *32*, 1971.
19. Kee, R.J., Miller, J.A. and Jefferson, T.H., *CHEMKIN: Fortran Chemical Kinetics Code Package*, Sandia Report, SAND80-8003. UC-4 (1980)
20. Lutz, A.E., Kee, R.J. and Miller, J.A., *SENKIN: A Fortran Program for Predicting Homogeneous Gas Phase Chemical Kinetics with Sensitivity Analysis*, Sandia Report, SAND87-8248. UC-4 (1988)
21. Golden, D. M., *J. Chem. Education* **1971**, *48*, 235.
22. Ritter, E. R. and Bozzelli, J. W., *Int'l J. Chem. Kinetics* **1991**, *23*, 767.
23. Perry, R. A., Atkinson, R. and Pitts, Jr., J. N., *J. Phys. Chem.* **1977**, *81*, 296.
24. Atkinson, R., Ashmann, S. M., Arey, J. and Carter and W. P. L., *Int. J. Chem. Kinet.* **1989**, *21*, 801.
25. Knispel, R., Koch, R. Siese, M. and Zetzch, C., *Ber. Bunsenges. Phys. Chem.* **1990**, *94*, 1375.
26. Atkinson, R., Carter, W. P. L., Darnell, K. R., Winer, A. M. and Pitts, J. N., *Int. J. Chem. Kinet.* **1980**, *12*, 779.
27. Atkinson, R., Carter, W. P. L. and Winer, A. M., *J. Phys. Chem.* **1983**, *87*, 1605.
28. Chepson, P. B., Edney, E. O. and Corse, E. W., *J. Phys. Chem.* **1984**, *88*, 4122.
29. Gery, M. W., Fox, D. L. and Jeffries, H. E., *Int. J. Chem. Kinet.* **1985**, *17*, 931.
30. Leone, J. A., Flagan, R. C. Grosjean, D. and Seinfeld, J. H., *Int. J. Chem. Kinet.* **1985**, *17*, 177.
31. Takagi, H., Washida, N., Akimoto, H. Nagasawa, K., Usui, Y. and Okuda, M., *J. Phys. Chem.* **1980**, *84*, 478.
32. Atkinson, R., Aschmann, S. M. and Arey, J., *Int. J. Chem. Kinet.* **1991**, *23*, 77.

33. Lonneman, W. A., Kopczynski, S. L., Darley, P. E. and Sutterfield, F. D., *Environ. Sci. Tech.* **1974**, *8*, 229.
34. Grosjean, D. and Fung, K., *J. Air Pollut. Control Assoc.* **1984**, *34*, 537.
35. Hendry, D. G., Baldwin, A. C. and Golden, D. M., *Computer Modeling of Simulated Photochemical Smog*, EPA-600/3-80-029, Feb. 1980.
36. Killus, J. P. and Whitten, G. Z., *Atmos. Environ.* **1982**, *16*, 1973.
37. Leone, J. A. and Seinfeld, J. H., *Int. J. Chem. Kinet.* **1984**, *16*, 159.
38. Atkinson, R. and Lloyd, A. C., *J. Phys. Chem. Ref. Data* **1984**, *13*, 315.
39. Atkinson, R., *J. Phys. Chem. Ref. Data* **1991**, *20*, 459.
40. James, D. G. L. and Suart, R. D., *Trans. Faraday Soc.* **1968**, *64*, 2752.
41. Shaw, R., Cruickshank, F. R. and Benson, S. W., *J. Phys. Chem.* **1967**, *71*, 4538.
42. Nicovich, J. M. and Ravishankara, A. R., *J. Phys. Chem.* **1984**, *88*, 2534.
43. McMillen, D. F. and Golden, D. M. In *Annual Review of Physical Chemistry*, Rabinovitch, B. S. (Ed.), Annual Reviews: Palo Alto, CA, **1982**.
44. Tsang, W., *J. Phys. Chem.* **1986**, *90*, 1152.
45. Chase, Jr., M. W. *et al.* (Ed.), "JANAF Thermochemical Tables, 3rd ed.", *J. Phys. Chem.* **1986**, *14*, Supplement No. 1.
46. Lay, T. H. and Bozzelli, J. W., "Hydrogen Atom Bond Increment Groups for Calculation of Thermodynamic Properties of Oxygenated Hydrocarbon Radical Species", to be published.
47. Dorofeeva, O. V., Gurvich, L. V. and Jorish, V. S., *J. Phys. Chem. Ref. Data* **1986**, *15*, 437.
48. Stewart, J. J. P. *MOPAC 6.0 : A General Molecular Orbital Package*, October, 1990. Frank J. Seiler Research Lab., US Air Force Academy, CO 80840.
49. Bauch *et al.*, *J. Phys. Chem. Ref. Data* **1992**, *21*, 595.
50. Kerr, J. A. and Parsonage, M. J. for reaction:  $\text{H} + \text{C}_6\text{H}_6 = \text{C}_6\text{H}_7$ , in *NIST Chemical Kinetic Database*, Ver. 5.0, by Mallard *et al.*, NIST Standard Reference Data, Gaithersburg, Maryland, 1993.



51. Benson, S. W., *J. Am. Chem. Soc.* **1965**, *87*, 972.
52. Chapter 3 of this dissertation.
53. Seakins, P. W., Pilling, M. J., Nitranen, J. T., Gutman, D. and Krasnoperov, L. N., *J. Phys. Chem.* **1992**, *96*, 9847.
54. The secondary allylic C-H bond energy (85.6 kcal/mol) is estimated from primary allylic C-H bond energy (88.2 kcal/mol, ref. 39) plus the increment of C-H bond energy from primary alkyl (101.1 kcal/mol, ref. 36) to secondary alkyl (98.45 kcal/mol, ref. 36) C-H bond energy.
55. The torsion frequency which corresponds to the hindered rotation of OH rotor on the ring body was excluded from the calculation of  $\Delta S_{298}^{\ddagger}$ , because this rotor is considered to contribute the entropy identical to both reactant and TS.
56. Tsang, W., *J. Phys. Chem.* **1992**, *96*, 8378.
57. Ritter, E. R., *J. Chem. Info. and Comp. Sci.* **1991**, *31*,400.
58. Seinfeld, J. H., *Atmospheric Chemistry and Physics of Air Pollution*, John Wiley & Sons Inc., New York, **1986**.